Quantitative analysis of new generation antidepressants using gas chromatography-mass spectrometry

Applications in clinical and forensic toxicology

Sarah Wille
Pharmacist

Thesis submitted to obtain the degree of
Doctor in Pharmaceutical Sciences

2008

Dean:
Prof. Dr. Jean-Paul Remon

Promoter :
Prof. Dr. Willy Lambert

TABLE OF CONTENTS

ionization

Summary

Samenvatting

Curriculum Vitae

ACKNOWLEDGMENTS DANKWOORD

LIST OF ABBREVIATIONS

ACN	acetonitrile
AD	antidepressant
AGNP	arbeitsgemeinschaft für neuropsychopharmakologie und pharmakopsychiatrie
AMP	adenosine monophosphate
amu	atomic mass unit
APCI	atmospheric pressure chemical ionization
BDNF	brain-derived neurotrophic factor
CI	confidence interval
CI(-mode)	chemical ionization
CRE	$cAMP/Ca^{2+}$-responsive element
CREB	$cAMP/Ca^{2+}$-responsive element binding protein
CRH	corticotrophin-releasing hormone
CYP	cytochrome
DAD	diode array detector
DDMC	didesmethylcitalopram
DMC	desmethylcitalopram
DMFluox	desmethylfluoxetine
DMMap	desmethylmaprotiline
DMMia	desmethylmianserin
DMMir	desmethylmirtazapine
DMSer	desmethylsertraline
DNA	deoxyribonucleic acid
DSM-IV	american psychiatric association diagnostic and statistical manual of mental disorders
DRI	dopamine reuptake inhibitor
ECD	electron capture detector
EDTA	ethylene diamine tetra-acetic acid
EI	electron ionization
EM	extensive metabolizer
ESI	electrospray ionization
eV	electron volt
Fd_6	hexa-deuterated fluoxetine
FDA	food and drug administration
F^{19} MRS	fluorine magnetic resonance spectroscopy
GABA	gamma-aminobutyric acid
GC	gas chromatography
HAM-D	hamilton depression rating scale
HFB-	heptafluorobutyryl-
HFBA	heptafluorobutyric anhydride
HFBI	heptafluorobutyryl imidazole
HPA	hypothalamic-pituitary-adrenal axis
HPLC	high pressure liquid chromatography
IM	intermediate metabolizer

I.S.	internal standard
LC	liquid chromatography
LLE	liquid/liquid extraction
LOQ	limit of quantification
m-cpp	m-chlorophenylpiperazine
MAOI	mono-amine oxidase inhibitor
MADRS	montgomery and asberg depression rating scale
Md_3	tri-deuterated mianserin
MeOH	methanol
MRP	multidrug resistance associated protein
MS	mass spectrometry
m/z	mass-to-charge ratio
NARI	selective noradrenaline reuptake inhibitor
NaSSA	noradrenergic and specific serotonergic antidepressant
NICI	negative ion chemical ionization
NPD	nitrogen phosphorus detector
ODMV	O-desmethylvenlafaxine
Pd_6	hexa-deuterated paroxetine
PICI	positive ion chemical ionization
PKA	cAMP-dependent protein kinase A
pK_a	dissociation constant
PM	poor metabolizer
P-gp	P-glycoprotein transporter
RE	relative error
RSD	relative standard deviation
RSK1-3	ribosomal S6 kinases
SARI	serotonin-2 antagonist and reuptake inhibitor
SCX	strong cation exchanger
SIM	selected ion monitoring
S/N	signal to noise ratio
SNRI	serotonin and noradrenaline reuptake inhibitor
SPE	solid phase extraction
SPME	solid phase micro extraction
SSRE	selective serotonin reuptake enhancer
SSRI	selective serotonin reuptake inhibitor
STA	systematic toxicological analysis
TCA	tricyclic antidepressant
TDM	therapeutic drug monitoring
TDM-GEN	therapeutic drug monitoring combined with genotyping
TIAFT	the international association of forensic toxicologists
trkB	tyrosine kinase B receptor
UGT	uridine diphosphate glucuronosyltransferase
UM	ultrarapid metabolizer
UV	ultraviolet
WCX	weak cation exchanger

STRUCTURE

This thesis gives an overview of the development of a gas chromatographic-mass spectrometric (GC-MS) method for new generation antidepressants (ADs) and their metabolites. The structure of the manuscript is build up as if the reader is following the sample analysis.

First a general overview of the ADs and the relevance of monitoring those compounds in clinical and forensic settings are given in **chapter I**, while **chapter II** gives an overview of the objectives of our research.

Thereafter the method development for sample analysis is described. **Chapter III** describes the solid phase extraction development for different biological matrices such as plasma, blood, brain and hair tissue. Because a GC-MS configuration was applied, derivatization of the extracts was evaluated and optimized (**chapter IV)**. After the sample preparation, the ADs and metabolites are separated and detected using gas chromatography-mass spectrometry. The chromatographic and mass spectrometric parameters for three ionization modes (electron ionization, positive and negative ion chemical ionization) were optimized for each compound as described in **chapter V**.

Having established a GC-MS procedure for new generation ADs, this method was validated based on the FDA guidelines concerning stability, linearity, sensitivity, selectivity, precision, and accuracy. The validation procedure is described in **chapter VI**.

The applicability of the developed and validated method is evaluated in **chapter VII and VIII**. Chapter VII describes the usefulness of the developed method in a clinical setting by describing a project in which the antidepressant/metabolite plasma concentration will be linked to the metabolization capacity of the individual patient. Chapter VIII describes the application of the procedure to post-mortem cases with matrices such as whole blood, brain tissue and hair.

A general conclusion is given in **chapter IX**.

Chapter I

Introduction:
depression,
use of antidepressants,
and relevance of antidepressant monitoring

I.1.   Foreword

Depression is a chronic or recurrent mood disorder that affects both economic and social functions of about 121 million people worldwide. According to the World Health Organization, depression will be the second leading contributor to the global burden of disease, calculated for all ages and both sexes by the year 2020 [1-3]. This common mental disorder presents a highly variable set of symptoms such as depressed mood, loss of interest or pleasure, feelings of guilt or low self-esteem, disturbed sleep or appetite, low energy, and poor concentration. These problems lead to substantial impairments in an individual's ability to take care of his or her everyday responsibilities. At its worst, depression can lead to suicide, a tragic fatality associated with the loss of about 850 thousand lives every year. Depression can be subdivided in bipolar disorder (manic-depression), dysthymia, and major depression (unipolar depression). This introduction will focus on major depression, discussing the onset of depression and the treatment, including the action mechanisms, side-effects and toxicity of the new generation antidepressants (ADs). Moreover, the potential value of therapeutic drug monitoring (TDM) and toxicological assays for these drugs is discussed in relation to their mode of action, drug interactions, metabolism and pharmacokinetic properties.

I.2.   Onset of depression

Epidemiologic studies show that about 40-50% of the risk of depression is genetic. However, no specific genes or genetic abnormality have been identified to date with certainty. In addition, factors such as stress, emotional trauma, viral infections, and certain processes in brain development also have an influence on the etiology of depression [4]. The neural circuitry underlying depression is not yet fully understood. It is likely that several brain regions (prefrontal and cingulated cortex, hippocampus, striatum, amygdale and thalamus) mediate the diverse symptoms of depression.

It seems that malfunction of the hypothalamic-pituitary-adrenal (HPA) axis plays an important role [5]. These malfunctions include an increased

corticotrophin-releasing hormone (CRH) level or an impaired cortisol negative feedback mechanism, stimulating the release of glucocorticoids from the adrenal cortex. This release of glycocorticoids leads to damage of the hippocampal neurons, resulting in impaired hippocampal function which contributes to some of the cognitive abnormalities of depression.

The evidence that monoamine systems including serotonergic, noradrenergic and dopaminergic systems are crucial in the pathophysiology of depression was already known in the early 1950's. Low serotonin activity and depletion of catecholamines in the central and peripheral nervous system was associated with depression. Therefore, several receptors and transporters of these monoamines became the target of medical treatment of depression.

Neurotrophic factors such as the brain-derived neurotrophic factor (BDNF) play a role, as they regulate the neural growth and plasticity as well as the survival of adult neurons and glia. The up-regulation of the expression of BDNF by ADs could oppose the cell death pathway.

On the other hand, the GABAergic system also seems to be critical as in depressed patients lower GABA levels are observed in the occipital cortex using magnetic resonance spectroscopy studies. In addition, the GABAergic system interacts with the serotonergic system, the noradrenergic system, the hypothalamic-pituitary-adrenal axis and neurotrophic factors.

I.3.   Action mechanisms of antidepressants

Monoamine neurotransmitters such as dopamine, serotonin and noradrenaline play an important role in the onset and treatment of depression, as depression can be improved by compounds that increase synaptic concentrations of these neurotransmitters. These increased concentrations can be achieved by various mechanisms such as blocking neurotransmitter transport (reuptake) and neurotransmitter auto-receptors or by inhibiting the mitochondrial enzyme monoamine oxidase which is responsible for the oxidative deamination of endogenous and xenobiotic monoamines [6, 7]. Neurotransmitter transporters and certain receptors are

safety-mechanisms that prevent overstimulation of receptors in the synapse by either transporting monoamines back into the neuron or diminishing the nerve impulse to release more neurotransmitter. When these transporters and receptors are blocked, the negative feed-back mechanism of the neuron is stopped, leading to a higher concentration of monoamines in the synapse. These are the action mechanisms of the tricyclic (TCA) and new generation ADs. However, while TCAs block the transport and receptors of noradrenaline and serotonin as well as muscarin cholinergic, H_1-histaminergic and $α_1$-adrenergic receptors, the new generation ADs work more selectively. Consequently, new generation ADs are subdivided on base of their selectivity for enhancing the synapse concentration of one or more neurotransmitters.

The classic monoamine hypothesis discussed above does not explain why the AD drug therapy is associated with a delay of a few weeks before a clinical effect, even though the onset of increased synaptic monoamine concentrations happens directly [5, 6, 8]. Therefore, the current view is that chronic adaptations in the brain function rather than acute increases in synaptic monoamine concentrations lead to the therapeutic effects of ADs. Thus, while monoamine synapses are still considered the immediate target of AD drugs, more attention is paid to long-term changes in signal transduction systems and gene expression, due to chronic use of ADs. Recent theories postulate a number of mechanisms that could cause these long-term changes, including activation of transcription factors such as the $cAMP/Ca^{2+}$-responsive element binding protein (CREB), but also activation of neurotrophic pathways and increased hippocampal neurogenesis.

I.3.1. Activation of transcription factors

When a monoamine neurotransmitter binds on its respective receptors, a signal will be transmitted to the cell interior, mostly through a G-protein. Once a G-protein is activated, it can regulate the behaviour of potassium or calcium ion-channels or second messenger systems, which on their turn regulate kinases. These kinases phosphorylate transcription factors, controlling gene expression by binding to several short sequences of

deoxyribonucleic acid (DNA). This reaction results in activation or repression of the expression of certain genes [9].

<u>Figure I.1.</u> Regulation of cAMP responsive element-binding protein (CREB) phosphorylation by ADs

Most clinically effective ADs alter noradrenaline or 5-HT neurotransmitter levels by a variety of mechanisms. Cell-surface receptors can respond to these neurotransmitters by altering intracellular second messengers, such as cAMP and Ca^{2+}, in addition to several kinases, such as cAMP-dependent protein kinase (PKA), Ca^{2+}–CaM-dependent kinases (CaMK), mitogen-activated protein kinase (MEK), extracellular signal-regulated protein kinase (ERK) and several forms of ribosomal S6 kinase (RSK_{1-3}). Kinases phosphorylate protein substrates such as the transcription factor CREB. CREB binds to a cAMP responsive element (CRE) in DNA to regulate gene expression. These CREB-target genes might ultimately modulate behavior, endocrine or cellular changes associated with chronic AD treatment. Adapted from [10].
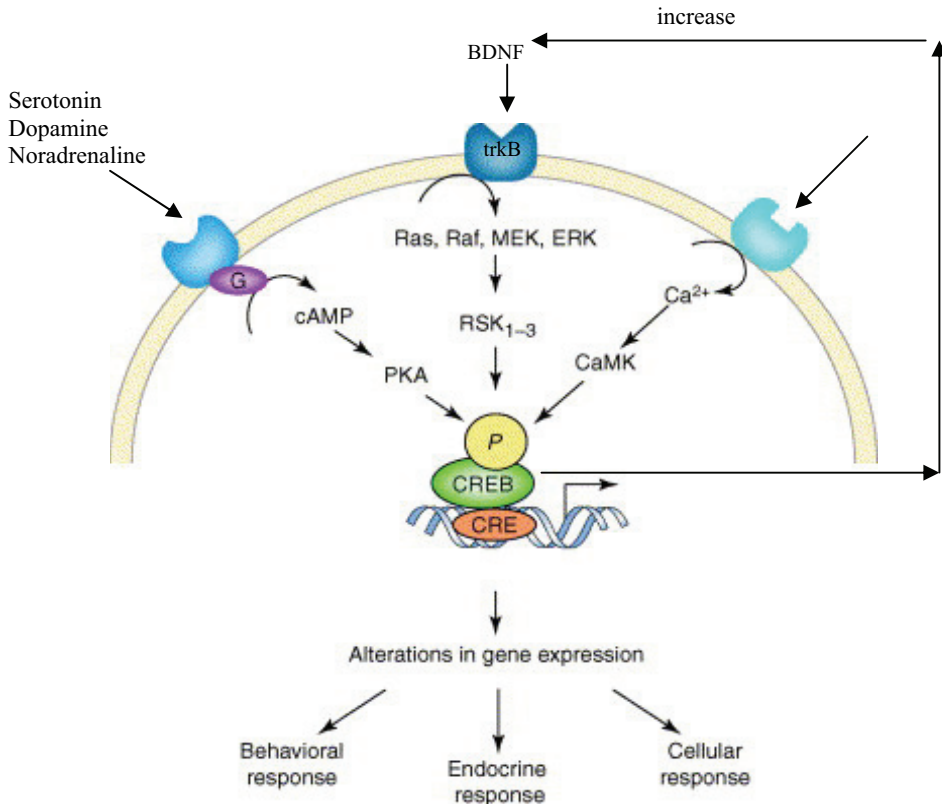
There are 3 mechanisms (Figure I.1.) that will result in the phosphorylation of the transcription factor CREB, which will then bind to a cAMP- and calcium-responsive element (CRE) in DNA and will result in regulation of gene expression important for AD effects. CREB regulates genes for neurotransmitter synthetic enzymes such as tyrosine hydroxylase, which is the rate-limiting enzyme in the biosynthesis of catecholamines. In addition, CREB regulates proteins involved in cell neurogenesis [10].

The first mechanism activates adenylyl cyclase through G-protein stimulation, which leads to an increased production of cAMP, enabling the activation of cAMP-dependent protein kinase A (PKA). This protein kinase A will then translocate to the nucleus and will phosphorylate a specific serine residue in the CREB protein.

The second mechanism is the activation of phospholipase C through α_1-adrenoceptors, leading to mobilization of Ca^{2+} and subsequent activation of Ca^{2+}-calmodulin-dependent kinases, which in their turn also phosphorylate CREB.

Another mechanism is started by neurotropic factors and cytokines that regulate certain receptors, influencing mitogen-activated protein kinase and intracellular signal-regulated protein kinase, which phosphorylate CREB through several forms of ribosomal S6 kinases (RSK_{1-3}) [11-13].

I.3.2. Activation of neurotrophic pathways

There have been reports indicating that chronic administration of ADs can prevent atrophy of neurons in the hippocampus caused by repeated stress by increasing the neurotrophic factor BDNF [10, 11, 14]. As BDNF binds to the tyrosine kinase B receptor (trkB) in the brain, an intracellular signalling cascade starts, which results in phosphorylation of CREB. In addition, a link between CREB and BDNF is suggested as enhanced CREB expression might lead to an upregulation of BDNF, because CREB would target the gene encoding for BDNF. On the other hand, BDNF would also induce neurogenesis [5, 9, 10].

I.3.3.   Increasing neurogenesis

Chronic AD treatment has shown to reverse the reduced hippocampal cell volume. This increased neurogenesis is observed in depressed humans using the Magnetic Resonance Imaging technique and in post-mortem studies. As a result, a hypothesis was postulated that the increasing neurogenesis could lead to the therapeutic effects of the ADs. The neurogenesis caused by ADs is possibly mediated through CREB, BDNF enhancement and the insulin-like growth factor, another neurotrophic factor.

Although the regulation of CREB and BDNF may be important in the actions of AD treatment, a lot of research still has to be done in this field, as these reactions are probably not the only targets of ADs. Therefore, the action mechanisms of ADs still partly remain unclear [10].

I.4.   **Classification of antidepressants**

Before 1980, depression was treated using tricyclic antidepressants (TCAs) and monoamine oxidase inhibitors (MAOI). However, their side-effects, toxicity, and severe drug-drug interactions combined with an advanced understanding of the central nervous system have led to the introduction of several 'new' ADs [15, 16].

Classes of these ADs are defined by their selectivity towards certain neurotransmitter transporters and receptors. The reuptake of serotonin and noradrenaline is selectively blocked by the Selective Serotonin Reuptake Inhibitors (SSRI) such as fluoxetine, fluvoxamine, sertraline, paroxetine, and citalopram, and the Selective Noradrenaline Reuptake Inhibitors (NARI) including reboxetine and viloxazine, respectively. The class of the Serotonin and Noradrenaline Reuptake Inhibitors (SNRI), however, combines the action mechanisms of the two previous classes by inhibiting the reuptake of both serotonin and noradrenaline, leading to dual-acting agents such as venlafaxine, milnacipran and duloxetine.

<u>Table I.1.</u> Classification of ADs based on their action mechanism, their influence on cytochrome P450 isoenzymes and on the neurotransmitter transporters and receptors

TCAs (tricyclic AD), MAOI (mono amine oxidase inhibitors), SNRI (serotonin and noradrenaline reuptake inhibitors), SSRI (selective serotonin reuptake inhibitors), NARI (selective noradrenaline reuptake inhibitors), SARI (serotonin-antagonist and reuptake inhibitors), NaSSA (noradrenergic and specific serotonergic antidepressants), SSRE (selective serotonin reuptake enhancer), DRI (dopamine reuptake inhibitor). NA (noradrenaline), 5-HT (serotonin), DA (dopamine), H_1 (histamine H_1 receptor), MA (muscarinic acetylcholine receptor), Alpha$_1$ (α_1-adrenergic receptor), Alpha$_2$ (α_2-adrenergic receptor). The ++++ means strong interaction with the transporters and receptors, + very low potency, to no potency at all.

Antidepressants	CYP isoenzymes		Neurotransmitter Transporters and Receptors							
	CYP inhibition	*CYP metabolism*	*Transporters*			*Receptors*				
			NA	5-HT	DA	H_1	MA	Alpha $_1$	Alpha $_2$	5HT
TCA										
1. Amitriptyline		2D6, 2C19, 2C9, 1A2, 3A4	+++	++++	+	+++++	+++	+++		++
2. Amoxapine			+++	+++	+	+++	+	+++		++
3. Clomipramine		2C19, 3A4, 2D6	+++	++++	+	+++	+++	+++		
4. Dosulepin			++++	++++						
5. Doxepin		2D6, 2C19, 2C9, 1A2	+++	+++		+++++	++	+++		
6. Imipramine		2D6, 2C19, 1A2, 3A4	+++	++++	+	++++	++	++		
7. Maprotiline		2D6, 1A2	++++				+			
8. Melitracen			++++	++++						
9. Nortriptyline		2D6, 3A4	++++							
10. Opipramol										
11. Trimipramine					++		++	++		++
MAOI										
1. Moclobemide	2C9, 2D6,1A2	2C19								
2. Phenelzine										
3. Trancylcypromine										
SNRI										
1. Duloxetine		1A2, 2D6	+++	++++	+	+	+			
2. Milnacipran	no inhibition		++++	++++						
3. Venlafaxine	Minimal: 2D6	2D6, 3A4	++	++++	+					
SSRI										
1. Citalopram	Minimal: 2D6, 2C19,1A2	2C19, 2D6,3A4		++++		+		+		
2. Fluoxetine	2D6, 2C9/19, 3A4	2D6, 2C	+	++++		+	+	+		+
3. Fluvoxamine	1A2, 2C19, 3A4,2C9	1A2,2D6	+	++++				+		
4. Paroxetine	2D6	2D6	+	++++	+		++			
5. Sertraline	Minimal: 2D6, 2C, 3A4,1A2	2D6, 2C9, 2C19, 3A4	+	++++	++		+	+		
NARI										
1. Reboxetine	Minimal: 2D6, 3A4	3A4	++++	+			+	+		
2. Viloxazine	3A4, 2C9, 2C19,1A2		++++	+						
SARI										
1. Nefazodone	3A4	2D6, 3A4		++++				+++		++++
2. Trazodone		2D6, 1A2, 3A4		++++		+		+++		++++
NaSSA										
1. Mianserin		1A2, 2D6, 3A4							++++	++++
2. Mirtazapine		1A2, 2D6, 3A4				+	+		++++	++++
SSRE										
1. Tianeptine		3A		++++						
DRI										
1. Bupropion	2D6	2B6	++		+++					

Mirtazapine and mianserin are receptor antagonists which block the noradrenaline α_2-auto- and hetero-receptors, as well as the 5-HT$_{2/3}$ receptors. However, mianserin, as in contrast to mirtazapine, has no indirect 5-HT$_{1a}$ stimulating effect through α_2-antagonism. Therefore mirtzapine is a Noradrenergic and Specific Serotonergic antidepressant (NaSSA), but this is

not clear for mianserin. Trazodone and nefazodone are Serotonin-2 Antagonists and Reuptake Inhibitors (SARI), combining antagonism of 5-HT$_2$ with serotonin reuptake blockade [3, 11, 15-18]. Bupropion is a dopamine reuptake inhibitor (Table I.1.).

I.5. Side-effects, drug-drug interactions and toxicity

The differences in side-effects and drug-drug interaction profile of the ADs are the result of their specific pharmacokinetic properties, interaction with the cytochrome P450 isoenzymes (CYP 450), and their affinity for different neurotransmitter sites.

The most relevant pharmacokinetic properties include the non-linear kinetics, half-life of the compound and its active metabolite (if relevant), as well as protein binding. Compounds that have non-linear kinetics (e.g. fluvoxamine) lead to disproportionate increases in drug plasma concentrations when using higher doses, resulting in a possible increase of side-effects. Due to the long half-life of compounds such as fluoxetine and especially of its active metabolite desmethylfluoxetine, attention should be paid to longer wash-out periods before starting other medication as drug-drug interactions could occur. Protein binding interactions do not seem to be of great importance for ADs, probably because basic drugs bind to α_1-acid glycoproteins rather than albumin and as a result do not displace drugs such as warfarin and digoxin that are tightly bound to albumin [19-21].

A lot of drug-drug interactions occur through the inhibition of CYP 450. The isoenzymes that are inhibited by ADs and the ones that metabolize the antidepressant drugs are shown in Table I.1. When evaluating the clinical significance of a potential interaction, several factors must be considered. These factors include the potency and the concentration of drug and inhibitor or inducer at the enzyme active site, the saturation of the CYP enzyme involved, the extent of metabolism by the drug through this enzyme, the presence of active metabolites and the therapeutic window of the substrate, genetic polymorphism, the patient (elderly, liver impairment) and the probability of concurrent use [22]. As a result of the inhibition, caution is

advised using (co-)medication with narrow therapeutic windows such as tricyclic antidepressants, theophylline, phenytoin, tolbutamide, carba-mazepine, terfenadine, astemizole, type 1C antiarrhythmics or antipsychotics [23].

The differences in side-effects of ADs depend on their potency of interaction with different transporters and receptors (Table I.1.) such as the noradrenaline, serotonin and dopamine transporter and the histamine, muscarinic and adrenergic receptors [6]. Side-effects caused by affinity for the serotonin transporter are gastrointestinal disturbances and nausea (5-HT_3), sexual dysfunction (5-HT_2), and extra pyramidal adverse effects [6, 24]. In addition, coadministration of MAOI with ADs that block the serotonin transporter can cause the deadly serotonin syndrome [25]. Blockade of the noradrenaline transporter can result in hypertension, tremors and tachycardia, while blockade of the dopamine transporter leads to psychomotor activation and aggravation of psychosis. Other common side-effects are sedation and weight gain caused by histamine H_1 receptor blockade, and postural hypotension, dizziness, reflex tachycardia caused by blockade of $α_1$-adrenergic receptors. As a result of muscarinic receptor binding, dry mouth, constipation, urinary retention, blurred vision, increased intra-ocular pressure, increased heart rate, disturbances in accommodation and hyperthermia occur [6, 21]. Cardiovascular symptoms are the most important side-effects seen for the TCAs and they are mediated by different mechanisms. Inhibition of $α_1$-noradrenergic receptors causes orthostatic hypotension, dizziness and possibly reflex tachycardia, while the quinidine-like effect (blockage of myocardial sodium channels) of the tricyclics is responsible for disturbances in conduction, which is reflected in changes in the electrocardiogram [26]. Hypertension and tachycardia may originate from the hyperadrenergic state which is induced by neurotransmitter reuptake inhibition. This may be followed by a period of catecholamine depletion, causing hypotension [26]. In therapeutic doses, most common cardiovascular effects include orthostatic hypotension and tachycardia, which may be more severe in elderly patients [27]. In overdose, cardiovascular effects may be life threatening [26, 28-30]. In patients with cardiovascular disease, the use of tricyclic antidepressants increases the risk of cardiac morbidity and sudden

cardiac death, particularly in the elderly patients [31-33]. Taking this into consideration, together with the growing evidence that personality [34] and depression may adversely affect cardiovascular health [32, 33, 35-37], several authors conclude that SSRIs may be a better alternative in depressed patients with concomitant cardiovascular disease [33, 35, 36, 38]. However, bleeding and cardiovascular effects seem to occur with SSRIs because of the serotonin effect on vascular smooth muscle. Therefore, there are also good reasons to believe that β-blockers such as propranolol and pindolol could interact with SSRI [39].

Thus, while the new generation ADs are almost equipotent as TCAs, they have less life-threatening side-effects, such as cardiotoxicity and are safer in overdose. The most reported side-effects are neurological, psychiatric, and gastrointestinal side-effects [40]. Recently though, it has been suggested that there might be an association between suicidal thoughts and the use of SSRIs [41, 42]. However, more research is needed to support this hypothesis. In addition, the FDA is also concerned about the use of SSRIs in children. Whittington et al. [43] concluded that risks could outweigh the benefits of SSRIs (except for fluoxetine) used to treat depression in children and young people. SSRIs, though, seem rather safe when used during pregnancy and breastfeeding, although more research and clinical experience will be needed to confirm this finding [44, 45]. On the other hand, Sanz et al. published a database analysis in which they concluded that withdrawal syndromes or neonatal convulsions are seen for all SSRIs, but especially after paroxetine use [46]. This could be due to the affinity of paroxetine towards the muscarinic receptors in combination with non-linear kinetics and self-limiting metabolism [46, 47]. In general, the SSRIs are the group of new generation ADs of which the side-effects are clearer, as this group is largely used and studied. For other groups of new generation ADs, more studies and time will probably be necessary to get a full image of the side-effects that may occur and the severity of those effects.

I.6.   Relevance of Therapeutic Drug Monitoring

The basic principle underlying Therapeutic Drug Monitoring (TDM) is that the plasma drug-concentration is related to the drug-concentration at the effector site, producing a certain clinical response. Thus, TDM provides an indirect estimation of the concentration of ADs in the brain tissue in relation with a certain effect. TDM is used to avoid drug toxicity, to assess patient compliance, to enhance drug response, and to increase cost-efficiency. TDM can be a valid tool to optimize AD pharmacotherapy, but is underutilized in the field of psychiatry. Among clinicians there is still an under-appreciation of the degree of pharmacokinetic variability found in patients and how that might have an impact on the patient's response to pharmacotherapy [48]. While TDM is used for TCAs as they have narrow therapeutic windows and can have severe side-effects, use of TDM will not become a standard procedure for new generation ADs as they have an unclear relationship between blood concentrations and therapeutic effects. Furthermore, therapeutic ranges of the new ADs seem quite broad, leading to the generally accepted notion of low toxicity. These compounds, however, also provide considerable adverse drug reactions and side-effects. Nowadays, psychiatric medication is prescribed in all imaginable combinations, increasing the possibility of drug-drug interactions [49]. Therefore, TDM could be of interest for monitoring patients with poor or ultrarapid metabolism by CYP 450 isoenzymes, and patients that are co-medicated with inhibitors or inducers of those isoenzymes. In addition, the side-effects of the new generation ADs and their delayed therapeutic effect lead to poor patient compliance. As over 40% of patients receiving psychotropic medications are non-compliant, monitoring of ADs use is crucial to provide an objective compliance check. For special patient populations such as children, adolescents, elderly and patients with liver and kidney impairment, TDM could provide valuable information for a cost-effective and more rational use of psychiatric drugs.

Thus, although it is unlikely that TDM will become a standard procedure for all AD agents and all patients, it can surely optimize AD treatment for special patient populations, patients with poor or ultrarapid metabolism due to CYP 450 isoenzymes or it can provide an alternative to a lengthy trial and error

dose titration process for patients with concomitant drug use. In addition, it can be used to monitor compliance [48-53]. In the future, advances in TDM will be made by increasing the knowledge of the brain and the influence of ADs on the brain, the genetic differences and the influences of those differences on plasma concentrations.

I.7. Selection of antidepressants and relevant issues for TDM

The ADs monitored in this work were selected based on their importance in the 7 major antidepressant markets (Japan, USA, France, United Kingdom, Italy, Spain, Germany) according to the Cognos Plus Study #11 [54] and on the AGNP-TDM Expert Group Consensus Guidelines [55].

Table I.2. Therapeutic and toxic range of several ADs and their active metabolites in plasma together with characteristics relevant for therapeutic drug monitoring

[1]Information between brackets concerns the metabolite. ActMet: Active metabolite in plasma; Vd: distribution volume; Fb: Fraction bound; pKa: Dissociation constant; Log P: Partition coefficient (octanol/water); $T_{1/2}$: half-life; Ther.C.: Therapeutic concentration range; Tox.C.: Toxic concentration; (L): Lethal concentration [56].

Compound	Mw	ActMet	Vd (l/kg)	Fb (%)	pKa	LogP	$T_{1/2}$ (h)	Ther.C (µg/l)	Tox.C. (µg/l)
Citalopram	324	Desmethylcitalopram Didesmethylcitalopram	12-16	50	9.5	3.74	25-40	20-200	(L)500
Fluoxetine	309	Desmethylfluoxetine	20-42	94.5	8.7 (9.37)[1]	4.05	96-144 (96-384)[1]	150-500 (100-500)[1]	1000 (900)[1]
Fluvoxamine	318		25	77	8.7	0.04	8-28	50-250	650
Maprotiline	277	Desmethylmaprotiline	23-70	90	10.5	4.5	20-70	75-250	300-800
Melitracen	291				7.05			10-100	
Mianserin	264	Desmethylmianserin	10-29	90	7.1	3.36	6-40	15-70	500-5000
Mirtazapine	265	Desmethylmirtazapine	10-14	85	9.9		20-40	20-100 (50-300sum)	1000-2000
Paroxetine	329		3-28	95		3.95	12-40	10-75	350-400
Reboxetine	313		0.39-2.8	97			13-15	50-160	
Sertraline	306	Desmethylsertraline	20	98	9.45	5.29	26	50-250	290/1600
Trazodone	372	m-Chlorophenylpiperazine	0.9-1.5	90	6.7	3.2	4-7	500-2500	4000
Venlafaxine	277	O-desmethylvenlafaxine	4-12	30	9.24 (9.74)[1]	0.43	4	200-400	1000-1500
Viloxazine	237		0.5-1.5	85-90	8.1	1.8	2-5	5000-10000peak	

The Cognos Plus Study demonstrates that monoamine oxidase inhibitors and TCAs (8% European market share 2004) are less frequently prescribed than SSRIs and SNRIs. In addition, compounds such as nefazodone, duloxetine and milnacipran were not determined as they were not commercially available in Belgium, while the TCAs melitracen and maprotiline were monitored as they are readily prescribed in Belgium. In addition, the (active) metabolites were monitored as suggested by the AGNP-TDM Expert Group

Consensus Guidelines, as metabolite/compound ratios could provide more information on the relation between plasma concentration and therapeutic effects. A summary of relevant information concerning AD drug monitoring is given in Table I.2. The stability of the ADs will be discussed in chapter III and VI.

I.7.1. Citalopram

1-[3-(Dimethylamino)propyl]-1-(4-fluorophenyl)-1,3-dihydroisobenzofuran-5-carbo-nitrile: mol. wt., 324.4; pK$_a$, 9.5; usual dose, 20-60 mg/day (escitalopram : 10-20 mg/day); therapeutic plasma concentration, 20 to 200 ng/ml; lethal concentration, 500 ng/ml [56] ; plasma half-life, 33 h [25-40 h]; plasma protein binding, 50%; distribution volume, 12-16 l/kg [57, 58].
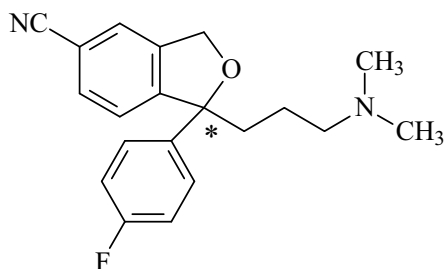
Citalopram is a selective inhibitor of neuronal serotonin (5-hydroxytryptamine) reuptake [40]. This antidepressant is the most selective serotonin reuptake inhibitor, but is less potent than paroxetine [40, 59]. Citalopram is a racemic mixture (S/R=1) with a blood or plasma ratio of the S/R form varing between 0.32 and 1.25. The S-enantiomer is pharmacologically active and accounts for 24 to 49% of the total plasma citalopram level, while the R-enantiomer appears to be pharmacologically inactive. Therefore, the S-enantiomer has been isolated and marketed in 2002 as escitalopram [59, 60]. Escitalopram shows greater efficacy than citalopram using equivalent doses of the S-enantiomer in non-clinical and in controlled randomised clinical experiments. R-Citalopram appears to exert an allosteric effect on the 5-HT transporter protein and therefore counteracts the effect of escitalopram. This could explain the more favourable clinical efficacy of escitalopram, also in comparison to other comparator antidepressants [61]. Not only a higher efficacy, but also a higher response and faster onset of the drug, leading to faster symptom relief, is seen when using

escitalopram [60]. TDM could be of interest for patients with liver impairment and for elderly. Citalopram and also escitalopram have low potency for clinically important pharmacokinetic drug-drug interactions in comparison with other SSRI. This is the result of the low capacity of citalopram to inhibit CYP 450. Thus, citalopram is a good choice for patients who have a multidrug therapy [62].

I.7.1.1. *Mechanism of action*

This selective inhibitor of serotonin reuptake has minimal affinity for α_1-adrenoreceptors and has low histamine H_1-receptor blocking potency [40].

I.7.1.2. *Pharmacokinetics*

Citalopram is well absorbed following oral administration with a bioavailability of approximately 80%. Peak plasma levels of citalopram usually occur within 2-4 hours [59]. After oral administration of doses between 20 and 60 mg/day, plasma levels of racemic citalopram and desmethylcitalopram ranged between 9 to 200 ng/ml and 10 to 105 ng/ml, respectively [62]. When the enantiomers are measured separately, concentration ranges of 9-106 ng/ml and 20-186 ng/ml are seen for S- and R-citalopram, while 4-38 ng/ml and 3-75 ng/ml are detected for S- and R- desmethylcitalopram [62]. However, there is considerable inter-individual variation in plasma concentrations which increases with dose, probably due to genetic factors [40, 63]. At steady-state, plasma concentrations of desmethylcitalopram and didesmethylcitalopram are one-half and one-tenth, respectively, of the parent drug level [64]. The steady-state plasma concentration of escitalopram is 19-37 ng/ml after treatment with a dose of 10 mg/day [65].

Citalopram is metabolized in the liver by mono- and di-N-demethylation through CYP2C19, and 2D6, respectively. Citalopram and escitalopram are also metabolized by CYP3A4 to an important extent [66]. Other metabolization pathways include oxidative deamination, N-oxide formation and glucuronidation. The mono-desmethyl metabolite, desmethylcitalopram, has about 20 to 50% of the pharmacological activity of the parent drug, but does not contribute to the overall antidepressant activity of citalopram as it has a poor blood-brain barrier penetration [67]. The metabolism of escitalopram is similar to that of citalopram. The elimination half-life is 35

hours for citalopram, 50 hours for desmethylcitalopram and 100 hours for didesmethylcitalopram [59]. The active S-enantiomer is more rapidly eliminated than the inactive R-enantiomer [62], probably because CYP2C19 is mainly implicated in the N-demethylation of the S-enantiomer rather than in that of R-citalopram. Moreover, 12% of a single dose is excreted in 24-hours urine, as well as an equal amount of desmethylcitalopram and minor quantities of other metabolites. However, about 65% of a dose is thought to be excreted via the faeces and small amounts of the drug are also excreted in breast milk [58]. On the other hand, escitalopram seems to be eliminated mainly in urine. Citalopram has a low plasma protein binding of about 50%. Thus, protein binding interactions do not seem to be of great importance [19].

I.7.1.3. *Drug concentrations and clinical effects*
The therapeutic concentration for citalopram ranges from 20 to 200 ng/ml [56]. However, no therapeutic window has been set for citalopram. Hiemke and Hartter stated that possible relationships between clinical outcome and serum concentrations might have been masked by the lack of stereospecific analysis [40]. In the dose range of 10-60 mg/day, citalopram shows linear pharmacokinetics for single as well as multiple-dose trials [64]. A lower initial dose should be considered for the elderly. This dose should not exceed 40 mg per day, because in elderly, for similar doses, average concentrations were 23% higher and the half-life was 31% longer in comparison with the younger population. Barak et al. [68] report that citalopram-induced bradycardia is more prevalent among elderly. Moreover, patients with liver impairment or multiple co-administered medications should also be monitored. On the other hand, dose adjustment is not required for renal impaired patients. However, because there are no data on the pharmacokinetics of citalopram in patients with chronic or severe renal impairment, caution is advisable in this case [59, 69]. Although citalopram is prescribed for children, FDA has not approved its use in children, as it may increase suicidal thoughts. In addition, Whittington et al. [43] reported an unfavourable risk-benefit balance for children as there is no evidence for efficacy, while the risk for suicide increased. Also for adults, one should monitor the worsening of depression and increased suicidal thinking [64]. On the other hand, citalopram did not seem to have an

increased effect on the rate of congenital birth defects as compared to those expected in the general population [45].

I.7.1.4. *Drug interactions, side-effects and toxicity*

Possible side-effects of citalopram include nausea and vomiting, increased sweating, headache, dry mouth, tremor, sedation, insomnia, mania, and sexual problems [59]. According to Bezchlibnyk-Butler et al. [59] and the FDA [64], the major citalopram-drug interactions involve some TCAs such as imipramine, but also warfarine, carbamazepine, sumatriptan, metoprolol and cimetidine. However, these interactions do not seem to have any clinical consequences. Because citalopram is only a weak inhibitor of CYP1A2, 2D6 and 2C19, the need for a decreased dose of drugs metabolized by those enzymes seems low [62]. As CYP3A4, 2D6 and 2C19 are involved in the metabolism of citalopram, potent inhibitors of these isoenzymes may decrease the clearance of citalopram. However, several reports [64] indicated that because citalopram is metabolized by multiple enzymes, inhibition of a single enzyme may not decrease citalopram clearance in an important way [64]. Patients should be cautioned for the risk of bleeding associated with the concomitant use of citalopram with NSAIDs, aspirin, or other drugs that affect coagulation [64]. Citalopram, though, should not be coadministered with a irreversible monoamine oxidase inhibitor as this can lead to the risk of serotonin syndrome [70]. In addition, after a MAOI treatment, a delay of 2 weeks before taking citalopram or vice versa should be considered. Citalopram is considered not to be of importance in fatal poisoning cases as Jonasson and Saldeen state that fatal blood concentrations range between 2000 and 6200 ng/g and between 600-5200 ng/g in combination with other drugs [71]. However, according to the TIAFT-list the lethal concentration of citalopram is 500 ng/ml [56].

I.7.1.5. *Analytical Methods*

Citalopram is determined with or without its metabolites using thin-layer chromatography, capillary electrophoresis [72], liquid chromatographic or gas chromatographic methods. Escitalopram can be determined in human plasma using LC-ESI-MS [73]. Moreover, several methods can separate the enantiomers by using a chiral stationary phase [74, 75]. Examples of these

chiral stationary phases used in liquid chromatography are Chiralcel OD [76], Chiral AGP [77] and Chirobiotic V [75]. Enantiomeric separation can also be achieved by using a chiral mobile phase additive such as beta-cyclodextrin [78]. Derivatization with a chiral reagent to form diastereoisomeric derivatives is not possible as citalopram is a tertiary amine that can not be derivatized [79].

In gas chromatography, NPD [80] and mass detectors [81, 82] are used. In liquid chromatography, UV (absorption at 230 or 240 nm) [75, 83], DAD [84-86], fluorescence [87-90], and mass detectors are applied. The LC-MS methods are utilized in both electrospray [73, 91, 92] and atmospheric pressure chemical ionization mode [93].

Sample preparation mostly consists of a liquid-liquid extraction [73, 76, 84-86, 88] after alkalinization, although recently a lot of solid phase extraction methods [76, 83, 87, 90, 92, 94, 95] are published. In addition, solid phase micro extraction (SPME) can be applied to extract citalopram from urine [82].

I.7.2. Fluoxetine

N-Methyl-3-[4-(trifluoromethyl)phenoxy]-3-phenylpropan-1-amine: mol. wt., 309.3; pK_a, 8.7; usual dose, 20 mg/day for depression (and 60 mg/day for bulimia nervosa); max.dose, 80 mg/day; therapeutic concentration, 150 to 500 ng/ml for fluoxetine (100 to 500 ng/ml for desmethylfluoxetine); plasma half-life, 4-6 days (4-16 for desmethylfluoxetine); plasma protein binding, 94.5%; distribution volume, 27 l/kg (20-42 l/kg); bioavailability 60% [56, 58].
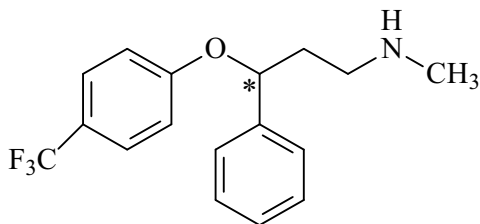
Fluoxetine is a selective inhibitor of neuronal serotonin reuptake and is approved by the FDA in 1987. It has been used to treat several disorders such as major depression, panic, bulimia nervosa, obsessive-compulsive behaviour, and premenstrual dysphoric disorder [64]. This racemic drug consists of S- and R-fluoxetine (50/50), which are both clinically relevant

[76]. The S-enantiomer, however, is eliminated more slowly and is the predominant enantiomer present in plasma at steady state. In addition, S-desmethylfluoxetine is also clinically relevant. TDM could be of interest for monitoring patients with liver impairment, with co-medication of drugs that either are metabolized by CYP2D6 or inhibit that enzyme, and for the elderly population. When using TDM, one has to be aware that changes in dose will not be fully reflected in plasma for several weeks, because of the long elimination half-lives of the parent drug and its major active metabolite. These long elimination half-lives, combined with the fact that fluoxetine inhibits its own metabolism are of great concern when using co-medication [64].

I.7.2.1. *Mechanism of action*

Fluoxetine is a potent and selective inhibitor of serotonin reuptake in the synapse, with little effect on other monoamine reuptake mechanisms or other neurotransmitter receptors. Fluoxetine was shown to have only weak affinity for various receptor systems, namely opiate, serotonergic $5HT_1$, dopaminergic, β-adrenergic, $α_2$-adrenergic, histaminergic, $α_1$-adrenergic, muscarinic, and serotonergic $5HT_2$ receptors.

I.7.2.2. *Pharmacokinetics*

Fluoxetine is well absorbed following oral administration and peak plasma fluoxetine concentrations usually occur within 4-8 hours (range 1.5-12 hours). After oral administration of a single 40-mg dose by healthy adults, peak plasma concentrations of approximately 15-55 ng/ml are obtained. However, there appears to be considerable inter-individual variation in plasma concentrations attained with a given dose. In addition, coadministration of fluoxetine and food, leads to a slower absorption rate but does not affect the overall extent of absorption of fluoxetine [76]. Following daily oral administration of the drug, steady-state plasma fluoxetine and desmethylfluoxetine concentrations generally are achieved within about 2-4 weeks. Although, the onset of antidepressant activity of fluoxetine usually occurs within the first 1-3 weeks of therapy, optimum therapeutic effect usually requires 4 weeks or more of drug administration. Fluoxetine is extensively demethylated in the liver by CYP2C9, 2C19 and 2D6 to the

primary active metabolite desmethylfluoxetine. The elimination half-life of the parent drug is 4 to 6 days, but it is increased to 4-16 days for desmethylfluoxetine. The plasma half-life of fluoxetine exhibits considerable inter-individual variation, which may be related to genetic differences in the rate of N-demethylation of the drug in the liver. On the other hand, fluoxetine inhibits isoenzyme CYP2D6 and thus its own metabolism. Further metabolism can occur by O-dealkylation, producing *p*-trifluoromethylphenol and hippuric acid. The drug and its metabolites are mainly excreted in urine, but also in the faeces and in breast milk. Due to extensive tissue distribution, fluoxetine has a high distribution volume of 20-42 l/kg. Fluoxetine is highly bound to plasma proteins (up to 94.5%), including albumin and α_1-acid glycoprotein. The extent of fluoxetine protein binding does not appear to be altered substantially in patients with hepatic cirrhosis or renal impairment, including those undergoing hemodialysis [76, 96].

I.7.2.3. *Drug concentrations and clinical effects*

The therapeutic concentration for fluoxetine ranges from 150 to 500 ng/ml and from 100 to 500 ng/ml for desmethylfluoxetine [56]. However, no consistent relationship has been described between plasma fluoxetine concentrations and clinical response. In addition, a considerable inter-individual variation in plasma concentrations attained with a given dose is observed. Because of the long half-life of fluoxetine and desmethylfluoxetine, a significant accumulation of these active compounds in chronic use, even when a fixed dose is used, is observed. Plasma concentrations of fluoxetine were higher than those predicted by single-dose studies, as fluoxetine's metabolism is not proportional to dose. Desmethylfluoxetine, however, appears to have linear pharmacokinetics [64]. A lower or less frequent dose should be considered in patients with liver impairment, for elderly patients and patients using multiple co-administered medications, while this is not routinely necessary for renal impaired patients. Diabetic patients should be monitored as fluoxetine can improve glucose tolerance and/or hypoglycaemia [96]. Fluoxetine use should be avoided by pregnant women in the third trimester due to increased hemorrhagic tendency and nervousness in infants [97].

I.7.2.4. *Drug interactions, side-effects and toxicity*

Possible side-effects of fluoxetine include allergic reactions, mania, weight loss, sexual problems, nausea, anxiety, and insomnia. Recently, several publications report the possibility of an increased risk for suicidal behaviour in patients treated with antidepressant medication. Serum levels of 1960 ng/ml fluoxetine (420 ng/ml desmethylfluoxetine) have been associated with seizures, while blood concentrations of 1300 to 6800 ng/ml fluoxetine and 900 to 5000 mg/l for desmethylfluoxetine have been associated with fatalities.

According to Messiha [98], the major fluoxetine-drug interactions involve the amino acids L-dopa and L-tryptophan, anorexants, anticonvulsants, antidepressants, anxiolytics, calcium channel blockers, cyproheptadine, lithium salts, and drugs of abuse. Fluoxetine should not be coadministered with a monoamine oxidase inhibitor as this can lead to hyperthermia, convulsions and coma. In addition, after fluoxetine treatment, a delay of 5 weeks before taking a MAOI should be considered, as fluoxetine and its metabolite have very long elimination half-lives. This washing out-period is also necessary for thioridazine, an antipsychotic used by schizophrenic patients. Thioridazine administration produces a dose-related prolongation of the QTc interval, which is associated with serious ventricular arrhythmias such as torsades de pointes-type arrhythmias and sudden death. This risk is expected to increase with fluoxetine-induced inhibition of thioridazine metabolism. The need for decreased dose of drugs metabolized by CYP2C9/19, 3A4 and 2D6 should be considered, as fluoxetine inhibits these enzymes. Consequently, co-medication with some antiarrhythmics, antipsychotics, β-blockers, and TCAs should be monitored [64, 96, 99, 100].

I.7.2.5. *Analytical Methods*

Fluoxetine is determined with or without its active metabolite using gas chromatographic, liquid chromatographic and micellar electrokinetic capillary chromatographic [101] methods. Some of these methods can separate the enantiomers of the compounds after derivatization with a chiral reagent [102] or by using a chiral stationary phase. Examples of these chiral stationary phases are hydrodex-beta-6-TBDM fused silica capillary columns used for GC purposes [103] or Chiralcel ODR, amylase-, beta-cyclodextrin-,

ovomucoid- and cellulose-based chiral columns [104-108] for liquid chromatography.

In gas chromatography, NPD [103, 109-111], ECD [76] and mass detectors in electron ionization mode [102, 112, 113] are used. In liquid chromatography, UV (absorption 230 nm) [87, 105, 107, 114-119], DAD [85], fluorescence [108, 120-122] and mass detectors are applied. The LC-MS methods are utilized in both electrospray ionization [76, 92, 123-126] and atmospheric pressure chemical ionization mode [127].

Sample preparation mostly consists of a liquid-liquid extraction after alkalinization [103, 107, 109, 116, 118, 122, 124, 127], although recently a lot of solid phase extraction methods are published. A large variety of sorbents such as apolar (C8), ion-exchange (SCX) and polymeric sorbents (Oasis HLB) [87, 92, 104, 111, 119, 121, 126] are used for extraction of fluoxetine and its metabolite from biological samples.

Most methods allow quantitative determination in the lower ng/ml range (LOQ between 1-20 ng/ml), and are thus suitable for therapeutic drug monitoring purposes [76].

I.7.3. Fluvoxamine

5-Methoxy-1[4-(trifluoromethyl)phenyl]-1-pentanone-O-(2-aminoethyl)oxime: mol. wt., 318.3; pKa, 8.7; usual dose: 100-300 mg/day of fluvoxamine maleate (max. 200 mg for children till 11 years old) [128]; therapeutic plasma concentration is 50-250 ng/ml, while 650 ng/ml results in toxic effects [56]; plasma half-life, 8 – 28 h (mean: 15 h); plasma protein binding, 77%; distribution volume, 25 l/kg [57, 58].
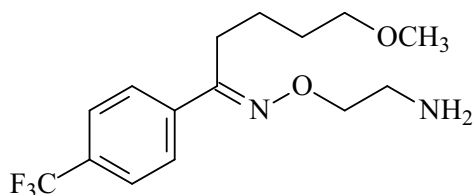
Fluvoxamine is a selective inhibitor of neuronal serotonin reuptake. The drug was introduced in 1983 and has been used to treat obsessive-compulsive disorder (only marked for this disorder in US) as well as depression, panic disorder, social phobia, post-traumatic stress disorder, eating disorders, and autism [40, 64, 129]. This compound does not have a chiral center, but the occurrence of a C=N double bound implies the existence of two isomers, E

(entgegen, trans) and Z (zusammen, cis) [130]. TDM could be of interest for monitoring patient compliance, patients with liver impairment and patients with co-medication of drugs that are metabolized by CYP1A2, 2C19 or 3A4 [131].

I.7.3.1. *Mechanism of action*

Fluvoxamine is a potent and selective inhibitor of serotonin reuptake in the synapse with little effect on other monoamine reuptake mechanisms or other neurotransmitter receptors, with the exception of σ_1-receptors [129]. These σ_1-receptors have a neuromodulatory role in the brain, which may result in a relevant response to anxiety, stress, depression, learning and cognitive processes, neuroprotection and antipsychotic activity [132].

I.7.3.2. *Pharmacokinetics*

Fluvoxamine is almost completely absorbed after oral administration, but undergoes an extensive first pass metabolism, resulting in a bioavailability of about 53%. The time to reach maximum plasma concentration is about 5 hours after a single dose of 100 to 300 mg. A dose proportionality study showed that patients treated with 100, 200 and 300 mg/day of fluvoxamine maleate during 10 days had fluvoxamine serum concentrations of 88, 283 and 546 ng/ml, respectively [64]. However, there appears to be considerable inter-individual variation in plasma concentrations attained with a given dose. As a result, a therapeutic window has not yet been established. Steady-state concentrations could be attained within 1 week, due to the relatively short half-life of 8-28 h. Because fluvoxamine exhibits non-linear kinetics, increased dosages led to increased half-lives. Consequently, steady-state conditions may not always be reached before 10 days of continuous treatment [40]. Fluvoxamine is extensively metabolized in the liver, and less than 4% is excreted unmetabolized in urine. The main metabolic degradation in the liver consists of N-acetylation, oxidative deamination and demethylation, resulting in 11 inactive metabolites, of which 9 could be structurally identified [40, 130] with the main metabolite identified as the 5-demethoxylated carboxylic acid [130]. Fluvoxamine is metabolized by the CYP isoenzymes CYP2D6 and 1A2, while the drug itself is a moderate inhibitor of CYP3A4, 2C9 and a potent inhibitor of 1A2, resulting in important

pharmacological interactions with other drugs [58, 100, 129]. On the other hand, fluvoxamine metabolism is increased in smokers [74]. Fluvoxamine has a distribution volume of 25 l/kg and a moderate plasma protein binding, mostly to albumin, of approximately 77%. Therefore, it makes drug interactions with restrictively protein-bound drugs unlikely to occur.

I.7.3.3. *Drug concentrations and clinical effects*

The therapeutic concentration for fluvoxamine in plasma ranges from 50 to 250 ng/ml [56]. However, no consistent relationship has been described between plasma fluvoxamine concentrations and clinical response [133]. In addition, a considerable inter-individual and gender specific variation in plasma concentrations attained for a given dose is observed [67].

Perhaps the inhibition of CYP1A2 by oral contraceptive drugs is the reason of the gender specific variation in plasma concentrations of fluvoxamine [74]. Moreover, a 23%-reduction in plasma concentration is seen for smokers as compared to non-smokers because cigarette smoke induces CYP1A2 metabolism [134].

Fluvoxamine does not appear to have linear pharmacokinetics after repeated administration of therapeutic dosages [40, 129], but rather an U-shaped relationship between drug concentrations and therapeutic response, probably due to auto inhibition of fluvoxamine metabolism [135]. A lower or less frequent dose should be considered in patients with hepatic cirrhosis, as the area under the concentration-time curve and the half-life are significantly increased [136]. On the other hand, dose adjustment is not necessary for the elderly and renal impaired patients [19]. Moreover, breast feeding during fluvoxamine treatment is considered safe [45, 137], as the penetration into breast milk is relatively low, with a milk to plasma concentration ratio of 0.29 [138].

I.7.3.4. *Drug interactions, side-effects and toxicity*

Possible side-effects of fluvoxamine are nausea, somnolence, asthenia, headache, dry mouth, and insomnia. It is associated with a low risk of suicidal behaviour, sexual dysfunction and withdrawal syndrome [129]. Although several fluvoxamine overdoses are reported, up to 12 g of the maleate salt were ingested without sequelae. According to the FDA [64] and

Perucca et al. [139], the major fluvoxamine-drug interactions involve the TCAs, MAOI, benzodiazepines, cardioactive drugs, carbamazepine, methadone, theophylline, warfarin, terfenadine, astemizole, cisapride and pimozide.

Fluvoxamine inhibits CYP isoenzymes such as CYP2D6, 2C19, 3A4, 1A2, and 2C9. Consequently, co-medication with drugs that are metabolized by one or more of these enzymes such as TCAs, warfarin, theophylline, propranolol, benzodiazepines, thioridazine, and neuroleptics such as clozapine and haloperidol should be monitored [22, 23, 64, 79, 131, 134]. On the other hand, concomitant use of fluvoxamine with the previous described drugs could lead to improvement of the therapeutic effects of these drugs [40].

Fluvoxamine should not be coadministered with a monoamine oxidase inhibitor as this leads to hyperthermia, convulsions and coma. In addition, a delay of 2 weeks before taking a MAOI should be considered after fluvoxamine treatment and vice versa [129]. This washing-out period is also necessary for thioridazine, cisapride and pimozide administration as it produces a dose-related prolongation of the QTc interval, which is associated with serious ventricular arrhythmias, such as torsades de pointes-type arrhythmias, and sudden death.

I.7.3.5. *Analytical methods*

Fluvoxamine is determined using gas chromatographic and liquid chromatographic methods in a variety of samples such as serum [91], plasma [85, 93], blood [140], urine [82, 140, 141], brain tissue [142], breast-milk [143], amniotic and umbilical fluids [144].

Gas chromatography combined with detectors such as FID [145], NPD [94], ECD [76, 142] and MSD [39, 76, 82, 141] is used. In liquid chromatography, the following detectors are applied: UV [76, 83, 84, 143, 144, 146-150], DAD [85, 86], fluorescence [76, 151, 152] and mass detectors in electrospray [91] as well as in atmospheric pressure chemical ionization mode [93]. When using UV detection, fluvoxamine gives a maximum absorption at 254 nm. Fluorescence detection of fluvoxamine was described after derivatization with dansylchloride [151] or 4-fluoro-7-nitro-2,1,3-benzoxadiazole [152].

Sample preparation mostly consists of a liquid-liquid extraction after alkalinization [76, 85, 86, 91, 93, 143, 151], although recently a lot of solid

phase extraction methods [76, 82, 83, 94, 95, 143, 145-148, 150, 153] are published. Moreover, methods using SPME [82, 153] and supported liquid membrane sample pre-treatment [154] are also utilized. Most methods allow quantitative determination in the lower ng/ml range (LOQ between 1.5-25 ng/ml), and are thus suitable for therapeutic drug monitoring purposes [76].

I.7.4. Maprotiline

N-Methyl-9,10 ethanoanthracene-9(10H)-propanamine: mol. wt., 277.4; pK_a, 10.5; usual dose, 30-150 mg/day; toxic plasma concentration from 300-800 ng/ml; therapeutic concentration, 75-250 ng/ml (100-600) [56]; plasma half-life, 20-70 h (36-105); plasma protein binding, 90%; distribution volume, 23-70 l/kg (14-22) [57, 58].
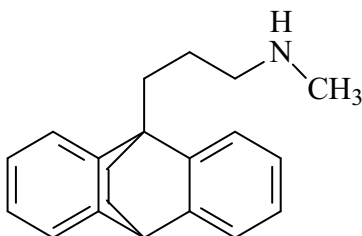
Maprotiline is a tetracyclic antidepressant, which is distinguished from conventional tricyclic antidepressants only by an ethylene bridge upon its molecular skeleton, creating a fourth ring [155]. It has been used in antidepressant therapy and has sedative as well as anti-aggressive properties. TDM could be of interest for monitoring patient compliance and when coadministration of CYP2D6 inhibitors and inducers occurs.

I.7.4.1. *Mechanism of action*
Maprotiline acts by blocking noradrenaline uptake and appears to have no influence on serotonin metabolism. In addition, the drug is a weak central acetylcholine antagonist [155].

I.7.4.2. *Pharmacokinetics*

Maprotiline is slowly, but completely absorbed from the gastrointestinal tract. The drug undergoes an important first pass metabolism. Mean steady state plasma concentrations are reached in 1 week. After administration of daily doses of 50, 100 and 150 mg, maprotiline concentrations were respectively 67, 143, and 216 ng/ml [155].

The main metabolic degradation pathway of the drug is demethylation via CYP2D6 and 1A2 [156], resulting in the active metabolite N-desmethylmaprotiline. In addition, N-oxidation into maprotiline N-oxide and hydroxylation followed by conjugation also occur. The drug is excreted in urine and faeces, mainly as metabolites. In addition, maprotiline can be found in the cerebrospinal fluid, even as in breast milk.

I.7.4.3. *Drug concentrations and clinical effects*

For patients treated with maprotiline, the therapeutic range in plasma is 75-250 ng/ml, although some authors report therapeutic ranges between 100-600 ng/ml. The sum of the therapeutic serum concentrations for maprotiline and desmethylmaprotiline is 100-400 ng/ml [56]. However, there seems to be a wide inter-individual variation in blood levels, perhaps due to the difference in individual body weights and CYP2D6 metabolism [155]. Maprotiline is well tolerated by elderly patients and there appears to be no increase in the incidence and severity of side-effects as compared to younger patients [155]. In patients with hepatic or renal damage, the drug should be used with caution. Since the drug is excreted in breast milk, with a level over 200 ng/ml in both breast milk and maternal blood after 5 days of treatment (50 mg, 3 times daily), the child should also be monitored during maprotiline therapy [155].

I.7.4.4. *Drug interactions, side-effects and toxicity*

Adverse effects of maprotiline (drowsiness, dry mouth) are largely the same as for the tricyclic antidepressants, but there seems to be a higher incidence of skin rashes [155]. However, most of the side-effects of maprotiline are mild and usually disappear with continued treatment or after reduction in dosage. Uncommon side-effects such as hallucinatory episodes, hypomania or mania, development of grand mal seizures, increase in serum

transaminases and alkaline phosphatase, decreased bilirubin, as well as severe neutropenia can occur during maprotiline therapy [155].

Since maprotiline is metabolized by enzymes of the CYP 450 family, the most important being CYP2D6, any other substance influencing this enzyme can have an effect on the plasma concentrations of maprotiline [157]. Moreover, coadministration with MAOI should be avoided, because of the risk of hyperpyretic crisis, convulsions and death. A wash out period of two weeks should be respected when a MAOI is replaced with maprotiline. A serum concentration of 1000-5000 ng/ml can be lethal [56]. The characteristic symptoms of maprotiline overdosage are neuromuscular in nature (tremor, ataxia, muscular twitching), while respiratory depression, drowsiness, convulsions, vertigo, hallucinations, confusion, mydriasis and disturbances of consciousness are also common [155].

I.7.4.5. *Analytical Methods*

Several methods for the analysis of maprotiline in biological samples have been published. Gas chromatography is used frequently in combination with a nitrogen-phosphorus detector [111, 158-160], but an MSD can also be used [95]. In addition, high pressure liquid chromatography is a frequently used method for the analysis of maprotiline, using UV [83, 161, 162] , DAD [163], as well as fluorescence detectors [164]. Moreover, Oztunc et al. described a TLC screening method using 7,7,8,8-tetracyanoquinodimethane as derivatization reagent to detect several antidepressants, including maprotiline [162], while Cakrt et al. published an isotachophoretic determination in combination with fluorimetric detection [165].

Common to these methods is the need for alkaline extraction from the biological medium prior to analysis [160, 162-164]. However, several solid phase extraction methods are also published [83, 95, 111, 161], while Ulrich and Zollinger described a SPME extraction of maprotiline from plasma samples [159].

I.7.5. Melitracen

mol. wt., 291; therapeutic plasma concentration from 10-100 ng/ml
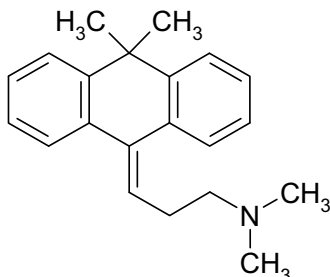
Melitracen is a not well documented tricyclic antidepressant that inhibits the reuptake of noradrenaline and serotonin. The side-effects are less intense in comparison with the other tricyclic antidepressants and is therefore still frequently prescribed.

I.7.6. Mianserin

1,2,3,4,10,14b-Hexahydro-2-methyldibenzo(*c,f*)-pyrazino(1,2-*a*)azepine: mol.   wt., 264.4; pK$_a$, 7.1; usual dose, 30-90 mg/day; max.dose, 200 mg/day; therapeutic concentration, 15 to 70 ng/ml; plasma half-life, 6-40 h; plasma protein binding, 90%; distribution volume, 13 (10-29) l/kg [57, 58].
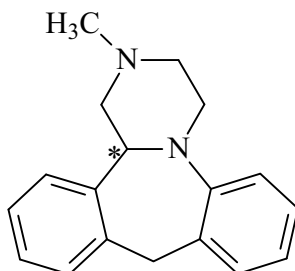
Mianserin is a noradrenergic and specific serotonergic antidepressant (NaSSA). Although the drug is not marketed in the USA, it is used to treat depression in most European countries. This compound is a racemic tetracyclic antidepressant, with the S-enantiomer being considered more potent [166]. TDM could be of interest for monitoring patient compliance.

I.7.6.1. *Mechanism of action*

Mianserin enhances noradrenergic and serotonergic neurotransmission through antagonism of the central α_2-adrenergic receptors and by a postsynaptic blockade of 5-HT$_2$ receptors (not the 5-HT$_3$ receptors).

I.7.6.2. *Pharmacokinetics*

Mianserin is well absorbed following oral administration, but it undergoes first-pass metabolism, resulting in a bioavailability of about 70%. After oral administration of 30 mg of mianserin, the plasma concentrations ranged between 3-13 ng/ml after 18 hours and 18-34 ng/ml at steady state. In addition, the concentration of desmethylmianserin ranged from 1-7 ng/ml and 3-24 ng/ml, respectively [167]. The active metabolite to parent drug ratio, desmethylmianserin/mianserin is about 0.3-0.4 [138,166]. Mianserin is metabolized by N-demethylation and 8-hydroxylation, to form the metabolites N-desmethylmianserin and 8-hydroxymianserin, respectively. N-oxidation of the drug also occurs but does not form a biologically active metabolite. Mianserin is metabolized in the liver through CYP2D6, 1A2, and 3A4 [166]. The mean plasma half-life of mianserin is 16 hours but the value is increased by age. About 30 to 40% of a single dose is excreted in 24 hours urine, mostly as metabolites, since only 5% unchanged drug is found in urine. Mianserin crosses the blood-brain barrier and the placenta, and is excreted in breast milk.

I.7.6.3. *Drug concentrations and clinical effects*

The therapeutic concentration for mianserin ranges from 15 to 70 ng/ml [56], while it ranges from 40-125 ng/ml for the sum of mianserin and its metabolite desmethylmianserin. Although the best clinical response was associated with a plasma concentration of less than 70 ng/ml, there seems to be no relationship between plasma concentrations and therapeutic response [138]. Mianserin, desmethylmianserin, and the sum of mianserin and its metabolite have significant linear kinetics [167]. Plasma concentrations of mianserin have been reported to increase significantly with age, in contrast with the metabolite concentrations that decreased, probably due to impaired demethylation in the elderly [138].

I.7.6.4. *Drug interactions, side-effects and toxicity*

The most frequently reported side-effects are drowsiness, convulsions and sedation [168]. Serious side-effects are the occurrence of blood diseases such as agranulocytosis, granulocytopenia, leucopenia or pancytopenia [168]. According to Nawishy et al. [169], plasma levels of mianserin are significantly reduced in epileptic patients treated with phenytoin, phenobarbitone and carbamazepine. Eap et al. concluded that carbamazepine reduced the plasma concentration of mianserin as it is an inducer of CYP3A4, which is involved in the metabolism of mianserin [166].

I.7.6.5. *Analytical Methods*

Mianserin is determined with or without its metabolites using capillary electrophoresis [170] and liquid or gas chromatographic methods. Several methods can separate the enantiomers by using a chiral stationary phase [171].

Nitrogen-phosphorus [94, 172] and MS detectors [95] are used in gas chromatography. In liquid chromatography, UV [173, 174], fluorescence [175], mass [176] and electrochemical [177] detectors are applied.

Liquid-liquid extraction after alkalinization [170] or solid phase extraction is utilized as sample preparation [94, 95, 174, 177].

I.7.7. Mirtazapine

1,2,3,4,10,14b-Hexahydro-2-methylpyrazino(2,1-*a*)pyrido(2,3-*c*)(2)-benzazepine: mol. wt., 265.4; pK$_a$, 7.1; usual dose, 15-45 mg/day; therapeutic concentration, 20 to 100 ng/ml; plasma half-life, 20-40 h; plasma protein binding, 85%; distribution volume, 10-14 l/kg [57, 58].
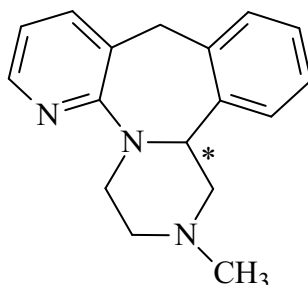
Mirtazapine is a noradrenergic and specific serotonergic antidepressant (NaSSA). The drug has been used to treat depression with or without anxiety

symptoms and sleep disturbances [64, 178]. This compound is a racemate and the S(+)- as well as the R(-)- enantiomer are pharmacologically active [178]. TDM could be of interest for monitoring patient compliance and patients with liver impairment.

I.7.7.1. *Mechanism of action*

Mirtazapine enhances noradrenergic and serotonergic neurotransmission through antagonism of the central α_2-adrenergic receptors and by a postsynaptic blockade of $5-HT_2$ and $5-HT_3$ receptors [178]. It has a weak affinity for $5-HT_1$ receptors and very weak muscarinic anticholinergic and histamine antagonist properties [179].

I.7.7.2. *Pharmacokinetics*

Mirtazapine is readily absorbed after oral administration, resulting in a bioavailability of 50% [180]. The time to reach maximum plasma concentration is about 2 hours and coadministration of food has minor effect on the rate, but not on the extent of absorption [180]. According to Timmer et al., the C_{max} at steady state ranges from 55 to 89 ng/ml for healthy males receiving 30 mg mirtazapine per day [180]. Mirtazepine has a plasma half-life from 20 to 40 hours, with an average of 37 hours in women, and 26 hours in men, while steady-state concentrations could be attained within 5 days [178]. In addition, mirtazapine has linear pharmacokinetics at dosages of 15-80 mg/day [180].

Mirtazapine is metabolized into its 8-hydroxy-metabolite by cytochrome 2D6 and 1A2. CYP3A4, however, metabolizes mirtazapine into the active N-desmethylmirtazapine and the inactive N-oxide. Moreover, conjugation of these metabolites also occurs. Although some metabolites have a pharmacological activity, they do not contribute significantly to the therapeutic effect, due to the low plasma concentrations. The drug is eliminated by excretion in urine and faeces in a few days after a single dose.

I.7.7.3. *Drug concentrations and clinical effects*

The therapeutic concentration for mirtazapine ranges from 20 to 100 ng/ml [56]. According to Grasmäder et al. 30 ng/ml is the threshold plasma concentration, resulting in a response to mirtazapine treatment [181].

Moreover, young males seem to need higher doses to reach the same plasma concentrations in comparison to female patients or elderly men. However, because no consistent relationship has been described between plasma mirtazapine concentrations and effect, the significance of these gender and age specific variation in plasma concentrations attained for a given dose is still unknown [180]. A decreased oral clearance and increased peak-plasma concentration, as well as time to reach that concentration is seen in patients with moderate or severe renal failure in comparison with the healthy population [178]. Because hepatic clearance of mirtazapine is reduced in patients with cirrhosis or hepatic impairment, dosage adjustments should be performed with caution [178].

I.7.7.4. *Drug interactions, side-effects and toxicity*

The most common side-effects are somnolence [181], dizziness, dry mouth, increased appetite and body-weight gain [182]. According to the FDA [64], following side-effects can also occur: agranulocytosis, increase in plasma cholesterol and triglycerides, seizures, mania and sexual problems. The increase in cholesterol and triglycerides is probably due to the increased appetite. Side-effects such as mania, seizures and agranulocytosis are rather rare [179, 182]. In addition, sexual dysfunction is less frequently than when using an SSRI [183].

As mirtazapine is unlikely to inhibit CYPs, the drug-drug interaction profile is favourable [178]. Moreover, as it is metabolized by several enzymes, it is unlikely that its metabolism would be affected by coadministration of a CYP1A2, 2D6 or 3A4-inhibitor [182]. Although coadministration of cimetidine, paroxetine [184], fluoxetine, carbamazepine and amitriptyline [185] increases the steady-state plasma concentration of mirtazapine, this increase was not considered to be clinically relevant [180]. Patients should be cautioned, though, not to use other central nervous system depressants (e.g. ethanol or diazepam) in combination with mirtazapine [182]. Mirtazapine should not be coadministered with a monoamine oxidase inhibitor as this can lead to hyperthermia, convulsions and coma. In addition, a delay of 2 weeks before taking a MAOI should be considered after mirtazapine treatment and vice versa [64].

I.7.7.5. *Analytical methods*

Mirtazapine and its metabolites are determined using gas and liquid chromatographic methods, as well as capillary electrophoresis [186] in a variety of samples such as plasma [86, 186-194], serum [188, 189], post-mortem blood [195] and urine [82, 196]. Some methods are able to separate the enantiomers using a chiral column [192, 193] or a chiral additive in the eluent such as carboxymethyl-beta-cyclodextrin [186].

Gas chromatography is used combined with an MSD [82, 195, 196]. In liquid chromatography, the following detectors are applied: fluorescence detectors [188-190, 194], UV [187, 193, 197], DAD [85, 86] and mass spectrometric detectors [191, 192].

Sample preparation mostly consists of a liquid-liquid extraction after alkalinization [85, 86, 187, 190-192, 195, 196]. Moreover, de Santana et al. published a method using liquid-phase microextraction (LPME) [193]. Recently, solid phase extraction [95, 194, 197] and solid phase microextraction methods [82] are also published.

Most methods allow quantitative determination in the lower ng/ml range, and are thus suitable for therapeutic drug monitoring purposes.

I.7.8. Paroxetine

(3S-trans)-3-[(1,3-Benzodioxol-5-yloxy)methyl]-4-(4-fluorophenyl)-piperidine : mol. wt., 329.4; pK$_a$, 9.9; usual dose, 10 up to 60 mg/day (max. 40 mg/day for elderly and patients with kidney or hepatic impairment) [198]; therapeutic concentrations in serum from 10 to 75 ng/ml; toxic serum concentrations from 350 to 400 ng/ml [56]; plasma half-life, 12-40 h; plasma protein binding, 95%; distribution volume, 3 - 28 l/kg [57, 58].
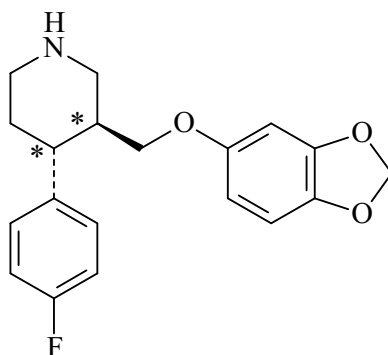
Paroxetine is a selective inhibitor of neuronal serotonin reuptake. The drug was approved in 1992 by the FDA and has been used to treat depression as

well as several disorders: panic, obsessive-compulsive disorder, posttraumatic stress, generalized and social anxiety [64, 199]. Paroxetine has the most clinical evidence supporting the use for anxiety of all SSRIs. This compound has two chiral centres, but it is used clinically as pure 3S, 4R-isomer [19]. TDM could be of interest for monitoring patient compliance, patients with liver and kidney impairment or for the elderly population. In addition, patients with co-medication of drugs that are metabolized by CYP2D6 should also be monitored.

I.7.8.1. *Mechanism of action*
Paroxetine is a potent and selective inhibitor of presynaptic serotonin reuptake and enhances serotonergic neurotransmission by prolonging serotonin activity at its postsynaptic receptors. It is a weak inhibitor of dopamine and noradrenaline transporters, while it displays some affinity for the muscarinic receptor, resulting in more anticholinergic symptoms such as dry mouth and constipation [20, 198, 200, 201].

I.7.8.2. *Pharmacokinetics*
Paroxetine is well absorbed without being affected by presence of food or antacids. The absolute bioavailability of paroxetine, though, is about 50%, due to first pass metabolism [19]. The time to reach maximum plasma concentration is about 5 hours after a single dose of 30 mg, while steady-state concentrations could be attained after 7 to 14 days in healthy volunteers administered 30 mg/day [198]. This dosage leads to an inter-individual variation in the plasma concentration from less than 1 to more than 150 ng/ml [138]. In addition, Rasmussen and Brosen reported plasma concentrations of 1-188 ng/ml in patients treated with paroxetine in doses of 20-60 mg/day [74]. As a result, a therapeutic window has not yet been established. Moreover, the small numbers of presently available studies do not suggest the existence of a plasma concentration-clinical response relationship for paroxetine [79].

Paroxetine is extensively metabolized after oral absorption, mainly by oxidation and demethylation, followed by conjugation. The CYP2D6 isoenzyme mainly regulates the O-demethylenation, leading to a cathechol type metabolite [58], which is further O-methylated and conjugated with

glucuronic acid and sulphate. Thus, the extensive metabolism in the liver leads to inactive glucuronide and sulphate metabolites [201]. On the other hand, a not yet identified low-affinity enzyme also plays a role in the paroxetine metabolism [67]. This enzyme is the primary enzyme used by CYP2D6 poor metabolizers [134].

The drug is widely distributed in the body, even in the central nervous system and in breast milk. Approximately 64% of a dose is excreted in urine, while the other 36% is excreted in the faeces. Less than 2% of a dose is excreted as the parent drug. Paroxetine has a high protein binding rate, leading to possible interactions with other high protein bound drugs [198].

I.7.8.3. *Drug concentrations and clinical effects*

The therapeutic concentration for paroxetine ranges from 10 to 75 ng/ml [56]. However, no consistent relationship has been described between plasma paroxetine concentrations and clinical response [201]. In addition, a considerable inter-individual variation in plasma concentrations attained for a given dose is observed. Paroxetine does appear to have nonlinear pharmacokinetics after repeated administration of therapeutic doses [79, 198, 201], probably due to saturation of CYP2D6 at higher paroxetine concentration, leading to further elimination by the lower affinity unidentified metabolite [100, 134]. A lower or less frequent dose should be considered in patients with hepatic cirrhosis, renal impairment and the elderly as the area under the concentration-time curve and the half-life are significantly increased [198]. Furthermore, paroxetine is not advised during the first three months of the pregnancy as it increases risk of birth defects, particularly heart defects [64]. In addition, withdrawal syndromes or neonatal convulsions are described for paroxetine during pregnancy [46, 47]. This could be due to the affinity of paroxetine towards the muscarinic receptors in combination with nonlinear kinetics, self-limiting metabolism and short half-life. Moreover, breast feeding during paroxetine treatment is considered safe, although this view should be considered as preliminary due to the lack of data [137]. Spigset and Hagg have calculated a milk/plasma ratio between 0.4 and 1, resulting in a relative dose of 1 to 3% in the infant [137].

I.7.8.4. *Drug interactions, side-effects and toxicity*

Possible side-effects of paroxetine are nausea, sexual dysfunction, somnolence, asthenia, headache, constipation, dizziness, sweating, tremor and decreased appetite [198]. Toxic effects may occur with concentrations exceeding 400 ng/ml. Caution is advised when paroxetine is coadministered with drugs that are metabolized by CYP2D6. As a result, paroxetine AUC are increased by 50% or decreased by 28%, due to co-medication with cimetidine or phenytoin, respectively [201]. Moreover, paroxetine may lead to enhancement of plasma concentrations of TCAs such as desipramine [22], antipsychotics (e.g. perphenazine [22]), and antiarrhythmics [134, 201]. On the other hand, paroxetine leads to a decrease in analgesic efficacy of codeine, oxycodone and hydrocodone as it inhibits their metabolism, leading to less of their active metabolites [22].

Paroxetine should not be coadministered with a monoamine oxidase inhibitor as this can lead to hyperthermia, convulsions and coma. In addition, a delay of 2 weeks before taking an irreversible MAOI and 1 day after treatment with a reversible MAOI should be considered after paroxetine treatment and vice versa [198]. This washing out-period is also necessary for thioridazine administration as it produces a dose-related prolongation of the QTc interval, which is associated with serious ventricular arrhythmias, such as torsades de pointes-type arrhythmias, and sudden death.

I.7.8.5. *Analytical methods*

Paroxetine is determined in a variety of samples such as serum, plasma and whole blood [87, 111] by using gas chromatographic and liquid chromatographic methods, as well as micellar electrokinetic capillary chromatographic methods [140] and TLC [76, 92]. Gas chromatography is used, combined with detectors such as NPD [76, 80, 111], ECD [202] and MSD [113]. Paroxetine is derivatized with pentafluorobenzyl carbamate or heptafluorobutyric anhydride before injection onto a GC-MS in negative ion chemical ionization mode or on a GC-ECD configuration [202-204]. In liquid chromatography, the following detectors are applied: UV [87, 146, 148, 205, 206], DAD [86], fluorescence [76, 80, 87, 151, 207, 208], coulometric detection [209], and mass detectors in electrospray [92, 210, 211] as well as in atmospheric pressure chemical ionization mode [93]. When using DAD, a

typical spectrum arises in acidic conditions with absorption at 233, 264, 270 and 293 nm. On the other hand, paroxetine could be determined using fluorescence detection with or without dansylchloride derivatization [76]. Some methods can separate the enantiomers of the compound after using a chiral stationary phase such as Chiralcel OD columns [212].

Sample preparation mostly consists of a liquid-liquid extraction after alkalinization [76, 80, 202, 203, 206, 211, 213], although recently a lot of solid phase extraction methods [76, 87, 92, 95, 111, 148, 208] are published.

Most methods allow quantitative determination in the lower ng/ml range (LOQ between 1-5 ng/ml), and are thus suitable for therapeutic drug monitoring purposes [76].

I.7.9. Reboxetine

(R,S)-2-((RS)-α-(2 Ethoxyphenoxy))benzylmorpholine: mol. wt., 313.4; usual dose, 8 mg/day; max.dose, 12 mg/day; therapeutic concentration, 50 to 160 ng/ml; plasma half-life, 13-15 h; plasma protein binding, 97%; distribution volume, 0.39-0.92 l/kg (1.9-2.8 l/kg) [57, 58].
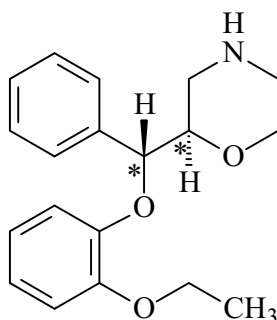
Reboxetine is a selective noradrenaline reuptake inhibitor (NARI) used in most European countries to treat depression. This compound is a antidepressant with two chiral centres, but only the (R,R)-(-) and the (S,S)-(+)-enantiomer (the most potent enantiomer) exist in commercial products [214]. TDM could be of interest for monitoring patient compliance, patients with liver impairment or for the elderly. In addition, monitoring patients who receive potent CYP3A inhibitors could be valuable [215]. However, it is a drug with a good tolerability and a low potency for drug-drug interactions.

I.7.9.1. *Mechanism of action*

Reboxetine enhances noradrenergic neurotransmission through inhibition of the noradrenaline reuptake. It also has a very weak inhibition of serotonin reuptake, but no inhibition of dopamine reuptake [214]. Reboxetine has no monoamine oxidase A inhibitory properties, and has very little affinity for α-adrenergic and muscarinic cholinergic receptors [16].

I.7.9.2. *Pharmacokinetics*

Reboxetine is rapidly and almost completely absorbed from the gastrointestinal tract. After oral administration of 4 mg of reboxetine, the plasma concentration achieved after about 2 hours was 111±28 ng/ml [215]. Peak plasma concentration may be increased in elderly and in patients with renal and hepatic impairment. Steady-state is achieved within 4 days after the start of administration [214]. In addition, reboxetine has significant linear kinetics through a dose of 5 mg [215]. Metabolism of reboxetine includes dealkylation, hydroxylation of the ethoxyphenoxy ring and morpholine ring oxidation, followed by conjugation [67, 214]. It is metabolized primarily in the liver through CYP3A4 [214, 215]. The mean plasma half-life of reboxetine ranges between 13-15 hours, but the value is increased by age and renal as well as hepatocellular dysfunction. The greatest part of a single dose is excreted in urine (about 77% in 5 days), which contains about 5% unchanged reboxetine, and at least 17 different metabolites. The rest of the drug is eliminated in the faeces. The drug has a high protein binding rate of 97%, particularly to α_1-acid glycoprotein.

I.7.9.3. *Drug concentrations and clinical effects*

The therapeutic concentration for reboxetine ranges from 50-160 ng/ml. While gender has no effect on reboxetine pharmacokinetics, plasma concentrations of the drug have been reported to increase significantly with age. Moreover, there appears to be a high degree of inter-subject variability of the pharmacokinetic parameters in the elderly. Therefore, the starting dose should be reduced by 50% and monitored in this population. Patients with mild or severe liver impairment should be monitored as the AUC values for reboxetine are substantially increased. Although reboxetine is cleared mainly via hepatic metabolism, the AUC and the half-life of reboxetine in

severe renal impaired patients are increased [215]. There are no data on effects of reboxetine exposure during pregnancy [45].

I.7.9.4. *Drug interactions, side-effects and toxicity*

The most frequently reported side-effects in short-term reboxetine trials are dry mouth, constipation, insomnia, increased sweating, tachycardia, vertigo, urinary hesitancy and/or retention, and impotence. Moreover, an increased heart rate was associated with reboxetine use, but the clinical significance of this finding is unknown [16, 216]. Occasional atrical and vertricular ectopic beats were also reported [217].

Reboxetine is a weak in vitro inhibitor of CYP2D6 and 3A4, but the inhibitory effect is unlikely to be relevant in vivo because it occurs at concentrations well above those achieved clinically [100, 218]. Therefore, drug interactions as seen for the SSRI are not common. Because CYP3A4 is involved in the metabolism of reboxetine, potent inhibitors of this isoenzyme such as ketoconazole may increase the plasma concentration of the drug [214, 215].

I.7.9.5. *Analytical Methods*

Reboxetine is determined with or without its metabolite O-desmethylreboxetine using capillary electrophoresis, liquid chromatographic or gas chromatographic methods. While MS detectors [113] are used in gas chromatography, UV [83, 219, 220], fluorescence [219, 221, 222], and mass [91] detectors are applied in liquid chromatography. Several methods can separate the enantiomers of the compound using a chiral stationary phase such as Chiral CBH (cellobiohydrolase), Chiral AGP (α_1-acid-glycoprotein) and ChiraGrom-2 [223]. Walters and Buist describe a method combining chiral derivatization and a chiral column to separate the enantiomers [221]. In addition, capillary electrophoresis is also used to separate reboxetine enantiomers [224].

Solid phase extraction is mostly used as sample preparation technique [95, 219, 221].

I.7.10. Sertraline

(1S,4S)-4-(3,4-Dichlorophenyl)-1,2,3,4-tetrahydro-N-methyl-1-naphtalenamine: mol. wt., 306.2 ; pK$_a$, 9.48 ± 0.04 (water); usual dose, 50 – 200 mg/day; toxic from 290 ng/ml; therapeutic concentration, 50 to 250 ng/ml; plasma half-life, 26 h; plasma protein binding, 98%; distribution volume, 20 l/kg [57, 58].
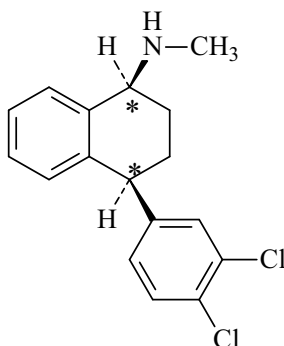
Sertraline is a selective inhibitor of neuronal serotonin reuptake. The drug has been used to treat depression as well as obsessive-compulsive disorder (also for children), panic disorder, post-traumatic stress, premenstrual dysphoric disorder and social anxiety disorder [64, 225]. This compound has two chiral centres, but the cis 1S, 4S-enantiomer is the most potent and is the one marketed as pharmaceutical form [40, 225]. TDM could be of interest for monitoring patient compliance, patients with liver impairment, elderly and patients with co-medication of drugs that are metabolized by CYP2D6.

I.7.10.1. *Mechanism of action*
Sertraline is a potent and selective inhibitor of serotonin reuptake in the synapse with little effect on other monoamine reuptake mechanisms or other neurotransmitter receptors, with the exception of the dopamine transporter, which is not considered to be of therapeutic consequence [225].

I.7.10.2. *Pharmacokinetics*
Sertraline is slowly absorbed from the gastrointestinal tract, resulting in a bioavailability greater than 44% [225]. The time to reach maximum plasma concentration is about 4-8 hours and coadministration of food increased peak plasma concentrations by approximately 25% [225]. Steady-state

concentrations could be attained within 1 week, due to the relatively short half-life of 26 h [226]. The therapeutic concentration for sertraline ranges from 50 to 250 ng/ml [56]. In addition, the plasma concentration of desmethylsertraline is higher than the parent drug concentration, with a ratio of sertraline/desmethylsertraline varying from 0.24 to 0.85 in patients after a dose of 100-300 mg/day [79]. However, there appears to be considerable inter-individual variation in steady state plasma concentrations (nearly 15-fold) attained with a given dose [225].

Sertraline is extensively metabolized in the liver, where it undergoes N-demethylation to form desmethylsertraline. Both the parent drug and the N-desmethylderivative are further metabolized by oxidative deamination, reduction, and hydroxylation followed by glucuronidation [58]. Sertraline is excreted in urine and faeces and is distributed in breast milk. Sertraline is metabolized by CYP2D6, 2C9, 2B6, 2C19 and 3A4 [225], while the drug itself is a moderate inhibitor of CYP2D6.

I.7.10.3. *Drug concentrations and clinical effects*

The therapeutic concentration for sertraline ranges from 50 to 250 ng/ml [56]. However, Goodnick describes that a concentration of 10 to 60 ng/ml may provide the maximal therapeutic benefit [138]. Therefore, there can be concluded that no consistent relationship has been described between plasma sertraline concentrations and clinical response. In addition, a considerable inter-individual and gender specific variation in plasma concentrations attained for a given dose is observed.

Sertraline appears to have linear pharmacokinetics at dosages of 50-200 mg/day [226]. A decreased clearance and prolonged half-life of sertraline is seen in the elderly, suggesting a higher steady-state concentration achieved later during long-term administration. However, the clinical significance of these effects is still unknown [225]. A prolonged half-life of sertraline is also seen for patients with liver disease, while the pharmacokinetics of sertraline did not change after single dose in renal impaired patients. As no data have been reported after multiple doses or for patients with severe renal dysfunction, caution is recommended for these groups [225]. Moreover, several studies reported that plasma concentrations of young men tended to

be lower than for women, probably due to either differences in the tissue distribution or in the metabolism [40, 226].

I.7.10.4. *Drug interactions, side-effects and toxicity*

Possible side-effects of sertraline are nausea, decreased libido, tremor, tachycardia, headaches and dry mouth. Co-medication with drugs that are metabolized by CYP2D6 should be monitored, as sertraline is a mild to moderate inhibitor of that enzyme [79]. Sertraline also slightly inhibits CYP1A2, 3A4, 2C19 and 2C9, while in vitro desmethylsertraline seems to be a more potent inhibitor of CYP3A4, due to the long half-life of the metabolite. Therefore, the period for potential drug-drug interactions could be prolonged after sertraline treatment [131]. However, sertraline appears to have a favourable drug interaction profile in vivo as compared to the other SSRIs [22, 100]. Caution is advised when sertraline is coadministered with warfarin (prothrombin time should be monitored) and when using high dosages of sertraline in combination with a TCA or vice versa [225].

Sertraline should not be coadministered with a monoamine oxidase inhibitor as this can lead to hyperthermia, convulsions and coma. In addition, a delay of 2 weeks before taking a MAOI should be considered after fluvoxamine treatment and vice versa [64]. This washing out-period is also necessary for pimozide administration as it produces a dose-related prolongation of the QTc interval, which is associated with serious ventricular arrhythmias, such as torsades de pointes-type arrhythmias, and sudden death [64].

I.7.10.5. *Analytical methods*

Sertraline and its metabolite are determined using gas chromatographic, liquid chromatographic, as well as micellar electrokinetic capillary chromatographic methods [227]. Gas chromatography combined with detectors such as ECD [79], NPD [80], and MSD [76, 82, 113, 195, 228-230] is used. UV [83, 84, 143, 231], DAD [85, 86], and mass detectors [232, 233] are applied in liquid chromatographic methods.

Sample preparation mostly consists of a liquid-liquid extraction after alkalinization [76, 80, 84-86, 151, 195, 230] although recently numerous solid phase extraction methods [76, 83, 95, 143, 228, 231] are published. Moreover, methods using SPME [82] were also utilized. Most methods allow

quantitative determination in the lower ng/ml range (LOQ between 1-10 ng/ml), and are thus suitable for therapeutic drug monitoring purposes [76].

I.7.11. Trazodone

2-(3-(4-(3-Chlorophenyl)-1-piperazinyl)propyl)-1,2,4-triazolo (4,3-*a*)-pyridine-3 (2H) – one: mol. wt., 371.9; pK$_a$, 6.7; usual dose, 100-300 mg/day; max.dose, 600 mg/day; therapeutic concentration, 500-2500 ng/ml ; plasma half-life, 4-7 h; plasma protein binding, 90%; distribution volume, 0.9-1.5 l/kg [57, 58].
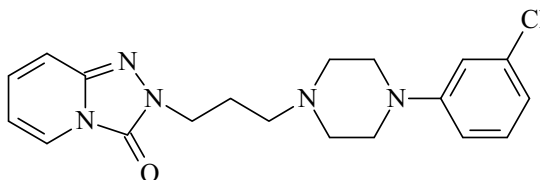
Trazodone is a serotonin antagonist and reuptake inhibitor. The drug has been used to treat depression, while it improves anxiety [234] and insomnia [235].

I.7.11.1. *Mechanism of action*

Trazodone blocks the reuptake of serotonin and blocks 5-HT$_{2a}$ as well as noradrenaline α$_1$-receptors. It blocks H$_1$ and noradrenaline α$_2$-receptors less potently, while it lacks anticholinergic activity [234, 236]. The active metabolite 1-(3-chlorophenyl)piperazine (m-cpp), has opposite activities, it releases serotonin and is a 5-HT$_{2c}$ and 5-HT$_{1a}$ receptor agonist [237]. These actions may contribute to the side-effects and action mechanism of trazodone [157] and are probably the reason why m-cpp is also encounterd in the drug scene.

I.7.11.2. *Pharmacokinetics*

Trazodone is readily and almost completely absorbed after oral administration. The time to reach maximum plasma concentration is about 1-2 hours and coadministration of food delays t$_{max}$ and decreases C$_{max}$ [138]. Steady-state plasma levels of trazodone range from 490 to 1210 ng/ml, while concentrations of m-cpp range from 10 to 30 ng/ml [238, 239]. Trazodone undergoes extensive hepatic metabolism, mainly through hydroxylation, N-

oxidation and N-dealkylation [157]. The two major metabolites are the pharmacologically active m-cpp, and beta-(3-oxo-s-triazolic(4,3-*a*)pyridin-2-yl)propionic acid (TPA). These metabolites are further glucuronated. While m-cpp is the major plasma metabolite, TPA (20%) is the main metabolite found in urine. Other urinary metabolites are p-hydroxytrazodone, and a dihydrodiol derivate (9%), even as their conjugation products. Trazodone is metabolized by CYP2D6, 1A2, and 3A4 [157].

I.7.11.3. *Drug concentrations and clinical effects*
The therapeutic concentration for trazodone ranges from 500-2500 ng/ml serum, while the toxic concentration is about 4000 ng/ml [56]. According to Otani et al., plasma concentrations of trazodone and m-cpp, after initial dosing, correlated well with those at steady state. However, there was a substantial accumulation of m-cpp due to the longer half-life of the metabolite [240]. Although there appears to be considerable inter-individual variation in trazodone metabolism and thus in steady state plasma concentrations attained with a given dose [157, 241], Mihara and Monteleone et al. have suggested a threshold plasma concentration of 714 ng/ml trazodone, necessary for a good antidepressant response [241, 242]. Trazodone appears to have linear pharmacokinetics. In addition, a considerable age and gender specific variation in plasma concentrations attained for a given dose is observed. The plasma concentrations were higher in females and in older patients [243]. Moreover, the plasma concentration of trazodone is lower in smokers compared to non-smokers [244]. Breast feeding during trazodone treatment is considered safe, as there is a minimal penetration of trazodone into breast milk (milk/plasma ratio of 0.14) [138].

I.7.11.4. *Drug interactions, side-effects and toxicity*
Possible side-effects of trazodone are sedation, particularly at high doses, orthostatic hypotension, nausea, drowsiness, vertigo and sexual dysfunction [236, 245]. These dysfunctions include increased libido, spontaneous orgasm and priapism [234]. Several case reports illustrate cardiovascular adverse effects such as orthostatic hypotension, ventricular arrhythmias, cardiac conduction disturbances, exacerbation of ischemic attacks and torsades de pointes [238, 246]. Especially, for the elderly, the side-effects of trazodone

such as sedation, dizziness and cardiotoxic effects raise considerable concerns. Caution is advised when trazodone is coadministered with fluoxetine, as excessive sedation has been reported. Moreover, trazodone in combination with other sedatives such as alcohol or other antidepressants should be observed carefully [245].

In addition, serotonin syndrome has been reported after coadministration with SSRIs, MAOI and TCAs [157, 238, 247, 248]. However, Prapotnik et al. did not observe drug interactions when trazodone was coadministered with fluoxetine or citalopram [243]. Trazodone should not be coadministered with a MAOI as this could lead to hyperthermia, convulsions and coma. Moreover, a few cases of warfarin-trazodone interactions have been reported [249]. Inhibitors of CYP2D6 (thioridazine) or CYP3A4 (ritonavir, ketonazole) increase the plasma concentration of trazodone in depressed patients [236, 250]. On the other hand, carbamazepine decreases trazodone plasma concentrations as it induces CYP3A4 [238]. Although trazodone has a low toxicity level, fatalities with blood concentrations around 9000 ng/ml and higher are observed in the literature, while noting the survival of patients even with significantly higher concentrations [238]. Most of the time, trazodone is coadministered with other drugs such as antidepressants, especially SSRIs and it is also used together with drugs of abuse [238, 251].

I.7.11.5. *Analytical methods*

Trazodone and m-cpp are determined using gas chromatographic and liquid chromatographic methods. Gas chromatography is mostly combined with an NPD [111, 252-254], but FID is also used [254]. Caccia et al. determined trazodone with a GC-NPD in plasma and brain tissues. They also analyzed m-cpp after heptafluorobutyryl derivatization with ECD and MSD [253]. UV detectors [173, 255-259] and DAD [260] are applied in liquid chromatographic methods. Ohkubo et al. combined UV detection for trazodone with coulometric electrochemical detection of m-cpp [257]. In addition, Siek [261] reported a high-performance thin-layer chromatographic method combined with a Camag TLC scanner for fluorescence-reflectance measurements. Although trazodone can not be detected with immunological methods, the metabolite of trazodone can be responsible for false-positive

results for amphetamine using polyclonal antibody assays (EMIT 1, Triage panel) [262].

Sample preparation mostly consists of a liquid-liquid extraction after alkalinization [173, 253-256, 258-260], although recently solid phase extraction methods are also published [111, 257].

I.7.12. Venlafaxine

1-(2-(Dimethylamino)-1-(4-methoxyphenyl]ethyl)cyclohexanol: mol. wt., 277.4; pK_a, 9.4; usual dose, 75 mg/day; max.dose, 375 mg/day ; therapeutic concentration, 250 to 750 ng/ml for the sum parent drug and metabolites; toxic concentration, 1000-1500 ng/ml; plasma half-life, 4 h; plasma protein binding, 30%; distribution volume, 6.8 l/kg (4-12 l/kg)[57, 58].
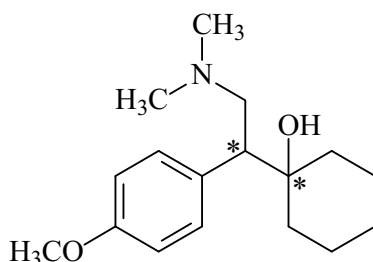
Venlafaxine is a selective noradrenaline and serotonin inhibitor (SNRI), introduced in 1993 to treat depression, generalized or social anxiety disorders. This compound exists as racemic antidepressant with both active R(+)- and S(-) – enantiomers [263]. TDM could be of interest for monitoring patient compliance and adjusting the dose for patients with liver and kidney impairment. However, it is a drug with a low potency for drug-drug interactions, due to its low protein binding as well as its weak inhibitory effect on the CYP 450 system.

I.7.12.1. *Mechanism of action*
Venlafaxine enhances noradrenergic and serotonergic neurotransmission through inhibition of the noradrenaline and serotonin reuptake. The (-) enantiomer inhibits reuptake of both serotonin and noradrenaline, while the (+) enantiomer primarily inhibits serotonin reuptake. Venlafaxine also inhibits, to a lesser extent, dopamine reuptake. Venlafaxine has no

monoamine oxidase inhibitory properties, and has no affinity for histamine, α_2 or β-adrenergic and muscarinic cholinergic receptors [263].

I.7.12.2. *Pharmacokinetics*

Venlafaxine is absorbed rapidly and almost complete (92%) after oral intake. The maximum plasma concentration is achieved after about 2 till 4 hours, while steady-state is achieved within 3 days of multidose therapy. In addition, venlafaxine and O-desmethylvenlafaxine have linear kinetics over the total daily dosage range of 75-450 mg. Venlafaxine is subject to an extensive first-pass metabolism in the liver. The main metabolite, O-desmethylvenlafaxine, has a pharmacological activity similar to that of the parent drug. This metabolite, however, has a longer elimination half-life, being 10 hours instead of 4. Other minor metabolites such as N-desmethylvenlafaxine and N,O-didesmethylvenlafaxine are also produced. Venlafaxine is metabolized primarily in the liver via CYP2D6, but also by CYP3A4 to yield the N-desmethylmetabolite [264]. The mean plasma half-life of venlafaxine is 4 hours, but is increased in patients suffering from renal and hepatic impairment. Approximately 87% of a single dose venlafaxine is excreted in urine within 48 hours, containing about 5% unchanged venlafaxine, unconjugated and conjugated O-desmethylvenlafaxine (29/26%), and minor metabolites (27%).

I.7.12.3. *Drug concentrations and clinical effects*

The therapeutic concentration for the sum of venlafaxine and its active metabolite O-desmethylvenlafaxine ranges from 250-750 ng/ml [56]. While gender has no effect on venlafaxine pharmacokinetics, plasma concentrations of the drug and its active metabolite have been reported to increase with age [264]. This observation might be due to a higher risk of drug interactions in the elderly (polypharmacy) and a physiologically age-related lower clearance [264]. However, no dosage adjustments are necessary in the elderly on the basis of age alone [265]. On the other hand, dosage of venlafaxine should be reduced (by 50%) for patients with moderate liver impairment as the hepatic clearance of both venlafaxine and O-desmethylvenlafaxine is decreased. In addition, the dosage should be reduced for renal impaired patients because of

the decreased venlafaxine renal clearance and the prolonged elimination half-life of both the parent drug and its active metabolite [67, 263].

Reis et al. found a reduction in O-desmethyl- and N,O-didesmethyl-venlafaxine plasma concentrations for smokers, compared to nonsmokers, indicating that CYP1A2 might have a role in the drug metabolism [264]. Venlafaxine administration seems quite safe during pregnancy and breastfeeding. Although there are reports of more spontaneous abortions when using venlafaxine, it did not attain statistical significance in comparison with pregnant women taking SSRIs or non-teratogenic agents [45]. However, it should only be used if the benefits clearly outweigh the risks.

I.7.12.4. *Drug interactions, side-effects and toxicity*

The most frequently reported side-effects of venlafaxine are nausea, headache, somnolence, dry mouth, insomnia, dizziness and sexual dysfunction. Moreover, a mild increased blood pressure was occasionally associated with venlafaxine use. This effect seems to be dose related and occurs most frequently at dosages of more than 300 mg per day.

Severe adverse arrhythmia is reported in several patients, which were all poor metabolizers of CYP2D6 and thus had the highest levels of venlafaxine in plasma [266]. Therefore, Kirchheiner et al. recommend 20% of the average venlafaxine dose for poor metabolizers. Although there is some concern about the influence of venlafaxine on the heart rate [267], some authors conclude that there is no direct effect on cardiac conduction and it is in fact a relatively safe choice of an antidepressant in people at risk of cardiac arrhythmias [268]. Venlafaxine has a low toxicity potential, despite the fact that there were 14 premarketing reports of overdose with venlafaxine, either alone or in combination with other drugs or alcohol. Seizures and increased QT intervals were also reported, but all of the patients made full recovery [268]. According to the TIAFT reference list a serum concentration of 6600 ng/ml is lethal [56].

Because venlafaxine is metabolized by CYP2D6, theoretically competitive inhibition by other drugs that are metabolized by this enzyme can occur. However, venlafaxine has a low affinity for inhibiting CYP2D6 and thus will not have a significant effect on the metabolism of other drugs, but other drugs (such as cimetidine) may rather affect the metabolism of venlafaxine

[263]. Moreover, as the drug has a low protein binding rate of 30%, drug interactions with high-protein bound drugs are not expected [263]. Venlafaxine, though, should not be coadministered with a monoamine oxidase inhibitor as this can lead to hyperthermia, convulsions and coma. While after venlafaxine treatment, a delay of 7 days before taking a MAOI should be considered, it is recommended that venlafaxine should not be used within 14 days of discontinuing treatment with an MAOI [263]. Moreover, venlafaxine causes a 70% increase in the AUC of coadministered haloperidol [100], and a 30% decrease of alprazolam plasma concentration [268].

I.7.12.5. *Analytical Methods*

Venlafaxine is determined in biological matrices with or without its metabolites using electrokinetic capillary chromatographic techniques [140, 269], liquid or gas chromatographic methods. NPD [270, 271] and MSD [82] are used in gas chromatography. In liquid chromatography detectors such as UV [83, 84, 272-274], DAD [85, 86], fluorescence [275], and mass detectors [92, 276] are applied. In addition, Rudaz et al. described a capillary electrophoresis method that separates the enantiomers of the compound using gamma-cyclodextrin as chiral selector [269].

Solid phase extraction [83, 92, 95, 276] or liquid-liquid extraction [84-86, 272-275] are mostly used as sample preparation techniques, however, solid-phase micro extraction techniques are also applied [82].

I.7.13. Viloxazine

2-((2-Ethoxyphenoxy) methyl) morpholine: mol. wt., 237.3; pK_a, 8.1; usual dose, 100-400 mg/day; max.dose, 400 mg/day; therapeutic concentration, 5000-10000 ng/ml (peak plasma concentration); plasma half-life, 2-5 h; plasma protein binding, 85-90%; distribution volume, 0.5-1.5 l/kg [57, 58].
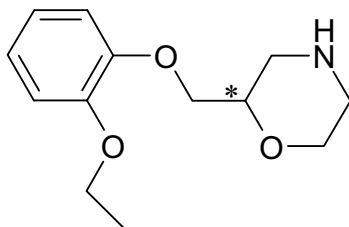
Viloxazine is a noradrenaline reuptake blocking antidepressant used to treat depression [138]. This compound is marketed as a racemate, but the (R)-(+) is less potent than the (S)-(-)-enantiomer [277]. Viloxazine has a good tolerability and a low potency for drug-drug interactions.

I.7.13.1. *Mechanism of action*
Viloxazine enhances noradrenergic neurotransmission through inhibition of the noradrenaline reuptake. It possibly also inhibits the reuptake of serotonin very weakly, but does not inhibit dopamine reuptake. In addition, the drug has no affinity for α-adrenergic and muscarinic cholinergic receptors [278].

I.7.13.2. *Pharmacokinetics*
The mean plasma half-life of viloxazine ranges between 2-5 hours, while the drug exhibits linear pharmacokinetics [138]. It is rapidly and almost completely absorbed from the gastrointestinal tract. Viloxazine is metabolized through hydroxylation, eventually followed by conjugation. The greatest part of a single dose is excreted in urine (about 90% in 24 h), which contains about 12 to 15% unchanged viloxazine, and 3% as its hydroxy metabolites, while the rest is excreted as glucuronide conjugates of 5-hydroxyviloxazine or hydroxylated 5-oxo metabolite.

I.7.13.3. *Drug concentrations and clinical effects*
The peak plasma concentration for viloxazine ranges from 5-10 μg/ml [56]. Steady state plasma concentrations of the drug have been reported to increase significantly with age, however, this does not seem to have a clinical impact.

I.7.13.4. *Drug interactions, side-effects and toxicity*
The most frequently reported side-effects of viloxazine are nausea and vomiting [279], but also palpitation, anxiety, constipation and dryness of the mouth are reported [280, 281].
Drug-drug interactions reported with viloxazine include anticonvulsants such as carbamazepine and phenytoin. In addition, viloxazine decreases the clearance of theophylline. These drug-drug interactions are due to inhibition of CYP3A4, 2C9, 2C19 and 1A2 by viloxazine [138, 157].

I.7.13.5. *Analytical Methods*

Viloxazine is determined by using liquid chromatographic or gas chromatographic methods. While MSD [95], NPD [271, 282, 283], ECD or FID are used in gas chromatography, UV [284]/ DAD [85] are applied in liquid chromatography.

Solid phase extraction [95, 271] or liquid-liquid extractions [282-284] are used as sample preparation techniques.

I.8. Relevance of antidepressant analysis in forensic toxicology

Although the new generation ADs have a low toxicity profile, analysis of forensic samples is of interest. Dispite the high suicide rate amoung depressed patients, acute intoxications with these new generation ADs in healthy individuals are rare and mostly concern very high concentrations, thus reflecting large intentional overdoses [39, 285, 286]. These highly prescribed ADs, however, are frequently coadministered with other legal or illegal drugs. Therefore, co-medication of these ADs can lead to synergy of adverse reactions and symptoms, a changed drug concentration due to inhibition or induction of CYP 450 isoenzymes, or result in a severe and possible life threatening interaction. The most common lethal intoxication observed for the new generation ADs is the serotonin syndrome. This serotonin syndrome leads to agitation, mental status change, diaphoresis, myoclonus, diarrhea, fever, hyperreflexia, tremor or incoordination and can eventually lead to death. The syndrome is caused by excessive serotonin levels that arise from an overdose of a serotonin reuptake inhibitor [287], but also by therapeutic amounts of multiple drugs with reuptake inhibition of serotonin, or by co-medication of a serotonin reuptake inhibitor and drugs that interfere with the metabolism of serotonin such as MAOI [70, 288-290]. Deaths due to serotonin syndrome may also occur due to the presence of predisposing factors, such as peripheral vascular disease, environmental hyperthermia, or seizure disorder [39].

In forensics, different matrices are used to determine ADs as compared to TDM. Blood is the most relevant post-mortem matrix as it gives a direct link

between the compound concentration and the effect. Plasma can not be obtained in most of the post-mortem cases, as plasma has to be separated from the blood cells within 2 hours by centrifugation, thus before cell lysis occurs. Brain tissue also has advantages as it is an isolated compartment in which putrefaction is delayed. In addition, the metabolic activity is lower, resulting in a more prominent presence of the original compounds as compared to degradation products [291]. Urine and hair analysis is a complementary approach to ADs detection as it yields a picture of long-term exposure over a time window of several days to several months, respectively. In addition, hair samples can be stored at room temperature for long periods without degradation of the compounds inside [292-293].

I.9.   References

[1]   Murray CJL, Lopez AD. Global burden of disease: a comprehensive assessment of mortality and disability from diseases, injuries, and risk factors in 1990 and projected to 2020, Harvard University Press, Harvard, 1996

[2]   Sampson SM. Treating depression with selective serotonin reuptake inhibitors: a practical approach. *Mayo Clin. Proc.* 2001; 76: 739-744

[3]   Uges DRA, Conemans JMH. Antidepressants and antipsychotics. Handbook of Analytical Separations, Elsevier, Amsterdam, 2000, pp. 742

[4]   Nestler EJ, Barrot M, DiLeone RJ, Eisch AJ, Gold SJ, Monteggia LM. Neurobiology of depression. *Neuron.* 2002; 34: 13-25

[5]   Taylor C, Fricker AD, Devi LA, Gomes N. Mechanisms of action of antidepressants: from neurotransmitter systems to signaling pathways. *Cell Signal.* 2005; 17: 549-557

[6]   Richelson E. Interactions of antidepressants with neurotransmitter transporters and receptors and their clinical relevance. *J. Clin. Psychiatry* 2003; 64: 5-12 Suppl. 13

[7]   Richelson E. Pharmacology of antidepressants. *Mayo Clin. Proc.* 2001; 76: 511-527

[8]   Schwaninger M, Weisbrod M, Knepel W. Progress in defining the mechanism of action of antidepressants - across receptors and into gene transcription. *CNS Drugs* 1997; 8: 237-243

[9]   Vetulani J, Nalepa I. Antidepressants: past, present and future. *Eur. J. Pharmacol.* 2000; 405: 351-363

[10]   Malberg JE, Blendy JA. Antidepressant action: to the nucleus and beyond. *Trends Pharmacol. Sci.* 2005; 26: 631-638

[11]   Yildiz A, Gönül A, Tamam L. Mechanism of actions of antidepressants: beyond the receptors. *Bull. Clin. Psychopharmacol.* 2002; 12: 194-200

[12]   Frey BN, Rodrigues da Fonseca MM, Machado-Vieira R, Soarese JC, Kapczinski F. Neuropathological and neurochemical abnormalities in bipolar disorder. *Rev. Bras. Psiquiatr.* 2004; 26: 180-188

[13]   Duman RS, Heninger GR, Nestler EJ. A molecular and cellular theory of depression. *Arch. Gen. Psychiatry* 1997; 54: 597-606

[14]   Dwivedi Y, Rizavi HS, Conley RR, Roberts RC, Tamminga CA, Pandey GN. Altered gene expression of brain-derived neurotrophic factor and receptor tyrosine kinase B in postmortem brain of suicide subjects. *Arch. Gen. Psychiatry* 2003; 60: 804-815

[15]   Pacher P, Kohegyi E, Kecskemeti V, Furst S. Current trends in the development of new antidepressants. *Curr. Med. Chem.* 2001; 8: 89-100

[16]   Kent JM. SNaRIs, NaSSAs, and NaRIs: new agents for the treatment of depression. *Lancet* 2000; 355: 911-918

[17]   Kent J. SNaRIs, NaSSAs, and NaRIs: new agents for the treatment of depression. *Lancet* 2000; 355: 2000-2000

[18]   Mann JJ. Drug therapy - The medical management of depression. *N. Engl. J. Med.* 2005; 353: 1819-1834

[19]   Vanharten J. Clinical pharmacokinetics of selective serotonin reuptake inhibitors. *Clin. Pharmacokinet.* 1993; 24: 203-220

[20]   Masand PS, Gupta S. Selective serotonin-reuptake inhibitors: an update. *Harv. Rev. Psychiatry* 1999; 7: 69-84

[21]   Rudorfer MV, Potter WZ. Metabolism of tricyclic antidepressants. *Cell. Mol. Neurobiol.* 1999; 19: 373-409

[22]   Sproule BA, Naranjo CA, Bremner KE, Hassan PC. Selective serotonin reuptake inhibitors and CNS drug interactions - A critical review of the evidence. *Clin. Pharmacokinet.* 1997; 33: 454-471

[23]   Nemeroff CB, DeVane CL, Pollock BG. Newer antidepressants and the cytochrome P450 system. *Am. J. Psychiatry* 1996; 153: 311-320

[24]   Stahl SM. Mechanism of action of serotonin selective reuptake inhibitors - serotonin receptors and pathways mediate therapeutic effects and side effects. *J. Affect. Disord.* 1998; 51: 215-235

[25]   Boyer WF, Shannon M. The serotonin syndrome. *N. Engl. J. Med.* 2005; 352: 1112-1119

[26]   Harrigan RA, Brady WJ. ECG abnormalities in tricyclic antidepressant ingestion. *Am. J. Emerg. Med.* 1999; 17: 387-393

[27]   Hardman J, Limberd L, Molinoff P, Ruddon R. Goodman and Gilman's the pharmacological basis of therapeutics In A. Goodman Gilman, Eds. *Goodman and Gilman's the pharmacological basis of therapeutics 9th Ed.* pp 1905. New York: McGraw-Hill, 1996

[28]   Kerr GW, McGuffie AC, Wilkie S. Tricyclic antidepressant overdose: a review. *Emerg. Med. J.* 2001; 18: 236-241

[29]   Thanacoody HK, Thomas SH. Tricyclic antidepressant poisoning: cardiovascular toxicity. *Toxicol. Rev.* 2005; 24: 236-241

[30]   Glauser J. Tricyclic antidepressant poisoning. *Cleve. Clin. J. Med.* 2000; 67: 704-706

[31]   Ray WA, Meredith S, Thapa PB, Hall K, Murray KT. Cyclic antidepressants and the risk of sudden cardiac death. *Clin. Pharmacol. Ther.* 2004; 75: 234-241

[32]   Roose SP. Treatment of depression in patients with heart disease. *Biol. Psychiatry* 2003; 54: 262-268

[33]   Cohen HW, Gibson G, Alderman MH. Excess risk of myocardial infarction in patients treated with antidepressant medications: Association with use of tricyclic agents. *Am. J. Med*. 2000; 108: 2-8

[34]   Denollet J, Sys SU, Stroobant N, Rombouts H, Gillebert TC, Brutsaert DL. Personality as independent predictor of long-term mortality in patients with coronary heart disease. *Lancet* 1996; 347: 417-421

[35]   Roose SP. Depression, anxiety, and the cardiovascular system: the psychiatrist's perspective. *J. Clin. Psychiatry* 2001; 62: 19-23

[36]   Roose SP. Considerations for the use of antidepressants in patients with cardiovascular disease. *Am. Heart J*. 2000; 140: 584-588

[37]   Glassman AH. Cardiovascular effects of antidepressant drugs: Updated. *Int. Clin. Psychopharmacol.* 1998; 13: S25-S30

[38]   Glassman AH. Cardiovascular effects of antidepressant drugs: Updated. *J. Clin. Psychiatry* 1998; 59: 13-18

[39]   Goeringer KE, Raymon L, Christian GD, Logan BK. Postmortem forensic toxicology of selective serotonin reuptake inhibitors: A review of pharmacology and report of 168 cases. *J. Forensic Sci.* 2000; 45: 633-648

[40]   Hiemke C, Hartter S. Pharmacokinetics of selective serotonin reuptake inhibitors. *Pharmacol. Ther.* 2000; 85: 11-28

[41]   Cipriani A, Barbui C, Geddes JR. Suicide, depression, and antidepressants. *BMJ* 2005; 330: 373-374

[42]   Licinio J, Wong ML. Depression, antidepressants and suicidality: a critical appraisal. *Nat. Rev. Drug Discov* 2005; 4: 165-171

[43]   Whittington CJ, Kendall T, Fonagy P, Cottrell D, Cotgrove A, Boddington E. Selective serotonin reuptake inhibitors in childhood depression: systematic review of published versus unpublished data. *Lancet* 2004; 363: 1341-1345

[44]   Goldstein DJ, Sundell K. A review of the safety of selective serotonin reuptake inhibitors during pregnancy. *Hum. Psychopharmacol.* 1999; 14: 319-324

[45]   Gentile S. The safety of newer antidepressants in pregnancy and breastfeeding. *Drug Saf.* 2005; 28: 137-152

[46]   Sanz EJ, De-las-Cuevas C, Kiuru A, Bate A, Edwards R. Selective serotonin reuptake inhibitors in pregnant women and neonatal withdrawal syndrome: a database analysis. *Lancet* 2005; 365: 482-487

[47]   Ruchkin V, Martin A. SSRIs and the developing brain. *Lancet* 2005; 365: 451-453

[48]   Burke MJ, Preskorn SH. Therapeutic drug monitoring of antidepressants - Cost implications and relevance to clinical practice. *Clin. Pharmacokinet.* 1999; 37: 147-165

[49]   Lundmark J, Bengtsson F, Nordin C, Reis M, Walinder J. Therapeutic drug monitoring of selective serotonin reuptake inhibitors influences clinical dosing strategies and reduces drug costs in depressed elderly patients. *Acta Psychiatr. Scand.* 2000; 101: 354-359

[50]   Mitchell PB. Therapeutic drug monitoring of psychotropic medications. *Br. J. Clin. Pharmacol.* 2000; 49: 303-312

[51]   Mitchell PB. Therapeutic drug monitoring of non-tricyclic antidepressant drugs. *Clin. Chem. Lab. Med.* 2004; 42: 1212-1218

[52]   Eap CB, Sirot EJ, Baumann P. Therapeutic monitoring of antidepressants in the era of pharmacogenetics studies. *Ther. Drug Monit.* 2004; 26: 152-155

[53]   Heller S, Hiemke C, Stroba G, Rieger-Gies A, Daum-Kreysch E, Sachse J, Hartter S. Assessment of storage and transport stability of new antidepressant and antipsychotic drugs for a nationwide TDM service. *Ther. Drug Monit.* 2004; 26: 459-461

[54]   Decision Resources Inc. The Antidepressant Market through 2014 - Focus on emerging therapies and new indications. *Cognos Plus Stud*y nº 11*, Massechussets, 2005; pp 176

[55]   Baumann P, Hiemke C, S. U, Eckermann G, Gaertner I, Kuss HJ, Laux G, Müller-Oerlinghausen B, Rao ML, Riederer P, Zernig G. The AGNP-TDM expert group consensus guidelines: therapeutic drug monitoring in psychiatry. *Pharmacopsychiatry* 2004; 37: 243-265

[56]   TIAFT. The international association of forensic toxicologists. *Tiaft bulletin* 26 1S (http: //www. tiaft. org/)

[57]   Council of the royal pharmaceutical society of Great Britain. Martindale -The extra Pharmacopoeia. In K. Parfitt, A.V. Parsons, S.C. Sweetman, Eds. *Martindale -The extra Pharmacopoeia*, pp 2363. London: The Pharmaceutical Press, 1993

[58]   Moffat AC, Osselton MD, Widdop B. Clarke's analysis of drugs and poisons in pharmaceuticals, body fluids and postmortem material. In Y.G. Laurent, Eds. *Clarke's analysis of drugs and poisons in pharmaceuticals, body fluids and postmortem material*, *3th Ed.* pp 1935. London: Pharmaceutical Press, 2004

[59]   Bezchlibnyk-Butler K, Aleksic I, Kennedy SH. Citalopram--a review of pharmacological and clinical effects. *J. Psychiatry Neurosci.* 2000; 25: 241-256

[60]   Sanchez C, Bogeso KP, Ebert B, Reines EH, Braestrup C. Escitalopram versus citalopram: the surprising role of the R-enantiomer. *Psychopharmacology* 2004; 174: 163-176

[61]   Kennedy SH, H.F. A, Lam RW. Efficacy of escitalopram in the treatment of major depressive disorder compared with conventional selective serotonin reuptake inhibitors and venlafaxine XR: a meta-analysis. *J. Psychiatry Neurosci.* 2006; 31: 122-131

[62]   Brosen K, Naranjo C. Review of pharmacokinetic and pharmacodynamic interaction studies with citalopram. *Eur. Neuropsychopharmacol.* 2001; 11: 275-283

[63]   Le Bloc'h Y, Woggon B, Weissenrieder H, Brawand-Amey M, Spagnoli J, Eap CB, Baumann P. Routine therapeutic drug monitoring in patients treated with 10-360 mg/day citalopram. *Ther. Drug Monit.* 2003; 25: 600-608

[64]   FDA. http://www.fda.gov.

[65]   Messer T, Schmauss M, Lambert-Baumann J. Efficacy and tolerability of reboxetine in depressive patients treated in routine clinical practice. *CNS Drugs* 2005; 19: 43-54

[66]   Rochat B, Amey M, Gillet M, Meyer UA, Baumann P. Identification of three cytochrome P450 isozymes involved in N-demethylation of citalopram enantiomers in human liver microsomes. *Pharmacogenetics* 1997; 7: 1-10

[67]   Caccia S. Metabolism of the newer antidepressants - An overview of the pharmacological and pharmacokinetic implications. *Clin. Pharmacokinet.* 1998; 34: 281-302

[68]   Barak Y, Swartz M, Levy D, Weizman R. Age-related differences in the side effect profile of citalopram. *Prog. Neuropsychopharmacol. Biol. Psychiatry* 2003; 27: 545-548

[69]   Joubert AF, Sanchez C, Larsen F. Citalopram. *Hum. Psychopharmacol.* 2000; 15: 439-451

[70]   Dams R, Benijts THP, Lambert WE, Van Bocxlaer JF, Van Varenbergh D, Peteghem CV, De Leenheer AP. A fatal case of serotonin syndrome after combined moclobemide-citalopram intoxication. *J. Anal. Toxicol.* 2001; 25: 147-151

[71]   Jonasson B, Saldeen T. Citalopram in fatal poisoning cases. *Forensic Sci. Int.* 2002; 126: 1-6

[72]   Andersen S, Halvorsen TG, Pedersen-Bjergaard S, Rasmussen KE, Tanum L, Refsum H. Stereospecific determination of citalopram and desmethylcitalopram by capillary electrophoresis and liquid-phase microextraction. *J. Pharm. Biomed. Anal.* 2003; 33: 263-273

[73]   Singh SS, Shah H, Gupta S, Jain M, Sharma K, Thakkar P, Shah R. Liquid chromatography-electrospray ionisation mass spectrometry method for the determination of escitalopram in human plasma and its application in bioequivalence study. *J. Chromatogr. B Biomed. Sci. Appl.* 2004; 811: 209-215

[74]   Rasmussen BB, Brosen K. Is therapeutic drug monitoring a case for optimizing clinical outcome and avoiding interactions of the selective serotonin reuptake inhibitors? *Ther. Drug Monit.* 2000; 22: 143-154

[75]   Zheng ZC, Jamour M, Klotz U. Stereoselective HPLC-assay for citalopram and its metabolites. *Ther. Drug Monit.* 2000; 22 219-224

[76]   Eap CB, Baumann P. Analytical methods for the quantitative determination of selective serotonin reuptake inhibitors for therapeutic drug monitoring purposes in patients. *J. Chromatogr. B Biomed. Appl.* 1996; 686: 51-63

[77]   Haupt D. Determination of citalopram enantiomers in human plasma by liquid chromatographic separation on a Chiral-AGP column. *J. Chromatogr. B Biomed. Sci. Appl.* 1996; 685: 299-305

[78]   El-Gindy A, Emara S, Mesbah MK, Hadad GM. Liquid chromatography determination of citalopram enantiomers using beta-cyclodextrin as a chiral mobile phase additive. *J. AOAC Int.* 2006; 89: 65-70

[79]   Baumann P. Pharmacokinetic-pharmacodynamic relationship of the selective serotonin reuptake inhibitors. *Clin. Pharmacokinet.* 1996; 31: 444-469

[80]   Lacassie E, Gaulier JM, Marquet P, Rabatel JF, Lachatre G. Methods for the determination of seven selective serotonin reuptake inhibitors and three active metabolites in human serum using high-performance liquid chromatography and gas chromatography. *J. Chromatogr. B Biomed. Sci. Appl.* 2000; 742: 229-238

[81]   Eap CB, Bouchoux G, Amey M, Cochard N, Savary L, Baumann P. Simultaneous determination of human plasma levels of citalopram, paroxetine, sertraline, and their metabolites by gas chromatography mass spectrometry. *J. Chromatogr. Sci.* 1998; 36: 365-371

[82]   Salgado-Petinal C, Lamas JP, Garcia-Jares C, Llompart M, Cela R. Rapid screening of selective serotonin re-uptake inhibitors in urine samples using

solid-phase microextraction gas chromatography-mass spectrometry. *Anal. Bioanal. Chem.* 2005; 382: 1351-1359

[83]   Frahnert C, Rao ML, Grasmader K. Analysis of eighteen antidepressants, four atypical antipsychotics and active metabolites in serum by liquid chromatography: a simple tool for therapeutic drug monitoring. *J. Chromatogr. B Analyt. Technol. Biomed. Life Sci.* 2003; 794: 35-47

[84]   Tournel G, Houdret N, Hedouin V, Deveaux M, Gosset D, Lhermitte M. High-performance liquid chromatographic method to screen and quantitate seven selective serotonin reuptake inhibitors in human serum. *J. Chromatogr. B Biomed. Sci. Appl.* 2001; 761: 147-158

[85]   Duverneuil C, de la Grandmaison GL, de Mazancourt P, Alvarez JC. A high-performance liquid chromatography method with photodiode-array UV detection for therapeutic drug monitoring of the nontricyclic antidepressant drugs. *Ther. Drug Monit.* 2003; 25: 565-573

[86]   Titier K, Castaing N, Scotto-Gomez E, Pehourcq F, Moore N, Molimard M. High-performance liquid chromatographic method with diode array detection for identification and quantification of the eight new antidepressants and five of their active metabolites in plasma after overdose. *Ther. Drug Monit.* 2003; 25: 581-587

[87]   Kristoffersen L, Bugge A, Lundanes E, Slordal L. Simultaneous determination of citalopram, fluoxetine, paroxetine and their metabolites in plasma and whole blood by high-performance liquid chromatography with ultraviolet and fluorescence detection. *J. Chromatogr. B Biomed. Sci. Appl.* 1999; 734: 229-246

[88]   Macek J, Ptacek P, Klima J. Rapid determination of citalopram in human plasma by high-performance liquid chromatography. *J. Chromatogr. B Biomed. Sci. Appl.* 2001; 755 279-285

[89]   Raggi MA, Pucci V, Mandrioli R, Sabbioni C, Fanali S. Determination of recent antidepressant citalopram in human plasma by liquid chromatography - Fluorescence detection. *Chromatographia* 2003; 57: 273-278

[90]   Meng QH, Gauthier D. Simultaneous analysis of citalopram and desmethylcitalopram by liquid chromatography with fluorescence detection after solid-phase extraction. *Clin. Biochem.* 2005; 38: 282-285

[91]   Gutteck U, Rentsch KM. Therapeutic drug monitoring of 13 antidepressant and five neuroleptic drugs in serum with liquid chromatography-electrospray ionization mass spectrometry. *Clin. Chem. Lab. Med*. 2003; 41: 1571-1579

[92]   He J, Zhou ZL, Li HD. Simultaneous determination of fluoxetine, citalopram, paroxetine, venlafaxine in plasma by high performance liquid chromatography-electrospray ionization mass spectrometry (HPLC-MS/ESI). *J. Chromatogr. B Biomed. Sci. Appl.* 2005; 820: 33-39

[93]   Kollroser M, Schober C. An on-line solid phase extraction - liquid chromatography - tandem mass spectrometry method for the analysis of citalopram, fluvoxamine, and paroxetine in human plasma. *Chromatographia* 2003; 57: 133-138

[94]   Martinez MA, de la Torre CS, Almarza E. A comparative solid-phase extraction study for the simultaneous determination of fluvoxamine, mianserin, doxepin, citalopram, paroxetine, and etoperidone in whole blood by capillary gas-liquid chromatography with nitrogen-phosphorus detection. *J. Anal. Toxicol.* 2004; 28: 174-180

[95]   Wille SMR, Maudens KE, Van Peteghem CH, Lambert WEE. Development of a solid phase extraction for 13 'new' generation antidepressants and their active

metabolites for gas chromatographic-mass spectrometric analysis. *J. Chromatogr. A* 2005; 1098: 19-29

[96]   Cheer SM, Goa KL. Fluoxetine - A review of its therapeutic potential in the treatment of depression associated with physical illness. *Drugs* 2001; 61: 81-110

[97]   Mhanna MJ, Bennet JB, Izatt SD. Potential fluoxetine chloride (Prozac) toxicity in a newborn. *Pediatrics* 1997; 100: 158-159

[98]   Messiha FS. Fluoxetine - adverse-effects and drug-drug interactions. *J. Toxicol. Clin. Toxicol.* 1993; 31: 603-630

[99]   Stokes PE, Holtz A. Fluoxetine tenth anniversary update: the progress continues. *Clin. Ther.* 1997; 19: 1135-1250

[100]   Spina E, Scordo MG, D'Arrigo C. Metabolic drug interactions with new psychotropic agents. *Fundam. Clin. Pharmacol.* 2003; 17: 517-538

[101]   Nevado JJB, Salcedo AMC, Llerena MJV. Micellar electrokinetic capillary chromatography for the determination of fluoxetine and its metabolite norfluoxetine in biological fluids. *J. Chromatogr. B Analyt. Technol. Biomed. Life Sci.* 2002; 769: 261-268

[102]   Eap CB, Gaillard N, Powell K, Baumann P. Simultaneous determination of plasma levels of fluvoxamine and of the enantiomers of fluoxetine and norfluoxetine by gas chromatography mass spectrometry. *J. Chromatogr. B Biomed. Appl.* 1996; 682: 265-272

[103]   Ulrich S. Direct stereoselective assay of fluoxetine and norfluoxetine enantiomers in human plasma or serum by two-dimensional gas-liquid chromatography with nitrogen-phosphorus selective detection. *J. Chromatogr. B Analyt. Technol. Biomed. Life Sci.* 2003; 783: 481-490

[104]   Pichini S, Pacifici R, Altieri I, Pellegrini M, Zuccaro P. Stereoselective determination of fluoxetine and norfluoxetine enantiomers in plasma samples by high-performance liquid chromatography. *J. Liq. Chromatogr. Relat. Technol.* 1996; 19: 1927-1935

[105]   Olsen BA, Wirth DD, Larew JS. Determination of fluoxetine hydrochloride enantiomeric excess using high-performance liquid chromatography with chiral stationary phases. *J. Pharm. Biomed. Anal.* 1998; 17: 623-630

[106]   Yu HW, Ching CB. Kinetic and equilibrium study of the enantioseparation of fluoxetine on a new beta-cyclodextrin column by high performance liquid chromatography. *Chromatographia* 2001; 54: 697-702

[107]   Gatti G, Bonomi I, Marchiselli R, Fattore C, Spina E, Scordo G, Pacifici R, Perucca E. Improved enantioselective assay for the determination of fluoxetine and norfluoxetine enantiomers in human plasma by liquid chromatography. *J. Chromatogr. B Analyt. Technol. Biomed. Life Sci.* 2003; 784: 375-383

[108]   Fukushima T, Naka-aki E, Guo XJ, Li FM, Vankeirsbilck T, Baeyens WRG, Imai K, Toyo'oka T. Determination of fluoxetine and norfluoxetine in rat brain microdialysis samples following intraperitoneal fluoxetine administration. *Anal. Chim. Acta.* 2005; 531: 163-163

[109]   Fontanille P, Jourdil N, Villier C, Bessard G. Direct analysis of fluoxetine and norfluoxetine in plasma by gas chromatography with nitrogen-phosphorus detection. *J. Chromatogr. B Biomed. Sci. Appl.* 1997; 692: 337-343

[110]   Ulrich S. Direct stereoselective assay of fluoxetine and norfluoxetine enantiomers in human plasma by two-dimensional gas chromatography with nitrogen-phosphorus selective detection. *Pharmacopsychiatry* 2002; 35: XI-XI

[111]   Martinez MA, de la Torre CS, Almarza E. A comparative solid-phase extraction study for the simultaneous determination of fluoxetine, amitriptyline, nortriptyline, trimipramine, maprotiline, clomipramine, and trazodone in whole blood by capillary gas-liquid chromatography with nitrogen-phosphorus detection. *J. Anal. Toxicol.* 2003; 27: 353-358

[112]   Lefebvre M, Marchand M, Horowitz JM, Torres G. Detection of fluoxetine in brain, blood, liver and hair of rats using gas chromatography mass spectrometry. *Life Sci.* 1999; 64: 805-811

[113]   Fathi M, Duparc MT, Morch F, Jayo M, Martin C, Hochstrasser D. Simultaneous determination of fluoxetine, norfluoxetine, paroxetine, sertraline and reboxetine in serum as acetvlated derivatives by gas chromatography-selected ion monitoring mass spectrometry (GC-SIM-MS). *Ther. Drug Monit.* 2005; 27: 217-218

[114]   Holladay JW, Dewey MJ, Yoo SD. Quantification of fluoxetine and norfluoxetine serum levels by reversed-phase high-performance liquid chromatography with ultraviolet detection. *J. Chromatogr. B Biomed. Sci. Appl.* 1997; 704: 259-263

[115]   Alvarez JC, Bothua D, Colignon I, Advenier C, Spreux-Varoquaux O. Determination of fluoxetine and its metabolite norfluoxetine in serum and brain areas using high-performance liquid chromatography with ultraviolet detection. *J. Chromatogr. B Biomed. Sci. Appl.* 1998; 707: 175-180

[116]   Meineke I, Schreeb K, Kress I, Gundert-Remy U. Routine measurement of fluoxetine and norfluoxetine by high-performance liquid chromatography with ultraviolet detection in patients under concomitant treatment with tricyclic antidepressants. *Ther. Drug Monit.* 1998; 20: 14-19

[117]   Molander P, Thomassen A, Kristoffersen L, Greibrokk T, Lundanes E. Simultaneous determination of citalopram, fluoxetine, paroxetine and their metabolites in plasma by temperature-programmed packed capillary liquid chromatography with on-column focusing of large injection volumes. *J. Chromatogr. B Analyt. Technol. Biomed. Life Sci.* 2002; 766: 77-87

[118]   Llerena A, Dorado P, Berecz R, Gonzalez A, Norberto MJ, de la Rubia A, Caceres M. Determination of fluoxetine and norfluoxetine in human plasma by high-performance liquid chromatography with ultraviolet detection in psychiatric patients. *J. Chromatogr. B Analyt. Technol. Biomed. Life Sci.* 2003; 783: 25-31

[119]   Li KM, Thompson MR, McGregor IS. Rapid quantitation of fluoxetine and norfluoxetine in serum by micro-disc solid-phase extraction with high-performance liquid chromatography-ultraviolet absorbance detection. *J. Chromatogr. B Analyt. Technol. Biomed. Life Sci.* 2004; 804: 319-326

[120]   Clausing P, Rushing LG, Newport GD, Bowyer JF. Determination of D-fenfluramine, D-norfenfluramine and fluoxetine in plasma, brain tissue and brain microdialysate using high-performance liquid chromatography after precolumn derivatization with dansyl chloride. *J. Chromatogr. B Biomed. Sci Appl.* 1997; 692: 419-426

[121]   Raggi MA, Mandrioli R, Casamenti G, Bugamelli F, Volterra V. Determination of fluoxetine and norfluoxetine in human plasma by high-pressure liquid chromatography with fluorescence detection. *J. Pharm. Biomed. Ana.I* 1998; 18: 193-199

[122]   Vlase L, Imre S, Leucuta S. Determination of fluoxetine and its N-desmethyl metabolite in human plasma by high-performance liquid chromatography. *Talanta* 2005; 66: 659-663

[123] Moraes MO, Lerner FE, Corso G, Bezzerra FAF, Moraes MEA, De Nucci G. Fluoxetine bioequivalence study: Quantification of fluoxetine and norfluoxetine by liquid chromatography coupled to mass spectrometry. *J. Clin. Pharmacol*. 1999; 39: 1053-1061

[124] Sutherland FCW, Badenhorst D, de Jager AD, Scanes T, Hundt HKL, Swart KJ, Hundt AF. Sensitive liquid chromatographic-tandem mass spectrometric method for the determination of fluoxetine and its primary active metabolite norfluoxetine in human plasma. *J. Chromatogr. A* 2001; 914: 45-51

[125] Li C, Ji ZH, Nan FJ, Shao QX, Liu P, Dai JY, Zhen J, Yuan H, Xu F, Cui J, Huang B, Zhang MY, Yu C. Liquid chromatography/tandem mass spectrometry for the determination of fluoxetine and its main active metabolite norfluoxetine in human plasma with deuterated fluoxetine as internal standard. *Rapid Commun. Mass Spectrom.* 2002; 16: 1844-1850

[126] Green R, Houghton R, Scarth J, Gregory C. Determination of fluoxetine and its major active metabolite norfluoxetine in human plasma by liquid chromatography-tandem mass spectrometry. *Chromatographia* 2002; 55: S133-S136

[127] Shen ZZ, Wang S, Bakhtiar R. Enantiomeric separation and quantification of fluoxetine (Prozac ®) in human plasma by liquid chromatography/tandem mass spectrometry using liquid-liquid extraction in 96-well plate format. *Rapid Commun. Mass Spectrom.* 2002; 16: 332-338

[128] Cheer SM, Figgitt DR. Spotlight on fluvoxamine in anxiety disorders in children and adolescents. *CNS Drugs* 2002; 16: 139-144

[129] Figgitt DP, McClellan KJ. Fluvoxamine - An updated review of its use in the management of adults with anxiety disorders. *Drugs* 2000; 60: 925-954

[130] Spigset O, Axelsson S, Norstrom A, Hagg S, Dahlqvist R. The major fluvoxamine metabolite in urine is formed by CYP2D6. *Eur. J. Clin. Pharmacol.* 2001; 57: 653-658

[131] Richelson E. Pharmacokinetic drug interactions of new antidepressants: a review of the effects on the metabolism of other drugs. *Mayo Clin. Proc.* 1997; 72: 835-847

[132] Carrasco JL, Sandner C. Clinical effects of pharmacological variations in selective serotonin reuptake inhibitors: an overview. *Int. J. Clin. Pract.* 2005; 59: 1428-1434

[133] Hartter S, Wetzel H, Hammes E, Torkzadeh M, Hiemke C. Serum concentrations of fluvoxamine and clinical effects - A prospective open clinical trial. *Pharmacopsychiatry* 1998; 31: 199-200

[134] Preskorn SH. Clinically relevant pharmacology of selective serotonin reuptake inhibitors - An overview with emphasis on pharmacokinetics and effects on oxidative drug metabolism. *Clin. Pharmacokinet.* 1997; 32: 1-21

[135] Devries MH, Raghoebar M, Mathlener IS, Vanharten J. Single and Multiple Oral Dose Fluvoxamine Kinetics in Young and Elderly Subjects. *Ther. Drug Monit.* 1992; 14: 493-498

[136] Vanharten J, Duchier J, Devissaguet JP, Vanbemmel P, Devries MH, Raghoebar M. Pharmacokinetics of fluvoxamine maleate in patients with liver-cirrhosis after single-dose oral-administration. *Clin. Pharmacokinet.* 1993; 24: 177-182

[137] Spigset O, Hagg S. Excretion of psychotropic drugs into breast milk - pharmacokinetic overview and therapeutic implications. *CNS Drugs* 1998; 9: 111-134

[138] Goodnick PJ. Pharmacokinetic optimization of therapy with newer antidepressants. *Clin. Pharmacokinet.* 1994; 27: 307-330

[139] Perucca E, Gatti G, Spina E. Clinical pharmacokinetics of fluvoxamine. *Clin. Pharmacokinet.* 1994; 27: 175-190

[140] Labat L, Deveaux M, Dallet P, Dubost JP. Separation of new antidepressants and their metabolites by micellar electrokinetic capillary chromatography. *J. Chromatogr. B Analyt. Technol. Biomed. Life Sci*. 2002; 773: 17-23

[141] Maurer HH, Bickeboeller-Friedrich J. Screening procedure for detection of antidepressants of the selective serotonin reuptake inhibitor type and their metabolites in urine as part of a modified systematic toxicological analysis procedure using cas chromatography-mass spectrometry. *J. Anal. Toxicol.* 2000; 24: 340-347

[142] Rotzinger S, Todd KG, Bourin M, Coutts RT, Baker GB. A rapid electron-capture gas chromatographic method for the quantification of fluvoxamine in brain tissue. *J. Pharmacol. Toxicol. Methods* 1997; 37: 129-133

[143] Hostetter AL, Stowe ZN, Cox M, Ritchie JC. A novel system for the determination of antidepressant concentrations in human breast milk. *Ther. Drug Monit.* 2004; 26: 47-52

[144] Hostetter A, Ritchie JC, Stowe ZN. Amniotic fluid and umbilical cord blood concentrations of antidepressants in three women. *Biol. Psychiatry* 2000; 48: 1032-1034

[145] Rodriguez J, Berzas JJ, Contento AM, Cabello MP. Capillary gas chromatographic determination of tamoxifen in the presence of a number of antidepressants in urine. *J. Sep. Sci.* 2003; 26: 915-922

[146] Bagli M, Rao ML, Sobanski T, Laux G. Determination of fluvoxamine and paroxetine in human serum with highperformance liquid chromatography and ultraviolet detection. *J. Liq. Chromatogr. Relat. Technol.* 1997; 20: 283-295

[147] Palego L, Marazziti D, Biondi L, Giannaccini G, Sarno N, Armani A, Lucacchini A, Cassano GB, Dell'Osso L. Simultaneous plasma level analysis of clomipramine, N-desmethylclomipramine, and fluvoxamine by reversed-phase liquid chromatography. *Ther. Drug Monit.* 2000; 22: 190-194

[148] Skibinski R, Misztal G, Olajossy M. High performance liquid chromatographic determination of fluvoxamine and paroxetine in plasma. *Chem. Analityczna* 2000; 45: 815-823

[149] Dallet P, Labat L, Richard M, Langlois MH, Dubost JP. A reversed-phase HPLC method development for the separation of new antidepressants. *J. Liq. Chromatogr. Relat. Technol.* 2002; 25: 101-111

[150] Ohkubo T, Shimoyama R, Otani K, Yoshida K, Higuchi H, Shimizu T. High-performance liquid chromatographic determination of fluvoxamine and fluvoxamino acid in human plasma. *Anal. Sci.* 2003; 19: 859-864

[151] Lucca A, Gentilini G, Lopez-Silva S, Soldarini A. Simultaneous determination of human plasma levels of four selective serotonin reuptake inhibitors by high-performance liquid chromatography. *Ther. Drug Monit.* 2000; 22: 271-276

[152] Higashi Y, Matsumura H, Fujii Y. Determination of fluvoxamine in rat plasma by HPLC with pre-column derivatization and fluorescence detection using 4-fluoro-7-nitro-2,1,3-benzoxadiazole. *Biomed. Chromatogr.* 2005; 19: 771-776

[153] Lamas JP, Salgado-Petinal C, Garcia-Jares C, Llompart M, Cela R, Gomez M. Solid-phase microextraction-gas chromatography-mass spectrometry for the analysis of selective serotonin reuptake inhibitors in environmental water. *J. Chromatogr. A* 2004; 1046: 241-247

[154]   Barri T, Jonsson JA. Supported liquid membrane work-up of blood plasma samples coupled on-line to liquid chromatographic determination of basic antidepressant drugs. *Chromatographia* 2004; 59: 161-165

[155]   Pinder RM, Brogden RN, Speight TM, Avery GS. Maprotiline - Review of Its Pharmacological Properties and Therapeutic Efficacy in Mental Depressive States. *Drugs* 1977; 13: 321-352

[156]   Brachtendorf L, Jetter A, Beckurts KT, Holscher AH, Fuhr U. Cytochrome P-450 enzymes contributing to demethylation of maprotiline in man. *Pharmacol. Toxicol.* 2002; 90: 144-149

[157]   Rotzinger S, Bourin M, Akimoto Y, Coutts RT, Baker GB. Metabolism of some "second"- and "fourth"-generation antidepressants: Iprindole, viloxazine, bupropion, mianserin, maprotiline, trazodone, nefazodone, and venlafaxine. *Cell. Mol. Neurobiol*. 1999; 19: 427-442

[158]   Drebit R, Baker GB, Dewhurst WG. Determination of Maprotiline and Desmethylmaprotiline in Plasma and Urine by Gas-Chromatography with Nitrogen Phosphorus Detection. *J. Chromatogr. B* 1988; 432: 334-339

[159]   Ulrich S, Martens J. Solid-phase microextraction with capillary gas-liquid chromatography and nitrogen-phosphorus selective detection for the assay of antidepressant drugs in human plasma *J. Chromatogr. B* 1997; 696 217-234

[160]   Keller T, Zollinger U. Gas chromatographic examination of postmortem specimens after maprotiline intoxication. *Forensic Sci. Int.* 1997; 88: 117-123

[161]   Bakkali A, Corta E, Ciria JI, Berrueta LA, Gallo B, Vicente F. Solid-phase extraction with liquid chromatography and ultraviolet detection for the assay of antidepressant drugs in human plasma. *Talanta* 1999; 49: 773-783

[162]   Oztunc A, Onal A, Erturk S. 7,7,8,8-Tetracyanoquinodimethane as a new derivatization reagent for high-performance liquid chromatography and thin-layer chromatography: rapid screening of plasma for some antidepressants. *J. Chromatogr. B* 2002; 774: 149-155

[163]   Aymard G, Livi P, Pham YT, Diquet B. Sensitive and rapid method for the simultaneous quantification of five antidepressants with their respective metabolites in plasma using high-performance liquid chromatography with diode-array detection. *J. Chromatogr. B* 1997; 700: 183-189

[164]   Waschgler R, Hubmann MR, Conca A, Moll W, Konig P. Simultaneous quantification of citalopram, clozapine, fluoxetine, norfluoxetine, maprotiline, desmethylmaprotiline and trazodone in human serum by HPLC analysis. *Int. J. Clin. Pharmacol. Ther.* 2002; 40: 554-559

[165]   Cakrt M, Buzinkaiova T, Polonsky J, Korinkova V. Spectrofluorimetric and isotachophoretic determination of maprotiline in human blood serum. *Electrophoresis* 2000; 21: 2834-2838

[166]   Eap CB, Yasui N, Kaneko S, Baumann P, Powell K, Otani K. Effects of carbamazepine coadministration on plasma concentrations of the enantiomers of mianserin and of its metabolites. *Ther. Drug Monit.* 1999; 21: 166-170

[167]   Otani K, Mihara K, Okada M, Tanaka O, Kaneko S, Fukushima Y. Prediction of plasma-concentrations of mianserin and desmethylmianserin at steady-state from those after an initial dose of mianserin. *Ther. Drug Monit.* 1993; 15: 118-121

[168]   Wakeling A. Efficacy and side-effects of mianserin, a tetracyclic anti-depressant. *Postgrad. Med. J*. 1983; 59: 229-231

[169]   Nawishy S, Hathway N, Turner P. Interactions of anticonvulsant drugs with mianserin and nomifensine. *Lancet* 1981; 2: 871-872

[170]   Eap CB, Powell K, Baumann P. Determination of the enantiomers of mianserin and its metabolites in plasma by capillary electrophoresis after liquid-liquid extraction and on-column sample preconcentration. *J. Chromatogr. Sci.* 1997; 35: 315-320

[171]   Tybring G, Otani K, Kaneko S, Mihara K, Fukushima Y, Bertilsson L. Enantioselective determination of mianserin and its desmethyl metabolite in plasma during treatment of depressed japanese patients. *Ther. Drug Monit.* 1995; 17: 516-521

[172]   Vink J, Vanhal HJM. Simplified method for determination of the tetracyclic anti-depressant mianserin in human-plasma using gas-chromatography with nitrogen detection. *J Chromatogr* 1980; 181: 25-31

[173]   Wong SHY, Waugh SW, Draz M, Jain N. Liquid-chromatographic determination of 2 antidepressants, trazodone and mianserin, in plasma. *Clin. Chem.* 1984; 30: 230-233

[174]   Hefnawy MM, Aboul-Enein HY. Fast high-performance liquid chromatographic analysis of mianserin and its metabolites in human plasma using monolithic silica column and solid phase extraction. *Anal. Chim. Acta* 2004; 504: 291-297

[175]   Wolf C, Schmid R. Liquid-chromatographic determination of mianserin in plasma by fluorescence detection after online photochemical-reaction. *J. Pharm. Biomed. Anal.* 1990; 8: 1059-1061

[176]   Chauhan B, Rani S, Guttikar S, Zope A, Jadon N, Padh H. Analytical method development and validation of mianserin hydrochloride and its metabolite in human plasma by LC-MS. *J. Chromatogr. B Analyt. Techno.l Biomed. Life Sci.* 2005; 823: 69-74

[177]   Brown LW, Hundt HKL, Swart KJ. Automated high-performance liquid-chromatographic method for the determination of mianserin in plasma using electrochemical detection. *J. Chromatogr.* 1992; 582: 268-272

[178]   Holm KJ, Markham A. Mirtazapine - A review of its use in major depression. *Drugs* 1999; 57: 607-631

[179]   Fawcett J, Barkin RL. Review of the results from clinical studies on the efficacy, safety and tolerability of mirtazapine for the treatment of patients with major depression. *J. Affect. Disord.* 1998; 51: 267-285

[180]   Timmer CJ, Sitsen JMA, Delbressine LP. Clinical pharmacokinetics of mirtazapine. *Clin. Pharmacokinet.* 2000; 38: 461-474

[181]   Grasmader K, Verwohlt PL, Kuhn KU, Frahnert C, Hiemke C, Dragicevic A, von Widdern O, Zobel A, Maier W, Rao ML. Relationship between mirtazapine dose, plasma concentration, response, and side effects in clinical practice. *Pharmacopsychiatry* 2005; 38: 113-117

[182]   Puzantian T. Mirtazapine, an antidepressant. *Am. J. Health Syst. Pharm.* 1998; 55: 44-49

[183]   Kasper S, PraschakRieder N, Tauscher J, Wolf R. A risk-benefit assessment of mirtazapine in the treatment of depression. *Drug Saf.* 1997; 17: 251-264

[184]   Ruwe FJL, Smulders RA, Kleijn HJ, Hartmans HLA, Sitsen JMA. Mirtazapine and paroxetine: a drug-drug interaction study in healthy subjects. *Hum. Psychopharmacol.* 2001; 16: 449-459

[185]   Sennef C, Timmer CJ, Sitsen JAA. Mirtazapine in combination with amitriptyline: a drug-drug interaction study in healthy subjects. *Hum. Psychopharmacol.* 2003; 18: 91-101

[186] Mandrioli R, Pucci V, Sabbioni C, Bartoletti C, Fanali S, Raggi MA. Enantioselective determination of the novel antidepressant mirtazapine and its active demethylated metabolite in human plasma by means of capillary electrophoresis. *J. Chromatogr. A* 2004; 1051: 253-260

[187] Romiguieres T, Pehourcq F, Matoga M, Begaud B, Jarry C. Determination of mirtazapine and its demethyl metabolite in plasma by high-performance liquid chromatography with ultraviolet detection. *J. Chromatogr. B Analyt. Technol. Biomed. Life Sci.* 2002; 775: 163-168

[188] Morgan PE, Tapper J, Spencer EP. Rapid and sensitive analysis of mirtazapine & normirtazapine in plasma/serum by HPLC with fluorescence detection. *J. Psychopharmacol*. 2002; 16: A64-A64

[189] Shams M, Hartter S, Hiemke C. Column switching and high performance liquid chromatography [HPLC] with fluorescence detection for automated analysis of venlafaxine, mirtazapine and demethylated metabolites in blood serum or plasma. *Pharmacopsychiatry* 2002; 35: X-X

[190] Ptacek P, Klima J, Macek J. Determination of mirtazapine in human plasma by liquid chromatography. *J. Chromatogr. B Analyt. Technol. Biomed. Life Sci* 2003; 794: 323-328

[191] Pistos C, Koutsopoulou M, Panderi I. A validated liquid chromatographic tandem mass spectrometric method for the determination of mirtazapine and demethylmirtazapine in human plasma: application to a pharmacokinetic study. *Anal. Chim. Acta* 2004; 514: 15-26

[192] Paus E, Jonzier-Perey M, Cochard N, Eap CB, Baumann P. Chirality in the new generation of antidepressants - Stereoselective analysis of the enantiomers of mirtazapine, N-demethylmirtazapine, and 8-hydroxymirtazapine by LC-MS. *Ther. Drug Monit.* 2004; 26: 366-374

[193] de Santana FJM, de Oliveira ARM, Bonato PS. Chiral liquid chromatographic determination of mirtazapine in human plasma using two-phase liquid-phase microextraction for sample preparation. *Anal. Chim. Acta* 2005; 549: 96-103

[194] Mandrioli R, Mercolini L, Ghedini N, Bartoletti C, Fanali S, Raggi MA. Determination of the antidepressant mirtazapine and its two main metabolites in human plasma by liquid chromatography with fluorescence detection. *Anal. Chim. Acta* 2006; 556: 281-288

[195] Paterson S, Cordero R, Burlinson S. Screening and semi-quantitative analysis of postmortem blood for basic drugs using gas chromatography/ion trap mass spectrometry. *J. Chromatogr. B Analyt. Technol. Biomed. Life Sci.* 2004; 813: 323-330

[196] Bickeboeller-Friedrich J, Maurer HH. Screening for detection of new antidepressants, neuroleptics, hypnotics, and their metabolites in urine by GC-MS developed using rat liver microsomes. *Ther. Drug Monit.* 2001; 23: 61-70

[197] Dodd S, Burrows GD, Norman TR. Chiral determination of mirtazapine in human blood plasma by high-performance liquid chromatography. *J Chromatogr B Biomed Sci Appl* 2000; 748: 439-443

[198] Wagstaff AJ, Cheer SM, Matheson AJ. Paroxetine: an update of its use in psychiatric disorders in adults (vol 62, pg 655, 2002). *Drugs* 2002; 62: 1461-1461

[199] Wagstaff AJ, Cheer SM, Matheson AJ, Ormrod D, Goa KL. Spotlight on paroxetine in psychiatric disorders in adults. *CNS Drugs* 2002; 16: 425-434

[200] Caley CF, Weber SS. Paroxetine- a selective reuptake inhibiting antidepressant. *Ann. Pharmacother.* 1993; 27: 1212-1222

[201]   Gunasekara NS, Noble S, Benfield P. Paroxetine - an update of its pharmacology and therapeutic use in depression and a review of its use in other disorders. *Drugs* 1998; 55: 85-120

[202]   Lai CT, Gordon ES, Kennedy SH, Bateson AN, Coutts RT, Baker GB. Determination of paroxetine levels in human plasma using gas chromatography with electron-capture detection. *J. Chromatogr. B Biomed. Sci. Appl.* 2000; 749: 275-279

[203]   Leis HJ, Windischhofer W, Raspotnig G, Fauler G. Stable isotope dilution negative ion chemical ionization gas chromatography-mass spectrometry for the quantitative analysis of paroxetine in human plasma. *J. Mass Spectrom.* 2001; 36: 923-928

[204]   Leis HJ, Windischhofer W, Fauler G. Improved sample, preparation for the quantitative analysis of paroxetine in human plasma by stable isotope dilution negative ion chemical ionisation gas chromatography-mass spectrometry. *J. Chromatogr. B Analyt. Technol. Biomed. Life Sci.* 2002; 779: 353-357

[205]   Foglia JP, Sorisio D, Kirshner M, Pollock BG. Quantitative determination of paroxetine in plasma by high-performance liquid chromatography and ultraviolet detection. *J. Chromatogr. B Biomed. Sci. Appl.* 1997; 693: 147-151

[206]   Zainaghi IA, Lanchote VL, Queiroz RHC. Determination of paroxetine in geriatric depression by high-performance liquid chromatography. *Pharmacol. Res.* 2003; 48: 217-221

[207]   Shin JG, Kim KA, Yoon YR, Cha IJ, Kim YH, Shin SG. Rapid simple high-performance liquid chromatographic determination of paroxetine in human plasma. *J. Chromatogr. B Biomed. Sci. Appl.* 1998; 713: 452-456

[208]   Lopez-Calull C, Dominguez N. Determination of paroxetine in plasma by high-performance liquid chromatography for bioequivalence studies. *J. Chromatogr. B Biomed. Sci. Appl.* 1999; 724: 393-398

[209]   Schatz DS, Saria A. Simultaneous determination of paroxetine, risperidone and 9-hydroxyrisperidone in human plasma by high-performance liquid chromatography with coulometric detection. *Pharmacology* 2000; 60: 51-56

[210]   Zhu ZM, Neirinck L. High-performance liquid chromatography-mass spectrometry method for the determination of paroxetine in human plasma. *J. Chromatogr. B Analyt. Technol. Biomed. Life Sci.* 2002; 780: 295-300

[211]   Segura M, Ortuno J, Farre M, Pacifici R, Pichini S, Joglar J, Segura J, de la Torre R. Quantitative determination of paroxetine and its 4-hydroxy-3-methoxy metabolite in plasma by high-performance liquid chromatography/electrospray ion trap mass spectrometry: application to pharmacokinetic studies. *Rapid Commun. Mass Spectrom.* 2003; 17: 1455-1461

[212]   Vivekanand VV, Kumar VR, Mohakhud PK, Reddy GO. Enantiomeric separation of the key intermediate of paroxetine using chiral chromatography. *J. Pharm. Biomed. Anal*. 2003; 33: 803-809

[213]   Weng ND, Eerkes A. Development and validation of a hydrophilic interaction liquid chromatography-tandem mass spectrometric method for the analysis of paroxetine in human plasma. *Biomed. Chromatogr*. 2004; 18: 28-36

[214]   Fleishaker JC. Clinical pharmacokinetics of reboxetine, a selective norepinephrine reuptake inhibitor for the treatment of patients with depression. *Clin. Pharmacokinet.* 2000; 39: 413-427

[215]   Hajos M, Fleishaker JC, Filipiak-Reisner JK, Brown MT, Wong EHF. The selective norepinephrine reuptake inhibitor antidepressant reboxetine: Pharmacological and clinical profile. *CNS Drug Rev.* 2004; 10: 23-44

[216]   Olver JS, Burrows GD, Norman TR. Third-generation antidepressants - Do they offer advantages over the SSRIs? *CNS Drugs* 2001; 15: 941-954

[217]   Versiani M. Reboxetine, the first selective noradrenaline reuptake inhibitor antidepressant: efficacy and tolerability in 2613 patients. *Int. J. Psychiat. Clin.* 2000; 4: 201-208

[218]   Gottweiss M, Hiemke C, Nenadic I, Wagner G, Kohler S, Schlosser R, Balogh A, Sauer H. Comparative study of reboxetine on CYP2D6 activity in patients and healthy volunteers. *Eur. J. Clin. Pharmacol.* 2005; 61: 706-707

[219]   Raggi MA, Mandrioli R, Casamenti G, Volterra V, Pinzauti S. Determination of reboxetine, a recent antidepressant drug, in human plasma by means of two high-performance liquid chromatography methods. *J. Chromatogr. A* 2002; 949: 23-33

[220]   Hartter S, Weigmann H, Hiemke C. Automated determination of reboxetine by high-performance liquid chromatography with column-switching and ultraviolet detection. *J. Chromatogr. B* 2000; 740: 135-140

[221]   Walters RR, Buist SC. Improved enantioselective method for the determination of the enantiomers of reboxetine in plasma by solid-phase extraction, chiral derivatization, and column-switching high-performance liquid chromatography with fluorescence detection. *J; Chromatogr. A* 1998; 828: 167-176

[222]   Frigerio E, Pianezzola E, Benedetti MS. Sensitive Procedure for the Determination of Reboxetine Enantiomers in Human Plasma by Reversed-Phase High-Performance Liquid-Chromatography with Fluorometric Detection after Chiral Derivatization with (+)-1-(9-Fluorenyl)Ethyl Chloroformate. *J. Chromatogr. A* 1994; 660: 351-358

[223]   Ohman D, Norlander B, Peterson C, Bengtsson F. Simultaneous determination of reboxetine and O-desethylreboxetine enantiomers using enantioselective reversed-phase high-performance liquid chromatography. *J. Chromatogr. A* 2002; 947: 247-254

[224]   Raggi MA, Mandrioli R, Sabbioni C, Parenti C, Cannazza G, Fanali S. Separation of reboxetine enantiomers by means of capillary electrophoresis. *Electrophoresis* 2002; 23: 1870-1877

[225]   DeVane CL, Liston HL, Markowitz JS. Clinical pharmacokinetics of sertraline. *Clin. Pharmacokinet.* 2002; 41: 1247-1266

[226]   Mauri MC, Laini V, Cerveri G, Scalvini ME, Volonteri LS, Regispani F, Malvini L, Manfre S, Boscati L, Panza G. Clinical outcome and tolerability of sertraline in major depression - A study with plasma levels. *Prog. Neuropsychopharmacol. Biol. Psychiatry* 2002; 26: 597-601

[227]   Lucangioli SE, Hermida LG, Tripodi VP, Rodriguez VG, Lopez EE, Rouge PD, Carducci CN. Analysis of cis-trans isomers and enantiomers of sertraline by cyclodextrin-modified micellar electrokinetic chromatography. *J. Chromatogr. A* 2000; 871: 207-215

[228]   Rogowsky D, Marr M, Long G, Moore C. Determination of sertraline and desmethylsertraline in human serum using copolymeric bonded-phase extraction, liquid-chromatography and gas-chromatography mass-spectrometry. *J. Chromatogr. B Biomed. Appl.* 1994; 655: 138-141

[229]   Eap CB, Bouchoux G, Amey M, Cochard N, Savary L, Baumann P. Simultaneous determination of human plasma levels of citalopram,

paroxetine, sertraline, and their metabolites by gas chromatography mass spectrometry. *J. Chromatogr. Sci.* 1998; 36: 365-371

[230] Kim KM, Jung BH, Choi MH, Woo JS, Paeng KJ, Chung BC. Rapid and sensitive determination of sertraline in human plasma using gas chromatography-mass spectrometry. *J. Chromatogr. B Analyt. Technol. Biomed. Life Sci.* 2002; 769: 333-339

[231] Casamenti G, Mandrioli R, Sabbioni C, Bugamelli F, Volterra V, Raggi MA. Development of an HPLC method for the toxicological screening of central nervous system drugs. *J. Liq. Chromatogr. Relat. Technol.* 2000; 23: 1039-1059

[232] Jain DS, Sanyal M, Subbaiah G, Pande UC, Shrivastav P. Rapid and sensitive method for the determination of sertraline in human plasma using liquid chromatography-tandem mass spectrometry (LC-MS/MS). *J. Chromatogr. B Analyt. Technol. Biomed. Life Sci.* 2005; 829: 69-74

[233] He LJ, Feng F, Wu J. Determination of sertraline in human plasma by high-performance liquid chromatography-electrospray ionization mass sprectrometry and method validation. *J. Chromatogr. Sci*. 2005; 43: 532-535

[234] Mir S, Taylor D. The adverse effects of antidepressants. *Curr. Opin. Psychiatr.* 1997; 10: 88-94

[235] Becker PM. Trazodone as a hypnotic in major depression. *Sleep Med.* 2004; 5: 7-8

[236] Saletu-Zyhlarz GM, Anderer P, Arnold O, Saletu B. Confirmation of the neurophysiologically predicted therapeutic effects of trazodone on its target symptoms depression, anxiety and insomnia by postmarketing clinical studies with a controlled-release formulation in depressed outpatients. *Neuropsychobiology* 2003; 48: 194-208

[237] Rotzinger S, Fang J, Coutts RT, Baker GB. Human CYP2D6 and metabolism of m-chlorophenylpiperazine. *Biol. Psychiatry* 1998; 44: 1185-1191

[238] Goeringer KE, Raymon L, Logan BK. Postmortem forensic toxicology of trazodone. *J. Forensic Sci.* 2000; 45: 850-856

[239] Suckow RF. A Simultaneous Determination of Trazodone and Its Metabolite 1-M-Chlorophenylpiperazine in Plasma by Liquid-Chromatography with Electrochemical Detection. *J. Liq. Chrom.* 1983; 6: 2195-2208

[240] Otani K, Mihara K, Yasui N, Ishida M, Kondo T, Tokinaga N, Ohkubo T, Osanai T, Sugawara K, Kaneko S. Plasma concentrations of trazodone and M-chlorophenylpiperazine at steady state can be predicted from those after an initial dose of trazodone. *Prog. Neuro-Psychopharmacol. Biol. Psychiatry* 1997; 21: 239-244

[241] Mihara K, Yasui-Furukori N, Kondo T, Ishida M, Ono S, Ohkubo T, Osanai T, Sugawara K, Otani K, Kaneko S. Relationship between plasma concentrations of trazodone and its active metabolite, m-chlorophenylpiperazine, and its clinical effect in depressed patients. *Ther. Drug Monit.* 2002; 24: 563-566

[242] Monteleone P, Gnocchi G, Delrio G. Plasma Trazodone Concentrations and Clinical-Response in Elderly Depressed-Patients - a Preliminary-Study. *J. Clin. Psychopharmacol.* 1989; 9: 284-287

[243] Prapotnik M, Waschgler R, Konig P, Moll W, Conca A. Therapeutic drug monitoring of trazodone: are there pharmacokinetic interactions involving citalopram and fluoxetine? *Int. J. Clin. Pharmacol. Ther*. 2004; 42: 120-124

[244] Mihara K, Kondo T, Suzuki A, Yasui-Furukori N, Ono S, Otani K, Kaneko S. Effects of genetic polymorphism of CYP1A2 inducibility on the steady-state

plasma concentrations of trazodone and its active metabolite m-chlorophenylpiperazine in depressed Japanese patients. *Pharmacol. Toxicol.* 2001; 88: 267-270

[245]   Brogden RN, Heel RC, Speight TM, Avery GS. Trazodone - a Review of Its Pharmacological Properties and Therapeutic Use in Depression and Anxiety. *Drugs* 1981; 21: 401-429

[246]   Mendelson WB. A review of the evidence for the efficacy and safety of Trazodone in insomnia. *J. Clin. Psychiatry* 2005; 66: 469-476

[247]   McCue RE, Joseph M. Venlafaxine- and trazodone-induced serotonin syndrome. *Am. J. Psychiat.* 2001; 158: 2088-2089

[248]   Adson DE, Erickson-Birkedahl S, Kotlyar M. An unusual presentation of sertraline and trazodone overdose. *Ann. Pharmacother.* 2001; 35: 1375-1377

[249]   Small NL, Giamonna KA. Interaction between warfarin and trazodone. *Ann. Pharmacother.* 2000; 34: 734-736

[250]   Greenblatt DJ, von Moltke LL, Harmatz JS, Fogelman SM, Chen GS, Graf JA, Mertzanis P, Byron S, Culm KE, Granda BW, Daily JP, Shader RI. Short-term exposure to low-dose ritonavir impairs clearance and enhances adverse effects of trazodone. *J. Clin. Pharmacol.* 2003; 43: 414-422

[251]   de Meester A, Carbutti G, Gabriel L, Jacques JM. Fatal overdose with trazodone: Case report and literature review. *Acta Clin. Belg.* 2001; 56: 258-261

[252]   Rifai N, Levtzow CB, Howlett CM, Parker NC, Phillips JC, Cross RE. The Determination of Trazodone by Capillary Column Gc with N-Selective Detection. *Clin. Chem.* 1988; 34: 1258-1258

[253]   Caccia S, Ballabio M, Fanelli R, Guiso G, Zanini MG. Determination of plasma and brain concentrations of trazodone and its metabolite, 1-m-chlorophenylpiperazine, by gas-liquid-chromatography. *J. Chromatogr.* 1981; 210: 311-318

[254]   Anderson WH, Archuleta MM. The capillary gas-chromatographic determination of trazodone in biological specimens. *J. Anal. Toxicol.* 1984; 8: 217-219

[255]   Waschgler R, Hubmann MR, Conca A, Moll W, Konig P. Simultaneous quantification of citalopram, clozapine, fluoxetine, norfluoxetine, maprotiline, desmethyl-maprotiline, and trazodone in human serum by HPLC analysis. *Pharmacopsychiatry* 2002; 35: XI-XI

[256]   Vatassery GT, Holden LA, Hazel DK, Dysken MW. Determination of trazodone and its metabolite, 1-m-chlorophenyl-piperazine, in human plasma and red blood cell samples by HPLC. *Clin. Biochem.* 1997; 30: 149-153

[257]   Ohkubo T, Osanai T, Sugawara K, Ishida M, Otani K, Mihara K, Yasui N. High-performance liquid-chromatographic determination of trazodone and 1-m-chlorophenylpiperazine with ultraviolet and electrochemical detector. *J. Pharm. Pharmacol.* 1995; 47: 340-344

[258]   Dorey RC, Narasimhachari N. HPLC analysis of the new antidepressants, amoxapine and trazodone. *Clin. Chem*. 1984; 30: 1035-1035

[259]   Mayol RF, Gammans RE, Labudde JA. Simultaneous determination in plasma of trazodone and its metabolite m-chlorophenylpiperazine using a new hplc method after single and multiple oral dosing in man. *J. Clin. Pharmacol.* 1984; 24: 406-406

[260]   Brown P, Tribby P. Analysis of trazodone by normal phase liquid-chromatography. *Clin. Chem.* 1990; 36: 1045-1045

[261]   Siek TJ. Determination of trazodone in serum by instrumental thin-layer chromatography. *J. Anal. Toxicol.* 1987; 11: 225-227

[262]   Roberge RJ, Luellen JR, Reed S. False-positive amphetamine screen following a trazodone overdose. *J. Toxicol. Clin. Toxicol.* 2001; 39: 181-182

[263]   Morton WA, Sonne SC, Verga MA. Venlafaxine - a structurally unique and novel antidepressant. *Ann. Pharmacother.* 1995; 29: 387-395

[264]   Reis M, Lundmark J, Bjork H, Bengtsson F. Therapeutic drug monitoring of racemic venlafaxine and its main metabolites in an everyday clinical setting. *Ther. Drug Monit.* 2002; 24: 545-553

[265]   Ereshefsky L, Dugan D. Review of the pharmacokinetics, pharmacogenetics, and drug interaction potential of antidepressants: Focus on venlafaxine. *Depress. Anxiety* 2000; 12: 30-44

[266]   Kirchheiner J, Brosen K, Dahl ML, Gram LF, Kasper S, Roots I, Sjoqvist F, Spina E, Brockmoller J. CYP2D6 and CYP2C19 genotype-based dose recommendations for antidepressants: a first step towards subpopulation-specific dosages. *Acta Psychiatr. Scand .*2001; 104: 173-192

[267]   Roseboom PH, Kalin NH. Neuropharmacology of venlafaxine. *Depress. Anxiety* 2000; 12: 20-29

[268]   Burnett FE, Dinan TG. Venlafaxine. Pharmacology and therapeutic potential in the treatment of depression. *Hum. Psychopharmacol.* 1998; 13: 153-162

[269]   Rudaz S, Calleri E, Geiser L, Cherkaoui S, Prat J, Veuthey JL. Infinite enantiomeric resolution of basic compounds using highly sulfated cyclodextrin as chiral selector in capillary electrophoresis. *Electrophoresis* 2003; 24: 2633-2641

[270]   Martinez MA, de la Torre CS, Almarza E. Simultaneous determination of viloxazine, venlafaxine, imipramine, desipramine, sertraline,and amoxapine in whole blood: comparison of two extraction/cleanup procedures for capillary gas chromatography with nitrogen-phosphorus detection. *J. Anal. Toxicol.* 2003; 27: 8A-8A

[271]   Martinez MA, de la Torre CS, Almarza E. Simultaneous determination of viloxazine, venlafaxine, imipramine, desipramine, sertraline, and amoxapine in whole blood: comparison of two extraction/cleanup procedures for capillary gas chromatography with nitrogen-phosphorus detection. *J. Anal. Toxicol.* 2002; 26: 296-302

[272]   Hicks DR, Wolaniuk D, Russell A, Cavanaugh N, Kraml M. A high-performance liquid-chromatographic method for the simultaneous determination of venlafaxine and O-desmethylvenlafaxine in biological-fluids. *Ther. Drug Monit.* 1994; 16: 100-107

[273]   Matoga M, Pehourcq F, Titier K, Dumora F, Jarry C. Rapid high-performance liquid chromatographic measurement of venlafaxine and O-desmethylvenlafaxine in human plasma - application to management of acute intoxications. *J. Chromatogr. B Biomed. Sci. Appl.* 2001; 760: 213-218

[274]   Raut BB, Kolte BL, Deo AA, Bagool MA, Shinde DB. A rapid and sensitive HPLC method for the determination of venlafaxine and O-desmethylvenlafaxine in human plasma with UV detection. *J. Liq. Chromatogr. Relat. Technol*. 2003; 26: 1297-1313

[275]   Waschgler R, Moll W, Konig P, Conca A. Quantification of venlafaxine and O-desmethylvenlafaxine in human serum using HPLC analysis. *Int. J. Clin. Pharmacol. Ther.* 2004; 42: 724-728

[276] Bhatt J, Jangid A, Venkatesh G, Subbaiah G, Singh S. Liquid chromatography-tandem mass spectrometry (LC-MS-MS) method for simultaneous determination of venlafaxine and its active metabolite O-desmethyl venlafaxine in human plasma. *J. Chromatogr. B Analyt. Technol. Biomed. Life Sci.* 2005; 829: 75-81

[277] Baker GB, Prior TI. Stereochemistry and drug efficacy and development: relevance of chirality to antidepressant and antipsychotic drugs. *Ann. Med.* 2002; 34: 537-543

[278] Greenwood DT. Viloxazine and Neurotransmitter Function. *Adv. Biochem. Psychopharmacol.* 1982; 31: 287-300

[279] Ban TA, McEvoy JP, Wilson WH. Viloxazine - a Review of the literature. *Int. Pharmacopsychiatry* 1980; 15: 118-123

[280] Altamura AC, Mauri MC, Guercetti G. Age, therapeutic milieu and clinical outcome in depressive patients treated with viloxazine - a study with plasma-levels. *Progr. Neuro. Psychopharmacol. Biol. Psychiatr.* 1986; 10: 67-75

[281] Maistrello I, Grassi G, Bertolino A, Valerio P, Pistollato G, Soverini S. Recognition of adverse drug-reactions in depressed-patients treated with viloxazine (Vicilan). *Adv. Biochem. Psychopharmacol.* 1982; 32: 369-373

[282] Fazio A, Crisafulli P, Primerano G, Dagostino AA, Oteri G, Pisani F. A sensitive gas-chromatographic assay for the determination of serum viloxazine concentration using a nitrogen phosphorus-selective detector. *Ther. Drug Monit.* 1984; 6: 484-488

[283] Groppi A, Papa P. One-step extraction procedure for gas-chromatographic determination of viloxazine as its acetyl derivative in human-plasma. *J. Chromatogr.* 1985; 337: 142-145

[284] Thomare P, Kergueris MF, Bourin M, Thomas L, Larousse C. Sensitive one-step extraction procedure for high-performance liquid-chromatographic determination of viloxazine in human plasma. *J. Chromatogr. B* 1990; 529: 494-499

[285] Kincaid RL, McMullin MM, Crookham SB, Rieders F. Report of a fluoxetine fatality. *J. Anal. Toxicol.* 1990; 14: 327-329

[286] Wenzel S, Aderjan R, Mattern R, Pedal I, Skopp G. Tissue distribution of mirtazapine and desmethylmirtazapine in a case of mirtazapine poisoning. *Forensic Sci. Int.* 2006; 156: 229-236

[287] Luchini D, Morabito G, Centini F. Case report of a fatal intoxication by citalopram. *Am. J. Forensic Med. Pathol.* 2005; 26: 352-354

[288] Rogde S, Hilberg T, Teige B. Fatal combined intoxication with new antidepressants. Human cases and an experimetnal study of postmortem moclobemide redistribution. *Forensic Sci. Int.* 1999; 100: 109-116

[289] Singer PP, Jones GR. An uncommon fatalilty due to moclobemide and paroxetine. *J. Anal. Toxicol.* 1997; 21: 518-520

[290] McIntyre IM, King VK, Staikos V, Gall J, Drummer OH. A fatality involving moclobeemide, sertraline, and pimozide. *J. Forensic Sci.* 1997; 42: 951-953

[291] Stimpfl T, Reichel S. Distribution of drugs of abuse with specific regions of the human brain. *Forensic Sci Int.* 2007; 170: 179-182

[292] Musshoff F, Madea B. Analytical pitfalls in hair testing. *Anal Bioanal Chem.* 2007; 388: 1475-1494

[293]   Pragst F, Balikova MA. State of the art in hair analysis for detection of drug and alcohol abuse. *Clin. Chim Acta*. 2006; 370: 17-49

Chapter II

Objectives

New generation antidepressants are highly prescribed drugs worldwide. Moreover, the use of antidepressant drugs will still increase as this mental disorder will become the second leading contributor to the global burden of disease, calculated for all ages and both sexes by the year 2020 according to the World Health Organization. As a result, analytical methods for the determination of new generation antidepressants gain more and more importance in the clinical and forensic field.

The general aim of this thesis was to develop and validate a gas chromatographic-mass spectrometric method for the simultaneous identification and quantification of new generation antidepressants and their metabolites in biological matrices. This method must be sensitive and straightforward, in such a manner that application in a routine laboratory can be easily performed. In addition, the method had to be useful for clinical as well as forensic applications. Therefore, the method was adapted for several matrices such as plasma, whole blood, brain tissue, and hair.

A second aim was to evaluate the applicability of the developed method for therapeutic drug monitoring of depressed patients. Individually guided dosing of antidepressants is not routinely applied in psychiatric clinics, but can be interesting in special patient populations which do not seem to benefit from antidepressant therapy. For these patients, a preliminary study was set-up to determine the link between the antidepressant/metabolite ratio in plasma, the metabolization profile of the individual patient and the final outcome of the antidepressant therapy.

The last aim of this thesis was to evaluate the usefulness of the gas chromatographic-mass spectrometric antidepressant determination method for forensic purposes. Although, new generation antidepressants are considered as less toxic (as compared to tricyclic antidepressants), they are often co-administered with other drugs which can result in interactions. Matrices such as blood and hair from forensic cases were analyzed to determine the antidepressant concentrations and the time of antidepressant use. In addition, brain concentrations were also measured as the brain is the target of antidepressant treatment.

Chapter III

Sample preparation:
Development and optimization of a solid phase
extraction procedure for several biological
matrices

III.1. Introduction

An important step in the development of an analytical method is the extraction of the compounds of interest from the biological matrix as this will have implications on the overall sensitivity and selectivity of the method. Sample preparation will not only lead to highly concentrated extracts, but can remove potential interfering matrix compounds, resulting in enhanced selectivity and a more reproducible method independent of variations in the sample matrix. Conventionally, liquid-liquid and solid-phase extraction methods (LLE and SPE) are chosen.

In liquid-liquid extraction the objective is to transfer the desired solutes from one liquid solution to another nonmiscible liquid. Liquid-liquid extraction is still frequently used in analytical toxicology, especially for (urgent) screening purposes when analysis of a wide range of (unknown) compounds instead of a target analysis is aimed. In addition, development of a LLE procedure is less time-consuming. The standard procedure for extracting antidepressants (ADs) is based on a LLE after alkalinization (pH ±9) with potassium borate or hydroxide, sodium carbonate, or sodium hydroxide. A variety of organic solvents is used such as heptane-isoamylalcohol, n-butyl chloride, diethyl ether or n-heptane-ethylacetate [1-9]. Sometimes a back extraction under acidic conditions (HCl) is applied, followed by a direct injection on the HPLC system [5, 7]. For GC-purposes, the ADs are extracted as above followed by an additional extraction step into an organic solvent after alkalinization [4, 6]. The back extraction technique leads to better removal of interfering compounds such as cholesterol, but for GC-MS the different extraction steps lead to loss of ADs, due to incomplete recovery. Thus, sensitivity is reduced and leads to detection problems for several ADs even in their therapeutic range. In addition, LLE is labourous, requires high-purity solvents and can result in the formation of emulsions with incomplete phase separation, the latter leading to impure extracts. Moreover, safe disposal of toxic solvents may be problematic and expensive [10].

Solid phase extraction (SPE) extracts and concentrates analytes from a liquid matrix by partitioning these analytes between a solid and a liquid phase. SPE aims to remove interfering compounds and to concentrate the analytes, with

good recovery and reproducible results. In addition, it should facilitate the rapid and efficient simultaneous processing of multiple samples [11]. SPE also has disadvantages including the cost of SPE material and the labourous optimization of the procedure. A SPE procedure consists of four consecutive steps: column conditioning, sample loading, column washing and elution of the compounds. When developing such procedure, suitable sorbent material, washing and eluting solvents have to be selected, according to the characteristics of the analytes and the matrix, and of the purpose of the analysis (screening or target analysis).

III.2. Experimental

III.2.1. Reagents

Venlafaxine.HCl and O-desmethylvenlafaxine maleate (ODMV) were kindly provided by Wyeth (New York, NY, USA). Mianserin.HCl, desmethyl-mianserin.HCl (DMMia), mirtazapine and desmethylmirtazapine maleate (DMMir) were a gift from Organon (Oss, The Netherlands). Sertraline.HCl, desmethylsertraline maleate (DMSer) and reboxetine methanesulphonate were a gift from Pfizer (Groton, CT, USA). Citalopram.HBr, desmethyl-citalopram.HCl (DMC), didesmethylcitalopram tartrate (DDMC), and melitracen.HCl were kindly provided by Lundbeck (Valby, Denmark). ACRAF (Roma, Italy) donated trazodone.HCl and its metabolite m-chlorophenyl-piperazine.HCl (m-cpp), while paroxetine.HCl hemihydrate was donated by GlaxoSmithKline (Erembodegem, Belgium). Viloxazine.HCl was a kind gift from AstraZeneca (Brussels, Belgium). Novartis Pharma (Basel, Switzerland) donated maprotiline.HCl and desmethylmaprotiline (DMMap). Fluvoxamine maleate was donated by Solvay Pharmaceuticals (Weesp, The Netherlands). Fluoxetine.HCl and desmethylfluoxetine.HCl (DMFluox) were purchased from Sigma-Aldrich (Steinheim, Germany).

Methanol, acetonitrile and water were all of HPLC-grade (Merck, Darmstadt, Germany). Ammonia-solution 25%, orthophosphoric acid (85%), NaOH (5 M), glycine and sodium dihydrogen phosphate monohydrate were also from Merck. Formic acid was purchased from Riedel-de Haën (Seelze, Germany). Phosphate buffer (25 mM) pH 2.5 was made by adding approximately 6.7 g

of $NaH_2PO_4.H_2O$ to 2.7 l of HPLC-water and adjusting the pH by adding phosphoric acid. The phosphate buffer (25 mM) pH 6.5 was made by dissolving 2.8 g in 1 l of HPLC-grade water and adjusting the pH with 5 M NaOH. The glycine HCl-buffer was made by adding 4.1 ml 0.2 M HCl to 50 ml of 0.1-M glycine solution (0.75 g/100 ml) and then diluting with water till 100 ml.

Fluoxetine-d_6 oxalate (Fd_6), mianserin-d_3 (Md_3) and paroxetine-d_6 maleate (Pd_6) (100 µg/ml MeOH) were purchased from Promochem (Molsheim, France) and were used as internal standards. Toluene (Suprasolv quality, Merck, Darmstadt, Germany) and 1- (heptafluorobutyryl) imidazole (HFBI) (Fluka, Bornem, Belgium) were applied for derivatization. Vials, glass inserts and viton crimp-caps were purchased from Agilent technologies (Avondale, PA, USA).

Blood was taken from healthy volunteers in dipotassium EDTA Vacutainers (Novolab, Geraardsbergen, Belgium). If plasma had to be obtained, the tubes were centrifuged at 1200 *g* for 10 minutes within 2 hours of the blood collection. After the plasma was removed, it was stored at -20°C. Drug-free hair was obtained from volunteers. Drug-free post-mortem brain tissue was obtained from the department of forensic medicine (Ghent University, Belgium).

III.2.2. Stock solutions

Stock solutions were prepared in methanol at a concentration of 1 mg/ml for each compound individually and stored at -20°C. Two mixtures of compounds were made due to the overlap of some compounds in the HPLC-method. Mixture 1 contained DMMir, ODMV, DMC, DDMC, reboxetine, paroxetine, maprotiline, fluoxetine, DMFluox and m-cpp. Mixture 2 contained mirtazapine, viloxazine, DMMia, citalopram, mianserin, fluvoxamine, DMSer, sertraline, melitracen, venlafaxine and trazodone. During the SPE development, a concentration of 1 µg/ml of each ADs was spiked in 1 ml HPLC-grade water.

For the protein binding disruption test, the same mixtures as for the SPE method development were used, but the compounds were spiked in therapeutic concentrations. A mixture of 100 ng DMMir, 150 ng ODMV, 30 ng DMC, 10 ng DDMC, 80 ng reboxetine, 75 ng paroxetine, 125 ng maprotiline, 250 ng fluoxetine, 500 ng DMFluox and 10 ng m-cpp (mixture 1) or a mixture of 100 ng mirtazapine, 100 ng viloxazine, 20 ng DMMia, 100 ng citalopram, 35 ng mianserin, 125 ng fluvoxamine, 125 ng DMSer , 125 ng sertraline, 50 ng melitracen, 375 ng venlafaxine and 100 ng trazodone (mixture 2) was spiked to 1 ml of plasma by evaporating the mixtures at 40°C with nitrogen and adding the plasma afterwards.

For the GC-MS experiments, a standard mixture was obtained by mixing the individual primary stock solutions and by further diluting with methanol until a concentration of 0.05 – 0.125 mg/ml, depending on the therapeutic range of the compound. After preparation, it was stored protected from light at approximately -20°C. Further dilution of the standard mixture with methanol resulted in working solutions with concentrations of 0.1, 1 or 10 μg/ml. Primary stock solutions of the internal standards (I.S.) fluoxetine-d_6, mianserin-d_3 and paroxetine-d_6 were prepared in methanol at a concentration of 10 μg/ml and were stored protected from light at 4°C. Twenty μl of each I.S. solution were spiked to 1 ml of plasma.

III.2.3. Mixer, sonicator, vacuum manifold, evaporator, and centrifuge

An Ultra Turrax mixer IKA T18 basic (Staufen, Germany) was used to homogenize the tissue samples. Sonication of samples was done using a 'Brandson 1510' (Brandson UL Transonics corporation, Danbury, CT, USA). A Visiprep TM Disposable liner vacuum manifold (Supelco, Bornem, Belgium) controlled the flow during the solid phase extraction procedure. Evaporation under nitrogen was conducted in a TurboVap LV evaporator from Zymark (Hopkinton, MA, USA). The centrifuge was a Mistral MSE 200 BRS (Drogenbos, Belgium).

III.2.4. High Pressure Liquid Chromatography (HPLC)

A LaChrom Elite HPLC (Merck-Hitachi, Darmstadt, Germany), consisting of a L2100 micro-pump, a L2200 autosampler, a L2300 column oven and a L2450 DAD, was used to monitor the SPE optimization and the protein binding disruption test. A LiChroCART 4-4 guard column combined with a C18 endcapped Purospher Star (Merck, Darmstadt, Germany) LiChroCART 125-3 (5 µm) column was used. The oven was set at 40 °C and the gradient run started at 85% phosphate buffer (25 mM, pH 2.5) and 15 % acetonitrile. At 20 minutes the organic phase contribution was 40 %, and at 25 minutes 50 %. From 25.1 until 35 minutes the column equilibrated under starting conditions. The flow rate of the mobile phase was held at 0.5 ml/min. The DAD measured from 210 till 380 nm and the chromatograms were integrated at 220 nm, except for mirtazapine and desmethylmirtazapine (300 nm). Aqueous solutions (wash solutions) were injected directly into the HPLC, while organic solvents (eluent) was evaporated to dryness under nitrogen at 40 °C and redissolved in 0.5 ml of the acetonitrile (15 %)-phosphate buffer mixture. A 50-µl aliquot was injected on the HPLC-column.

III.2.5. Gas chromatography – Mass spectrometry (GC-MS)

A HP 6890 GC system was used, equipped with a HP 5973 mass selective detector, a HP 7683 split/splitless auto injector and a G1701DA Chem Station, version D.02.00 data processing unit (Agilent Technologies, Avondale, PA, USA).

Chromatographic separation was achieved on a 30m x 0.25mm I.D., 0.25-µm J&W-5ms column from Agilent Technologies (Avondale, PA, USA). The initial column temperature was set at 90°C for 1 min, ramped at 50°C/min to 180°C where it was held for 10 min, whereafter the temperature was ramped again at 10°C/min to 300°C.

The pulsed splitless injection temperature was held at 300°C while purge time and injection pulse time were set at 1 and 1.5 min, respectively. Meanwhile, the injection pulse pressure was 170 kPa and 1 µl of the sample,

resolved in 50 µl of toluene, was injected. Ultrapure Helium with a constant flow of 1.3 ml/min was used as carrier gas.

The mass selective detector temperature conditions were 230°C for the EI-source, 150°C for the quadrupole and 300°C for the transferline, whereas an electron voltage of 70 eV was used. The spectra were monitored in selected ion monitoring (SIM) mode for quantification (Table III.1.).

Table III.1. Monitored ions in SIM mode

The use of internal standards fluoxetine-d_6, mianserin-d_3, paroxetine-d_6 are indicated by 1, 2, and 3, respectively.

Compounds	M-ion	M-ion HFB	EI		
			Quant	ion 1	ion 2
Venlafaxine 2	277	259	58	259	121
m-cpp 1	196	392	392	166	394
Viloxazine 1	237	433	433	240	296
DMFluox 1	295	491	330	117	226
Fluvoxamine 1	318	514	258	240	514
ODMV 2	263	441	58	245	
Fluoxetine 1	309	505	344	117	486
Fluoxetine-d_6	315	511	350	123	492
Mianserin 2	264	264	264	193	220
Mianserin-d_3	267	267	267	193	220
Mirtazapine 2	265	265	195	208	265
Melitracen 2	291	291	58	202	291
DMMia 2	250	446	446	193	249
DMSer 3	291	487	274	487	489
DMMir 2	251	447	447	250	195
Reboxetine 3	313	509	371	138	509
Citalopram 3	324	324	58	238	324
DMMap 3	263	459	431	191	459
Maprotiline 3	277	473	445	191	473
Sertraline 3	305	501	274	501	503
DDMC 3	296	492	238	208	474
DMC 3	310	506	238	208	488
Paroxetine 3	329	525	525	138	388
Paroxetine-d_6	332	531	531	138	394
Trazodone	371	371	205	371	356

For the GC-MS method the ADs had to be derivatized after SPE. Thus, after evaporation of the solid phase extracts under nitrogen at 40°C, 50 µl of HFBI was added and the sample was heated at 85°C for 30 min. Thereafter, 0.5 ml of HPLC-water and 2 ml of toluene were added. After vortexing and centrifuging the sample at 1121 *g* for 10 min, the toluene layer was transferred and evaporated at 40°C [12]. The evaporated extract was resolved in 50 µl of toluene.

III.3. Solid phase extraction development

The development of a solid phase extraction for new generation ADs is described in the first section of this chapter. In the second part, the developed method was optimized for different matrices. The method was developed by extracting AD spiked water samples, using a high pressure liquid chromatographic method with diode array detection (HPLC-DAD) as monitoring technique. The advantage of this monitoring technique is the ability to analyze aqueous phases without a drying or extraction step. In addition, no derivatization was necessary. Thus, the choice of sorbent, the conditioning step, loading step, washing and eluting step were optimized using HPLC. However, during the initial development procedure, we always considered the implications of our choice for the final gas chromatographic-mass spectrometric (GC-MS) method.

III.3.1. Choice of SPE sorbent

There is a range of SPE sorbents, all with different kinds of interactions occurring between the analytes of interest and the active sites on the sorbent [10]. These interactions include both hydrophobic interactions such as Van Der Waals forces and hydrophilic interactions such as dipole-dipole, induced dipole-dipole, hydrogen bonding and π-π interaction. Other mechanisms include electrostatic attractions between charged groups on the compound and on the sorbent surface, as well as molecular recognition mechanisms [13]. The SPE sorbents that involve only one of the above interactions are reversed phase, normal phase, ion-exchange, immuno-affinity and molecularly imprinted polymers, while mixed modes combine several interaction mechanisms.

The choice of the interaction mode depends on the demands of the method such as screening or target analysis, the aimed sensitivity, and final composition of the extract (organic or aqueous (GC versus HPLC)). Not only the chemical characteristics of the functional groups on the sorbent are relevant, but also the characteristics of the back-bones on which these functional groups are attached. These back-bones are either silica-or polymer based. The silica-based sorbents have a large variation of functional groups

available, are relatively inexpensive and are stable within a pH range of approximately 2 to 7.5. The polymer-sorbents (styrene-divinylbenzene) are more hydrophobic, more retentive and stable within a pH range of 0 to 14.

The tested SPE sorbents were selected because of their potential interaction with the ADs. Four different categories of SPE sorbents were selected. The *silica based apolar sorbents* (reversed phase sorbents) are tested as they extract rather apolar compounds from polar matrices such as plasma, using hydrophobic interaction mechanisms. The apolar sorbents studied were Bond Elut C_{18} (200 mg tubes, Varian, Middelburg, The Netherlands), Empore HD C_8 (6 ml, 10 nm, Chrompack-Varian, Middelburg, The Netherlands) and RP-select B Lichrolut (200 mg tubes, Merck, Darmstadt, Germany). *Polymeric sorbents* were of interest because of their combined polar and apolar properties. They do not always require a conditioning step and are able to extract analytes over a large polarity range. Therefore, they could lead to a better extraction of the more polar metabolites in combination with the ADs. The SPE-tubes Focus (50 mg, Varian), Strata X (200 mg, Phenomenex, Bester, Amstelveen, The Netherlands) and Oasis HLB (200 mg, Waters, Milford, MA, USA) were selected. *Ion-exchange sorbents* were selected as they focus on ionic interactions between the analytes of interest and the functional groups on the sorbent. Based on this mechanism, the positively charged ADs can be extracted from a biological matrix using a cation exchange sorbent. When using a cation exchange mode, the choice between a weak (carboxylic acid with pKa 4.8) or a strong cation exchanger (sulphonic acid with pKa <1) can be made. The strong and weak cation exchangers (200 mg) from Phenomenex were evaluated as ion-exchange sorbents. Cerify Bond Elut (130 mg, Varian) and Strata XC (200 mg, Phenomenex) were two *mixed modes* combining cation-exchange properties with, respectively, a hydrophobic C_8 phase or a styrene-divinylbenzene polymer.

The choice of sorbent depends on the ability to have a selective, high and reproducible retention of the ADs. In addition, the ease of use in combination with the final chromatographic technique, thus GC-MS, is essential.

Figure III.1. Decision scheme for the SPE development
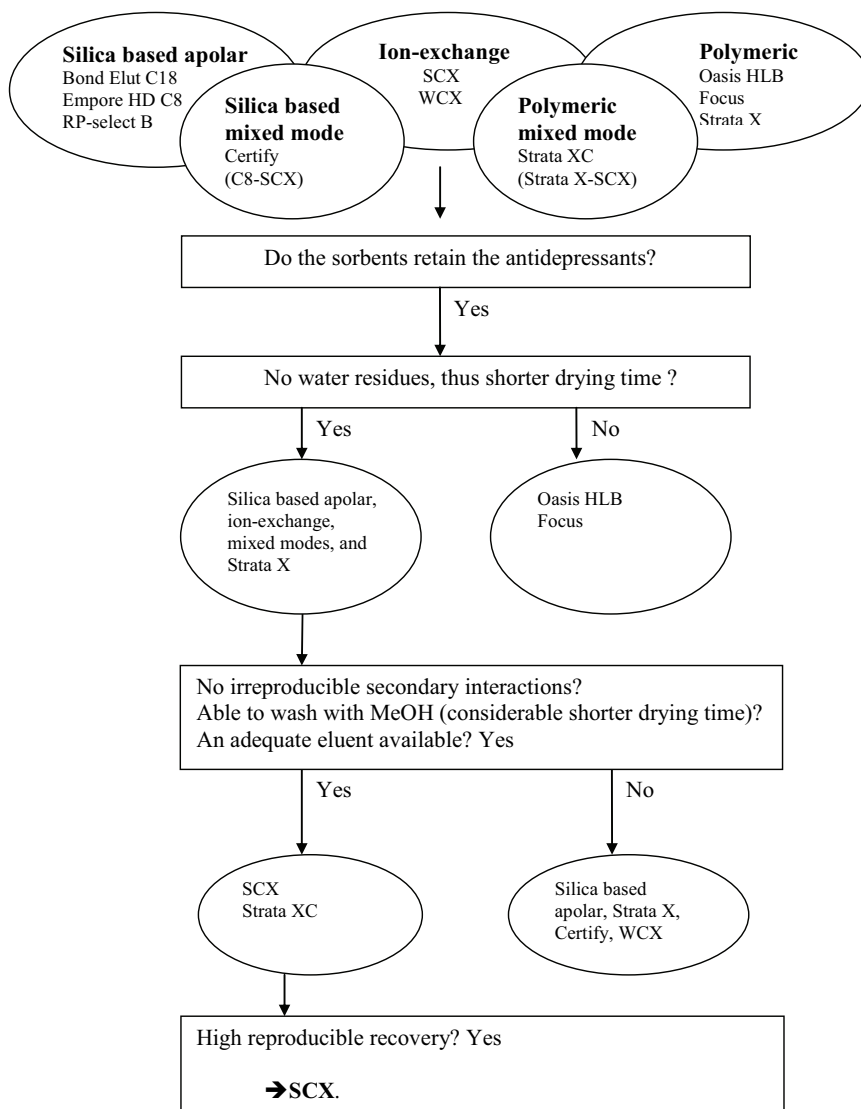
The decision scheme in Figure III.1. was used to select the best SPE sorbent for our purposes. The retention onto the SPE sorbents was examined first. Water samples, spiked with 1 µg/ml of each AD, were loaded onto the conditioned columns. Then 2 ml of HPLC-grade water was loaded to wash the column. The wash solution was collected and analyzed by HPLC. In addition, the compounds were eluted with methanol-2% formic acid or methanol-5% ammonia for the SCX and Strata XC phase. The eluent was analyzed to

evaluate the retention onto the column. The eluent was evaporated under nitrogen at 40 °C and redissolved in 1 ml of the mobile phase (starting conditions) of the HPLC. Fifty µl of this extract was injected onto the HPLC.

All sorbents retained the ADs, however, two of the polymeric sorbents (Focus and Oasis HLB) also retained a lot of water, probably due to their hydrophilic character. This necessitates a longer drying step, especially if gas chromatography is used as the final analytical method, because derivatization requires moisture free extracts [11, 14]. Therefore, these two phases were not used for further experiments. Because all sorbents retained the ADs very well, the further selection of sorbents was done during the optimization of the loading, washing and eluting conditions. As shown in Figure III.1. several findings during optimization of the SPE method (discussed in paragraph III.3.2) lead to the conclusion that the strong-cation exchangers gave the best results.

III.3.2. Choice of loading, washing and eluting conditions

Before loading the sample onto a SPE sorbent, a *conditioning step* is necessary for reproducible interaction with the compounds. This conditioning step consists of solvation of the SPE sorbent with methanol and the same aqueous solution as in the loading step to ensure the same environment during sample load. Before conditioning, the final eluent was passed through the column, to elute possible contaminants of the column. Thus, the column was conditioned with 3 ml of eluent, 2 ml of methanol, followed by 3 ml aqueous solution.

The *loading conditions* were optimized according to the SPE sorbent. When loading the samples on the silica based apolar phases, three different pH values were used. The ADs were spiked (1 µg/ml) in HPLC-grade water, in a water-formic acid mixture with pH 2.89 or a water-ammonia mixture with pH of 10.80. For the C_{18}, C_8 and RP Select B, a slight difference was observed in retention at different pH's. Silica based apolair sorbents may still contain a limited number of unreacted or 'free' silanols. These silanols provide polar, acidic patches on the column surface capable of binding amines through hydrogen bonding and cation exchange mechanisms. Since the ionization of

the ADs depends on the loading conditions, interactions with these residual silanols may cause an enhanced retention. These secondary interactions could be interesting, but are not reproducible as the degree of endcapping, and thus the number of free silanol functions can change from batch to batch. When evaluating ion-exchange phases, the pH during the loading and eluting step is again very important. For these sorbents a phosphate buffer with pH 6.5 or 2.5 was used to load and retain the compounds onto the sorbent. The pH during the loading step should be two pH units lower than the pKa of the compounds and two pH units higher than the sorbent. At this pH, approximately 99% of the groups are charged. A loading pH of 6.5 or 2.5 was chosen, according to the choice of a weak cation- (carboxyl pKa is 4.8) or a strong cation exchanger (sulphonic acid pKa < 1). Especially for trazodone and mirtazapine, a loading pH of 2.5 resulted to a better retention onto the strong cation exchanger (SCX).

A *wash step* was introduced and optimized to elute as much as possible interfering matrix compounds, without eluting the ADs. Methanol/water (50/50, 70/30, 90/10, by vol.) and pure methanol were tested by washing with 5 ml after sample load. The washing solvent, as well as the elution solvent were analyzed. While pure methanol eluted several compounds (especially trazodone) from the C_{18}, C_8, RP Select B, WCX, Certify and Strata X sorbents, it did not elute any compound from the strong ion-exchangers. Certify is a mixed mode of C_8 and a strong cation exchanger, however, methanol did elute ADs from the sorbent, perhaps because of the slightly lower bed mass and the higher contribution of apolar processes as compared to ion-exchange mechanisms. The WCX, in contrast to the strong cation exchangers, gave a slight elution of some compounds, probably because the ionic interaction of the sorbent with the ADs is weaker (Figure III.2.A). The use of pure organic solvents for washing is interesting as it shortens the drying time before elution and leads to clean and moisture free extracts.

Several possibilities for *eluting* the compounds were also studied. Conditioning and loading of the samples were done as described above. After drying, two times 1.2 ml (5 bed volumes) of eluent were added, collected separately and analyzed. The tested eluting solvents were pure methanol, methanol-2% formic acid, methanol-2% ammonia and methanol-5%

ammonia. A fast, reproducible elution with a limited volume of solvent is the most interesting. Therefore, it is advantageous if elution happens with the first 1.2 ml of the eluent. Methanol-2% formic acid and methanol with 2% ammonia gave good results for most of the sorbents. For the strong cation exchangers 5% ammonia in methanol gave the highest elution within 5 bedvolumes (Figure III.2.B). Methanol-acid and methanol-base work on the secondary interactions of the silica based phases. Under acidic conditions the silanol functions are not charged, while under basic conditions the ADs are not. For the strong cation exchangers acidic conditions were not successful, as even at low pH the sulphonic groups remain negatively charged.

Figure III.2. Comparison of washing (A) and eluting (B) conditions for the SPE sorbents

A
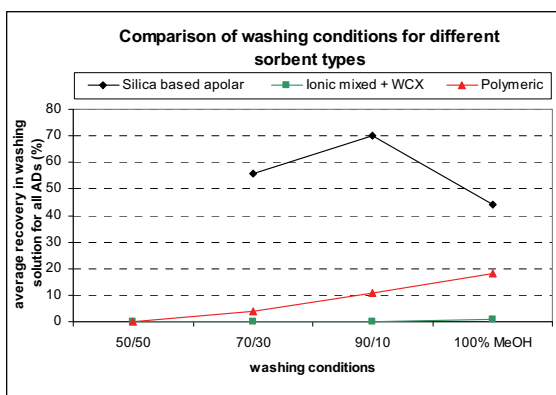
B
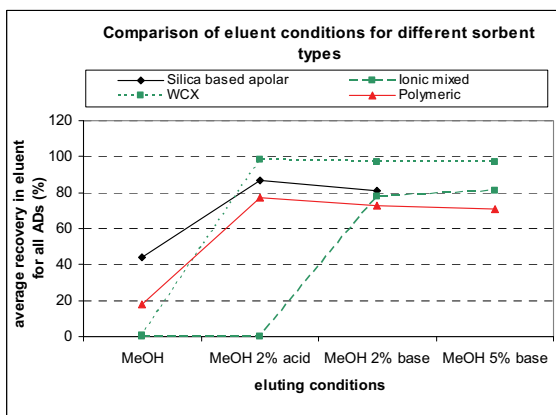
III.3.3. Final SPE method of ADs spiked in water samples

During the optimization of the loading, washing and eluting conditions, a final selection of the most useful SPE sorbent was made (Figure III.1.). Consequently, SPE tubes that retained water, SPE tubes that had irreproducible secondary interactions (silica based) and/or loss of compounds during the methanol wash were all left out for further investigation. Only the SCX and Strata XC sorbent were selected. Because the 'new' generation ADs have an amine-function a cation exchange mechanism was plausible. Retention on both the SCX and Strata XC phases is based on this mechanism, but Strata XC being a mixed-mode phase combining ion-exchange and a styrene-divinylbenzene polymer, shows hydrophobic and aromatic interactions as well. Combining different interaction mechanisms can be interesting to extract a variety of compounds, but can also lead to co-extraction of matrix compounds that are not of interest, leading to higher background in the final analysis.

Table III.2. Recovery of ADs by a strong cation exchanger (SCX) or Strata XC from water samples as determined by HPLC-DAD

Recovery %								
Compound	SCX	Strata XC	Compound	SCX	Strata XC	Compound	SCX	Strata XC
Venlafaxine	105	100	Mianserin	91	81	Citalopram	90	82
m-cpp	115	105	Mirtazapine			Maprotiline	92	78
Viloxazine	85	67	Melitracen	88	80	Sertraline	84	73
DMFluox	103	121	DMMia	87	75	DDMC	97	65
Fluvoxamine	93	87	DMSer	86	68	DMC	96	92
ODMV	108	94	DMMir			Paroxetine	90	84
Fluoxetine	89	94	Reboxetine	98	96	Trazodone	83	81

The recoveries for both columns were high and comparable as demonstrated in Table III.2. However, the recoveries were slightly, but constantly lower using Strata XC as compared to SCX. This result was also confirmed when analyzing plasma samples (n=5) by GC-MS using the two SPE tubes as described in our publication about the development of this solid phase extraction [12]. Perhaps, the difference in recoveries can be explained due to the domination of the ion-exchange mechanism on the retention. When using a mixed-mode, the ion-exchange groups are less numerous. On the other hand, methanol is not a good disruptor of hydrophobic and dipolar

interactions [15]. Therefore, a small percentage of acetonitrile in the methanol-ammonia eluent would probably neutralize these non-ionic interactions during elution, leading to enhanced recovery yields for the Strata XC.

Thus we decided to use the strong cation exchanger SCX for the further SPE procedure. It consisted of a conditioning step with 3 ml of eluent, 2 ml of methanol and 3 ml of phosphate buffer pH 2.5 followed the sample load. After a wash step (4 ml of methanol) using −20 kPa vacuum, the column was dried for 2 minutes at -50 kPa. Finally, the compounds were eluted with 2 ml of 5% ammonia in methanol. The solid phase tubes were again dried for 1 minute using −50 kPa vacuum.

<u>Figure III.3.</u> HPLC chromatogram of AD mixture 1 and 2 after SPE extraction from water using SCX

Mixture 1 contains in order of elution: ODMV, m-cpp, venlafaxine, DDMC, DMC, reboxetine, paroxetine, maprotiline, DMFluox, and fluoxetine. Mixture 2 contains in order of elution: viloxazine, trazodone, DMMia, citalopram, mianserin, fluvoxamine, DMSer, sertraline, and melitracen.
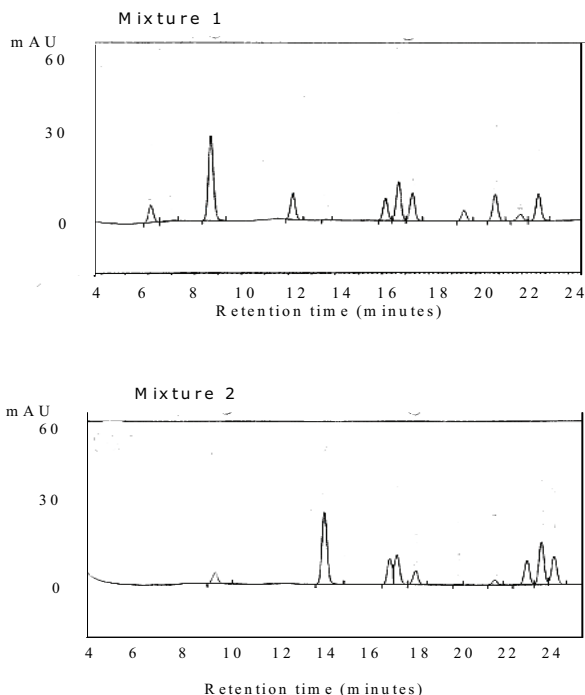
III.4. Optimization of the SPE procedure for extraction of ADs from biological matrices

The developed SPE procedure was now optimized for biological matrices such as plasma, blood, brain tissue and hair samples, as the extraction of ADs from these matrices is of interest in the field of clinical toxicology (plasma) and forensic toxicology (blood, brain, hair).

For plasma and blood, the developed SPE method had to be optimized due to their protein content. Most new generation ADs are highly bound to the plasma proteins, mainly to α_1-glycoprotein and to a lesser extent to albumin and lipoproteins. ADs bind to α_1-glycoprotein due to ionic interactions and their lipophilicity. Albumin preferably binds the hydrophobic and anionic compounds, thus less the positively charged ADs [16-20]. When using SPE as sample preparation, protein binding can lower the analyte recovery, as the active sites of the compounds that would normally interact with the sorbent are not available for this interaction. Another problem caused by protein binding is that proteins, as large molecules, prohibit penetration in the sorbent pores. As a result, the drug is carried through the sorbent bed by the protein instead of being retained [21].

For brain tissue, the sample preparation had to be adapted because of its solid nature. In addition, the lipophilic ADs are not easily extracted from the brain, as this matrix contains proteins and has a high lipid content.

Hair samples also have a solid nature, and can not just pass the SPE sorbent. Moreover, ADs are incorporated in the hair structure during the process of keratinization, preferentially in the cell membrane complex of the hair cortex containing proteins and a protein-lipid structure [22]. Thus, the ADs had to be extracted from the hair shafts prior to the SPE procedure.

While the protein binding disruption in plasma was studied using an HPLC-DAD system, the optimization of SPE for blood, brain and hair was done using a GC-MS configuration (paragraph III.2.5.). The recoveries for the different optimized methods were all obtained using the final GC-MS configuration.

III.4.1. SPE optimization for plasma samples

Because most of the ADs are highly bound to plasma proteins, a disruption of this protein binding is necessary to obtain high recoveries from the SPE sorbent. There are several ways to disrupt the binding. Dilution in combination with a slow sorbent pass-through of the sample is used to decrease the protein binding of drugs. In addition, before loading onto the SPE sorbent bed a sonication or centrifugation step is often applied [23-27]. On the other hand, changes in protein binding depend on temperature, pH, protein content and molecules that compete for the same sites on the protein. Thus, change of pH or addition of salt can also modify the protein binding. Denaturation of the protein by adding organic solvents to the sample is another method used. The above mentioned protein binding disruption methods were tested. However, as an ion-exchange procedure is used, addition of salts was not tested as they could interact with the SPE sorbent, leading to lower recovery of the compounds of interest.

Plasma samples (1 ml) were spiked with therapeutic concentrations of ADs and equilibrated overnight at 4°C, to simulate the protein binding. Afterwards the spiked plasma was submitted to SCX SPE-tubes after a deproteinization with different reagents. Standard mixtures were also analyzed as these represent 100% of free ADs. Acid (2% H_3PO_4), glycine-buffer, methanol and acetonitrile were tested for their capacity to break the protein bond. Dilution of the sample with phosphate buffer (pH 2.5; 25 mM) in combination with slow pass-through of the sample was also tested. The procedures for the acid/buffer and for the organic solvents involved addition of 3 ml of the substances to the plasma, and a vortex step followed by centrifugation for 10 minutes at 1121 g. The glycine-buffer required an extra 10 minutes equilibration-stirring time before centrifugation. The top layer was then removed and, respectively, 4 to 6 ml of phosphate buffer was added to the acid/buffer top layer and the organic top layer. The diluting procedure was achieved by adding 4 ml of phosphate buffer buffer pH 2.5 to the plasma, a vortex and centrifugation step.

When testing the different methods, it seemed that the organic solvents such as methanol and acetonitrile gave the worst results. Organic solvents lead to

a quick protein denaturation, but also to co-precipitation of the ADs and thus loss of these ADs. The glycine buffer and dilution method gave the best results (Figure III.4.).

Figure III.4. Comparison of protein binding disruption methods

The average recovery of all ADs was calculated for the different protein binding disruption methods (n=5 for each method and each AD). The lowest and highest recovery value (for a specific AD) obtained for each method are indicated.
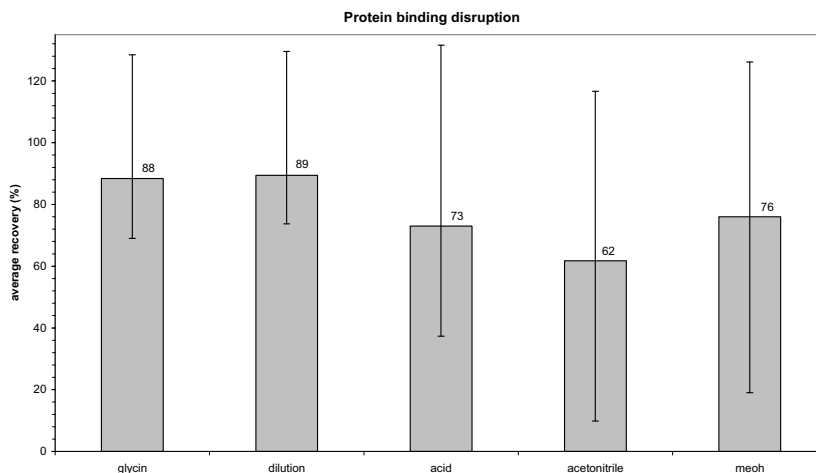
It was clear that a pH change of the sample led to a higher amount of unbound ADs. At pH 3 the proteins (iso-electric point of a_1-glycoprotein: 3.53) [28] will carry less negative charges than under physiological conditions, thus the ADs that are positively charged in those conditions, will show less ionic interactions [17]. In addition, at the iso-electric point there is no net charge and thus the solubility of the protein decreases, leading to a fractional protein precipitation. Not only the pH was of importance as a significant difference in ADs liberation was seen between the acid method and the glycine or dilution method when using an ANOVA-test ($p < 0.02$, except for DMSer and DDMC). Glycine wil compete with ADs for the binding sites on the a_1-glycoproteins. Dilution will change the equilibration status of bound and unbound ADs; thus will weaken the protein-drug binding. Moreover, dilution increases the time of eventual contact of the drugs with the adsorbent. Because of practical considerations, the method of choice for protein binding disruption was dilution of the plasma samples (1 ml) with

phosphate buffer pH 2.5 (4 ml, 25 mM) and a centrifugation step at 1200 *g* for 10 minutes. The sample was thereafter transferred to the SPE procedure.

III.4.2. SPE optimization for blood samples

For the blood samples, dilution of the sample with the phosphate buffer pH 2.5 resulted in a disruption of the protein binding of the ADs and in an ideal loading pH for the SPE as for the plasma samples. However, in contrast to plasma samples, the diluted blood sample was not centrifuged as it leads to irreproducible and lower extraction efficiencies (Table III.3.).

Table III.3. Differences in recovery after centrifugation or sonication of the diluted blood sample (n=6, *n=5)

Low, 20 ng/ml; Mid, 200 ng/ml; High, 500 ng/ml

compound	Recovery (%) (RSD%)					
	Blood centrifugated			Blood sonicated		
	Low	Mid	High	Low	Mid	High
Venlafaxine	38 (38)	99 (16)	99 (8)	51* (21)	101 (14)	93 (7)
m-cpp	52 (46)	83 (5)	80 (21)	92 (14)	93 (9)	101 (7)
Viloxazine	76 (31)	87 (5)	79 (15)	91 (8)	97 (10)	105 (7)
DMFluox	71 (38)	64 (9)	62 (17)	93 (12)	93 (6)	100 (6)
Fluvoxamine	86 (22)	81 (6)	72 (16)	95 (13)	99 (18)	104 (9)
ODMV		82 (29)	62 (24)	100 (15)	95 (30)	103 (20)
Fluoxetine	42 (34)	62 (7)	64 (14)	80 (9)	89 (7)	100 (5)
Mianserin	73 (7)	75 (9)	75 (5)	87 (6)	99 (8)	104 (3)
Mirtazapine	89 (7)	84 (11)	84 (3)	79 (10)	98 (8)	99 (4)
Melitracen	62 (10)	75 (9)	63 (11)	80 (8)	100 (9)	101 (5)
DMMia	42 (14)	84 (11)	78 (16)	82 (16)	102 (13)	92 (7)
DMSer	54 (32)	34 (28)	51 (25)	94* (15)	92 (11)	102 (5)
DMMir	67 (12)	116 (9)	97 (12)	83 (12)	103 (12)	94 (6)
Reboxetine	73 (14)	67 (13)	87 (16)	87 (12)	92 (8)	105 (7)
Citalopram	94 (17)	60 (13)	75 (9)	84 (21)	89 (14)	106 (13)
DMMap	66 (38)	48 (10)	60 (23)	91* (14)	79 (23)	96 (14)
Maprotiline	44 (35)	51 (16)	67 (19)	83 (14)	76 (14)	96 (5)
Sertraline	25 (46)	30 (15)	30 (23)	73 (18)	82 (17)	93 (17)
DDMC	102 (38)	76 (6)	80 (13)	85 (15)	87 (19)	97 (10)
DMC	60 (37)	69 (6)	79 (17)	84 (15)	82 (13)	96 (5)
Paroxetine	42 (34)	59 (9)	67 (17)	92 (18)	81 (12)	95 (4)

The separation of supernatant from the cell debris was not very clear and probably leads to these irreproducible results. Moreover, co-precipitation of ADs with the red blood cell fragments can lead to recovery loss, because ADs are bound to red blood cell membranes due to their amphiphilic character. ADs are also bound to proteins attached in the bilayer structure of this membrane [29, 30]. Thus, before the sample was transferred to the SPE

procedure, 1 ml of blood was diluted with 4 ml of a 25-mM phosphate buffer pH 2.5 and sonicated for 15 minutes.

III.4.3. SPE optimization for brain samples

For brain tissue, the sample preparation had to be adapted due to the lipid content of the brain and the lipophilic ADs (Table III.4.). Brain tissue (1 g) was spiked with 500 ng of each AD and was mixed after addition of 2 ml of acetonitrile, or a mixture of acetonitrile (2 ml) and 0.5 ml potassium carbonate buffer (1M pH 9.5). After centrifugation for 15 minutes at 1850 g, the top-layer was removed. The top-layer was then evaporated and redissolved in phosphate buffer (pH 2.5; 25 mM) or diluted with this buffer. After dilution of the acetonitrile phase with phosphate buffer, the pH was 6-7. Therefore, compounds such as mirtazapine, mianserin and Md$_3$ with a pKa of about 7.05 will not be positively charged and thus not trapped by the cationic phase. The pH of the diluted sample was thus adapted to 2-3 with orthophosphoric acid before it was submitted to the SPE-procedure.

Table III.4. indicates that extraction with acetonitrile is necessary to have high and reproducible extraction efficiencies. Acetonitrile disrupts the hydrophobic and dipolar interactions and extracts the ADs from the lipid rich matrix. An evaporation step of the acetonitrile phase seemed unnecessary and even led to a higher variation. Therefore the acetonitrile phase could be diluted before SPE leading to a shorter analysis time. The potassium carbonate buffer in combination with acetonitrile lead to higher extraction efficiencies, especially for melitracen, desmethylmianserin, desmethyl-mirtazapine, sertraline and desmethylsertraline.

In conclusion, before the sample was transferred to the SPE procedure, 1 g of brain tissue was mixed with 2 ml of acetonitrile and 0.5 ml of potassium carbonate buffer (1M pH 9.5). After centrifugation, the top layer was diluted with 4 ml of 25-mM phosphate buffer pH 2.5.

Table III.4. Differences in SPE recovery of ADs from brain tissue using a phosphate buffer (pH 2.5; 25 mM), acetonitrile (ACN) and phosphate buffer, ACN and evaporation, and ACN with a potassium carbonate buffer as sample pre-treatment

compound	Recovery (%) (RSD%)			
	buffer*	ACN + buffer	ACN	ACN + base
Venlafaxine	74 (11)	67 (6)	83 (21)	90 (18)
m-cpp	32 (42)	76 (3)	67 (15)	84 (6)
Viloxazine	61 (16)	80 (6)	63 (12)	83 (13)
DMFluox	8 (68)	60 (6)	39 (14)	75 (11)
Fluvoxamine	18 (49)	66 (5)	43 (7)	77 (10)
ODMV	73 (23)			
Fluoxetine	8 (68)	71 (5)	47 (21)	70 (6)
Mianserin	13 (63)	71 (7)	66 (35)	90 (15)
Mirtazapine	42 (27)	67 (1)	65 (26)	78 (20)
Melitracen	17 (124)	49 (8)	63 (30)	100 (13)
DMMia	12 (99)	48 (10)	68 (30)	95 (6)
DMSer	4 (58)	36 (2)	21 (34)	71 (3)
DMMir	39 (70)	63 (6)	76 (26)	98 (9)
Reboxetine	33 (42)	86 (7)	44 (30)	70 (4)
Citalopram	35 (30)	66 (12)	36 (23)	62 (15)
DMMap	5 (63)	43 (14)	25 (28)	61 (20)
Maprotiline	6 (63)	56 (17)	37 (33)	66 (20)
Sertraline	4 (80)	47 (1)	45 (34)	107 (6)
DDMC	22 (35)	78 (5)	54 (18)	77 (15)
DMC	27 (33)	84 (4)	56 (23)	74 (10)
Paroxetine	5 (68)	58 (3)	31 (30)	60 (9)

n=3
*n=5

III.4.4. SPE optimization for hair samples

ADs have to be extracted from the solid hair strains before SPE. The most common procedures involve the use of methanol or aqueous acids, and solubilization of the hair by digestion of the hairshaft with aqueous sodium hydroxide or specific enzymes [22].

Methanol is used together with sonication to liberate the drugs from the swelling hair through diffusion. While this method is very useful for neutral and lipophilic compounds, it seems that AD drugs are not easily liberated from hair with this method [31]. Extraction of basic drugs from hair using aqueous acids or buffer solutions is based on protonation. Digestion of the hair with sodium hydroxide leads to solubilization of the hair and to a high extraction efficiency for basic compounds. Enzymatic digestion by pronase and proteinase K can hydrolyze hair proteins and reduce disulfide bonds in

the hair. However, most of the time enzymatic extracts have a very high impurity level. Moreover, Couper et al. [31, 32] found that TCAs were better extracted using sodium hydroxide as compared to methanol, enzymatic digestion or an aqueous acid.

Tuhe first concern before extracting ADs from hair is their stability in the extraction solutions. ADs were spiked in concentrations around 500 ng/ml in different extraction media. Stability in methanol was not determined at this point, as the ADs stock solutions in methanol (1 mg/ml) were stable for at least 3 months. The stability in sodium hydroxide at different concentrations, temperature and contact time was tested. Indeed, Uges and Conemans [1] described that most ADs (TCAs) are not stable under alkaline conditions in daylight. Several conditions were selected whereby the hair samples were fully dissolved. Temperature seemed critical for hair solubilization, and a higher temperature allowed a shorter contact time with the sodium hydroxide. The sodium hydroxide concentration varied from 0.25 to 1 M, the temperatures used were 55, 80 and 100°C, and the duration for solubilization, depending on the NaOH concentration and temperature ranged from 10 till 90 minutes. The stability of the compounds was also tested in a 0.1-M HCl medium and in a phosphate buffer (pH 2.5, 25 mM) for 18 hours at 55°C. These conditions were chosen according to the extraction methods seen in literature [31].

Digesting hair (±20 mg) at 100°C during 10 minutes with 1 M NaOH gave good results and was preferred because of the short contact time. However, as depicted in Figure III.5., it is clear that some compounds are not stable in this alkaline medium under these conditions. Instability was observed for venlafaxine (30% loss), citalopram, DMC and DDMC (60-93% loss). No degradation was observed in acidic environment, except for fluvoxamine when 0.1 M HCl was used.

Because of stability reasons it would be better to select the extraction with phosphate buffer. In addition, this method results in an easy sample handling as the extraction solution can be transferred to the SPE sorbent directly. However, according to Couper et al. [32] the extraction efficiency by an aqueous acid is about 50% as compared to the sodium hydroxide digestion

method. Indeed, when hair is solubilized, the matrix is totally destroyed and the analytes are liberated from the hair. Extraction with an aqueous acid or buffer will only recover the analytes in the outher layers and will not penetrate the core of the hair shaft. Because of sensitivity and stability issues the two procedures were necessary for post-mortem hair analysis.

Figure III.5. Stability of ADs during extraction from hair samples (n=2)
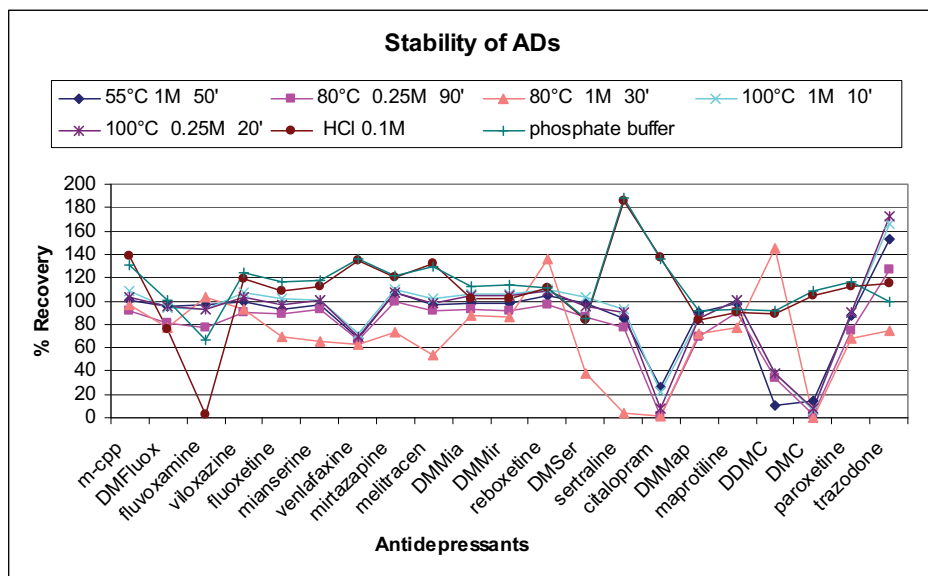
The final sample preparation for hair samples consisted of a wash step in HPLC-grade water for 5 minutes, and a rinse with 3 times 1 ml of methanol to remove possible external contamination and dirt from the surface of the hair. Thereafter, hair samples were cut in segments of approximately 2 cm. The hair segments were digested in a sodium hydroxide solution (1 M, 1 ml) for 10 minutes at 100°C. Before SPE, the samples were diluted with phosphate buffer and the pH was adapted to 2-3 with orthophosphoric acid. If compounds were not stable in the sodium hydroxide solution such as citalopram, DMC, DDMC and venlafaxine, hair segments were soaked in 4 ml of the phosphate buffer (pH 2.5; 25 mM) for 18 hours at 55°C and sonicated for 1 hour.

III.4.5. Recovery of ADs using SPE from plasma, blood, brain tissue

The recovery for each analyte was determined at low (20 ng), medium (200 ng) and high (500 ng) or super high (1000 ng) concentration. Therefore, standard working solutions were spiked in blank samples before (extraction samples) or after sample preparation (control samples). Each experiment was repeated six times. Outliers were eliminated when the obtained results deviated more than ± 3 standard deviations from the mean (*n=5). Since quantification was performed by the peak area ratios of the target analytes and the internal standard, the internal standards were always added after sample pre-treatment, before derivatization, and the resultant peak area ratios were compared. The recovery was expressed by its average and relative standard deviation (RSD).

Recovery of ADs from hair is not determined as spiked samples do not reflect reality. Compounds are incorporated in the interior of the hair through diffusion from blood, sweat or sebum. When samples are spiked, the compounds are spiked onto the hair, and this would lead to false high recoveries.

Table III.5. SPE recovery of ADs from plasma, blood and brain tissue (n=6)

compound	Plasma						Blood						Brain					
	Low		Mid		High		Low		Mid		High		Mid		High		S.High	
Venlafaxine	104	(3)	95	(4)	95	(2)	51*	(21)	101	(14)	93	(7)	38	(19)	46	(17)	45*	(13)
m-cpp	91	(4)	92	(7)	96	(5)	92	(14)	93	(9)	101	(7)	85	(16)	99	(8)	80	(9)
DMFluox	107*	(12)	91	(7)	91*	(5)	93	(12)	93	(6)	100	(6)	82	(12)	79	(5)	69	(10)
Viloxazine	104	(14)	96	(5)	92	(5)	91	(8)	97	(10)	105	(7)	58	(7)	62	(4)	56*	(8)
Fluvoxamine	102	(2)	104	(8)	97	(18)	95	(13)	99	(18)	104	(9)	44	(16)	43	(7)	35*	(10)
Fluoxetine	98	(12)	94	(2)	96	(2)	80	(9)	89	(7)	100	(5)	75	(8)	71	(5)	73	(6)
Mianserin	95	(4)	94	(3)	94	(3)	87	(6)	99	(8)	104	(3)	81	(11)	80	(5)	81	(7)
Mirtazapine	95	(6)	92	(3)	93	(3)	79	(10)	98	(8)	99	(4)	77	(11)	78	(7)	85	(5)
Melitracen	101	(5)	93	(3)	93	(3)	80	(8)	100	(9)	101	(5)	75	(13)	83	(6)	80*	(8)
DMMia	101	(4)	98	(4)	91	(2)	82	(16)	102	(13)	92	(7)	70	(9)	81	(10)	78*	(15)
DMSer	98	(11)	88	(7)	104	(10)	94*	(15)	92	(11)	102	(5)	77	(6)	70	(11)	76	(6)
DMMir	99	(4)	95	(2)	92	(3)	83	(12)	103	(12)	94	(6)	74	(12)	78	(8)	78	(11)
Reboxetine	99	(3)	97	(3)	95	(1)	87	(12)	92	(8)	105	(7)	51	(18)	60	(8)	59*	(4)
Citalopram	88	(8)	87	(9)	94	(5)	84	(21)	89	(14)	106	(13)	61	(16)	73	(5)	78*	(4)
Maprotiline	72*	(14)	88	(3)	90	(6)	83	(14)	76	(14)	96	(5)	54	(12)	59	(8)	81	(6)
DMMap	92	(15)	86	(5)	86	(6)	91*	(14)	79	(23)	96	(14)	51	(15)	57	(10)	78	(4)
Sertraline	82	(6)	89	(11)	96	(5)	73	(18)	82	(17)	93	(17)	90	(16)	73	(3)	82*	(11)
DDMC	94*	(11)	85	(7)	88	(6)	85	(15)	87	(19)	97	(10)	69	(10)	69	(7)	74	(8)
DMC	80	(13)	88	(4)	90	(5)	84	(15)	82	(13)	96	(5)	66	(4)	69	(3)	68*	(4)
Paroxetine	94	(11)	91	(2)	95	(2)	92	(18)	81	(12)	95	(4)	72	(11)	73	(7)	80	(6)

*n=5

Table III.5. indicates high, reproducible and concentration independent recoveries ranging from 82-105% for all ADs from plasma. The recoveries for ODMV and trazodone are not shown in this table as they are not reproducible using GC-MS as detection technique, due to an irreproducible derivatization

(chapter IV) and problematic chromatography (chapter V), respectively. The SCX extraction leads to reproducible and high recovery from blood for most compounds if no centrifugation step is included (Table III.3.). Recoveries from blood range between 73-106 %, except for venlafaxine (51%). The recoveries from blood samples are comparable to these from plasma.

ADs recoveries from plasma and blood were determined at low (20 ng/ml), mid (200 ng/ml) and high (500 ng/ml) concentrations, while brain tissue recoveries were determined at mid, high and super high concentration (1000 ng/g). This was chosen as brain concentrations found in literature were much higher than blood or plasma concentrations [33-35]. The extraction efficiencies for brain tissue are slightly lower than for plasma and blood. Especially venlafaxine and fluvoxamine gave low extraction efficiencies. However, recovery of the ADs from brain tissue is reproducible.

III.5. Conclusion

A solid phase extraction using a strong cation exchanger was developed for the new generation ADs and their metabolites. The final SPE procedure conditioned the sorbent with 3 ml of eluent, 2 ml of methanol and 3 ml of phosphate buffer pH 2.5 followed by the sample load. After a wash step (4 ml of methanol) using −20 kPa vacuum, the column was dried for 2 minutes at -50 kPa. Finally, the compounds were eluted with 2 ml of 5% ammonia in methanol. The solid phase tubes were again dried for 1 minute using −50 kPa vacuum.

The sample treatment before the load procedure onto the SPE sorbent was optimized for several biological matrices such as plasma, blood, and brain tissue as they have a different protein and lipid content. The samples were always diluted with 4 ml of the 25-mM phosphate buffer pH 2.5 and the pH was adapted with orthophosphoric acid if necessary, before loading onto the strong cation exchanger. In addition, plasma was centrifuged at 1200 g for 10 minutes, while blood was sonicated for 15 minutes. Brain tissue had to be treated by an acetonitrile/K_2CO_3 (2/0.5 ml/g) mixture before dilution with the buffer, due to the lipophilic matrix. Solubilization of the hair was necessary before SPE extraction. 1M NaOH at 100°C during 10 minutes was used for

this purpose. For instable compounds such as venlafaxine, citalopram and its metabolites, hair was extracted using phosphate buffer (pH 2.5; 25mM) during 18 hours at 55°C and sonication for 1 hour.

<u>Figure III.6.</u> Sample preparation scheme
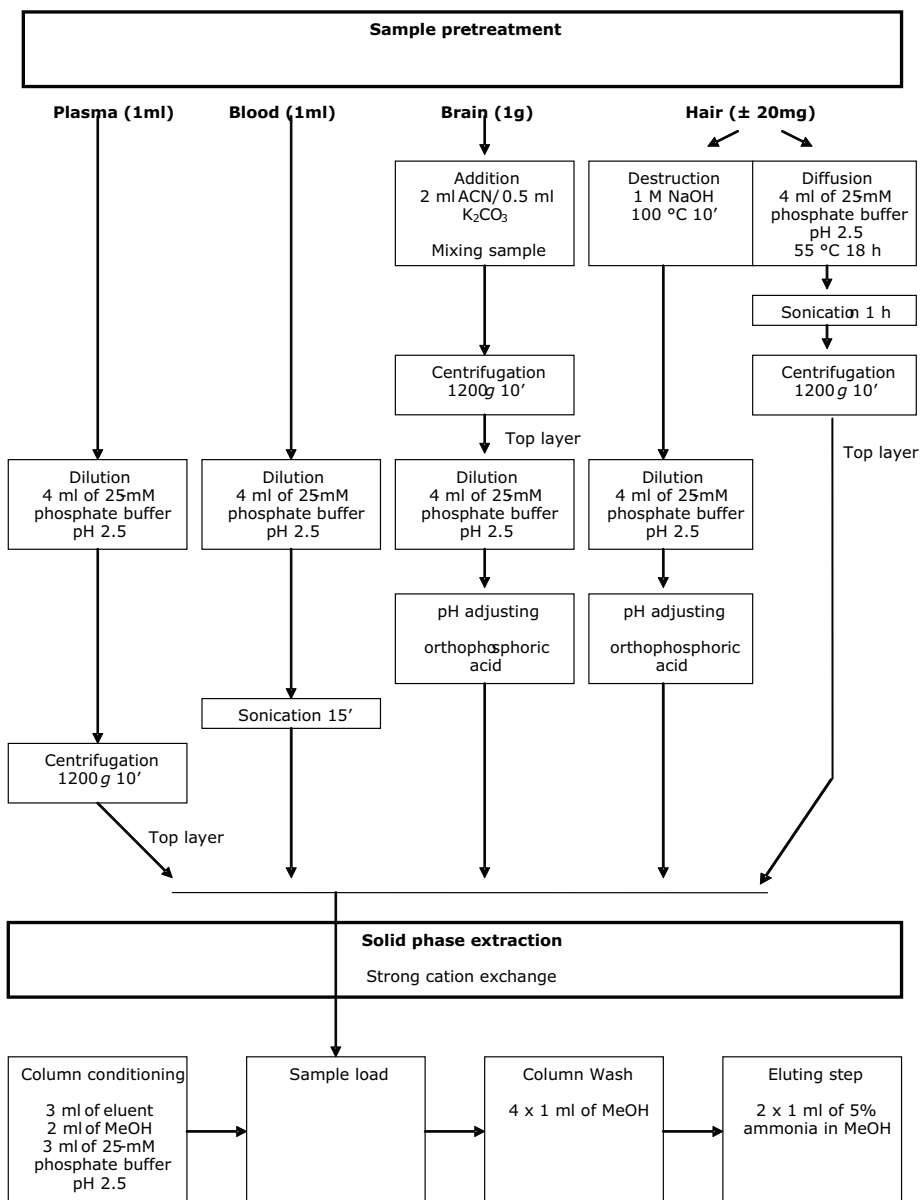
When these procedures were followed as indicatied in Figure III.6., the recoveries for the ADs from the different matrices were high and reproducible.

III.6. References

[1]   Uges DRA, Conemans JMH. Antidepressants and antipsychotics. Handbook of Analytical Separations, Elsevier, Amsterdam, 2000, pp. 742

[2]   Goeringer KE, Raymon L, Christian GD, Logan BK. Postmortem forensic toxicology of selective serotonin reuptake inhibitors: A review of pharmacology and report of 168 cases. *J. Forensic Sci*. 2000; 45: 633-648

[3]   Kim KM, Jung BH, Choi MH, Woo JS, Paeng KJ, Chung BC. Rapid and sensitive determination of sertraline in human plasma using gas chromatography-mass spectrometry. *J. Chromatogr. B* 2002; 769: 333-339

[4]   Eap CB, Bouchoux G, Amey M, Cochard N, Savary L, Baumann P. Simultaneous determination of human plasma levels of citalopram, paroxetine, sertraline, and their metabolites by gas chromatography mass spectrometry. *J. Chromatogr. Sci*. 1998; 36: 365-371

[5]   Titier K, Castaing N, Scotto-Gomez E, Pehourcq F, Moore N, Molimard M. High-performance liquid chromatographic method with diode array detection for identification and quantification of the eight new antidepressants and five of their active metabolites in plasma after overdose. *Ther. Drug Monit.* 2003; 25: 581-587

[6]   Lacassie E, Gaulier JM, Marquet P, Rabatel JF, Lachatre G. Methods for the determination of seven selective serotonin reuptake inhibitors and three active metabolites in human serum using high-performance liquid chromatography and gas chromatography. *J. Chromatogr. B* 2000; 742: 229-238

[7]   Duverneuil C, de la Grandmaison GL, de Mazancourt P, Alvarez JC. A high-performance liquid chromatography method with photodiode-array UV detection for therapeutic drug monitoring of the nontricyclic antidepressant drugs. *Ther. Drug Monit.* 2003; 25: 565-573

[8]   Gutteck U, Rentsch KM. Therapeutic drug monitoring of 13 antidepressant and five neuroleptic drugs in serum with liquid chromatography-electrospray ionization mass spectrometry. *Clin. Chem. Lab. Med.* 2003; 41: 1571-1579

[9]   Gupta RN. Drug level monitoring-antidepressants. *J. Chromatogr.* 1992; 576: 183-211

[10]   Walker V, Mills GA. Solid-phase extraction in clinical biochemistry. *Ann. Clin. Biochem.* 2002; 39: 464-477

[11]   Huck CW, Bonn GK. Recent developments in polymer-based sorbents for solid-phase extraction. *J. Chromatogr. A* 2000; 885: 51-72

[12]   Wille SMR, Maudens KE, Van Peteghem CH, Lambert WEE. Development of a solid phase extraction for 13 'new' generation antidepressants and their active metabolites for gas chromatographic-mass spectrometric analysis. *J. Chromatogr. A* 2005; 1098: 19-29

[13]   Van Horne KC. Sorbent extraction technology. Analytichem International, 1985, pp. 142

[14]   Pyrzynska K. Novel selective sorbents for solid-phase extraction. *Chem. Anal*. 2003; 48: 781-795

[15]   Snyder LR, Kirkland JJ, Glajch JL. Practical HPLC method development. John Wiley and sons, Inc., Hoboken, 1997, pp. 765

[16]   Kratochwil NA, Huber W, Müller F, Kansy M, Gerber PR. Predicting plasma protein binding of drugs: a new approach. *Biochem. Pharmacol.* 2002; 64: 1355-1374

[17]   Fournier T, Medjoubi N, Porquet D. Alpha-1-acid glycoprotein. *Biochim. Biophys. Acta* 2000; 1482: 157-171

[18]   Bertucci C, Domenici E. Reversible and covalent binding of drugs to human serum albumin: Methodological approaches and physiological relevance *Curr. Med. Chem.* 2002; 9: 1463-1481

[19]   Pike E, Skuterud B, Kierulf P, Bredesen JE, Lunde PKM. The relative importance of alubmin, lipoproteins and orosomucoid for drug serum binding. *Clin. Pharmacokinet.* 1984; 9: 84-85 S81

[20]   Piafsky KM. Disease-induced changes in the plasma binding of basic drugs. *Clin. Pharmacokinet.* 1980; 5: 246

[21]   Varian. Handbook of sorbent extraction technology. 1998; pp. 138

[22]   Pragst F, Balikova M. State of the art in hair analysis for detection of drug and alcohol abuse. *Clin. Chim. Acta* 2006; 370: 17-49

[23]   Martinez MA, de la Torre CS, Almarza E. A comparative solid-phase extraction study for the simultaneous determination of fluvoxamine, mianserin, doxepin, citalopram, paroxetine, and etoperidone in whole blood by capillary gas-liquid chromatography with nitrogen-phosphorus detection. *J. Anal. Toxicol.* 2004; 28: 174-180

[24]   Frahnert C, Rao ML, Grasmader K. Analysis of eighteen antidepressants, four atypical antipsychotics and active metabolites in serum by liquid chromatography: a simple tool for therapeutic drug monitoring. *J. Chromatogr. B* 2003; 794: 35-47

[25]   Molander P, Thomassen A, Kristoffersen L, Greibrokk T, Lundanes E. Simultaneous determination of citalopram, fluoxetine, paroxetine and their metabolites in plasma by temperature-programmed packed capillary liquid chromatography with on-column focusing of large injection volumes. *J. Chromatogr. B* 2002; 766: 77-87

[26]   Bakkali A, Corta E, Ciria JI, Berrueta LA, Gallo B, Vicente F. Solid-phase extraction with liquid chromatography and ultraviolet detection for the assay of antidepressant drugs in human plasma. *Talanta* 1999; 49: 773-783

[27]   Lai CK, Lee T, Au KM, Chan AYW. Uniform solid-phase extraction procedure for toxicological drug screening in serum and urine by HPLC with photodiode-array detection. *Clin. Chem.* 1997; 43: 312-325

[28]   Pruvost A, Ragueneau I, Ferry A, Jaillon P, Grognet JM, Benech H. Fully automated determination of eserine N-oxide in human plasma using on-line solid-phase extraction with liquid chromatography coupled with electrospray ionization tandem mass spectrometry. *J. Mass Spectrom.* 2000; 35: 625-633

[29]   Fisar Z, Fuksova K, Sikora J, Kalisova L, Velenovska M, Novotna M. Distribution of antidepressants between plasma and red blood cells. *Neuroendocrinol. Lett.* 2006; 27: 307-313

[30]   Hinderling PH. Red blood cells: a neglected compartment in pharmacokinetics and pharmacodynamics. *Pharmacol. Rev.* 1997; 49: 279-295

[31]   Couper FJ, McIntyre IM, Drummer OH. Extraction of psychotropic drugs from human scalp hair. *J. Forensic Sci.* 1995; 40: 83-86

[32]   Couper FJ, McIntyre IM, Drummer OH. Detection of Antidepressant and Antipsychotic-Drugs in Postmortem Human Scalp Hair. *J. Forensic Sci.* 1995; 40: 87-90

[33]   Martin A, Pounder DJ. Postmortem Toxicokinetics of Trazodone. *Forensic Sci. Int.* 1992; 56: 201-207

[34]   Bolo NR, Hode Y, Nedelec JF, Laine E, Wagner G, Macher JP. Brain pharmacokinetics and tissue distribution in vivo of fluvoxamine and fluoxetine by fluorine magnetic resonance spectroscopy. *Neuropsychopharmacol.* 2000; 23: 428-438

[35]   Wenzel S, Aderjan R, Mattern R, Pedal I, Skopp G. Tissue distribution of mirtazapine and desmethylmirtazapine in a case of mirtazapine poisoning. *Forensic Sci. Int.* 2006; 156: 229-236

Chapter IV

Derivatization

IV.1. Introduction

Derivatization is a common sample preparation technique before gas chromatographic analysis. This reaction modifies the chemical functionality of a compound to increase its volatility and stability. In addition, it reduces analyte adsorption onto the column, leading to less tailing and thus an improved peak shape. Furthermore, it can improve detector response by adding specific functional groups onto the compounds and it can facilitate the separation of the compounds-of-interest from other substances present in the extract. The choice of derivatizing reagent depends on the functional groups of the compounds-of-interest and the demands of the user [1, 2].

Gas chromatographic analysis of free (underivatized) amines such as ADs is generally unsatisfactory due to adsorption and decomposition of the analytes on the column. These effects increase from tertiary to secondary amines and are the worst for primary amines. Therefore, the predominant reason for derivatization of the ADs is the improvement of their chromatographic characteristics by decreasing their polarity. The antidepressants (ADs) monitored in this work can be chemically classified as ADs containing an alcohol, a primary, secondary or tertiary amine. These ADs, except for the tertiary amine group, contain active hydrogens which can be derivatized (Figure IV.1.)

The three most applied derivatization reactions are silylation, alkylation and acylation.

Silylation replaces active hydrogens by a silyl group and reduces the polarity and hydrogen bonding of the compound. However, the excess of derivatization product will also be injected onto the gas chromatographic system which leads to contamination of the whole system and in-situ derivatization of all injected compounds. In addition, silicium dioxide deposits in the ion source can affect the mass selective detector [3, 4]. Therefore, a gas chromatographic system reserved only for silylated samples is necessary and this was not an option in the laboratory.

<u>Figure IV.1.</u> Structures of ADs with indication of the replaced hydrogen functions during derivatization (italic functions)

Bold functions are those that are demethylated in the metabolization process. The arrow indicates the N-dealkylation of the piperazinyl nitrogen resulting in the formation of m-chlorophenylpiperazine. 1: Venlafaxine, 2: Fluvoxamine, 3: Sertraline, 4: Maprotiline, 5: Trazodone, 6: Citalopram, 7: Paroxetine, 8: Viloxazine, 9: Fluoxetine, 10: Reboxetine, 11: Mirtazapine, 12: Mianserin, 13: Melitracen.
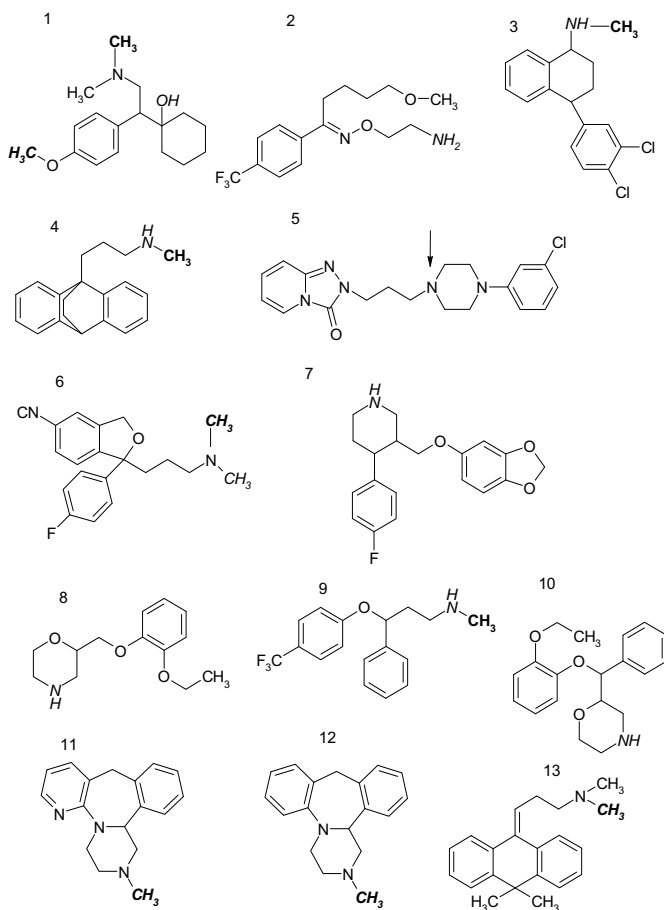
Alkylation involves replacement of active hydrogens by an alkyl group. In this case the polarity of the compound will be decreased and the volatility will increase.

The *acylation* reaction converts compounds that contain active hydrogens (NH, OH, SH groups) into amides, esters or thioesters through the action of an activated carboxylic acid. Besides advantages such as decreased polarity,

increased volatility and stability, another advantage of acylation can be the increased sensitivity of the derivative with electron capture or negative ion chemical ionization mass detection due to the combination of halogen atoms and the carbonyl group. Moreover, acylation benefits the formation of fragmentation-directing derivatives for gas chromatographic-mass spectrometric analysis. Therefore, the acylation reaction was chosen as most promising derivatization reaction for the monitored ADs.

The two acylation reactions tested were the acetylation reaction, using acetic anhydride and pyridine, and heptafluorobutyrylation. Derivatization with acetic anhydride was the first choice, as this reagent is largely used in systematic toxicological analysis [5-8]. However, when negative ion chemical ionization became an option during the research period, 1-(heptafluoro-butyryl) imidazole (HFBI) and heptafluorobutyric anhydride (HFBA) became first choice because of detection and sensitivity issues [1, 2].

Pentafluorobenzyl chloroformate was another interesting option as it contained fluorine atoms which would increase sensitivity in negative ion chemical ionization mode such as for the HFB-reagents, but in addition, it is directly applicable in an aqueous environment and it could derivatize tertiary amines [9]. However, as our aim was to analyze ADs and their demethylated metabolites pentafluorobenzyl chloroformate could not be applied. No difference would be observed between the derivatized parent compound and its demethylated metabolite as the reagent rather replaces the hydrogen atom than the methyl group on the nitrogen-function in the metabolite structure.

Thus acetic anhydride (acetylation), heptafluorobutyric anhydride and hepta-fluorobutyryl imidazole (heptafluorobutyrylation) were used as derivatization reagents and their respective optimized derivatization procedures for the ADs are discussed in this chapter.

IV.2. Experimental

IV.2.1. Reagents

ADs standards used during optimization of the derivatization were the same as described in chapter III (III.2.1.). Pyridine, acetic anhydride, and heptafluorobutyric anhydride (HFBA) were purchased from Sigma-Aldrich (Steinheim, Germany), while 1-(heptafluorobutyryl) imidazole (HFBI) was purchased at Pierce (Perbio, Erembodegem, Belgium). Promochem (Molsheim, France) delivered mianserin-d_3 (100 µg/ml MeOH). Water (HPLC-grade), ammonia-solution 25%, triethylamine and toluene (Suprasolv) were purchased from Merck (Darmstadt, Germany).

IV.2.2. Preparation of standard solutions

Primary stock solutions of each individual AD were prepared in methanol at a concentration of 1 mg/ml and stored at -20°C. A standard mixture 0.1 mg/ml was obtained by mixing these individual primary stock solutions.

Depending on the type of experiment, the ADs concentrations were chosen. For determination of spectra primary stock solutions were used. For comparison of the different derivatization reagents, 40 ng on-column was used to detect underivatized compounds in scan mode. For comparison of HFB-reagents, 4 ng was injected onto the column and monitored in selected ion monitoring mode.

When validating the final derivatization procedure, a standard mixture was obtained by mixing the individual primary ADs stock solutions and by further diluting with methanol until a concentration of 0.05-0.125 mg/ml, depending on the therapeutic range of the compound. After preparation, it was stored protected from light at approximately -20°C. Further dilution of the standard mixture with methanol resulted in working solutions with concentrations of 0.1, 1 or 10 µg/ml.

IV.2.3. Instrumentation

All experiments were carried out on a HP 6890 GC system, equipped with a HP 5973 mass selective detector and a G1701DA Chem Station, version D.02.00 data processing unit (Agilent Technologies, Avondale, PA, USA). The first experimental set-up contained a HP 7683 on-column auto injector. Later on the injector was changed to a HP 7683 split/splitless auto injector due to practical considerations as described in chapter V.

Evaporation under nitrogen was conducted in a TurboVap LV evaporator from Zymark (Hopkinton, MA, USA). The heater was a multi-block from Lab-line (Tiel, The Netherlands).

IV.2.4. Gas chromatographic parameters

Chromatographic separation was achieved on a 30m x 0.25mm I.D., 0.25-µm J&W-5ms column from Agilent Technologies (Avondale, PA, USA). The start condition of the column temperature was set depending on the injector type and injection solvent (chapter V.3.). For the on-column (methanol) and split/splitless injector (toluene), a starting temperature of 50 °C for 1 min or 90 °C for 1 min was applied, respectively. Thereafter the temperature of the column was ramped at 50°C/min to 180°C where it was held for 10 min, whereafter the temperature was ramped again at 10°C/min to 300°C. Ultrapure helium at a constant flow of 1.3 ml/min was used as carrier gas.

When the split/splitless auto injector was used, the pulsed splitless injection temperature was held at 300°C, the purge time and pulse activation time were set at 1 and 1.5 min, respectively. Meanwhile, the injection pulse pressure was 170 kPa.

For each injection type 1 µl of the sample, redissolved in 50 µl toluene or methanol, was injected. While toluene was used as injection solvent during the further development and validation of the GC-MS method (chapter V), methanol was used as redissolving and injection solvent for determination of several spectra in the beginning of our research.

IV.2.5. Mass spectrometric parameters

The mass selective detector temperature conditions were 230°C for the EI-source, 150°C for the quadrupole and 300°C for the transferline, whereas an electron voltage of 70 eV was used. The mass selective detector was used in scan mode for optimization of the derivatization reactions. When comparing the heptafluorobutyrylation reagents and validating the final derivatization method, the mass selective detector was used in selected ion monitoring mode as described in chapter III (III.2.5. Table III.1.)

IV.3. Acetylation

IV.3.1. Optimization of acetylation reaction

The acetylation procedure was not optimized for ADs. The chosen acetylation conditions were already successfully applied in our laboratory for benzodiazepines and were tested for ADs [10,11]. The evaporated methanolic AD stock-solution was acetylated with a mixture of 200 µl of acetic anhydride and 200 µl of pyridine. The derivatization occurred at room temperature after 30 minutes.

IV.3.2 Acetylation reaction with antidepressants

Acetylation occurs for alcohols, secondary and primairy amines, but not for tertiary amines. The alcohol and amine functions react with acetic anhydride, and this reaction is catalyzed by pyridine that acts as an acceptor for the acidic byproduct formed during the reaction. This reaction is a result of an nucleophilic mechanism, leading to a carbonyl addition intermediate followed by elimination of acetic acid (byproduct) and resulting in the acetylated AD [1]. The reaction scheme is depicted in Figure IV.2. After derivatization the moleculair mass gain is 42 amu, as a free hydrogen atom is replaced by an acetylgroup.

Figure IV.2. Acetylation reaction scheme
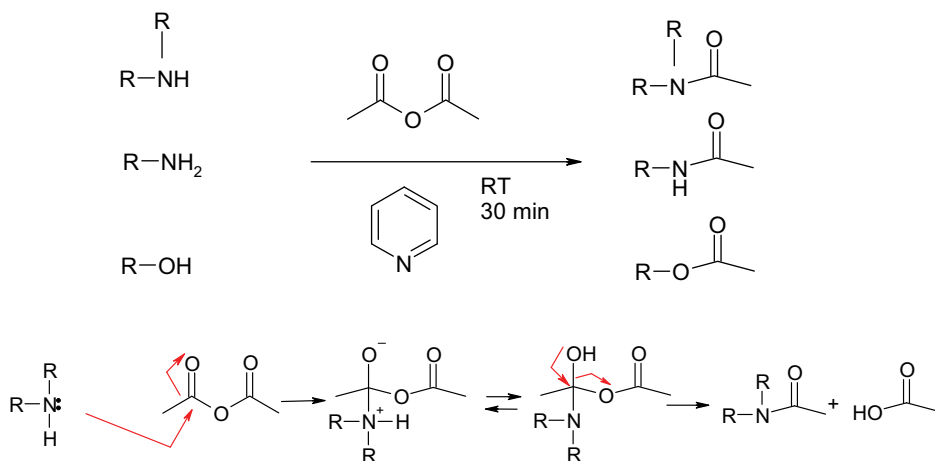
IV.3.2.1. *ADs containing an alcohol function*

Venlafaxine and its metabolite O-desmethylvenlafaxine (ODMV) are the only monitored compounds that contain at least one alcohol function. The structure of venlafaxine containing one hydroxyl-function is shown in Figure IV.3.A. Venlafaxine is demethylated to its metabolite ODMV which then contains 2 alcohol functions that can possibly be derivatized.

After the acetylation procedure, two peaks were detected in the chromatograms of both acetylated venlafaxine and its metabolite ODMV. Figure IV.3. gives the example of venlafaxine. When studying the spectra before and after derivatization, a mass gain of 42 amu is observed for one of the two peaks in the chromatogram (B) after derivatization. Therefore, successful acetylation of the alcohol function could be concluded. However, for the other peak a loss of 18 amu is observed and dehydration of the molecule is suspected (C).

ODMV acetylation occurs in the same way as its parent compound. Maurer et al. [5] describe an acetylation reaction for ODMV as for venlafaxine, but on the demethylated oxygen atom (underlined), leaving the other alcohol function underivatized. The second ODMV-peak after derivatization is the acetylated compound without the aliphatic alcohol, as this function is dehydrated.

Acetylation of venlafaxine and ODMV does not lead to one derivative, resulting in the problem of possibly irreproducible quantitative results. This effect should be kept in mind during validation of the method.

<u>Figure IV.3.</u> Derivatization of venlafaxine with acetic anhydride

Chromatogram and corresponding mass spectra of underivatized venlafaxine (A, black trace) and venlafaxine after acetylation (red trace): derivatized (B) and dehydrated (C)

Abundance

Time-->

A

m/z-->
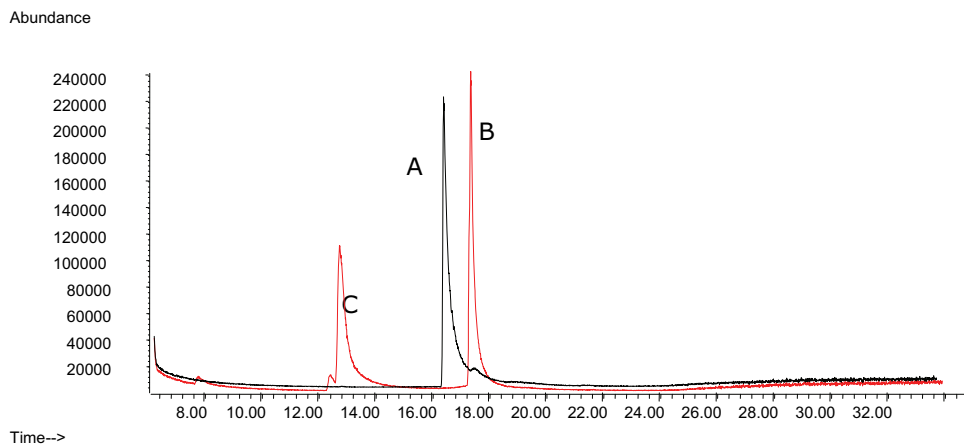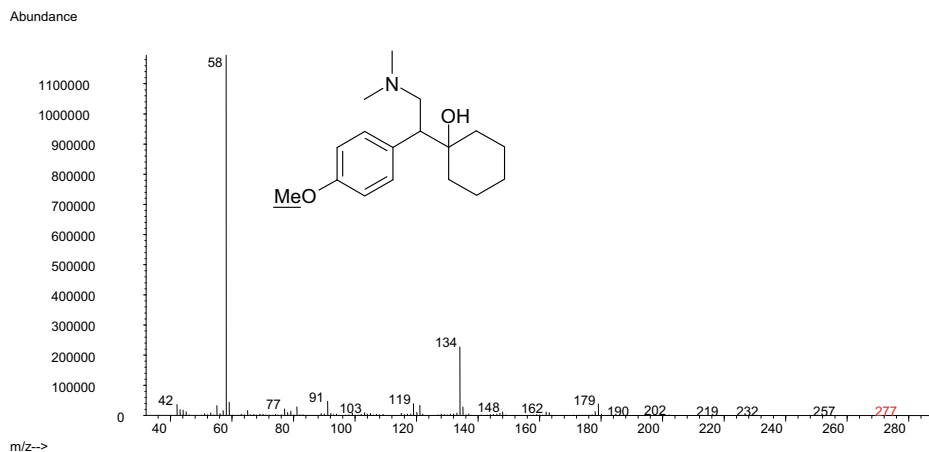
B
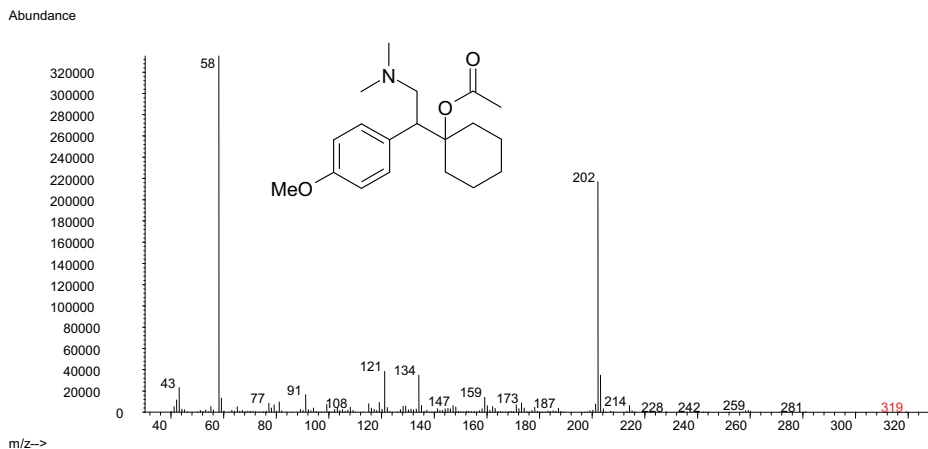
C
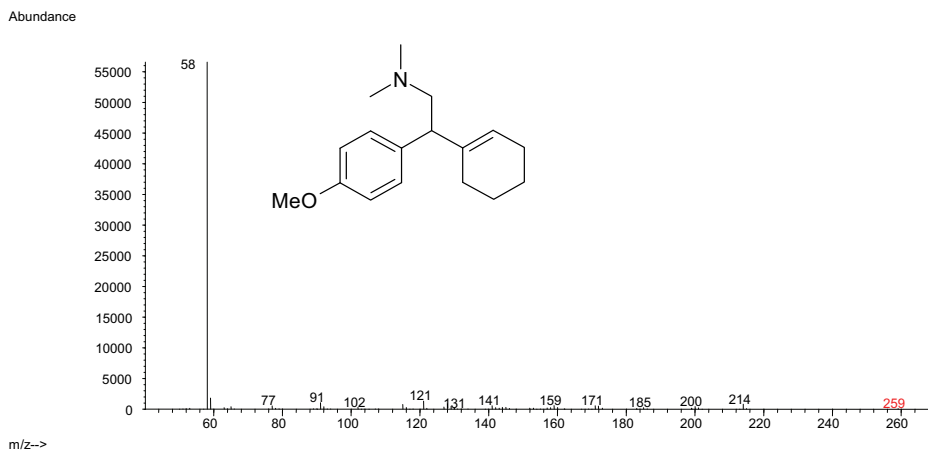
IV.3.2.2. *ADs containing a primary amine function*

Fluvoxamine is the only AD that contains a primary amine function. However, the demethylated metabolites of sertraline, maprotiline and fluoxetine, and the didesmethylated metabolite of citalopram also contain a primary amine function. During acetylation of these compounds one of the free hydrogen atoms on the nitrogen atom acts as leaving group.

After the acetylation procedure, the retention times of the peaks are increased and spectra have a molecular ion mass gain of 42 amu (Table IV.1.). This leads to the conclusion that primary amines are easily derivatized with acetic anhydride and pyridine.

Figure IV.4. Derivatization of fluvoxamine with acetic anhydride

A: mass spectrum underivatized; B: derivatized

A
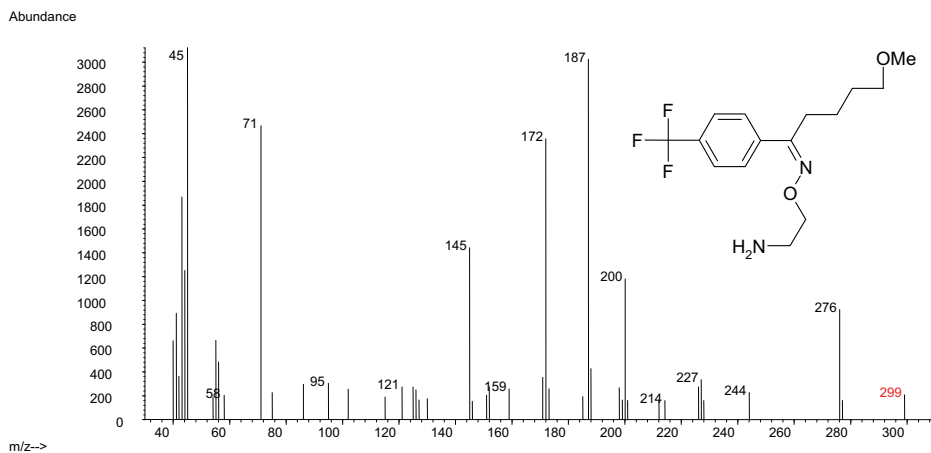
B
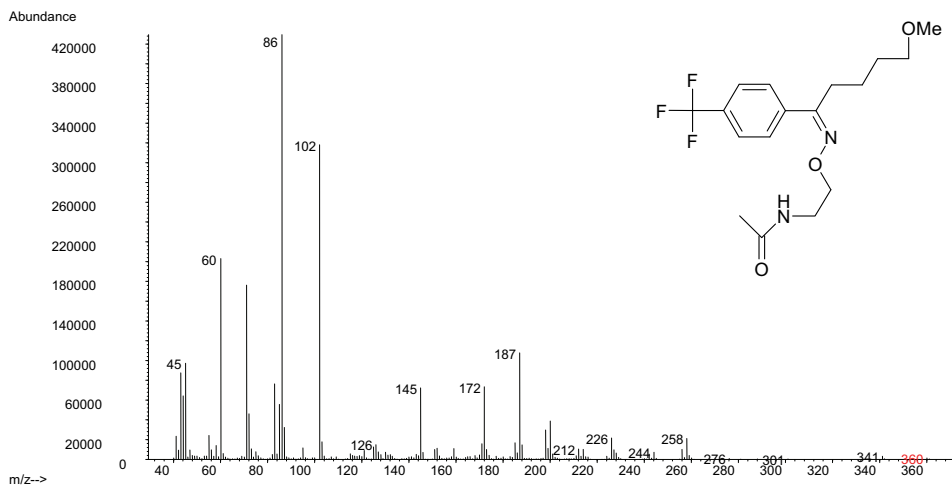
For fluvoxamine (shown in Figure IV.4.), it seems that an addition of 61 amu occurs after acetylation as the molecular ion of underivatized fluvoxamine is 299, while the derivatized form is 360 amu. However, using the theoretical molecular weight of fluvoxamine, which is 318, an addition of 42 amu is demonstrated. The difference of 61 amu according to the spectra shown above is explained by the fragmentation pattern of underivatized fluvoxamine

that looses a fluorine atom (loss of 19 amu) resulting in the monitored ion of 299 amu in stead of 318 amu.

IV.3.2.3. *ADs containing secondary amine functions*

<u>Figure IV.5.</u> Derivatization of secondary amines with acetic anhydride with spectra before (A) and after (B) derivatization. Viloxazine is given as an example

A

B
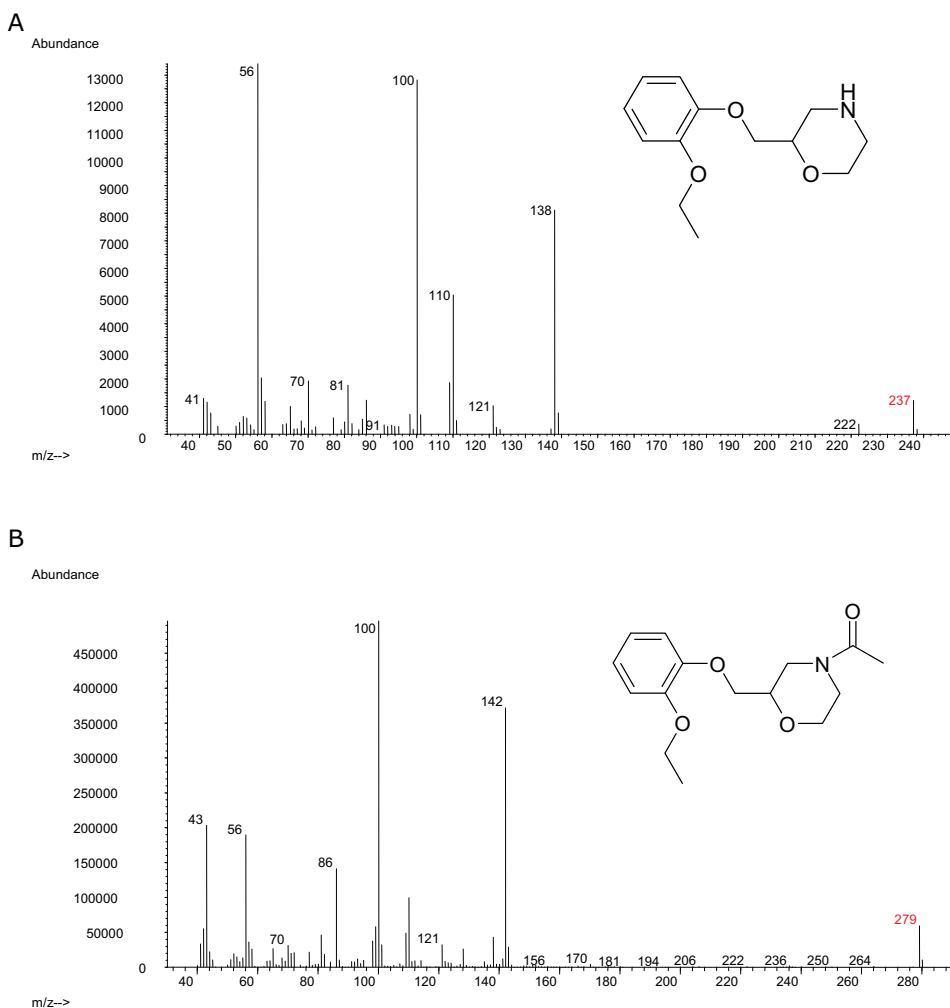
Several ADs discussed in this work are secondary amines. These ADs are fluoxetine, viloxazine, maprotiline, reboxetine, sertraline, and paroxetine. In

addition, several metabolites also contain a secondary amine function, leading to a free and thus replacable hydrogen atom: desmethylcitalopram, desmethylmirtazapine, desmethylmianserin and m-cpp.

As demonstrated in Table IV.1. a mass gain of 42 amu is seen for these compounds, concluding that the derivatization reaction is successful. Figure IV.5. demonstrates the acetylation of viloxazine as an example.

IV.3.2.4. *Tertiary amines*

Several ADs contain tertiary amine functions that can not be derivatized using acetic anhydride and pyridine. These ADs are citalopram, mirtazapine, mianserin, melitracen and trazodone. Spectra before and after derivatization are identical for these compounds (Figure IV.6.), therefore we can conclude that the compounds are stable during the derivatization conditions. This is important in forensic analysis as the content of the sample is unknown and every sample will be analyzed identically and thus will undergo the derivatization reaction.

Figure IV.6. Mass spectrum of mianserin after passing the derivatization procedure
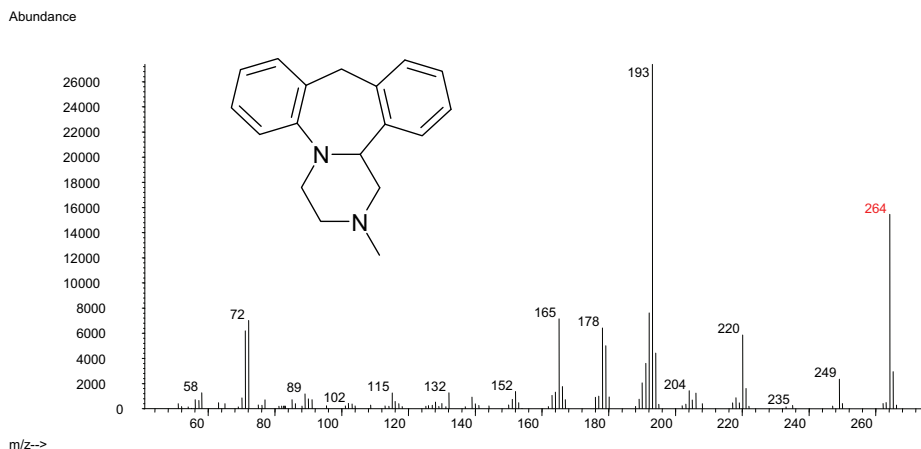
IV.3.3. Conclusion

Most ADs and their metabolites can be derivatized using pyridine and acetic anhydride at room temperature after 30 minutes as demonstrated in Table IV.1. This derivatization procedure results in a much better peak shape, leading to an enhanced sensitivity.

ADs containing tertiary amines in their structure can not be derivatized, but their peak shape is already satisfactory as tertiary amines show less adsorption onto the analytical column.

Acetylation of venlafaxine and its metabolite ODMV results in two derivatization products; an acetylated and a dehydrated product, which can lead to irreproducible quantitative results.

Table IV.1. Retention time (t_r) and molecular ion of each AD before and after acetylation

ADs	Before derivatization			After acetylation	
	M^+-ion theor.	t_r	M^+-ion monitored	t_r	M^+-ion monitored
		min.	amu	min.	amu
Alcohols					
Venlafaxine	277.41	16.4	277	12.6	259 (-H_2O)
				17.3	319 (AC)
ODMV	263.38	18.9	263	16.5	287 (AC-H_2O)
				19.1	305 (AC)
Primary amines					
Fluvoxamine	318.34	11.2	299	18.9	360
DMFluox	295.30	9.6	295	19.7	327
DMMap	263.38	19.6	263	24.3	305
DMSer	292.20	20.1	292	24.1	334
DDMC	296.34	20.9	296	25.4	338
Secondary amines					
Fluoxetine	309.33	10.2	309	19.0	351
Maprotiline	277.41	19.9	277	24.2	319
Paroxetine	329.37	22.8	329	25.9	371
Reboxetine	313.40	21.0	313	23.6	355
Sertraline	306.23	20.3	306	24.3	348
Viloxazine	237.30	10.4	237	18.6	279
DMC	310.37	21.0	310	25.3	352
DMMia	250.34	19.2	250	23.3	292
DMMir	251.33	19.9	251	23.9	293
m-cpp	196.70	7.7	196	17.9	238
Tertiary amines					
Citalopram	324.40	20.7	324	20.7	324
Melitracen	291.44	19.3	291	19.3	291
Mianserin	264.37	18.2	264	18.2	264
Mirtazapine	265.36	18.9	265	18.9	265
Trazodone	371.87	29.8	371	29.8	371

IV.4. Heptafluorobutyrylation

For the heptafluorobutyrylation two reagents, 1-(heptafluorobutyryl) imidazole (HFBI) and heptafluorobutyric anhydride (HFBA), were tested. Because our first GC-MS configuration was equipped with a cold on-column injector, HFBI was used. This derivatization reagent results in the formation of the non aggressive byproduct imidazole, while the acid HFBA can result in column damage. However, later on, the injector in our GC-MS system was changed to a split/splitless configuration and the HFBA reagent was re-evaluated.

IV.4.1. Optimization of HFBI reaction

IV.4.1.1. *Experimental*

The derivatization step was optimized in duration, temperature and quantity of HFBI. Derivatization parameters such as temperature were changed from 45-105°C and duration from 15-60 minutes. Quantities of HFBI were varied from 20 till 200 µl. In addition, an extraction was optimized using toluene and water to remove excess of the HFBI derivatization reagent and by-products. The ratio of water/toluene was varied from 0.5/1 till 0.5/2. These parameters were optimized through peak height and area, variation and completeness of the reaction.

Twenty µl of a 0.1-mg/ml ADs mix was evaporated to dryness and derivatized under different conditions. Before injection of the samples, mianserin-d_3 (200 ng / 50 µl) was added, as this I.S. can be analyzed without derivatization.

IV.4.1.2. *Results*

For derivatization of the analytes of interest with HFBI, addition of 20 µl of reagent resulted in a complete reaction. No significant difference (T-test $p>0.05$) was seen between the different amounts of HFBI. However, because a 50-µl volume ensured adequate moistening of the reaction vial, this amount of HFBI was chosen.

The reaction at 85°C during 30 minutes gave the highest yield with an acceptable variation. Although, there was no significant difference in

temperature, 85°C was necessary to get a complete derivatization of sertraline.

The duration of the derivatization did not affect the procedure significantly. Therefore, 30 minutes were selected as this resulted in the least variation for an acceptable derivatization reaction time.

Usually, the excess of derivatization reagent and byproducts are removed after derivatization, as they can damage the GC-column. Due to the inert imidazole byproduct of HFBI, damage of the column is minimized, however, the injection needle can still be clogged. Moreover, when using NICI-MS detection, the excess of reagent must be eliminated to minimize detector noise and to obtain adequate sensitivity. Evaporation of the excess of HFBI was not an option as it led to crystallization of the derivatization product. Therefore, a simple extraction step was applied, resulting in the transfer of the derivatized compounds in the toluene layer, while the excess of reagent and byproducts remain in the aqueous phase. When 2 ml of toluene and 0.5 ml of water were used, the underivatized compounds were extracted more efficiently into the toluene layer. The toluene phase was evaporated with nitrogen at 40°C and the extract was redissolved in 50 µl of toluene.

Figure IV.7. Optimization of HFBI derivatization (n=3)
Errorflags indicate ± one standard deviation
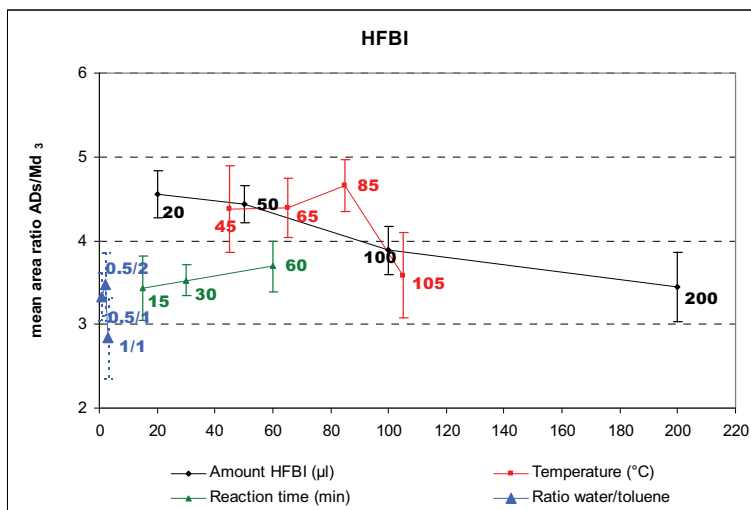
IV.4.2. Optimization of HFBA reaction

IV.4.2.1. *Experimental*

The derivatization step was optimized in duration, temperature and quantity of HFBA. Derivatization parameters such as temperature were changed from 45-105°C and duration from 15-60 minutes. HFBA was diluted with chloroform or toluene in concentrations of 10-50%. These parameters were optimized through peak height and area, variation and completeness of reaction.

Twenty µl of a 0.1-mg/ml ADs mix was evaporated to dryness and derivatized under different conditions. Before injection of the samples, mianserin-d_3 was added, as this I.S. can be analyzed without derivatization.

IV.4.2.2. *Results*

Heptafluorobutyric anhydride was dissolved in chloroform or mixed with toluene at percentages varying from 10-50%. Chloroform and toluene were chosen, respectively because ADs and the HFBA solution are easily dissolved in chloroform, while HFB-derivatives are highly soluble in toluene. In addition, due to the derivatization temperature, a low percentage of HFBA can be dissolved in the toluene fraction. As depicted in Figure IV.7. a mix of 10% HFBA in toluene (total volume of 100 µl) resulted in the best derivatization results. The percentage of HFBA can be kept low. This is an advantage as the anhydride can damage the column and can lead to higher background especially when the mass analyzer is used in negative ion chemical ionization mode.

A derivatization temperature of 105 °C was selected as this resulted in the highest reaction yield. Although higher variation was seen at this temperature, 105 °C was necessary for the derivatization reactions of venlafaxine and its metabolite. Heptafluorobutyrylation reactions with amines generally proceed at low temperature, while hydroxyl derivatizations are slower and thus heat is recommended [1]. However, the reaction yield for venlafaxine and ODMV was still not complete and in addition, dehydration products were noticed (IV.4.3.1.).

The ADs were derivatized during 5 minutes as this resulted in the best signal with the least variation for most compounds. No significant difference in

signal was seen between 5 and 15 minutes of reaction time (T-test: p=0.36). After longer reaction times some compounds showed a decrease in signal, possibly due to degradation.

The excess of derivatization reagent was evaporated by nitrogen at 40°C and the extract was redissolved in 50 µl of toluene.

<u>Figure IV.8.</u> Optimization of HFBA derivatization (n=3)

Errorflags indicate ± one standard deviation
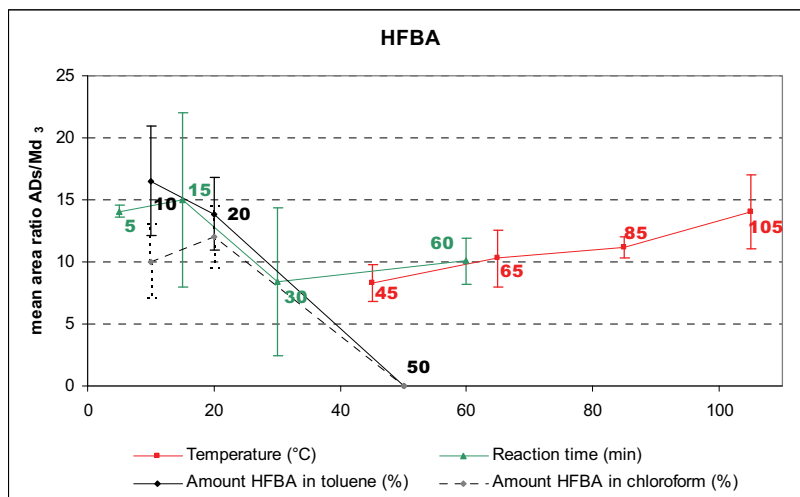
IV.4.3. Heptafluorobutyrylation of antidepressants

The acylation reaction with both HFBI and HFBA replaces a labile hydrogen atom attached to the nitrogen atom, for a less polar, stable group. HFB-acylation occurs for alcohols, secondary and primairy amines, but not for tertiary amines. The alcohol and amine functions react with heptafluoro-butyrylimidazole and heptafluorobutyric anhydride, forming a carbonyl addition intermediate and finally resulting in heptafluorobutyrylated ADs and their respective byproducts, the neutral imidazole or heptafluorobutyric acid. The reaction scheme is depicted in Figure IV.9. After derivatization the molecular mass gain is 196 amu, as a free hydrogen atom is replaced by a heptafluorobutyryl-group.

Figure IV.9. Heptafluorobutyrylation reaction scheme
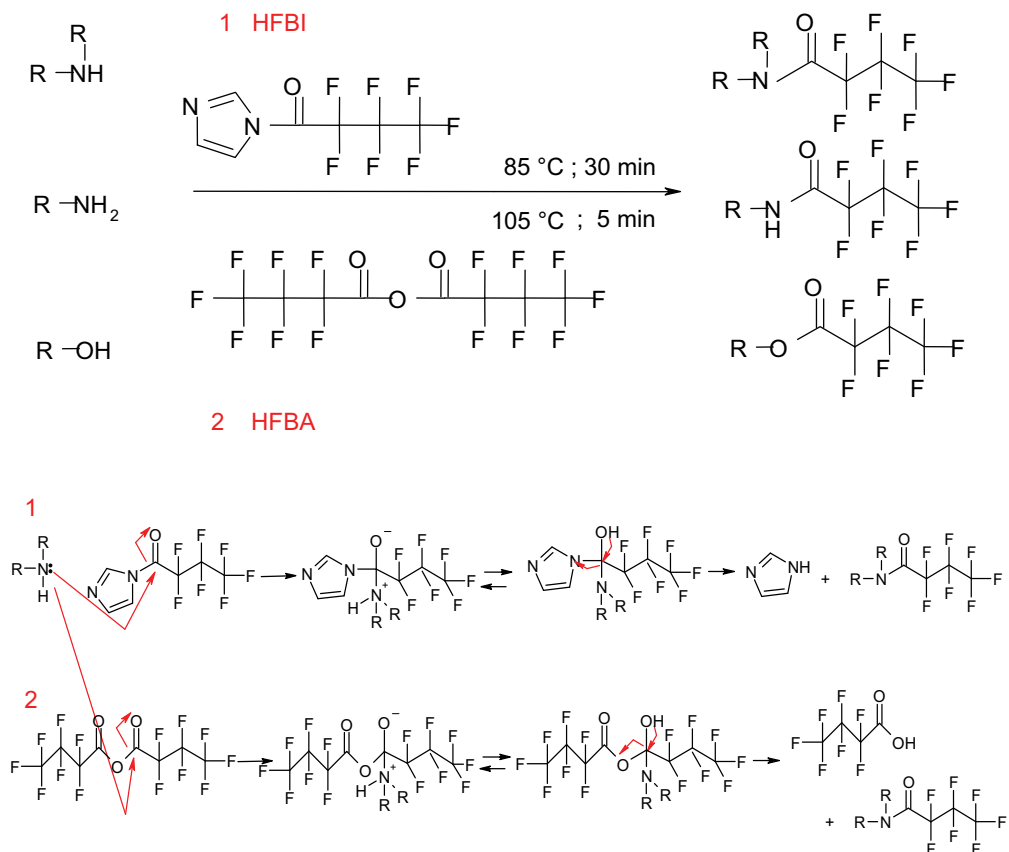
IV.4.3.1. *ADs containing an alcohol function*

Although HFB-reagents can derivatize alcohol functions, a dehydration of tertiary alcohols such as in venlafaxine and its metabolite ODMV is observed [2]. This reaction eliminates possible hydrogen bridges, thus leading to a better peak shape of the derivatized analyte. The rate of the dehydration reaction depends on the type of HFB-reagent and on the temperature during each derivatization reaction.

Figure IV. 10. shows the chromatograms of venlafaxine after HFBI and HFBA derivatization. When using HFBI one peak arises in the chromatogram and the spectrum demonstrates a loss of 18 amu, thus loss of water. No HFB-venlafaxine was observed. After HFBA derivatization, the dehydration product

was also observed, but in combination with a large underivatized venlafaxine peak. Again, no HFB-venlafaxine was observed, leading to the conclusion that venlafaxine can not be heptafluorobutyrylated. In addition, the dehydration seems to result in a higher reaction yield when using HFBI. The spectra of underivatized and dehydrated venlafaxine were already shown in Figure IV.3., as heptafluorobutyrylation and acetylation result in the same dehydrated venlafaxine peak.

<u>Figure IV.10.</u> Derivatization of venlafaxine with heptafluorobutyrylimidazole (red trace) and heptafluorobutyric anhydride at 105 °C (black trace)

A, underivatized venlafaxine; B, dehydrated venlafaxine
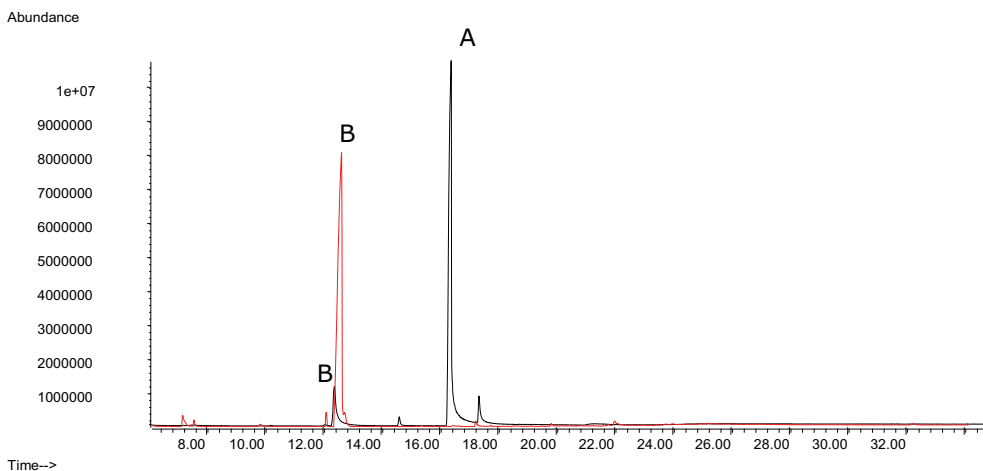
For ODMV a similar dehydration reaction as for venlafaxine was observed. In addition, for both reagents a HFB-derivative could be suspected, however, due to pronounced fragmentation of the compound in electron ionization mode the spectra were difficult to interprete. During the further optimization of our GC-MS method, the formation of both the HFB-derivative and its dehydrated form was confirmed in the PICI mode. However, heptafluoro-butyrylation of ODMV led to irreproducible derivatization results. Moreover, for the HFBI reagent the dehydrated underivatized ODMV reaction seemed to be favourable, while the HFBA derivatization led to the derivatized dehydrated ODMV molecule. However this reaction was uncomplete.

IV.4.3.2. *ADs containing a primary amine function*

Primary amines such as fluvoxamine and the metabolites desmethyl-maprotiline, as well as desmethylsertraline are all heptafluorobutyrylated as observed in the spectra by a mass gain of 196 and a retention time shift. The mass spectrum of HFB-fluvoxamine is shown in Figure IV. 11., while the spectrum of underivatized fluvoxamine was already shown in Figure IV.4.A.

Figure IV.11. Spectrum of heptafluorobutyrylated fluvoxamine
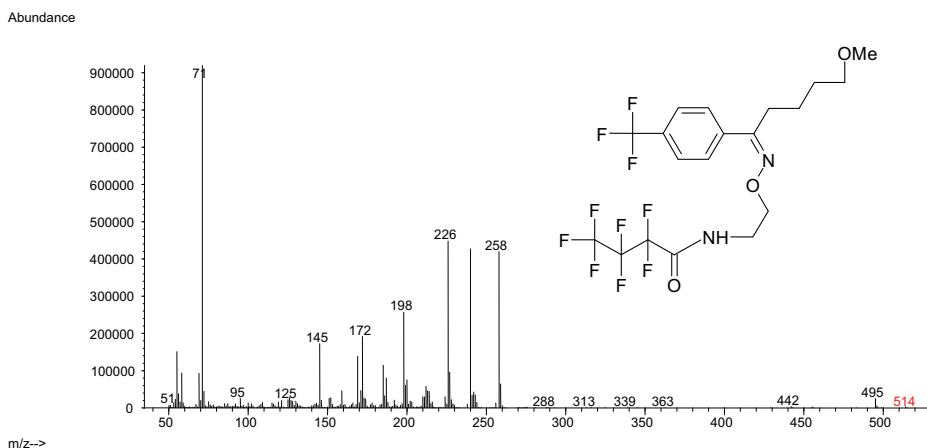
Didesmethylcitalopram is also heptafluorobutyrylated, however, a mass gain of 178 amu is observed instead of 196 amu. This phenomenon is due to water loss after the tetrahydrofurane-ring opening during fragmentation in the ion source.

Derivatization of desmethylfluoxetine with HFB-reagents probably leads to HFB-desmethylfluoxetine, but this reaction can not be confirmed using the spectra before and after derivatization as a mass gain of only 35 amu is noticed. The derivatized molecule is fragmented very easily and therefore the molecular ion is not detected (Table IV.2.).

IV.4.3.3. *ADs containing secondary amine functions*

The derivatization reaction was successful for all secondary amines, as a mass gain of 196 amu was observed in the spectra after derivatization. However, for fluoxetine a gain of 177 amu was noticed in stead of 196, due to a loss of a fluorine atom (19 amu) during fragmentation.

Figure IV.12. gives the spectrum of HFB-viloxazine as an example (underivatized viloxazine is shown in Figure IV.5.A). As demonstrated by this example, it is clear that heptafluorobutyrylation can increase the selectivity through more abundant higher m/z-fragments as compared to underivatized or acetylated viloxazine.

<u>Figure IV.12.</u> Derivatization with HFB-reagents of the secondary amines. Spectrum of heptafluorobutyrylated viloxazine
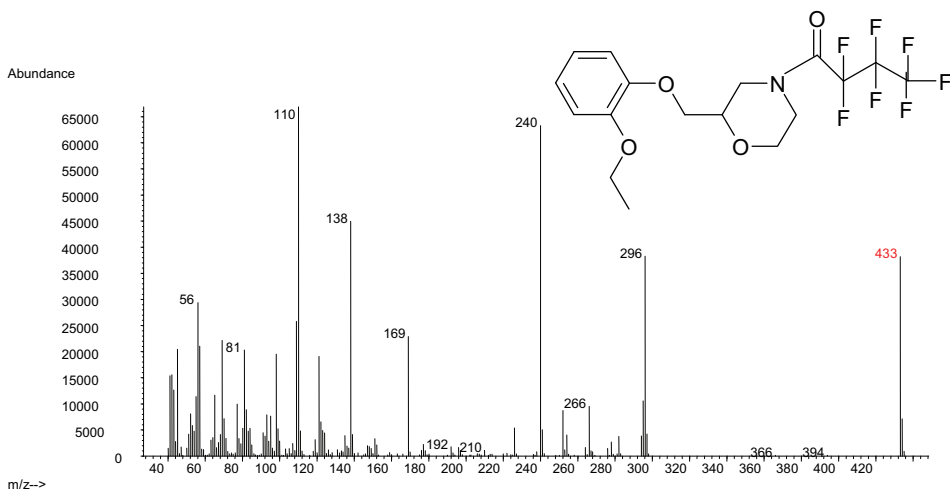
IV.4.3.4. *Tertiary amines*

Tertiary amines such as citalopram, mirtazapine, mianserin, melitracen and trazodone are not derivatized through heptafluorobutyrylation. Spectra before and after derivatization are identical for these compounds. The compounds showed no degradation under HFB-derivatization conditions.

IV.4.4. Conclusion

Most ADs and their metabolites can be heptafluorobutyrylated using 50 µl of HFBI at 85 °C during 30 minutes or 10% HFBA in toluene (100 µl) at 105 °C during 5 minutes. Heptafluorobutyrylation leads to a better peak shape for most ADs and a mass gain of the molecular ion with 196 amu (Table IV.2.).

The improved peak shape results in higher sensitivity, while the mass gain can result in higher selectivity.

While primary and secondary amines are derivatized, ADs containing tertiary amines can not be derivatized, but their peak shape is satisfactory as tertiary amines show less adsorption onto the analytical column.

Venlafaxine and its metabolite ODMV both contain an alcohol function and result in different derivatization yields when using HFBA or HFBI. Both reagents lead to dehydration of venlafaxine. ODMV is dehydrated simultaneously with a heptafluorobutyrylation of the phenolic function. However, when applying the HFBI reagent, non-derivatized but dehydrated ODMV is also observed and is even the main derivatization product.

Table IV.2. Retention time (t_r) and molecular ion of each AD before and after heptafluorobutyrylation

ADs	M^+-ion theor.	Before derivatization		After Heptafluorobutyrylation	
		t_r	M^+-ion monitored	t_r	M^+-ion monitored
		min.	amu	min.	amu
Alcohols					
Venlafaxine	277.41	16.4	277	12.6	259 (-H_2O)
ODMV	263.38	18.9	263	10.3	441 (HFB-H_2O)
				14.6	245 (-H_2O)
Primary amines					
Fluvoxamine	318.34	11.2	299	14.9	514
DMFluox	295.30	9.6	295	14.5	330
DMMap	263.38	19.6	263	21.2	459
DMSer	292.20	20.1	292	20.6	487
DDMC	296.34	20.9	296	22.7	474
Secondary amines					
Fluoxetine	309.33	10.2	309	15.9	486
Maprotiline	277.41	19.9	277	21.9	473
m-cpp	196.70	7.7	196	13.1	392
Paroxetine	329.37	22.8	329	23.2	525
Reboxetine	313.40	21.0	313	20.7	509
Sertraline	306.23	20.3	306	21.9	501
Viloxazine	237.30	10.4	237	14.5	433
DMC	310.37	21.0	310	22.7	506
DMMia	250.34	19.2	250	20.2	446
DMMir	251.33	19.9	251	20.6	447
Tertiary amines					
Citalopram	324.40	20.7	324	20.7	324
Melitracen	291.44	19.3	291	19.3	291
Mianserin	264.37	18.2	264	18.2	264
Mirtazapine	265.36	18.9	265	18.9	265
Trazodone	371.87	29.8	371	29.8	371

IV.5. Choice of acylation procedure

IV.5.1. Acetylation versus heptafluorobutyrylation

When comparing the three optimized acylation procedures, the acetylation procedure was not selected because of three reasons.

The first reason is the option of NICI monitoring. HFBI or HFBA are excellent derivatization agents for NICI as they contain seven fluorine atoms, resulting in detectability of the derivatized ADs when using this highly sensitive ionization mode. When HFB-derivatization is used, only one sample preparation would be necessary to analyze the ADs in the 3 ionization modes, namely electron ionization, positive and negative ion chemical ionization.

The second reason is the volatility of the heptafluorobutyryl-derivatives. HFB-acylation was chosen as derivatization reaction in EI as it leads to a quantitative formation of stable derivatives, which are more volatile than their acetylated forms, resulting in a considerable shorter retention time (Table IV.1. and IV.2.). Moreover, HFB-derivatization leads to enhanced sensitivity as seen in Figure IV.13.

Figure IV. 13. Comparison of an underivatized (black trace), acetylated (red trace) and heptafluorobutyrylated (green trace) ADs mix (40 ng on-column).
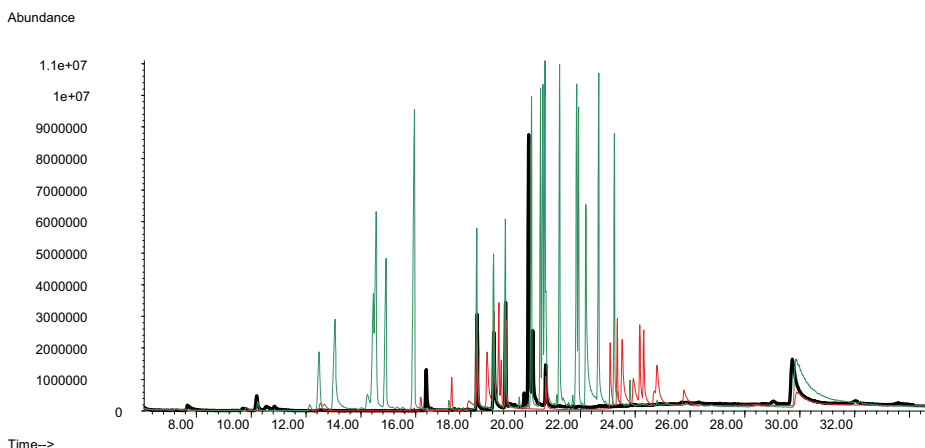
The final reason was the difference in mass gain after acetylation (42 amu) and heptafluorobutyrylation (196 amu). The shift of the main fragment ions to high mass ranges, mostly results in a lower background when analyzing biological samples. High-mass ions have greater diagnostic value, since they are more specific than low-mass ions, which can be easily affected by interference from the fragment ions of contaminants and/or column bleeding [12]. Thus a higher mass gain leads to more selectivity.

IV.5.2. Heptafluorobutyrylimidazole versus heptafluorobutyric anhydride

IV.5.2.1. *Experimental*

The optimized derivatization HFB-procedures were compared by derivatization of ADs mixtures containing 200 ng of each AD. Mianserin-d_3 was used as I.S. (200 ng) and was added before injection (before evaporating and redissolving the sample). The samples were evaporated under nitrogen and redissolved in 50 µl of toluene. The extracts were analyzed in EI in SIM mode after injection of 1 µl.

IV.5.2.2. *Results*

When evaluating both optimized derivatization procedures, the ratio between the peak area of the ADs and the I.S. as well as the variation on this ratio were compared (Figure IV.14.). A T-test was performed and a significant difference ($p \leq 0.05$) with higher ratios for the HFBA derivatization was seen for ODMV, sertraline, desmethylsertraline, fluvoxamine and desmethyl-maprotiline. For the other ADs, the ratio was higher with HFBI derivatization or not significantly different as compared to HFBA derivatization. Especially for the non-derivatized tertiary ADs, HFBA derivatization conditions resulted in a decreased signal. This decrease is observed for mianserin, mirtazapine, melitracen, and citalopram and will lead to sensitivity problems for the determination of those compounds at low therapeutic concentrations.

<u>Figure IV.14.</u> Comparison of the optimized HFBA and HFBI derivatization procedures (n = 5)

Error bars indicate ± one standard deviation
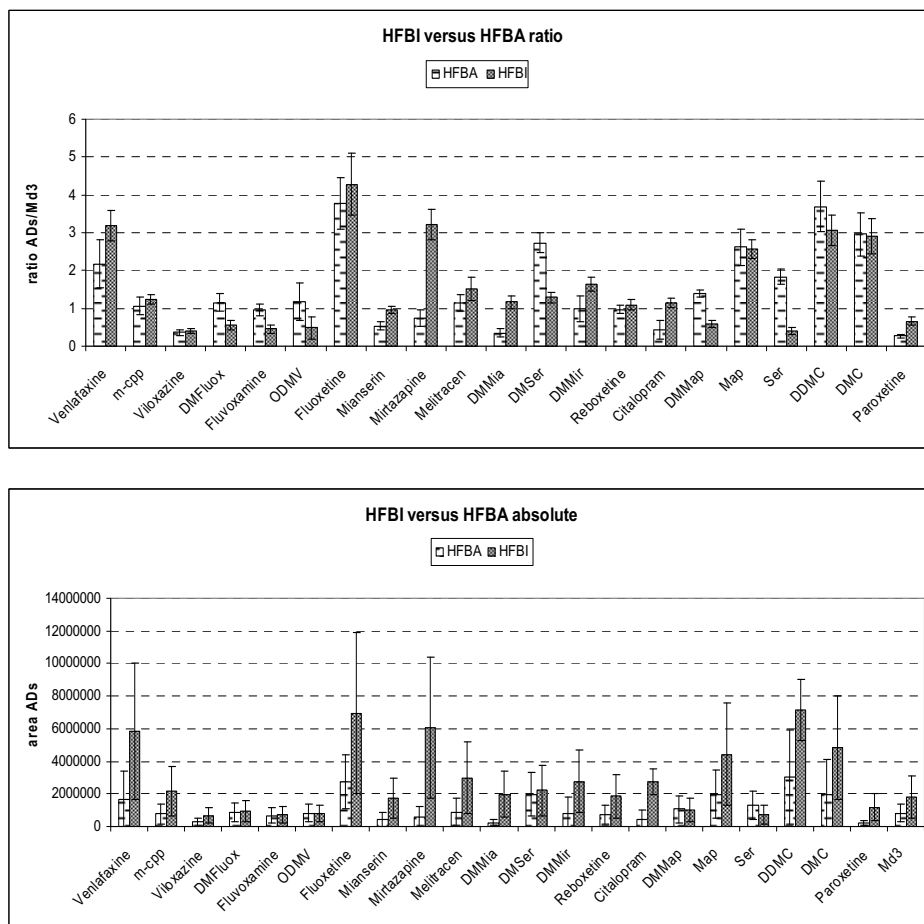
Because the I.S. mianserin-d_3 is also a tertiary amine, the ratio ADs versus I.S. will lead to a different conclusion than plotting absolute peak areas (Figure IV.14.). A possible cause of the decreased sensitivity for tertiary amines could be a decreased solubility, due to the acidic environment of the HFBA derivatization, which leads to the formation of quaternary amines that are much less soluble in organic phases. In addition, some of the acidic derivatization product may still remain in the extract, leading to degradation of the column film or activity in the injector or possible instability of the ADs. Therefore, addition of triethylamine during derivatization with HFBA was

tested to increase the reaction yield and to neutralize the acidic byproduct. For mianserin and mirtazapine slighty better results were observed, however, triethylamine was not used as it led to problems during evaporation of the HFBA extract. Addition of ammonia (5% in methanol) also resulted in higher areas for the tertiary amines. However, the yield of derivatized ADs was lower, probably due to methanol decreasing the stability of the derivatives.

Another difference between HFBA and HFBI is the way the excess of reagent is removed. Moreover, both derivatization reagents produce byproducts that need to be removed before injection onto the column. The acidic byproduct of HFBA is aggressive for the column phase. However, the byproduct and the excess of reagent can be evaporated under nitrogen after derivatization, leading to a shorter and less labour intensive derivatization. The HFBI by-product is the neutral imidazole and is not aggressive for the column. It is, however, still better to remove this byproduct and left-over HFBI to increase the sensitivity by diminishing analytical noise especially under NICI conditions. For this procedure, an extraction step with 0.5 ml of water and 2 ml of toluene is necessary, whereby the toluene is evaporated and the extract is redissolved in 50 µl of toluene before injection onto the analytical column (1 µl). This efficient clean-up procedure is, however, more time demanding. In addition, although the derivatives are stable in case of amines, they are susceptible to hydrolysis in the case of alcohols. Because of this extraction step, a difference in reaction yield is observed for the derivatization rate of ODMV when using HFBA or HFBI.

IV.5.3. Conclusion

HFB acylation was chosen instead of acetylation because it leads to a quantitative formation of stable derivatives, which are more volatile than acetyl-derivatives, resulting in a considerable shorter retention time. In addition, heptafluorobutyrylation increases sensitivity in NICI mode and results in one sample preparation for the 3 ionization modes used in GC-MS.

Both heptafluorobutyrylation reagents have their pros and cons: HFBA leads to a shorter procedure, while HFBI does not result a decreased signal for ADs

containing a tertiary amine. Because we wanted to screen and quantitate as much ADs as possible in one run, HFBI derivatization was chosen, despite the longer procedure and the pronounced hydrolysis of ODMV.

IV.6. Final derivatization procedure

The final derivatization procedure was as follows: after evaporation of the solid phase extracts under nitrogen at 40°C, 50 µl of HFBI was added and the sample was heated at 85°C for 30 min. Thereafter, 0.5 ml of HPLC-grade water and 2 ml of toluene were added. After vortexing and centrifuging the sample at 1121 g for 10 min, the toluene layer was removed and evaporated at 40°C.

IV.7. Validation of final derivatization procedure

Intra- and inter batch precision, and linearity of the derivatization reaction as well as stability of the HFB-derivatives were evaluated as these parameters are important for a successful derivatization.

IV.7.1. Precision

IV.7.1.1. *Experimental*
Precision was evaluated at three different levels, i.e. 0.2-0.4 (low), 2-4 (medium), and 5-15 ng/µl (high), depending on the compound. Mianserin-d_3 (4 ng/µl) was used as internal standard and was added before injection. Intra- and inter batch precision was assessed by five determinations per concentration in one day or on five separate days, respectively, and was measured using RSD.

IV.7.1.2. *Results*
The precision of the derivatization reaction is acceptable for most compounds. The intra- and inter batch precision of ODMV after derivatization is not acceptable for the low concentration. While citalopram has a rather high intra batch variation, the inter batch variation fulfilled the limit of 15%

RSD. The inter batch precision of fluvoxamine and desmethylsertraline was also slightly elevated.

Table IV.3. Precision data of the HFB-derivatization procedure (n=5)

	Precision (% RSD)								
	Concentration on-column (ng/µl)			Intra batch precision			Inter batch precision		
	Low	Mid	High	Low	Mid	High	Low	Mid	High
Venlafaxine	0.4	4	10	8	4	2	5	6	7
m-cpp	0.4	4	10	14	13	4	12	9	5
Viloxazine	0.2	2	5	8	7	3	14	7	3
ODMV	0.4	4	10	17	10	13	25	9	6
DMFluox	0.5	5	15	2	4	3	11	5	3
Fluvoxamine	0.5	5	15	4	5	3	17	5	3
Fluoxetine	0.5	5	15	3	5	3	8	6	4
Mianserin	0.4	4	10	4	4	3	6	4	3
Mirtazapine	0.4	4	10	2	5	6	9	5	9
Melitracen	0.2	2	5	6	3	2	5	4	3
DMMia	0.4	4	10	1	5	3	9	5	3
DMSer	0.4	4	10	4	5	3	6	18	3
DMMir	0.4	4	10	3	5	3	7	7	3
Reboxetine	0.2	2	5	4	5	3	5	5	4
Citalopram	0.4	4	10	16	3	5	14	6	4
DMMap	0.25	2.5	6	3	4	5	4	4	5
Maprotiline	0.25	2.5	6	2	5	3	7	4	3
Sertraline	0.5	5	15	2	6	3	12	4	3
DDMC	0.2	2	5	7	5	2	12	7	3
DMC	0.2	2	5	14	7	5	9	5	3
Paroxetine	0.2	2	5	4	5	2	16	4	3

IV.7.2. Linearity

IV.7.2.1. *Experimental*

The linearity of the derivatization reaction was determined by analyzing samples ranging from ± 0.2 till ± 10 ng/µl of the individual ADs. Mianserin-d_3 (4 ng/µl) was used as internal standard and was added before injection. The slope, the range for the intercept and the coefficient of determination were evaluated.

IV.7.2.2. *Results*

Overall the derivatization reaction is quantitative, leading to linear responses. For ODMV and mirtazapine the reaction is not linear as seen by their coefficient of determination 0.968 and 0.954, respectively. Mirtazapine is a tertiary amine and is not derivatized, perhaps the extraction step in toluene leads to the non-linearity. However, this is not seen for other tertiary compounds such as mianserin and citalopram. ODMV is dehydrated; perhaps

this reaction depends on the concentration of the metabolite. During validation of the method in different matrices ODMV derivatization led to irreproducible results as already discussed before.

<u>Table IV.4.</u> Linearity data of the HFB-derivatization procedure (n=5)

	Linearity				
	Slope		Y-intercept		Coeficient of determination
	best fit	cv%	min	max	R^2
Venlafaxine	0.02602	7	-0.1492	0.1071	0.997
m-cpp	0.00440	6	-0.0207	0.0051	0.997
Viloxazine	0.00124	4	-0.0032	0.0085	0.998
ODMV	0.01090	5	-0.2346	0.0171	0.968
DMFluox	0.00480	4	-0.0023	0.0079	0.998
Fluvoxamine	0.00466	4	-0.0340	-0.00004	0.998
Fluoxetine	0.01096	5	0.0492	0.0800	0.998
Mianserin	0.00512	4	0.0249	0.0462	0.998
Mirtazapine	0.01080	11	0.3748	0.4974	0.954
Melitracen	0.01494	5	0.0175	0.1232	0.997
DMMia	0.00402	4	0.0088	0.0300	0.998
DMSer	0.00964	4	-0.0621	0.0814	0.993
DMMir	0.00250	3	0.0060	0.0413	0.996
Reboxetine	0.00320	5	0.0112	0.0269	0.999
Citalopram	0.01986	4	-0.0049	0.0997	0.997
DMMap	0.01088	6	0.0138	0.0903	0.999
Maprotiline	0.00568	4	0.0397	0.0761	0.998
Sertraline	0.00502	5	-0.0538	0.0198	0.996
DDMC	0.01412	5	-0.0984	-0.0275	0.997
DMC	0.01366	3	0.0030	0.0489	0.999
Paroxetine	0.00120	6	-0.0036	0.0074	0.998

IV.7.3. Stability of the derivatives

IV.7.3.1. *Experimental*

The stability of the HFB-derivatives was evaluated by analyzing a sample at low and at high concentration directly after derivatization (day 0) and leaving that sample in the autosampler tray for four days. The peak area of the compounds was analyzed and compared each day. No internal standard was used as this could compensate for losses, leading to erroneous conclusions.

IV.7.3.2. *Results*

At low concentration, it seems that the derivatized extracts are concentrated during their stay in the autosampler tray. On day 1 a loss of 5 and 34% is observed for HFB-didesmethylcitalopram and dehydrated ODMV. The loss of didesmethylcitalopram is acceptable, but not the loss of ODMV (Figure IV.15.A).

A loss is observed for underivatized mirtazapine after 2 days. All other compounds and HFB-derivatives are stable for 4 days in the autosampler (loss below 13%). The concentration of ODMV and desmethylcitalopram seems to increase after several days. The only explanation that could be given is that degradation products of other compounds interfere in the measurement of those two compounds (Figure IV.15.B).

In conclusion, it seems that the HFB-derivatives are stable at least for 24 hours at room temperature for most compounds. The dehydrated ODMV is demonstrated to be unstable. In addition, it is susceptable to wrongful quantitation due to degradation products of other ADs.

Figure IV.15. Stability of heptafluorobutyrylated ADs at low and high concentration

A
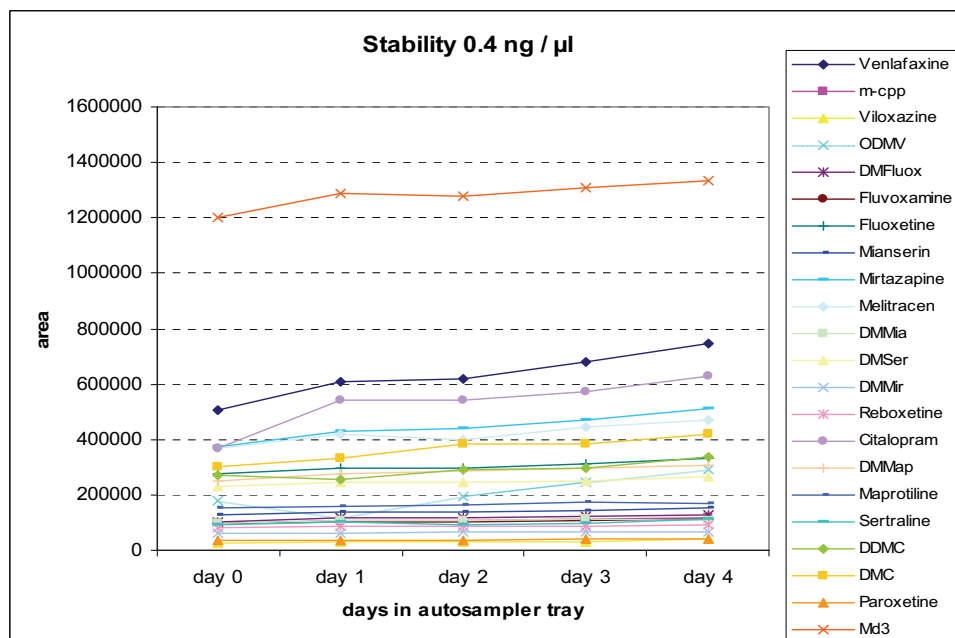
B
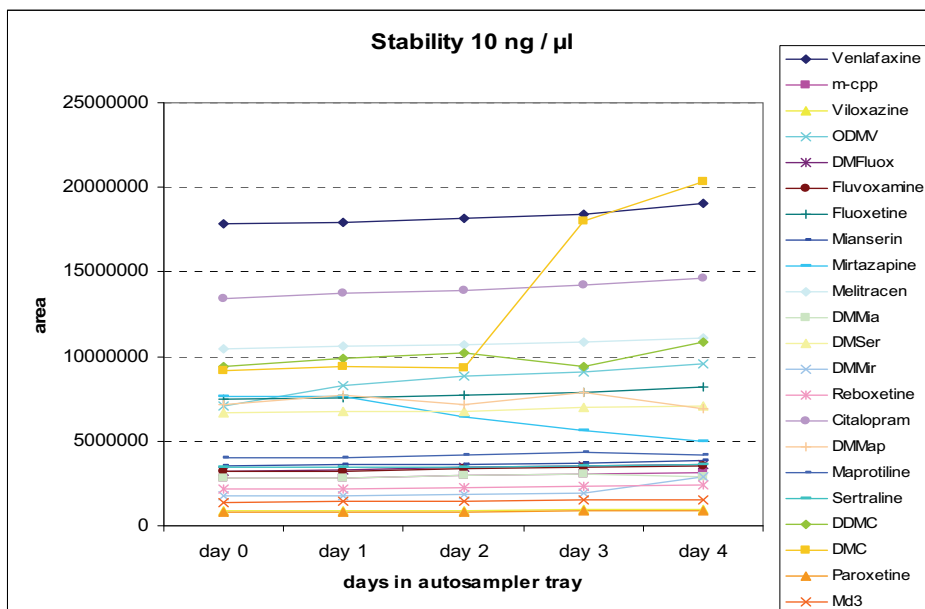
IV.8. Conclusion

In this chapter we selected the best derivatization procedure for the new generation ADs. It is, however, clear that every derivatization reaction has its pros and cons and the final choice of reagent and procedure depends on the demands of the analyst.

Structural information of the ADs led to the conclusion that acylation was a promising technique, leading to an improvement of peak shape for most ADs. The choice of acylation reagent was less straightforward.

Acylation using acetic anhydride and pyridine resulted in a good derivatization for all ADs containing primary or secondary amines. However, as a single sample preparation for three possible ionization modes including negative ion chemical ionization was required, it was not reached. Heptafluorobutyrylation was an option to avoid this drawback of acetylation. This reaction results in high sensitivity when using negative ion chemical ionization due to the addition of the seven fluorine atoms in combination with

the carbonylgroup after derivatization. Moreover, heptafluorobutyrylation led to more volatile derivatives, leading to a shorter analysis time.

Heptafluorobutyrylimidazole and heptafluorobutyric anhydride were compared as heptafluorobutyrylation reagents. Although HFBI led to a longer derivatization procedure and a clean-up step including water and toluene was necessary, this procedure was selected. The main reason was the loss of tertiary amines during the HFBA procedure due to solubility problems, leading to losses in sensitivity for citalopram, meltiracen, mianserin, and mirtazapine. However, it is clear that depending on the specific ADs and needs of the analyst, both heptafluorobutyryl reagents have their specific benefits. We selected HFBI as derivatization reagent for our further method development, because derivatization of most compounds is reproducible and resulted in stable derivatives. Moreover, a linear response was observed. Only the reaction of ODMV was characterized by various reaction products, instability and non-linearity.

IV.9. References

[1]   Blau K, King G. Handbook of derivatives for chromatography. London: Heyden, 1978, pp 576.

[2]   Watson D. Gaschromatography: a practical approach. Oxford: Oxford University Press, 1993,pp 456.

[3]   Preu M, Guyot D, Petz M. Development of a gas chromatography–mass spectrometry method for the analysis of aminoglycoside antibiotics using experimental design for the optimisation of the derivatisation reactions *J. Chromatogr. A* 1998; 818: 95-108

[4]   Preu M, Petz M. Development and optimisation of a new derivatisation procedure for gas chromatographic–mass spectrometric analysis of dihydrostreptomycin Comparison of multivariate and step-by-step optimisation procedures *J. Chromatogr. A* 1999; 840: 81-91

[5]   Maurer HH, Pfleger K, Weber AA. Mass Spectral and GC Data of drugs, poisons, pesticides, pollutants and their metabolites (Vol.2). Weinheim: Wiley-VCH Verlag, 2007, pp 201.

[6]   Maurer HH, Bickeboeller-Friedrich J. Screening procedure for detection of antidepressants of the selective serotonin reuptake inhibitor type and their metabolites in urine as part of a modified systematic toxicological analysis procedure using cas chromatography-mass spectrometry. *J. Anal. Toxicol.* 2000; 24: 340-347

[7]   Bickeboeller-Friedrich J, Maurer HH. Screening for detection of new antidepressants, neuroleptics, hypnotics, and their metabolites in urine by GC-MS developed using rat liver microsomes. *Ther. Drug Monit.* 2001; 23: 61-70

[8]   Baker GB, Coutts RT, Holt A. Derivatization with acetic anhydride: applications to the analysis of biogenic amines and psychiatric drugs by gas chromatography and mass spectrometry. *J. Pharmacol. Toxicol. Meth.* 1994; 31: 141-148

[9]   Kataoka H. Derivatization reactions for the determination of amines by gas chromatography and their applications in environmental analysis. *J. Chromatogr. A* 1996; 733: 19-34

[10]   Borrey D, Meyer E, Lambert W, Van Calenbergh S, Van Peteghem C, De Leenheer A. Sensitive gas chromatographic-mass spectrometric screening of acetylated benzodiazepines *J. Chromatogr. A* 2001; 910: 105-118

[11]   Borrey D, Meyer E, Lambert W, Van Peteghem C, De Leenheer A. Simultaneous determination of fifteen low-dosed benzodiazepines in human urine by solid-phase extraction and gas chromatography-mass spectrometry. *J. Chromatogr. B* 2001, 765: 187-197

[12]   Segura J, Ventura R, Jurado C. Derivatization procedures for gas chromatographic-mass spectrometric determination of xenobiotics in biological samples, with special attention to drugs of abuse and doping agents. *J. Chromatogr. B* 1998; 713: 61-90

Chapter V

Gas chromatographic-mass spectrometric method development

V.1. Introduction

Over the years, several chromatographic methods have been developed for the determination of antidepressants (ADs) in biological matrices. A lot of determination methods describe the analysis of one single or a mixture of a few ADs. Moreover, several multi-analysis methods are described in the literature. Chapter I gives an overview of these methods including capillary electrophoresis [1, 2], high performance liquid chromatography with UV [3-6], fluorescence [7, 8] or mass spectrometric detection [9-12], as well as gas chromatography combined with nitrogen-phosphorus [13, 14] or mass detection (GC-MS) [15-18].

Our aim was to develop a quantitative multi-ADs method for the new generation ADs and their metabolites in biological materials. The ADs monitored in this work were selected based on their importance in the 7 major AD markets (Japan, USA, France, United Kingdom, Italy, Spain, Germany) according to the Cognos Plus Study #11 [19]. In addition, the (active) metabolites were monitored as suggested by the AGNP-TDM Expert Group Consensus Guidelines [20], as metabolite/compound ratios could provide more information on the relation between plasma concentration and therapeutic effects. In conclusion, a quantitative chromatographic method was developed for citalopram, fluoxetine, fluvoxamine, maprotiline, melitracen, mianserin, mirtazapine, paroxetine, reboxetine, sertraline, trazodone, viloxazine, and venlafaxine and their metabolites (desmethyl-citalopram, didesmethylcitalopram, desmethylfluoxetine, desmethyl-maprotiline, desmethylmianserin, desmethylmirtazapine, desmethyl-sertraline, m-chlorophenylpiperazine, and O-desmethylvenlafaxine).

The method of choice was a gas chromatographic-mass spectrometric method, as it is sensitive and selective, providing the best separation power for compounds that are volatile under GC conditions. The major success of the application of modern GC in clinical and forensic toxicology is firstly due to the very high efficiencies of separation which can be achieved with capillary columns, secondly to the high sensitivity of the detection and finally to the precision and accuracy of the data from quantitative analyses of very

complex mixtures. In contrast, LC-MS methods have the great advantage that no derivatization is needed, leading to shorter sample preparation times and thus higher-throughput. However, the absence of ion suppression effect observed in LC-MS, availability, high separation power and comparative low cost of the equipment still make GC-MS instruments very attractive in many laboratories.

In this chapter, the choice of sample introduction, the parameters for the separation on the analytical column and the detector conditions will be discussed (Figure V.1.). All of these optimized parameters will result in a GC-MS method for ADs that will be evaluated and validated in chapter VI. For validation, internal standards will be used and therefore, the choice of the internal standards will also be discussed in this chapter.

<u>Figure V.1.</u> The gas chromatographic system

1, the gas supply; 2, the injector; 3, the oven containing the column; 4, the mass selective detector.
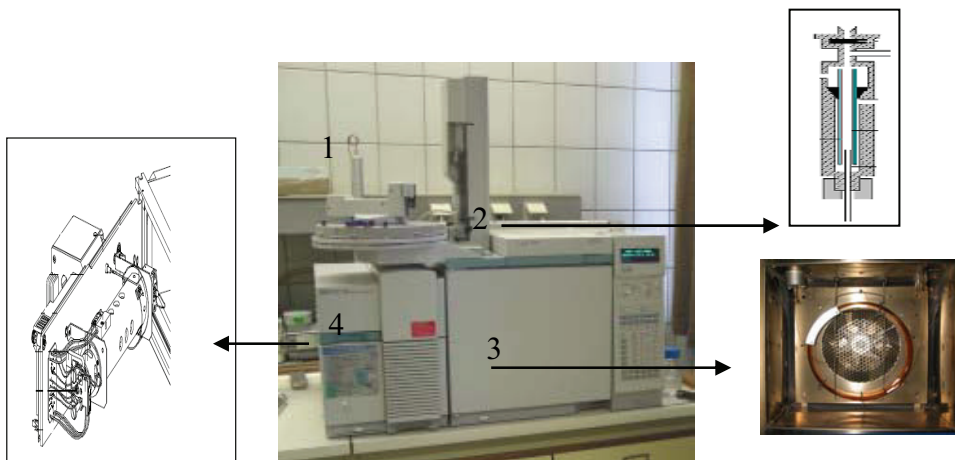
V.2. Experimental

V.2.1. Reagents

ADs standards used during optimization of the gas chromatographic-mass spectrometric method were the same as described in chapter III (III.2.1.).

Fluoxetine-d_6 oxalate (Fd_6), mianserin-d_3 (Md_3) and paroxetine-d_6 maleate (Pd_6) (100 µg/ml MeOH) were purchased from Promochem (Molsheim, France) and were used as internal standards. Toluene (Suprasolv quality, Merck, Darmstadt, Germany) and 1-(heptafluorobutyryl) imidazole (HFBI) (Fluka, Bornem, Belgium) were applied for derivatization. Vials, glass inserts and viton crimp-caps were purchased from Agilent technologies (Avondale, PA, USA).

V.2.2. Stock solutions

Stock solutions were prepared in methanol at a concentration of 1 mg/ml for each compound individually and stored at -20°C. These stock solutions were further diluted with methanol to working solutions of 0.1 mg/ml. For detection of mass spectra 20 µl of this solution was derivatized and redissolved in 50 µl of toluene of which 1 µl was injected.

The stock solutions were also used to prepare a standard mixture by mixing the individual primary stock solutions and by further diluting with methanol until a concentration of 0.05 – 0.125 mg/ml was obtained, depending on the therapeutic range of the compound. After preparation, it was stored protected from light at approximately -20°C. This mixture was used to optimize the gas chromatographic parameters. Twenty µl of this mixture was derivatized and redissolved in 50 µl of toluene of which 1 µl was injected.

V.2.3. Equipment

A HP 6890 GC system was used, equipped with a HP 5973 mass-selective detector, and a G1701DA Chem Station, version D.02.00 data processing unit (Agilent Technologies, Avondale, PA, USA). The mass selective detector was used in scan to determine the injection conditions, the separation parameters and the mass spectra.

Evaporation under nitrogen was conducted in a TurboVap LV evaporator from Zymark (Hopkinton, MA, USA). The heater was a multi-block from Lab-line (Tiel, The Netherlands).

V.3. Gas chromatographic parameters

V.3.1. Sample introduction

V.3.1.1. *Cold on-column versus split/splitless injection*

A very important step in gas chromatography is the introduction of the sample onto the capillary column. There are two basic types of injectors for capillary columns: vaporization (Figure V.2.A) and cold-on column (Figure V.2.B) [21].

Vaporization injectors include split and splitless injectors and are the most common injector types. All vaporization injectors function basically in the same manner. A syringe is used to pierce the septum and introduce the sample into the vaporization chamber. This vaporization chamber contains a heated glass liner in which the volatile components of the sample are rapidly vaporized due to the high temperature. A carrier gas line supplies carrier gas to the interior of the injector body and usually enters near the top of the injector. This carrier gas mixes with the sample vapours and the vaporized volatiles are introduced into the column by the movement of the carrier gas.

Figure V.2.   Schematic overview of vaporization (A) and cold on-column injectors

A. Split/Splitless injector

B. Cold on-column injector
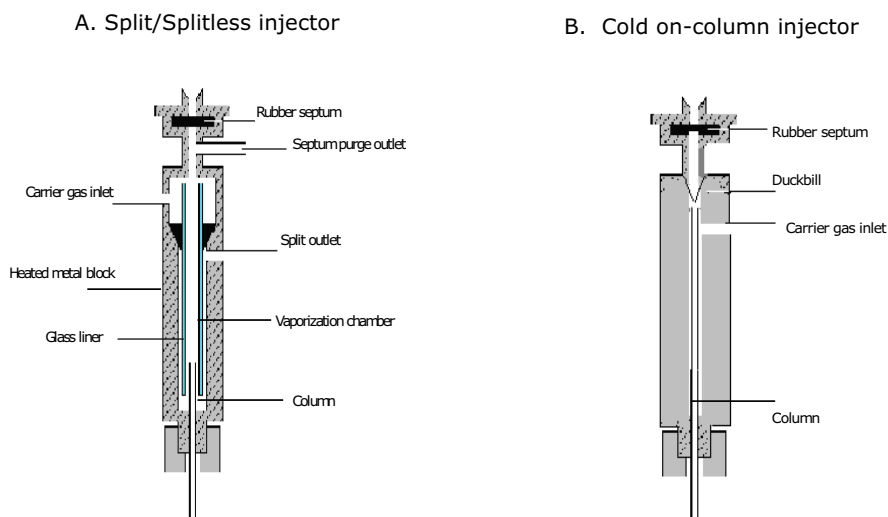
The difference between a split and splitless injector is the amount of sample introduced onto the column. While splitless injectors do not split the sample, introducing most of the vaporized sample onto the column, split injectors split the vaporized sample into two unequal portions with the smaller fraction going to the column and the larger fraction being discarded through the split outlet. The discarded fraction is determined by the split ratio. Split injectors are used for highly concentrated samples (0.1-10 µg/µl), because only a limited amount of sample finally reaches the column, preventing column overloading. Splitless injectors are, on the contrary, suitable for trace level analyses, as no portion of the sample is discarded, resulting in introduction of most of the volatiles onto the column [21, 22].

The cold on-column injector eliminates the vaporization proces as it injects the sample directly onto the capillary column. The injector is usually kept at ambient temperature since immediate sample vaporization is not required. The characteristics of a cold on-column injector make it ideal for high boiling point compounds as they are directly injected onto the column and are not vaporized. In addition, this injection technique is ideal for heat sensitive compounds. However, as the whole sample is introduced onto the column, non-volatile compounds can result in pronounced column contamination [21, 23].

Our first GC configuration contained a cold on-column injector. Although this injector resulted in highly reproducible results, it was not robust due to the use of a retention gap. The retention gap was necessary to enlarge the lifetime of the analytical column and it was connected to the analytical column by a press-fit connection. These connections can result in small airleaks if not installed properly or after several injections. In addition, matrices such as plasma, whole blood and brain tissue are dirty matrices leading to column contamination and thus a high maintenance level of the GC configuration. The major field of application of vaporization injectors, however, is the analysis of 'dirty' samples, because the involatile material is deposited inside the injector and not on the column as with cold-on column injectors [22]. Therefore, the injector type was changed to a vaporization injector. The splitless mode was preferred because of sensitivity issues as concentrations of picograms or nanograms per injection volume (1 µl) would be monitored.

V.3.1.2. *Splitless injection optimization*

Choice of injection solvent

Methanol was used as injection solvent in the beginning of our research as a lot of compounds of interest in clinical and forensic applications are easily dissolved in this rather polar solvent. Later on, toluene was used for several reasons.

First of all, the HFB-derivatives are very soluble in toluene. Secondly, the vapour volume generated by methanol is much higher as compared to toluene. This vapour volume should be taken into account when optimizing the sample introduction as a high vapour volume can lead to backflush of the vaporized sample in the injector. This backflush leads to loss of the sample and possible injector contamination. According to Grob [22], the volumes of undiluted vapour generated by 1 µl of toluene or methanol, calculated for an injector at 250 °C and a carrier gas inlet pressure of 28 kPa are respectively, 260 and 750 µl. As a result of this large difference in vapour volume, a larger volume of the sample redissolved in toluene can be injected as compared to methanol before the effect of backflush occurs. In addition, injection of 1 µl of toluene leads to a short and homogeneous flooded zone onto the apolar stationary phase, while injection of polar solvents leads to a poor wettability of the column, thus formation of droplets and a long and inhomogeneous flooded zone, which can result in peak broadening or distortion [24]. Finally, the boiling point of toluene is 110.6 instead of 64.7 °C, which leads to higher possible starting column temperatures when using a cold on-column or splitless injection technique, resulting in a shorter analysis time.

Choice of inlet liner

A splitless single tapered (taper down) inlet liner (4 mm I.D.) containing deactivated glass wool was chosen. While glass wool can lead to adsorption of some compounds, it has several advantages. If dirty samples such as plasma, blood and brain tissue extracts are injected, non-evaporating material is retained on the glass wool and will not be transferred to the column. In addition, deposition of the sample liquid onto the wool prevents wild movement through the vaporizing chamber during the vaporization of the sample.

Injection temperature

The injector temperature should be high enough to evaporate the compounds instantly without any degradation. Excessively low injector temperatures may cause incomplete vaporization of the sample, especially for high boiling compounds, leading to broad or tailing peaks and discrimination [21, 25].

The injection temperature was varied from 200 till 300 °C for the injection of an extracted sample (40 ng/µl for each AD; n=3).

As depicted in Figure V.3., 200 °C was adequate for full vaporization of most compounds. However, for the high boiling compounds, such as trazodone, 300 °C resulted in a faster evaporation and thus a better sample transfer onto the column. Therefore, an injection temperature of 300 °C was chosen for our final analysis.

Figure V.3.   Influence of injection temperature on sample transfer onto the column. Errorbars indicate ± one standard deviation
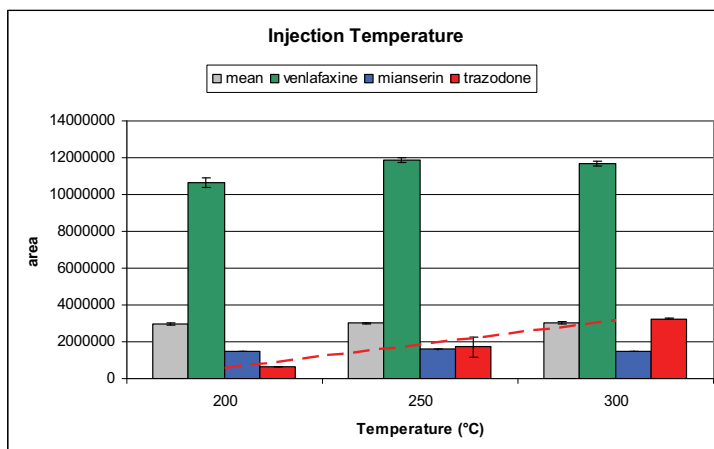
Inlet Pressure

The inlet pressure during injection is important for a rapid transfer of the vaporized sample into the column. A rapid sample transfer results in a high efficiency and less sample backflush. According to Grob [22], the vapour plug in the liner is steadily growing during sample transfer as a result of diffusion. At low gas flow rates, this broadening is more pronounced than the transfer to the column. This effect leads to incomplete sample transfer and broad

peaks. High carrier gas flows create a rapid sample transfer and a short initial sample band onto the column leading to narrow peaks. Therefore, it would be interesting to use high carrier gas flows. However, a continuous high carrier gas flow will result in high carrier gas linear velocities and thus reduced resolution. As a result, the carrier gas pressure is increased during injection, and thereafter reduced to an ideal gas flow during separation of the sample compounds on the column. This short pressure increase during injection is called pulsed injection [21].

Pulsed splitless injections with very high flow rates improve sample transfer dramatically, however, because column flow rates are much less for a gas chromatograph with mass spectrometric detection, the improvements with pulsed injection are less drastic for these GC-MS configurations [22, 26]. The pulsed splitless injection also leads to a shorter residence time in the liner, leading to less time for adsorption onto the active sites in the injector and less time for degradation of the analytes.

Pulsed splitless injection can also result in less matrix-induced response enhancement. Erney et al. [27] and Poole [28] describe the increase of sample transfer from hot vaporizing injectors because of matrix compounds as these reduce the thermal stress and mask active sites in the injector responsible for adsorption and decomposition of the monitored analytes. This is a problem that mostly occurs for thermally labile compounds and compounds that are predisposed to adsorb on surfaces encountered by the sample during its transfer to the column. Because pulsed splitless injection leads to shorter contact time between sample and active sites in the injector this matrix enhancement is reduced. In contrast, Grob [22] describes a response decrease due to the matrix and residual 'dirt' in the injector because of evaporation problems. It is thus clear that the matrix-effect in the vaporization injector is not straightforward and a pulsed injection will not always diminish these problems. Therefore, all our sample calibration will occur in the same matrix as the actual samples and the pulsed splitless injection was mainly used to provide rapid sample transfer to the column and thus lead to sharper peaks in the chromatogram.

For the optimization of the inlet pressure, a mixture of ADs (40 ng/µl) was extracted from plasma and derivatized before injection at various inlet pressures from 10.7 (1.3 ml/min He flow) to 30 psi. When comparing the

areas at different inlet pressures, an increase of compound transfer onto the column is seen for the high boiling compounds as demonstrated in Figure V.4. An inlet pressure of 25 psi was selected as this led to less discrimination of the high boiling points and to a smaller variation as compared to 30 psi.

Figure V.4. Influence of inlet pressure during splitless injection

Errorbars indicate ± one standard deviation
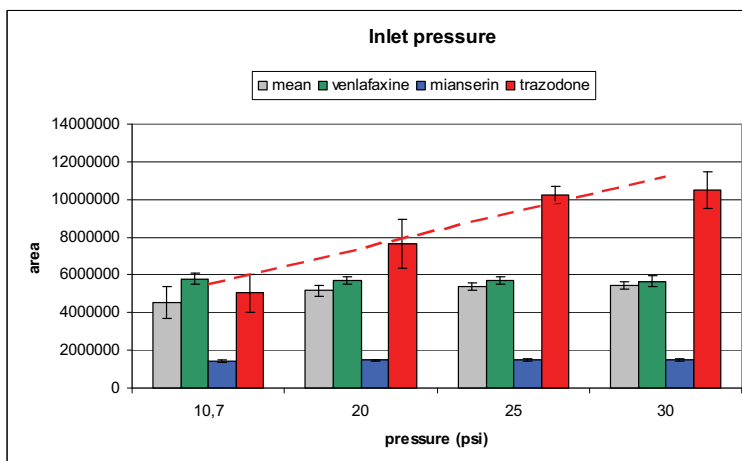
Purge activation time

During splitless injection, purge and split valves are closed, to ensure that the sample mixed with carrier gas will flow into the column. After a certain time, the valves are opened and the carrier gas flow that previously flowed into the column, will now be swept out of the injector through the slit line. The purge activation time, the time whereafter the purge of the splitless injector is opened, needs to be chosen carefully as a short purge activation time will lead to sample loss, while too long purge activation can result in an increased solvent front, a higher ratio of compound degradation and adsorption. The best purge activation time depends on the carrier gas flow rate and the volatility of the sample compounds. Typical purge activation times are 15-90 seconds [21, 22].

The purge activation and splitless activation time was optimized. ADs (40 ng/ µl) were injected after sample preparation with a purge activation time of 0.5-1.5 minutes. These conditions were chosen by calculating the theoretical

purge activation time. The purge activation time should occur when at least 1.5 volumes of carrier gas have swept the injector. The sweep rate of the liner is calculated by deviding the liner volume (1.01 cm^3) through the column flow rate (2.6 ml/min during injection). The sweep rate is 0.39 minutes or 23 seconds, thus as a result the purge activation time should be at least 35 seconds [21]. A purge activation time of 1 minute was selected experimentally, because no gain in peak area was observed after 1.5 minutes (Figure V.5.).

Figure V.5. Influence of purge activation time during splitless injection (n=3) Errorbars indicate ± one standard deviation
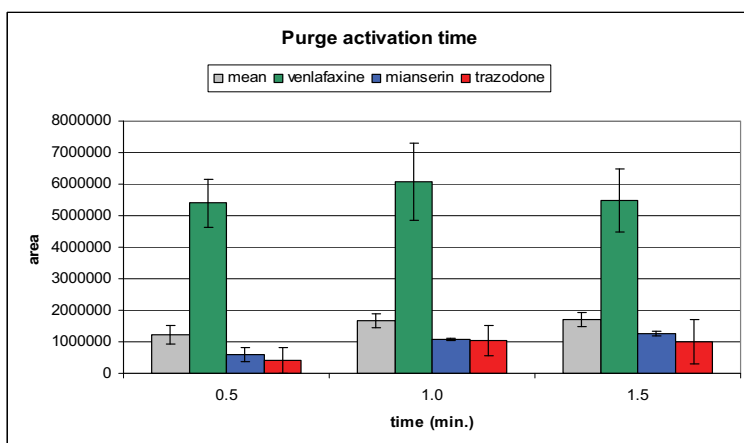
Pulse time

The pulse time is a parameter that must be optimized when applying a pulsed splitless injection type. It is the time whereafter the inlet pressure is dropped to the carrier gas pressure necessary for the separation step. During injection the pressure is high to ensure almost complete and fast sample transfer onto the column. However, this inlet pressure will create a too high linear velocity and thus less resolution. Therefore a time is set at which the pressure is decreased.

The pulse time should be 0.1 to 0.5 minutes longer then the purge activation time [29]. Therefore, a pulse time of 1.1 and 1.5 minutes was tested during the injection of a mixture of ADs (40 ng/µl).

Especially for the high boiling compounds an increase in signal was observed if the inlet pressure stayed high for 1.5 minutes. As a result, the pulse time was set for that period.

Figure V.6. Influence of pulse time during splitless injection (n=3)
Errorbars indicate ± one standard deviation
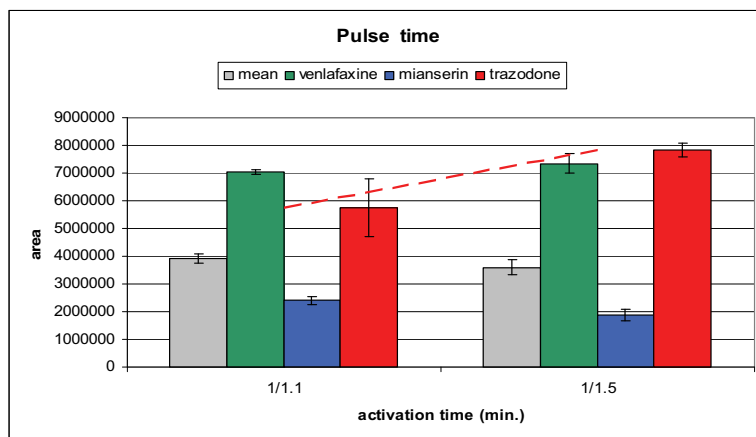
V.3.2. Chromatographic separation

The chromatographic separation of the ADs mixture occurs on a capillary column residing in an oven whose temperature is controlled. The vaporized compounds move through the column at the same rate as the carrier gas. However, as the column wall is coated with a thin film of polymeric material (stationary phase) compounds will react in a different way with this film, resulting in a slowed down movement of the compounds. This retention onto the column will be different for each compound due to their differences in chemical structures and physical properties. In addition, the length and diameter of the column, the chemical structure and amount of stationary phase, the column temperature all will affect the compound retention. As result each compound will leave the column at a different time and will be measured separately by the detector.

V.3.2.1. *Column choice*

The 5% phenylmethylpolysiloxane phase was applied as it is the most common general purpose column which is used a lot in clinical and forensic routine laboratories. Non-polar stationary phases are preferable to use, because they have higher maximum temperatures, are more durable, and result in less column bleed. The 5% phenylmethylpolysiloxane phase will interact with the ADs through strong dispersion interaction and a weak hydrogen bonding interaction. Dispersion is the primary separation mechanism and it is related to the intermolecular attraction between the compound and stationary phase. The polarization property of the compound and its solubility in the stationary phase plays a major role in this type of interaction. This interaction can be related to the vapour pressure of the compound, or simplified to the boiling points of compounds: the higher the boiling point of a compound, the more retention onto the column. Due to the 5% of phenyl groups onto the methylpolysiloxane backbone, hydrogen bonding can also occur with the ADs containing amine functions.

The capillary column dimensions selected were the standard dimensions. A column length of 30 meter results in a good resolution and acceptable retention times. The column has a diameter of 0.25 mm, which is the largest diameter that can be applied for GC-MS systems because the mass spectrometer has a maximum pumping capacity of 1-2 ml/min carrier gas. Carrier gas volumes of columns with inner diameters of 0.32 mm or greater exceed this flow rate. Columns with internal diameters smaller than 0.25 mm result in higher efficiency and resolution, however, the column capacity will decrease. A 0.25-mm ID column was chosen as this column still has an acceptable efficiency and resolution, but also has a higher capacity range [21, 30]. The film thickness of the stationary phase is 0.25 µm, resulting in a high efficiency, an acceptable capacity and acceptable column bleed. Thinner column films whould result in higher efficiencies and shorter retention times, however, slightly thicker films shield compounds from active sites on the surface of the tubing, reducing peak tailing [21].

In conclusion, a "common" column was used due to practical considerations in a routine forensic and clinical laboratory. This column was a 30 m x 0.25 mm I.D. x 0.25 µm film 5% phenylmethylpolysiloxane column (5-MS J&W column from Agilent technologies, Avondale, PA, USA). On this column

several analyses can be performed without a column switch. This reduces the number of columns needed, and thus reduces complexity and cost. Of course some dimensions could be better to create a higher throughput (filmthickness, I.D., column length). However, the column that was chosen provides acceptable retention, separation and peak shape.

V.3.2.2. *Choice of carrier gas and flow rate*

Helium was provided as carrier gas for the GC-MS configurations in our laboratory. A constant helium flow rate was prefered over a constant pressure of the carrier gas during analysis due to the sensitivity of mass selective detectors to flow changes. A constant flow helps to establish a constant pressure in the mass ion source, thereby normalizing ion fragmentation patterns across the range of column temperatures [31].

The flow rate was chosen according to the Van Deemter curve and the speed of analysis. The recommended average linear velocity of helium in our analytical column (30 m, 0.25 μm film, 0.25 mm I.D.) ranges from 30-40 cm/sec [21]. Therefore, the flow rate was varied from 0.7-1.6 ml/min. A flow of 0.7 results in a linear velocity of 31 cm/sec for our analytical column, which is near the minimum of the Van Deemter curve, leading to the best separation power. A flow of 1.6 ml/min results in a linear velocity of 47 cm/sec and leads to shorter retention times onto the column, but results in less resolution. Finally, a constant flow rate of 1.3 ml/min was chosen as this resulted in an acceptable separation for most compounds and an exceptable analysis time for the late eluting compounds such as trazodone.

V.3.2.3. *Optimization of temperature program*

In common practical gas chromatographic separations using splitless injection as sample introduction, the sample is introduced at a column temperature below the boiling point of the solvent. Under these conditions, the injected vaporized sample will condense and form a liquid droplet on the column, which then forms a flooded zone that is short and homogeneous. As the column temperature is increased, the solvent starts to evaporate from the front of the flooded zone. Eventually, only a small droplet of solvent remains at the end of the flooded zone which traps the highly volatile compounds. When the solvent and highly volatile solutes have started their

chromatographic process, the moderately volatile and high-boiling compounds are distributed over the length of the original flooded zone. They are dissolved in the stationary phase as long as the column temperature is low. As the column temperature is increased, they will evaporate, and chromatography will start over the length of the flooded zone. The length of this zone will determine the initial band width: short flooded zones mean small initial bands and no broadening. Long and inhomogeneous zones mean large initial bands and peak broadening. For an effective solvent effect of the low-boiling compounds, the initial oven temperature should be at least 20 °C lower than the boiling point of the solvent. For effective thermal focusing of high-boiling compounds, the initial oven temperature should be at least 80 °C lower than the elution temperature of the solutes [24].

In our case, an initial column temperature of 90 °C was chosen to create a small flooded zone after injection of 1 µl of toluene, as this temperature is 20°C lower than the boiling point of toluene. In addition, most compounds start to elute at about 180 °C, and this is 90 °C higher than the starting conditions, resulting in a thermal focusing effect of these compounds.

The dependence of GC retention on vapour pressure means that mixtures containing compounds with a wide range of boiling points cannot be separated satisfactory in an isothermal run. The more volatile components may be well enough resolved, but the higher boiling materials will only be eluted with long retention times and very broad peaks [30]. Due to the choice of the temperature gradient the analysis time was reduced and a better peak shape and detection was observed for the late eluting compounds such as paroxetine and trazodone [32]. Several temperature gradients were applied for the ADs mixture and the final temperature program was as follows: the initial column temperature was set at 90 °C for 1 min, ramped at 50 °C/min to 180 °C where it was held for 10 min, whereafter the temperature was ramped again at 10 °C/min to 300 °C (5'). However, chromatographic problems were observed for trazodone during further analysis and therefore the run-time during validation was shortend by cooling the column down directly after it reached the temperature of 300 °C. Trazodone did not elute in a reproducible way from the column (sometimes it eluted, sometimes not) probably due to adsorption onto the liner, inlet seal, and onto the aging column.

<u>Figure V. 7.</u> Chromatographic separation of 13 new generation ADs and 8 of their metabolites

Compounds indicated in red are not fully separated. Compounds in order of elution are venlafaxine, m-cpp, norfluoxetine, viloxazine, fluvoxamine, fluoxetine, mianserin, mirtazapine, melitracen, DMMia, DMMir, reboxetine, DMSer, DMMap maprotiline, sertraline, DDMC, DMC, paroxetine, and trazodone
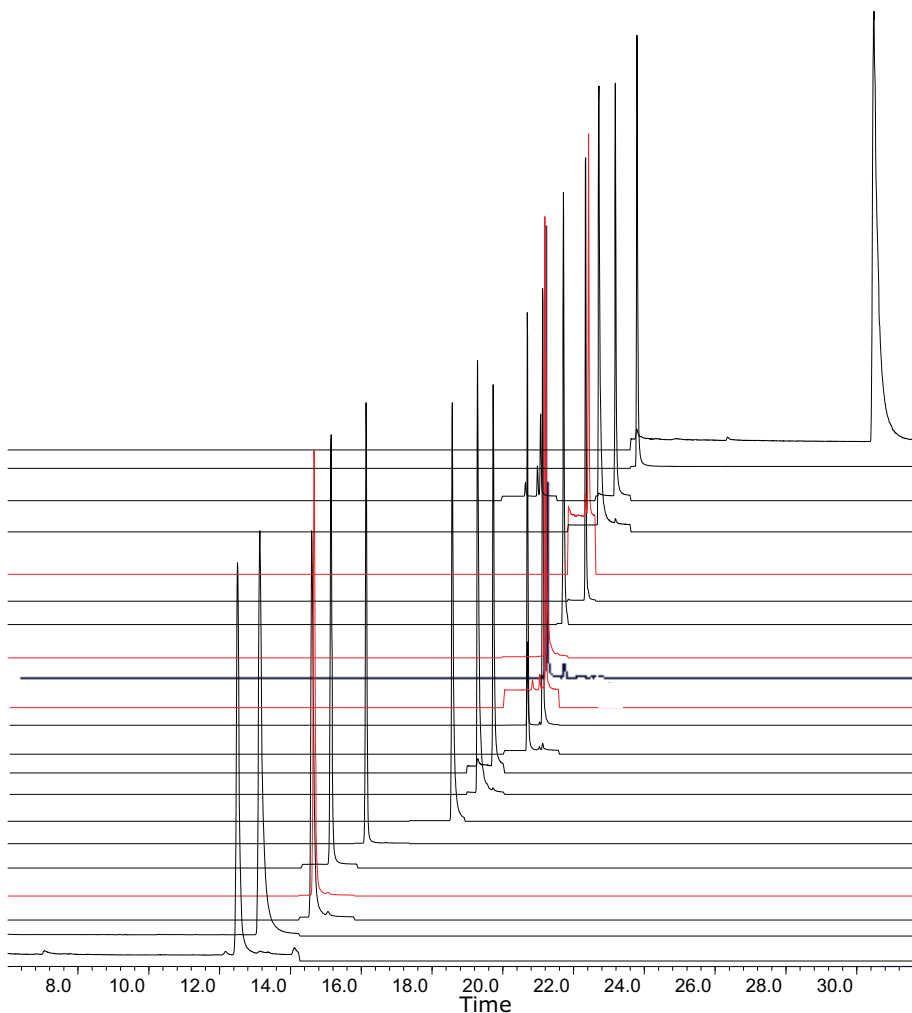
Figure V.7. shows the compounds in order of their retention times. Not all compounds are base-line separated. Viloxazine and desmethylfluoxetine coelute, while desmethylsertraline, desmethylmirtazapine, reboxetine and citalopram elute very close to each other. Maprotiline and sertraline also have a slight overlap. Although a base-line separation is still state of the art, due

to the selectivity of the mass spectrometer it is not necessary. The monitored ions for each ADs are specific and different from the overlapping compounds. Therefore, the separation problems do not result in identification or quantification problems. In addition, when analyzing 'real' samples, the problem of co-eluting peaks will be rather rare.

V.3.3. Internal standard choice

Choosing the appropriate internal standard is an important aspect to achieve acceptable method performance. Ideally, isotopically labelled internal standards for all analytes should be used, but only fluoxetine-d_6 oxalate, maprotiline-d_3, mianserin-d_3, and paroxetine-d_6 maleate were commercially available during our method development period. However, before a deuterated analogue can be used as internal standard, the mass spectrum must be evaluated for 'cross' contribution. Due to ionization, the deuterated I.S. can produce the same fragment ions as the parent compound, leading to wrongful quantification.

Table V.1. Choice of internal standard

	I.S. choice		
	Fluoxetine-d_6	Mianserin-d_3	Paroxetine-d_6
Structural analog	Fluoxetine DMFluox	Mianserin DMMia Mirtazapine DMMir	Paroxetine
Retention time	m-cpp Viloxazine Fluvoxamine	Melitracen	Reboxetine Citalopram DDMC DMC Sertraline DMSer Maprotiline DMMap
Variation and reponse ratio		Venlafaxine ODMV	

Maprotiline-d_3 was not useful as it fragmented easily in EI-mode to the ion with m/z 445, which was the molecular and quantifier ion of maprotiline.

Therefore, only 3 I.S.s were used for the validation process. The I.S.s used, were selected on structural analogy (deuterated versus their cold products), retention time, and on base of the response ratio of the compound versus I.S. and its variation. In addition, for the metabolites always the same I.S. was used as for the parent compound. A concentration of 200 ng/ml of each I.S. was chosen as this concentration was in the mid range of the monitored therapeutic window.

V.3.4. Conclusion: gas chromatographic method

During optimization of the gas chromatographic method a lot of attention was paid to the sample introduction. Splitless vaporization injection was chosen due to sensitivity and robustness concerns. However, as incomplete sample transfer from the injector liner to the column, discrimination, and poor peak focussing on the top of the column are the most widely observed problems in splitless injections, this injection type was evaluated concerning inlet temperature, purge activation time and inlet pressure to ensure minimal negative effects. In order to accelerate and maximize the sample transfer, a pulsed splitless injection was selected in which the high inlet pressure was used to increase the mass transfer to the column and to reduce the band spreading. In addition, an initial oven temperature was selected 20 °C lower than the boiling point of the solvent, resulting in accelerated sample transfer due to the vacuum created upon recondensation of the solvent in the column and a better peak shape due to solvent trapping. The discrimination of high boiling compounds was diminished due to optimization of the injection temperature, the purge activation time and an increase in inlet pressure.

The separation occurred on a non-polar 5% phenylmethylpolysiloxane column with general purpose dimensions to avoid GC-MS downtime due to column switching in the forensic or clinical routine laboratory. Although not all compounds were base-line separated, the choice of column and temperature program resulted in adequate separation and an acceptable retention time for most compounds. Although a lot of parameters were optimized for high boiling point compounds such as trazodone, this compound did not lead to

reproducible chromatographic results. Trazodone demonstrates adsorption probably onto an older column, a 'dirty' liner and probably onto the inlet seal. Therefore, this compound was not monitored during validation.

The final gas chromatographic method conditions were as follows: the pulsed splitless injection temperature was held at 300 °C, while purge time and injection pulse time were set at 1 and 1.5 min, respectively. Meanwhile, the injection pulse pressure was 25 psi and 1 µl of the sample, redissolved in 50 µl of toluene, was injected. Ultrapure Helium with a constant flow of 1.3 ml/min was used as carrier gas. Chromatographic separation was achieved on a 30 m x 0.25 mm i.d., 0.25-µm J&W-5ms column from Agilent Technologies (Avondale, PA, USA). The initial column temperature was set at 90 °C for 1 min, ramped at 50 °C/min to 180 °C where it was held for 10 min, whereafter the temperature was ramped again at 10 °C/min to 300°C. The separation of the ADs and their active metabolites was achieved in 24.8 minutes.

V.4. Mass spectrometric parameters

Once the compounds are separated on the GC capillary column, the vaporized compounds leave the column and enter the mass selective detector (MSD). The mass analyzer will ionize the sample, filter the ions and finally detect the ions. The mass analyzer consists of three essential parts: the ion source, the quadrupole and the detector (Figure V.8.).

The sample molecules will first enter the ion source, which is the part of the analyzer where sample molecules are ionized and fragmented. There are different types of *ion sources* as vaporized sample compounds can be ionized and fragmented using electron ionization or chemical ionization. An ion source that operates by electron ionization (EI) will ionize and fragment sample molecules through high energy electrons (70 eV) emitted by a filament. In the chemical ionization (CI) modes the energy of the fragmentation reaction is diminished by adding a reaction gas such as methane (133 Pa) into the ion source. This reagent gas is ionized in electron ionization to the primary ions $CH_4^{+\cdot}$ and CH_3^+. These primary ions react with

the excess of methane to give secondary ions which will then react with the sample molecules [33]. Thus in chemical ionization modes bimolecular processes are used to generate analyte ions and involve the transfer of an electron, a proton or other charged species between the reactants. After the ionization step in EI or CI, the voltage on the repeller will then push the ions through several electrostatic lenses that will lead the ions in a thight beam towards the mass filter (Figure V.9.).

Electron ionization is the traditional method as toxicological libraries use this 70 eV EI mode. However, EI mass spectra suffer from frequent absence of the molecular ion due to extensive fragmentation. Chemical ionization is a softer ionization technique and often results in highly abundant quasi-molecular ions.

Figure V.8. Mass analyzer consisting of an ion source, quadrupole mass filter, detector and heaters (adapted from Agilent Technologies)

Mass filter contact

Mass filter cable kit

Mass filter heater assembly

Ion source (inside radiator)

Source heater assembly

Magnet assembly

Repeller

Feedthrough board
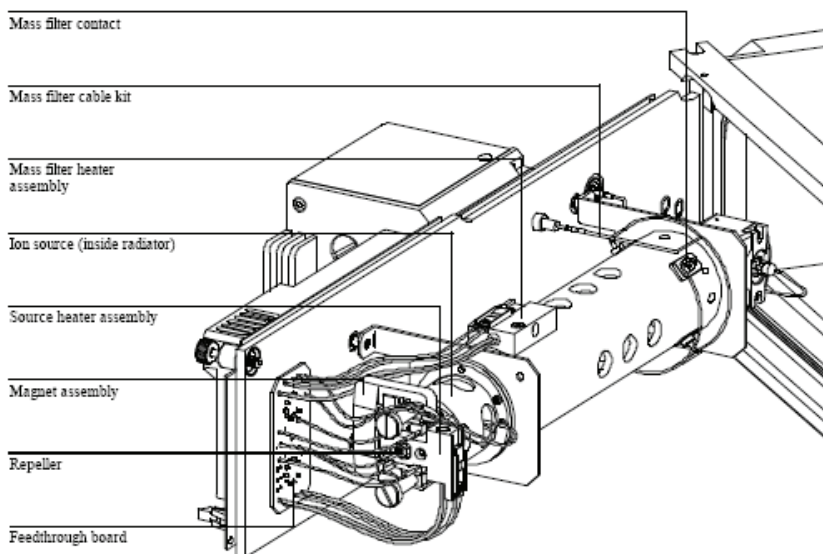
<u>Figure V.9.</u> Disassembly of an EI ion source (adapted from Agilent technologies)
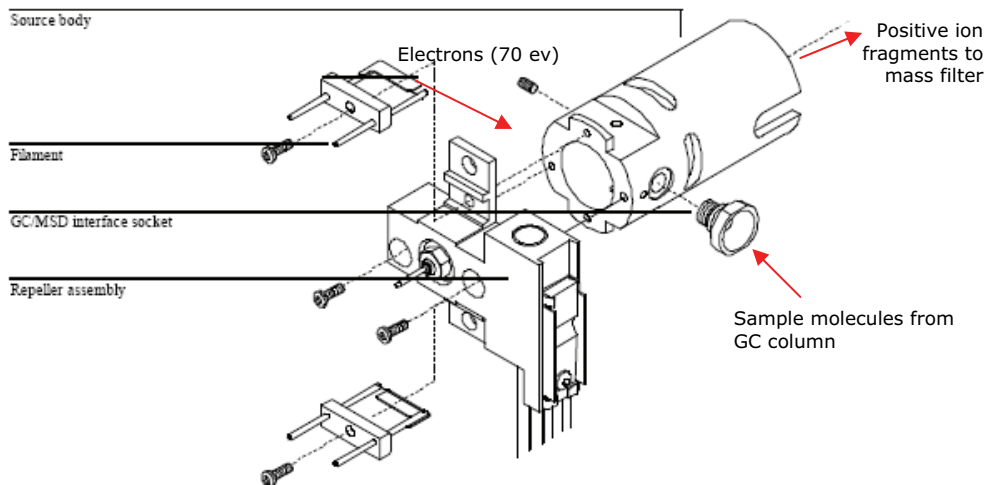
The mass filter, which is a quadrupole in our GC-MS configuration, filters and separates ions according to their mass-to-charge ratio (m/z). The quadrupole consists of four hyperbolic surfaces creating a complex electric field necessary for mass selection. The mass filter can work in scan mode, monitoring a whole range of m/z values, or in selected ion monitoring (SIM) mode, whereby only a few selected m/z values are measured (Figure V.10.).

Once the fragments pass the quadrupole, they reach the detector which consists of a *high energy conversion dynode* coupled to an *electron multiplier*. The high energy dynode attracts the positive ions and when a positive ion hits the dynode, electrons are emitted. These electrons are attracted to the positive electron multiplier horn, in which they cascade through, liberating more and more electrons as they go. At the end of the horn, the current generated by the electrons is carried towards a signal amplifier board and towards the data processor (Figure V.10.).

<u>Figure V. 10.</u> Fragment selection through mass filter and detection

1: quadrupole mass filter; 2: high energy dynode; 3: electron multiplier
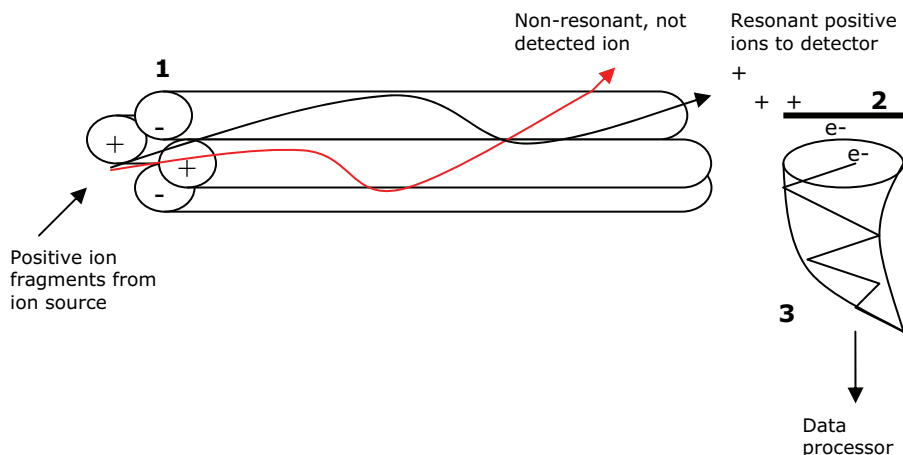
V.4.1. Optimization of mass selective detector parameters

The mass parameters for the electron ionization mode (EI) were not optimized, as the 'traditional' conditions in which the spectra of the commercially available libraries were obtained were chosen. In EI, the mass-selective detector temperature conditions were 230 °C for the EI-source, 150 °C for the quadrupole and 300 °C for the transferline, whereas an electron voltage of 70 eV was used.

For the chemical ionization modes another ion source was used and parameters such as temperature of the source and quadrupole were optimized. The manufacture guidelines were followed and the abundances of the quasi-molecular ions were compared. The mass selective detector temperature conditions in positive ion chemical ionization (PICI) were as in EI, except for the ion source temperature, which was 250 °C. The methane reagent gas entered the ion source at a constant flow of 1 ml/min. For the MSD conditions in negative ion chemical ionization (NICI) special attention was paid to optimize ion source temperature and ion focus potential as these parameters have the most effect on the abundance of the molecular ions in

NICI mode [34]. For NICI-mode the transferline was kept at 280 °C, the ion source at 150 °C and the quadrupole at 106 °C, with an electron energy of 170 eV. The electron emission (100 µA) was optimized to give best peak intensity, as this parameter is compound specific. Methane was used as reagent gas with a flow of 2 ml/min.

Parameters for the repeller, ion focus and entrance lens were not optimized, but adapted as indicated by the weekly tuning reports.

V.4.2. Spectra of the derivatized ADs after electron ionization

The result of the impact of the high-energy electron beam onto molecules in vapour fase results in a spectrum of positive ions separated on the basis of mass/charge (m/z). The positive fragment ions in combination with the molecular ion will be plotted against their abundance and these spectra exhibit a characteristic pattern for each specific compound. The spectra obtained in the electron ionization (EI) mode give structural information and it is the traditional ionization technique applied in chromatographic methods for comprehensive screening procedures in clinical and forensic toxicology. Because of the robustness of the system, ionization occurs very precise, allowing identification of unknown compounds by comparison of their mass spectrum with a large collection of reference mass spectra in commercially available libraries.

In this paragraph, the spectra for the different (heptafluorobutyrylated) ADs obtained in EI are shown. The spectra were obtained in scan mode, and the selected fragments (V.4.5., Table V.1.) for the selected ion mode will be discussed.

V.4.2.1. *Venlafaxine and O-desmethylvenlafaxine*
The fragments selected for venlafaxine were m/z 259, the molecular ion of the dehydrated venlafaxine molecule, 121 and 58. The last two fragments are not specific as demonstrated in Figure V. 11. The fragment with m/z 58 was chosen as quantifier due to its high abundance. HFBI derivatization of O-demethylvenlafaxine leads to a dehydrated product and a derivatized

dehydrated product. Both of these products are severly fragmented in EI, especially to the highly abundant m/z 58 ion that is typical for dimethylated tertiary amines.

<u>Figure V.11.</u> Spectra and fragmentation pattern of venlafaxine (A) and O-desmetylvenlafaxine (B) after HFB-derivatization
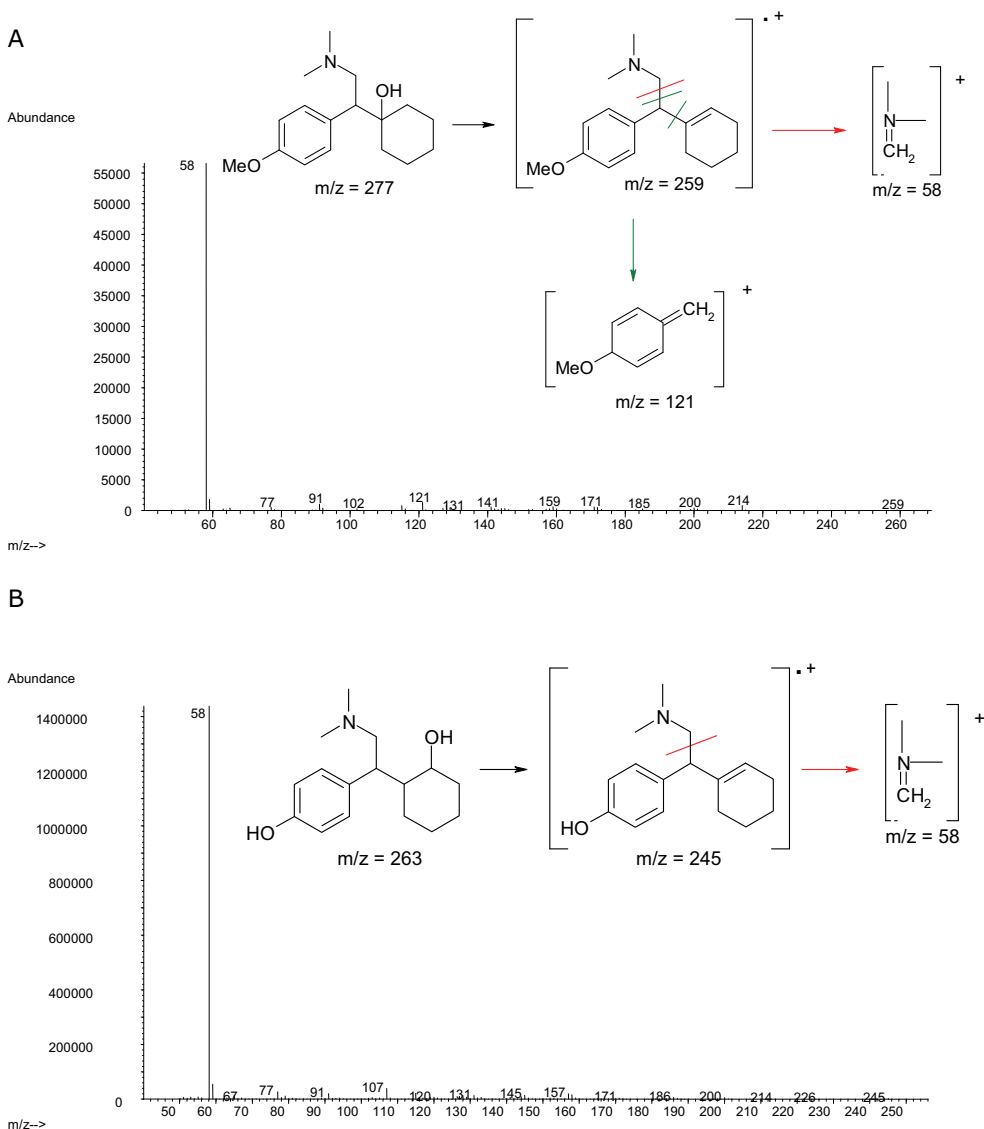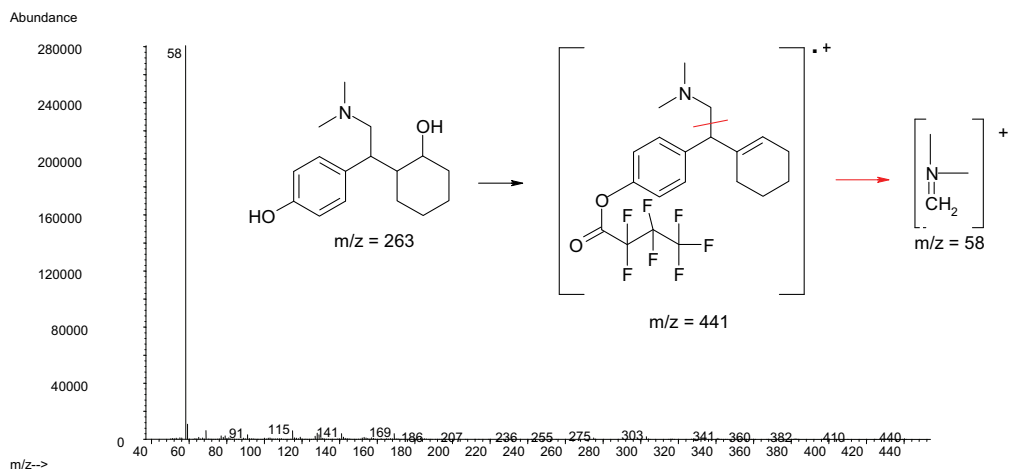
V.4.2.2. *Viloxazine*

Heptafluorobutyrylated viloxazine has a high abundant molecular ion at m/z 433 even when using EI. Fragment m/z 296 is formed by a heterolytic cleavage of the O-C binding indicated by the red trace in Figure V.12. The fragment m/z 240 is probably a result of two homolytical cleavages (demonstrated by the green trace) due to the oxygen and nitrogen heteroatoms in the ringstructure, finally resulting in a positive charge on the nitrogen atom.

Figure V.12. Spectrum and fragmentation pattern of HFB-viloxazine

Abundance
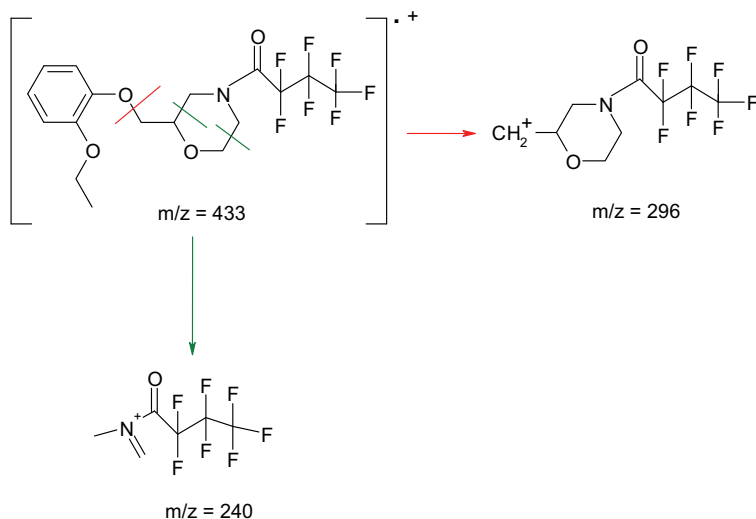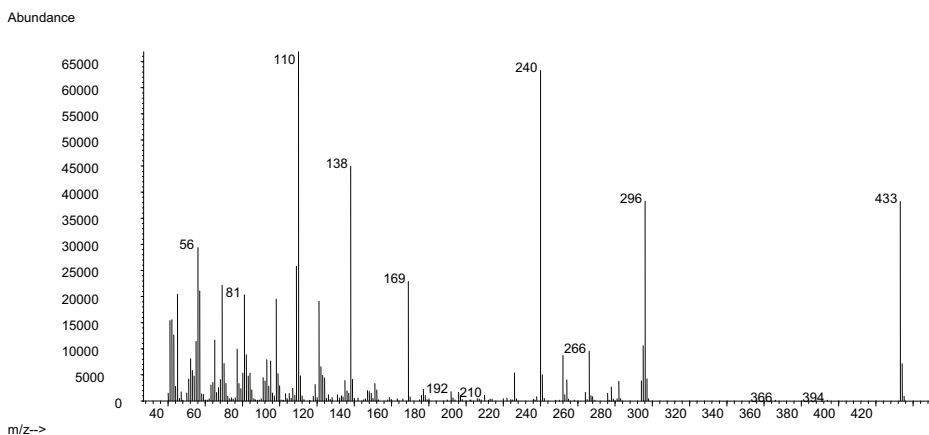
V.4.2.3. *Fluvoxamine*

<u>Figure V.13.</u> Spectra and fragmentation pattern of HFB-fluvoxamine
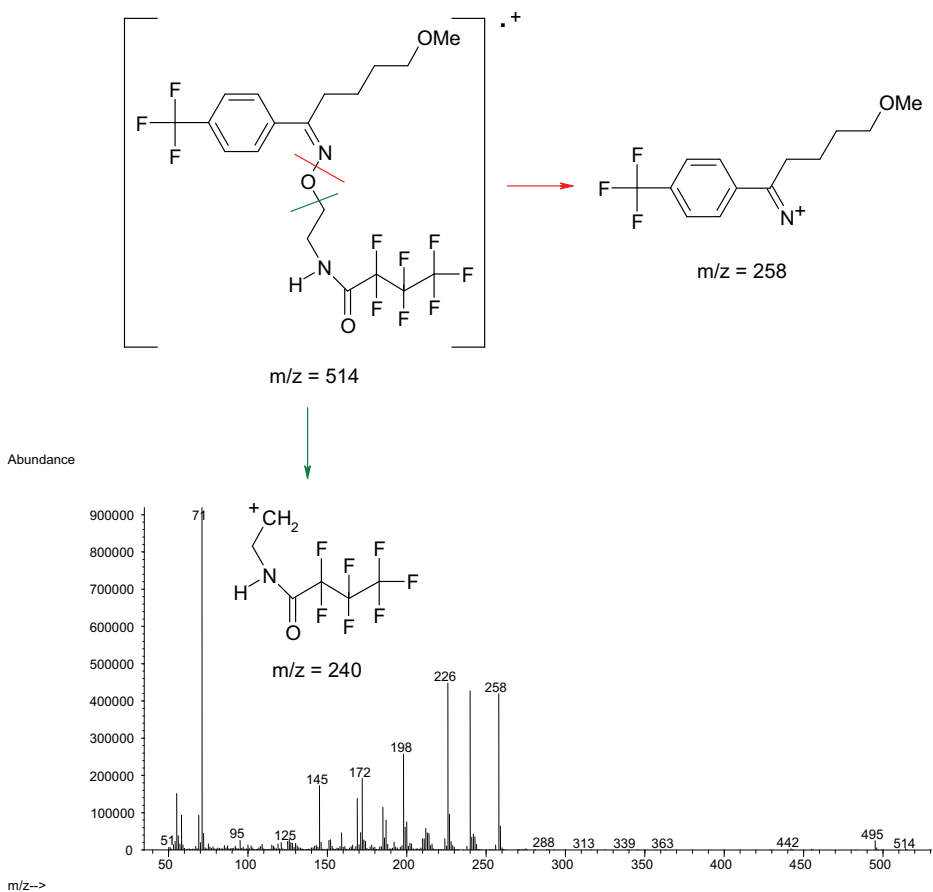
Abundance

For heptafluorobutyryl-fluvoxamine the molecular ion m/z 514 was selected because of the selectivity. In addition, the fragments 258 and 240 were chosen based on their m/z values and for the abundance of the two fragments. Both fragment ions, m/z 258 and 240, were formed by a heterolytic cleavage as indicated in Figure V.13. Ion m/z 240 is not that specific as it consists largely of the HFB-function, thus a lot of derivatized products could lead to such a fragment. However, ions m/z 226 (fragment 240 amu – CH_2) and ion 198 (HFB) are also related to the derivatization product. No selectivity problems, however, occurred during validation of this method with the selected ions for fluvoxamine. In addition, according to the NCCLS-guidelines [35], one of the selected ions may originate from the derivatization product.

V.4.2.4. *Fluoxetine, fluoxetine-d₆ and desmethylfluoxetine*

For heptafluorobutyrylated fluoxetine, the m/z 344 fragment was chosen as quantification ion because it has a relative high abundance and is more specific than ion m/z 240 or 117. The molecular ion is only seen in low abundance. Ion m/z 344 is a result of a heterolytic cleavage, in which a pair of electrons 'moves' together towards the charged oxygen atom. The 117 amu fragment is achieved by a McLafferty rearrangement followed by a heterolytic cleavage leaving the charge on the carbon after the cleavage of the C-O bound (Figure V.14. A). Fragment m/z 117 was preferred over 240 as it gave more structural information, as fragment m/z 240 mostly contained the HFB-part. In addition, ion m/z 117 resulted in a higher abundance. The fragmentation pattern of derivatized fluoxetine-d₆ results in the same fragments but with 6 amu difference due to the deuterated functions. Fragmentation of desmethylfluoxetine occurs in the same manner as for its parent compound.

<u>Figure V.14.</u> Spectra and fragmentation patterns of heptafluorobutyrylated fluoxetine (A), fluoxetine-d$_6$ (B) and desmethylfluoxetine (C)

A

B

C

m/z = 491

- F

m/z = 472

m/z = 117

Abundance

2600000

2200000

1800000

1400000

1000000

600000

200000

m/z = 330

m/z-->
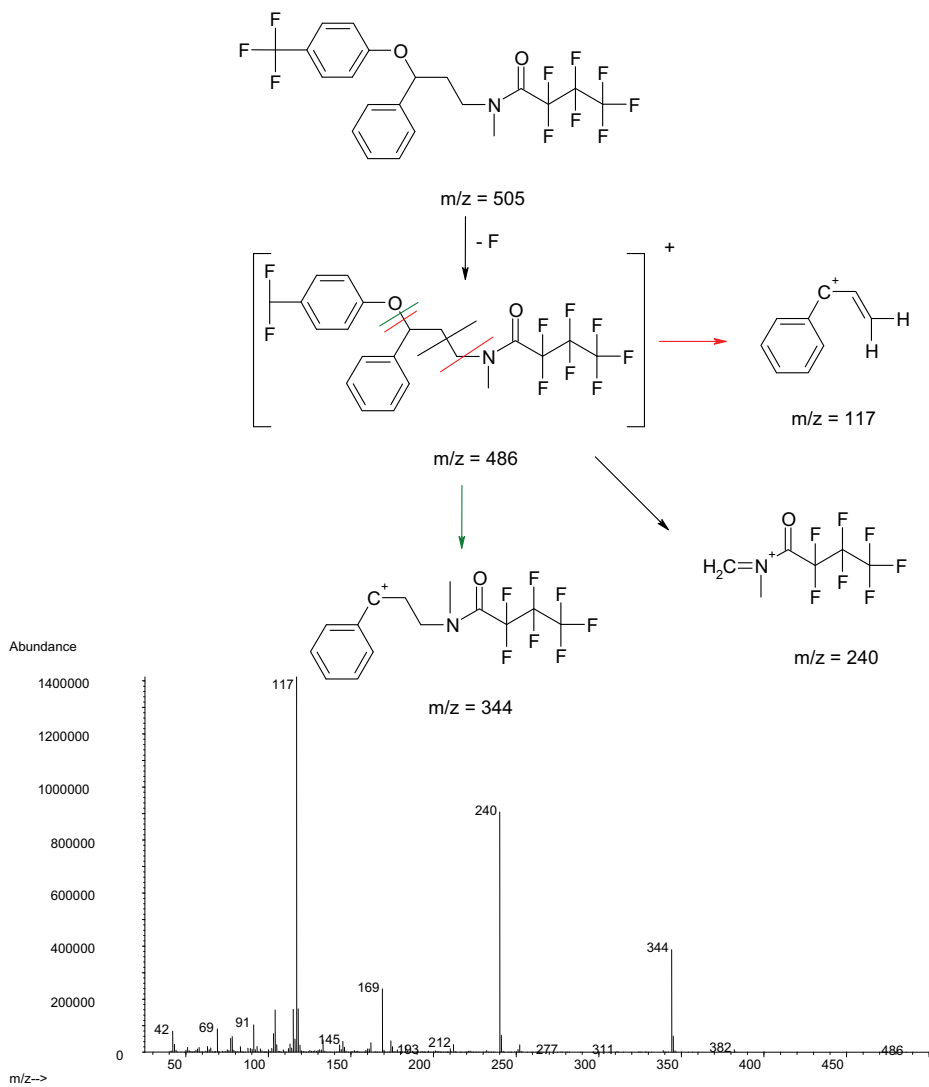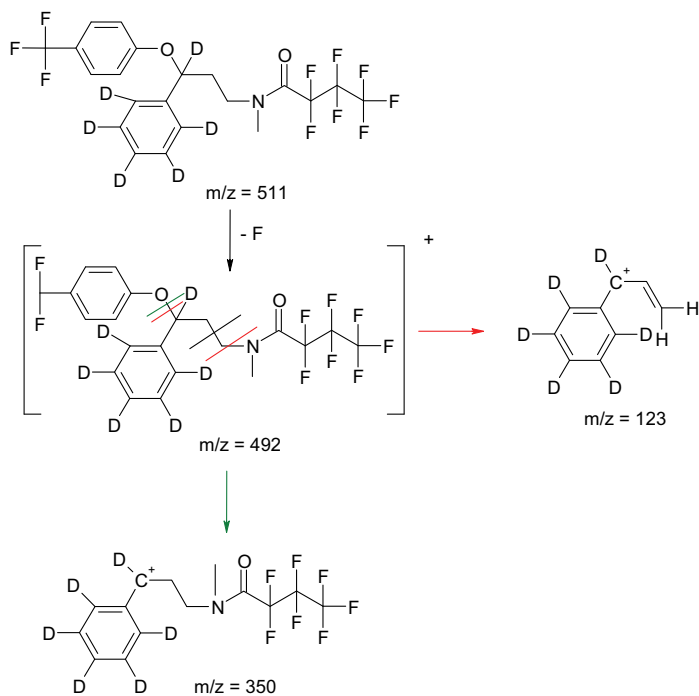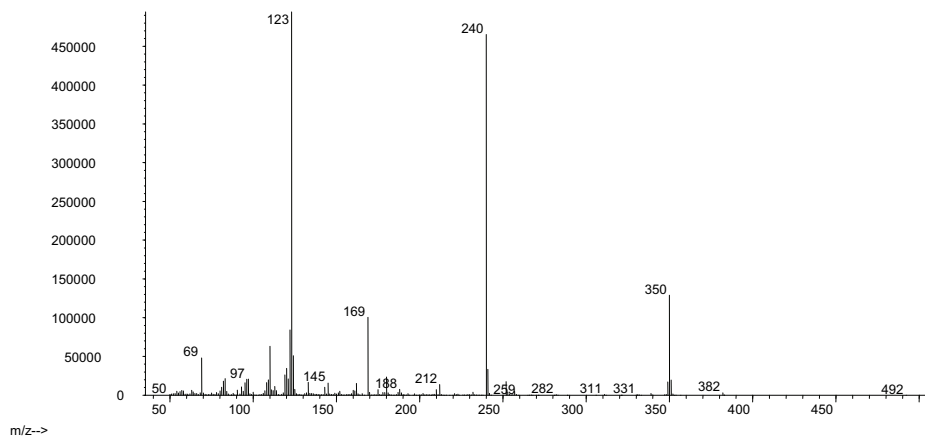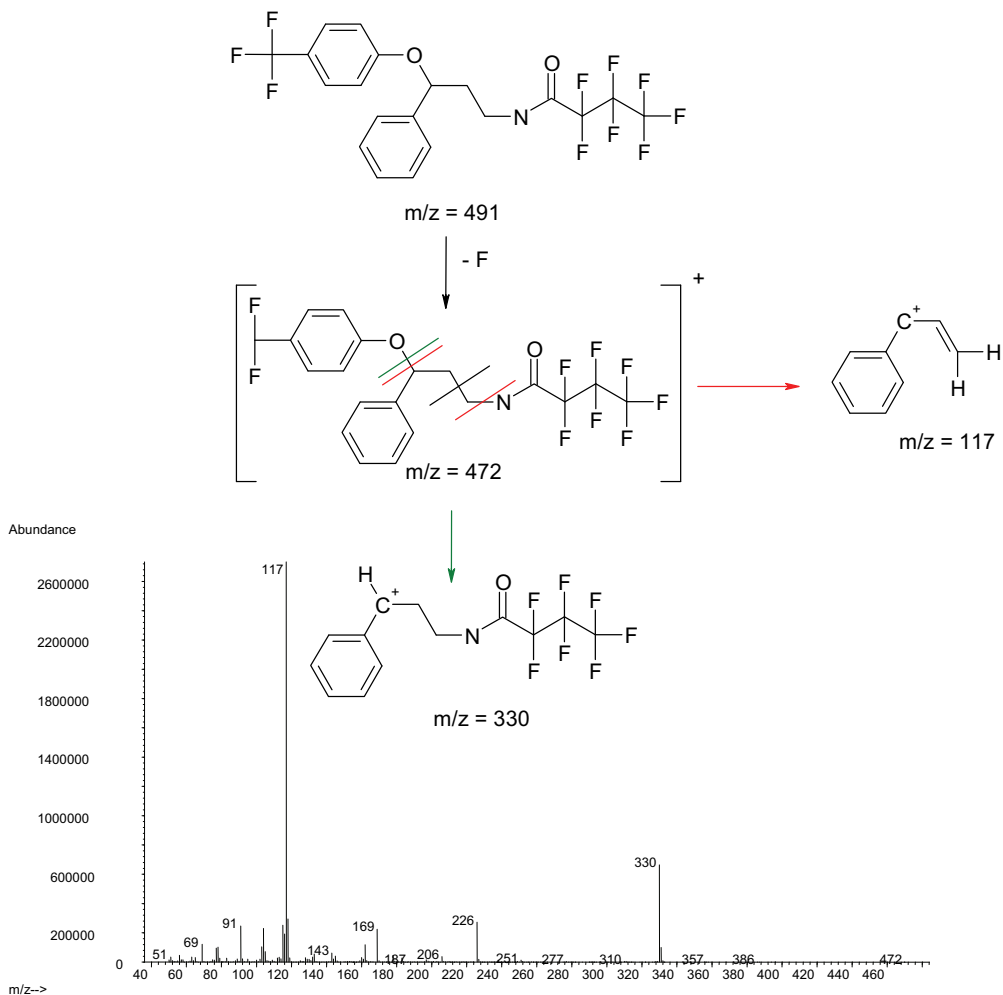
V.4.2.5. *Mianserin, mianserin-d3 and desmethylmianserin*

Mianserin and deuterated mianserin have the same fragment ions, only their molecular ion has a difference of 3 amu due to the deuterium atoms. Fragment m/z 193 and 220 are products of heterolytic and homolytical cleavages due to the nitrogen atoms. In the spectrum of desmethylmianserin ion m/z 193 is also the base peak. However, the derivatized metabolite has a highly abundant molecular ion of m/z 446 and is fragmented to ion m/z 249 (Figure V.15)

Figure V.15. Spectra and fragmentation patterns of mianserin (A), mianserin-d$_3$ (B) and HFB-desmethylmianserin (C)

R= H   m/z = 264
R= D   m/z = 267

m/z = 220

A

m/z = 193

B
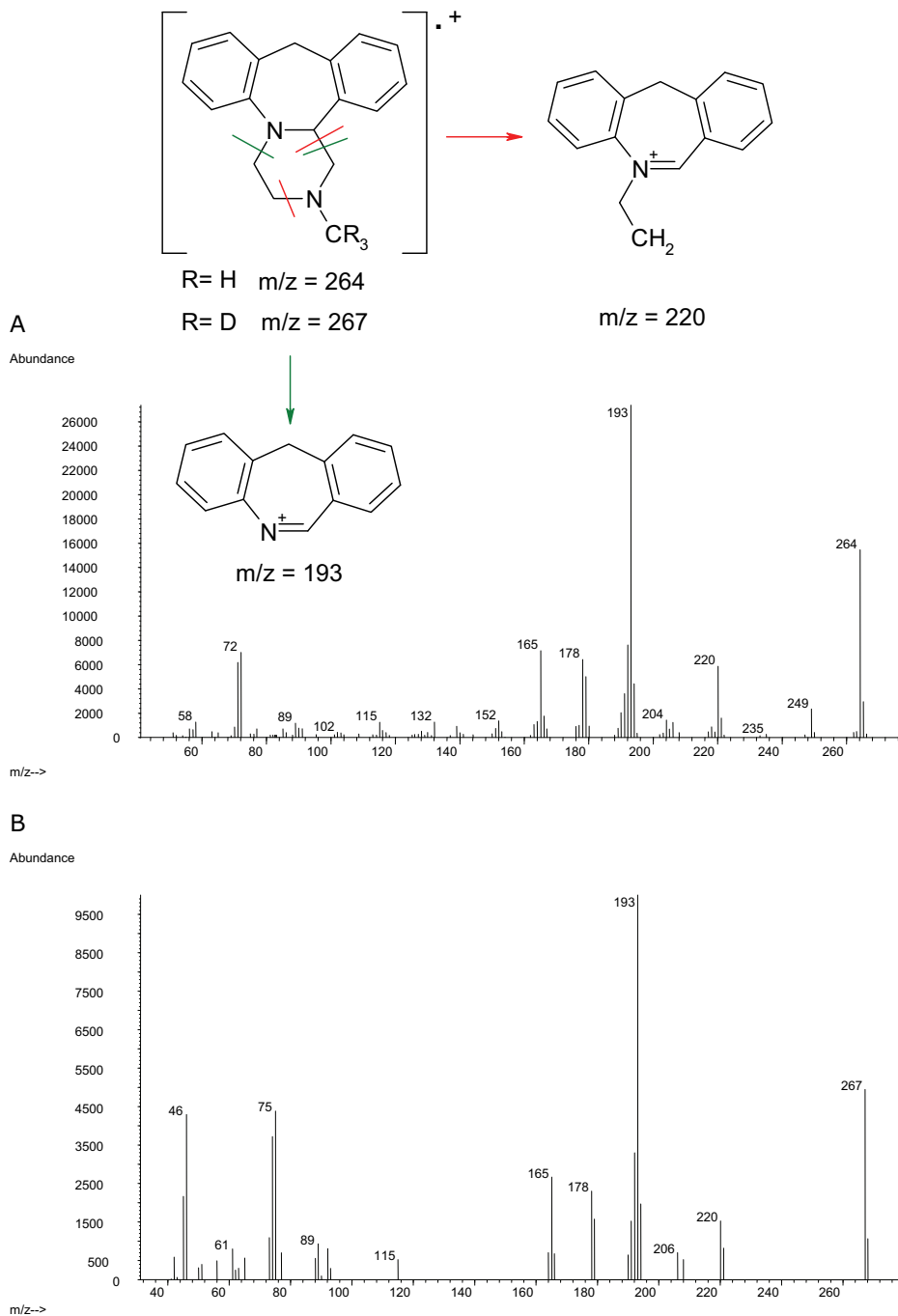
C
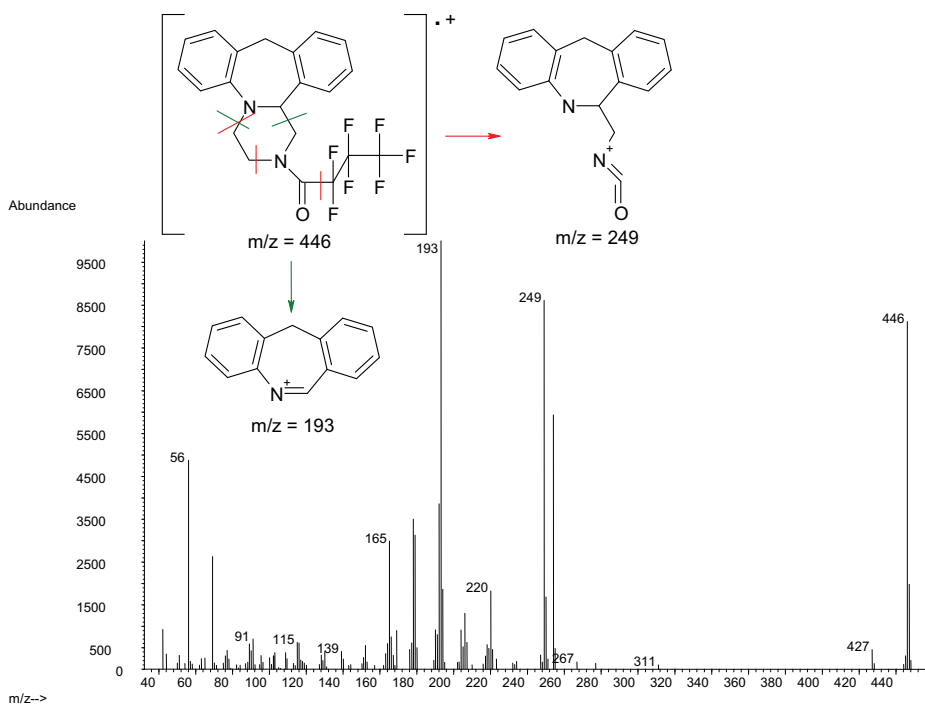
V.4.2.6. *Mirtazapine and desmethylmirtazapine*

Figure V.16. Spectra and fragmentation patterns of mirtazapine (A), and HFB-desmethylmirtazapine (B)

A

Abundance

m/z-->

B

m/z = 447

m/z = 250

Abundance

m/z = 195

m/z-->
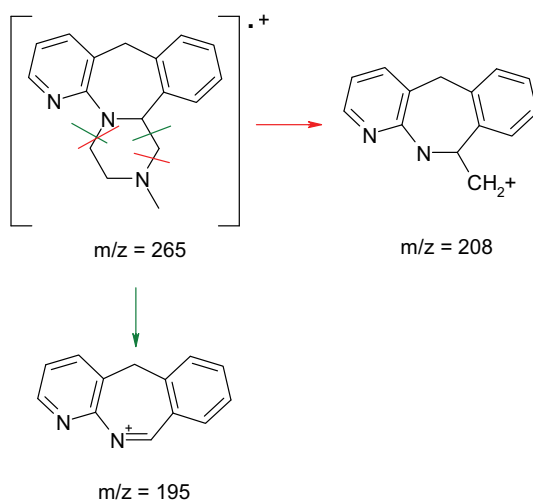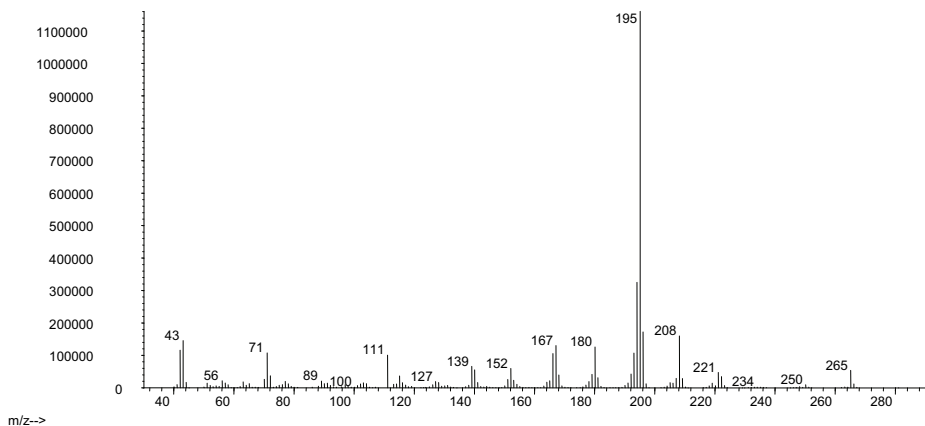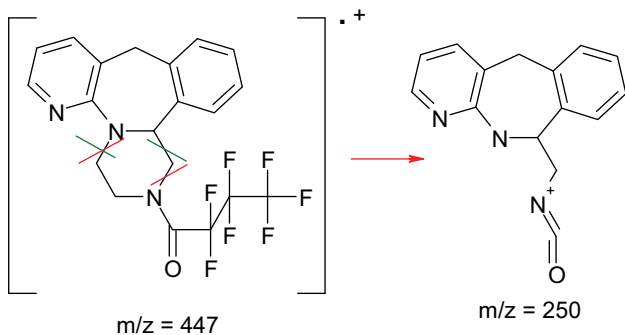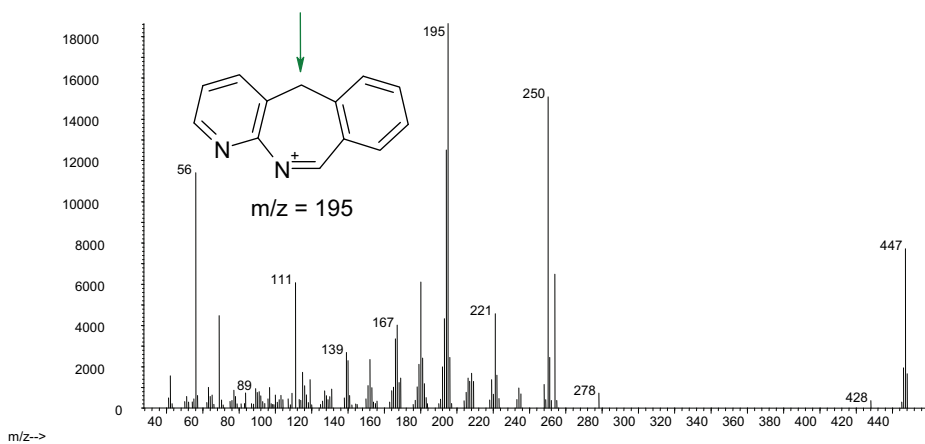
Mirtazapine is not derivatized and the molecular ion is cleary observed in its EI spectrum. Fragments m/z 195 and 208 are observed due to heterolytic cleavages next to the nitrogen atoms and homolytic cleavage of the ß-bound of the nitrogen atoms. Desmethylmirtazapine is derivatized with HFBI and the

fragmentation pattern is also determined by cleavage of the ring structure due to the N-atoms.

V.4.2.7. *Melitracen*

Melitracen is extensively fragmented in EI to the unspecific ion m/z 58.

<u>Figure V.17.</u> Spectrum and fragmentation pattern of melitracen
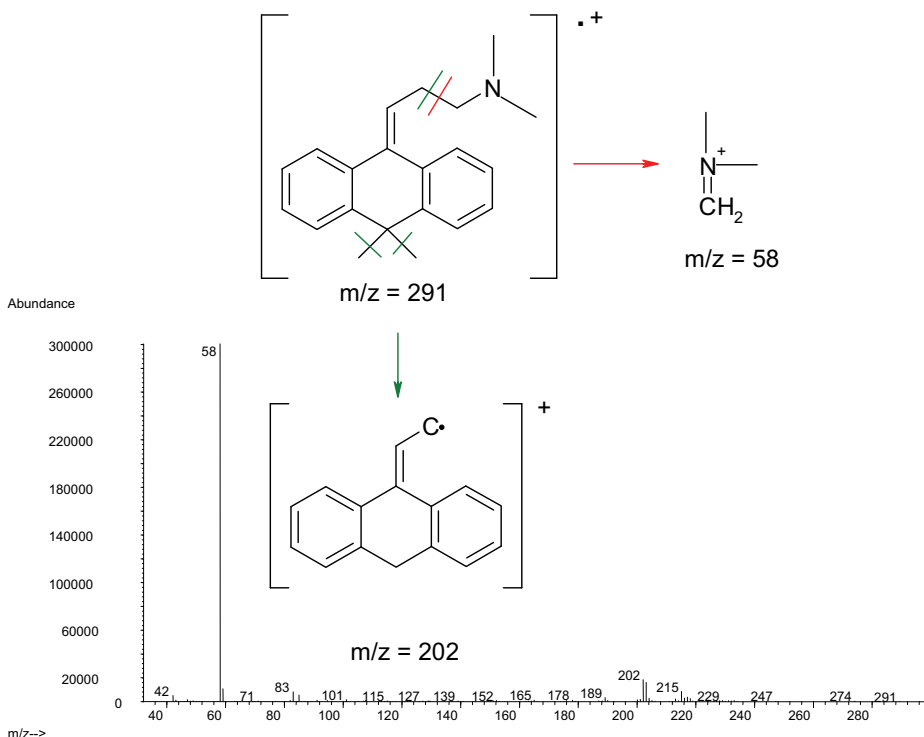
V.4.2.8. *Reboxetine*

For HFB-reboxetine the molecular ion of 509 amu was selected as well as fragment m/z 371, due to its selectivity and relative high abundance, and m/z 138. Fragment 91 amu was not selected as this ion represents a tropylium ion and is not specific. Fragment m/z 371 was obtained from a heterolytic cleavage as indicated in Figure V.18, while fragment m/z 138 was obtained after a rearrangement of a H-atom.

Figure V.18. Spectra and fragmentation pattern of HFB-reboxetine
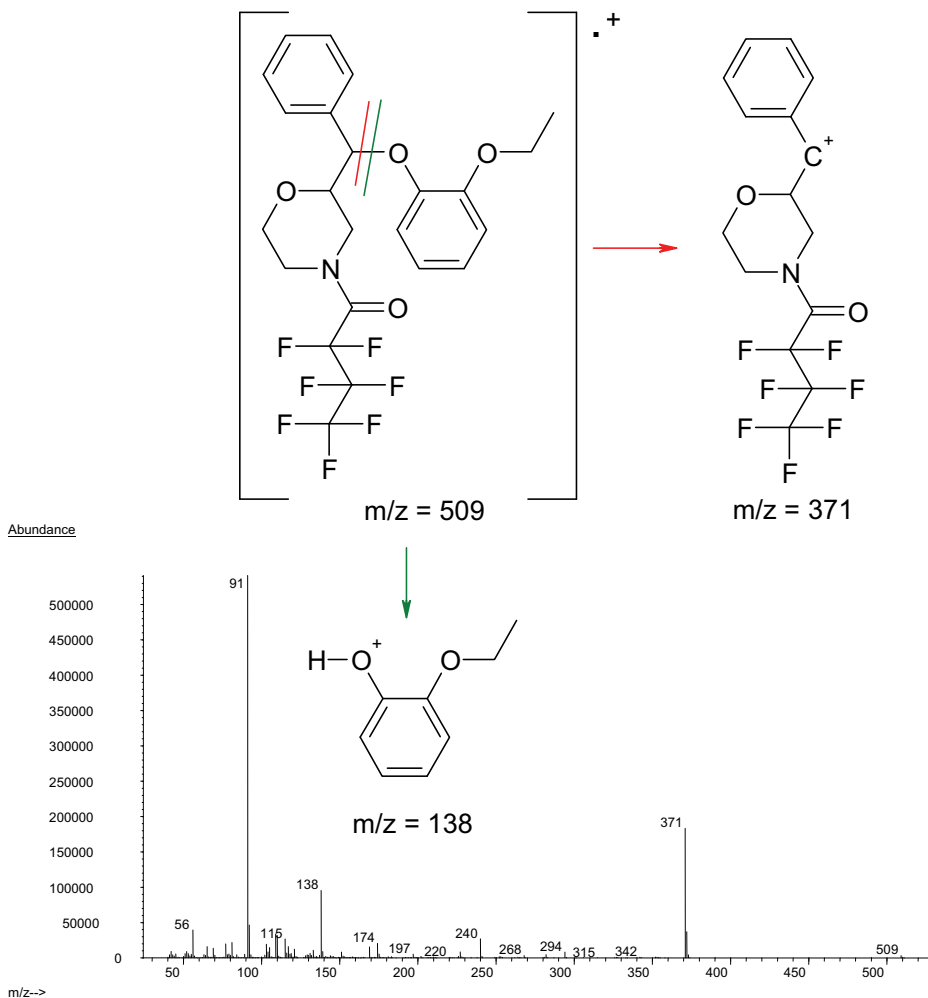
V.4.2.9. *Citalopram, desmethylcitalopram and didesmethylcitalopram*

Citalopram was highly fragmented to ion 58 amu, which is common for dimethyl tertiary amines. In addition, due to C-C cleavage next to the O-heteroatom a stable 238 amu fragment is formed. This fragment is also noticed in the spectra of desmethyl- and didesmethylcitalopram. In addition, for the metabolites of citalopram a loss of 18 amu, thus water, was observed in the spectra.

Figure V.19. Spectra and fragmentation patterns of citalopram (A), and its heptafluorobutyrylated metabolites desmethylcitalopram (B) and dides-methylcitalopram (C)

A

$m/z = 58$

Abundance

$m/z = 324$

$m/z = 238$

m/z-->

R = CH$_3$ $m/z = 506$

R = H $m/z = 492$

$m/z = 488$

$m/z = 474$

$m/z = 238$

$m/z = 208$

B

Abundance

m/z-->

C

Abundance

m/z-->
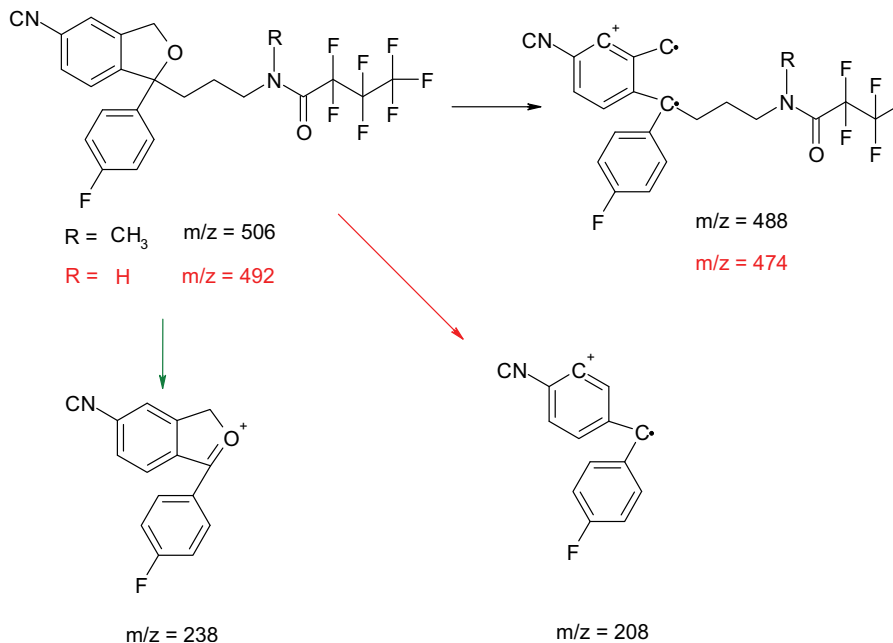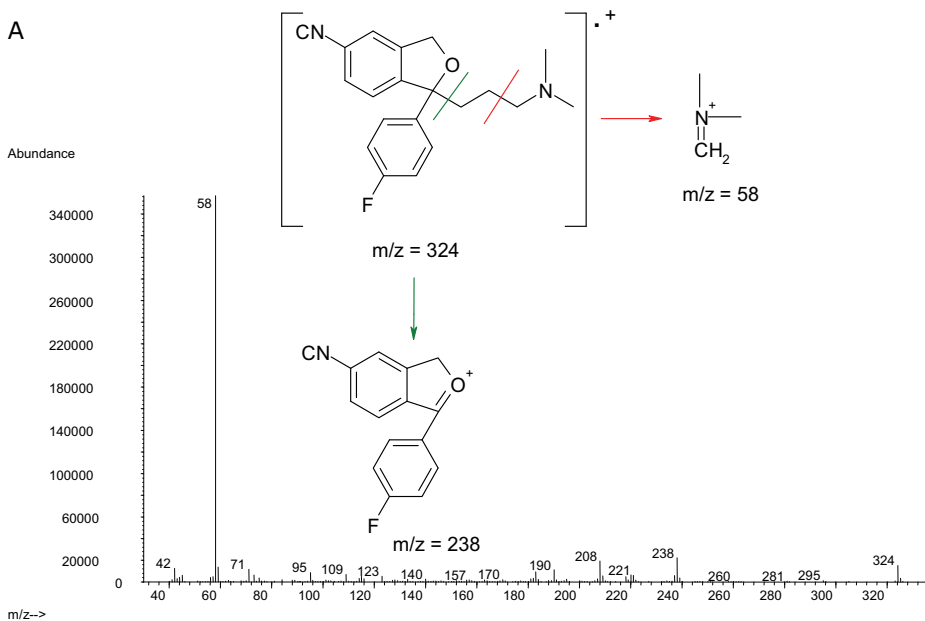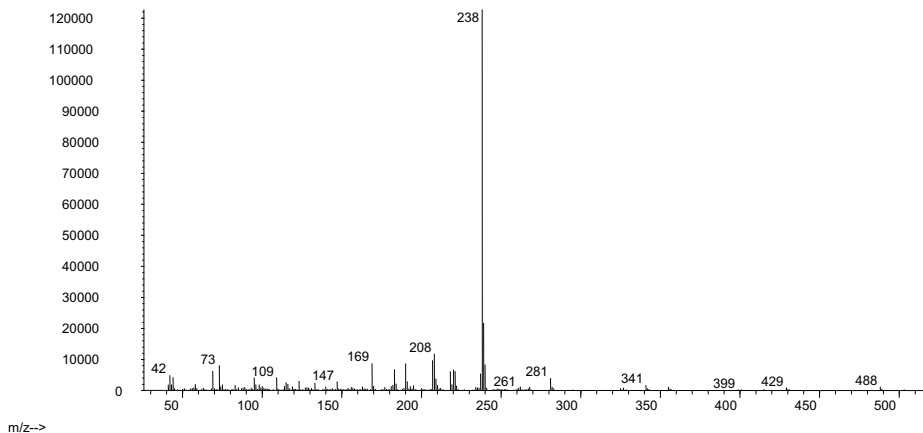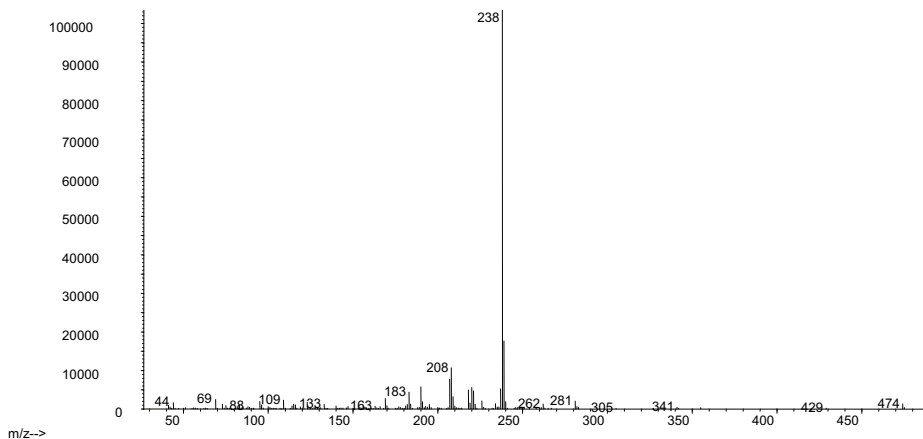
V.4.2.10. *Maprotiline and desmethylmaprotiline*

Maprotiline was monitored by the low abundance molecular ion, the m/z 445 fragment, which is a result of a retro-Diels-Alder rearrangement and a m/z 191 fragment resulting from the rearrangement and a homolytic cleavage of the ß-bond from the 3-ring complex. For desmethylmaprotiline the same fragmentation pattern occurs.

Figure V.20. Spectra and fragmentation patterns of HFB-maprotiline (A) and HFB-desmethylmaprotiline (B)

A
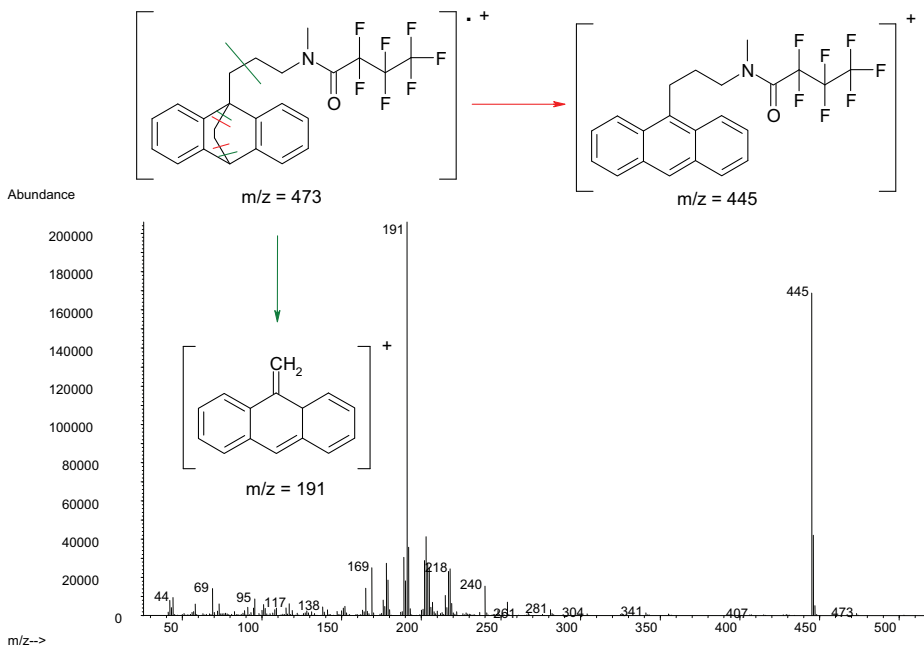
B
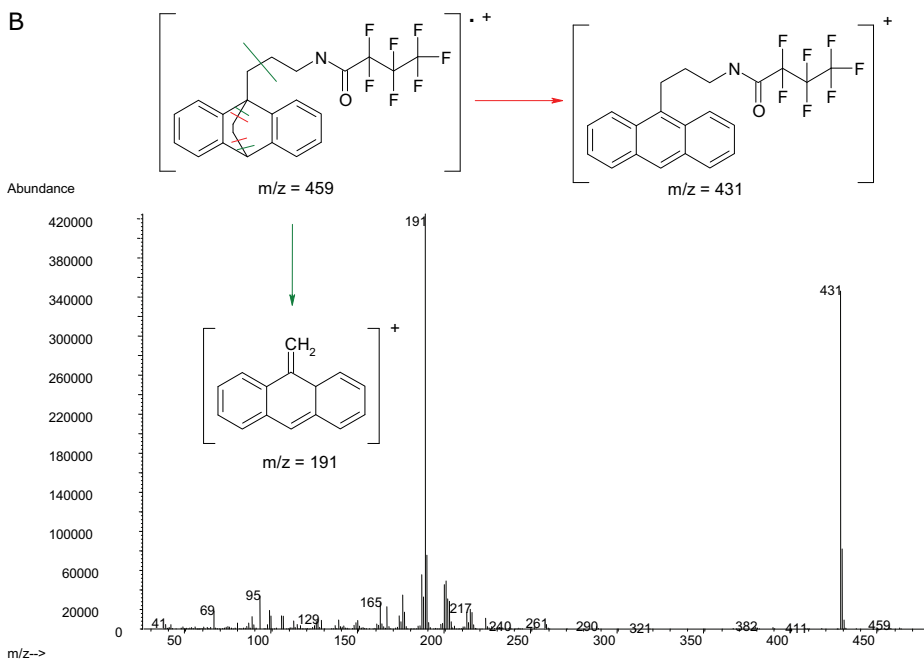
V.4.2.11. *Sertraline and desmethylsertraline*

Sertraline contains two chlorine atoms and therefore isotopes were monitored, viz. m/z 501 and 503. The most specific high abundant ion was m/z 274 and is a result of a McLafferty rearrangement. For desmethylsertraline, the same fragmentation pattern and isotopes were monitored (m/z 274, 487, 489)

<u>Figure V.21.</u> Spectra and fragmentation patterns of derivatized sertraline (A) and desmethylsertraline (B)

A

B

Abundance
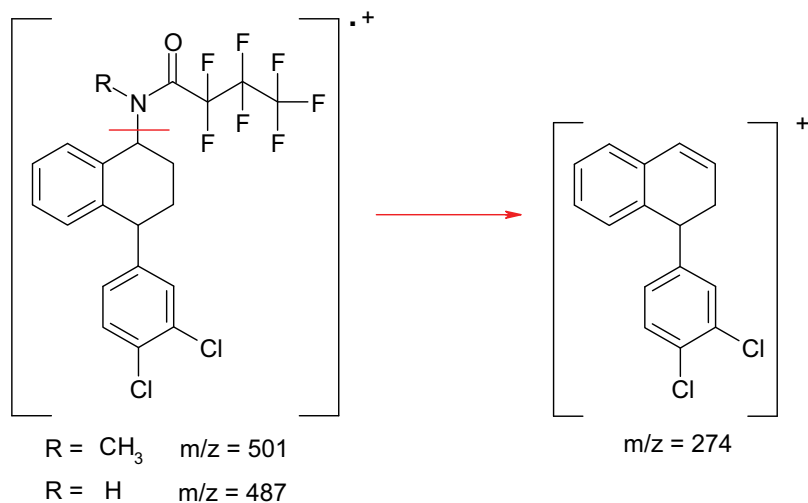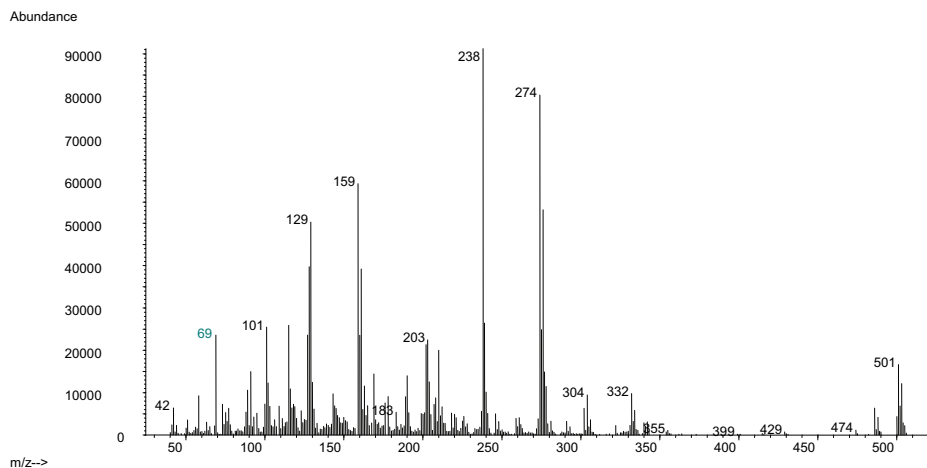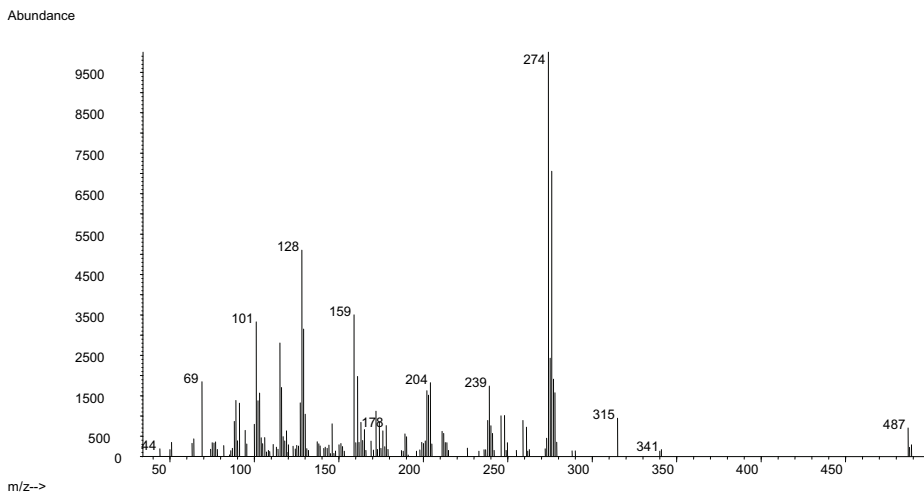
V.4.2.12. *Paroxetine and paroxetine-d$_6$*

The fragmentation of paroxetine and paroxetine-d$_6$ occurs in the same way. Fragments m/z 388 and 394 are products of a heterolytic cleavage next to the O atom. The m/z 138 fragment is a result of a ß-bond cleavage next to the substituted aromatic ring.

<u>Figure V.22.</u> Spectra and fragmentation patterns of derivatized paroxetine (A) and paroxetine-d$_6$ (B)

R = H   m/z = 525
R = D   m/z = 531

m/z = 388
m/z = 394

m/z = 138

A

Abundance

m/z-->

B

Abundance

m/z-->
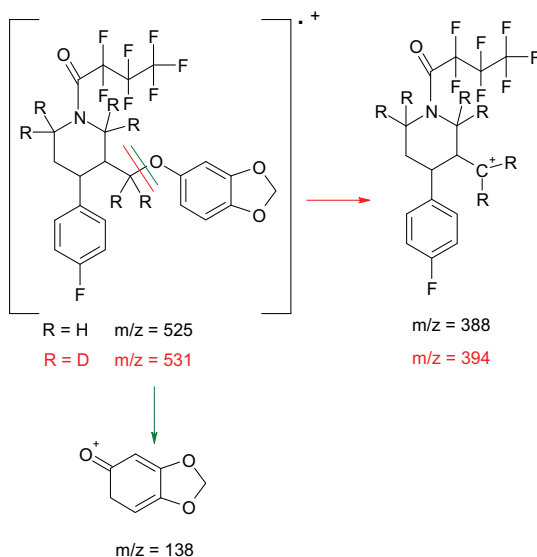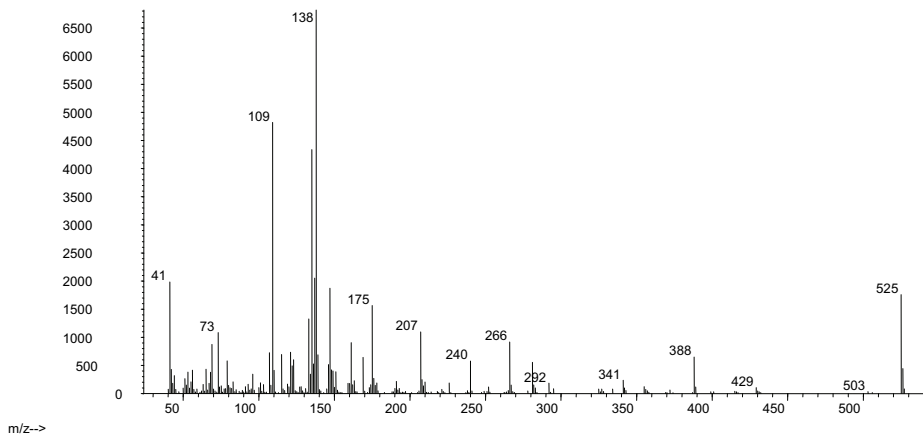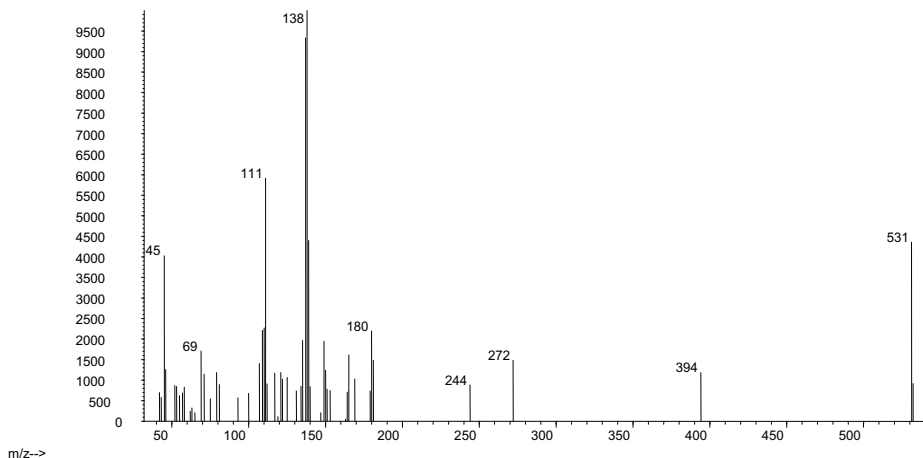
V.4.2.13. *Trazodone and m-chlorophenylpiperazine*

Ionization and fragmentation of trazodone and its heptafluorobutyrylated metabolite occur through heterolytical and homolytical cleavage due to the nitrogen atoms in the piperazine ring. For trazodone, the 'ion-cluster' around the base peak of 205 amu is caused by several fragments as indicated in Figure V.23. Fragment 207 amu probably results from fragment m/z 209 by loss of 2 hydrogen atoms in the piperazine ring to ensure stability. Because of the chlorine atom, isotope peaks can occur, however, the fragmentation

pattern that would result in a fragment with the chlorine atom and a m/z 205 (207) was not found.

Figure V.23. Spectra and fragmentation patterns of trazodone (A) and HFB-m-chlorophenylpiperazine (B)
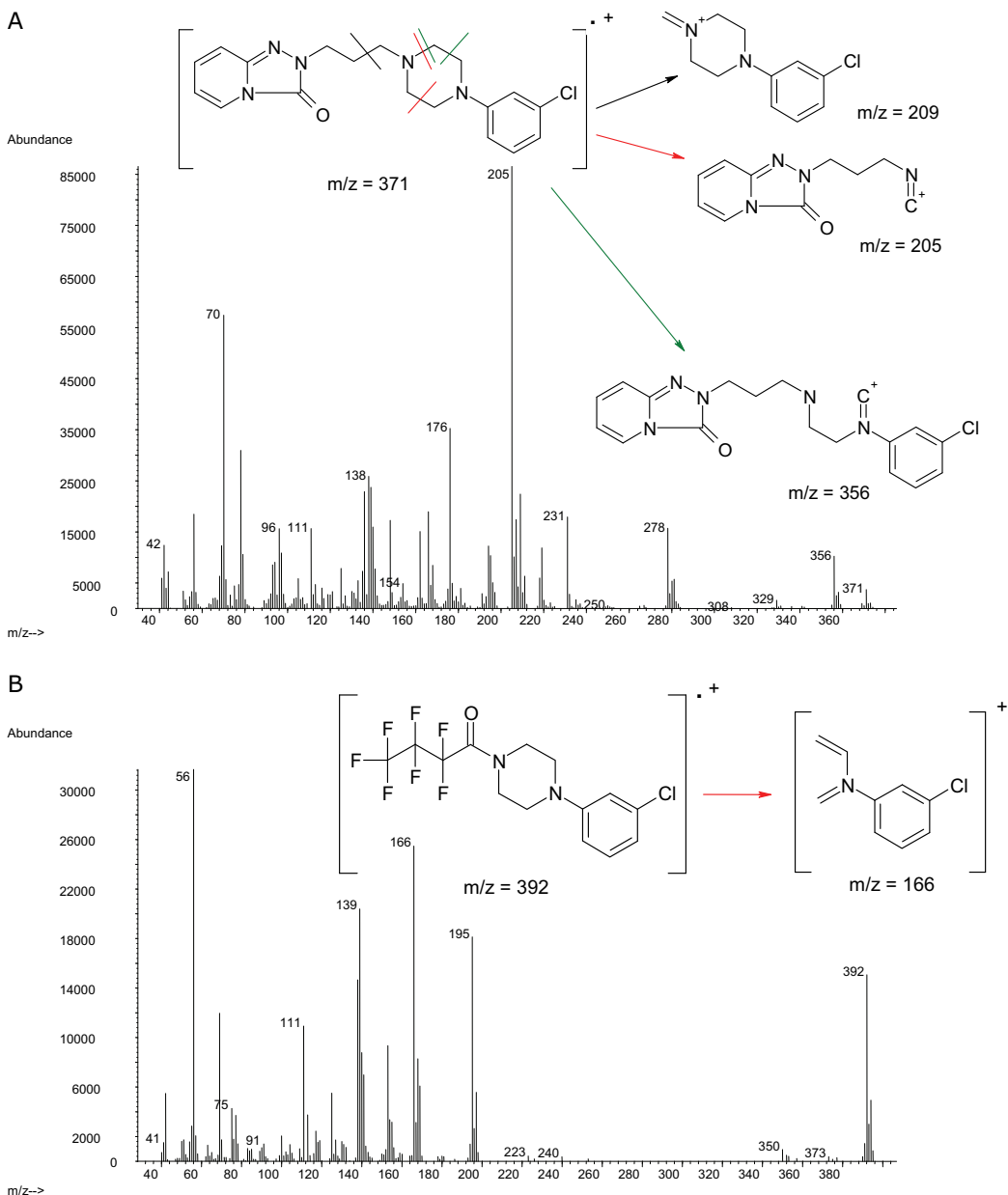
V.4.3. Spectra of the derivatized ADs after positive ion chemical ionization

Electron ionization led to extensive fragmentation of several ADs. Therefore, positive ion chemical ionization (PICI) was applied as this ionization technique leads to less fragmentation and often gives molecular mass information. For this reason, PICI could provide more selectivity.

Figure V.24. Positive ion chemical ionization reaction using methane gas [36]

Formation of major reagent gas ions when using methane gas

$CH_4 + e^- \rightarrow CH_4^{+\cdot} + 2\ e^-$

$\rightarrow CH_3^+ + H^\cdot + 2\ e^-$

$CH_4 + CH_4^{+\cdot} \rightarrow CH_5^+ + CH_3^\cdot$

$CH_4 + CH_3^+ \rightarrow C_2H_5^+ + H_2$
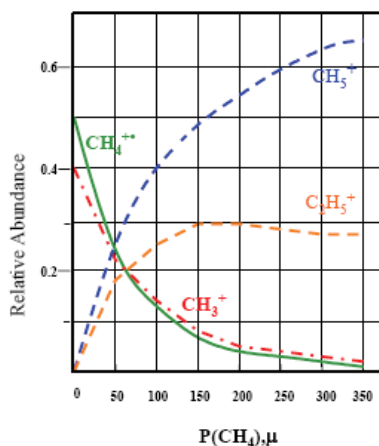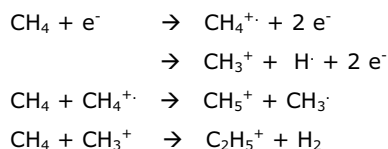
Formation of sample ions

Proton transfer

$CH_5^+ + M \rightarrow [M—H]^+ + CH_4$ $\qquad$ m/z = M+1

Hydride abstraction

$CH_5^+ + M \rightarrow [M - H]^+ + CH_4 + H_2$ $\qquad$ m/z = M-1

Addition

$C_2H_5^+ + M \rightarrow [M— C_2H_5]^+$ $\qquad$ m/z = M+29

$C_3H_5^+ + M \rightarrow [M— C_3H_5]^+$ $\qquad$ m/z = M+41

Methane is used as reagent gas in our chemical ionization MSD configuration. At first, the methane gas is ionized through electron ionization due to electrons emerging from the filaments of the ion source. This electron impact reaction combined with ion-molecule reactions results in the creation of

several reagent gas ions (CH_5^+ and $C_2H_5^+$). To ensure a high reaction yield and reproducible ionization condition, the pressure in the CI-ion source is set at about 133 Pa. The last step of the ionization process is the reaction of the reagent gas ions with the sample molecules, resulting in stable sample ions (Figure V.24.).

For a reaction to occur between a reactant ion and a sample molecule, the reaction must be exothermic. The more exothermic a reaction is, the more fragmentation will occur. There are three types of interaction between the methane reagent gas ions and the sample molecules in the ion source: proton transfer, hydride abstraction, and addition.

Proton transfer occurs if the proton affinity of the analyte is greater than that of the reagent gas. In that case, the protonated reagent gas will transfer its proton onto the analyte, forming a positively charged analyte ion with an additional weight of 1 amu. Because methane has a low proton affinity (127 kcal/mol) most of the analytes will have a higher proton affinity and the proton transfer reaction will be exothermic.

During the formation of reagent ions, various reactant ions can be formed that have high hydride-ion affinities. If the hydride-ion affinity of a reactant ion is higher than the hydride-ion affinity of the ion formed, then the analyte will loose a H^-. This process is called *hydride abstraction* and usually occurs for saturated hydrocarbons when using methane gas.

However, for many analytes, proton-transfer and hydride-abstraction chemical ionization reactions are not thermodynamically favourable. In these cases, reagent gas ions are often reactive enough to combine with the analyte molecules by condensation or association. These reactions are the *addition reactions* (Figure V.24.)*.*

In this paragraph, the spectra for the different (heptafluorobutyrylated) ADs obtained in PICI with methane gas are shown. The spectra were obtained in scan mode, and the fragments chosen for the selected ion mode will be discussed.

V.4.3.1. *Venlafaxine and O-desmethylvenlafaxine*

Dehydrated venlafaxine (A) and O-desmethylvenlafaxine (B indicated in red) are ionized in the same way. Protonation, hydride abstraction and addition of $C_2H_5^+$ result in ions with m/z 260 (246), 258 (244) and 288 (274), respectively. The same reactions are also observed for heptafluoro-butyrylated O-desmethylvenlafaxine (C indicated in green), leading to ions with m/z 442, 440, and 470.

Figure V. 25. PICI spectrum and fragmentation of venlafaxine (A, black trace) and dehydrated O-desmethylvenlafaxine (B, red) and heptafluorobutyrylated ODMV (C, green)

A
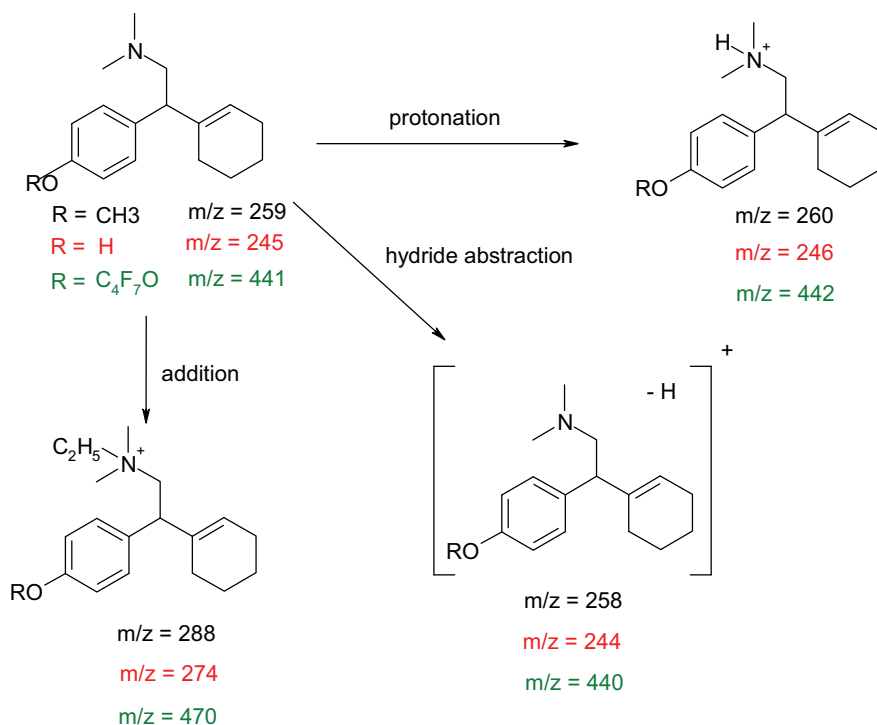
Abundance
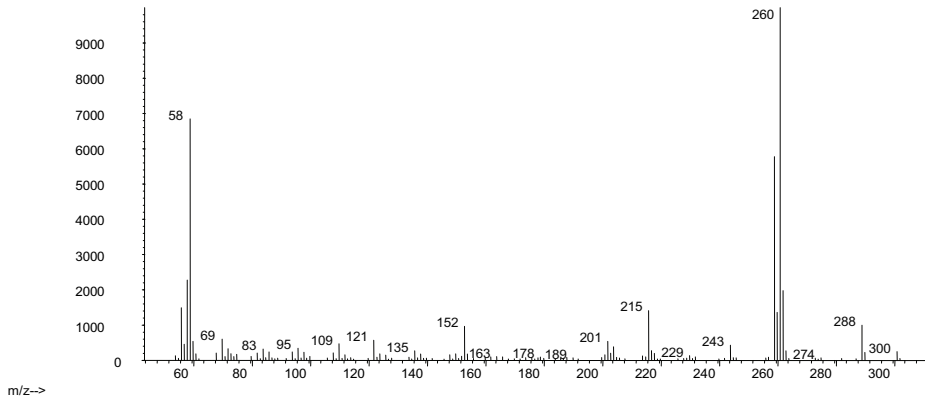
B

Abundance
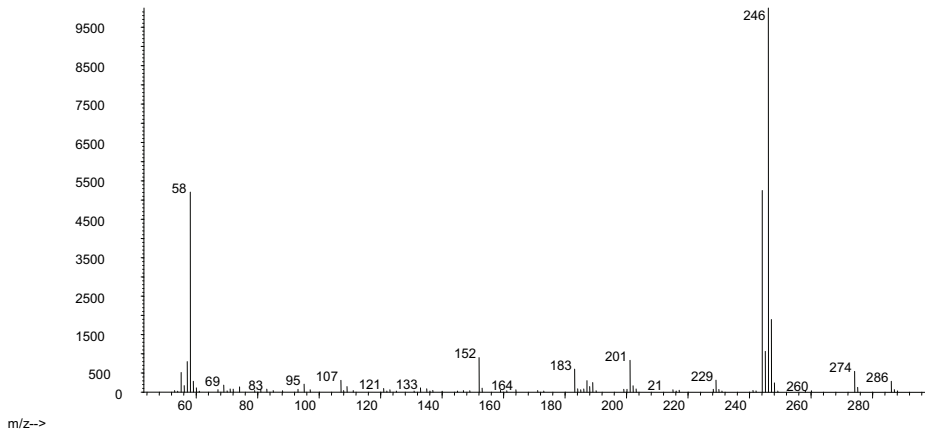
C

Abundance
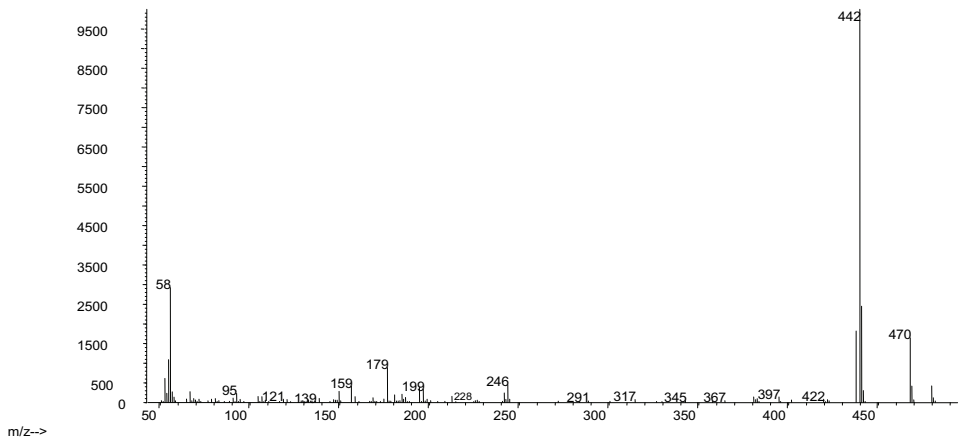
V.4.3.2. *Viloxazine*

Although PICI is a soft ionization technique, viloxazine is still fragmented to ion m/z 296 as with EI. In addition, a fragment m/z 414 is noticed which demonstrates the loss of a fluorine atom from the derivatization moiety. In addition to these fragmentation reactions, the protonation of the viloxazine molecule is also observed.

<u>Figure V. 26.</u> PICI spectrum and fragmentation of HFB-viloxazine
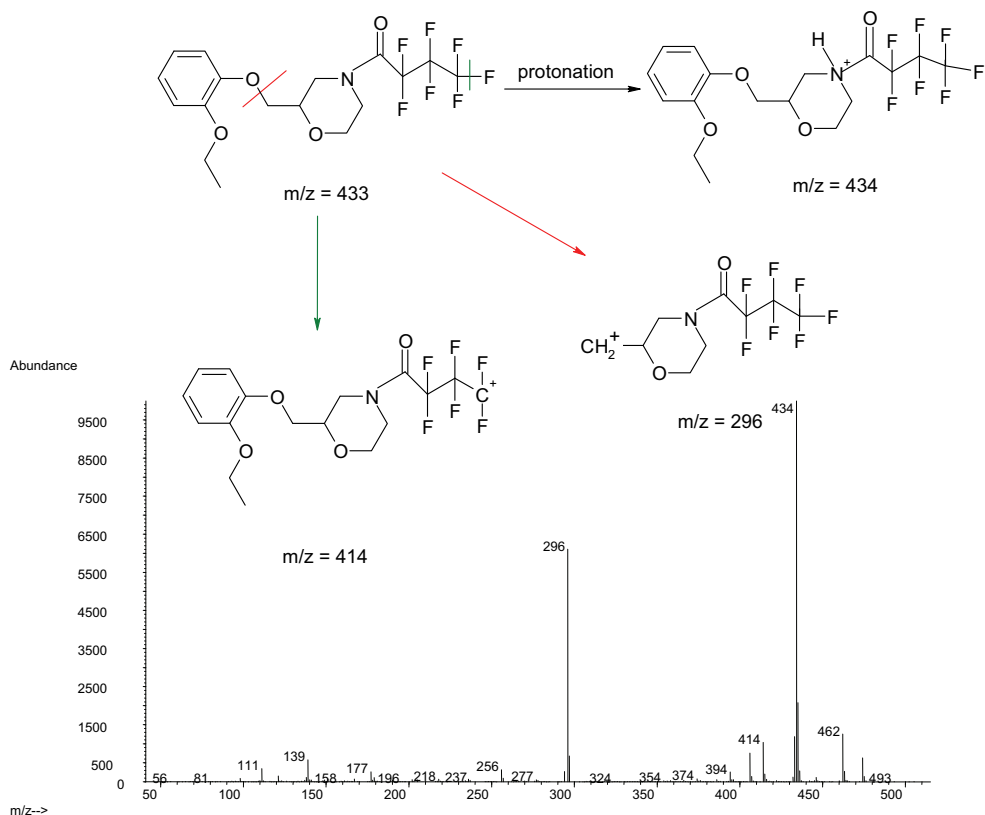
V.4.3.3. *Fluvoxamine*

Heptafluorobutyrylated fluvoxamine is fragmentated to m/z 258 and m/z 495, respectively, due to heterolytic cleavage of the N-O bound and a C-F bound. Due to a protonation reaction the quasi-molecular ion m/z 515 is formed.

<u>Figure V. 27.</u> PICI spectrum and fragmentation of HFB-fluvoxamine
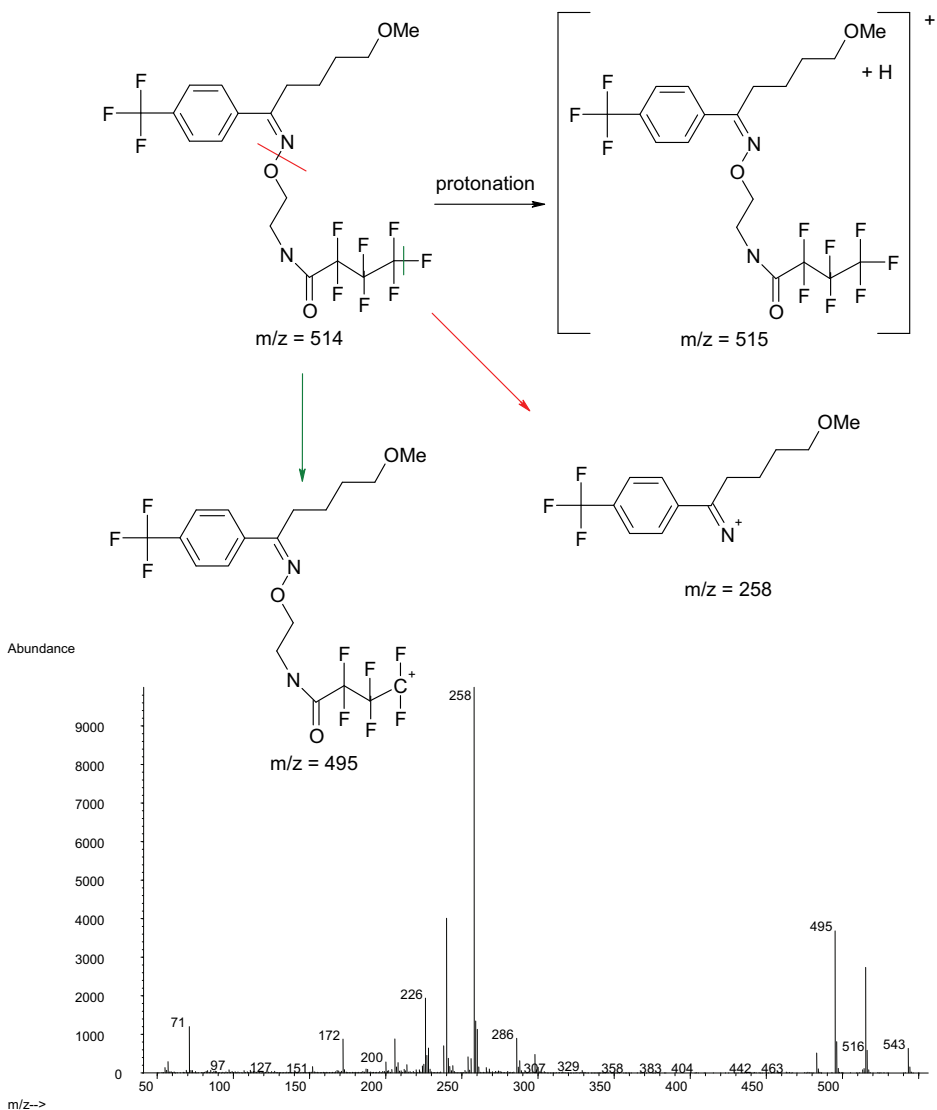
V.4.3.4. *Fluoxetine, fluoxetine-d$_6$ and desmethylfluoxetine*

Even in PICI, the molecular ion of heptafluorobutyrylated fluoxetine, fluoxetine-d$_6$ and desmethylfluoxetine is not observed. The addition of C$_2$H$_5^+$ is thermodynamically favourable and leads to m/z 534 and 540 for fluoxetine and fluoxetine-d$_6$, respectively. Other reactions are fragmentation reactions as in EI. These reactions are heterolytical cleavages.

Figure V. 28. PICI spectra and fragmentation patterns of heptafluoro-butyrylated fluoxetine (A), fluoxetine-d$_6$ (B) and desmethylfluoxetine (C)

R = H   m/z = 505
R = D   m/z = 511

addition

m/z = 534
m/z = 540

m/z = 344
m/z = 350

m/z = 486
m/z = 492

A

Abundance

m/z-->
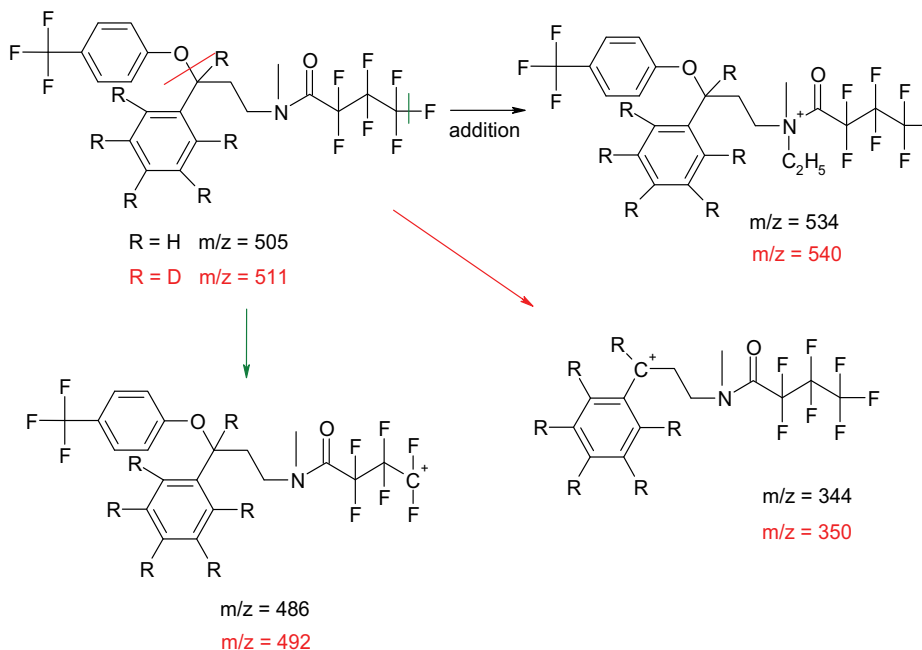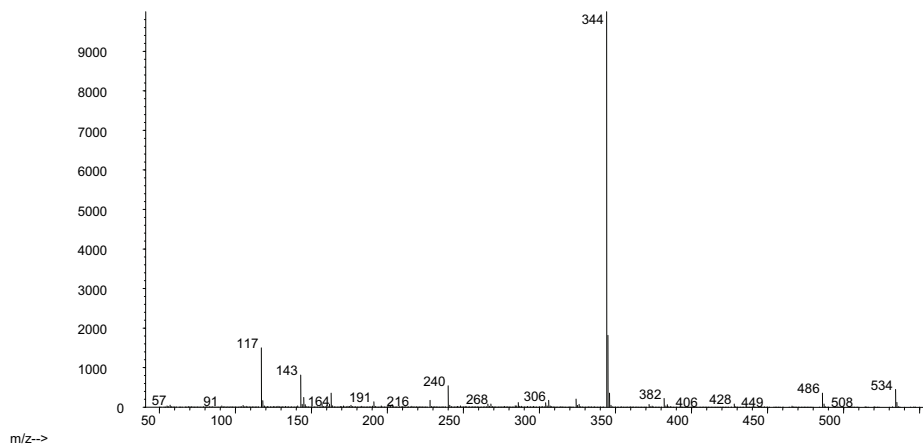
B
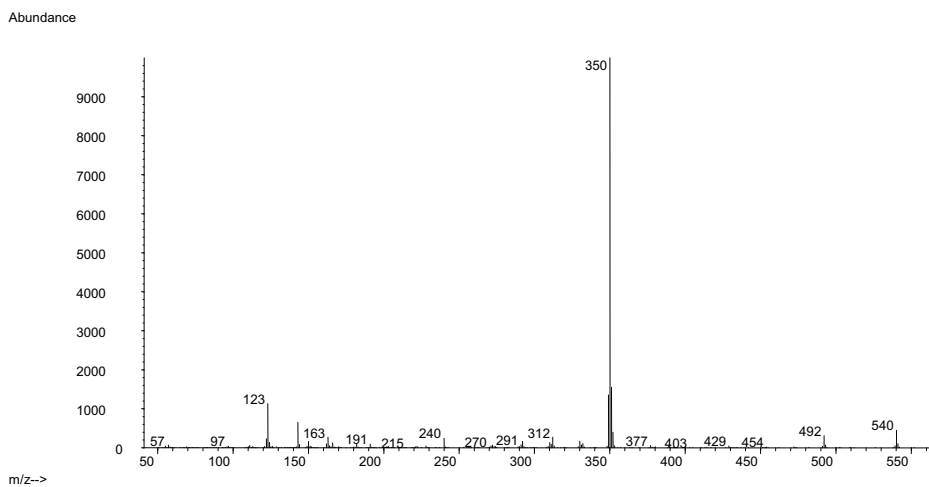
C
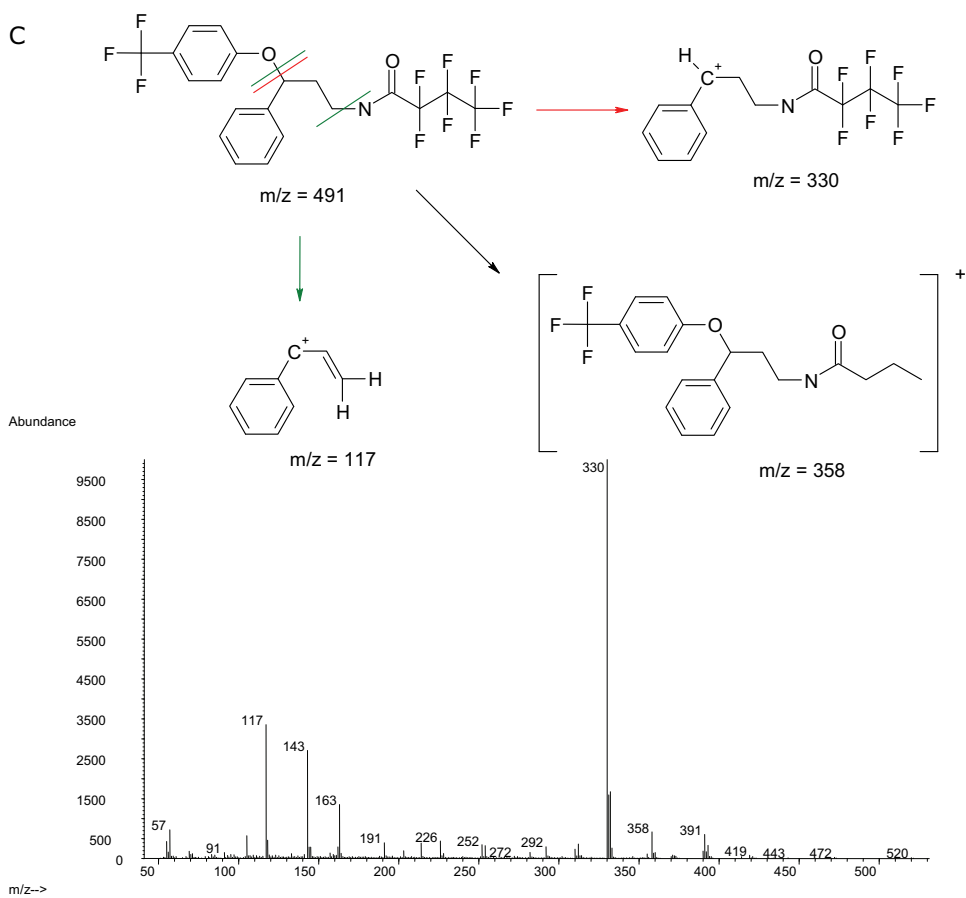
V.4.3.5. *Mianserin, mianserin-d₃ and desmethylmianserin*

<u>Figure V. 29.</u> PICI spectra and fragmentation patterns of mianserin (A), mianserin-d₃ (B) and HFB-desmethylmianserin (C)

protonation

addition

addition

R = H   m/z 264

R = D   m/z 267

R = H   m/z 265

R = D   m/z 268

C₂H₅   CR₃

R = H   m/z 293

R = D   m/z 296

C₃H₅   CR₃

R = H   m/z 305

R = D   m/z 308

A

Abundance

m/z-->

B
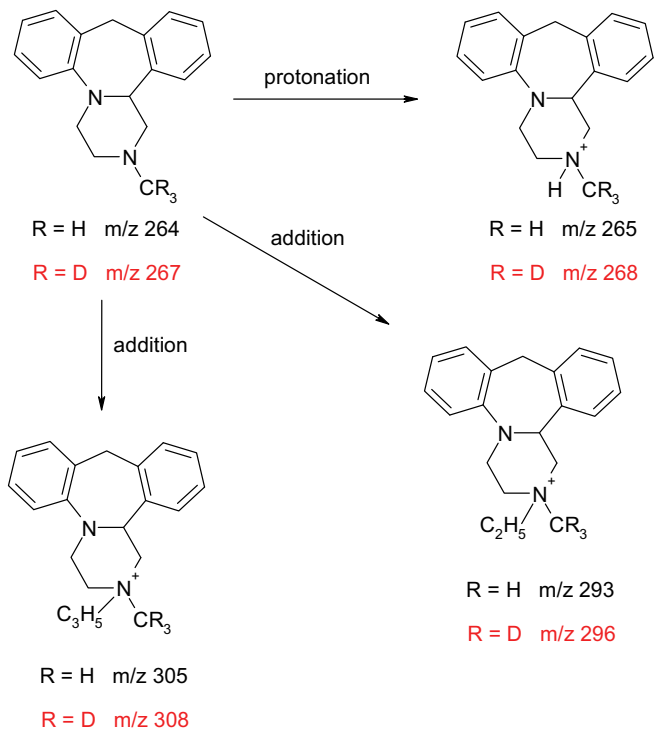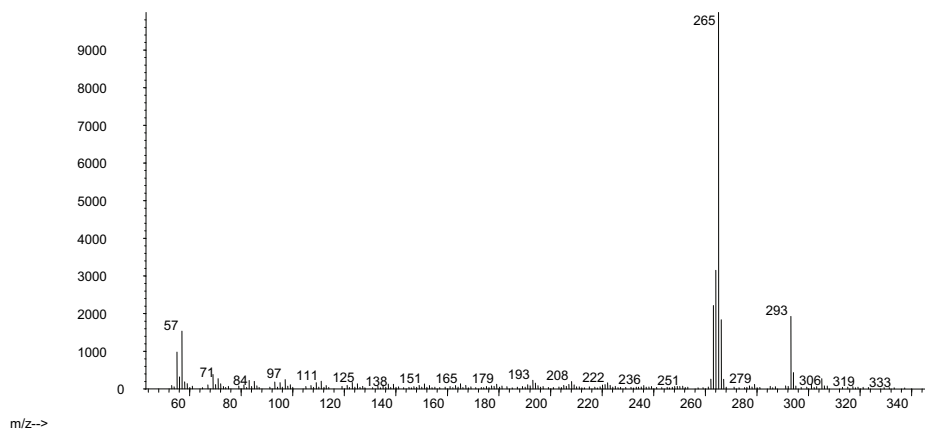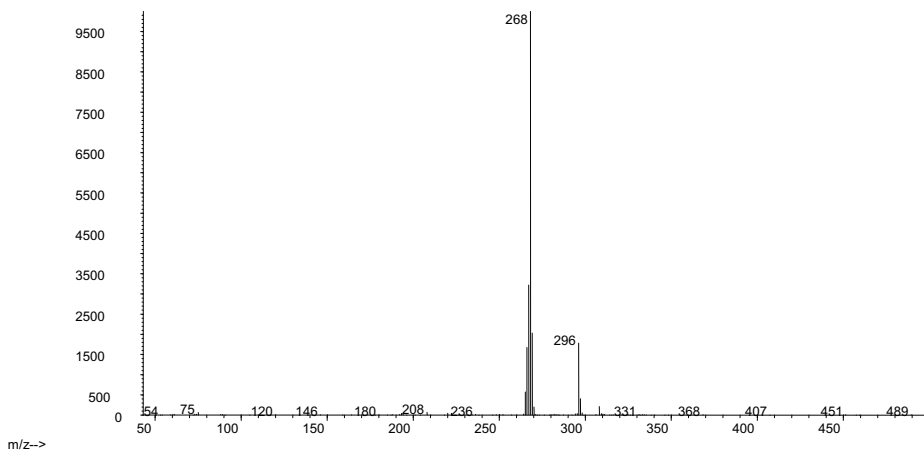
C
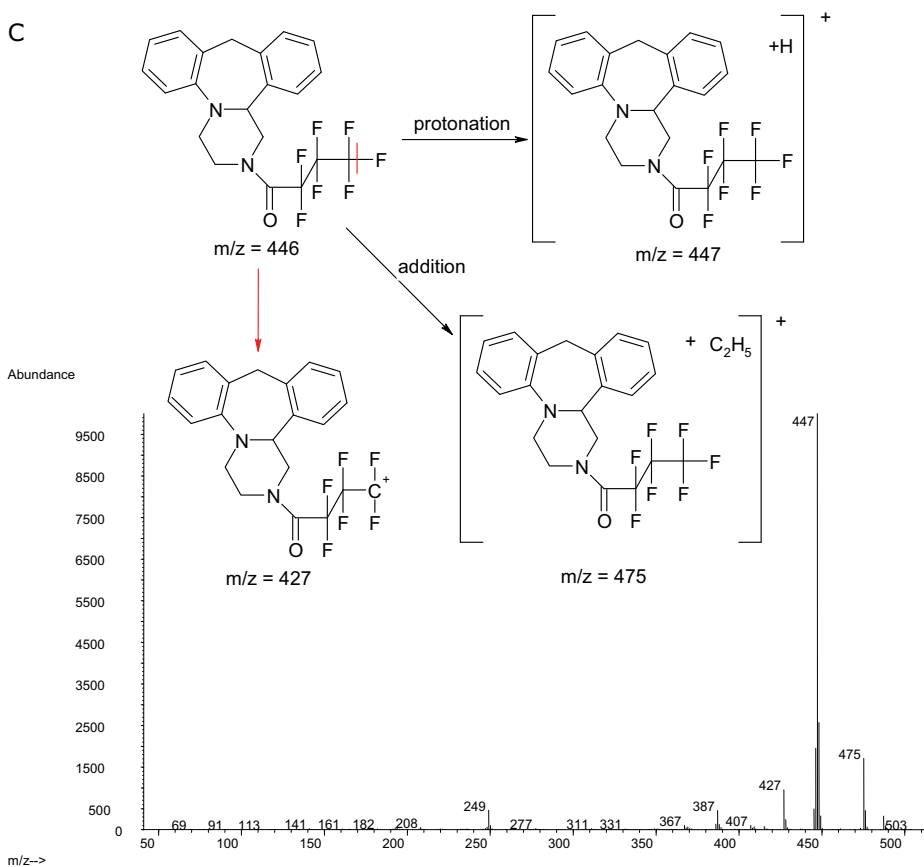
For analytes such as mianserin, PICI leads to a proton transfer and addition reaction, and not to severe fragmentation. The reagent gas ions $C_2H_5^+$ and $C_3H_5^+$ are added to the mianserin and deuterated mianserin molecule. For heptafluorobutyrylated desmethylmianserin protonation and addition also occurs. In addition, fragmentation with a loss of a fluorine atom is also observed resulting in an ion with m/z 427.

V.4.3.6. *Mirtazapine and desmethylmirtazapine*

For mirtazapine and desmethylmirtazapine the same reactions are noticed as for mianserin and desmethylmianserin due to their structural analogy.

Figure V. 30. PICI spectra and fragmentation patterns of mirtazapine (A), and HFB-desmethylmirtazapine (B)

B
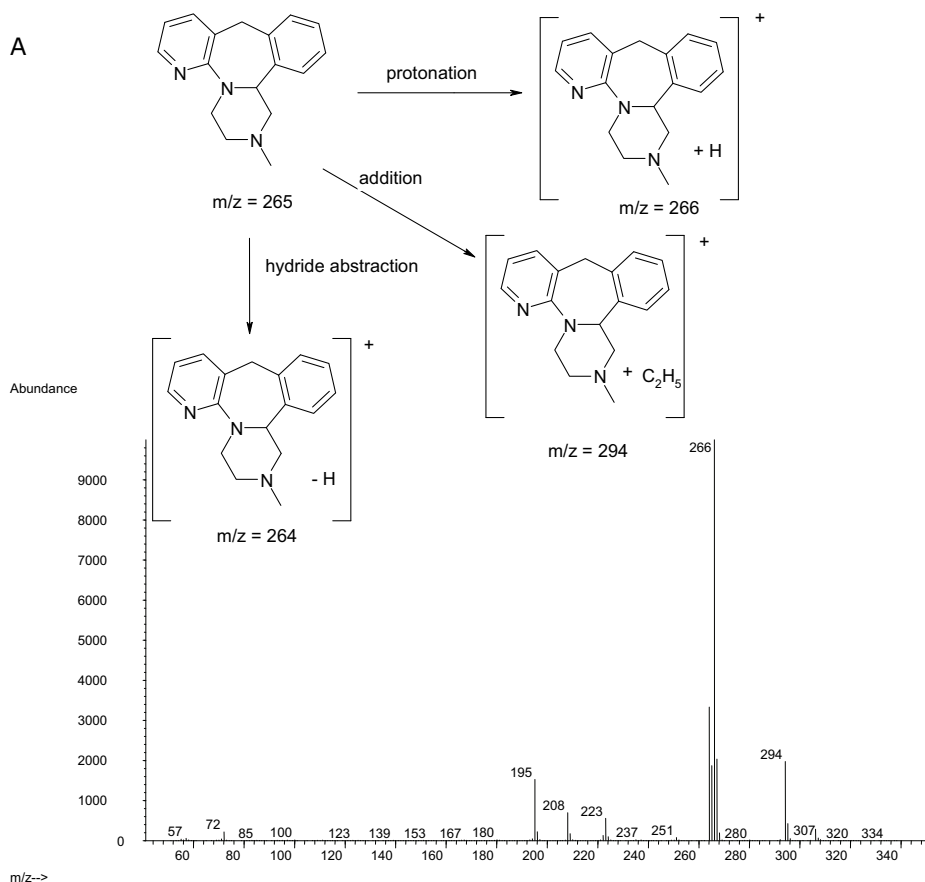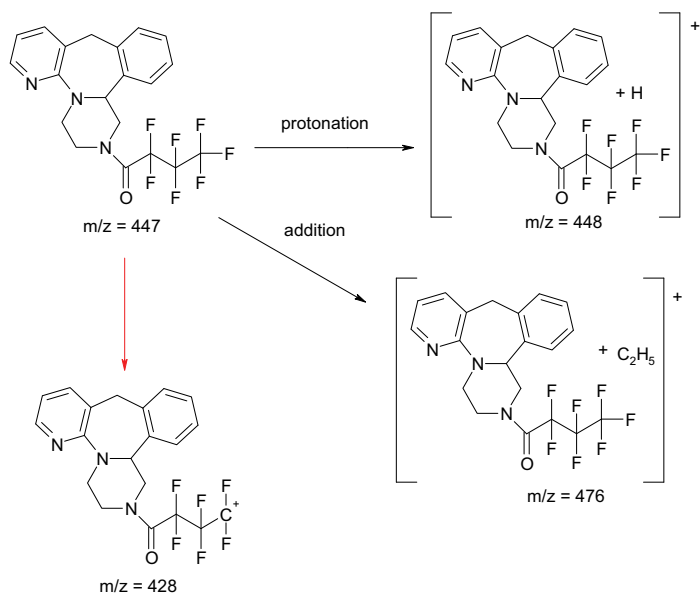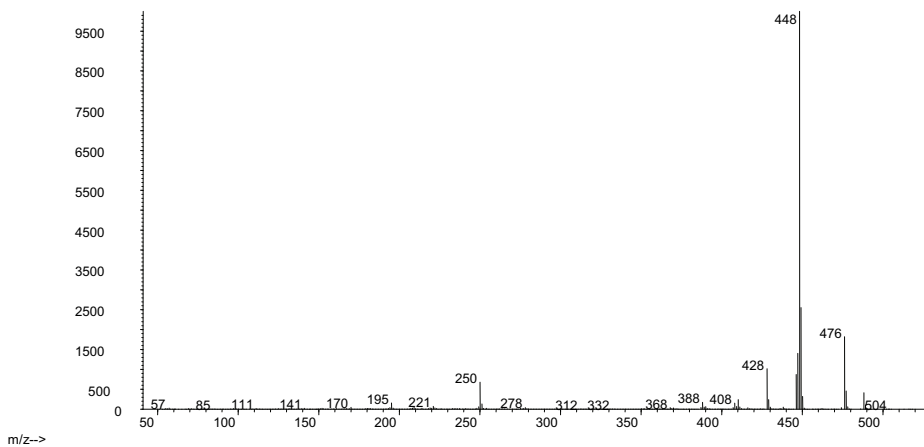
V.4.3.7. *Melitracen*

Melitracen undergoes protonation, addition and hydride abstraction resulting in ions with m/z 292, 320 and 290, respectively.

Figure V. 31. PICI spectrum and fragmentation of melitracen
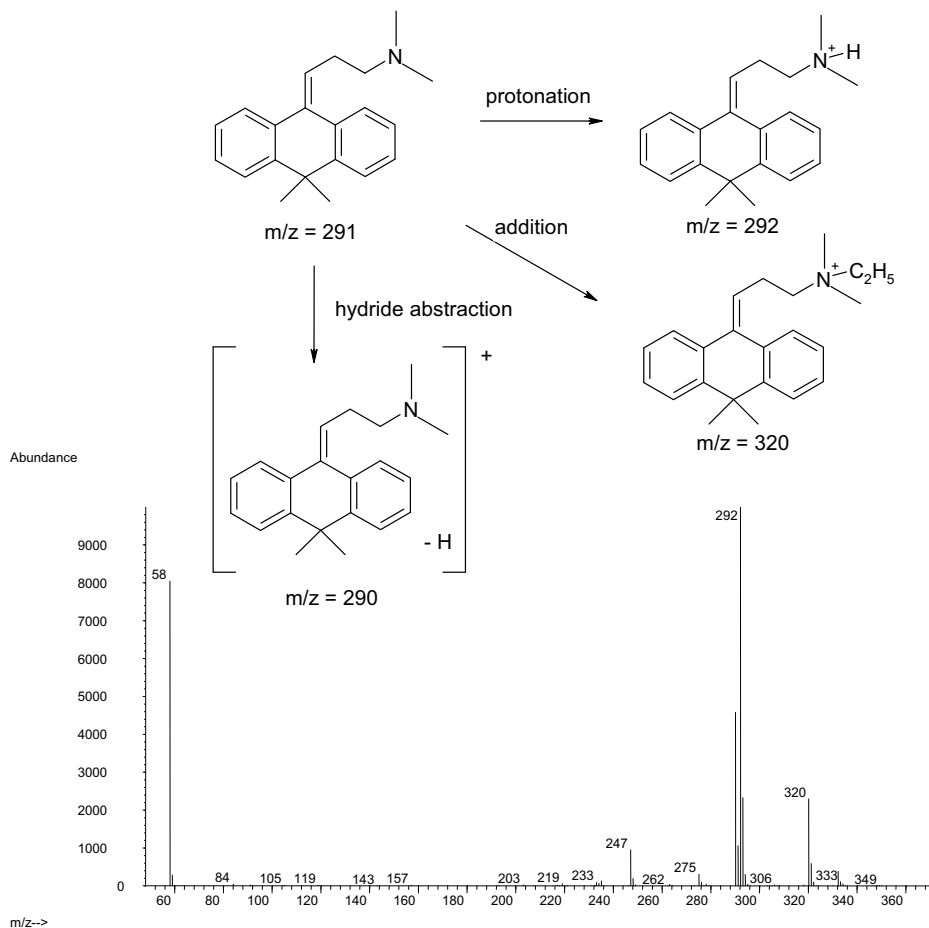
V.4.3.8. Reboxetine

Reboxetine is fragmentated in PICI to ion m/z 372 and 490 due to heterolytic cleavage of the bound next to a heteroatom. For ion m/z 372 the heterolytic cleavage is followed by a loss of water. In addition to these fragments, the protonated quasi-molecular ion 510 amu is also noticed with acceptable abundance in the mass spectrum.

<u>Figure V. 32.</u> PICI spectrum and fragmentation of HFB-reboxetine
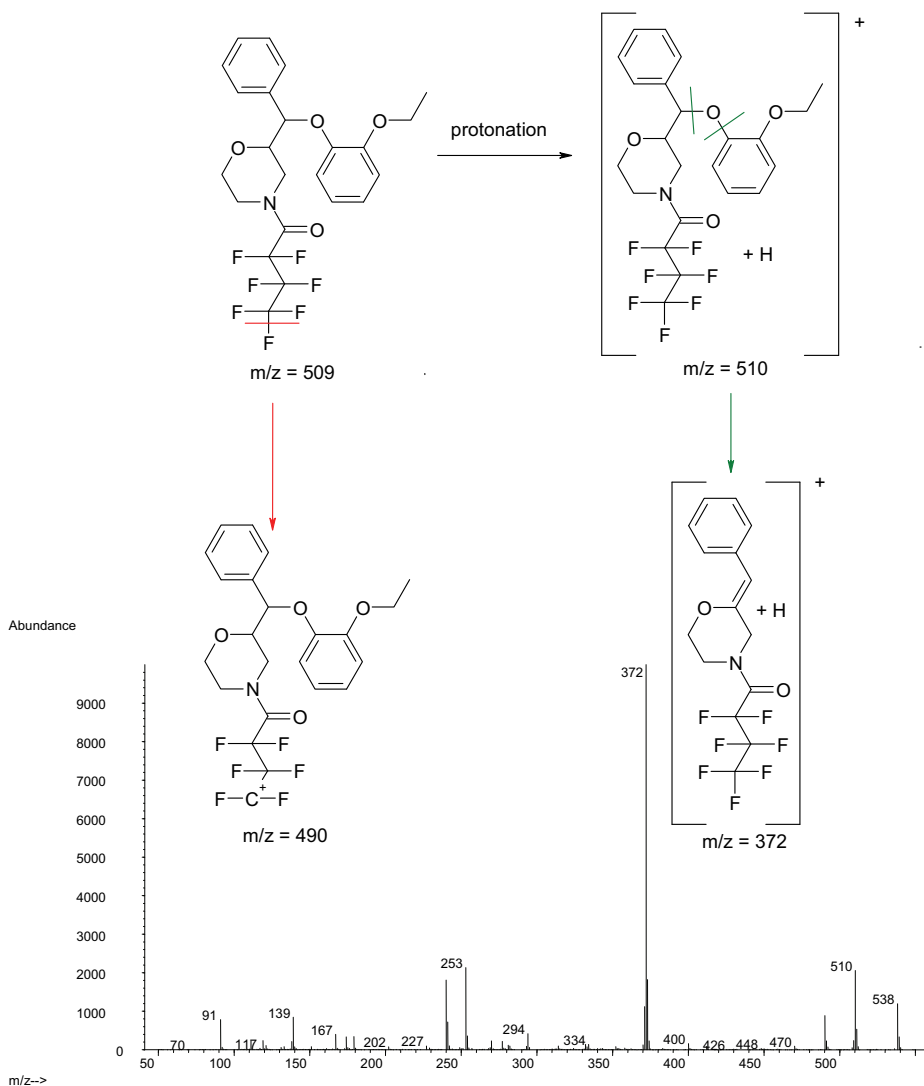
V.4.3.9. *Citalopram, desmethylcitalopram and didesmethylcitalopram*

Ionization in positive ion chemical ionization mode of citalopram occurs by protonation, addition of $C_2H_5^+$ reagent gas ion and abstraction of a fluorine atom. Desmethylcitalopram and didesmethylcitalopram ionize through protonation and addition. Moreover, loss of water (-18 amu) and protonation result in fragment ions with m/z 489 and 475.

Figure V. 33. PICI spectra and fragmentations of citalopram (A), HFB-desmethylcitalopram (B) and HFB-didesmethylcitalopram (C)

A

B

Abundance

m/z-->
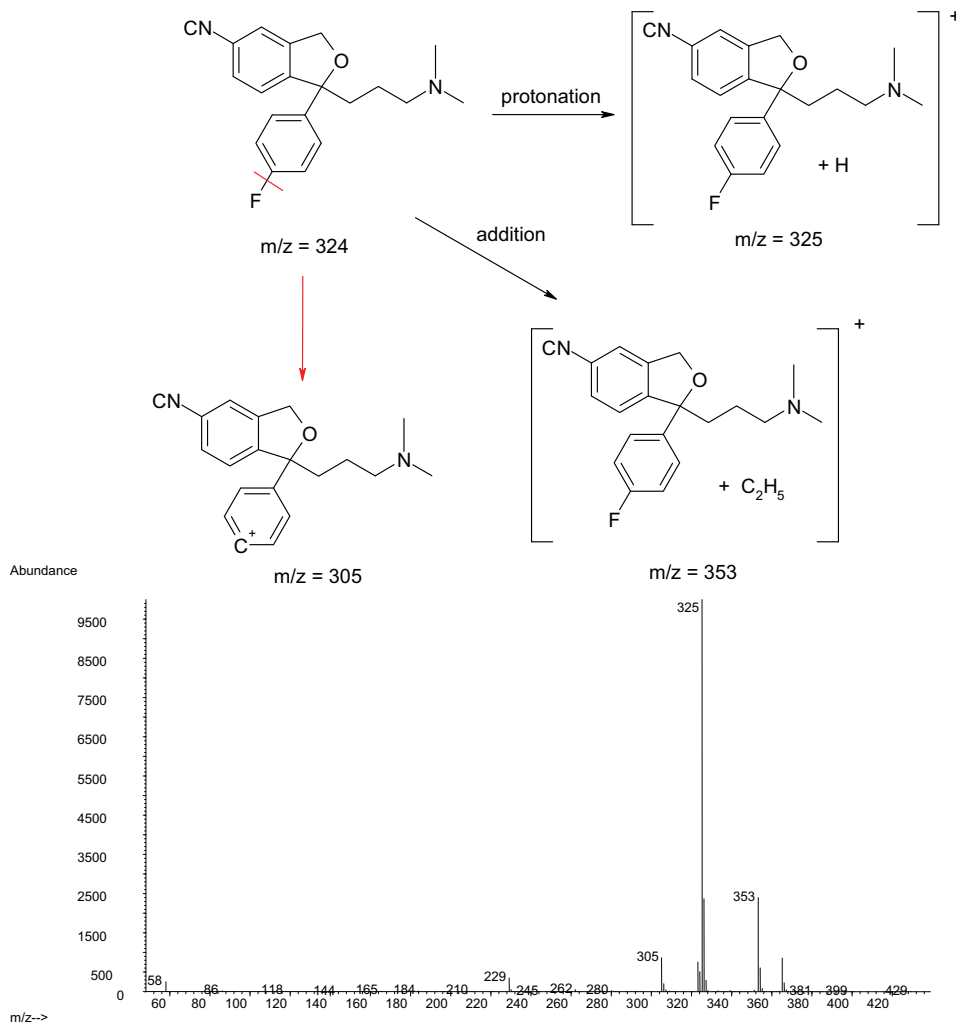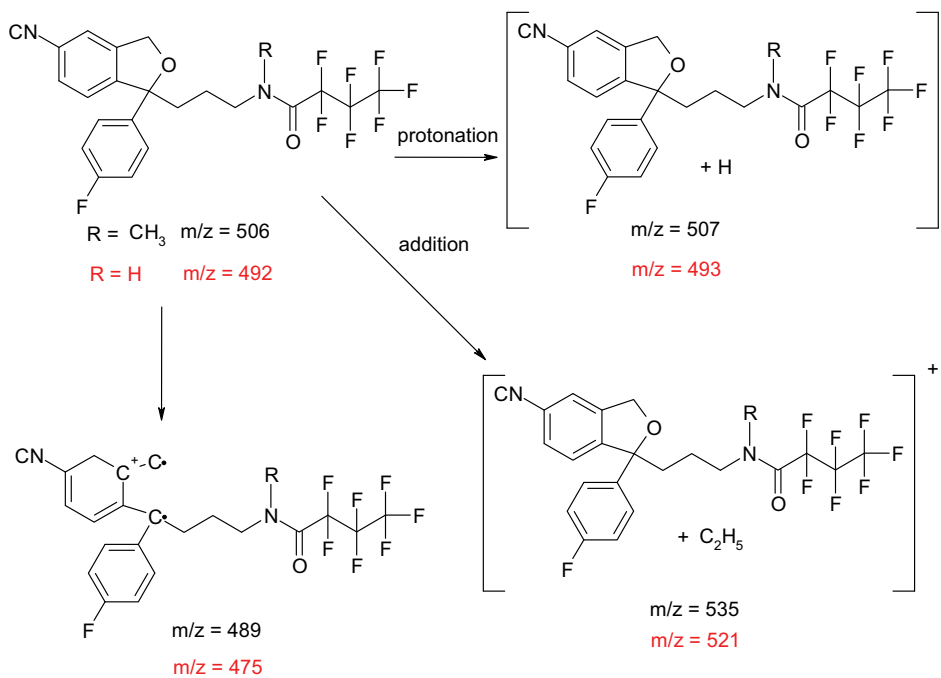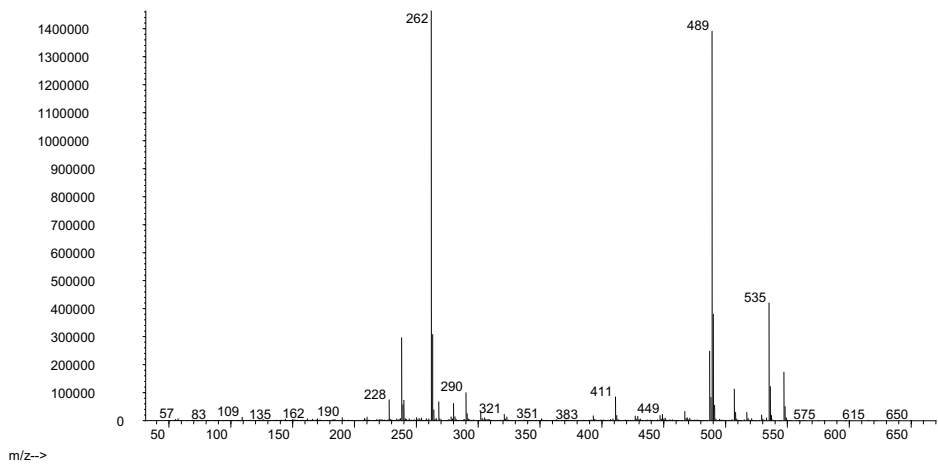
C

Abundance
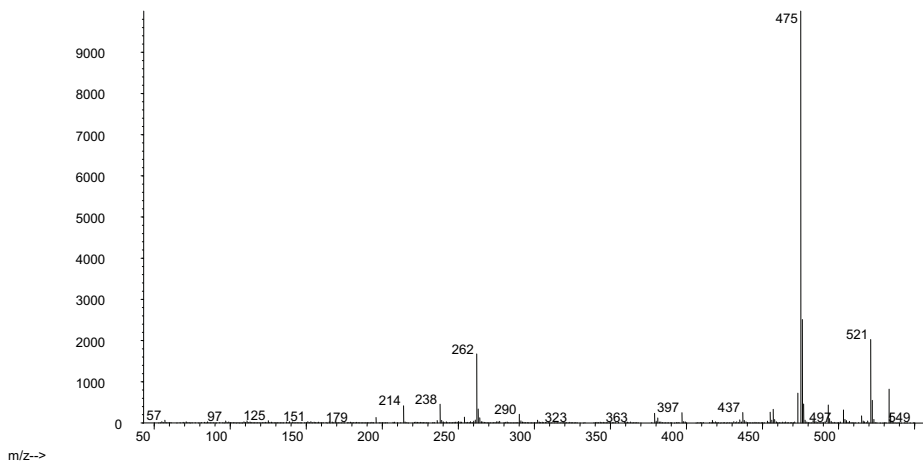
V.4.3.10. *Maprotiline and desmethylmaprotiline*

Ionization of heptafluorobutyrylated maprotiline and its metabolite are a result of protonation, and losses of fluorine atoms as indicated in Figure V.34. For HFB-desmethylmaprotiline, a fragment of m/z 431 is observed due to a retro-Diels-Alder rearrangement.

Figure V. 34. PICI spectra and fragmentations of heptaflurobutyrylated maprotiline (A) and desmethylmaprotiline (B)

A

Abundance

B
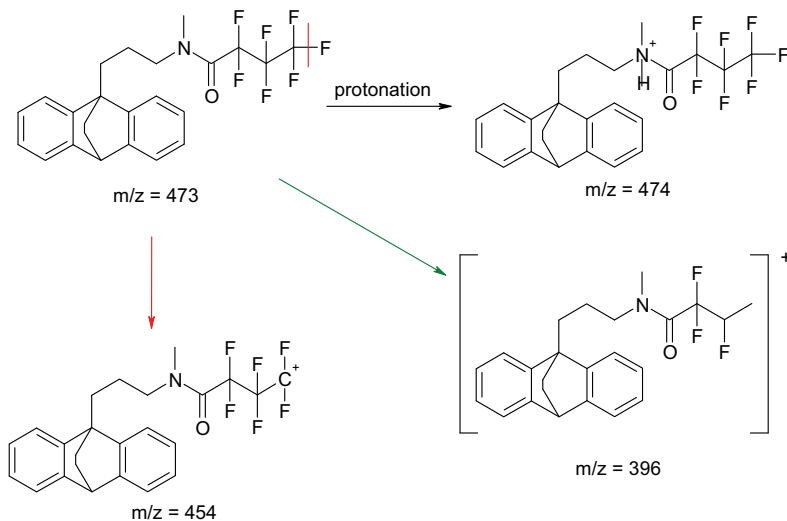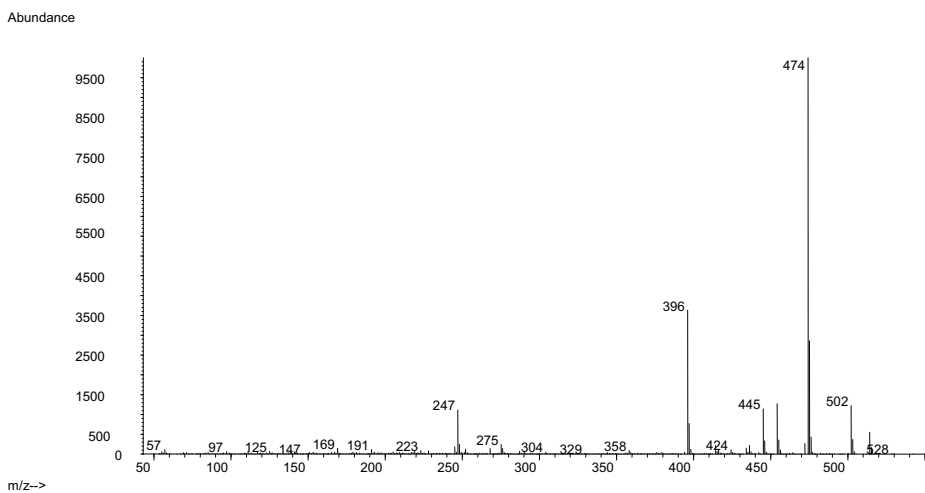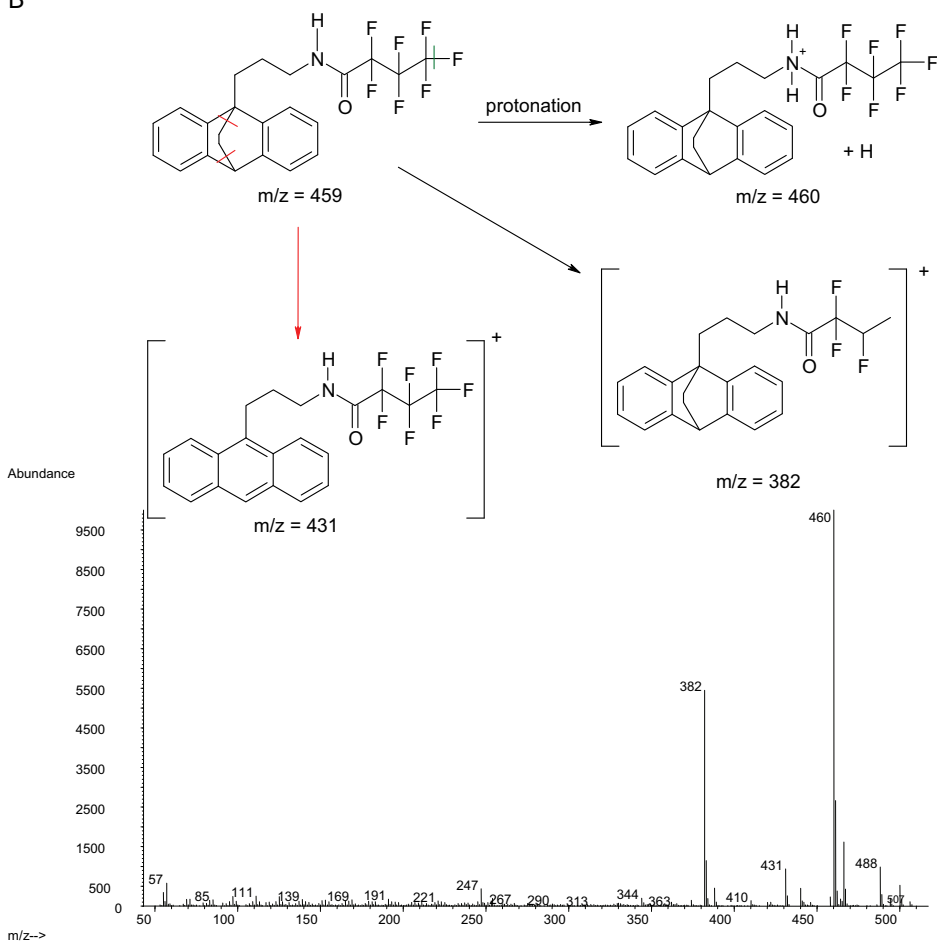
Abundance

V.4.3.11. *Sertraline and desmethylsertraline*

Sertraline and desmethylsertraline are still fragmented in positive ion chemical ionization mode. In PICI the most abundant fragment is the same as for EI, however, the fragment is protonated leading to an m/z-value of 275. The fragment m/z 277 is due to the isotopes of the chlorine atoms on the structure. The calculated molecular weight of HFB-sertraline and HFB-desmethylsertraline is 502 and 488, respectively. Therefore ions m/z 501 and 487 are the quasi-molecular ions after hydride extraction.

Figure V. 35. PICI spectra and fragmentations of heptafluorobutyrylated sertraline (A) and desmethylsertraline (B)

B

Abundance
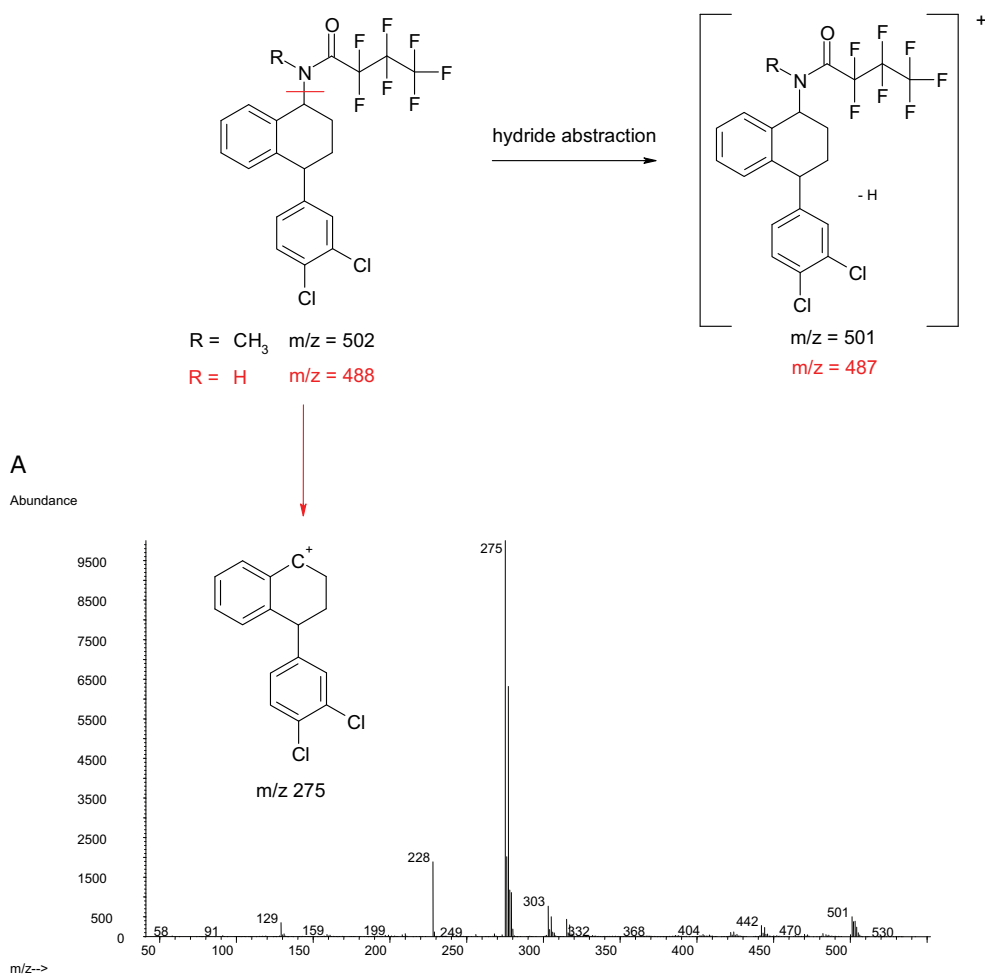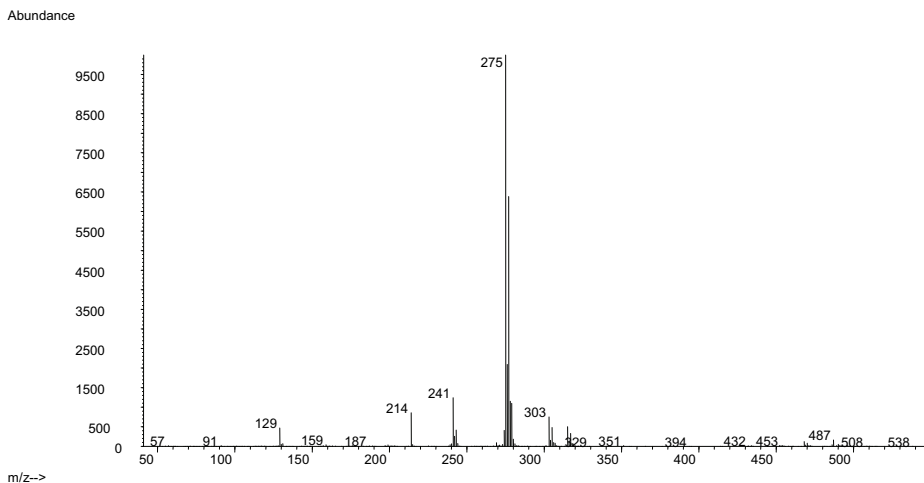
V.4.3.12. *Paroxetine and paroxetine-d$_6$*

Protonation and addition of paroxetine during positive ion chemical ionization leads to ion m/z 526 and 554. Loss of 19 amu due to loss of a fluorine atom results in ion m/z 506. These reactions also occur for paroxetine-d$_6$, resulting in ions with 6 amu more than nondeuterated paroxetine.

Figure V. 36. PICI spectra and fragmentation patterns of heptafluoro-butyrylated paroxetine (A) and paroxetine-d$_6$ (B)

A

Abundance

R = D   m/z = 531
R = H   m/z = 525

protonation

+ H
m/z = 532
m/z = 526

addition

+ C$_2$H$_5$
m/z = 560
m/z = 554

m/z = 512
m/z = 506

B

Abundance

m/z-->
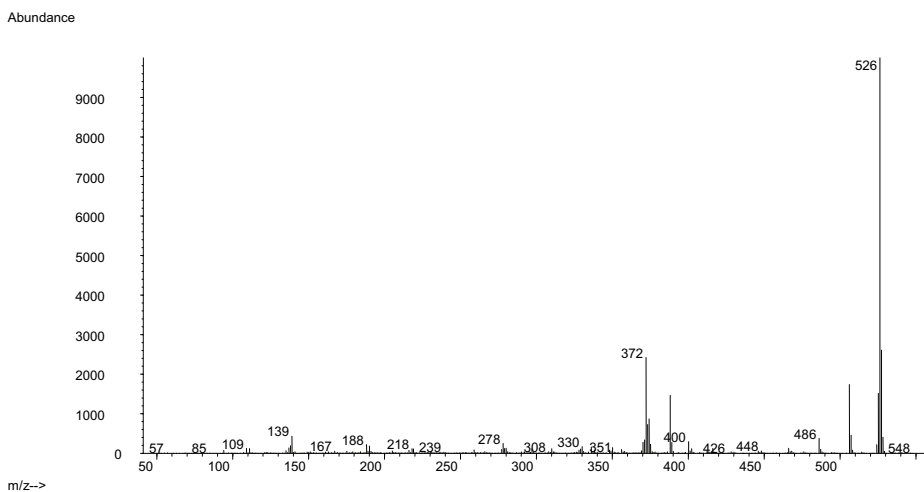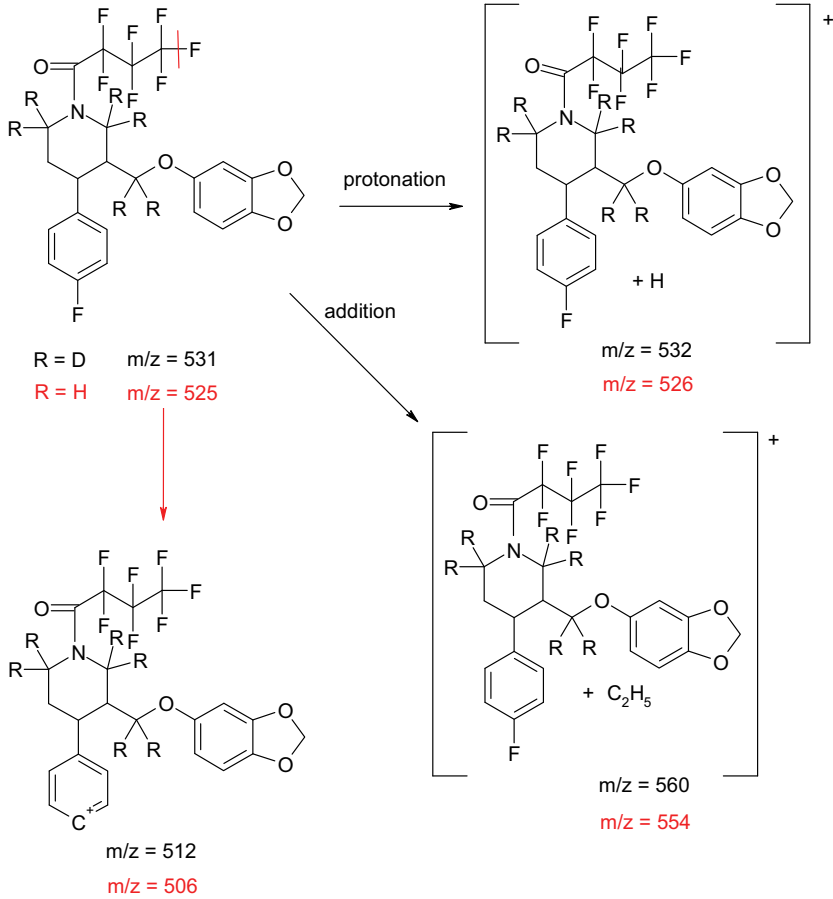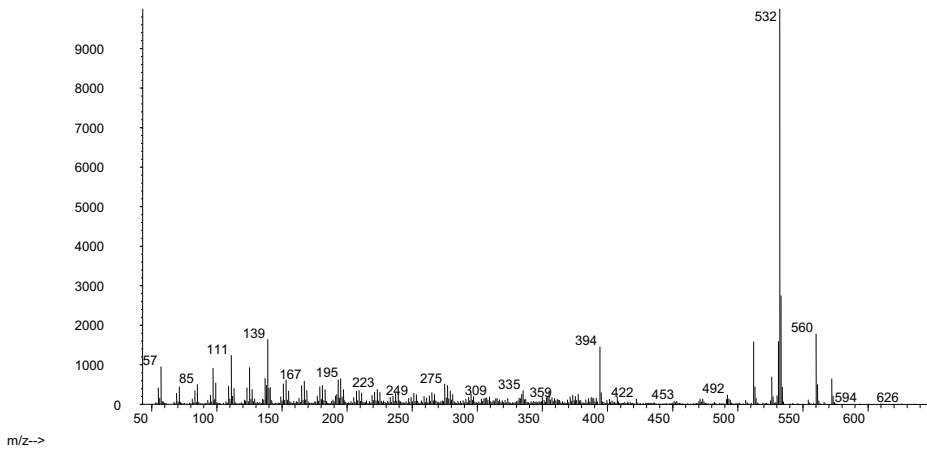
V.4.3.13. *Trazodone and m-chlorophenylpiperazine*

Ionization of trazodone occurs through protonation, addition and fragmentation. Fragmentation occurs at the C-Cl bound, resulting in a loss of a chlorine atom (Figure V.37). Heptafluorobutyrylated m-chlorophenyl-piperazine is protonated and fragmented by loss of fluorine atoms.

Figure V. 37. PICI spectra and fragmentations of trazodone (A) and HFB-m-cpp (B)

A
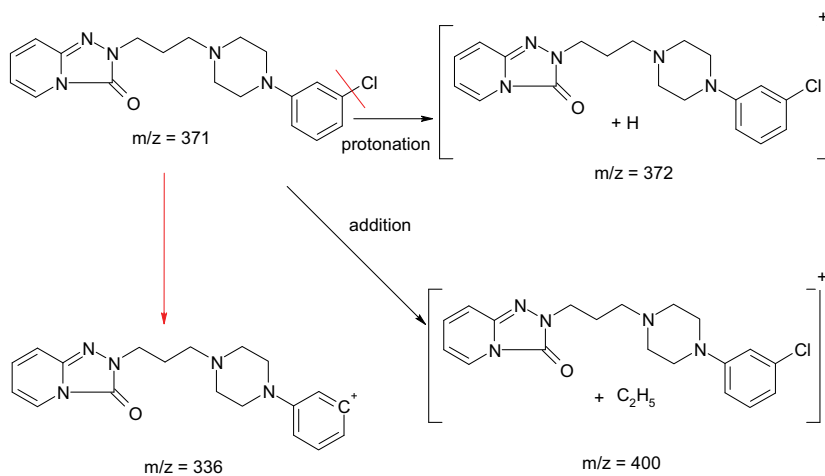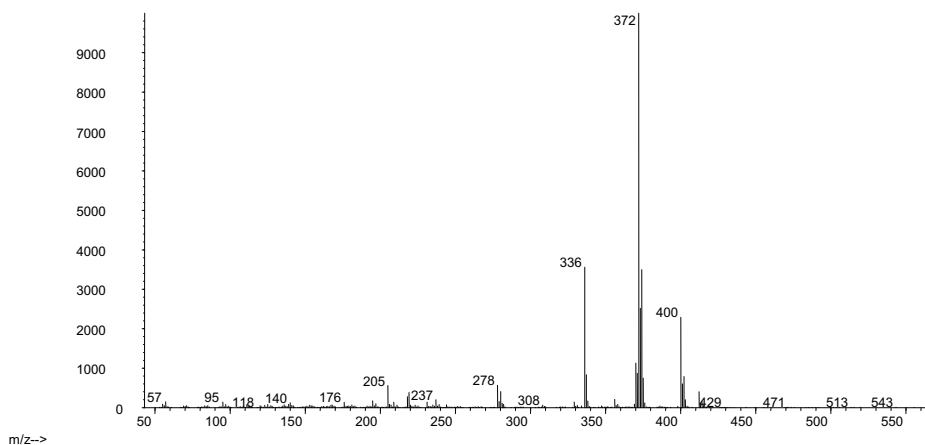
B
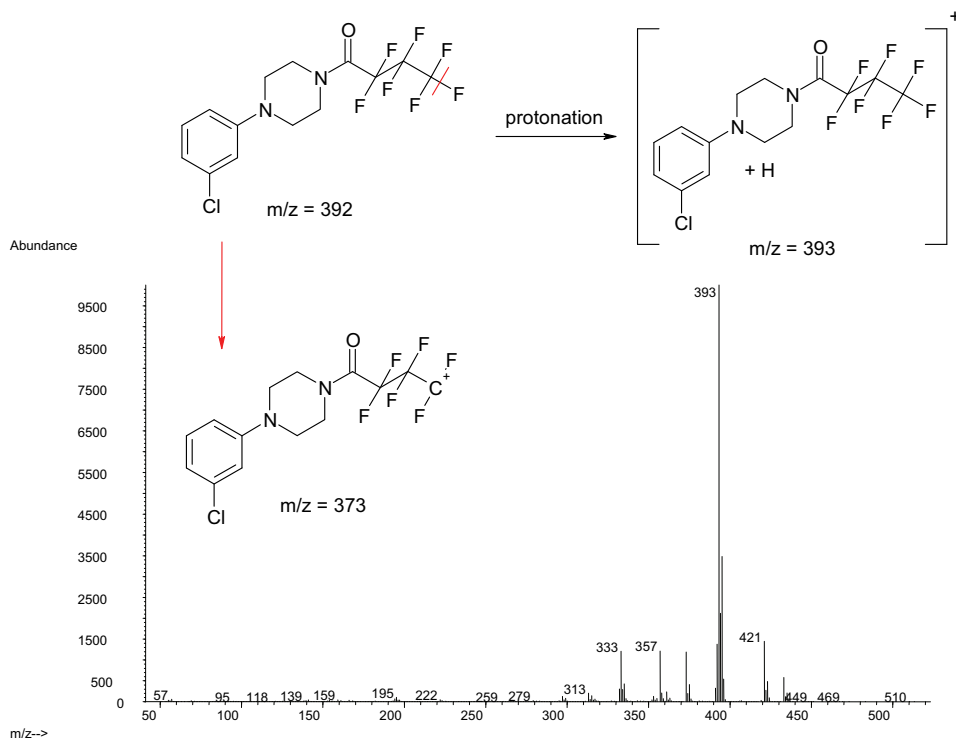
V.4.4. Spectra of the derivatized ADs after negative ion chemical ionization

Negative ion chemical ionization (NICI) is a soft ionization technique and therefore it leads to less fragmentation as compared to EI. In addition, NICI can improve sensitivity compared to PICI or EI with a factor 10 to 1000 times depending on the number of electronegative moieties, either present in their original structure or obtained after derivatization [37, 38]. Because most of the ADs were derivatized with heptafluorobutyrylimidazole, NICI was validated as ionization technique to improve the detection limit.

Negative ion chemical ionization occurs in the same chemical ionization source as in the PICI mode. In the CI plasma, both positive and negative ions are formed simultaneously. The negative quasi-molecular ions that are formed are detected because the MSD is operating with reversed polarity of

all the analyzer voltages, thus extracting negative ions from the source and not the positive ions as in PICI or EI.

<u>Figure V.38.</u> Negative ion chemical ionization reaction using methane gas
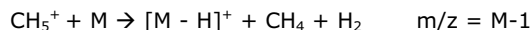
Formation of reagent gas ions when using methane gas

$CH_4 + e^-_{(230\ eV)} \rightarrow CH_4^{+\cdot} + 2\ e^-_{(thermal)}$
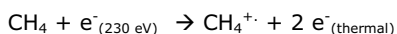
Formation of sample ions

Electron capture:
$MX + e^-_{(thermal\ 0-2\ eV)} \rightarrow MX^{\cdot-}$

Dissociative electron capture:
$MX + e^-_{(thermal\ 0-15\ eV)} \rightarrow M^{\cdot} + X^-$

Ion pair formation
$MX + e^-_{(thermal)} \rightarrow M^+ + X^- + e^-$

The reagent gas, methane in our case, is bombarded with high energy electrons from a filament. As a result, lower energy electrons called thermal electrons are produced and these electrons are then captured by the sample analytes. There are several chemical mechanisms for negative ion chemical ionization. The three most common mechanisms are electron capture, dissociative electron capture, and ion pair formation. The *electron capture reaction* is the primary mechanism in negative ion chemical ionization. When the sample molecule fragments or dissociates afer the electron capture reaction, the reaction is called *dissociative electron capture*. The dissociative electron capture reaction leads to a lower quasi-molecular ion and sensitivity as compared to the electron capture reaction. *Ion pair formation* seems similar to dissociative electron capture, however, the electron is not captured by the created fragments. During ion pair formation, the molecule fragments in such way that the electrons are distributed unevenly and positive as well as negative ions are generated. Another unwanted reaction can occur during NICI: ion-molecule reactions. These reactions compete with the electron

capture reactions, resulting in decreased sensitivity. Ion-molecule reactions are a result of traces of water, oxygen or other contaminants that are ionized by electrons from the filament and react with the sample molecules through addition.

In the following paragraph, the spectra for the different (heptafluoro-butyrylated) ADs obtained in NICI with methane gas are discussed. The spectra were obtained in scan mode, and the fragments chosen for the selected ion mode will be discussed.

V.4.4.1. *Venlafaxine and O-desmethylvenlafaxine*

Dehydrated venlafaxine and O-demethylvenlafaxine are not detected in NICI mode as they do not contain the highly electronegative moiety containing 7 fluorine atoms after the heptafluorobutyrylimidazole derivatization (IV.4.3.1.). ODMV can be derivatized, however, this derivatization reaction is irreproducible as discussed in chapter IV. The spectrum of derivatized ODMV in NICI mode shows extensive fragmentation to the heptafluorobutyryl-reagent fragment (Figure V.39.).

Figure V.39. NICI spectrum and fragmentation of HFB-ODMV
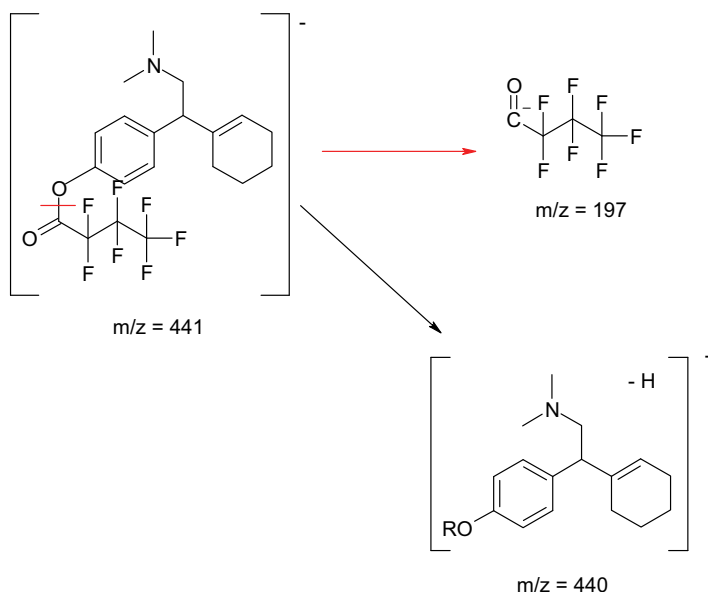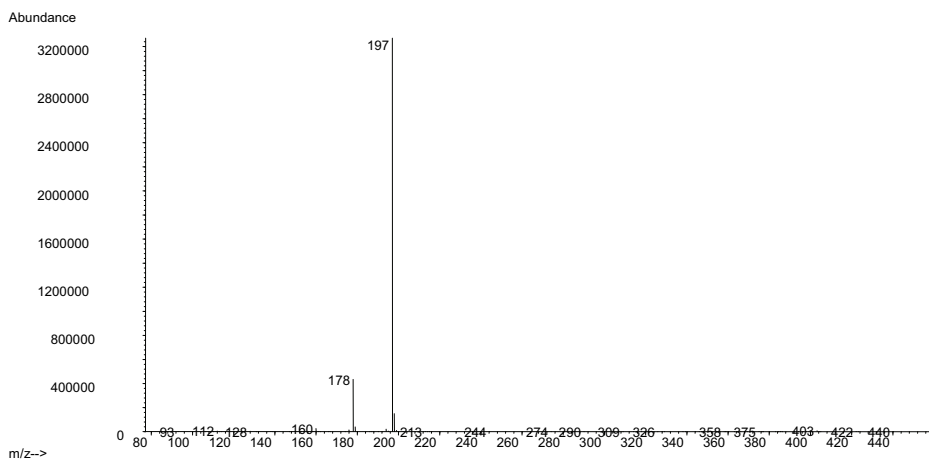
V.4.4.2. *Viloxazine*

Heptafluorobutyrylated viloxazine shows a very low abundant molecular ion in NICI. Several losses of 20 amu are observed resulting in fragments with m/z 413, 393 and 373. These losses indicate a loss of hydrogen and a fluorine atom.

<u>Figure V. 40.</u> NICI spectrum and fragmentation of HFB-viloxazine

Abundance

m/z-->
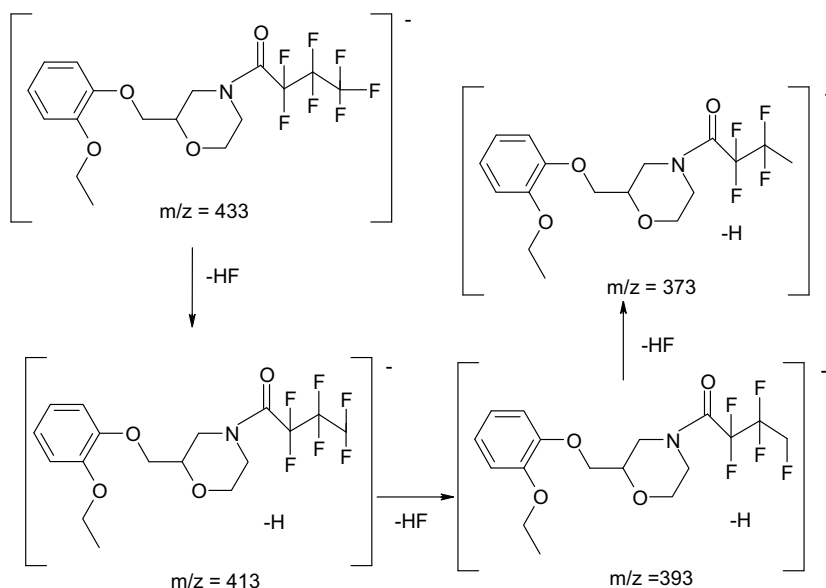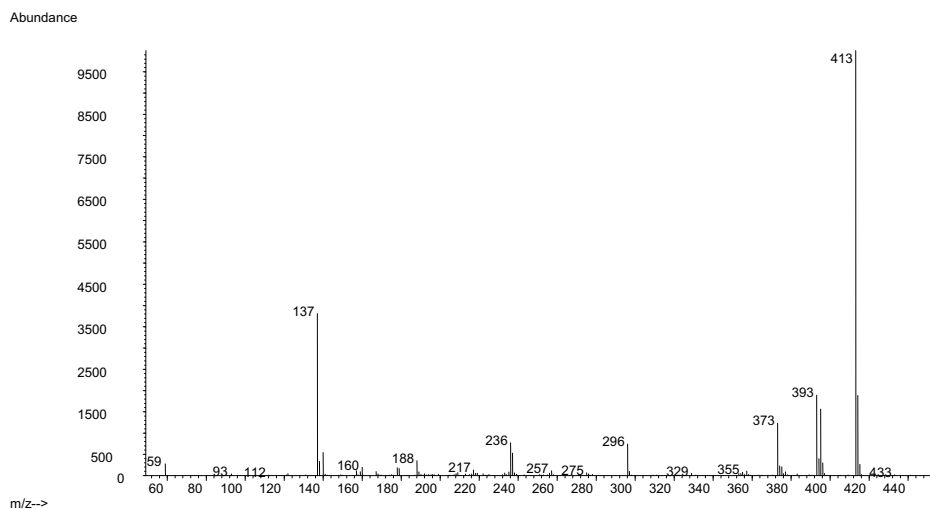
V.4.4.3. *Fluvoxamine*

Figure V. 41. NICI spectrum and fragmentation of HFB-fluvoxamine

Abundance

m/z-->
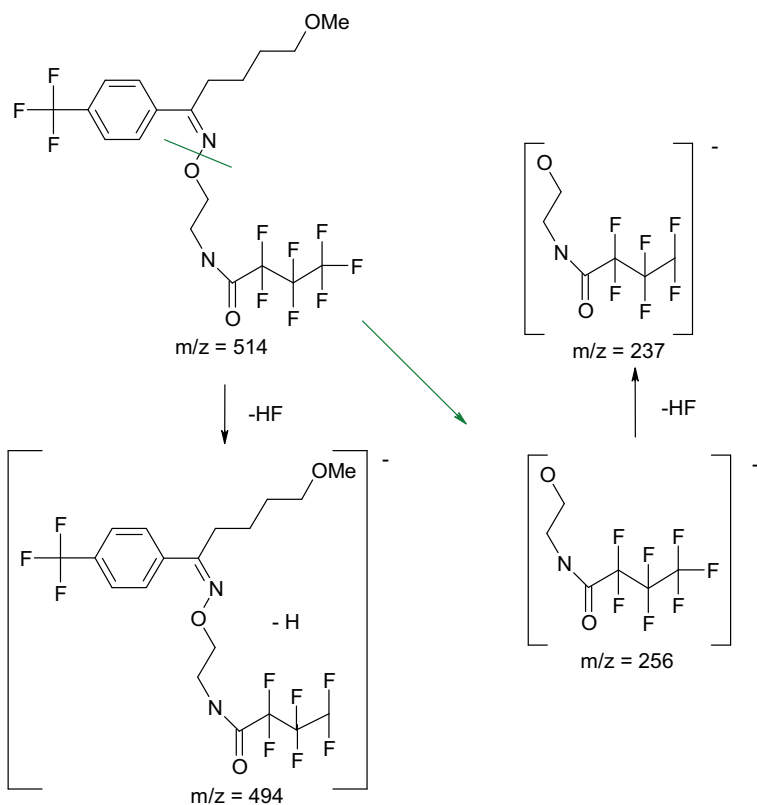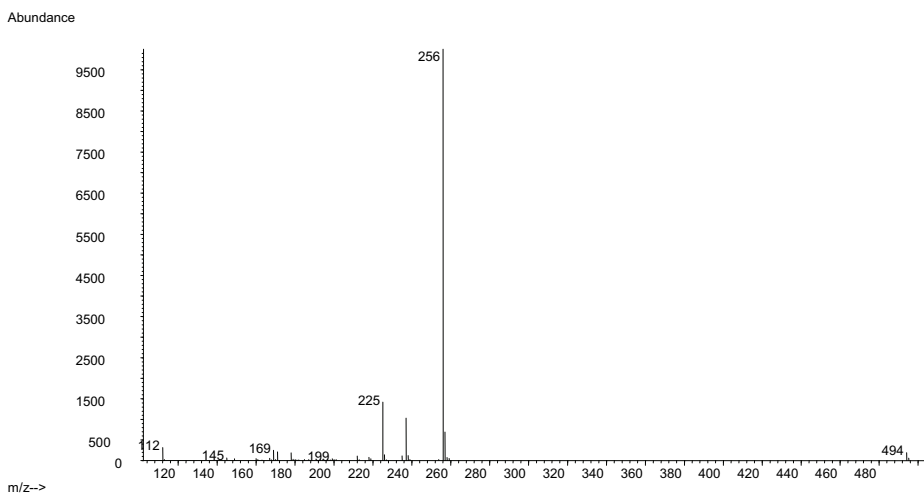
No electron capture reaction is observed for fluvoxamine in NICI mode. Dissociative electron capture reactions result in ions with m/z 494 (loss of HF), 256 and 237. The last two ions demonstrate fragmentation even in the 'soft' NICI ionization technique.

V.4.4.4. *Fluoxetine, fluoxetine-d$_6$ and desmethylfluoxetine*

The molecular ion of fluoxetine, fluoxetine-d$_6$ and desmethylfluoxetine is observed and is a result of the electron capture reaction during negative ionization. For fluoxetine and fluoxetine-d$_6$ two times a loss of HF is observed in addition to the molecular ion. For desmethylfluoxetine, again, a loss of HF is observed together with a fragment m/z 329.

<u>Figure V. 42.</u> NICI spectra and fragmentations of heptafluorobutyrylated fluoxetine (A), fluoxetine-d_6 (B) and desmethylfluoxetine (C)

R = H   m/z = 505
R = D   m/z = 511

-HF

m/z = 485
m/z = 491

-HF

m/z = 465
m/z = 471

A

Abundance

m/z-->
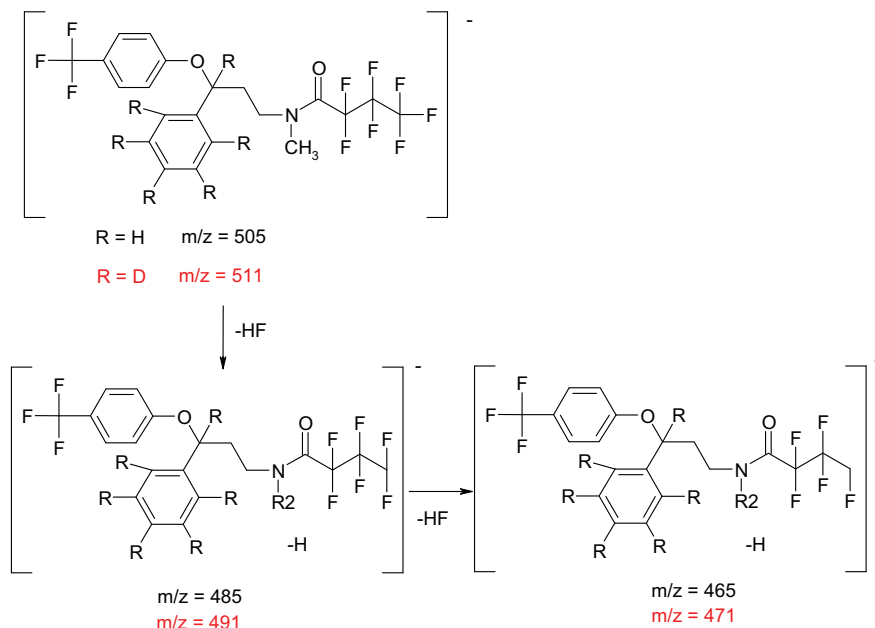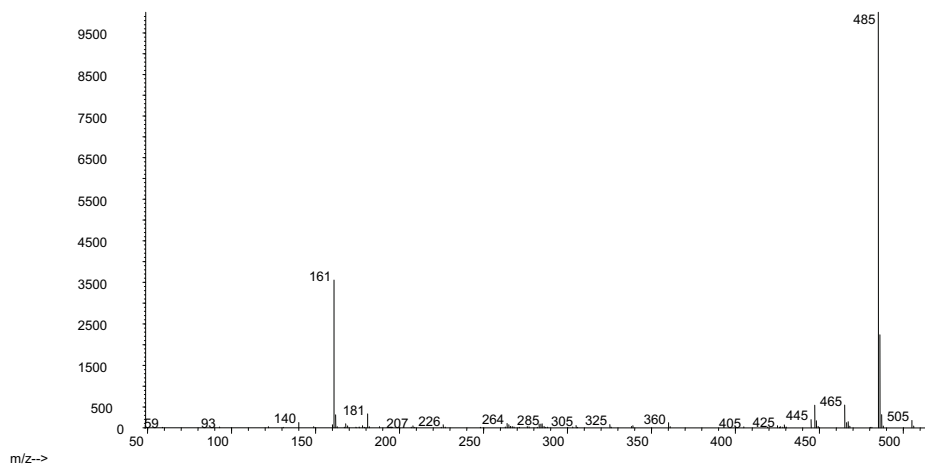
B
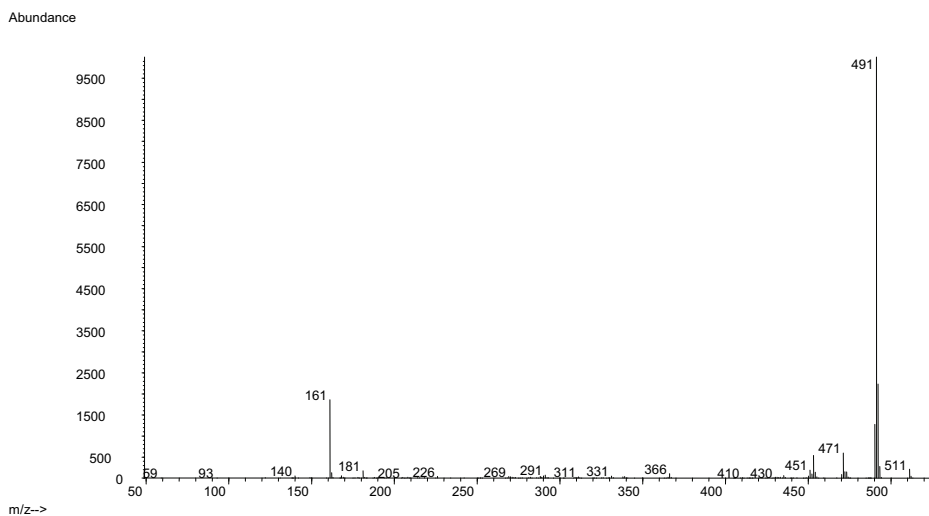
C
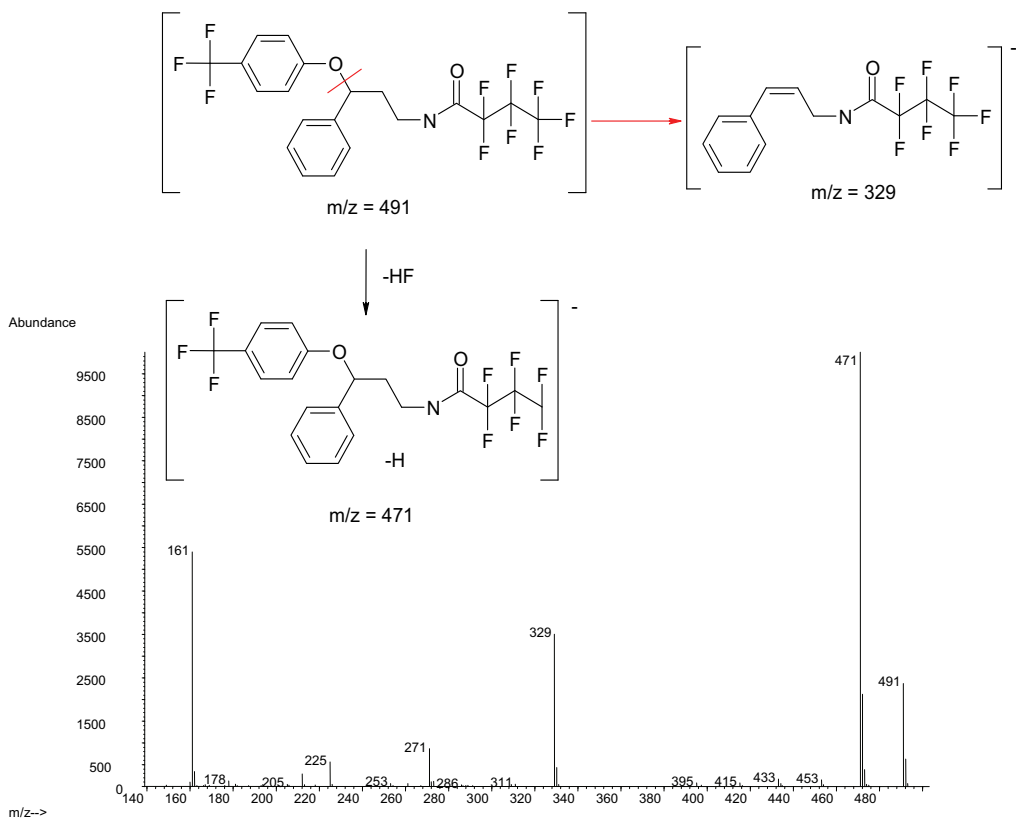
V.4.4.5. *Mianserin, mianserin-d$_3$ and desmethylmianserin*

Mianserin and mianserin-d$_3$ are not derivatized and are not detected in NICI mode. Desmethylmianserin demonstrates losses of 20 amu, thus loss of HF.

<u>Figure V. 43.</u> NICI spectra and fragmentation of HFB-desmethylmianserin
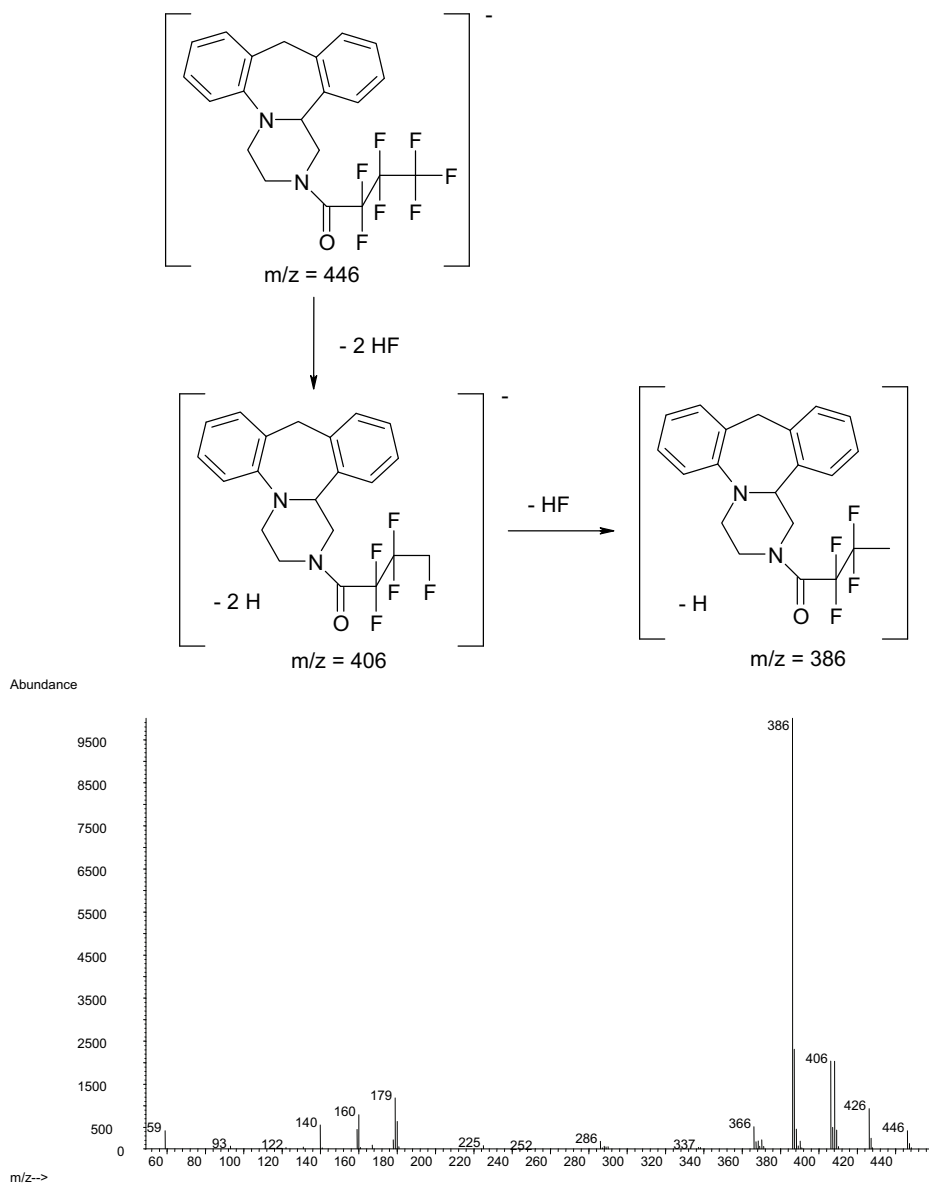
V.4.4.6. *Mirtazapine and desmethylmirtazapine*

Mirtazapine is not derivatized and is thus not detected in NICI mode. Desmethylmirtazazpine shows the same ionization pattern as desmethyl-mianserin as it is a structural analogue.

Figure V. 44. NICI spectrum and fragmentation of HFB-desmethylmirtazapine
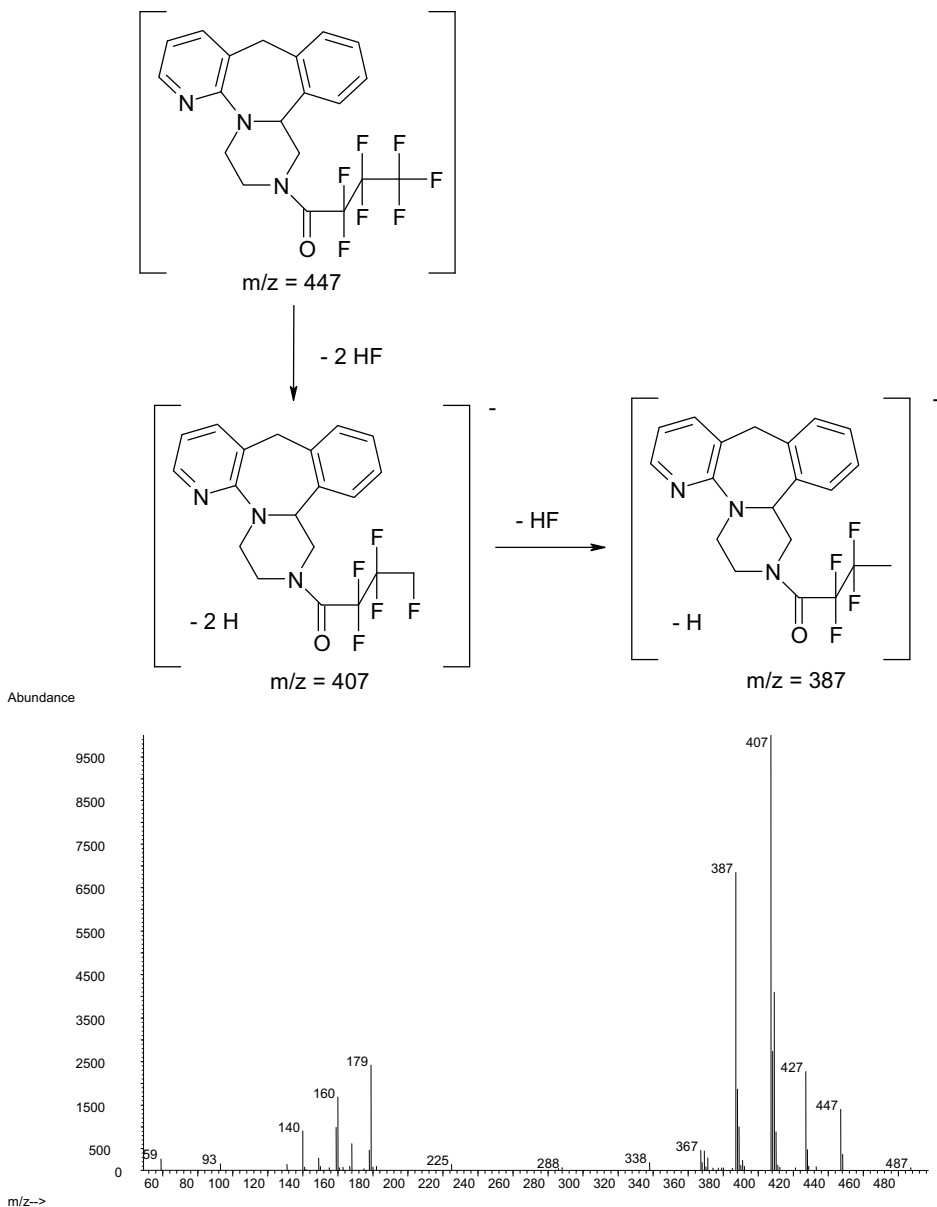
V.4.4.7. *Melitracen*

Melitracen is a tertiary amine that is not derivatized and thus not detected in NICI mode.

V.4.4.8. *Reboxetine*

The molecular ion of heptafluorobutyrylated reboxetine is not detected in the spectrum of reboxetine. Losses of 20 amu due to loss of HF can be observed in the spectrum and ion m/z 489 is chosen as this fragment results in the highest m/z ratio and is the most abundant ion in the spectrum. Reboxetine is still fragmented in NICI mode, and therefore two fragments with m/z 296 and 312 are chosen because of their structural information.

Figure V. 45. NICI spectrum and fragmentation of HFB-reboxetine

Abundance
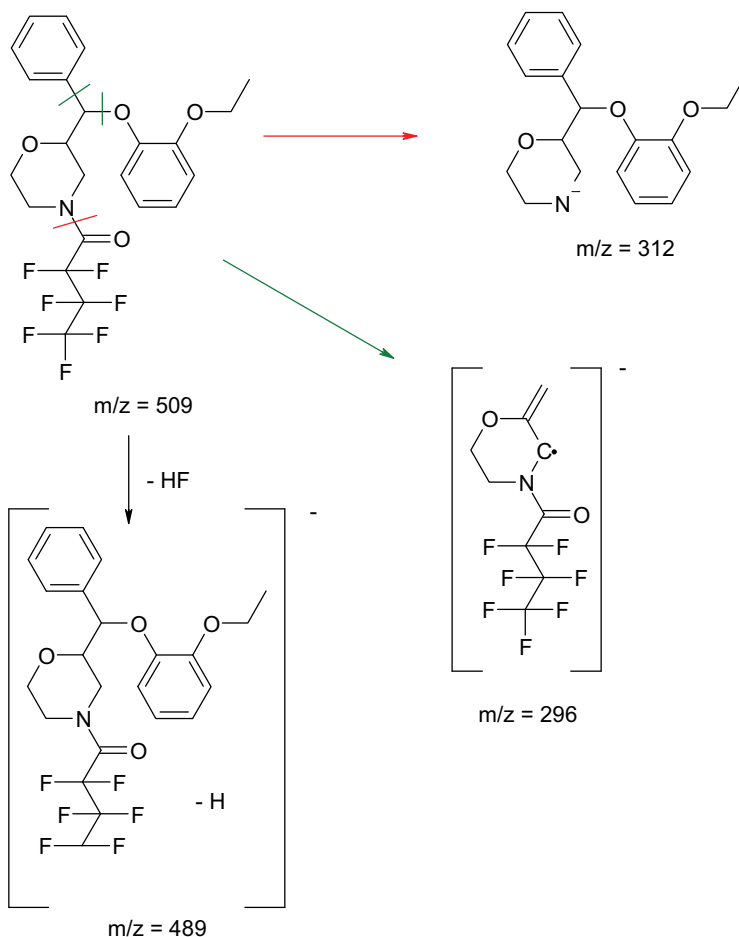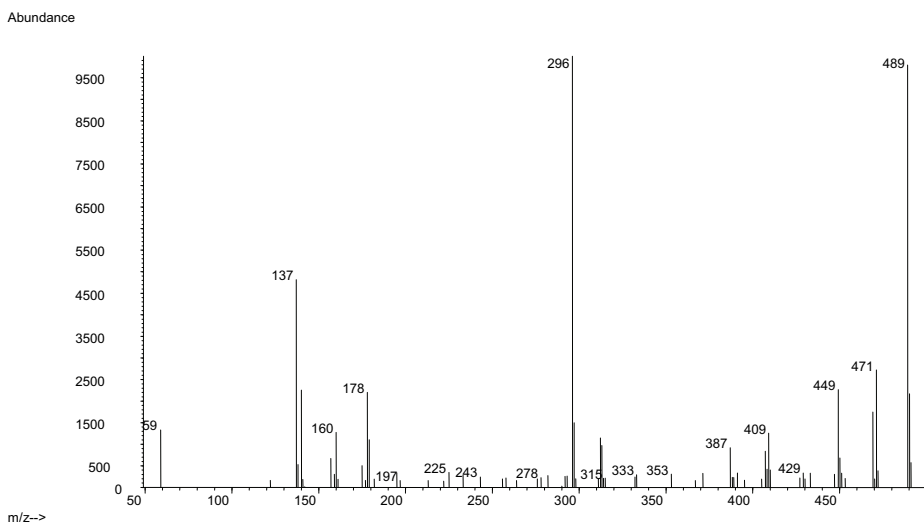
V.4.4.9. *Citalopram, desmethylcitalopram and didesmethylcitalopram*

Although citalopram contains one fluorine atom in its underivatized structure, its electron affinity is too low for the molecule to be detected in NICI mode. The derivatized metabolites of citalopram, however, can be detected.

<u>Figure V. 46.</u> NICI spectra and fragmentations of HFB-desmethyl- (A) and didesmethylcitalopram (B)

R = CH$_3$ m/z = 506
R = H   m/z = 492

- HF

m/z = 486
m/z = 472

- HF

m/z = 466
m/z = 452

A

Abundance

B
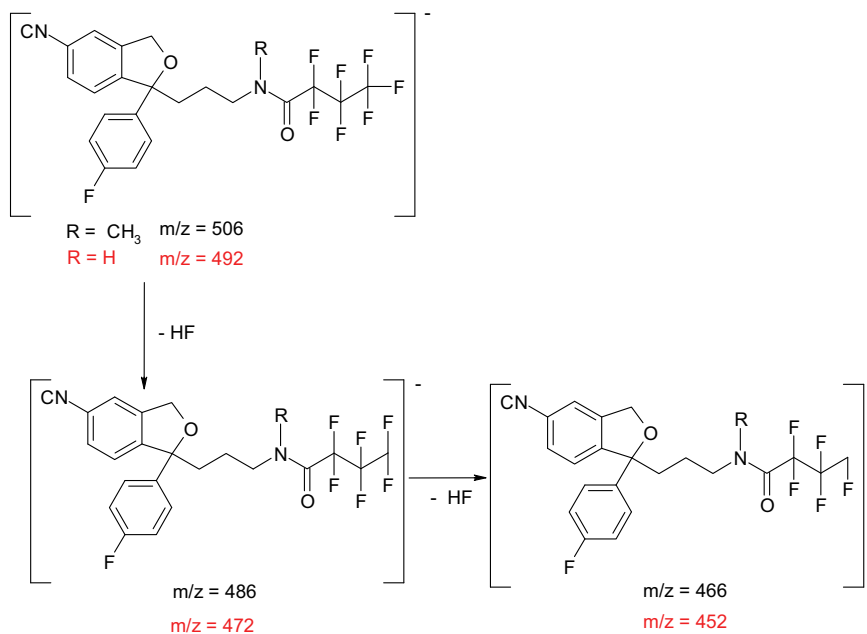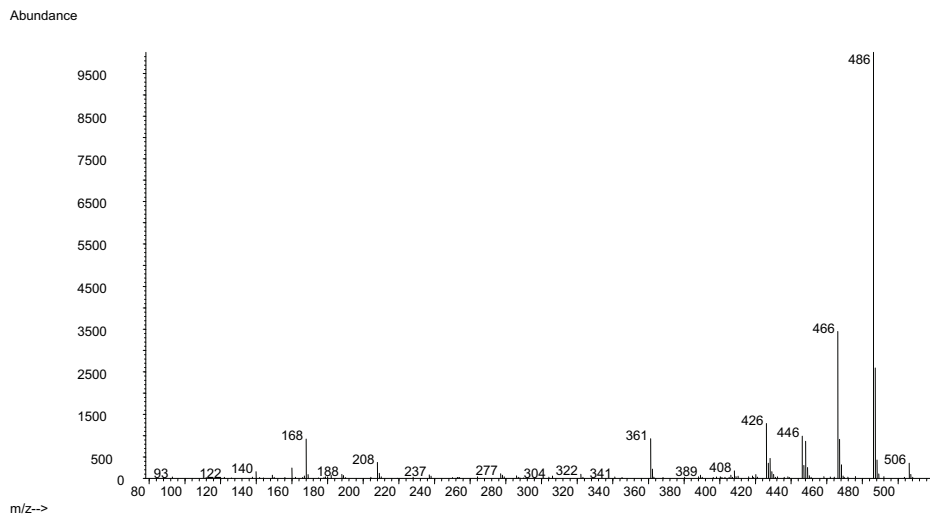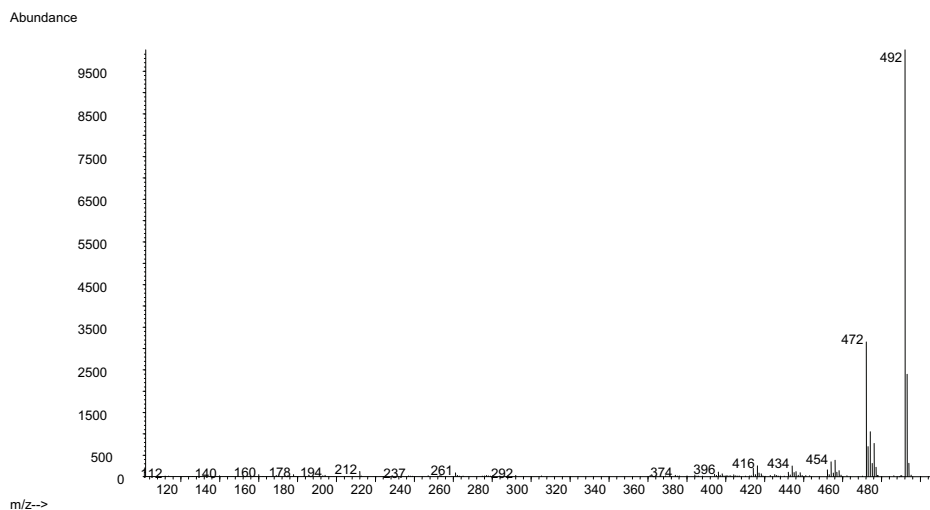
Abundance

For didesmethylcitalopram a clear negative molecular ion (482 amu) is detected as a result of electron capture. The molecular ion of desmethylcitalopram (506 amu) is less abundant, and this metabolite is more stable after a loss of HF. For the two metabolites of citalopram the dissociative electron capture reaction during negative ion chemical ionization leads to most of the fragment ions in the spectra.

V.4.4.10. *Maprotiline and desmethylmaprotiline*

Dissociative electron capture is the dominant reaction type occurring during negative ion chemical ionization of maprotiline and desmethylmaprotiline as indicated in Figure V.47.

Figure V. 47. NICI spectra and fragmentations of HFB-maprotiline (A) and HFB-desmethylmaprotiline (B)

A

B

Abundance

m/z-->
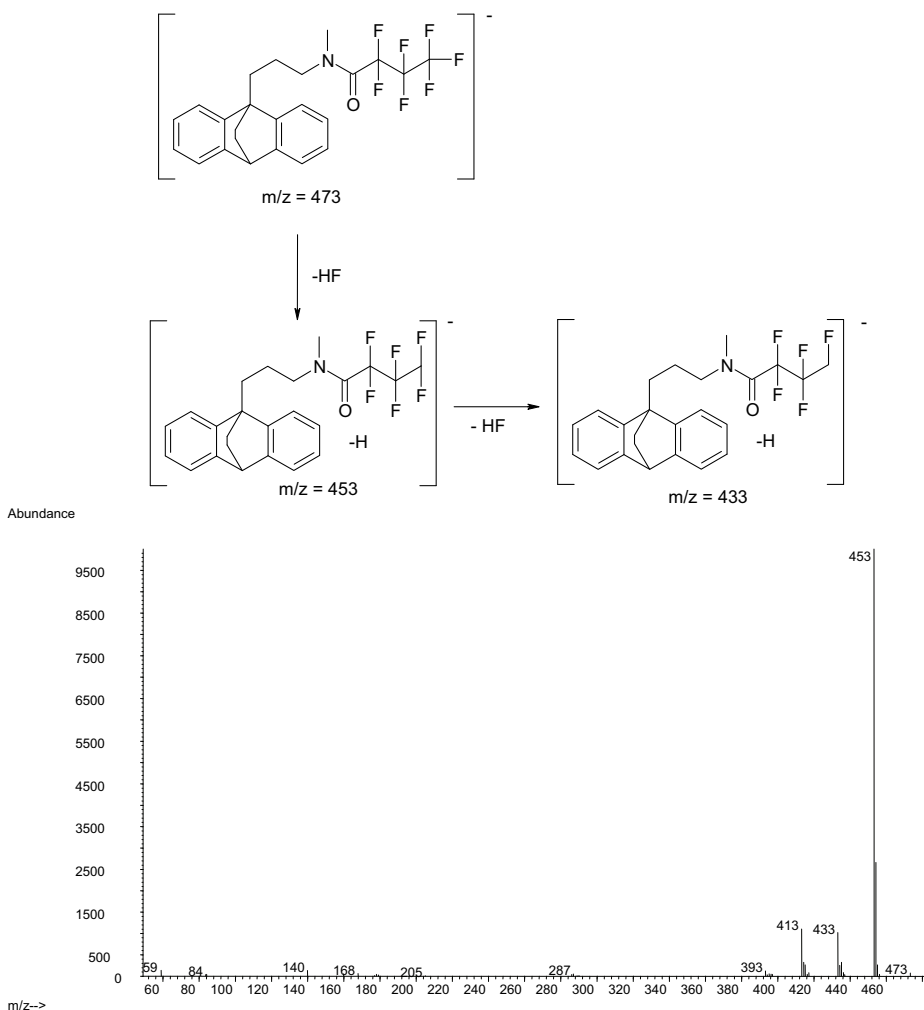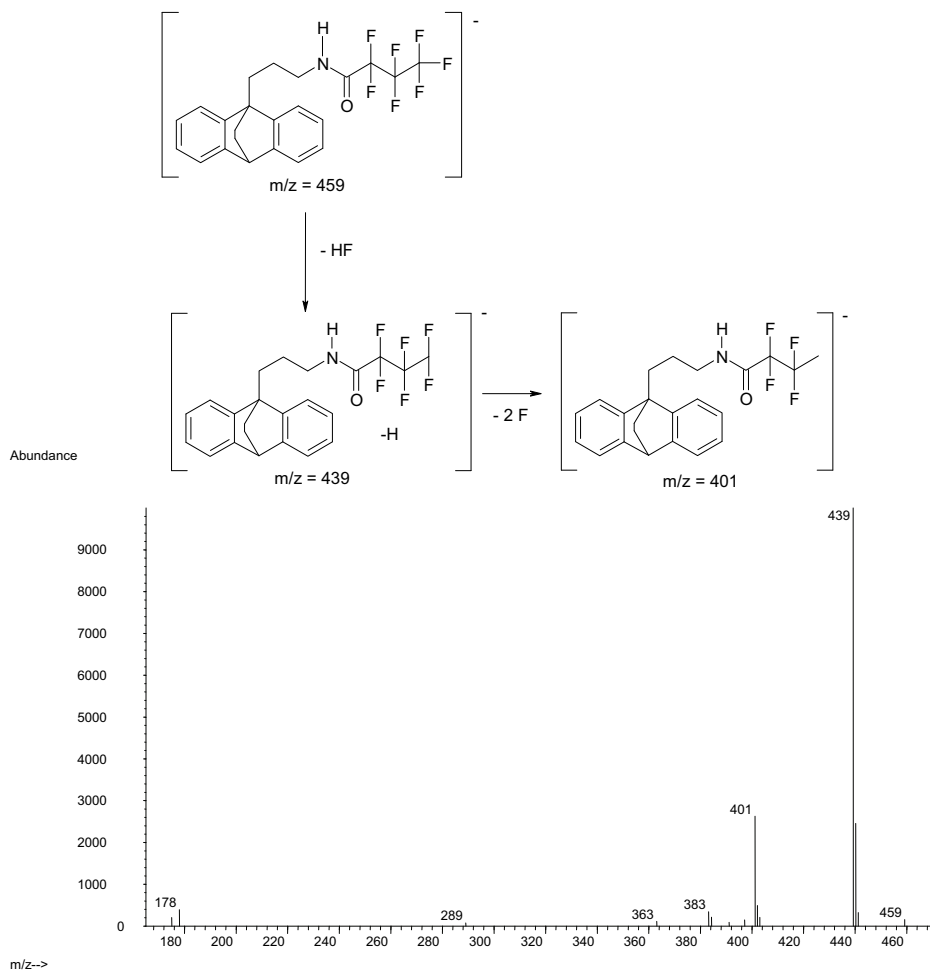
V.4.4.11. *Sertraline and desmethylsertraline*

Heptafluorobutyrylated sertraline demonstrates losses of HF and leads to ions with m/z 501, 481, 461, 441 as the highest abundant ions. Negative ionization of the HFB-derivative of the desmethylsertraline also results in a loss of HF (m/z 467). In addition a loss of one chlorine atom in combination with a fluorine atom can be suspected (Figure V.48).

Figure V. 48. NICI spectra and fragmentations of heptafluororbutyrylated sertraline (A) and desmethylsertraline (B)

A

m/z = 501

- HF

m/z = 481

- H

- 2 HF

m/z = 441
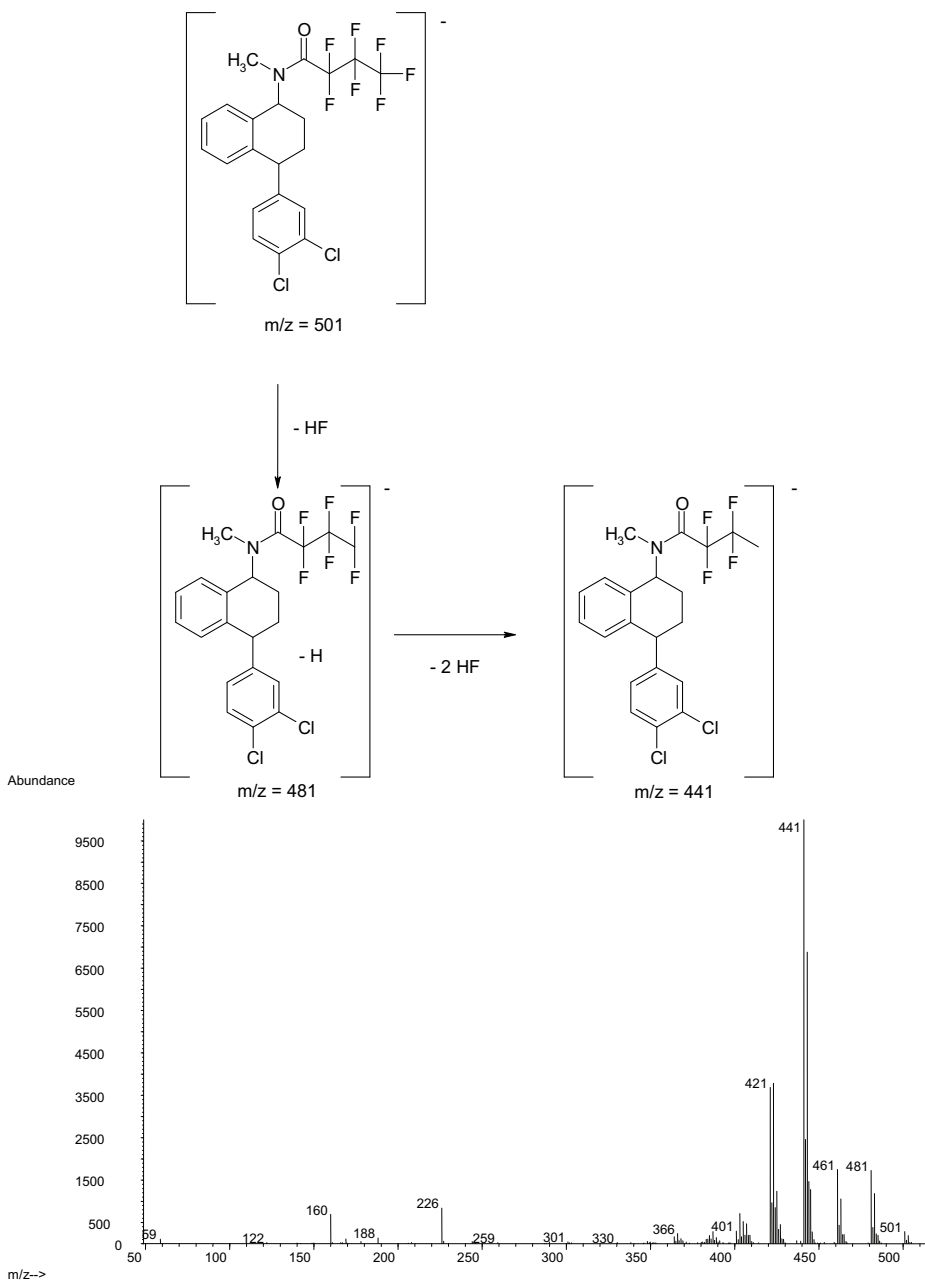
B
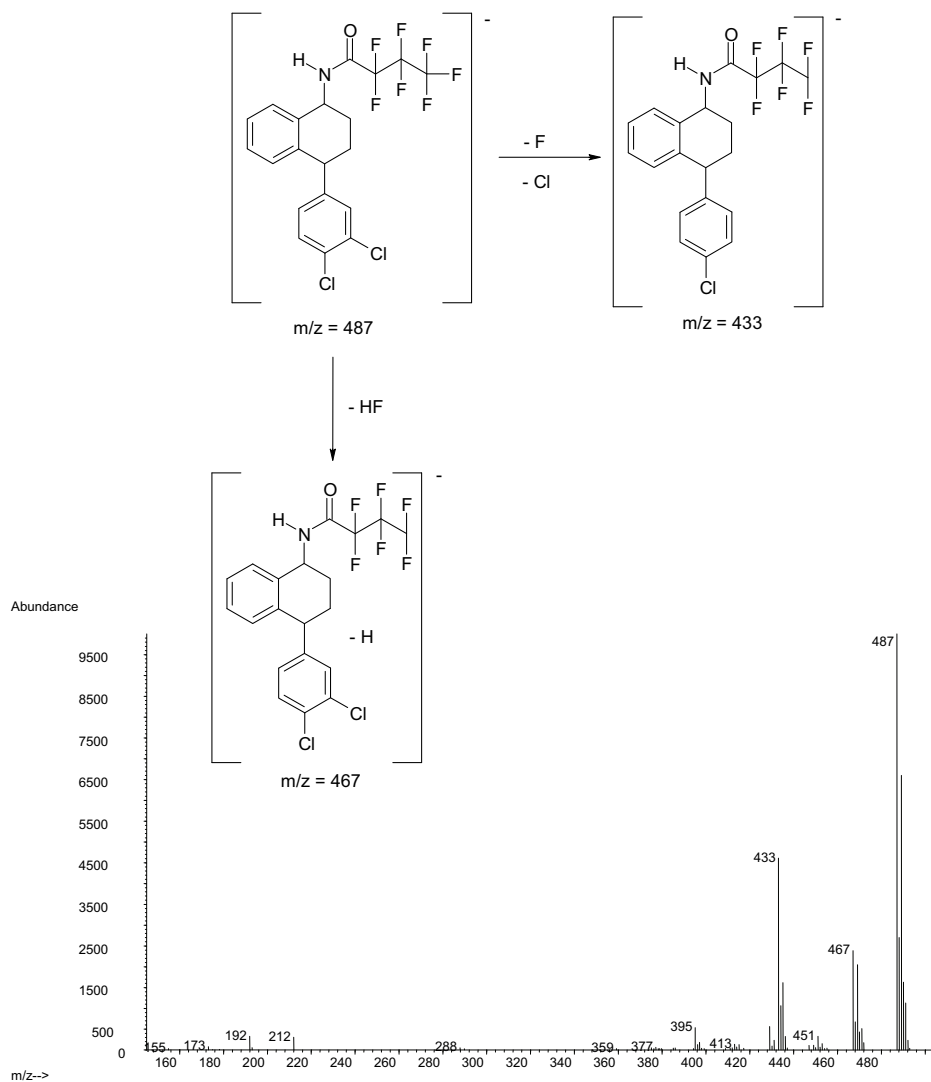
V.4.4.12. *Paroxetine and paroxetine-d₆*

Dissociative electron capture is the dominant reaction type occurring during negative ion chemical ionization of paroxetine and paroxetine-d$_6$ as indicated in Figure V.49.

<u>Figure V. 49.</u> NICI spectra and fragmentation patterns of HFB-paroxetine (A) and HFB-paroxetine-d$_6$ (B)

A

Abundance

m/z-->

B

Abundance

m/z-->
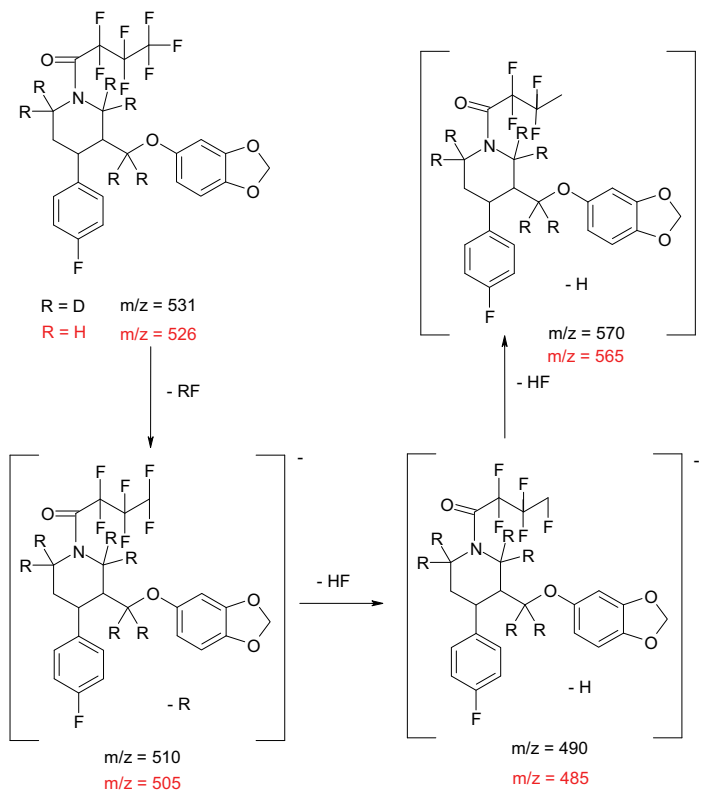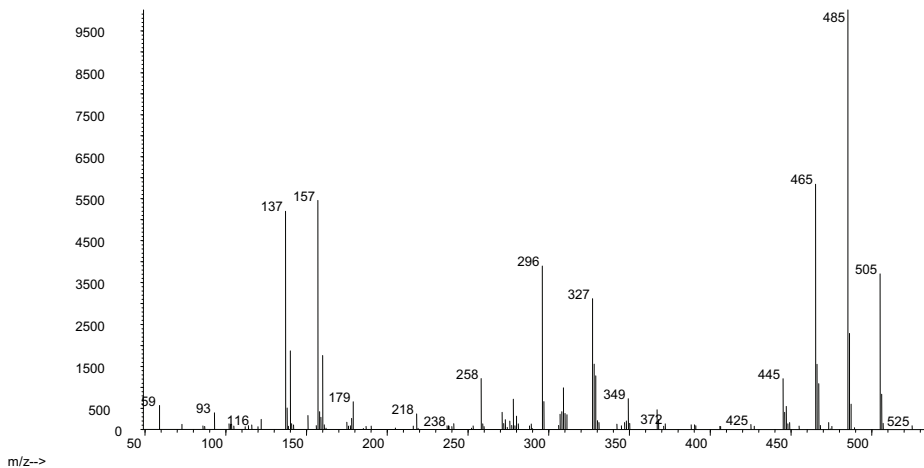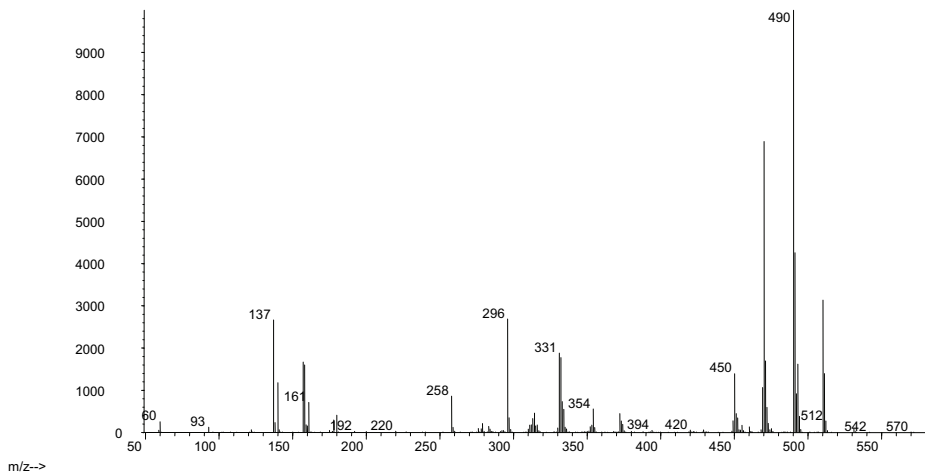
V.4.4.13. *Trazodone and m-chlorophenylpiperazine*

Trazodone is not detected in NICI mode as this tertiary amine can not be derivatized using heptafluorobutyrylimidazole. The metabolite of trazodone, m-chlorophenylpiperazine, can be heptafluorobutyrylated and demonstrates losses of 20 amu due to loss of HF fragments.

<u>Figure V. 50.</u> NICI spectrum and fragmentation of of HFB-m-cpp

Abundance

m/z-->
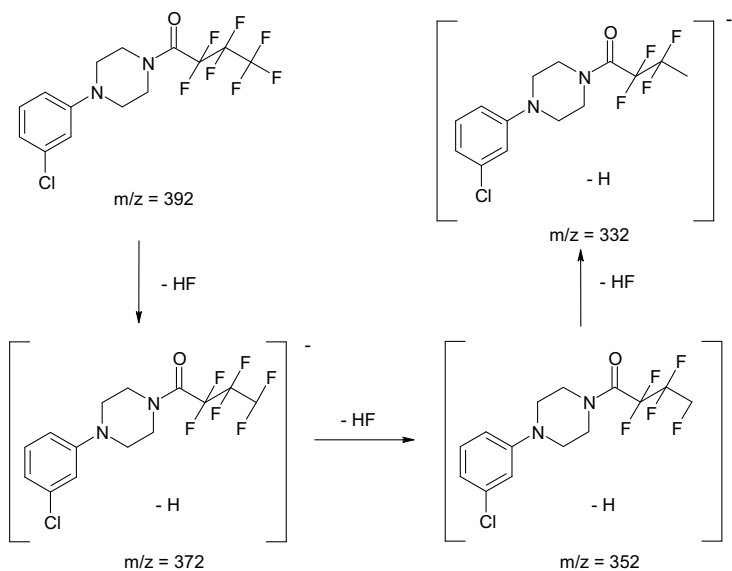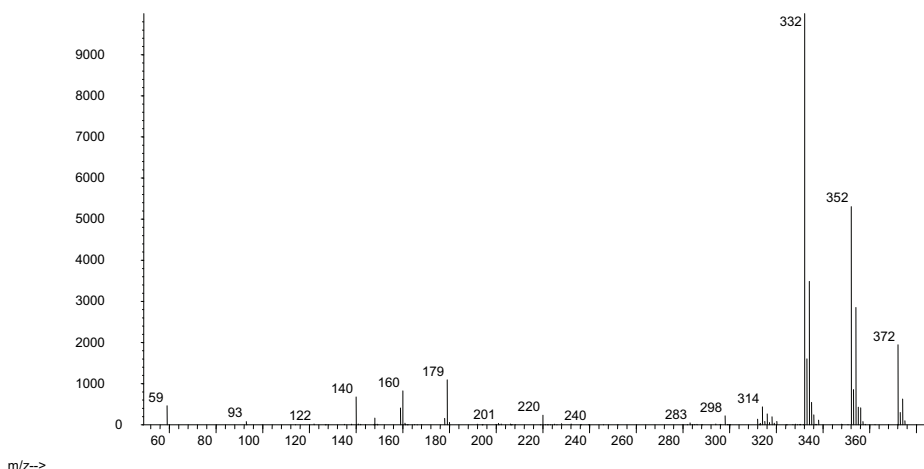
V.4.5. Conclusion: mass spectrometric detection

The enormous benefit of a mass analyzer is the identification of compounds not only on basis of their retention time, but in combination with the spectra of the compounds. Fragment masses can be selected which allow the detection and determination of the corresponding compounds undisturbed by the presence of other species within the mixture to be analyzed, even without complete separation.

The mass analyzer can be used in scan or in SIM (selected ion monitoring) mode. In scan mode a whole range of mass to charge ratios are detected, while in SIM only specific m/z ratios are monitored. Because low concentrations (ng/ml range) of ADs had to be monitored, SIM should be used as this method results in high sensitivity as compared to scan mode. When working in SIM mode, the relative ion abundance ratios of three ions can be used to identify a compound. The selection of the monitored ions depends on their abundance and their selectivity. In general, ions of higher abundance are selected due to their greater reproducibility and lower limit of detection. The selected ions must be diagnostic of the structure of the compound to increase method selectivity. Structurally significant ions should be selected over ions that have greater abundance but are not diagnostic. If sufficiently abundant, the molecular ion should be selected as this ion gives a

lot of information concerning the detected compound. Sometimes ions from the derivatization moiety are monitored, but only one of the three selected ions should be originating from this group. The spectra of each AD were discussed in the previous paragraph (V.4.) and the monitored ions for each compound are summarized in Table V. 1.

Table V.1. Selected ions for each antidepressant in electron and positive or negative ion chemical ionization

( ), Relative intensity %; 1,2,3, numbers indicate the I.S. used for this compound (respectively, fluoxetine-d_6, mianserin-d_3, paroxetine-d_6)

Compounds	Time window (min.)	M-ion	M-ion HFB	EI Quant	ion 1	ion 2	PICI Quant	ion 1	ion 2	NICI Quant	ion 1	ion 2
ODMV 2 (HFB)	6.00 - 14.00	263	441	58	440 (0.1)	441 (0.02)	442	440 (46)	470 (44)	197	440 (0.02)	441 (0.005)
Venlafaxine 2		277	259	58	259 (0.38)	121 (2.9)	260	258 (56)	288 (10)		not detected	
m-cpp 1		196	392	392	166 (64)	394 (34)	393	395 (33)	373 (9.6)	332	372 (21)	352 (48)
Viloxazine 1	14.00-15.50	237	433	433	240 (112)	296 (82)	434	296 (63)	414 (10)	413	393 (24)	373 (20)
DMFluox 1		295	491	330	117 (337)	226 (0.20)	330	358 (6.6)	117 (36)	471	491 (29)	329 (39)
Fluvoxamine 1		318	514	258	240 (93)	514 (1.9)	495	258 (304)	515 (65)	256	237 (11)	494 (1.6)
ODMV 2 (-H_2O)		263	441	58	245 (1.2)		246	244 (53)	274 (5.5)		not detected	
Fluoxetine 1	15.50 - 17.00	309	505	344	117 (197)	486 (0.23)	344	486 (3.2)	534 (4.0)	485	505 (2.4)	465 (7.1)
Fluoxetine-d_6		315	511	350	123 (200)	492 (0.27)	350	492 (4.8)	540 (5.6)	491	511 (1.9)	471 (7.7)
Mianserin 2	17.00 - 18.50	264	264	264	193 (166)	220 (43)	265	293 (18)	305 (2.4)		not detected	
Mianserin-d_3		267	267	267	193 (245)	220 (58)	268	296 (19)	308 (3.8)		not detected	
Mirtazapine 2	18.50 - 19.50	265	265	195	208 (16)	265 (6.2)	266	264 (31)	294 (17)		not detected	
Melitracen 2		291	291	58	202 (7.8)	291 (0.10)	292	290 (45)	320 (20)		not detected	
DMMia 2	19.50 - 21.00	250	446	446	193 (57)	249 (72)	447	427 (7.4)	475 (14)	386	406 (20)	446 (4.3)
DMSer 3		291	487	274	487 (9.9)	489 (6.8)	275	277 (67)	487 (1.1)	487	467 (24)	433 (35)
DMMir 2		251	447	447	250 (123)	195 (81)	448	428 (7.3)	476 (13)	407	387 (68)	447 (13)
Reboxetine 3		313	509	371	138 (21)	509 (2.2)	372	510 (6.6)	490 (5.3)	296	489 (83)	312 (18)
Citalopram 3	21.00 -21.30	324	324	58	238 (6.4)	324 (4.6)	325	305 (10)	353 (22)		not detected	
DMMap 3		263	459	431	191 (93)	459 (0.90)	460	382 (56)	431 (10)	439	459 (5.9)	401 (28)
Maprotiline 3	21.30 - 22.05	277	473	445	191 (77)	473 (0.80)	474	454 (11)	396 (37)	453	473 (3.3)	433 (11)
Sertraline 3		305	501	274	501 (32)	503 (22)	275	277 (66)	501 (3.0)	441	481 (20)	501 (4.1)
DDMC 3	22.05 - 23.00	296	492	238	208 (8.5)	474 (1.5)	475	521 (20)	493 (4.0)	492	472 (43)	452 (2.6)
DMC 3		310	506	238	208 (7.2)	488 (1.4)	489	507 (5.7)	535 (21)	486	466 (27)	506 (6.2)
Paroxetine 3	23.00 - 24.80	329	525	525	138 (186)	388 (25)	526	506 (15)	554 (17)	485	465 (45)	505 (45)
Paroxetine-d_6		332	531	531	138 (164)	394 (27)	532	512 (16)	560 (18)	490	470 (89)	510 (27)
Trazodone	24.80 - 31.00	371	371	205	371 (4.9)	356 (10)	372	400 (23)	336 (36)		not detected	

Electron ionization is the traditional ionization method and results in compound specific fragments. However, for compounds such as citalopram, melitracen, venlafaxine, and ODMV, the extreme fragmentation results in the aspecific high abundance quantifier ion at m/z 58 and inherent loss of specificity. The chemical ionization mass spectra are characterized by less fragmentation. When applying positive ion chemical ionization, the quasi-molecular MH^+ ion, due to the proton affinity of the compound will be monitored in most cases. Moreover, addition reactions are constantly monitored in the spectra of the ADs. Although the 'softer' positive ion chemical ionization mode is used, some compounds such as fluoxetine still fragment easily. According to the NCCLS guidelines [35], the ion derived from the intact molecule or an ion closely related to the molecular species

should be monitored. Therefore protonated molecular ions and ions created through addition were first choice for our SIM method. When using negative ion chemical ionization, compounds that are not derivatized such as venlafaxine, citalopram, melitracen, mianserin, mirtazapine and trazodone are not detected. Although, some of these compounds contain electronegative moieties, they are still not detected as one or two heteroatoms do not result in sufficient electron affinity for NICI-detectability. For the derivatized ADs, the electron capture reaction does not occur in a high abundance. The dissociative electron capture reaction, however, leads to high abundant fragment ions for which in most cases a constant loss of HF-fragments is observed. Some compounds are still fragmented and result in the same fragment-ions as in EI.

The final mass-spectral determination occurred in SIM mode in different time frames as indicated in Table V.1. Within each time frame, several ions were monitored at a dwell time of at least 30 msec to ensure enough monitoring cycles per minute for a good peak shape. Because detection of ADs is based on the ratio of the selected ions (Table V.1.) attention must be paid to the variation of these ion ratios. Since the ionization process of the chemical ionization is based on the kinetics of chemical reactions, the reproducibility of ion-relative abundances in chemical ionization is somewhat lower than for EI. Therefore, ion ratios compared to a standard run in the same batch should be within 25% variation and not within 20% as for EI.

V.5. Conclusion

A GC-MS method for the simultaneous determination of 'new' ADs (venlafaxine, viloxazine, fluvoxamine, fluoxetine, mianserin, mirtazapine, melitracen, reboxetine, citalopram, maprotiline, sertraline, and paroxetine) and their active metabolites was developed. The metabolite of venlafaxine, O-desmethylvenlafaxine, was not included in the analyzed mixture due to derivatization problems discussed in chapter IV. In addition, fragmentation in all three ionization modes led to aspecific fragment ions or very low abundant (quasi)molecular ions. Because of irreproducible chromatographic results for trazodone this compound was not analyzed as this would lead to problems during quantification.

The final gaschromatographic-mass spectrometric method conditions were as follows: the pulsed splitless injection temperature was held at 300°C, while purge time and injection pulse time were set at 1 and 1.5 min, respectively. Meanwhile, the injection pulse pressure was 25 psi and 1 µl of the sample, redissolved in 50 µl of toluene, was injected. Ultrapure Helium with a constant flow of 1.3 ml/min was used as carrier gas. Chromatographic separation was achieved on a 30m x 0.25mm i.d., 0.25-µm J&W-5ms column from Agilent Technologies (Avondale, PA, USA). The initial column temperature was set at 90°C for 1 min, ramped at 50°C/min to 180°C where it was held for 10 min, whereafter the temperature was ramped again at 10°C/min to 300°C. The separation of the ADs and their active metabolites was achieved in 24.8 minutes. Identification and quantification were based on selected ion monitoring in electron (EI) and chemical ionization (CI) modes. For each AD the most specific and high abundance ions were selected in the three ionization modes.

V.6. References

[1]   Labat L, Deveaux M, Dallet P, Dubost JP. Separation of new antidepressants and their metabolites by micellar electrokinetic capillary chromatography. *J. Chromatogr. B* 2002; 773: 17-23

[2]   Andersen S, Halvorsen TG, Pedersen-Bjergaard S, Rasmussen KE. Liquid-phase microextraction combined with capillary electrophoresis, a promising tool for the determination of chiral drugs in biological matrices. *J. Chromatogr. A* 2002; 963: 303-312

[3]   Raggi MA, Mandrioli R, Casamenti G, Volterra V, Pinzauti S. Determination of reboxetine, a recent antidepressant drug, in human plasma by means of two high-performance liquid chromatography methods. *J. Chromatogr. A* 2002; 949: 23-33

[4]   Llerena A, Dorado P, Berecz R, Gonzalez A, Norberto MJ, de la Rubia A, Caceres M. Determination of fluoxetine and norfluoxetine in human plasma by high-performance liquid chromatography with ultraviolet detection in psychiatric patients. *J. Chromatogr. B* 2003; 783: 25-31

[5]   Hostetter AL, Stowe ZN, Cox M, Ritchie JC. A novel system for the determination of antidepressant concentrations in human breast milk. *Ther. Drug Monit.* 2004; 26: 47-52

[6]   Titier K, Castaing N, Scotto-Gomez E, Pehourcq F, Moore N, Molimard M. High-performance liquid chromatographic method with diode array detection for identification and quantification of the eight new antidepressants and five of their active metabolites in plasma after overdose. *Ther. Drug Monit.* 2003; 25: 581-587

[7]   Lacassie E, Gaulier JM, Marquet P, Rabatel JF, Lachatre G. Methods for the determination of seven selective serotonin reuptake inhibitors and three active

metabolites in human serum using high-performance liquid chromatography and gas chromatography. *J. Chromatogr. B* 2000; 742: 229-238

[8]   Suckow RF, Zhang MF, Cooper TB. Sensitive and selective liquid-chromatographic assay of fluoxetine and norfluoxetine in plasma with fluorescence detection after precolumn derivatization. *Clin. Chem.* 1992; 38: 1756-1761

[9]   Goeringer KE, McIntyre IM, Drummer OH. LC-MS analysis of serotonergic drugs. *J. Anal. Toxicol.* 2003; 27: 30-35

[10]   Kollroser M, Schober C. Simultaneous determination of seven tricyclic antidepressant drugs in human plasma by direct-injection HPLC-APCI-MS-MS with an ion trap detector. *Ther. Drug Monit.* 2002; 24: 537-544

[11]   Kirchherr H, Kuhn-Velten WN. Quantitative determination of forty-eight antidepressants and antipsychotics in human serum by HPLC tandem mass spectrometry: a multi-level, single-sample approach. *J. Chromatogr. B* 2006; 843: 100-113

[12]   Sauvage FL, Gaulier JM, Lachatre G, Marquet P. A fully automated turbulent-flow liquid chromatography-tandem mass spectrometry technique for monitoring antidepressants in human serum. *Ther. Drug Monit.* 2006; 28: 123-130

[13]   Ulrich S, Martens J. Solid-phase microextraction with capillary gas-liquid chromatography and nitrogen-phosphorus selective detection for the assay of antidepressant drugs in human plasma. *J. Chromatogr. B* 1997; 696: 217-234

[14]   Martinez MA, de la Torre CS, Almarza E. Simultaneous determination of viloxazine, venlafaxine, imipramine, desipramine, sertraline, and amoxapine in whole blood: Comparison of two extraction/cleanup procedures for capillary gas chromatography with nitrogen-phosphorus detection. *J. Anal. Toxicol.* 2002; 26: 296-302

[15]   Maurer HH, Bickeboeller-Friedrich J. Screening procedure for detection of antidepressants of the selective serotonin reuptake inhibitor type and their metabolites in urine as part of a modified systematic toxicological analysis procedure using cas chromatography-mass spectrometry. *J. Anal. Toxicol.* 2000; 24: 340-347

[16]   Bickeboeller-Friedrich J, Maurer HH. Screening for detection of new antidepressants, neuroleptics, hypnotics, and their metabolites in urine by GC-MS developed using rat liver microsomes. *Ther. Drug Monit.* 2001; 23: 61-70

[17]   Eap CB, Bouchoux G, Amey M, Cochard N, Savary L, Baumann P. Simultaneous determination of human plasma levels of citalopram, paroxetine, sertraline, and their metabolites by gas chromatography mass spectrometry. *J. Chromatogr. Sci.* 1998; 36: 365-371

[18]   Goeringer KE, Raymon L, Christian GD, Logan BK. Postmortem forensic toxicology of selective serotonin reuptake inhibitors: A review of pharmacology and report of 168 cases. *J. Forensic Sci.* 2000; 45: 633-648

[19]   Cognos Plus Study nr.11, Massachusetts: Decision Resources Inc, 2005, pp.176

[20]   Baumann P, Hiemke C, S. U, Eckermann G, Gaertner I, Kuss HJ, Laux G, Müller-Oerlinghausen B, Rao ML, Riederer P, Zernig G. The AGNP-TDM expert group consensus guidelines: therapeutic drug monitoring in psychiatry. *Pharmacopsychiatry* 2004; 37: 243-265

[21]   Rood D. A practical guide to the care, maintenance, and troubleshooting of capillary gas chromatographic systems. Weinheim: Wiley-VCH, 1999, pp 323.

[22]   Grob K. Split and splitless injection in capillary gas chromatography. Heidelberg: Hüthig Buch Verlag, 1993, pp 547.

[23]   Grob K. On-column injection in capillary gas chromatography: basic technique, retention gaps, solvent effects. Heidelberg: Hüthig Buch Verlag, 1991, pp 591.

[24]   David F, Sandra P, Stafford SS. Application of retention gaps for optimized capillary GC. *Application note Hewlett Packard* 1994; Note 228-245

[25]   Wang FS, Shanfield H, Zlatkis A. Injection temperature effects using on-column and Split sampling in capillary gas chromatography. *J. High Resolut. Chrom. Chrom. Comm.* 1983; 6: 471-479

[26]   Wylie PL, Uchiyama K. Improved gas chromatographic analysis of organophosphorus pesticides with pulsed splitless injection. *J. AOAC Int.* 1996; 79: 571-577

[27]   Erney DR, Gillespie AM, Gilvydis DM, Poole CF. Explanation of the matrix-induced chromatographic response enhancement of organophosphorus pesticides during open-tubular column gas-chromatography with splitless or hot on-column injection and flame photometric detection. *J. Chromatogr.* 1993; 638: 57-63

[28]   Poole CF. Matrix-induced response enhancement in pesticide residue analysis by gas chromatography. *J. Chromatogr. A* 2007; 1158: 241-250

[29]   Agilent. Operating manual: Inlets. Wilmington: Agilent Technologies, 2000, pp 254

[30]   Bartle KD, Tipler A, Dawes PA, Baugh PJ, Watson D, Flanagan RJ, Taylor DR, Best GA, Dawson JP, Harriman GE, Evershed RP, Jackson P. Gas Chromatography: a practical approach. Oxford: Oxford university press, 1993, pp 427

[31]   Hinshaw JV. GC connections. Computer-Controlled Pneumatics. *LC-GC* 1995; 8: 634

[32]   Deelder RS, De Jong GJ, van den Berg JHM. Chromatografie. Houten: Bohn Stafleu Van Loghum, 1994

[33]   Silverstein R, Webster F. Spectrometric identification of organic compounds. New York: John Wiley and sons, 1998, pp 482.

[34]   Stemmler EA, Hites RA. A systematic study of instrumental parameters affecting electron capture negative ion mass spectra. *Biomed. Environ. Mass Spectrom.* 1988; 15: 659-667

[35]   NCCLS. Gas chromatography/mass spectrometry (GC/MS) confirmation of drugs; approved guideline. Wayne: National Committe on Clinical Laboratory Standards, 2001, pp 32

[36]   Harrison AG. Chemical ionization mass spectrometry. Boca Raton: CRC Press, 1992, pp 208

[37]   Maurer HH, Kraemer T, Kratzsch C, Peters FT, Weber AA. Negative ion chemical ionization gas chromatography-mass spectrometry and atmospheric pressure chemical ionization liquid chromatography-mass spectrometry of low-dosed and/or polar drugs in plasma *Ther. Drug Monit*. 2002; 24: 117-124

[38]   Maurer HH. Role of gas chromatography-mass spectrometry with negative ion chemical ionization in clinical and forensic toxicology, doping control, and biomonitoring. *Ther. Drug Monit.* 2002; 24: 247-254

Chapter VI

Validation

VI.1. Introduction

Depression is a chronic or recurrent mood disorder that affects economic and social functions of about 121 million people worldwide, and can eventually lead to suicidal behaviour. According to the World Health Organization, depression will be the second leading contributor to the global burden of disease, calculated for all ages and both sexes by the year 2020 [1, 2]. Therefore, the prescription rate of antidepressants (ADs) will increase, resulting in a growing interest for determination methods in the clinical and forensic field. Detection and quantification of ADs in plasma is a valid tool to optimize AD pharmacotherapy for special patient populations and for monitoring patient compliance [3-8]. Analytical methods for the detection of ADs in blood and tissues are of interest in the field of forensic toxicology as they are often involved in intoxications [9-14]. Validation of these methods is necessary to demonstrate the validity of the assay's performance and to be sure that the obtained results are reliable.

The ADs that we monitored are the 'new' generation ADs as these are the most prescribed AD drugs in the seven major markets (Japan, USA, France, United Kingdom, Italy, Spain, Germany) nowadays, according to the Cognos Plus Study 11 [15]. The 'new' generation ADs include the Selective Serotonin Reuptake Inhibitors (SSRIs: fluoxetine, fluvoxamine, sertraline, paroxetine and citalopram), the Selective Noradrenaline Reuptake Inhibitors (reboxetine and viloxazine), the Serotonin and Noradrenaline Reuptake Inhibitors (venlafaxine), the Noradrenergic and Specific Serotonergic ADs (mirtazapine and mianserin), and the Serotonin-2 antagonists and Reuptake Inhibitors such as trazodone [16-21]. These ADs are monitored in combination with their (active) metabolites as the latter can also contribute to the overall therapeutic and toxic effect. In addition, metabolites can give extra information about the time of ingestion, the metabolic capacity, and compliance. These metabolites, i.e. desmethylmirtazapine, O-desmethyl-venlafaxine, m-chlorophenylpiperazine, desmethylcitalopram, didesmethyl-citalopram, desmethylmianserin, desmethylfluoxetine, desmethylsertraline, desmethylmaprotiline, were chosen according to the AGNP-TDM expert group consensus guidelines [22].

Over the years, several chromatographic methods have been developed for the determination of these ADs in biological matrices. These methods include capillary electrophoresis [23, 24], high performance liquid chromatography with ultra-violet (UV) [25-28], fluorescence [29, 30] or mass spectrometric detection [31-33], as well as gas chromatography combined with nitrogen-phosphorus [34, 35] or mass detection (GC-MS) [12, 36-38]. In clinical toxicology, GC-MS is still the method of choice as it is sensitive and selective, providing the best separation power for compounds that are volatile under GC conditions. Electron ionization (EI) is the traditional method for comprehensive screening procedures, allowing identification of unknown compounds by comparison of their mass spectrum with a large collection of reference mass spectra in commercially available libraries. In addition, EI leads to a number of fragment ions providing additional structural information. However, due to the extensive fragmentation of some ADs in the EI-mode, the positive ion chemical ionization mode (PICI) provides more selectivity as this technique often gives molecular mass information. Negative ion chemical ionization (NICI) can improve sensitivity as compared to PICI or EI for the determination of compounds with electronegative moieties, either present in their original structure or obtained after derivatization [39, 40]. In this chapter a comparison between EI mode and the chemical ionization modes (CI, both PICI and NICI) was made during validation of the developed GC-MS method for the simultaneous quantification of most new generation ADs and their metabolites in plasma. Moreover, the same GC-MS method was validated for blood and brain tissue in PICI mode for post-mortem investigation purposes.

VI.2. Experimental

VI.2.1. Reagents

Venlafaxine.HCl was provided by Wyeth (New York, NY, USA). Organon (Oss, The Netherlands) donated mianserin.HCl, desmethylmianserin.HCl, mirtazapine, and desmethylmirtazapine maleate, while sertraline.HCl, desmethylsertraline maleate, and reboxetine methanesulphonate were a gift from Pfizer (Groton, CT, USA). Lundbeck (Valby, Denmark) offered

citalopram.HBr, desmethylcitalopram.HCl, didesmethylcitalopram tartrate hydrate (DDMC), and melitracen.HCl. ACRAF (Roma, Italy) provided trazodone.HCl and its metabolite m-chlorophenylpiperazine.HCl, whereas paroxetine.HCl hemi-hydrate was donated by GlaxoSmithKline (Erembodegem, Belgium) and viloxazine.HCl by AstraZeneca (Brussels, Belgium). Fluvoxamine maleate and maprotiline.HCl were provided by Solvay Pharmaceuticals (Weesp, The Netherlands) and Novartis Pharma (Basel, Switzerland), respectively. Fluoxetine.HCl, desmethylfluoxetine.HCl and 1-(heptafluorobutyryl) imidazole (HFBI) were purchased from Sigma-Aldrich (Steinheim, Germany). Promochem (Molsheim, France) delivered fluoxetine-d_6 oxalate, mianserin-d_3, maprotiline-d_3 and paroxetine-d_6 maleate (100 µg/ml in MeOH). The following reagents were purchased from Merck (Darmstadt, Germany): ammonia-solution 25%, orthophosphoric acid (85%), sodium dihydrogenium phosphate monohydrate, methanol and water (HPLC grade), and toluene (Suprasolv).

The strong cation exchanger (Strata SCX with 200 mg sorbent mass) was obtained from Phenomenex (Bester, Amstelveen, The Netherlands). Vials, glass inserts and viton crimp-caps were purchased from Agilent technologies (Avondale, PA, USA).

Drug-free blood and hair were obtained from healthy volunteers. EDTA plasma was harvested from the blood within 2 hours after a 10-min centrifugation period at 1200 g. Drug-free post-mortem brain tissue samples were obtained from the department of forensic medicine (Ghent University, Belgium).

VI.2.2. Preparation of standard solutions and calibrators

Primary stock solutions of each individual AD were prepared in methanol at a concentration of 1 mg/ml and stored at -20°C. A standard mixture was obtained by mixing these individual primary stock solutions and by further diluting with methanol to a concentration of 0.05 – 0.125 mg/ml, depending on the therapeutic range of the compound. After preparation, it was stored protected from light at approximately -20°C. Further dilution of the standard

mixture with methanol resulted in working solutions with concentrations of 0.1, 1 or 10 µg/ml. For the preparation of sample calibrators, 20 to 100 µl of a working solution were spiked to 1 ml of plasma or blood to have a concentration range from 10 till 500 ng/ml. For NICI mode only 250 µl of the 1 ml spiked plasma was used. When spiking brain tissue (1 g), a 50-µl Hamilton injection needle was used to introduce the compounds directly into the tissue. A concentration range from 50 to 1000 ng/g was used for brain tissue samples.

Samples were equilibrated at 4°C overnight. Primary stock solutions of the internal standards (I.S.) fluoxetine-d_6, mianserin-d_3 and paroxetine-d_6 were prepared in methanol at a concentration of 10 µg/ml and were stored protected from light at 4°C. Twenty µl of each I.S. solution were spiked to 1 ml of plasma, blood or 1 g of brain tissue.

VI.2.3. Instrumentation

All experiments were carried out on a HP 6890 GC system, equipped with a HP 5973 mass-selective detector, a HP 7683 split/splitless auto injector and a G1701DA Chem Station, version D.02.00 data processing unit (Agilent Technologies, Avondale, PA, USA).

An Ultra Turrax mixer IKA T18 basic (Staufen, Germany) was used to homogenize the tissue samples. Sonication was done using a 'Brandson 1510' (Brandson UL Transonics corporation, Danbury, CT, USA). A Visiprep TM Disposable liner vacuum manifold (Supelco, Bornem, Belgium) controlled the flow during the solid phase extraction. Evaporation under nitrogen was conducted in a TurboVap LV evaporator from Zymark (Hopkinton, MA, USA). The heater was a multi-block from Lab-line (Tiel, The Netherlands).

VI.2.4. Sample preparation

A short résumé of the sample preparation is given in this paragraph. The optimization of the sample preparation is described in chapter III, and the sample preparation according to each matrix is schematically presented in

Figure III.6. (chapter III, p 105). The derivatization procedure is described in detail in chapter IV. I.S.s (200 ng in EI, PICI and 50 ng in NICI / ml plasma) were added to the samples. Thereafter, samples were prepared for the loading step onto the SPE tube according to the matrix. Plasma samples were diluted with 4 ml of phosphate buffer (pH 2.5; 25 mM), centrifuged and submitted to the solid phase extraction procedure (SPE). Blood samples were also diluted with the phosphate buffer, sonicated for 15 minutes and transferred to the SPE without centrifugation. Brain tissue was mixed after addition of 2 ml of acetonitrile and 0.5 ml of potassium carbonate buffer (1M pH 9.5) and centrifuged for 15 minutes at 1850 g. The top-layer was removed and diluted with phosphate buffer (pH 2.5; 25 mM). The pH of the diluted sample was adapted to 2-3 with orthophosphoric acid before it was submitted to the SPE-procedure. Hair samples were washed in HPLC-water (5 minutes), and rinsed 3 times with 1 ml of methanol. Thereafter, they were cut in segments of approximately 2 cm. The hair fragments were digested in a sodium hydroxide solution (1M, 1 ml) for 10 minutes at 100°C or they were soaked in 4 ml of phosphate buffer (pH 2.5; 25 mM) for 18 hours at 55°C and sonicated for 1 hour. Then the samples were diluted with phosphate buffer and the pH was adapted to 2-3 with orthophosphoric acid if necessary.

The SPE procedure consisted of conditioning the strong cation exchanger with 3 ml of the final eluting solvent, 2 ml of methanol and 3 ml of phosphate buffer, followed by loading of the sample. Then, a wash step with 4 times 1 ml of methanol followed using −20 kPa vacuum. After 2 minutes drying time at -50 kPa, the compounds were eluted with 2 ml of 5% ammonia in methanol. Finally, a vacuum of -50 kPa was used during 1 minute to collect all the eluting solvent.

After evaporation of the solid phase extracts under nitrogen at 40°C, 50 µl of HFBI was added and the sample was heated at 85°C for 30 min. Thereafter, 0.5 ml of HPLC-grade water and 2 ml of toluene were added. After vortexing and centrifuging the sample at 1121 g for 5 min, the toluene layer was transferred and evaporated at 40°C [41]. The residue was dissolved in 50 µl of toluene.

VI.2.5. Gas chromatographic parameters

The pulsed splitless injection temperature was held at 300°C, while purge time and injection pulse time were set at 1 and 1.5 min, respectively. Meanwhile, the injection pulse pressure was 170 kPa and 1 µl of the sample, redissolved in 50 µl toluene, was injected. Chromatographic separation was achieved on a 30m x 0.25mm ID, 0.25-µm J&W-5ms column from Agilent Technologies (Avondale, PA, USA). The initial column temperature was set at 90°C for 1 min, ramped at 50°C/min to 180°C where it was held for 10 min, whereafter the temperature was ramped again at 10°C/min to 300°C. Ultrapure helium with a constant flow of 1.3 ml/min was used as carrier gas.

VI.2.6. Mass spectrometric parameters

In EI mode, the mass selective detector temperature conditions were 230°C for the EI-source, 150°C for the quadrupole and 300°C for the transferline, whereas an electron voltage of 70 eV was used. The mass parameters for the electron ionization mode were not optimized, as the 'traditional' conditions in which the spectra of the commercially available libraries were obtained were chosen.

The mass selective detector temperature conditions in PICI were as in EI, except for the ion source temperature (PICI/NICI source), which was 250°C, and the electron energy (140 eV). Ion source temperature and ion focus potential have the highest effect on the abundance of the molecular ions in NICI mode [42]. These parameters were optimized according to Agilent's guidelines and weekly tuning parameters. For NICI-mode the transferline was kept at 280°C, the ion source at 150°C and the quadrupole at 106°C, with an electron energy of 170 eV. The electron emission (100 µA) was optimized to give best peak intensity, as this parameter is compound specific. Methane was used as reagent gas with a flow of 1 and 2 ml/min for PICI and NICI, respectively. The spectra were monitored in selected ion monitoring (SIM) mode for quantification (Table VI.1.).

Table VI.1. Quantifier and qualifier ions of the ADs in electron and chemical ionization mode

Relative intensity of ions as compared to the quantifier ion are shown between brackets. I.S.: 1 (Fluoxetine-d_6); 2 (Mianserin-d_3); 3 (Paroxetine-d_6)

Compounds	Time window	M-ion	M-ion HFB	EI			PICI			NICI		
	(min.)			Quant	ion 1	ion 2	Quant	ion 1	ion 2	Quant	ion 1	ion 2
Venlafaxine 2	6.00 - 14.00	277	259	58	259 (0.38)	121 (2.9)	260	258 (56)	288 (10)	not detected		
m-cpp 1		196	392	392	166 (64)	394 (34)	393	395 (33)	373 (9.6)	332	372 (21)	352 (48)
Viloxazine 1	14.00-15.50	237	433	433	240 (112)	296 (82)	434	296 (63)	414 (10)	413	393 (24)	373 (20)
DMFluox 1		295	491	330	117 (337)	226 (0.20)	330	358 (6.6)	117 (36)	471	491 (29)	329 (39)
Fluvoxamine 1		318	514	258	240 (93)	514 (1.9)	495	258 (304)	515 (65)	256	237 (11)	494 (1.6)
Fluoxetine 1	15.50 - 17.00	309	505	344	117 (197)	486 (0.23)	344	486 (3.2)	534 (4.0)	485	505 (2.4)	465 (7.1)
Fluoxetine-d_6		315	511	350	123 (200)	492 (0.27)	350	492 (4.8)	540 (5.6)	491	511 (1.9)	471 (7.7)
Mianserin 2	17.00 - 18.50	264	264	264	193 (166)	220 (43)	265	293 (18)	305 (2.4)	not detected		
Mianserin-d_3		267	267	267	193 (245)	220 (58)	268	296 (19)	308 (3.8)	not detected		
Mirtazapine 2	18.50 - 19.50	265	265	195	208 (16)	265 (6.2)	266	264 (31)	294 (17)	not detected		
Melitracen 2		291	291	58	202 (7.8)	291 (0.10)	292	290 (45)	320 (20)	not detected		
DMMia 2	19.50 - 21.00	250	446	446	193 (57)	249 (72)	447	427 (7.4)	475 (14)	386	406 (20)	446 (4.3)
DMSer 3		291	487	274	487 (9.9)	489 (6.8)	275	277 (67)	487 (1.1)	487	467 (24)	433 (35)
DMMir 2		251	447	447	250 (123)	195 (81)	448	428 (7.3)	476 (13)	407	387 (68)	447 (13)
Reboxetine 3		313	509	371	138 (21)	509 (2.2)	372	510 (6.6)	490 (5.3)	296	489 (83)	312 (18)
Citalopram 3	21.00 -21.30	324	324	58	238 (6.4)	324 (4.6)	325	305 (10)	353 (22)	not detected		
DMMap 3		263	459	431	191 (93)	459 (0.90)	460	382 (56)	431 (10)	439	459 (5.9)	401 (28)
Maprotiline 3	21.30 - 22.05	277	473	445	191 (77)	473 (0.80)	474	454 (11)	396 (37)	453	473 (3.3)	433 (11)
Sertraline 3		305	501	274	501 (32)	503 (22)	275	277 (66)	501 (3.0)	441	481 (20)	501 (4.1)
DDMC 3	22.05 - 23.00	296	492	238	208 (8.5)	474 (1.5)	475	521 (20)	493 (4.0)	492	472 (43)	452 (2.6)
DMC 3		310	506	238	208 (7.2)	488 (1.4)	489	507 (5.7)	535 (21)	486	466 (27)	506 (6.2)
Paroxetine 3	23.00 - 24.80	329	525	525	138 (186)	388 (25)	526	506 (15)	554 (17)	485	465 (45)	505 (45)
Paroxetine-d_6		332	531	531	138 (164)	394 (27)	532	512 (16)	560 (18)	490	470 (89)	510 (27)

VI.3. Method Validation

The developed GC-MS method was validated in plasma, blood and brain tissue based on the FDA guidelines [43]. Bioanalytical method validation includes all of the procedures that demonstrate that a particular method used for quantitative measurement of analytes in a given biological matrix is reliable and reproducible for the intended use. The fundamental parameters for validation include accuracy, precision, selectivity, sensitivity, reproducibility, linearity and stability. In plasma, validation parameters such as stability and recovery were evaluated only in EI mode, while parameters such as sensitivity, selectivity, linearity, intra and inter batch precision, and accuracy were analyzed and compared in the three ionization modes (EI, PICI, NICI). Validation parameters were re-evaluated for blood and brain tissue, while only selectivity was checked for hair samples. The validation parameters for the post-mortem matrices, (whole blood, brain tissue and hair) were obtained using the PICI mode.

VI.3.1. Stability

VI.3.1.1. *Experimental*

Stability of compounds or their derivatives is very important during method validation. Compounds should be stable in their matrix to allow correct analytical data and interpretation of the results. In addition, compounds should be stable during sample handling (stable at certain temperatures, in the solvents used,…) and finally if derivatization occurs, the derivatized compounds should be stable during the analytical run. Therefore, the analyte stability determinations comprised of stock solution stability, stability of the compounds in their matrix and stability of the heptafluorobutyryl-derivatives. Stability of ADs in plasma, blood and brain tissue was determined as long-term stability (2 months, -20°C), short-term stability (4 hours, room temperature), and freeze-thaw cycle stability (3 cycles). The stability of HFB-derivatives was checked after a period of 14 days at -20°C and after 24 hours at room temperature in the autosampler.

For all stability determinations, except for the autosampler stability, the concentrations of the analytes were calculated from daily calibration curves and an acceptance interval of 85-115% was applied for the ratio of the mean stability sample concentration versus the mean control concentration. Moreover, an acceptance interval of 80-120% of the control sample means was applied for the 90% confidence interval of the stability samples. All analyte stability determinations and storage stability tests of the derivatized extracts were determined at low, mid and high concentrations, except for the long-term stability (low and high), with 6 repetitions for plasma and 5 repetitions for blood and brain tissue. Controls and stability samples were prepared at the same time and analyzed before and after treatment.

Autosampler stability of the derivatives was evaluated at low and high concentration over a period of 24 hours. Ten samples of each concentration were extracted and derivatized. Thereafter, the extracts obtained at each concentration were pooled and redivided in 10 aliquots to be transferred to 10 autosampler vials, leaving each vial reinjected after 4 hours and 8 minutes under the conditions of a regular analytical run. The absolute peak areas corresponding to each compound were plotted at each concentration versus injection time. The slopes of the obtained curves were determined

whereby a negative slope would indicate instability. The concentration at time zero as well as after 24 hours was calculated from these curves. The percentage loss was determined from these results.

VI.3.1.2. *Results and discussion*

Stock solutions in methanol (1 mg/ml) are stable for at least 3 months. In addition, these new ADs seem to be stable in blood and plasma samples [44]. According to our experiments (Table VI.2.), long-term instability was seen for venlafaxine, melitracen and citalopram at low and high and for sertraline at high concentrations in plasma. However, short-term stability was no problem as the ADs were stable in plasma after 4 hours at room temperature, because the ratio of the mean stability sample concentrations versus mean control concentrations as well as their 90% confidence interval (CI) fulfilled the acceptance criteria. The freeze-thaw stability for most compounds also fulfilled the acceptance criteria, except for maprotiline, desmethylmaprotiline and sertraline who showed a decrease in concentration at the low level (70-77%, 90% CI 61-81%). Overall, the stability of compounds in plasma is acceptable.

As observed in Table VI.2., the short-term and freeze-thaw stability of ADs at low concentration was better in plasma than in blood. Compounds such as m-cpp, viloxazine, desmethyfluoxetine, melitracen, desmethylsertraline, reboxetine, citalopram, desmethylmaprotiline and maprotiline did not fulfil the acceptance criteria; however, this instability was not seen for medium and high ADs concentrations in blood. For long-term storage, an instability was observed for venlafaxine and sertraline (low and high concentrations) and for melitracen and citalopram (low concentration). Thus the same compounds show a decrease in concentration in plasma and blood after long-term storage.

In brain tissue, freeze-thaw instability was seen for m-cpp and citalopram, while short-term instability was only seen for m-cpp. ADs at low concentrations are not stable in brain tissue after long-term storage. At high concentrations, only m-cpp showed significant losses.

Overall, the stability of ADs is acceptable in plasma and blood. However, long-term instability for citalopram, venlafaxine, sertraline and melitracen is problematic if samples have to be stored for long period. In brain tissue, the

stability is dependent on the spiked concentration, and especially the long-term storage led to degradation.

<u>Table VI.2.</u> Stability data of ADs and their HFB-derivatives in plasma, blood and brain tissue

% IV, percentage of initial value; 90%CI, 90 percent confidence interval

Stability — Long-term stability

	Low plasma %IV	Low plasma 90% CI	Low blood %IV	Low blood 90% CI	Low brain %IV	Low brain 90% CI	Med plasma %IV	Med plasma 90% CI	Med blood %IV	Med blood 90% CI	Med brain %IV	Med brain 90% CI	High plasma %IV	High plasma 90% CI	High blood %IV	High blood 90% CI	High brain %IV	High brain 90% CI
Venlafaxine	16	15-18	58	36-80									13	13-14	75	72-79	107	103-110
m-cpp	96	87-104	88	86-99	46	15-77							90	88-93	93	89-97	64	60-67
Viloxazine	96	93-99	86	77-95									94	91-97	92	91-92	88	84-92
DMFluox	87	83-90	90	85-96									86	83-89	100	99-100	99	97-100
Fluvoxamine	98	95-100	127	121-135									96	93-99	104	103-105	110	105-114
Fluoxetine	111	107-114	98	94-101	18	13-22							90	86-93	91	91-92	91	90-92
Mianserin	96	93-99	98	94-105									88	85-90	91	90-91	90	89-91
Mirtazapine	91	88-95	94	79-109	37	33-41							74	72-76	90	89-91	86	83-89
Melitracen	15	14-15	43	32-55									13	12-13	89	87-91	91	87-95
DMMia	116	113-118	97	92-102									101	99-102	77	71-82	83	73-93
DMSer	86	76-95	105	97-113	115	87-143							87	83-92	103	98-108	97	96-98
DMMir	129	124-135	80	71-88									102	100-104	78	73-82	83	77-89
Reboxetine	101	99-104	96	95-98									89	88-90	90	87-94	116	108-123
Citalopram	22	21-23			23	12754							11	10-11	95	91-99	115	92-137
DMMap	89	86-93	131	123-139	45	35-55							103	99-106	110	105-114	111	104-118
Maprotiline	113	109-117	102	99-105	47	33-60							99	98-101	94	92-97	100	95-105
Sertraline	131	117-144	82	77-87	124	79-169							77	75-80	65	58-73	158	130-185
DDMC	94	91-97	94	89-98									89	86-92	108	102-114	99	90-109
DMC	97	95-98	103	93-112									85	85-86	91	88-95	92	88-96
Paroxetine	86	80-92	108	104-112	12	7-17							94	93-96	91	89-92	85	83-86

Short-term stability

	Low plasma %IV	Low plasma 90% CI	Low blood %IV	Low blood 90% CI	Low brain %IV	Low brain 90% CI	Med plasma %IV	Med plasma 90% CI	Med blood %IV	Med blood 90% CI	Med brain %IV	Med brain 90% CI	High plasma %IV	High plasma 90% CI	High blood %IV	High blood 90% CI	High brain %IV	High brain 90% CI
Venlafaxine	117	113-121	129	107-151	165	89-241	102	98-105	106	95-117	98	91-105	98	96-101	93	84-101	101	88-113
m-cpp	94	90-97	87	78-96	55	51-58	97	93-101	92	90-94	98	88-108	95	92-99	102	100-104	74	53-95
Viloxazine	98	95-101	70	63-77	93	90-95	97	95-99	94	93-95	88	85-91	99	98-99	106	104-108	94	91-97
DMFluox	89	85-93	77	65-88	94	83-105	109	101-117	96	93-99	85	81-89	104	99-110	112	111-113	113	105-122
Fluvoxamine	85	82-88	94	86-102	113	108-119	108	98-118	99	94-104	92	87-97	106	99-112	111	109-112	126	121-132
Fluoxetine	103	100-106	99	97-102	95	88-101	100	98-102	101	100-102	103	102-104	102	99-106	101	100-102	101	93-95
Mianserin	105	102-107	107	97-117	92	85-98	99	96-103	103	101-105	98	94-101	101	100-102	100	99-101	94	95-101
Mirtazapine	103	101-106	96	91-101	112	107-117	101	98-104	104	100-107	91	88-94	98	97-100	99	98-100	98	80-96
Melitracen	112	108-117	77	74-80	149	140-159	98	95-101	102	97-106	85	76-94	97	95-99	105	103-107	88	80-98
DMMia	116	113-120	158	123-194	81	76-86	103	100-105	106	101-110	87	76-99	95	93-97	92	87-97	89	92-116
DMSer	104	100-108	79	74-84	88	82-94	102	96-108	92	90-96	109	100-119	96	85-102	112	109-115	104	88-105
DMMir	115	110-119	134	105-162	91	84-98	105	102-107	107	101-112	92	81-102	96	94-98	94	87-101	97	94-114
Reboxetine	102	99-105	58	52-64	153	133-173	96	94-99	96	93-98	128	123-134	102	99-106	105	103-107	104	94-114
Citalopram	92	87-97	67	56-78	179	145-213	94	88-99	95	89-102	94	82-106	99	94-104	109	103-114	87	80-93
DMMap	90	87-92	66	59-73	100	96-103	107	101-113	92	89-95	112	101-123	99	96-103	110	106-114	118	97-139
Maprotiline	103	102-105	80	76-83	94	89-99	97	95-99	93	92-94	105	96-113	97	95-99	99	98-100	96	89-103
Sertraline	94	85-104	118	100-135	135	129-141	86	82-90	111	104-117	114	101-126	131	124-137	81	76-86	124	111-137
DDMC	90	87-92	158	137-179	178	153-202	106	100-113	95	92-98	107	100-114	95	92-99	109	107-112	113	107-120
DMC	105	102-109	88	82-93	113	105-121	93	92-94	99	97-101	100	96-105	97	96-99	99	98-101	102	93-112
Paroxetine	100	98-102	94	93-96	103	102-105	100	97-102	98	97-99	100	99-101	101	101-102	101	100-102	93	92-94

Freeze-thaw stability

	Low plasma %IV	Low plasma 90% CI	Low blood %IV	Low blood 90% CI	Low brain %IV	Low brain 90% CI	Med plasma %IV	Med plasma 90% CI	Med blood %IV	Med blood 90% CI	Med brain %IV	Med brain 90% CI	High plasma %IV	High plasma 90% CI	High blood %IV	High blood 90% CI	High brain %IV	High brain 90% CI
Venlafaxine	113	110-115	104	82-125	165	118-212	106	102-109	95	85-105	103	95-112	103	98-108	103	99-106	93	88-97
m-cpp	111	105-118	83	78-89	67	55-79	103	98-108	93	87-99	99	82-115	108	105-112	61	55-67		
Viloxazine	103	102-105	70	60-79	101	79-123	100	97-103	92	86-99	90	86-95	96	95-98	112	110-114	97	95-98
DMFluox	96	86-107	80	70-90	94	91-105	93	88-99	97	92-102	86	83-89	101	98-105	118	115-121	108	101-114
Fluvoxamine	96	85-107	98	74-122	98	91-105	95	88-101	100	94-106	94	90-98	103	98-108	116	113-119	121	117-124
Fluoxetine	97	96-99	99	98-100	100	95-105	99	94-104	102	100-105	101	100-102	97	93-101	103	102-103	105	100-109
Mianserin	104	98-110	108	98-119	99	95-103	102	97-108	107	104-109	96	95-98	102	101-102	96	94-99		
Mirtazapine	98	91-104	97	92-101	99	84-115	108	102-114	101	95-107	87	83-91	100	93-107	101	100-102	99	97-101
Melitracen	96	91-101	79	74-83	135	124-147	105	101-108	96	87-106	82	79-85	102	97-106	101	100-102	99	95-99
DMMia	105	101-109	114	93-136	85	78-92	109	105-113	97	88-106	109	98-119	103	98-108	97	94-99	110	106-114
DMSer	101	87-115	85	79-92	108	97-119	86	82-91	101	97-105	111	106-117	95	87-103	117	115-119	92	93-101
DMMir	105	102-108	104	79-130	86	77-85	110	103-116	98	88-108	104	95-113	108	100-115	99	97-102	111	108-114
Reboxetine	109	106-112	63	55-70	128	105-152	102	99-106	100	93-107	132	118-145	95	99-110	101	93-108		
Citalopram	103	99-108	80	70-89	103	71-135	100	94-105	97	90-105	83	77-90	95	91-98	113	110-117	76	71-81
DMMap	70	61-79	70	64-75	97	92-101	94	91-97	96	93-99	100	94-106	99	89-108	112	110-114	89	82-63
Maprotiline	78	74-82	80	70-90	98	91-105	110	94-126	97	93-101	101	96-106	96	92-101	100	98-102	86	83-89
Sertraline	73	63-82	119	112-126	159	134-184	138	126-150	102	89-114	105	96-113	81	72-86	114	102-126		
DDMC	106	98-114	147	120-174	128	113-143	101	96-106	100	96-103	95	89-101	101	98-104	114	111-117	96	89-103
DMC	86	82-90	91	78-105	98	90-105	99	98-100	104	100-108	100	98-101	95	94-96	102	100-104	108	104-112
Paroxetine	92	88-96	90	86-93	104	100-108	98	94-102	101	99-103	102	101-102	95	91-99	104	102-105	95	93-97

	Freeze stability HFB-derivatives																
	Low concentration						Medium concentration						High concentration				
	plasma		blood		brain		plasma		blood		brain		plasma		blood		brain
	% IV	90% CI	% IV	90% CI	% IV	90% CI	% IV	90% CI	% IV	90% CI	% IV	90% CI	% IV	90% CI	% IV	90% CI
Venlafaxine	113	110-116					104	101-107					96	95-97		
m-cpp	133	130-138					111	105-106					106	102-110		
Viloxazine	117	114-120					113	111-115					106	104-108		
DMFluox	91	85-98					102	95-110					94	90-98		
Fluvoxamine	94	89-99					100	92-109					95	92-98		
Fluoxetine	114	111-116					106	104-108					100	96-103		
Mianserin	106	101-111					103	99-107					99	96-101		
Mirtazapine	109	106-111					107	104-110					96	94-98		
Melitracen	104	99-109					102	99-106					95	94-96		
DMMia	111	105-117					114	111-118					105	104-106		
DMSer	96	85-107					110	103-117					108	102-114		
DMMir	114	110-119					118	114-121					109	106-111		
Reboxetine	109	106-112					103	100-105					96	95-96		
Citalopram	125	119-130					95	92-99					82	80-83		
DMMap	94	87-101					103	96-109					101	94-105		
Maprotiline	117	111-123					110	107-112					105	103-108		
Sertraline	110	96-124					80	77-84					78	75-81		
DDMC	95	90-100					113	108-118					98	94-102		
DMC	118	112-123					101	99-103					99	98-100		
Paroxetine	107	100-113					103	100-106					99	97-101		

The autosampler stability overnight of the analytes at high concentrations showed tolerable losses (less than 11%) after 24 hours, except for DMMap (16%) (Figure VI.1.). At low concentration, the resulting positive slopes for all compounds indicated a concentration effect of the extract due to evaporation during analysis. This concentration effect masked the stability results. Special Viton caps and glass inserts were used to prevent the evaporation of toluene, but still a concentration effect was observed, this was more pronounced for low concentration extracts according to Raoult's law (P_i (vapour pressure of solvent with added solute) = x_i (mole fraction).P_i* (vapour pressure of pure solvent). The higher the amount of solute that is added to a pure solvent, the more the vapour pressure of that solvent will be depressed. During this experiment no internal standards were used, however, internal standards will compensate for this concentration effect when analyzing real samples.

The derivatives were also preserved at -20°C, to check if derivatized extracts could be analyzed after 2 weeks. This is of interest, when the ion source has to be switched from EI to PICI and NICI mode. No degradation of the derivates was observed even after 2 weeks of storage at -20°C, except for sertraline (mid and high) (Table VI.2.)

<u>Figure VI.1.</u> Autosampler stability at low and high therapeutic AD concentration

% IV, percentage of initial value

Autosampler stability at 20 ng/ml
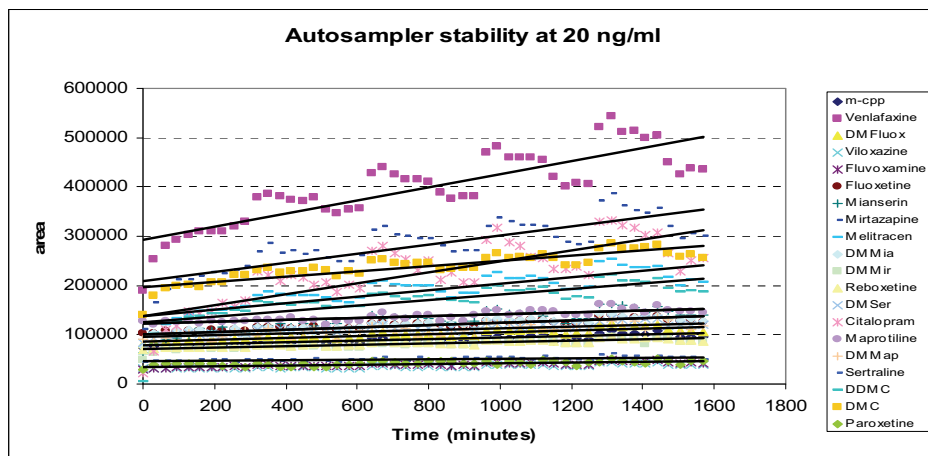
	Stability curve low	% IV low after 24 hours		Stability curve high	% IV high after 24 hours
m-cpp	y = 15.694x + 77737	130	m-cpp	y = -157x + 3338834	93
Venlafaxine	y = 133.63x + 293263	167	Venlafaxine	y = -680x + 13960186	93
DMFluox	y = 18.944x + 86151	133	DMFluox	y = -198x + 4165379	93
Viloxazine	y = 6.8955x + 30501	133	Viloxazine	y = -89x + 1486308	91
Fluvoxamine	y = 8.1224x + 33332	136	Fluvoxamine	y = -95x + 1873421	93
Fluoxetine	y = 18.293x + 106066	125	Fluoxetine	y = -238x + 4531469	92
Mianserin	y = 36.887x + 98957	155	Mianserin	y = -239x + 4453838	92
Mirtazapine	y = 92.967x + 208715	166	Mirtazapine	y = -546x + 9644458	92
Melitracen	y = 66.024x + 136504	171	Melitracen	y = -527x + 7909464	90
DMMia	y = 23.82x + 101287	135	DMMia	y = -310x + 4732498	90
DMMir	y = 16.303x + 67311	136	DMMir	y = -201x + 3142142	91
Reboxetine	y = 12.764x + 72432	126	Reboxetine	y = -198x + 3427683	91
DMSer	y = 18.807x + 98952	128	DMSer	y = -266x + 4105396	90
Citalopram	y = 110.85x + 138287	218	Citalopram	y = -736x + 10346314	90
Maprotiline	y = 20.035x + 122051	247	Maprotiline	y = -360x + 4885553	89
DMMap	y = 17.919x + 94866	128	DMMap	y = -404x + 3720341	84
Sertraline	y = 5.5116x + 46215	118	Sertraline	y = -127x + 1798923	90
DDMC	y = 57.253x + 124531	168	DDMC	y = -339x + 7330348	93
DMC	y = 52.103x + 197707	139	DMC	y = -579x + 8820070	90
Paroxetine	y = 5.6402x + 37896	122	Paroxetine	y = -79x + 1430291	92

Autosampler stability at 500 ng/ml
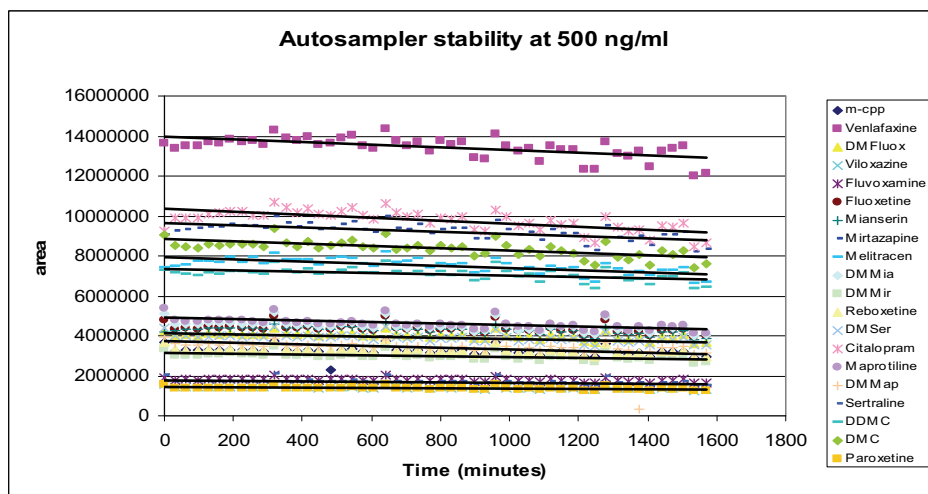
VI.3.2. Recovery

VI.3.2.1. *Experimental*

The recovery for each analyte was determined at low, medium and high concentration (n=6). Therefore, standard working solutions were spiked in blank matrix samples before (extraction samples) or after sample preparation (control samples). Since quantification was performed by the peak area ratios of the target analytes and the internal standard, the internal standards were always added after sample pretreatment, before derivatization, and the resulting peak area ratios were compared. The recovery was expressed by its average and relative standard deviation (RSD).

VI.3.2.2. *Results and discussion*

The SCX extraction leads to reproducible and high recovery from blood for most compounds if no centrifugation step is included (Table VI.3.) and range between 73-106 %, except for venlafaxine (51%). The recoveries from blood samples are comparable to the recovery from plasma.

Table VI.3. Recovery of ADs from plasma, blood and brain tissue

compound	Plasma						Blood						Brain					
	Low		Mid		High		Low		Mid		High		Mid		High		S.High	
Venlafaxine	104	(3)	95	(4)	95	(2)	51*	(21)	101	(14)	93	(7)	38	(19)	46	(17)	45*	(13)
m-cpp	91	(4)	92	(7)	96	(5)	92	(14)	93	(9)	101	(7)	85	(16)	99	(8)	80	(9)
DMFluox	107*	(12)	91	(7)	91*	(5)	93	(12)	93	(6)	100	(6)	82	(12)	79	(5)	69	(10)
Viloxazine	104	(14)	96	(5)	92	(5)	91	(8)	97	(10)	105	(7)	58	(7)	62	(4)	56*	(8)
Fluvoxamine	102	(2)	104	(8)	97	(18)	95	(13)	99	(18)	104	(9)	44	(16)	43	(7)	35*	(10)
Fluoxetine	98	(12)	94	(2)	96	(2)	80	(9)	89	(7)	100	(5)	75	(8)	71	(5)	73	(6)
Mianserin	95	(4)	94	(3)	94	(3)	87	(6)	99	(8)	104	(3)	81	(11)	80	(5)	81	(7)
Mirtazapine	95	(6)	92	(3)	93	(3)	79	(10)	98	(8)	99	(4)	77	(11)	78	(7)	85	(5)
Melitracen	101	(5)	93	(3)	93	(3)	80	(8)	100	(9)	101	(5)	75	(13)	83	(6)	80*	(8)
DMMia	101	(4)	98	(4)	91	(2)	82	(16)	102	(13)	92	(7)	70	(9)	81	(10)	78*	(15)
DMSer	98	(11)	88	(7)	104	(10)	94*	(15)	92	(11)	102	(5)	77	(6)	70	(11)	76	(6)
DMMir	99	(4)	95	(2)	92	(3)	83	(12)	103	(12)	94	(6)	74	(12)	78	(8)	78	(11)
Reboxetine	99	(3)	97	(3)	95	(1)	87	(12)	92	(8)	105	(7)	51	(18)	60	(8)	59*	(4)
Citalopram	88	(8)	87	(9)	94	(5)	84	(21)	89	(14)	106	(13)	61	(16)	73	(5)	78*	(4)
Maprotiline	72*	(14)	88	(3)	90	(6)	83	(14)	76	(14)	96	(5)	54	(12)	59	(8)	81	(6)
DMMap	92	(15)	86	(5)	86	(6)	91*	(14)	79	(23)	96	(14)	51	(15)	57	(10)	78	(4)
Sertraline	82	(6)	89	(11)	96	(5)	73	(18)	82	(17)	93	(17)	90	(16)	73	(3)	82*	(11)
DDMC	94*	(11)	85	(7)	88	(6)	85	(15)	87	(19)	97	(10)	69	(10)	69	(5)	74	(8)
DMC	80	(13)	88	(4)	90	(5)	84	(15)	82	(13)	96	(5)	66	(4)	69	(3)	68*	(4)
Paroxetine	94	(11)	91	(2)	95	(2)	92	(18)	81	(12)	95	(4)	72	(11)	73	(7)	80	(6)

*n=5

ADs recoveries from plasma and blood are determined at low (20 ng/ml), mid (200 ng/ml) and high (500 ng/ml) concentrations, while brain tissue recoveries were determined at mid, high and super high concentration (1000 ng/g). This super high level was chosen as brain concentrations found in literature were much higher than blood or plasma concentrations [45-47].

The extraction efficiencies for brain tissue are slightly lower than for plasma and blood. Especially venlafaxine and fluvoxamine gave low extraction efficiencies. However, recovery of the ADs from brain tissue is reproducible. Recovery of ADs from hair is not determined as spiked samples do not reflect reality. Compounds are incorporated in the interior of the hair through diffusion from blood, sweat or sebum. When samples are spiked, the compounds are spiked onto the hair and this would lead to false high recoveries.

VI.3.3. Selectivity

VI.3.3.1. *Experimental*
Selectivity, defined as the ability to differentiate and quantify the analyte in the presence of other components in the sample, was evaluated by analyzing blank plasma samples of 10 different individuals to observe possible co-eluting interferences in EI, PICI, and NICI. Blank samples of whole blood were obtained from five healthy volunteers. For brain tissue three individuals were tested at six different locations, i.e. cerebellum, the brain stem, the frontal, temporal, parietal, and occipital lobe. These locations were selected as the structure of the lobes, cerebellum and brain stem differ from each other. Two blank hair samples were also checked. The selectivity of the post-mortem matrices was analyzed in PICI mode only.

In addition, zero samples (I.S. spiked to blank plasma) were analyzed to check for absence of analyte ions in the peak of the I.S.

VI.3.3.2. *Results and discussion*
Ten blank plasma samples were checked for interferences and thus selectivity of the method. In EI, a lot of endogenous compounds are seen in the chromatogram, but most of them are chromatographically separated and they do not interfere with quantification. However, only 10 blank samples were screened for interferences, and these are most likely to occur for compounds with the ion m/z 58 as quantifier ion as this ion is very unspecific. The CI-techniques have more selectivity; however, in PICI an interference was seen for venlafaxine in plasma, blood and brain tissue. In NICI, no interferences were detected.

Figure VI.2. Overlays of blank chromatograms with a trace of a low concentration mixture (20 ng / 200 ng for brain tissue) in plasma (A), whole blood (B), brain tissue (C). For hair samples (D) blanks in the 2 extraction modes are shown.

Aa, plasma in PICI; Ab, plasma in NICI; Ac plasma in EI. D; full line: blank hair using sodium hydroxide; dotted line, blank hair using phosphate buffer. Chromatograms are set to the same scale to compare in selectivity and sensitivity, except for Ac. Total ion currents of all monitored ions in SIM are shown in the chromatograms. 1, venlafaxine; 2, m-chlorophenylpiperazine; 3, desmethylfluoxetine; 4, viloxazine; 5, fluvoxamine, 6, fluoxetine, 7, fluoxetine-d_6, 8, mianserin, 9, mianserin-d_3; 10, mirtazapine, 11, melitracen, 12, desmethylmianserine, 13, desmethylsertraline; 14, desmethyl-mirtazapine; 15, reboxetine; 16, citalopram; 17, desmethylmaprotiline; 18, maprotiline; 19, sertraline; 20, didesmethylcitalopram; 21, desmethylcitalopram; 22, paroxetine; 23, paroxetine-d_6

A
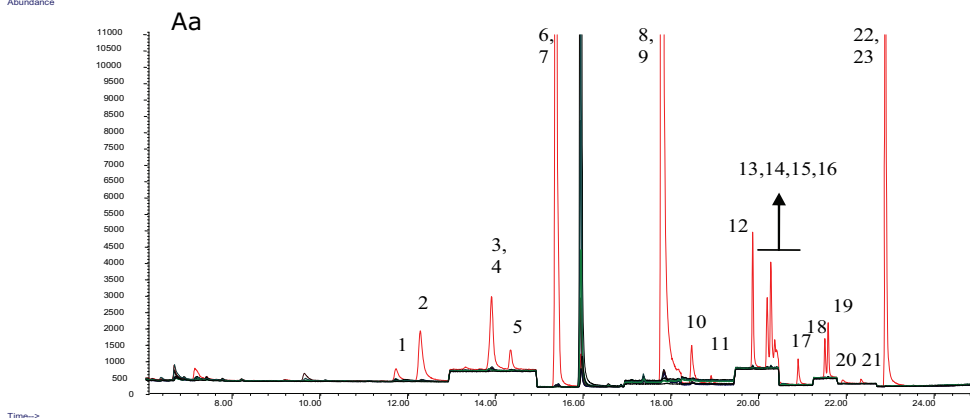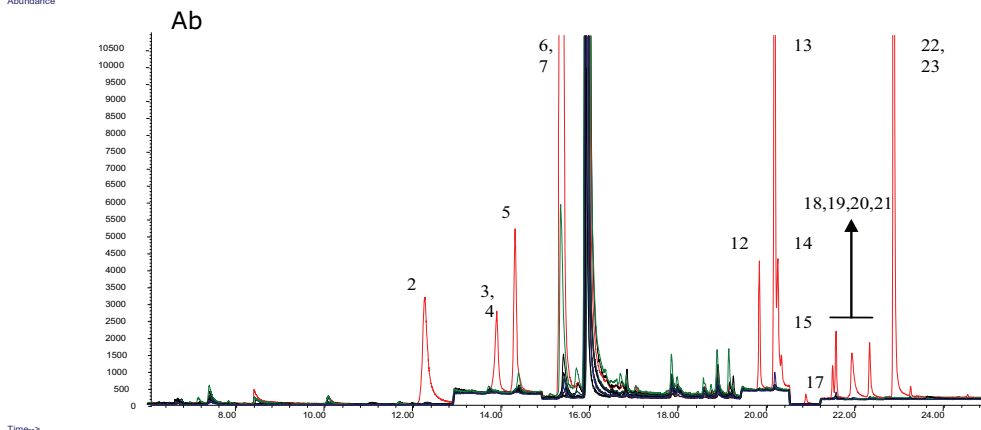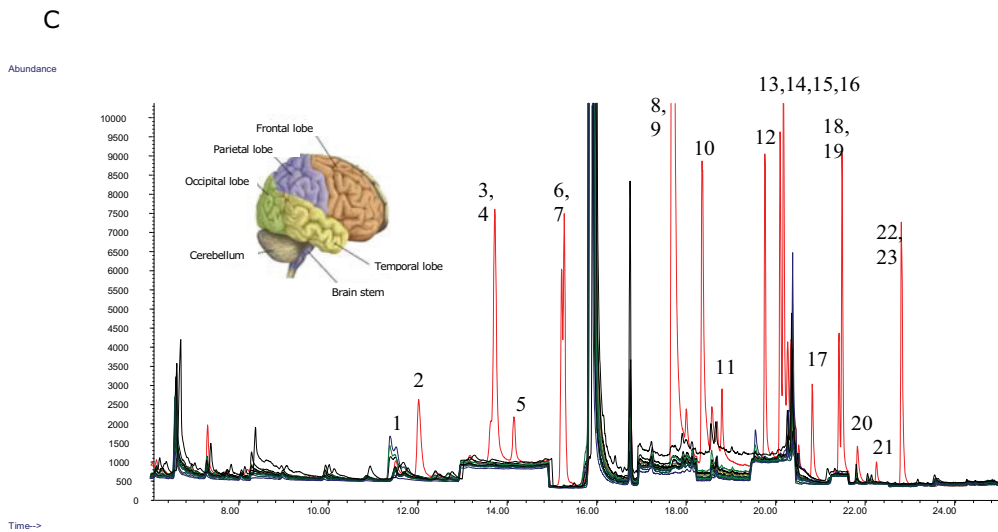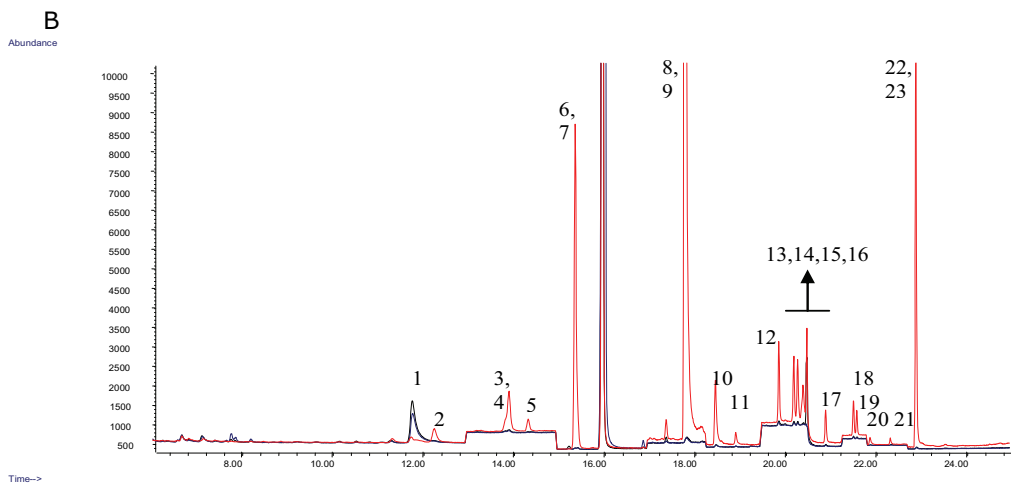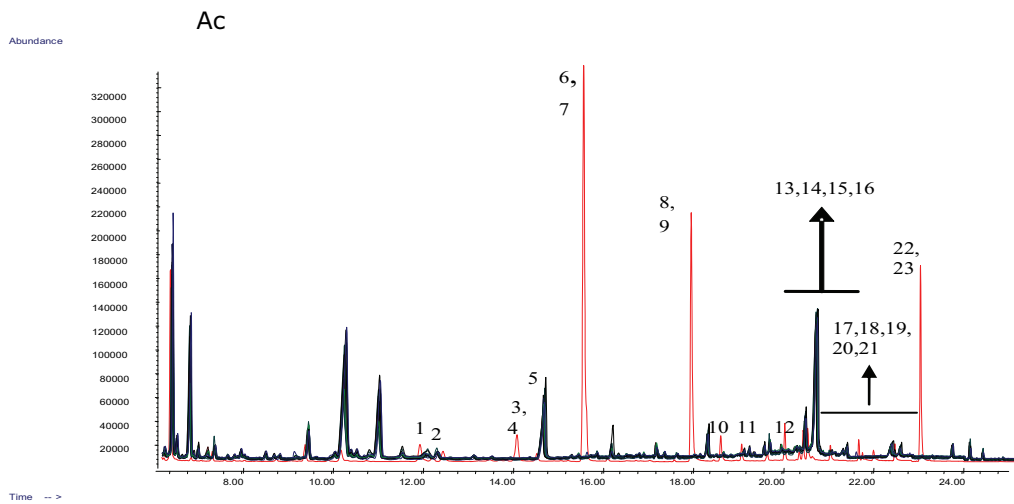
D
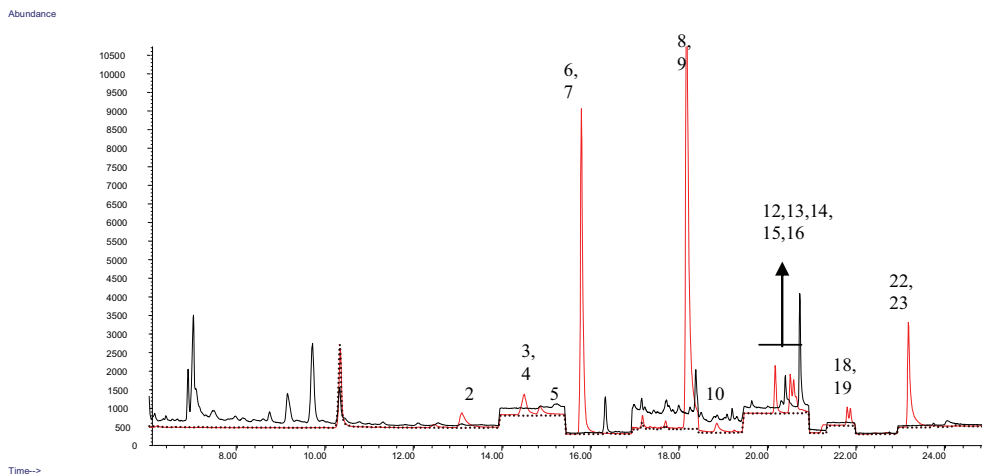
Zero-plasma samples spiked with each I.S. separately were analyzed for analyte ions. The fragmentation patterns of the deuterated standard were checked for the molecular ion of their non-deuterated analogues. The spectra of fluoxetine-d_6, paroxetine-d_6 and mianserin-d_3 contained respectively 0.75, 0.26 and 1.88 % of the quantifier ion of their non-deuterated analogue in EI mode. In PICI mode, the fluoxetine-d_6 spectrum contained 0.4% of the quasi-molecular ion of fluoxetine, while the paroxetine-d_6 spectrum contained 0.2% of its non-deuterated form. These low percentages of non-deuterated forms did not interfere with the quantification. However, mianserin-d_3 fragmentation led to a relative high abundant quasi-molecular ion of mianserin (9.8%), which was demonstrated by the positive intercept of the calibration curve for mianserin. In NICI mode, mianserin-d_3 is not detected as it contains no electronegative moieties. Fluoxetine-d_6 and paroxetine-d_6 fragmentation resulted in 0.02 and 0.06 % of their non-deuterated analogue in their spectrum, respectively.

VI.3.4. Linearity

VI.3.4.1. *Experimental*
Quantification was based on target ion/I.S. ratios (Table VI.1.). Therefore, seven-point curves for plasma, whole blood or hair and 6 point-curves for brain tissue were constructed using internal standardization. Calibration

ranged from the sub therapeutic (10 ng/ml) till high therapeutic concentration (500 ng/ml) of the individual ADs in plasma and blood. For brain tissue, calibration ranged from 50 till 1000 ng/g. Calibrator samples were fortified blank matrix samples and were treated in a way similar to the unknowns. Hair samples were quantitated using a calibration curve from pure standards ranging from 10 till 500 ng/ml.

The weighting factor and regression type were applied to the data of plasma samples through the least percentage relative error (%RE), which is the regressed concentration minus the nominal standard concentration divided by the nominal standard concentration. The sum of the squares of the %RE of all data points for a given curve estimation was calculated, in order to facilitate comparison [48, 49].

VII.3.4.2. *Results and discussion*

For determination of the most appropriate calibration curve, both calibration curve equation type (linear versus quadratic) and weighting factor were considered. Primarily, data heteroscedasticity was shown for all analytes by a F-test on the lowest and the highest concentration level, at the 99% confidence level. Secondly, the most appropriate calibration curve equation was determined by calculating the percent relative error at each calibrator level and for each compound.

The %RE is the percent deviation of the experimental value calculated with the Chemstation software from the nominal value. At each of the 7 calibrator levels, three %RE values were obtained, originating from the experiment being performed in triplicate. All %RE values were converted into positive values if necessary and the sum of the squares of the 3 values was calculated for each calibrator. These 3 values were summed up for all compounds at all levels, and this final sum for each calibrator type is shown in Table VI.4. The calibration type with the lowest value is considered to be the best fit for our data.

Table VI.4. Sum of % Relative Error for each type of calibration curve in the different ionization modes

Sum % Relative Error			
Calibration curve	Ionization mode		
	EI	PICI	NICI
linear	5069	46907	23323
linear, 1/x	3305	17680	6662
linear, $1/x^2$	3153	11335	4561
quadratic	/	21324	15299
quadratic, 1/x	/	7274	4629
quadratic, $1/x^2$	/	4909	3695

A linear curve with a $1/x^2$-weighting factor was applied for the EI results. For PICI and NICI, a second-order polynomial function with a weighting factor of $1/x^2$ provided better equations and resulted in least sum of residual squares. Especially for PICI, a large difference was seen in the sum of residual squares. Small deviations from linearity caused by curvature are often noticed for data obtained by chromatographic analysis. Nevertheless, traditionally, linear curves are more commonly used as compared to quadratic curves. This is mainly because of the level of complexity of the latter, especially from a historical point of view, as the appropriate software to perform the complicated calculation was not available. Nowadays, most analytical software includes the option of quadratic calibration and statistical software is more accessible. Thus, quadratic calibration curves provide a tool to account for curvature and can provide higher quality data when used appropriately. In addition, Kirkup and Mulholland conclude that a slight curvature in calibration data is often noticed and the choice of calibration curves depends upon the analyst's requirements and desired constraints about quantities as the prediction interval for estimated analyte concentrations [49]. Although the deviations from linearity for most compounds are small in PICI and NICI, as can be derived from the low quadratic term representing the bending of the curve (Table VI.5.), quadratic regression resulted in a lower %RE. In NICI, quadratic regression resulted in better inter batch precision and accuracy for highly concentrated samples. In

EI, no curvature is detected as seen in Figure VI.3., and therefore the simplest approach, thus the linear regression was chosen.

<u>Figure VI.3.</u> Representative calibration curves in EI, PICI and NICI for desmethylmirtazapine

Each curve has a weighting factor of $1/x^2$

Calibration curve desmethylmirtazapine EI

$y = 0,0052x + 0,008$
$R^2 = 0,9998$

Calibration curve desmethylmirtazapine PICI

$y = 0,0086x - 0,2765$
$R^2 = 0,9856$

$y = 7E\text{-}06x^2 + 0,005x - 0,0813$
$R^2 = 0,9976$

Calibration curve desmethylmirtazapine NICI

$y = 0,0015x - 0,028$
$R^2 = 0,9763$

$y = 2E\text{-}06x^2 + 0,0007x + 0,0005$
$R^2 = 0,9974$
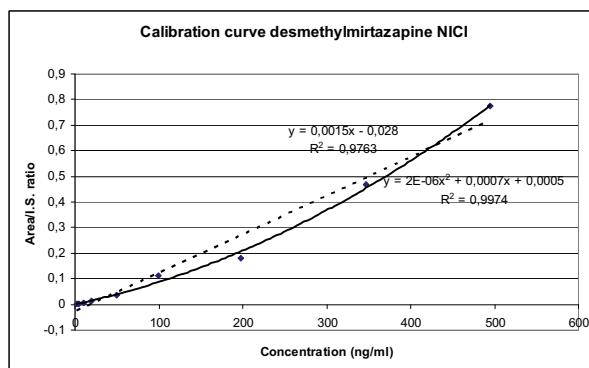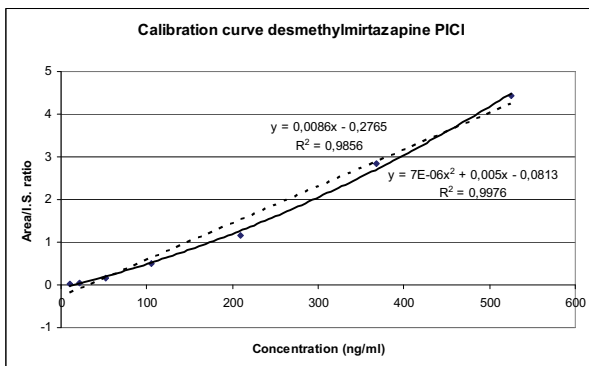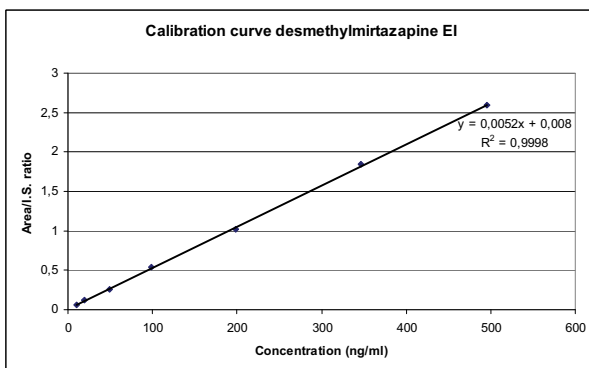
It seems that the slight curvature in the calibration data is dependent on the type of ionization. Chaler et al. also described polynomial calibration data for the chemical ionization modes and these data seem to depend on the type of mass spectrometer, i.e. differences in ion source construction (such as path length of the ion source), the eventual contamination of the ion source, and tuning parameters [50]. Moreover, variations in CI mass spectra resulting from changes in sample concentration and from co-eluting electron capturing agents have been observed [42, 51]. These variations are not caused by increased pressure in the source while the compounds pass through, but probably because of an increase in the residence time of ions within the source due to electronegative compounds. Rudewicz et al. [51] state that under the conditions of high pressure and high electron current, positive ions and negative particles diffuse together at the ambipolar diffusion rate (to the source walls). When electron capturing compounds enter the source, the rapidly moving electrons are converted into much more slowly moving negative ions, thus decreasing the ambipolar diffusion rate and increasing the residence time of ions within the source. This enhances positive reagent ion abundance and an increase in the extent of conversion of reactant ions to sample ions. Perhaps, this phenomenon could explain the non-linear response seen in CI mode as HFBI-derivatized sample compounds and endogenous compounds are strong electronegative substances.

Finally, for assessment of the correct weighting factor the strategy reported by Almeida and co-workers [48] was followed. The choice of the weighting factor was based on the sum of all %RE values. After comparison of $1/x$ and $1/x^2$ weighted regressions, $1/x^2$ was chosen because it resulted in improved calibration results.

Best fit calibration curves and the variations are indicated in Table VI.5. While EI calibration curves are stable for at least one week and show less variation, daily calibration curves for chemical ionization modes are suggested as differences in source contamination can lead to different results.

Table VI.5. Calibration curve data obtained in plasma (EI, PICI and NICI mode; n=7), blood and brain tissue (PICI mode; n=5)

Linearity Electron Ionization

plasma linear curve $1/x^2$

	Slope				y-intercept		C of determination
	best fit	95% CI	CV%		best fit	95% CI	R^2
Venlafaxine	0.019479	0.018763 - 0.020194	5		0.027357	0.007274 - 0.047441	0.990
m-cpp	0.004428	0.004213 - 0.004643	7		-0.001340	-0.011150 - 0.008464	0.987
Viloxazine	0.003513	0.003382 - 0.003646	5		0.0010533	-0.000827 - 0.002934	0.992
DMFluoxetine	0.004072	0.003781 - 0.004363	10		0.004882	-0.001530 - 0.011296	0.993
Fluvoxamine	0.001666	0.001493 - 0.001840	14		-0.000121	-0.003096 - 0.002853	0.992
Fluoxetine	0.005009	0.004940 - 0.005077	2		0.010610	0.005668 - 0.015552	0.995
Mianserin	0.004731	0.004610 - 0.004851	3		0.018086	0.016214 - 0.019957	0.994
Mirtazapine	0.014250	0.014049 - 0.014451	2		0.019407	0.007985 - 0.030829	0.996
Melitracen	0.021836	0.021469 - 0.022202	2		0.008699	-0.008410 - 0.004479	0.995
DMMia	0.006421	0.006186 - 0.006657	5		0.011116	0.006672 - 0.023142	0.992
DMSer	0.006643	0.006308 -0.006978	7		0.012372	-0.000543 - 0.017786	0.993
DMMir	0.003883	0.003757 - 0.004009	4		0.005640	0.001475 - 0.009831	0.992
Reboxetine	0.011757	0.011574 - 0.011940	2		0.005197	0.001367 - 0.009067	0.996
Citalopram	0.016250	0.015027 - 0.017473	10		0.030432	-0.057140 - -0.012050	0.991
DMMap	0.009857	0.009153 - 0.010561	10		0.009317	0.006165 - 0.019969	0.993
Maprotiline	0.014071	0.013691 - 0.014451	4		0.010312	0.011314 - 0.026592	0.994
Sertraline	0.002588	0.002342 - 0.002833	13		0.006739	-0.004163 - 0.005821	0.989
DDMC	0.01630	0.0151060 - 0.17540	10		0.016748	-0.013366 - 0.011448	0.991
DMC	0.032779	0.032313 - 0.033244	2		0.028201	-0.013220 - 0.028559	0.994
Paroxetine	0.005024	0.004945 - 0.005102	2		0.002290	0.004639 - 0.008032	0.996

Linearity Positive Chemical Ionization

plasma quadratic curve $1/x^2$

	quadratic term		linear term		y-intercept		C of determination
	best fit	95% CI	best fit	95% CI	best fit	95% CI	R^2
Venlafaxine	0.00000124	0.00000108 - 0.00000139	0.000350	0.000301 - 0.000399	0.001622	0.000183 - 0.003062	0.988
m-cpp	0.00000599	0.00000540 - 0.00000658	0.002810	0.002615 - 0.003005	0.004799	-0.002278 - 0.011876	0.991
Viloxazine	0.00000755	0.00000672 - 0.00000839	0.001280	0.001155 - 0.001405	0.000354	0.000268 - 0.000976	0.992
DMFluoxetine	0.00000338	0.00000276 - 0.00000401	0.001863	0.001618 - 0.002108	-0.000720	-0.004651 - 0.003212	0.990
Fluvoxamine	0.00000029	0.00000023 - 0.00000036	0.000132	0.000109 - 0.000155	0.000107	-0.000281 - 0.000495	0.989
Fluoxetine	0.00000560	0.00000512 - 0.00000608	0.004262	0.004089 - 0.004435	0.010023	0.005497 - 0.014549	0.994
Mianserin	0.00000091	0.00000051 - 0.00000130	0.004821	0.004630 - 0.005012	0.094671	0.089759 - 0.099584	0.994
Mirtazapine	0.00000309	0.00000287 - 0.00000332	0.001851	0.001753 - 0.001949	-0.004877	-0.006333 - -0.003421	0.990
Melitracen	0.00000181	0.00000164 - 0.00000198	0.000345	0.000322 - 0.000368	0.000310	0.000193 - 0.000426	0.993
DMMia	0.00000532	0.00000456 - 0.00000608	0.002545	0.002308 - 0.002782	-0.002524	-0.005076 - 0.000028	0.991
DMSer	0.00000415	0.00000300 - 0.00000531	0.003621	0.003165 - 0.004077	0.003413	-0.003691 - 0.010516	0.996
DMMir	0.00000586	0.00000494 - 0.00000678	0.002860	0.002529 - 0.003144	-0.012370	-0.016769 - -0.007971	0.995
Reboxetine	0.00000796	0.00000573 - 0.00001019	0.004611	0.004327 - 0.004894	-0.005180	-0.006864 - -0.003496	0.989
Citalopram	0.00000974	0.00000879 - 0.00001068	0.003192	0.002840 - 0.003544	-0.011306	-0.015282 - -0.007330	0.981
DMMap	0.00000187	0.00000102 - 0.00000272	0.002013	0.001790 - 0.002236	0.000678	-0.000771 - 0.002126	0.987
Maprotiline	0.00000485	0.00000425 - 0.00000545	0.002860	0.001881 - 0.003839	-0.002086	-0.003656 - -0.000515	0.988
Sertraline	0.00000179	0.00000146 - 0.00000212	0.001966	0.001610 -0.002323	0.002327	-0.003762 - 0.008416	0.989
DDMC	0.00000362	0.00000253 - 0.00000470	0.000730	0.000593 - 0.000867	0.002276	0.000893 - 0.001899	0.996
DMC	0.00000653	0.00000596 - 0.00000710	0.000796	0.000728 - 0.000863	0.001396	0.000675 - 0.003876	0.994
Paroxetine	0.00000625	0.00000486 - 0.00000765	0.004128	0.003996 - 0.004260	0.004914	0.003462 - 0.006367	0.995

blood quadratic curve $1/x^2$

	quadratic term		linear term		y-intercept		C of determination
	best fit	95% CI	best fit	95% CI	best fit	95% CI	R^2
Venlafaxine	0.00000103	0.00000093 - 0.00000113	0.000319	0.000288 - 0.000350	0.002002	0.001089 - 0.002916	0.993
m-cpp	0.00000866	0.00000632 - 0.0001099	0.005981	0.005037 - 0.006925	0.005188	-0.011320 - 0.021699	0.983
Viloxazine	0.00001303	0.00001000 - 0.00001605	0.002719	0.002173 - 0.003265	-0.001006	-0.005990 - 0.003983	0.985
DMFluoxetine	0.00000669	0.00000495 - 0.00000843	0.003852	0.003193 - 0.004511	-0.027780	-0.072980 - 0.017421	0.986
Fluvoxamine	0.00000140	0.00000097 - 0.00000183	0.000463	0.000260 - 0.000667	0.004456	-0.006630 - 0.015545	0.986
Fluoxetine	0.00000742	0.00000725 - 0.00000758	0.005361	0.005129 - 0.005593	0.012036	0.007663 - 0.016409	0.996
Mianserin	0.00000345	0.00000292 - 0.00000397	0.008010	0.007907 - 0.008113	0.094540	0.088443 - 0.100637	0.991
Mirtazapine	0.00000467	0.00000426 - 0.00000507	0.001804	0.001658 - 0.001950	-0.004271	-0.006270 - -0.002270	0.986
Melitracen	0.00000188	0.00000173 - 0.00000203	0.000372	0.000324 - 0.000420	0.000429	0.000235 - 0.000622	0.992
DMMia	0.00000455	0.00000417 - 0.00000492	0.002424	0.001948 - 0.002900	0.000273	-0.00128 - 0.001823	0.995
DMSer	0.00000946	0.00000446 - 0.00001446	0.011540	0.007503 - 0.015577	-0.000324	0.033720 - 0.033071	0.993
DMMir	0.00000573	0.00000464 - 0.00000681	0.002898	0.002031 - 0.003765	-0.009352	-0.015360 - -0.003340	0.995
Reboxetine	0.00000957	0.00000660 - 0.00001253	0.006910	0.006756 - 0.007064	0.008584	0.000886 - 0.016283	0.981
Citalopram	0.00001299	0.00000987 - 0.00001611	0.006000	0.005002 - 0.006998	-0.021860	-0.025960 - -0.017760	0.976
DMMap	0.00001179	0.00000840 - 0.00001517	0.008950	0.008549 - 0.009352	-0.001574	-0.011080 - 0.007928	0.975
Maprotiline	0.00000826	0.00000756 - 0.00000896	0.005222	0.004956 - 0.005488	0.003592	0.000290 - 0.007479	0.989
Sertraline	-0.00000022	0.00000090 - 0.00000045	0.001708	0.001398 - 0.002017	0.010198	0.005693 - 0.014702	0.957
DDMC	0.00004633	0.00002980 - 0.00006286	0.006266	0.004532 - 0.008000	0.020052	0.001870 - 0.041978	0.995
DMC	0.00000469	0.00000384 - 0.00000554	0.001603	0.001422 - 0.001784	0.004016	0.003204 - 0.004828	0.995
Paroxetine	0.00001082	0.00000963 - 0.00001200	0.005560	0.005494 - 0.005626	0.005766	0.003255 - 0.008277	0.994

brain quadratic curve $1/x^2$

	quadratic term		linear term		y-intercept		C of determination
	best fit	95% CI	best fit	95% CI	best fit	95% CI	R^2
Venlafaxine	0.00000042	0.00000018 - 0.00000067	0.000609	0.000273 - 0.000944	0.032960	0.018082 - 0.047838	0.990
m-cpp	0.00000288	0.00000115 - 0.00000461	0.008320	0.007644 - 0.008996	0.056070	-0.007817 - 0.119957	0.984
Viloxazine	0.00001150	0.00000970 - 0.00001239	0.008520	0.007662 - 0.009378	-0.043620	-0.061838 - -0.025402	0.989
DMFluoxetine	0.00000220	0.00000192 - 0.00000248	0.005503	0.004466 - 0.006540	-0.077520	-0.106269 - -0.048771	0.997
Fluvoxamine	0.00000050	0.00000042 - 0.00000058	0.008020	0.000599 - 0.001005	-0.012876	-0.022395 - -0.003357	0.996
Fluoxetine	0.00000235	0.00000166 - 0.00000304	0.006700	0.006330 - 0.007070	0.054920	0.030333 - 0.079507	0.998
Mianserin	0.00000071	0.00000028 - 0.00000115	0.008860	0.008351 - 0.009369	0.186140	0.110836 - 0.261444	0.996
Mirtazapine	0.00000074	0.00000032 - 0.00000116	0.003870	0.003448 - 0.004292	-0.036960	-0.057910 - -0.016010	0.995
Melitracen	0.00000155	0.00000121 - 0.00000190	0.001565	0.001388 - 0.001742	0.004534	-0.001701 - 0.010769	0.994
DMMia	0.00000053	-0.00000093 - 0.00000200	0.011500	0.010078 - 0.012922	-0.101060	-0.233092 - 0.030972	0.992
DMSer	0.00000641	0.00000554 - 0.00000727	0.005388	0.004925 - 0.005851	0.046900	0.020888 - 0.072912	0.992
DMMir	0.00000186	0.00000087 - 0.00000285	0.006671	0.005749 - 0.007594	-0.078248	-0.190940 - 0.034445	0.990
Reboxetine	-0.00000089	-0.00000150 - -0.00000028	0.009475	0.009037 - 0.009913	0.099175	0.078130 - 0.120220	0.991
Citalopram	-0.00000243	-0.00000435 - -0.00000051	0.015560	0.013387 - 0.017733	-0.039100	-0.401209 - 0.323009	0.988
DMMap	-0.00000138	-0.00000227 - -0.00000050	0.008380	0.008009 - 0.008751	-0.304200	-0.047738 - -0.013102	0.994
Maprotiline	0.00000103	0.00000032 - 0.00000174	0.005790	0.005567 - 0.006013	0.012388	0.010343 - 0.014433	0.995
Sertraline	0.00000511	0.00000361 - 0.00000661	0.004626	0.002931 - 0.006321	0.137914	0.053785 - 0.222043	0.983
DDMC	0.00001924	0.00001491 - 0.00002357	0.003069	0.001658 - 0.004480	0.088974	0.036594 - 0.141354	0.996
DMC	0.00001098	0.00001002 - 0.00001194	0.002382	0.001985 - 0.002779	0.047000	0.035464 - 0.058536	0.994
Paroxetine	0.00000471	0.00000393 - 0.00000548	0.006440	0.006230 - 0.006650	0.018180	0.011024 - 0.025336	0.997

Linearity Negative Chemical Ionization

plasma quadratic curve $1/x^2$

	quadratic term		linear term		y-intercept		C of determination
	best fit	95% CI	best fit	95% CI	best fit	95% CI	R^2
m-cpp	0.00000147	0.00000067 - 0.00000227	0.0034	0.002967 - 0.003833	0.000465	-0.000629 - 0.001559	0.990
Viloxazine	0.00000199	0.00000191 - 0.00000207	0.000755	0.000718 - 0.000792	0.000298	0.000041 - 0.000554	0.991
DMFluoxetine	0.00000051	0.00000039 - 0.00000064	0.0010	0.000896 - 0.001133	0.000760	0.000148 - 0.001372	0.992
Fluvoxamine	0.00000036	-0.0000021 - 0.00000093	0.0044	0.004062 - 0.004732	0.001318	-0.000498 - 0.003134	0.989
Fluoxetine	0.00000068	0.00000345 - 0.00000446	0.0042	0.003917 - 0.004483	0.045971	0.001915 - 0.007279	0.996
DMMia	0.00000364	0.00000343 - 0.00000384	0.001106	0.001050 - 0.001161	0.000211	-0.000185 - 0.000607	0.991
DMSer	0.00002343	0.00001349 - 0.00003337	0.023086	0.020551 - 0.025620	0.015154	-0.000808 - 0.031117	0.989
DMMir	0.00000271	0.00000250 - 0.00000292	0.000514	0.000484 - 0.000544	0.000196	-0.000048 - 0.000441	0.990
Reboxetine	0.00000700	0.00000606 - 0.00000794	0.002714	0.002430 - 0.002998	0.001684	0.000267 - 0.003101	0.986
DMMap	0.00000274	0.00000207 - 0.00000342	0.001682	0.001508 - 0.001856	0.000369	-0.000165 - 0.000902	0.987
Maprotiline	0.00001386	0.00001266 - 0.00001506	0.005251	0.005017 - 0.005486	0.002071	-0.000108 - 0.004249	0.988
Sertraline	0.00000392	0.00000223 - 0.00000561	0.002794	0.002552 - 0.003036	0.005209	0.002161 - 0.008256	0.973
DDMC	0.00008010	0.00005262 - 0.00010757	0.036670	0.024920 - 0.048420	-0.005964	-0.018890 - 0.006963	0.987
DMC	0.00002294	0.00002040 - 0.00002548	0.014074	0.012949 - 0.015200	0.001354	-0.001767 - 0.004475	0.992
Paroxetine	0.00000583	0.00000493 - 0.00000674	0.005757	0.005406 - 0.006108	0.001710	0.000559 - 0.002862	0.992

VI.3.5. Sensitivity

VI.3.5.1. *Experimental*

The sensitivity of the method was evaluated by determining the limit of quantification (LOQ). LOQ was defined as the lowest standard, spiked to the matrix, with a signal-to-noise ratio ≥ 10, an acceptable precision (RSD less than 20%) and accuracy (80-120%). This parameter was evaluated in SIM total ion mode (quantifier and qualifiers monitored). Six or five repetitions were applied in plasma and post-mortem samples (blood and brain), respectively.

VI.3.5.2. *Results and discussion*

All LOQs indicated in Table VI.6. gave a S/N > than 10. In addition, the precision and accuracy were also determined for these concentrations in plasma, blood and brain tissue. The LOQs in plasma ranged from 5 till 12.5 ng/ml, however, for mianserin and sertraline the accuracy did not meet the criteria and therefore the LOQs should be 20 and 25 ng/ml. The LOQs of all ADs show that the sensitivity even for subtherapeutic concentrations is adequate when monitoring plasma concentrations. The LOQ value for the compounds in PICI is not better than in EI, because in addition to the quasi-molecular ions, only low abundance fragment ions are created, leading to a loss in sensitivity as the qualifiers are not detected anymore. NICI is much more sensitive as compared to EI and PICI. The sample loaded on the SPE-tubes was downsized from 1 ml to 250 µl, because of the enhanced sensitivity of the system. This can be an advantage in clinical analysis where sample volume can be a limiting factor. The sensitivity for plasma samples is, however, worse than for pure standards, probably due to derivatization of endogenous molecules, increasing the background signal. While the

concentrations shown in Table VI.6. for NICI mode gave a S/N> 10 and an acceptable intra batch precision and accuracy, the inter batch precision results for most compounds did not fulfil the <20% variation criterion. A LOQ of 2.5-6.25 ng/ml depending on the compound would give better inter batch precision results.

Table VI.6. Limit of quantification in plasma, blood and brain tissue
* n-1

	LOQ									
	Spiked concentration					Accuracy (%)				
	Plasma (ng/ml)			Blood (ng/ml)	Brain (ng/g)	Plasma (ng/ml)			Blood (ng/ml)	Brain (ng/g)
compound	EI	PICI	NICI	PICI	PICI	EI (n=6)	PICI (n=6)	NICI (n=6)	PICI (n=5)	PICI (n=5)
venlafaxine	10	10		20	50	92	93*		109	85
m-cpp	10	10	2	10	50	101	101*	85	107	103
viloxazine	5	5	1	5	25	98	101	90	115	102
DMFluox	12.5	12.5	2.5	12.5	62.5	100	97	104	109	101
fluvoxamine	12.5	12.5	2.5	12.5	62.5	91	86*	86	105	101
fluoxetine	12.5	12.5	2.5	12.5	62.5	94	98	97	111	98
mianserin	10	10		20	50	*131*	*134*		79	99
mirtazapine	10	10		10	50	92	100		110	103
melitracen	5	5		10	25	104	95		110	100
DMMia	10	10	2	20	50	89	93	95	98	99
DMSer	10	10	2	10	50	91	104*	112	75	100
DMMir	10	10	2	20	50	117	118	101	96	107
reboxetine	5	5	1	5	25	92	99	81	111	96
citalopram	10	10		10	50	103	104		101	81
DMMap	6	6	1.2	6	30	113	102	105	114	104
maprotiline	6	6	1.2	6	30	89	99	112	108	97
sertraline	12.5	12.5	2.5	25	62.5	108	103	85	117	100
DDMC	5	5	1	10	25	135	118	80	83	100
DMC	5	5	1	5	25	95	79	83	113	102
paroxetine	5	5	1	5	25	101	100	97	106	99

	Intra batch precision (RSD%)					Inter batch precision (RSD%)				
	Plasma (ng/ml)			Blood (ng/ml)	Brain (ng/g)	Plasma (ng/ml)			Blood (ng/ml)	Brain (ng/g)
compound	EI (n=5)	PICI (n=5)	NICI (n=5)	PICI (n=5)	PICI	EI (n=6)	PICI (n=6)	NICI (n=6)	PICI (n=5)	PICI (n=5)
venlafaxine	9	13		15	15	17	23*		14	3
m-cpp	7	13	7	14	10	20	16*	33	3	2
viloxazine	4	9	9	12	15	7	8	25	9	3
DMFluox	5	4	5	8	11	15	19	28	6	1
fluvoxamine	5	7	6	10	10	19	17	27	3	2
fluoxetine	1	4	7	3	3	9	8	24	1	0.5
mianserin	10	4		2	4	12	11		10	2
mirtazapine	7	10		12	9	8	9		7	1
melitracen	4	18		8	17	9	19		14	3
DMMia	11	10	4	14	21	19	15	20	6	2
DMSer	6	6	7	11	17	12	22*	22	4	2
DMMir	9	8	5	*22*	12	9	14	25	9	3
reboxetine	2	4	13	9	27	14	14	35	3	16
citalopram	11	8		13	23	17	5		3	4
DMMap	4	6	10	14	13	1	33	11	4	6
maprotiline	2	6	4	14	8	9	18	40	4	7
sertraline	8	14	13	11	15	27	37	26	16	8
DDMC	8	16	2	18	6	18	30	20	9	6
DMC	3	9	4	16	7	19	32	43	5	5
paroxetine	2	2	4	11	4	13	16	12	3	1

While the LOQs in blood are higher for some compounds than in plasma, sensitivity, even for subtherapeutic concentrations, is adequate for most compounds. For brain tissue, citalopram and reboxetine demonstrated a variation in precision at the LOQ level above 20% at the indicated spiked concentrations (25-62.5 ng/g). However, the concentration in brain tissue is

usually much higher in patients with therapeutic drug levels in blood, thus sensitivity for most compounds will not be a problem. LOQ was not checked for hair samples as spiking onto hair does not reflect the incorporation in the hair structure.

VI.3.6. Precision

VI.3.6.1. *Experimental*

Precision was evaluated over the linear dynamic range at three different levels, i.e. 20 (low), 200 (medium), and 500 ng (high) for 1 ml plasma and blood. For brain tissue the concentrations were 200, 500 and 1000 ng/g. Intra and inter batch precision in plasma was assessed by six determinations per concentration in one day or on six separate days, respectively, and was measured using RSD. For the post-mortem matrices, 5 repetitions for intra and inter batch precision were performed.

VI.3.6.2. *Results and discussion*

The intra batch precision in plasma of all compounds fulfilled the acceptance criteria for all concentrations in EI as well as CI modes. For inter batch precision, venlafaxine gave bad results in PICI, possibly due to interference of a co-eluting peak. m-Chlorophenylpiperazine showed a high variation at low concentration, but fulfilled the criteria at medium and high concentrations in EI and CI modes. The inter batch precision for sertraline and DDMC was not acceptable over the total concentration range in NICI mode.

In blood, the intra and inter batch precision was acceptable for all compounds, however, the inter batch variation for sertraline is rather high.

Intra batch precision for brain tissue samples was acceptable, except the intra batch precision for citalopram at low concentration.

Table VI.7. Precision data
*n-1

			Precision																	
	Spiked concentration (ng/ml)			Intra batch (RSD%)									Inter batch (RSD%)								
Plasma	Low	Mid	High	Low (n=5)			Mid (n=6)			High (n=6)			Low (n=6)			Mid (n=6)			High (n=6)		
				EI	PICI	NICI	EI	PICI	NICI	EI	PICI	NICI	EI	PICI	NICI	EI	PICI	NICI	EI	PICI	NICI
Venlafaxine	20	200	500	3	7		5	8		1	8		14	30		5	24		9	4	
m-cpp	20	200	500	3	6	6	7	7	10	6	4	3	18	31	14	9	11	15	11	10	17
Viloxazine	10	100	250	3	5	6	3	2	9	3	2	8	10	11	13	6	5	7	5	4	6
DMFluox	25	250	625	11	11	11	12	11	11	6	4	10	12	10	13	14	14	11	10	14	12
Fluvoxamine	25	250	625	10	11	11	14	13	14	5	4	9	12	12	14	12	12	9	9	14*	12
Fluoxetine	25	250	625	4	3	3	4	4	5	5	4	3	7	6	8	5	6	5	2	4	6
Mianserin	20	200	500	4	5		5	5		3	3		6	5		6	8		3	5	
Mirtazapine	20	200	500	4	3		5	3		3	2		6	7		7	7		2	3	
Melitracen	10	100	250	7	10		5	6		1	4		5	11		4	10		2	4	
DMMia	20	200	500	8	6	4	4	3	11	1	2	8	13	9	11	7	7	9	5	6	6
DMSer	20	200	500	7	12	13	9	12	11	8	7	4	10	15*	12	6	26	15	15	7*	17
DMMir	20	200	500	6	6	2	4	4	10	2	2	11	14	7	11	8	9	8	5	4	10
Reboxetine	10	100	250	4	4	5	3	5	6	1	4	8	7	8*	16	5	6	6	3	5	7
Citalopram	20	200	500	11	7		8	4		3	4		10	13		8	14*		7	5	
DMMap	12	125	300	3	11	7	8	12	7	5	6	7	12	12	9	12	15	13	11	12*	15
Maprotiline	12	125	300	5	7	3	3	6	3	3	4	5	8	9	8	7	9	4	4	6	7
Sertraline	25	250	625	8	10	10	7	10	7	7	8	9	13	10*	31	12	15*	33	12	14*	38
DDMC	10	100	250	7	10	11	9	12	9	5	9	8	14	10	43	9	10*	37	8	11*	52
DMC	10	100	250	7	9	7	2	3	4	1	3	3	12	9	8	5	7	6	4	3	7
Paroxetine	10	100	250	6	7	3	4	4	8	2	3	6	11	5	12	5	7	7	1	4	5

	Spiked concentration (ng/ml)			Intra batch (RSD%)			Inter batch (RSD%)		
Blood	Low	Mid	High	Low (n=5) PICI	Mid (n=5) PICI	High (n=5) PICI	Low (n=5) PICI	Mid (n=5) PICI	High (n=5) PICI
Venlafaxine	20	200	500	15	8	7	14	14	1
m-cpp	20	200	500	13	4	6	10	8	5
Viloxazine	10	100	250	15	5	10	3	13	4
DMFluox	25	250	625	11	9	8	8	12	5
Fluvoxamine	25	250	625	12	11	7	6	13	5
Fluoxetine	25	250	625	2	1	1	2	9	1
Mianserin	20	200	500	2	3	2	10	0.5	1
Mirtazapine	20	200	500	4	6	3	9	7	3
Melitracen	10	100	250	8	6	3	14	11	2
DMMia	20	200	500	14	12	2	6	10	2
DMSer	20	200	500	11	8	3	4	7	3
DMMir	20	200	500	22	12	3	9	11	1
Reboxetine	10	100	250	9	3	4	14	9	4
Citalopram	20	200	500	14	12	8	6	13	5
DMMap	12	125	300	13	9	3	8	5	3
Maprotiline	12	125	300	7	4	5	5	9	1
Sertraline	25	250	625	11	14	11	16	8	19
DDMC	10	100	250	18	9	6	9	2	2
DMC	10	100	250	10	4	3	10	8	2
Paroxetine	10	100	250	7	3	2	2	11	1

	Spiked concentration (ng/g)			Intra batch (RSD%)			Inter batch (RSD%)		
Brain	Low	Mid	High	Low (n=5) PICI	Mid (n=5) PICI	High (n=5) PICI	Low (n=5) PICI	Mid (n=5) PICI	High (n=5) PICI
Venlafaxine	200	500	1000	10	15	7	4	7	3
m-cpp	200	500	1000	13	15	9	5	14	1
Viloxazine	100	250	500	6	13	11	2	5	1
DMFluox	250	625	1250	3	8	9	11	13	1
Fluvoxamine	250	625	1250	7	7	8	6	3	1
Fluoxetine	250	625	1250	4	3	7	10	10	1
Mianserin	200	500	1000	11	5	7	4	5	4
Mirtazapine	200	500	1000	3	6	5	6	5	3
Melitracen	100	250	500	14	3	13	2	2	4
DMMia	200	500	1000	8	10	14	6	3	6
DMSer	200	500	1000	9	3	12	12	13	2
DMMir	200	500	1000	11	7	12	15	9	7
Reboxetine	100	250	500	12	11	12	10	10	3
Citalopram	200	500	1000	16	13	15	4	4	3
DMMap	125	300	600	4	8	14	12	6	2
Maprotiline	125	300	600	4	2	9	7	7	1
Sertraline	250	625	1250	6	7	15	7	10	3
DDMC	100	250	500	15	13	12	4	3	0.5
DMC	100	250	500	14	11	10	5	6	1
Paroxetine	100	250	500	2	2	5	14	13	1

VI.3.7. Accuracy

VI.3.7.1. *Experimental*

Accuracy was evaluated with separately prepared individual primary stock solutions, mixtures and working solutions of all standards. It was calculated over the linear dynamic range at three different concentration levels, i.e. low, medium, and high. The analyte concentrations were calculated from daily

calibration curves and the accuracy was calculated by the ratio of this calculated concentration versus the spiked concentration.

VI.3.7.2. *Results and discussion*

The low concentrations were underestimated for most of the compounds in EI, PICI and NICI mode in plasma. While didesmethylcitalopram was overestimated in plasma at mid and high concentrations in EI and PICI mode, it was underestimated in NICI mode. However, an acceptable accuracy was seen for most compounds in all three matrices and ionization modes (Table VI.8.).

In blood, the low concentrations were again underestimated. This phenomenon was not seen in brain tissue. Maybe the underestimated values for the low concentration samples in plasma and blood are due to the surface of the laboratory glassware, which is slightly acidic and can adsorb ADs as they are amines. Therefore, silanized glassware could be used or a small amount of an alcohol such as butanol (1%) could be added to the redissolving solvent to reduce this adsorption by competition for the adsorptive sites on the glass surface.

Table VI.8. Accuracy data
*n-1

Plasma											
Spiked concentration (ng/ml)			(n=7; NICI n=6)								
Low	Mid	High	Low			Mid			High		
			EI	PICI	NICI	EI	PICI	NICI	EI	PICI	NICI
Venlafaxine	20	200	500	81	76		98	102		106	97	
m-cpp	20	200	500	88*	101	83	106	110	92	114	108	108
Viloxazine	10	100	250	85	85	75	105	106	85	110	102	91
DMFluox	25	250	625	89	83	84	104	107*	98	105	99	100
Fluvoxamine	25	250	625	84	78	80	107	92	93	107	107*	100
Fluoxetine	25	250	625	82	83	89	93	93	95	99	98	101
Mianserin	20	200	500	112	114*		127	128		135	132	
Mirtazapine	20	200	500	82	76		89	93		94	90	
Melitracen	10	100	250	87	82		101	96		105	98	
DMMia	20	200	500	86	81	83	99	99	88	103	101	94
DMSer	20	200	500	88*	77*	90	101*	86	108	99	98*	98
DMMir	20	200	500	103	91	86	107	107	87	113	107	93
Reboxetine	10	100	250	83	76*	77	98	100	90	104	99	91
Citalopram	20	200	500	77	76		98	96*		105	85	
DMMap	12	125	300	116*	87	81	112	108	100	106	108	89
Maprotiline	12	125	300	84	79	82	89	90	100	94	90*	101
Sertraline	25	250	625	91*	94*	94	99	94*	85	123	115*	94
DDMC	10	100	250	116	113	55	138	125*	64	139	128*	54
DMC	10	100	250	86*	81	80	97	88	92	99	95	96
Paroxetine	10	100	250	93	89	81	97	99	89	105	104	93

Blood						
Spiked concentration (ng/ml)				(n=5)		
	Low	Mid	High	Low PICI	Mid PICI	High PICI
Venlafaxine	20	200	500	109	106	101
m-cpp	20	200	500	71	102	95
Viloxazine	10	100	250	83	104	94
DMFluox	25	250	625	74	103	94
Fluvoxamine	25	250	625	78	102	94
Fluoxetine	25	250	625	86	99	98
Mianserin	20	200	500	79	98	95
Mirtazapine	20	200	500	92	99	95
Melitracen	10	100	250	110	100	100
DMMia	20	200	500	98	105	98
DMSer	20	200	500	75	91	96
DMMir	20	200	500	96	103	99
Reboxetine	10	100	250	83	99	94
Citalopram	20	200	500	79	109	93
DMMap	12	125	300	75	101	95
Maprotiline	12	125	300	82	103	97
Sertraline	25	250	625	117	101	97
DDMC	10	100	250	83	107	110
DMC	10	100	250	96	109	109
Paroxetine	10	100	250	85	100	98

Brain						
Spiked concentration (ng/g)				(n=5)		
	Low	Mid	High	Low PICI	Mid PICI	High PICI
Venlafaxine	200	500	1000	97	104	100
m-cpp	200	500	1000	86	96	96
Viloxazine	100	250	500	88	101	99
DMFluox	250	625	1200	92	95	99
Fluvoxamine	250	625	1200	93	102	98
Fluoxetine	250	625	1200	90	96	99
Mianserin	200	500	1000	94	101	97
Mirtazapine	200	500	1000	87	94	97
Melitracen	100	250	500	94	104	102
DMMia	200	500	1000	89	105	100
DMSer	200	500	1000	91	100	95
DMMir	200	500	1000	90	98	101
Reboxetine	100	250	500	92	100	101
Citalopram	200	500	1000	93	105	100
DMMap	125	300	600	94	106	97
Maprotiline	125	300	600	91	104	98
Sertraline	250	625	1200	105	104	99
DDMC	100	250	500	115	105	111
DMC	100	250	500	108	105	108
Paroxetine	100	250	500	89	98	99

VI.4. Conclusion

A gas chromatographic-mass spectrometric method (GC-MS) for the simultaneous determination of the 'new' ADs (mirtazapine, viloxazine, venlafaxine, trazodone, citalopram, mianserin, reboxetine, fluoxetine, fluvoxamine, sertraline, maprotiline, melitracen, paroxetine) and their active metabolites (desmethylmirtazapine, O-desmethylvenlafaxine, m-chloro-

phenylpiperazine, desmethylcitalopram, didesmethylcitalopram, desmethyl-mianserin, desmethylfluoxetine, desmethylsertraline, desmethylmaprotiline) is validated in plasma, blood and brain tissue using different ionization modes.

Sample preparation consisted of a strong cation exchange mechanism and derivatization with heptafluorobutyrylimidazole. The GC separation was performed in 24.8 minutes. Identification and quantification were based on selected ion monitoring in electron and chemical ionization modes. Calibration by linear and quadratic regression for electron and chemical ionization, respectively, utilized deuterated internal standards and a weighting factor $1/x^2$. Limits of quantitation were established between 5-12.5 ng/ml in EI and positive ion chemical ionization (PICI), and 1-6.25 ng/ml in negative ion chemical ionization (NICI) for plasma. For blood the limit of quantification ranged from 5-20 ng/ml in PICI, while the limit of quantification in brain tissue ranged from 25-62.5 ng/g.

During validation stability, sensitivity, precision, accuracy, recovery, linearity and selectivity were evaluated for each ionization mode and were demonstrated to be acceptable for most compounds. While it is clear that not all compounds can be quantitated either due to irreproducible validation results and chromatographic problems (trazodone) or due to derivatization problems (O-desmethylvenlafaxine), this method can quantitate most new ADs in the therapeutic range in plasma in different ionization modes, and in blood and brain tissue.

Electron ionization is the traditional method for comprehensive screening procedures due to the easy library search mechanism. This ionization, however, leads to high fragmentation of citalopram, melitracen, and venlafaxine, resulting in the aspecific high abundance quantifier ion at m/z 58 and inherent loss of specificity, especially for demanding matrices such as post-mortem blood and brain tissue. Chemical ionization (CI) is a 'softer' ionization technique, thus providing more selectivity through molecular mass information. However, due to less fragmentation, the qualifier ions had low abundancy, leading to loss of sensitivity. NICI leads to improved sensitivity

due to heptafluorobutyrylimidazole derivatization, allowing smaller sample volumes. However, efficient sample preparation stays necessary because of detectable derivatized endogenous compounds. On the other hand, underivatized tertiary amines such as citalopram, melitracen, mianserin, and mirtazapine are not detected.

Chemical ionization modes can surely provide advantages, however, the system is less robust and harder to optimize. The presence of impurities in the reagent gas, radical species in the ion source plasma (formed by trace amounts of oxygen, water or chlorinated solvents), air leaks and interactions with the ion source walls can lead to variations in spectra and thus difficulties during analysis. In addition, in routine clinical analysis, changing the EI and CI source can be time consuming. Therefore, EI is still the ionization mode of choice in clinical analysis due to time concerns. For routine toxicological analyses, PICI mode can be of interest when highly fragmented compounds such as citalopram, venlafaxine and melitracen have to be monitored, but interferences are still seen for venlafaxine. While the NICI mode leads to loss of information because it does not detect the underivatized tertiary amine ADs, it leads to remarkably enhanced sensitivity for the derivatized ADs. This could be very interesting in clinical analysis and TDM of samples from children where often only a limited amount of sample is available.

VI.5. References

[1]   Murray CJL, Lopez AD. Global burden of disease: a comprehensive assessment of mortality and disability from diseases, injuries, and risk factors in 1990 and projected to 2020, Harvard University Press, Harvard, 1996 (WHO: http://www.who.int/mental_health.)

[2]   Sampson SM. Treating depression with selective serotonin reuptake inhibitors: a practical approach. *Mayo Clin. Proc.* 2001; 76: 739-744

[3]   Lundmark J, Bengtsson F, Nordin C, Reis M, Walinder J. Therapeutic drug monitoring of selective serotonin reuptake inhibitors influences clinical dosing strategies and reduces drug costs in depressed elderly patients. *Acta Psychiatr. Scand.* 2000; 101: 354-359

[4]   Burke MJ, Preskorn SH. Therapeutic drug monitoring of antidepressants - Cost implications and relevance to clinical practice. *Clin. Pharmacokinet.* 1999; 37: 147-165

[5]   Mitchell PB. Therapeutic drug monitoring of psychotropic medications. *Br. J. Clin. Pharmacol.* 2000; 49: 303-312

[6]   Mitchell PB. Therapeutic drug monitoring of non-tricyclic antidepressant drugs. *Clin. Chem. Lab. Med.* 2004; 42: 1212-1218

[7]   Eap CB, Sirot EJ, Baumann P. Therapeutic monitoring of antidepressants in the era of pharmacogenetics studies. *Ther. Drug Monit.* 2004; 26: 152-155

[8]   Heller S, Hiemke C, Stroba G, Rieger-Gies A, Daum-Kreysch E, Sachse J, Hartter S. Assessment of storage and transport stability of new antidepressant and antipsychotic drugs for a nationwide TDM service. *Ther. Drug Monit.* 2004; 26: 459-461

[9]   de Meester A, Carbutti G, Gabriel L, Jacques JM. Fatal overdose with trazodone: Case report and literature review. *Acta Clin. Belg.* 2001; 56: 258-261

[10]   Azaz-Livshits T, Hershko A, Ben-Chetrit E. Paroxetine associated hepatotoxicity: A report of 3 cases and a review of the literature *Pharmacopsychiatry* 2002; 35: 112-115

[11]   Goeringer KE, McIntyre IM, Drummer OH. Postmortem tissue concentrations of venlafaxine. *Forensic Sci. Int.* 2001; 121: 70-75

[12]   Goeringer KE, Raymon L, Christian GD, Logan BK. Postmortem forensic toxicology of selective serotonin reuptake inhibitors: A review of pharmacology and report of 168 cases. *J. Forensic Sci.* 2000; 45: 633-648

[13]   Kelly CA, Dhaum N, Laing WJ, Strachan FE, Good AM, Bateman DN. Comparative toxicity of citalopram and the newer antidepressants after overdose. *J. Toxicol.-Clin. Toxicol.* 2004; 42: 67-71

[14]   Adson DE, Erickson-Birkedahl S, Kotlyar M. An unusual presentation of sertraline and trazodone overdose. *Ann. Pharmacother.* 2001; 35: 1375-1377

[15]   Decision Resources Inc. The Antidepressant Market through 2014 - Focus on emerging therapies and new indications. *Cognos Plus Stud*y n° 11*, Massachussets,* 2005; pp 176

[16]   Yildiz A, Gönül A, Tamam L. Mechanism of actions of antidepressants: beyond the receptors. *Bull. Clin. Psychopharmacol.* 2002; 12: 194-200

[17]   Uges DRA, Conemans JMH. Antidepressants and antipsychotics. Handbook of Analytical Separations, Elsevier, Amsterdam, 2000, pp. 742

[18]   Pacher P, Kohegyi E, Kecskemeti V, Furst S. Current trends in the development of new antidepressants. *Curr. Med. Chem.* 2001; 8: 89-100

[19]   Kent JM. SNaRIs, NaSSAs, and NaRIs: new agents for the treatment of depression. *Lancet* 2000; 355: 911-918

[20]   Kent J. SNaRIs, NaSSAs, and NaRIs: new agents for the treatment of depression. *Lancet* 2000; 355: 2000

[21]   Mann JJ. Drug therapy - The medical management of depression. *N. Engl. J. Med.* 2005; 353: 1819-1834

[22]   Baumann P, Hiemke C, S. U, Eckermann G, Gaertner I, Kuss HJ, Laux G, Müller-Oerlinghausen B, Rao ML, Riederer P, Zernig G. The AGNP-TDM expert group consensus guidelines: therapeutic drug monitoring in psychiatry. *Pharmacopsychiatry* 2004; 37: 243-265

[23]   Labat L, Deveaux M, Dallet P, Dubost JP. Separation of new antidepressants and their metabolites by micellar electrokinetic capillary chromatography. *J. Chromatogr. B* 2002; 773: 17-23

[24]   Andersen S, Halvorsen TG, Pedersen-Bjergaard S, Rasmussen KE. Liquid-phase microextraction combined with capillary electrophoresis, a promising

tool for the determination of chiral drugs in biological matrices. *J. Chromatogr. A* 2002; 963: 303-312

[25] Raggi MA, Mandrioli R, Casamenti G, Volterra V, Pinzauti S. Determination of reboxetine, a recent antidepressant drug, in human plasma by means of two high-performance liquid chromatography methods. *J. Chromatogr. A* 2002; 949: 23-33

[26] Llerena A, Dorado P, Berecz R, Gonzalez A, Norberto MJ, de la Rubia A, Caceres M. Determination of fluoxetine and norfluoxetine in human plasma by high-performance liquid chromatography with ultraviolet detection in psychiatric patients. *J. Chromatogr. B* 2003; 783: 25-31

[27] Hostetter AL, Stowe ZN, Cox M, Ritchie JC. A novel system for the determination of antidepressant concentrations in human breast milk. *Ther. Drug Monit.* 2004; 26: 47-52

[28] Titier K, Castaing N, Scotto-Gomez E, Pehourcq F, Moore N, Molimard M. High-performance liquid chromatographic method with diode array detection for identification and quantification of the eight new antidepressants and five of their active metabolites in plasma after overdose. *Ther. Drug Monit*. 2003; 25: 581-587

[29] Lacassie E, Gaulier JM, Marquet P, Rabatel JF, Lachatre G. Methods for the determination of seven selective serotonin reuptake inhibitors and three active metabolites in human serum using high-performance liquid chromatography and gas chromatography. *J. Chromatogr. B* 2000; 742: 229-238

[30] Suckow RF, Zhang MF, Cooper TB. Sensitive and selective liquid-chromatographic assay of fluoxetine and norfluoxetine in plasma with fluorescence detection after precolumn derivatization. *Clin. Chem.* 1992; 38: 1756-1761

[31] Goeringer KE, McIntyre IM, Drummer OH. LC-MS analysis of serotonergic drugs. *J. Anal. Toxicol.* 2003; 27: 30-35

[32] Kirchherr H, Kuhn-Velten WN. Quantitative determination of forty-eight antidepressants and antipsychotics in human serum by HPLC tandem mass spectrometry: a multi-level, single-sample approach. *J. Chromatogr. B* 2006; 843: 100-113

[33] Sauvage FL, Gaulier JM, Lachatre G, Marquet P. A fully automated turbulent-flow liquid chromatography-tandem mass spectrometry technique for monitoring antidepressants in human serum. *Ther. Drug Monit.* 2006; 28: 123-130

[34] Ulrich S, Martens J. Solid-phase microextraction with capillary gas-liquid chromatography and nitrogen-phosphorus selective detection for the assay of antidepressant drugs in human plasma. *J. Chromatogr. B* 1997; 696: 217-234

[35] Martinez MA, de la Torre CS, Almarza E. Simultaneous determination of viloxazine, venlafaxine, imipramine, desipramine, sertraline, and amoxapine in whole blood: Comparison of two extraction/cleanup procedures for capillary gas chromatography with nitrogen-phosphorus detection. *J. Anal. Toxicol.* 2002; 26: 296-302

[36] Maurer HH, Bickeboeller-Friedrich J. Screening procedure for detection of antidepressants of the selective serotonin reuptake inhibitor type and their metabolites in urine as part of a modified systematic toxicological analysis procedure using cas chromatography-mass spectrometry. *J. Anal. Toxicol* 2000; 24: 340-347

[37]   Bickeboeller-Friedrich J, Maurer HH. Screening for detection of new antidepressants, neuroleptics, hypnotics, and their metabolites in urine by GC-MS developed using rat liver microsomes. *Ther. Drug Monit.* 2001; 23: 61-70

[38]   Eap CB, Bouchoux G, Amey M, Cochard N, Savary L, Baumann P. Simultaneous determination of human plasma levels of citalopram, paroxetine, sertraline, and their metabolites by gas chromatography mass spectrometry. *J. Chromatogr. Sci.* 1998; 36: 365-371

[39]   Maurer HH, Kraemer T, Kratzsch C, Peters FT, Weber AA. Negative ion chemical ionization gas chromatography-mass spectrometry and atmospheric pressure chemical ionization liquid chromatography-mass spectrometry of low-dosed and/or polar drugs in plasma *Ther. Drug Monit.* 2002; 24: 117-124

[40]   Maurer HH. Role of gas chromatography-mass spectrometry with negative ion chemical ionization in clinical and forensic toxicology, doping control, and biomonitoring *Ther. Drug Monit.* 2002; 24: 247-254

[41]   Wille SMR, Maudens KE, Van Peteghem CH, Lambert WEE. Development of a solid phase extraction for 13 'new' generation antidepressants and their active metabolites for gas chromatographic-mass spectrometric analysis. *J. Chromatogr. A* 2005; 1098: 19-29

[42]   Stemmler EA, Hites RA. A systematic study of instrumental parameters affecting electron capture negative ion mass spectra. *Biomed. Environ. Mass Spectrom.* 1988; 15: 659-667

[43]   US Department of Health and Human Services Food and Drug Administration-Center for Drug Evaluation and Research (CDER), Guidance for Industry, Bioanalytical Method Validation, Rockville, 2001

[44]   Heller S, Hiemke C, Stroba G, Rieger-Gies A, Daum-Kreysch E, Sachse J, Hartter S. Assessment of storage and transport stability of new antidepressant and antipsychotic drugs for a nationwide TDM service *Ther. Drug Monit.* 2004; 26: 459-461

[45]   Martin A, Pounder DJ. Postmortem Toxicokinetics of Trazodone. *Forensic Sci. Int.* 1992; 56: 201-207

[46]   Bolo NR, Hode Y, Nedelec JF, Laine E, Wagner G, Macher JP. Brain pharmacokinetics and tissue distribution in vivo of fluvoxamine and fluoxetine by fluorine magnetic resonance spectroscopy. *Neuropsychopharmacol.* 2000; 23: 428-438

[47]   Wenzel S, Aderjan R, Mattern R, Pedal I, Skopp G. Tissue distribution of mirtazapine and desmethylmirtazapine in a case of mirtazapine poisoning. *Forensic Sci. Int.* 2006; 156: 229-236

[48]   Almeida AM, Castel-Branco MM, Falcao AC. Linear regression for calibration lines revisited: weighting schemes for bioanalytical methods. *J. Chromatogr. B* 2002; 774: 215-222

[49]   Kirkup L, Mulholland M. Comparison of linear and non-linear equations for univariate calibration. *J. Chromatogr. A* 2004; 1029: 1-11

[50]   Chaler R, Villanueva J, Grimalt JO. Non-linear effects in the determination of paleotemperature $U^{k'37}$ alkenone ratios by chemical ionization mass spectrometry. *J. Chromatogr. A* 2003; 1012: 87-93

[51]   Rudewicz P, Feng T, Blom K, Munson B. Effect of electron capture agents in chemical ionization mass spectrometry. *Anal. Chem.* 1984; 56: 2610-2611

Chapter VII

Therapeutic drug monitoring and
pharmacogenetics of antidepressants

VII.1. Foreword

This chapter describes a preliminary study concerning personalized anti-depressant (AD) treatment. So far most compelling evidence in pharmacogenetics of ADs has been gathered for an effect of CYP2D6 polymorphisms (i.e. variations in a specific metabolic enzyme) on AD drug plasma levels [1]. Therefore, in this study, therapeutic drug monitoring (TDM) is combined with *CYP2D6* genotyping (GEN) to ensure a good medical treatment. Despite the low toxicity of ADs, physicians must be aware that depression is a chronic disease leading to a long period of drug intake. In addition, these patients mostly use a whole range of drugs, which increases the risk of adverse effects. There are no clear guidelines to get an optimized therapy, especially because a lot of factors (environmental, genetic) will influence the final outcome. Nowadays, AD treatment is largely based on trial and error combined with the experience of the physician. At first, we wanted to link the genotype of a large group of depressed patients with their plasma concentration and effects; however, it was hard to gather enough patients for a significant large scale study. Moreover, blood samples are not taken on a routine base in psychiatric clinics. Therefore, as an example of the TDM-GEN procedure, we will discuss a case report in which a healthy volunteer showed adverse effects after intake of a single dose of mianserin (30 mg/day). In addition, the TDM-GEN procedure that would be used for depressed patients will be described.

VII.2. Introduction

In spite of the enormous progress in the knowledge of depression and the design of ADs during the past decades, treatment of depression is far from being optimal. There is a delayed time of onset of clinical improvement, remission rates are high and a significant number of patients, about 30-50 %, have an insufficient response or do not respond at all. In addition, side-effects are often noticed and about 40 % of all patients are non-compliant, probably largely due to these side-effects [1-8].

In the psychiatric clinic, depression is treated with 'optimal doses' of ADs that are defined through population-based dose-effect relationships, thus doses

are based on the average plasma levels of the drug obtained in the population at a certain dosage. However, a large inter-individual variability between dose, plasma concentrations and final effects are observed during treatment with ADs. Variability of the ADs plasma concentrations is determined by different factors such as environmental (e.g. compliance, co-medication, diet, smoking habit) and physiological factors (e.g. age, sex, liver disease, impared kidney function), as wel as by genetic variability of pharmacokinetic (metabolism) or pharmacodynamic (transporters, targets) parameters (Figure VII.1.) [1, 4, 5, 8-10].

One of the most important factors of the inter-individual variability of AD plasma concentrations and effects is the metabolism of ADs due to cytochrome P450 isoenzymes. Especially CYP2D6 is of interest, as this enzyme (partially) metabolizes about 25 % of all drugs. Polymorphisms (i.e. variations) in the genetic sequence may result in a lack of this enzyme (gene deletion), a partially functional enzyme (mutation of a single nucleotide) or a high amount of active enzyme (gene amplification) and thus lead to differences in drug metabolism. Based on these genetic variations, different patient groups can be distinguished from poor (PM) to ultrarapid (UM) metabolizers. For these patients the 'optimal average dose' used in clinical practice can lead to problems. For poor metabolizers, a lot of side-effects may occur as high ADs plasma concentrations are reached because of the slower rate of metabolism. Ultrarapid metabolizers, on the other hand, often do not respond to AD treatment, because their high rate of metabolism leads to subtherapeutic concentrations [11].

In the clinical field, therapeutic drug monitoring (TDM) is known to be a valid tool to optimize pharmacotherapy as it enables the clinician to adjust the dosage of drugs according to the pharmacokinetic characteristics of the individual patient. The usefulness of TDM for the new generation ADs is, however, under discussion because of the low toxicity profile, the large therapeutic window and the poor plasma concentration-effect relationship. In addition, dose adjustments based on TDM can only occur at steady-state of the drug, thus only after a couple of weeks of treatment, and these first weeks of treatment are crucial for patient compliance [12, 13]. As a result,

for optimal and rational use of ADs, all factors of variability should be considered and if possible monitored during (a problematic) therapy. As the variability of the ADs plasma concentrations is due to environmental factors, underlying diseases as well as genetic variables, TDM combined with pharmacogenetics (TDM-GEN) and qualitative diagnostic tests could give a better idea of the individual patient's response to a drug and can finally result in a personalized medicine [5].

Figure VII.1. Schematic overview of the drug route towards site of action, with indication of factors influencing drug plasma concentration and effect

A, after drug intake, plasma concentrations for one dose differ due to compliance, environmental, physiological and genetic factors. The genetic variability for CYP2D6 metabolism is indicated. B, for one plasma concentration, a different brain concentration can occur due to genetic variation of the transport system. C, variations also occur in receptors, transporters, and biosynthesis enzymes resulting in a different effect. Adapted from [10, 14].
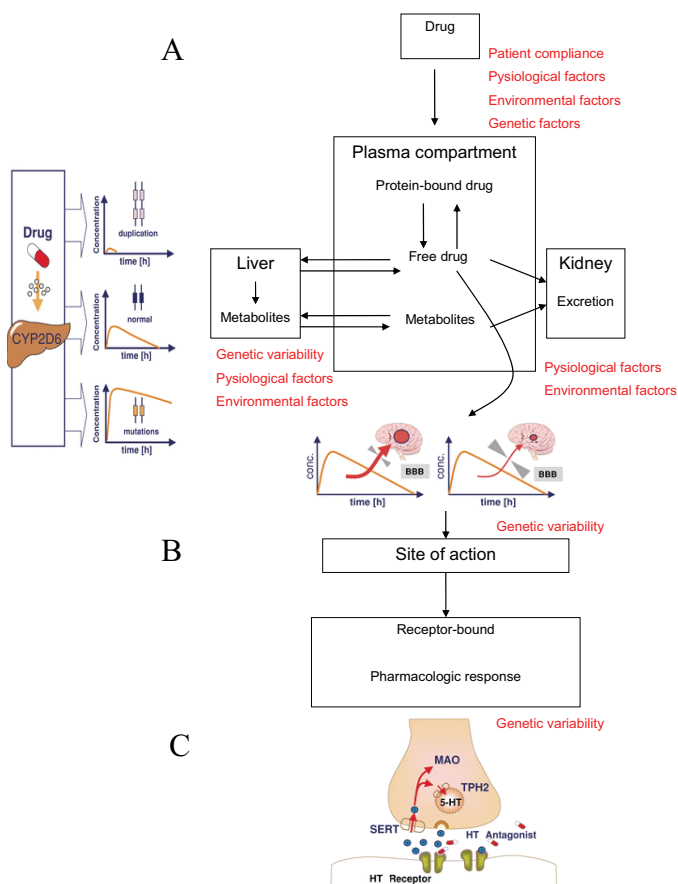
VII.2.1. Patient information and qualitative diagnostic tests

The diagnosis of depression is done by depression rating scales as no objective parameters such as plasma concentration of certain markers can indicate the state of the depression. The three most popular rating scales are the Hamilton Depression Rating Scale (HAM-D), the Montgomery and Asberg Depression Rating Scale (MADRS) and the American Psychiatric Association Diagnostic and Statistical Manual of Mental Disorders (DSM-IV).

The HAM-D is a multiple choice questionnaire originally published in 1960 by Max Hamilton, which rates the severity of symptoms observed in depression such as low mood, insomnia, agitation, anxiety and weight-loss. The total scores range between 0-52 and are interpreted as follows: 0-7 = normal /not-depressed; 8-13 = possibly/mildly depressed mood; 14-15 moderately depressed; 19-27 severely depressed; > 27 very severely depressed [15].

The MADRS is a commonly used scale to determine the severity of depression in elderly patients without dementia. It rates the severity of depression by observing symptoms such as low mood, insomnia, appetite, concentration problems, agitation, negative and suicidal thoughts. A score of 20 leads to the conclusion of a slightly depressed mood, while a score higher than 30 means a severely depressed state of the patient.

The DSM rating scale was first published in 1952 by the American Psychiatric Association and the last revision DSM-IV was published in 1994. This publication is a categorical classification system of 297 mental health disorders into five levels. The first level (axis 1) includes clinical disorders, including major mental disorders, as well as developmental and learning disorders. This is the category in which depression is situated. Depression is categorized as a recurrent or single episode mental disorder and is subdivided in mild, moderate, or severe depression with or without psychotic features [16].

The results of these qualitative diagnostics should be linked to quantitative TDM results to link the state of the patient to the obtained plasma concentrations [16]. In addition, information concerning the patient's physiology, habits (e.g. smoking, diet), co-medication, comorbidity and genetic parameters should be obtained to get as much information as

possible to ensure a good interpretation of the TDM-GEN results in order to finally result in an individualized and adequate therapy without side-effects.

VII.2.2. Therapeutic drug monitoring

Therapeutic drug monitoring of ADs in plasma is the only way to estimate the brain concentration and thus the concentration at the effector-site of the drugs. However, as discussed above, there is a large variability in AD plasma concentrations and it is difficult to link a plasma concentration to an effect due to inter-individual variations as a result of environmental, physiological and genetic factors [5]. Therefore, the interdisciplinary TDM group of the Arbeitsgemeinschaft für Neuropsychopharmakologie und Pharmakopsychiatrie (AGNP) has worked out consensus guidelines to assist psychiatrists and laboratories to optimize the use of TDM of psychotropic drugs. Five research-based levels of recommendation were defined with regard to routine monitoring of plasma concentrations of 65 psychoactive drugs. For new generation ADs, TDM is recommended or useful to detect non-compliance, for patients with a lack of clinical response or adverse effects at recommended doses, and when interactions are suspected. Moreover, for special patient groups such as children, adolescents, pregnant women and elderly, monitoring could be of interest because of variations in pharmacokinetic behaviour. As ADs can be used chronically, monitoring can be used to prevent relapse or recurrence [2, 13].

TDM is only useful if therapeutic windows are postulated, to link plasma concentrations to effects. Both TIAFT [17] and the AGNP-group [13] have proposed therapeutic windows for several ADs and these were already discussed in chapter I of this thesis. During TDM, high plasma concentrations can indicate adverse effects and toxicity due to poor metabolism or interactions, while low plasma concentrations could lead to a suspicion of ultrarapid metabolism or non-compliance. TDM demonstrates the effect of all possible pharmacokinetic variables, and can result in dose adjustments, but it does not show the underlying problem such as genetic variations or co-medication. However, there are also reports that demonstrate the usefulness of TDM for phenotyping purposes. Through the plasma concentration ratio of

an AD and its metabolite, the pharmacokinetic phenotype of an individual can be measured. Van der Weide et al. [12] and Veefkind et al. [18] have demonstrated a difference in metabolic ratio between the phenotypes for venlafaxine, and used these data to optimize AD therapy. Based on these studies, individuals can be classified as poor, intermediate, extensive and ultrarapid metabolizers. The reseach group of Kirchheiner even went a step further and gave dose recommendations for extensive, intermediate and poor metabolizers of CYP2D6 for 16 ADs based on their plasma concentrations [8, 19]. Figure VII.2. demonstrates that dose adjustments for citalopram and sertraline will not be necessary for the different CYP 2D6 phenotypes, while the importance of personalized AD treatment increases from trazodone, mianserin, venlafaxine, paroxetine to maprotiline treatment [19]. It is therefore clear, that TDM of ADs can be of interest to determine the patient's phenotype and to adjust AD dosages based on their plasma concentrations.

Figure VII.2. Dose adjustment of ADs according to their CYP2D6 phenotype [19]
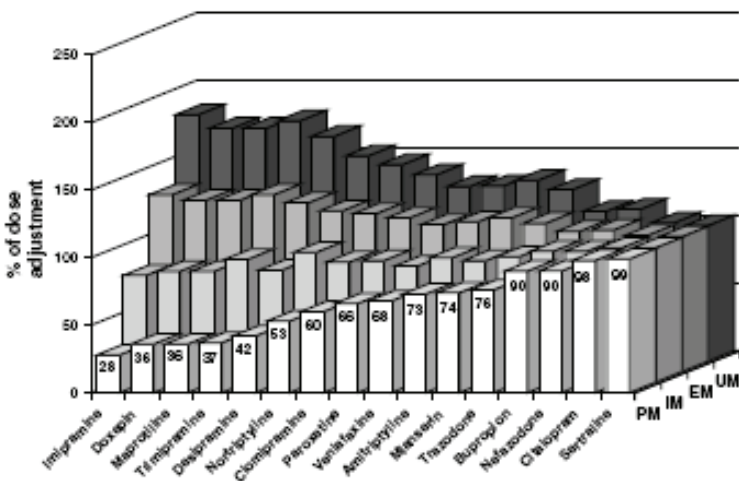
VII.2.3. Genetic variability

Genetic factors are believed to play a major role in the variation of treatment response and the incidence of adverse effects to medication. Genetic variability occurs in enzymes playing a role in drug metabolism, at the target sites [8, 9, 20, 21] and in transport proteins located in the intestinal mucosa and in the blood-brain barrier, such as P-glycoprotein [8, 21-24].

During the past 30 years, a lot of research has been done concerning cytochrome P450 isoenzymes polymorphisms. Especially polymorphisms of *CYP2D6*, encoding the debrisoquine hydroxylase enzyme, are of high clinical relevance for the metabolism and thus plasma concentration of ADs [9]. The *CYP2D6* gene is located on chromosome 22, and over 70 functionally different alleles have been reported for this enzyme. However, only 15 encode an enzyme with 'abnormal' functionality [1]. The differences are due to gene deletion, gene duplication or mutations and result in defective, qualitatively altered, diminished or enhanced rates of drug metabolism [9]. In general, four phenotypes can be identified: poor metabolizers (PM), lacking the functional enzyme; intermediate metabolizers (IM), who are heterozygous for one deficient allele or carry two alleles that cause reduced activity; extensive metabolizers (EM), who have two normal alleles; and ultrarapid metabolizers (UM), who have multiple gene copies [11]. The distribution of these four phenotypes is different for different ethnic groups (Figure VII.3.). Although the incidence of PM or UM is not so high, readily 35-50 million people in Europe are expected to exhibit problems during therapy with a CYP2D6 substrate [9]. However, it is clear that the extent of these potential problems largely depends on the relative contribution of the respective CYP enzyme to the total elimination of the drug and the therapeutic index of the drug [19].

Figure VII.3. Ethnic variability in the frequency of CYP2D6 polymorphism
Adapted from [9]. Red trace indicates frequency of poor metabolizers, black trace the
ultrarapid metabolizers
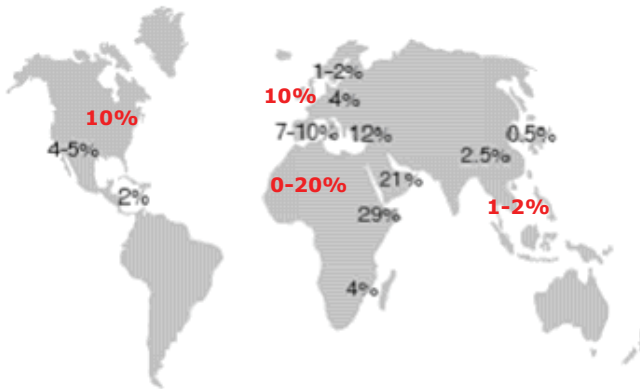
The number of known *CYP2D6* gene variants is growing. However,
genotyping for only the 6 most common defective alleles will predict the
CYP2D6 phenotype (poor, ultrarapid or normal metabolism) with about 95-
99% certainty [9, 25]. Therefore, *CYP2D6*3, *4, *5, *6, *7, *8, and *CYP2D6*
duplications were monitored in our CYP genotyping assays (Figure VII.4.).

There are different mechanisms that lead to total loss of function. Several
alleles have single base pair mutations or small insertions and deletions that
interrupt the reading frame or that interfere with correct splicing, ultimately
leading to prematurely terminated protein products (*CYP2D6*3, *4, *6, *8).
*CYP2D6*7, on the other hand, encodes a full-length but non-functional
protein, while *CYP2D6*5 refers to *CYP2D6* gene deletion. Poor metabolizers
are homozygous for one of these alleles or heterozygous for 2 of these non-
functional alleles. Ultrarapid metabolizers are detected by determining alleles
with increased function, thus gene duplications. Patients having at least one
decreased or normal functioning allele are intermediate or extensive
metabolizers, and their metabolization patterns are not clinically relevant for
AD therapy [4, 26].

<u>Figure VII.4.</u> Structure of functional and non-functional *CYP2D6* alleles and their influence on final protein activity

Adapted form [9, 26]. The 9 exons are indicated by numbered boxes with DNA polymorphisms indicated on top (*del* deletion, *ins* insertion). Predicted amino acid changes and translation termination (*ter*) codons are indicated below. Frequencies of variation in the Caucasian population are indicated in red.

VII.3. Experimental

VII.3.1. Patient selection

The TDM-GEN method described in this chapter can be used for any depressed patient treated with a novel AD that is metabolized by CYP2D6 (Table VII.1.). In this preliminary study, we will focus on mianserin and therefore, a 30 mg dose of Lerivon® was administered to a healty volunteer. This volunteer gave an informed consent for the study, which was supervised by a medical doctor. Lerivon® was purchased from a local pharmacist by the research group.

Table VII.1. List of ADs that are (partially) metabolized by CYP2D6, their influence on CYP 450, transporters and receptors (summary of chapter I)

Antidepressants	CYP isoenzymes			Neurotransmitter Transporters and Receptors								
	CYP metabolism	CYP inhibition		Transporters				Receptors				
			NA	5-HT	DA	P-glycoprotein	H₁	MA	Alpha₁	Alpha₂	5HT
Citalopram	2C19, 2D6,3A4	(Minimal: 2D6, 2C19,1A2)		++++		substrate	+		+		
Fluoxetine	2D6, 2C	2D6, 2C9/19, 3A4	+	++++		inhibitor	+	+	+		+
Fluvoxamine	1A2,2D6	1A2, 2C19, 3A4,2C9	+	++++		substrate/inhibitor	+		+		
Maprotiline	2D6, 1A2		++++					+			
Mianserin	1A2, 2D6, 3A4									++++	++++
Mirtazapine	1A2, 2D6, 3A4					no effects	+	+		++++	++++
Paroxetine	2D6	2D6	+	++++	+	substrate/inhibitor		++			
Sertraline	2D6, 2C9, 2C19, 3A4	Minimal: 2D6, 2C, 3A4,1A2	+	++++	++	inhibitor		+	+		
Trazodone	2D6, 1A2, 3A4			++++		inducer	+		+++		++++
Venlafaxine	2D6, 3A4	Minimal: 2D6	++	++++	+	substrate/inhibitor					

VII.3.2. Therapeutic drug monitoring

TDM is based on trough steady-state plasma concentrations, and therefore blood should be collected at least 5 drug intakes after changes of dose. As the average half-life of mianserin is about 16 hours, this implies that blood should be collected after at least 4 days of therapy. In clinical practice, the appropriate sampling time for most psychoactive drugs is one week after stable daily dosing. In addition, TDM blood samples should be taken at minimum steady-state concentrations, just before intake of the daily dose or at least 12-17 hours after the last dosage [2].

For our preliminary study, 5 ml of blood was drawn into an EDTA tube 15 hours after intake of the daily dose (30 mg mianserin). The blood samples were centrifuged within two hours at 1200 *g* for 10 minutes. The harvested plasma was stored at -20 °C before analysis with the GC-MS method with electron ionization as described in chapter VI (VI.2.).

VII.3.3. Determination of genetic variability

The method development for *CYP2D6* genotyping was done in the Laboratory of Molecular Biology at 'Erasmus ziekenhuis Antwerpen' by Ph. Liesbeth Daniels, under the supervision of Prof. Dr. Hugo Neels, whom we both gratefully acknowledge.

DNA was extracted from whole blood collected in EDTA-tubes. First, strong detergents were added to distroy the cell membrane and to inactivate the nucleases of the blood cells. This was followed by repeated extractions with phenol, resulting in discharge of the denaturated proteins and nucleic acids. Ethanol is added to precipitate and separate the smaller molecules from the nucleic acids, and to separate DNA from RNA due to differences in solubility. In addition, during the extraction, specific enzymes were used to discharge unwanted nucleic acids such as RNA.

After extraction of DNA, specific fragments of the double stranded DNA molecule were amplified by polymerase chain reactions (PCR), as only these

fragments are of interest. PCRs are in fact copying reactions of single DNA strands using thermal cycle programs. First, the double stranded DNA is denatured into two single strands at a relatively high temperature. Thereafter, at lower temperatures, primers will anneal to complementary, specific and defined sequences on each of the two single DNA strands. These primers are extended (elongation reaction) with nucleotides complementary to the single stranded DNA template by a DNA polymerase, resulting in a copy of the desired sequence. For each step of the copying reaction (annealing and elongation step), specific temperatures are used. After making the first copy, the temperature increases again to obtain single DNA strands and the procedure is started all over. As a result, another copy of the input DNA strand but also of the short copy made in the first round of synthesis is made and these reactions finally lead to a logarithmic amplification of the desired DNA sequence. These amplification reactions are checked by analyzing the amplified sequences with gelelectrophoresis using ethidiumbromide, a DNA intercalating UV-active compound, as detection reagent.

The PCR reaction used for the determination of *CYP2D6* polymorphisms in this thesis is the Real-Time PCR in combination with melting curve analysis, using a LightCycler. A classical PCR reaction is used for pre-amplification of a 1654 bp fragment of the *CYP2D6* gene for analysis of polymorphisms *3,*4,*6,*7 and *8. This PCR reaction occurs before the actual Real-Time PCR to circumvent interferences due to the highly homologous *CYP2D7* and *CYP2D8* pseudogenes [26]. The difference between Real-Time PCR and ordinary PCR reactions is that the former enables detection and quantification of the DNA amplification in 'real time' due to fluorescent dyes on hybridization probes that bind to a specific sequence. For each DNA fragment, two hybridization probes are used that will bind on specific sequences next to each other. One probe will be excited in the LightCycler and will transfer energy (FRET, fluorescence resonance energy transfer) to the other (acceptor) probe. This acceptor probe will also be excitated, leading to fluorescence detection.

<u>Figure VII. 5.</u> PCR reaction in combination with melting curve analysis

A, PCR reaction: denaturation of the double stranded DNA, annealing of primers and elongation step by the DNA polymerase are shown; B, hybridization probes anneal at specific sequences, the donor probe excites the acceptor probe, which leads to fluorescence. A melting curve is constructed by measuring fluorescence with increasing temperatures. At a certain point (the melting point) the probes will be denatured and loose their fluorescence. Based on [27].
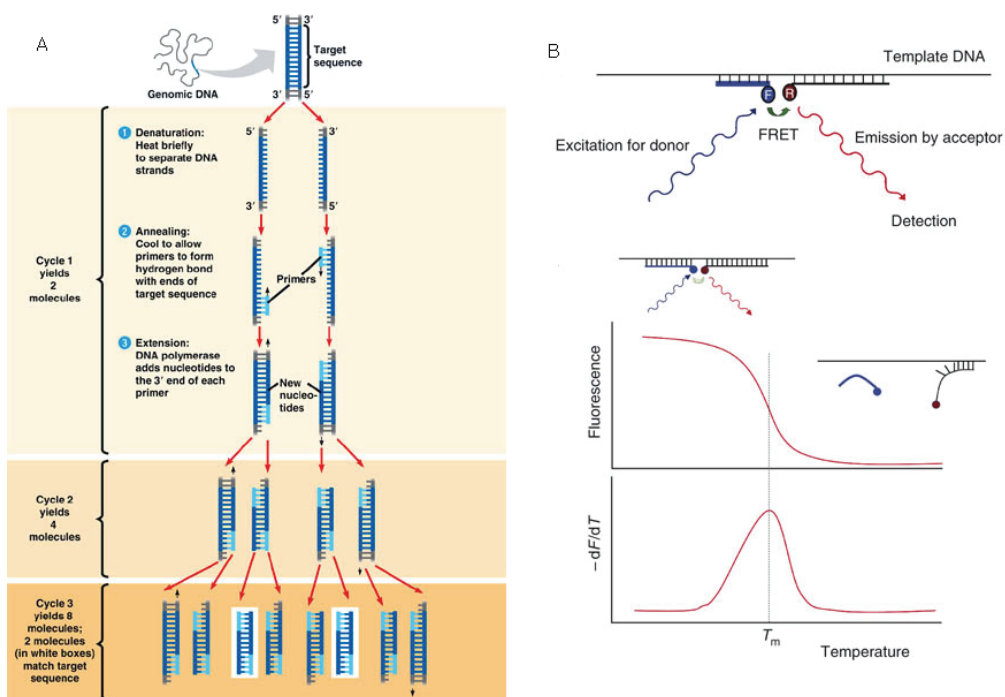
The final detection of the different *CYP2D6* polymorphisms was done by melting curve analysis after the Real-Time PCR. A melting curve is obtained by increasing the temperature, which results in disruption of the double stranded DNA and loss of hybridization probe binding, thus loss in fluorescence. DNA strands are linked by hydrogen bonds with weaker bonds between the nucleotides adenine and thymine, 2 hydrogen bonds, than between guanine and cytosine (3 hydrogen bonds). As a result, differences in the melting profile will occur for the different polymorphisms of *CYP2D6* (Figure VII.5.B.).

Another reaction used for the determination of *CYP2D6* polymorphisms is the sequencing reaction. This reaction determines the nucleotide order (guanine,

cytosine, thymine and adenine) of a specific DNA fragment. The sequencing reaction can be compared with a classical PCR, thus a single stranded DNA is used as template, primers anneal to initiate the reaction, DNA polymerase will elongate the primers with nucleotides, etc. However, dideoxynucleotides labeled with different dyes, exciting at a different wavelength, are also added during the PCR. These dideoxynucleotides will terminate the DNA strand elongation as they lack a 3'-OH group required for the formation of a phosphodiester bond between two nucleotides during elongation, resulting in DNA fragments that vary in length. All the produced DNA fragments will then be separated based on their length, and because the four kinds of dideoxynucleotides are labelled with a different fluorescent molecule, the sequence of the DNA fragment is obtained (Figure VII.6.)

Figure VII.6. DNA sequencing
Adapted from [28].
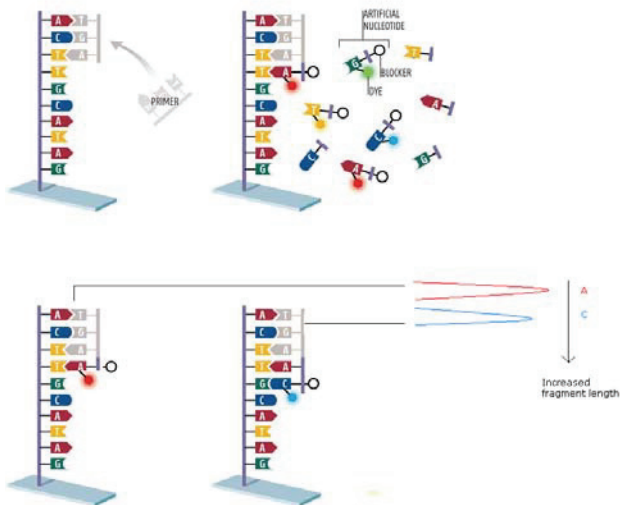
VII.3.3.1. *DNA extraction from EDTA-blood samples*

DNA was extracted from the EDTA-supplemented blood with a QiAmp DNA Blood Mini Kit (QIAGEN, Venlo, The Netherlands). Two hundred µl of blood sample was added to 20 µl QIAGEN protease in a 1.5-ml eppendorf tube. Thereafter, 200 µl lysis-buffer was added, vortexed for 15 seconds and then incubated for 10 minutes at 56 °C. After incubation, 200 µl of ethanol (96-

100 %) was added and mixed. The final mixture was loaded onto a QIAamp spin column and this column was centrifuged for 1 minute at 3585 g. The spin column was thereafter washed; first with 500 µl AW1 buffer and then with AW2 buffer. After both washing steps the column was centrifuged and the wash solutions were disposed off. Finally, the DNA was eluted from the spin column by adding 200 µl of elution buffer. The elution buffer was allowed to soak the phase during 5 minutes at room temperature before collection of the eluate through centrifugation of the tube at 3585 g during 1 minute. This eluate was stored at 4°C.

VII.3.3.2. *Pre-amplification of a 1654 bp DNA fragment of cytochrome 2D6*
For gene deletion and duplication, purified DNA obtained in VII.3.3.1 was used for the Real-Time polymerase chain reactions. For the analysis of alleles *3,*4,*6,*7, and *8, a 1654 bp pre-amplified fragment of *CYP2D6* was used as template. The GeneAmp PCR (Applied Biosystems, Toronto, Canada) equipment was used for pre-amplification of this fragment.

Table VII.2. Primers and probes used for determination of *CYP2D6* duplication, deletion, and allelic variations [29-31]

	Sequence	Site
Primer		
1654bp-F	5'-CAAGGTGGATGCACAAAGAGT-3'	3076
1654bp-R	5'-ACACTCCTTCTTGCCTCCTAT-3'	4702
Del-F	5'-ACCGGGCACCTGTACTCCTCA-3'	17307
Del-R	5'-GCATGAGCTAAGGCACCCAGAC-3'	-3518
Dup-F	5'-CCCTCAGCCTCGTCACCTCAC-3'	-595
Dup-R	5'-CACGTGCAGGGCACCTAGAT-3'	13524
*3 primer-F	5'-TGGCTGGCAAGGTCCTACG-3'	4100
*3 primer-R	5'-TGGGCTCACGCTGCACATT-3'	4560
*4 primer-F	5'-AGAGGCGCTTCTCCGTGTC-3'	3283
*4 primer-R	5'-CAGGTGAGGGAGGCGATCA-3'	3533
Probe		
Reb Sens	5'-TGCTGCCTCCCACTCTGCAGTGCTC-Fluorescein-3'	-2272 / 15062
Reb Anch	5'-LCRed640-ATGGCTGCTCAGTTGGACCCACGCT-phosphate-3'	-2298 / 15035
*3 Sens	5'-TCCCAGGTCATCCGTGCTCA-Fluorescein-3'	3460
*3 Anch	5'-LCRed670-TTAGCAGCTCATCCAGCTGGGTCAG-phosphate-3'	3436
*4 Sens	5'-CGACCCCTTACCCGCATCTCCC-Fluorescein-3'	3319
*4 Anch	5'-LCRed640-CCCCAAGACGCCCCTTT-phosphate-3'	3291
*6 Sens	5'-CCTCGGTCACCCACTGCTCCAGC-Fluorescein-3'	4161
*6 Anch	5'-LCRed640-CTTCTTGCCCAGGCCCAAGTTGC-phosphate-3'	4135

The 1654 bp fragment was amplified using the 1654bp forward (F) and reverse (R) primers (Table VII.2.) at a concentration of 0.25 and 0.5 μM, respectively. For the amplification, AmpliTaq Gold Polymerase (1.5 U, Applied Biosystems), deoxynucleotide triphosphates (0.3 mM), magnesium chloride (1.7 mM), PCR gold buffer and DNA (125 ng) were added and mixed together with the primer to get a final volume of 50 μl. The thermal cycler programme started at 95 °C for 3 min. Thereafter, 35 cycles of 30 sec at 95 °C, 30 sec at 62 °C, and 1:30 min at 72 °C were applied for amplification of the 1654 bp fragment. The final elongation occurred for 6 min at 72 °C. The amplified fragment was stored at 4 °C.

VII.3.3.3. *Confirmation of the amplification reaction*
The correct amplification of the 1654 bp fragment was confirmed by gel electrophoresis. PCR products were resolved by a 0.8 % agarose gel and ethidiumbromide staining. The 0.8 % agarose gel was obtained by adding 2.4 g of agarose to 300 ml 1 x Tris-EDTA buffer. This solution was heated, mixed and stored in a hot water bath at 56 °C for at least 15 minutes. Thereafter, 10 μl ethidiumbromide was added to the mixture and the gel could be poured. A DNA ladder (1 kb) was resolved on the gel simultaneously with the PCR products.

VII.3.3.4. *Real-Time PCR reactions in the LightCycler*
A LightCycler system from Roche (Brussels, Belgium) was used to determine gene deletion and duplication or allelic variations by using Real-Time PCR and melting-curve analysis. In this paragraph, the primers, hybridization probes, content of the reaction mixtures, as well as PCR cycle and melting curve conditions are described.
The primers (Del-F/Del-R; Dup-F/Dup-R) for the *gene deletion and duplication* were obtained from Eurogentec S.A. (Seraing, Belgium) and their sequences are indicated in Table VII.2. Detection of the DNA fragments was realized by using one common pair of hybridization probes (Rep Sens and Rep Anch), both corresponding to sequences in the second half of the large direct repeats immediately downstream of *CYP2D6* and *CYP2D7*. The reaction mixtures for gene deletion and duplication were prepared separately. The Expand Long Template PCR System enzyme mixture and its buffer (1.3 U,

Roche) were used in a final volume of 20 µl for both reactions. Deoxynucleotide triphosphates (0.3 mM) and 125 ng of DNA were also added to the mixture. The concentration of the forward primers was always 0.5 µM, while the concentration of the reverse primers was 0.5 or 1 µM for duplication and deletion, respectively. The concentration of the hybridization probes was 0.2 µM for forward and 0.4 µM for reverse probes. The following amplification program was used: 2 minutes at 95 °C, followed by 32 cycles, each comprising 10 sec at 95°C and 133 sec at 68°C. Before melting curve analysis, a final elongation at 68 °C occurred for 7 minutes. The melting curve analysis started at 55 °C and finished at 78 °C with a ramp speed of 1.2 °C/sec [29].

Two pairs of primers, purchased from Eurogentec S.A., were used for the detection of *CYP2D6**3,*4, and *6 (Table VII.2.). One pair (*3 primers) was used for the determination of *3, while the other pair (*4 primers) were used for *4, and *6. For each allelic variation, different hybridization probes (Tib MolBiol, Berlin, Germany) were used (Table VII.2.). The reaction mixtures for *3 and for *4 - *6 were separately prepared as different primers and probes are necessary for these reactions. The LC480 genotyping master kit from Roche was used in a final volume of 20 µl for both reactions. The concentration of primers and hybridization probes was always 0.5 µM and 0.2 µM, respectively. Five µl of a 1/400 dilution of the 1654 bp fragment of *CYP2D6*, obtained as described in VII.3.3.2, was added to this mixture. The following cycle program was used: 5 minutes at 95 °C, followed by 30 amplification cycles for the *3 analysis and 35 cycles for the *4 - *6 reaction. Each amplification cycle comprised 5 sec at 95°C, 10 sec at 60 °C (*3) or 65 °C (*4 - *6), and 2:12 minutes at 72 °C. Thereafter, melting curve analysis started at 95 °C for 1 min., then 60 °C for 20 seconds and finally a temperature gradient from 40 to 75 °C with a ramp speed of 1.5 °C/sec [30].

VII.3.3.5. *Sequencing*

If the result of the Real-Time PCR and melting curve analysis were not straightforward or for analysis of the *7 and *8 allelic variations, sequencing was applied. First, the amplified 1654 bp fragment (VII.3.3.2.) was purified with a QIAquick PCR purification Kit (Westburg, Leusden, The Netherlands). Thus, 50 µl of the PCR fragment is mixed with 250 µl of PB-buffer and

vortexed. This mixture was transferred to a QIAquick spin column, which thereafter was centrifuged at 3595 g during 1 minute. The eluent was transferred to the waste and the spin column was washed with 750 µl washing buffer and centrifuged. Finally, the purified DNA fragment was eluted in an eppendorf tube with 30 µl of elution buffer and a centrifugation step of 1 min at 3595 g.

This purified DNA fragment was then diluted 1/10 and used for the sequencing reaction. Two µl of the diluted sample was added to 1 µl of primer (*3 or *4 F/R Table VII.2.) and 17 µl of a sequencing mix to obtain a reaction volume of 20 µl. The sequencing mix used for the cycle reaction was prepared as follows: 4 µl of a ready reaction mix (Big Dye Terminator Sequencing kit, Applied Biosystems) and 2 µl of a sequencing buffer were added to 11 µl of HPLC-water.

The next step in the sequencing reaction is a purification step, leading to a loss of excess of reagents by the use of a DyeEx Spin Kit (Westburg). The DyeEx Spin column has to be prepared by centrifugation at 3595 g for 3 minutes before the cycle sequencing reaction mix (20 µl) is added to the gel surface of the spin column. Thereafter, the eluate is collected through centrifugation (3 minutes, 3595 g) and devided over the cups of the reaction plate. The reaction plate was heated at 96 °C until full evaporation of the sample. The extract was then redissolved in 20 µl of deionized formamide and heated again at 96 °C for 3 minutes. After this clean-up step, the DNA can finally be sequenced by the ABI PRISM 310 Genetic Analyzer (Applied biosystems).

VII.3.3.6. *Quality control*

During the analysis of CYP2D6 polymorphisms, positive and negative controls were also analyzed as quality control. For the negative control water was analyzed in the same way as the samples. The positive controls CYP2D6*3, *4, and *6 were obtained from ParagonDX (Morrisville, USA), while DNA obtained from a patient positive for gene duplication was applied as positive control for the gene duplication reaction.

VII.4. Case Report

VII.4.1. Patient information and qualitative diagnostic tests

<u>Figure VII.7.</u> Patient information sheet

Antidepressant TDM:	**Patient information**	**25 march 2008**
Patient	X	
Antidepressant therapy	Lerivon (mianserin 30 mg/day)	
Therapy duration	1 day	
Last administration	22:30 24 march	
Blood draw	13:30 25 march	
Psyiological factors		
Gender	female	
Co morbidity (e.g. liver, kidney)	/	
Environmental factors		
Diet	/	
Co-medication	Desorelle 20 mg	
Qualitative Test		
HAM-D score	/	
Side-effects, complaints	OVERDOSE: seizures, unsteady walk, unconsciousness	
CYP 2D6 phenotype	intermediate metabolism	
TDM result	9 ng/ml mianserin	
	5 ng/ml desmethylmianserin	
Results interpretation:	Stop mianserin medication:	
	intermediate metabolism and drug interaction	

The patient information sheet of the volunteer is shown in Figure VII.7. This volunteer was a young female without depression symptoms. She had no liver or kidney impairment, and the only co-medication was an oral contraceptive. The HAM-D score was not taken as the volunteer was not depressed. A dose of 30 mg was administered as mianserin dosages range from 30-90 mg per day for depressed patients. Nine hours after the intake of 30 mg of mianserin, severe adverse reactions were noticed. Although this dose is a normal daily dosage of depressed patients, overdose symptoms

such as queasiness, dizziness, unsteady walking, and finally seizures and unconsciousness were observed. A blood sample was drawn 15 hours after the drug intake for monitoring purposes. Due to the severe adverse reactions, intake of mianserin was immediately stopped.

VII.4.2. Therapeutic drug monitoring

A blood sample drawn 15 hours after a single adiminstration of 30 mg mianserin was analyzed with the developed GC-MS method. However, because of the low plasma concentrations in the sample, extrapolation was necessary and resulted in a semi-quantitative analysis. A plasma concentration of 9 ng/ml mianserin and 5 ng/ml desmethylmianserin was observed.

According to TIAFT [17], the therapeutic window ranges from 15-70 ng/ml mianserin in steady state conditions. Otani et al. [32] monitored the plasma concentration after 18 hours of a single mianserin (30 mg) intake and concluded that the concentrations ranged from 3-13 ng/ml for mianserin and 1-7 ng/ml for desmethylmianserin. In this study, however, plasma concentrations were not linked to an effect and in addition, differences in metabolism and thus differences in plasma concentrations for poor versus rapid metabolisers were not discussed. Therefore, although the results obtained from the current case are situated in this range, the plasma concentration of this case cannot be interpreted unambiguously. In addition, interpretation of the plasma concentration – effect relationship is even harder as desmethylmianserin retains pharmacological properties indicative of antidepressant activity. The metabolite is slightly less potent than the parent compound as a noradrenaline uptake inhibitor and antagonist at pre-synaptic adrenoreceptors, but is more active as a serotonin uptake inhibitor [33]. The side-effects observed in this case report, such as queasiness and dizziness, would be a result of $5HT_3$- and α_1-receptors blockage, however, mianserin blocks $5HT_2$- and α_2-receptors quite selectively according to recent knowledge and literature (chapter I; I.4-I.5.-I.7.6.).

From this case report, we can conclude that a dose of 30 mg mianserin can result in a mianserin plasma concentration of about 9 ng/ml 15 hours after intake and that this concentration was determined after adverse reactions indicative of overdose.

<u>Figure VII.8.</u> Chromatogram of the plasma sample obtained from a volunteer taking 30 mg of mianserin
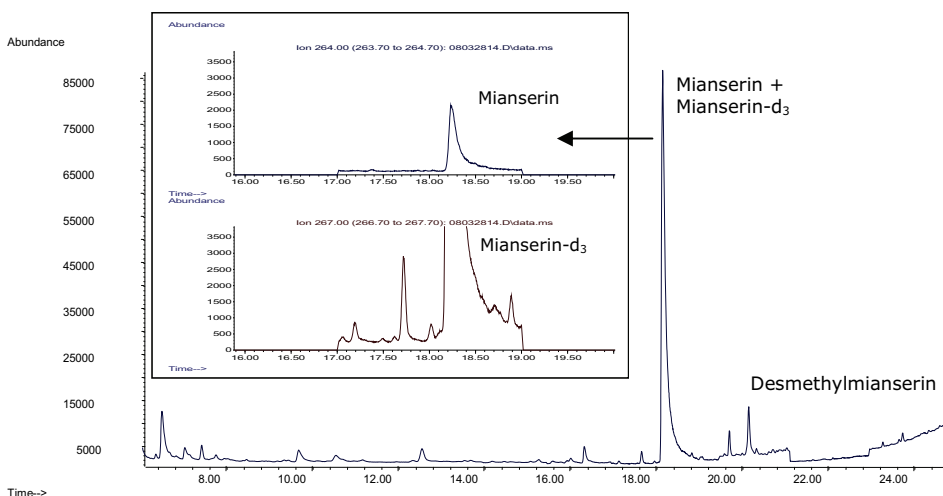
VII.4.3. Determination of CYP2D6 polymorphisms

Mianserin is metabolized by CYP1A2, CYP2D6 and CYP3A4. However, only CYP2D6 polymorphisms (duplication, deletion, *3, *4, *6, *7 and *8) were determined as these variations were monitored in the Laboratorium of our co-workers (Molecular Biology, Erasmus Ziekenhuis, Antwerp). Duplication, deletion, *3,*4 and *6 were determined using Real-Time PCR. In addition, for duplication and deletion, the DNA fragments were separated and detected using gelelectrophoresis. Sequencing reactions were done to check *7 and *8 and to confirm the Real-Time PCR results of *3, *4 and *6.

The volunteer was homozygous wildtype (no polymorphisms) for the *CYP2D6*3 and *6 variations (Figure VII.9.) as the melting peak of the subject overlapped with that of the wildtype control. For *4, however, the

melting peaks of the Real-Time PCR demonstrated that the subject was heterozygous for the *4 variation as two peaks were observed, one corresponding with the wildtype and one with the *4 variant (Figure VII.9.B). This result was confirmed by sequencing of the 1654 bp fragment as both a guanine and adenine were identified on the 1934 position (Figure VII.9.C). Sequencing also confirmed that the volunteer was homozygous wildtype for the *6, *7 and *8 variations.

Figure VII. 9. Real-Time PCR and melting curve analysis of *CYP2D6**3 (A), *4, *6 (B) and sequencing result for *CYP2D6**4 (C).

A
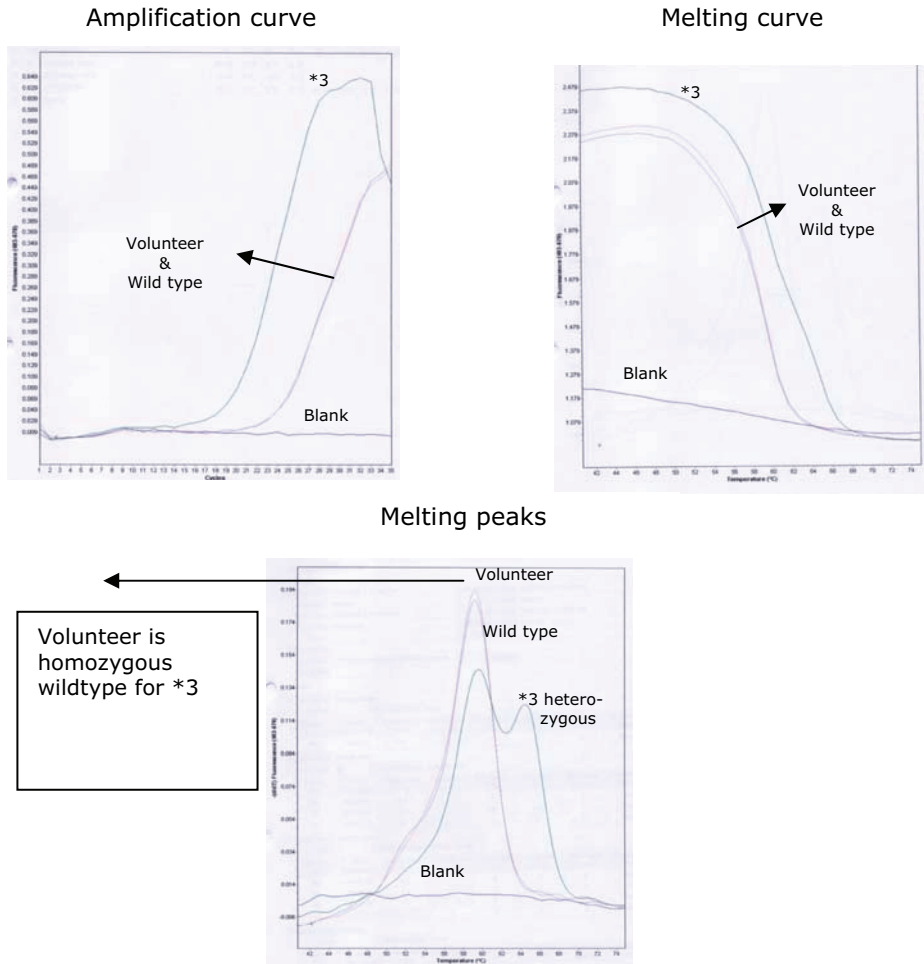
B

Amplification curve
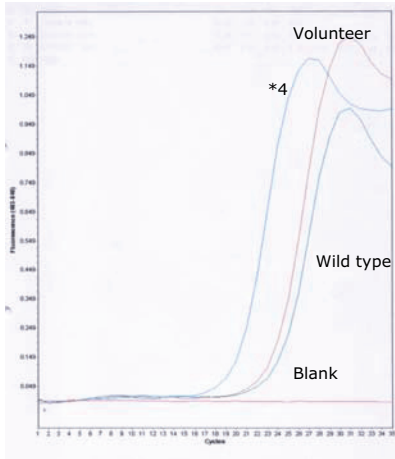
Melting curve
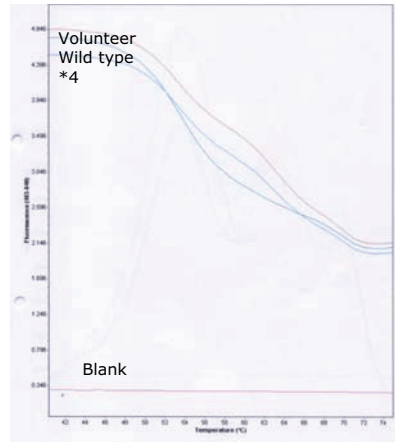
Melting peaks
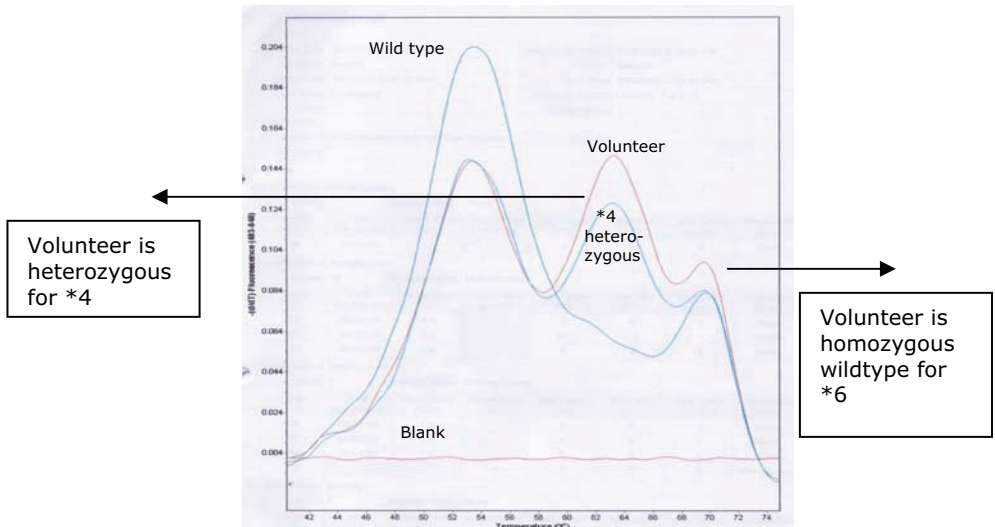
C
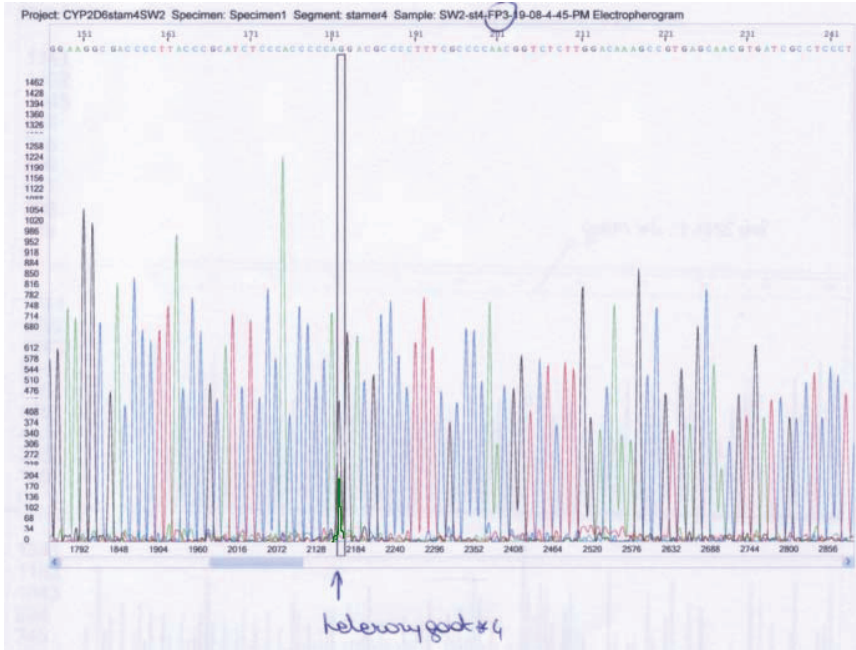
Figure VII.10. shows the ethidiumbromide-stained gel for analysis of *CYP2D6* deletion and duplication. While in the controls for *CYP2D6* duplication and deletion, 3.5 and 3.2 kbp fragments were amplified, respectively, no bands corresponding to these sizes were observed for the volunteer. This result was confirmed by using Real-Time PCR and melting curve analysis (results not shown).

<u>Figure VII.10.</u> Gelelectrophoresis of gene deletion and duplication fragments of *CYP2D6*
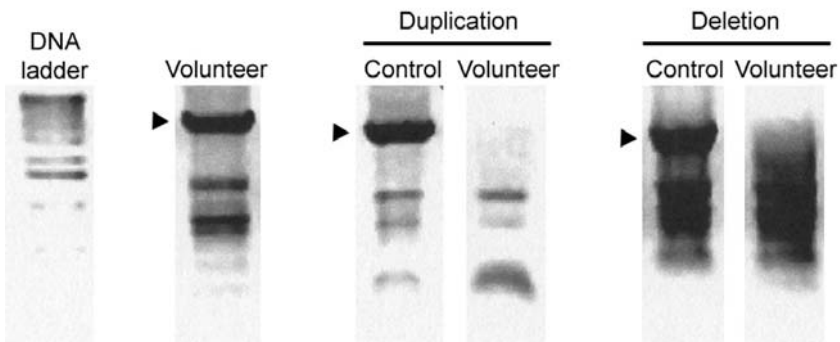
Determination of deletion, duplication, *3, *4, *6, *7, and *8 led to the conclusion that the volunteer has at least one non-functional allelic (*4) variant for *CYP2D6*. The prevalence of non-functional allelic variants for CYP2D6 was found to be 20.7% in a healthy Dutch population according to Tamminga et al. [34]. In addition, the most frequently observed null allele was *CYP2D6*4, which accounted for 89% of all null alleles.

Determination of the phenotype of CYP2D6 through the determined genotype results is described in Table VII.3. Because the volunteer has at least one non-functional allele, the phenotype of the subject likely corresponds to an intermediate metabolizer [25, 35].

Table VII.3. Genotype translation into phenotype

Gene-activity*	Phenotype
1- nX1 (gene duplication)	ultrarapid
1-1	extensive
1-0.5	
1-0	intermediate
0.5-0.5	
0.5-0	
0-0	poor

*
gene-activity 0 (non-active allel) = *3 - 8; *11 - 16; *19 - 21; *38, *40, *42
gene-activity 0.5 (decreased activity allel)= *9, *10, *17, *29, *36, *41
gene-activity 1 (active allel)= *1, *2, *33, *35

VII.4.4. TDM-GEN discussion for the case report

The volunteer appears to be an intermediate metabolizer of CYP2D6 substrates as determined by the Real-Time PCR method in combination with melting curve analysis, gelelectrophoresis and sequencing. According to Kirchheiner et al. [19], the therapy of this phenotype would benefit with a slightly lower dose (90%), thus a dose of 27 mg. However, normal dosages should not lead to severe adverse reactions. In addition, Mihara et al. [36] conclude that 30 mg is the ideal dose for intermediate metabolizers, while it

was suboptimal for normal metabolizers. As a result, the intermediate metabolism of CYP2D6 substrates by the volunteer is not likely to be the underlying cause of the overdose reaction that occurred in the case report. However, Otani et al. [32] calculates the required dose of mianserin after 18 hours of a single intake of 30 mg of mianserin through the sum of mianserin and desmethylmianserin plasma concentrations. For the case report, Otani et al. would suggest a dose of 20 mg/day.

Mianserin is not only metabolized by CYP2D6. The study of Mihara et al. [36] suggests that the CYP2D6 enzyme plays a major role in metabolization of the S-mianserin enantiomer, while metabolization of the R-enantiomer is catalyzed by CYP1A2 and CYP3A4. Moreover, while for CYP2D6 genetic determinants prevail over environmental factors such as smoking, use of oral contraceptive steroids or caffeine consumption [37, 38], CYP1A2 is inhibited by oral contraceptives [37, 39]. In case of inhibition of an enzyme, extensive or intermediate metabolizers may be converted to poor metabolizers of substrates of that particulary enzyme [6]. Thus, in the case report, mianserin metabolization by CYP2D6 is slower due to the genetic variation *CYP2D6*4*, while the other metabolization route via CYP1A2 is possibly inhibited by the intake of Desorelle®, an oral contraceptive, possibly leading to slightly elevated plasma concentrations and finally to the severe side-effects.

When analyzing the blood samples, plasma concentrations of about 9 ng/ml mianserin and 5 ng/ml desmethylmianserin were found. As already mentioned, comparison of these results with the ones obtained by Otani et al. [32] reveals that these can be considered as normal therapeutic concentrations. However, the plasma concentration for mianserin after one intake of 30 mg ranged from 3-13 and no indication of metabolism rate was suggested. Moreover, we must be aware that the mianserin in our case report was measured after 15 hours of intake and no toxic symptoms were observed at that point of time. The mianserin plasma concentrations observed in our case are not extremely high, and no reports have been found that linked such plasma concentrations with the observed side-effects.

In this case, the developed TDM-GEN does not provide an answer with respect to the cause of the adverse reactions. Probably it will be the result of the co-medication and the genetic variations in the metabolism of mianserin, combined with (genetic) variability of the targets in the brain and the serotonin transporter. Variability in the P-glycoprotein transporter is probably not so important in the case of mianserin, as for mirtazapine, a structural analogue, no variations in concentrations due to P-glycoprotein poly-morphism were observed [1, 40].

VII.5. Conclusion

The applicability of the developed TDM-GEN method is demonstrated in this chapter and it is clear that this method may support the therapy of a subset of psychiatric patients with new generation ADs, especially patients suffering from side-effects or not responding to therapy or special patient populations such as the elderly, children, patients with liver and kidney impairment, or patients with a lot of co-medication.

Retrospective genotyping can explain many cases of non-response or adverse drug reactions in patients treated with CYP2D6 substrates. However, the genotyping of patients is probably of most interest when therapy is started. The advantage of genotyping is that it needs to be performed only once in a lifetime for each patient. The genotype and its resulting phenotype, together with the information concerning the patient's depressed state, co-medication and co-morbidity can lead to a more rational choice of AD therapy and necessary dose. Once therapy is started, TDM can be used to monitor compliance and to link plasma concentrations to the clinical effect and side-effects in the patient (Figure VII.11).

However, the interpretation of results obtained from the developed TDM-GEN method still needs to overcome some problems and more research has to be done before personalized AD treatment will be state of the art.

First of all, dose recommendations based on differences in pharmacokinetics are not automatically helpful for prediction of treatment response, since

correlation between plasma concentrations and efficacy is very poor in AD therapy. Therefore, more research should be done concerning the link between dose, plasma concentration, brain concentration and effect, and between plasma concentrations and genetic, environmental and physiological factors.

<u>Figure VII.11.</u> TDM-GEN procedure in clinical practice.

Adapted from [8, 19].
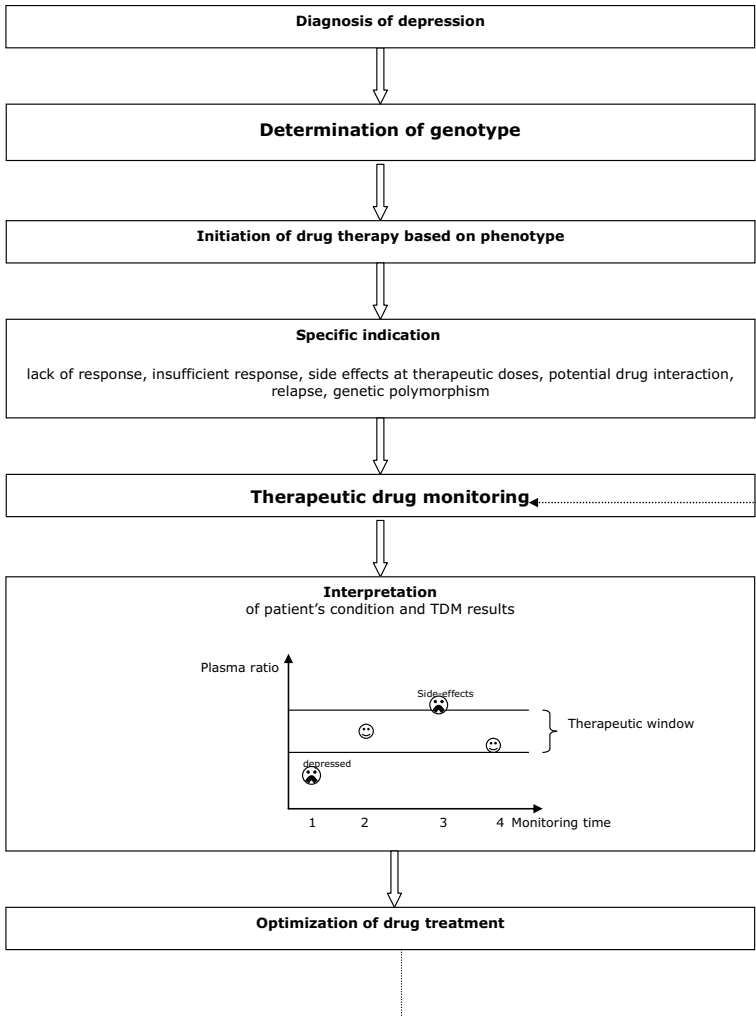
Secondly, it needs to be kept in mind that determination of *CYP2D6* genotype and phenotype will definitely not always result in a straightforward answer

concerning the final pharmacokinetic effects. The pharmacokinetic effects of the polymorphous isoenzyme finally depends on several factors such as the importance of that specific enzyme for the metabolism of the ADs, and the potency of the AD and its metabolite [4]. In addition, the enzyme can be induced by co-administered drugs and variations in other CYP enzymes that partially metabolize the substrate can also influence the pharmacokinetic effects. Moreover, due to the complexity of drug response, single mutations in one gene, such as the *CYP2D6*, are unlikely to cause the observed variability in response. Therefore, more information should be obtained concerning polymorphisms of other CYP isoenzymes, metabolizing enzymes (UGT), variations in transporters (P-gp, MRP2) and targets.

Finally, the developed TDM-GEN method should be applied to a large group of psychiatric patients to determine its value, to link plasma concentration ratios of ADs and their metabolites to a phenotype and, if possible, to their (side-) effects. Eventually, dose adjustments for each phenotype could be postulated for the new generation ADs.

VII.6. References

[1]   Binder E, Holsboer F. Pharmacogenomics and antidepressant drugs. *Ann. Med.* 2006; 38: 82-94

[2]   Baumann P, Hiemke C, S. U, Eckermann G, Gaertner I, Kuss HJ, Laux G, Müller-Oerlinghausen B, Rao ML, Riederer P, Zernig G. The AGNP-TDM expert group consensus guidelines: therapeutic drug monitoring in psychiatry. *Pharmacopsychiatry* 2004; 37: 243-265

[3]   Oscarson M. Pharmacogenetics of drug metabolising enzymes: importance for personalised medicine. *Clin. Chem. Lab. Med.* 2003; 41: 573-580

[4]   Bondy B. Pharmacogenomics in depression and antidepressants. *Dialogues Clin. Neurosci.* 2005; 7: 223-230

[5]   Eap CB, Sirot EJ, Baumann P. Therapeutic monitoring of antidepressants in the era of pharmacogenetics studies. *Ther. Drug Monit.* 2004; 26: 152-155

[6]   Mitchell PB. Therapeutic drug monitoring of psychotropic medications. *Br. J. Clin. Pharmacol.* 2000; 49: 303-312

[7]   Kirchheiner J, Seeringer A. Clinical implications of pharmacogenetics of cytochrome P450 drug metabolizing enzymes. *Biochim. Biophys. Acta* 2007; 1770: 489-494

[8]   Kirchheiner J, Nickchen K, Bauer M, Wong ML, Licinio J, Roots I, Brockmöller J. Pharmacogenetics of antidepressants and antipsychotics: the contribution of allelic variations to the phenotype of drug response. *Mol. Psychiat.* 2004; 9: 442-473

[9]   Ingelman-Sundberg M, Oscarson M, McLellan RA. Polymorphic human cytochrome P450 enzymes: an opportunity for individualized drug treatment *Trend. Pharmacol. Sci.* 1999; 20: 342-349

[10]   Eichelbaum M, Ingelman-Sundberg M, Evans WE. Pharmacogenomics and individualized drug therapy. *Ann. Rev. Med.* 2006; 57: 119-137

[11]   Ingelman-Sundberg M. Pharmacogenetics of cytochrome P450 and its applications in drug therapy: the past, present and future. *Trend. Pharmacol. Sci.* 2004; 25: 193-200

[12]   Van der Weide J, Van Baalen-Benedek EH, Kootstra-Ros JE. Metabolic ratios of psychotropics as indication of cytochrome P450 2D6/2C19 genotype. *Ther. Drug Monit.* 2005; 27: 478-483

[13]   Baumann P, Ulrich S, Eckermann G, Gerlach M, Kuss HJ, Laux G, Müller-Oerlinghausen B, Rao ML, Riederer P, Zernig G, Hiemke C. The AGNP-TDM expert group consensus guidelines: focus on therapeutic monitoring of antidepressants. *Dialogues Clin. Neurosci.* 2005; 7: 231-247

[14]   Pippenger CE. Principles of drug utilization. Palo Alto: Syva Co., 1978

[15]   Hamilton M. A rating Scale for depression. *J. Neurol. Neurosurg. Psychiat.* 1960; 23: 56-62

[16]   Bengtsson F. Therapeutic drug monitoring of psychotropic drugs (TDM nouveau). *Ther. Drug Monit.* 2004; 26: 145-151

[17]   TIAFT. The international association of forensic toxicologists. *Tiaft bulletin* 26 1S (http: //www. tiaft. org/).

[18]   Veefkind AH, Haffmans PMJ, Hoencamp E. Venlafaxine serum levels and CYP2D6 genotype. *Ther. Drug Monit.* 2000; 22: 202-208

[19]   Kirchheiner J, Brosen K, Dahl ML, Gram LF, Kasper S, Roots I, Sjoqvist F, Spina E, Brockmoller J. CYP2D6 and CYP2C19 genotype-based dose recommendations for antidepressants: a first step towards subpopulation-specific dosages. *Acta Psychiatr. Scand.* 2001; 104: 173-192

[20]   Kirchheiner J, Bertilsson L, Bruus H, Wolff A, Roots I, Bauer M. Individualized medicine-implementation of pharmacogenetic diagnostics in antidepressant drug treatment of major depressive disorders. *Pharmacopsychiatry* 2003; 36: S235-S243

[21]   Bishop JR, Ellingrod VL. Neuropsychiatric pharmacogenetics: moving toward a comprehensive understanding of predicting risks and response. *Pharmacogenomics* 2004; 5: 463-477

[22]   Ejsing TB, Linnet K. Influence of P-glycoprotein inhibition on the distribution of the tricyclic antidepressant nortriptyline over the blood-brain barrier. *Hum. Psychopharmacol. Clin. Exp.* 2005; 20: 149-153

[23]   Uhr M, Grauer MT, Holsboer F. Differential enhancement of antidepressant penetration into the brain in mice with abcb1ab (mdr1ab) P-glycoprotein gene disruption. *Biol. Psychiat.* 2003; 54: 840-846

[24]   Abou El Ela A, Härtter S, Schmitt U, Hiemke C, Spahn-Langguth H, Langguth P. Identification of P-glycoprotein substrates and inhibitors among psychoactive compounds - implications for pharmacokinetics of selected substrates. *Pharm. Pharmacol.* 2004; 56: 967-975

[25]   Ingelman-Sundberg M, Sim SC, Gomez A, Rodriguez-Antona C. Influence of cytochrome P450 polymorphisms on drug therapies: pharmacogenetic, pharmacoepigenetic and clinical aspects. *Pharmacol. Therapeut.* 2007; 116: 496-526

[26]   Zanger U, Raimundo S, Eichelbaum M. Cytochrome P450 2D6: overview and update on pharmacology, genetics, biochemistry. *Naunyn-Schmiedebergs Arch. Pharmacol.* 2004; 369: 23-37

[27]   Chiou CC, Luo JD, Chen TL. Single-tube reaction using peptide nucleic acid as both PCR clamp and sensor probe for the detection of rare mutations. *Nat. Protocols* 2007; 1: 2604-2612

[28]   DNA sequencing race hots up. *New Scientist magazine* 2005; 2495: 10

[29]   Müller B, Zöpf K, Bachofer J, Steimer W. Optimized strategy for rapid cytochrome P450 2D6 genotyping by real-time long PCR. *Clin. Chem.* 2003; 49: 1624-1631

[30]   Stamer UM, Bayerer B, Wolf S, Hoeft A, Stüber F. Rapid and reliable method for cytochrome P450 2D6 genotyping. *Clin. Chem.* 2002; 48: 1412-1417

[31]   BLAST (PubMed). *http:// www. ncbi.nlm.nih.gov/blast/Blast.cgi*

[32]   Otani K, Mihara K, Okada M, Tanaka O, Kaneko S, Fukushima Y. Prediction of plasma-concentrations of mianserin and desmethylmianserin at steady-state from those after an initial dose of mianserin. *Ther. Drug Monit.* 1993; 15: 118-121

[33]   Otani K, Kaneko S, Sasa H, Tsuyoshi K, Fukushima Y. Is there a therapeutic window for plasma concentratin of mianserin plus desmethylmianserin? *Hum. Psychopharmacol. Clin. Exp.* 1991; 6: 243-248

[34]   Tamminga WJ, Wemer J, Oosterhuis B, de Zeeuw RA, De Leij LFMH, Jonkman JHG. The prevalence of CYP2D6 and CYP 2C19 genotypes in a population of healthy dutch volunteers. *Eur. J. Clin. Pharmacol.* 2001; 57: 717-722

[35]   WINAp, Pharmacogenomics, lecture POAKC, Rotterdam, 2007

[36]   Mihara K, Otani K, Tybring G, Dahl ML, Bertilsson L, Kaneko S. The CYP2D6 genotype and plasma concentrations of mianserin enantionmers in relation to therapeutic response to mianserin in depressed Japanese patients. *J. Clin. Psychopharmacol.* 1997; 17: 467-471

[37]   Bock KW, Schrenk D, Forster A, Griese EU, Mörike K, Brockmeier D, Eichelbaum M. The influence of environmental and genetic factors on CYP2D6, CYP1A2 and UDP-glucuronosyltransferases in man using sparteine, caffeine, and paracetamol as probes. *Pharmacogenetics* 1994; 4: 209-218

[38]   Tamminga WJ, Wemer J, Oosterhuis B, Wieling J, Wilffert B, De Leij LFM, de Zeeuw RA, Jonkman JHG. CYP2D6 and CYP2C19 activity in a large population of dutch healthy volunteers: indications for oral contraceptive-related gender differences. *Eur. J. Clin. Parmacol.* 1999; 55: 177-184

[39]   Callahan MM, Robertson RS, Branfman AR, McComish MF, Yesair DW. Comparison of caffeine metabolism in three nonsmoking populations after oral administration of radiolabeled cafeine. *Drug Metab. Dispos.* 1983; 11: 211-217

[40]   Sandson NB, Armstrong SC, Cozza KL. An overview of psychotropic drug-drug interactions. *Psychosomatics* 2005; 46: 464-494

Chapter VIII

Monitoring of antidepressants in forensic toxicology

VIII.1. Introduction

In forensic toxicology, analysis of a wide range of unknown compounds is aimed, to situate the cause of death. Although the new generation ADs have a low toxicity profile, they are often screened in forensic cases. Acute intoxications with new generation ADs are rare and frequently follow an intentional ingestion of a huge amount of these substances [1-9]. These highly prescribed drugs, however, are frequently used together with other legal or illegal drugs and can result in synergy of symptoms. In addition, drug interactions can lead to adjusted drug concentrations due to inhibition of cytochrome P450 isoenzymes. Furthermore severe, life-threatening interactions such as the serotonin syndrome have been described [10-13]. The new generation ADs are often used by drug addicts under a methadone maintained treatment because of their safety profile [14, 15], thus ADs can be detected in these overdoses as well. Therefore, analytical methods for the detection of ADs in blood and tissues are of interest in the field of forensic toxicology as they are often involved in various kinds of intoxications [3, 6-9, 16].

VIII.1.1. Urine and blood analysis

Urine gives an indication of the history of drug use, while blood is the main post-mortem matrix as it gives a direct link between the compound concentration and the effect. However, interpretation of the blood concentrations in post-mortem cases is not always straightforward. Several problems have to be addressed such as changed concentrations due to post-mortem redistribution, blood loss and trauma, stability of ADs, genetic factors influencing metabolism, and place of blood sampling (femoral, cardial). In addition, for the interpretation of the AD blood concentrations, reference values in of plasma or serum are used [17]. However, it is clear that whole blood AD concentrations can slightly differ from their plasma concentration due to binding of amphiphilic ADs onto the red blood cell membranes. Moreover, ADs are also stored in the cytoplasm of the red blood cells. Partitioning of drugs into red blood cells, however, depends on their protein binding, as only free drugs can enter the cell, and on the structure of the

compound [18, 19]. Therefore, the difference between blood and plasma concentrations will not differ a lot for the highly plasmabound ADs. Although TIAFT has good reference values of ADs in serum, Reis et al. [20] determined the femoral toxic blood concentrations for several ADs. In this study, 8591 post-mortem cases were analyzed, however, only a few percentages of these cases, involved intoxications with a single AD. This study gives an idea about toxic ADs concentrations in blood. One must keep in mind, though, that the described concentrations are not cut-off levels for toxicity of ADs. The comparison of the serum concentrations (TIAFT) and concentrations in whole blood as described by Reis et al. [20] is shown in Table VIII.1. In addition, other parameters such as post-mortem interval (stability issues) and post-mortem redistribution, thus place of blood collection, can make the interpretation even harder.

<u>Table VIII.1.</u>   Toxic and lethal blood concentrations

AD: antidepressant; Met.: metabolite; % Intox: percentage of post-mortem cases in which only one AD caused the intoxication; TIAFT: toxic or lethal (L) ADs concentrations in serum described by The International Association of Forensic Toxicologists; * case report; REIS: range of lethal ADs concentrations in blood according to Reis et al. [20].

AD	Met.	% Intox	TIAFT (µg/ml) Serum	REIS (µg/g) Blood
Citalopram		2	L 0.5	1.5-27 / mean 6.5
	DMC			0.2-1.3 / mean 0.5
	DDMC			
Fluoxetine		3	1.5-2	1.5-6.1 / mean 2.2
	DMFluox		0.4 / L 0.9-5	0.4-1.2 / mean 0.5
Fluvoxamine		3	0.65	5.4-16
Maprotiline		11	0.3-0.8 / L 1-5	2.3-16 / mean 5.1
	DMMap		sum 0.75-1	
Melitracen				
Mianserin		1	0.5-5	1.6-8.6 / mean 2.8
	DMMia		sum 0.3-0.5 /L 2	1.4-1.9 / mean 1.5
Mirtazapine		1		1-4.3 / mean 2.3
	DMMir		sum 1	0.2-2.5 / mean 0.7
Paroxetine		1	0.3	1.2-4.2 / mean 2.2
Reboxetine				
Sertraline		1	0.29* ; 1.6*	1.1-2.5 / mean 1.4
	DMSer			0.4-3 / mean 1.6
Trazodone			4 / L 12-15	
	m-cpp			
Venlafaxine		3		6.7-95 / mean 31
	ODMV		sum 1-1.5 / L 6.6*	1.3-12 / mean 2.9
Viloxazine				

VIII.1.2. Brain tissue

In forensics, brain tissue has several advantages over blood as it is an isolated compartment in which putrefaction can be delayed. In addition, the metabolic activity is lower, resulting in a more prominent presence of the original compounds as compared to degradation products [21]. Lipophilic compounds such as ADs are easily passed through the blood-brain barrier by passive diffusion. The final drug uptake into the brain, however, depends on a variety of factors such as lipophilicity, protein binding and molecular weight of the compound, but also on the blood-brain barrier and the affinity of each AD for efflux transport systems such as P-glycoprotein. Venlafaxine and paroxetine are known to be exported from the brain through this P-glycoprotein, which shows genetic variability [22]. The final AD concentration in brain will thus depend on a range of factors. Once the ADs are located in the brain, they will bind in disitinct brain regions containing different amounts of noradrenaline, serotonin and dopamine neurons (Fig.VIII.1) [23].

<u>Figure VIII.1.</u> Noradrenaline (norepinephrine) and serotonin pathways indicated in the brain [23].
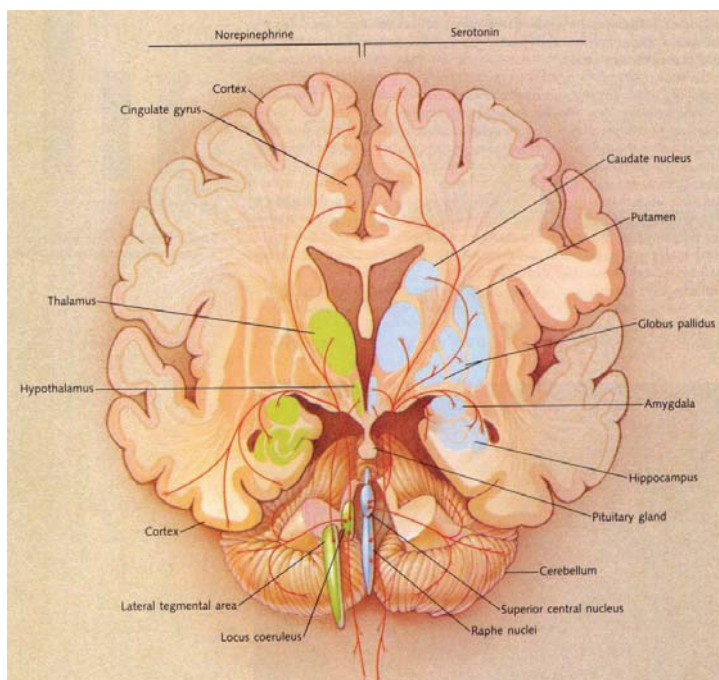
Since concentration of drugs of abuse found in the brain better reflect drug concentration at their site of action, brain specimens could be useful in the determination of the role of ADs and other drugs in the cause of death. In order to analyze brain specimens in routine forensic analysis, a comprehensive database with reliable reference values concerning ADs concentrations and their effects should be created. However, literature data concerning brain concentrations of new generation ADs are scarce. Martin and Pounder [24] describe two cases of trazodone intoxication in combination with alcohol. The blood concentrations were respectively 14.4 and 15.5 µg/ml, while the brain concentrations were 48.6 and 20.9 µg/g. Wenzel et al. [2] observed a mirtazapine overdosage in combination with sertraline, and amitriptyline. A femoral blood concentration of 1.03 µg/ml mirtazapine and 0.88 µg/ml sertraline was detected in combination with a brain concentration of 0.56 µg/g for mirtazapine, 4.95 µg/g for desmethylmirtazapine and 2.57 µg/g for sertraline. Bolo et al. [25] did not analyze post-mortem cases, but used Fluorine Magnetic Resonance Spectroscopy (F^{19} MRS) to analyze steady-state brain concentration in depressed patients. Patients with a plasma concentration of 0.356 ± 0.099 µg/ml fluvoxamine and 0.534 ± 0.309 µg/ml fluoxetine demonstrated a steady-state brain concentration of 3.816 ± 1.59 and 4.017 ± 2.163 µg/g, respectively. Renshaw et al. [26] also used F^{19} MRS to determine fluoxetine brain levels. Their conclusion was that brain concentrations of fluoxetine and desmethylfluoxetine were 2.6 times higher than their plasma concentrations, this in contrast with the above mentioned study of Bolo et al. [25] in which the ratio was 10.

It is clear that more study is definetely needed before a link between AD brain concentrations and their effect will be established. However, brain tissue is of interest in forensic investigation as the detection window of ADs will be longer due to the isolation of the matrix. Moreover, determination of ADs drug concentrations in brain tissue can also be helpful in ADs research. The main principle of TDM is to monitor a blood or plasma concentration, to estimate the drug concentration at the site of action [27]. However, as the final action site of ADs is the brain, brain concentrations can lead to a better understanding of ADs effects. More information could help solving questions such as the unclear blood concentration-effect relationship, the action

mechanisms of the ADs, and the delayed therapeutic effect of ADs. Other questions about the regional distribution, and possible accumulation of these drugs in the brain could also be studied.

VIII.1.3. Hair

Hair analysis is a complementary approach for the detection of ADs as it yields a picture of long-term (chronic) exposure over a time window. This time window depends on the length of the hair, with each 0.6 to 1.4 cm of hair describing the use per month. In addition, the sample can be stored at room temperature for a long time without degradation [28, 29].

The hair shaft germinates from the papilla in the highly vascularized hair follicles embedded in the dermis of the skin. The hair shafts consists of an outer cuticle, an inner medulla and a central cortex and is composed of lipids, trace elements, polysaccharides, water and fibrous proteins, as well as keratinocytes and melanocytes (pigment), both generated from the basal membrane of the hair follicles. Drugs are incorporated in the hair by passive diffusion from blood capillaries into the growing hair cells, before final keratinization of the hair follicle. Besides incorporation from blood during the germination stage of the hair, ADs can also be incorporated from surrounding tissues or from sebum and sweat during further growth of the hair. Several factors influence the drug incorporation; the melanin content (pigmentation of the hair), as well as the lipophilicity and the basicity of the drug. Because the intracellular pH of keratinocytes is more acidic than plasma, ADs are trapped into the keratinocytes and thus in the hairstructure. First non-ionized AD molecules will diffuse across the cell membrane because of their lipophilic characteristics; thereafter they will partially ionize and form ionic interactions with the keratinocytes (isoelectric point ± 6). In addition, melanocytes have a pH of 3-5, and will also trap the charged AD. Uncharged AD will bind to melanin in the melanocytes (Figure VIII.2.) through ionic and Van der Waals interactions. Binding to melanin and is an important mechanism, as concentration of basic drugs is ten times higher in pigmented hair.

<u>Figure VIII.2.</u> Structure of the hair shaft and the incorporation mechanisms

1-4 are the incorporation mechanisms of drugs in hair: 1, incorporation from blood; 2, sebum; 3, sweat, 4; delayed incorporation from surrounding tissues. Adapted from [29].
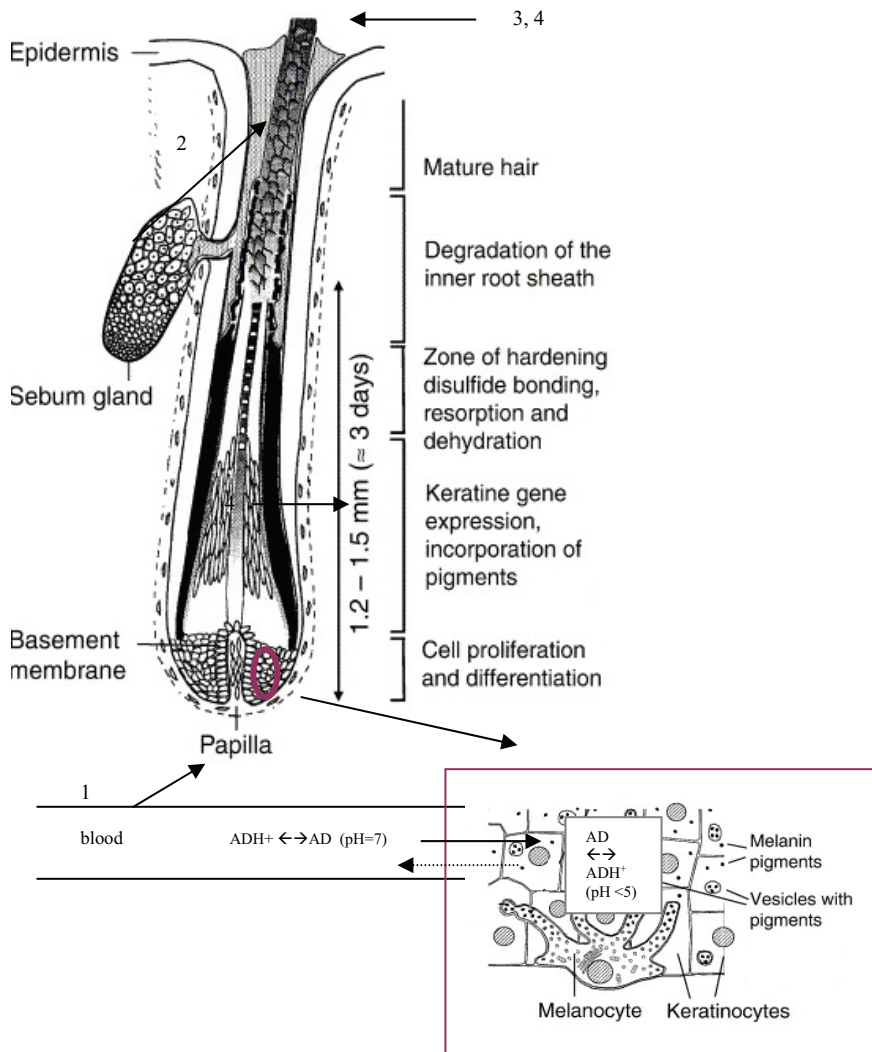
Few articles deal with the extraction of new generation ADs from hair. Smyth et al. [30] described an LC-MS method for determination of sertraline and paroxetine in hair. The obtained concentrations were 1.9 ng sertraline / mg and 0.25 ng paroxetine / mg. Another LC-MS method for maprotiline, citalopram and their metabolites was optimized by Müller et al. [31]. A hair

sample analyzed from a suicide case after a maprotiline overdose contained 3.1 ng maprotiline per milligram hair. The hair sample containing citalopram was obtained from a depressed patient in therapy during the past 4 months. In the latter hair sample, concentrations of 1107 ng/mg in the first segment of 2 cm and 557 ng/mg in the second segment (2 cm) were obtained for citalopram. One case of mianserin detection in hair using a GC-MS was described by Couper et al. [32], this case represented a concentration of 9.2 ng/mg hair. Pragst et al. [33] analyzed maprotiline in hair and were the only authors that linked the hair concentration with plasma concentrations. A hair concentration of 1.4 till 40 (with a mean of 7.4) ng/mg maprotiline was found, while the plasma concentration varied from 0.05 till 0.24 (with a mean of 0.14). However, they concluded that 'there is no way to estimate the daily dose or steady state plasma concentration from the hair concentration or to conclude, whether the drug really was taken every day or the prescribed dose was taken.'

Interpretation of the ADs concentrations in hair are very difficult, due to variations in hair growth (depending on race, sex, age and state of health [29]), but also due to differences in sampling place, possible external hair contamination, cosmetic hair treatment, and individual hair pigmentation [34]. Moreover, the link between blood/plasma and hair concentration is not yet described. This link is difficult to establish because of variations in drug metabolism, but also because the lack of knowledge concerning drug incorporation tendency into the hair. Therefore, more research should be done, regarding the link between hair and plasma concentration. Untill then, the different segments of the hair can only give an idea of the time of consumption of several ADs.

VIII.2. Experimental

VIII.2.1. Samples and reagents

The case report samples were obtained from the department of forensic medicine (Ghent University, Belgium). The reagents necessary for sample preparation are described in Chapter III. The derivatization reagent 1-

(heptafluorobutyryl) imidazole (HFBI) was purchased from Sigma-Aldrich (Steinheim, Germany). Promochem (Molsheim, France) delivered the internal standards fluoxetine-d_6 (Fd_6) oxalate, mianserin-d_3 (Md_3) and paroxetine-d_6 maleate (Pd_6) (100 µg/ml in MeOH). Vials, glass inserts and viton crimp caps were purchased from Agilent technologies (Avondale, PA, USA).

VIII.2.2. High Pressure Liquid Chromatography (HPLC)

A LaChrom HPLC (Merck-Hitachi, Darmstadt, Germany), consisting of a L1700 pump, a L7200 autosampler, a L7360 column oven and a L7455 DAD was used. A PurospherStar RP-8 endcapped 4 x 4 mm guard column combined with a C8 endcapped PurospherStar (Merck, Darmstadt, Germany) LiChroCART 125 mm – 4 mm I.D. (5 µm) column was used for the analysis of trazodone and m-cpp using a HPLC-DAD configuration. The gradient run started at 95% A (860 ml of water / 40 ml of phosphate buffer 250 mM, pH 2.3 / 100 ml of methanol) and 5% B (40 ml of phosphate buffer / 210 ml of water/ 750 ml of methanol). At 8 minutes, the B phase contribution was 25%, and at 16 minutes 55%. Then, during 8 minutes the gradient switched to 95% B. After 5 minutes, the run was switched to the starting conditions and equilibrated for 12 minutes before the next injection. The DAD measured from 220 till 350 nm and chromatograms were integrated at 230 nm. This method was used for analysis of trazodone and m-cpp, with a total run time of 30 minutes and m-cpp and trazodone eluting, respectively, at 11.25 and 15.16 minutes.

VIII.2.3. Gas Chromatography – Mass Spectrometry (GC-MS)

Chromatographic separation was achieved on a 30m x 0.25mm i.d., 0.25-µm J&W-5ms column from Agilent Technologies (Avondale, PA, USA). The initial column temperature was set at 90°C for 1 min, ramped at 50°C/min to 180°C where it was held for 10 min, whereafter the temperature was ramped again at 10°C/min to 300°C.

The pulsed splitless injection temperature was held at 300°C, while purge time and injection pulse time were set at 1 and 1.5 min, respectively.

Meanwhile, the injection pulse pressure was 25 psi and 1 µl of the sample, resolved in 50 µl toluene, was injected. The separation of the derivatized ADs and their active metabolites was achieved in 24.8 minutes. The helium flow was constantly delivered at 1.3 ml/min during analysis.

The mass selective detector temperature conditions were 250°C for the source, 150°C for the quadrupole and 300°C for the transferline. Methane was used as reagent gas in PICI mode with a flow of 1 ml/min. The spectra were monitored in selected ion monitoring (SIM) mode for quantification (Table VIII.2.). This method was validated for plasma, blood, and brain tissue and is discussed in detail in chapters V and VI.

<u>Table VIII.2.</u> Ions monitored in PICI SIM

Compounds	M-ion	M-ion HFB	PICI		
			Quant	ion 1	ion 2
Venlafaxine 2	277	259	260	258 (56)	288 (10)
m-cpp 1	196	392	393	395 (33)	373 (9.6)
Viloxazine 1	237	433	434	296 (63)	414 (10)
DMFluox 1	295	491	330	358 (6.6)	117 (36)
Fluvoxamine 1	318	514	495	258 (304)	515 (65)
ODMV 2 (-H$_2$O)	263	441	246	244 (53)	274 (5.5)
Fluoxetine 1	309	505	344	486 (3.2)	534 (4.0)
Fluoxetine-d$_6$	315	511	350	492 (4.8)	540 (5.6)
Mianserin 2	264	264	265	293 (18)	305 (2.4)
Mianserin-d$_3$	267	267	268	296 (19)	308 (3.8)
Mirtazapine 2	265	265	266	264 (31)	294 (17)
Melitracen 2	291	291	292	290 (45)	320 (20)
DMMia 2	250	446	447	427 (7.4)	475 (14)
DMSer 3	291	487	275	277 (67)	487 (1.1)
DMMir 2	251	447	448	428 (7.3)	476 (13)
Reboxetine 3	313	509	372	510 (6.6)	490 (5.3)
Citalopram 3	324	324	325	305 (10)	353 (22)
DMMap 3	263	459	460	382 (56)	431 (10)
Maprotiline 3	277	473	474	454 (11)	396 (37)
Sertraline 3	305	501	275	277 (66)	501 (3.0)
DDMC 3	296	492	475	521 (20)	493 (4.0)
DMC 3	310	506	489	507 (5.7)	535 (21)
Paroxetine 3	329	525	526	506 (15)	554 (17)
Paroxetine-d$_6$	332	531	532	512 (16)	560 (18)

Relative intensity % between brackets
IS: 1 (fluoxetine-d$_6$); 2 (mianserin-d$_3$); 3 (paroxetine-d$_6$)

VIII.3. Case reports

Five post-mortem cases are discussed to demonstrate the usefulness of the optimized and validated GC-MS method in forensic toxicology. Urine, stomach content and blood were screened using our laboratory systematic toxicological screening (STA) system to situate each case. Matrices such as whole blood, brain tissue and hair were thereafter analyzed using our

developed GC-MS method. Femoral blood was obtained, while six different locations were analyzed in the brain tissue, i.e. frontal, parietal, temporal and occipital lobe, the cerebellum and the brainstem. Hair samples were sampled at the vertex site of the head and cut into segments of approximately 2 cm after a wash to eliminate external contamination. However, for case 1 and 2 there was not enough blood to perform the GC-MS analysis. Hair samples were only available for case 3 and 4.

ADs were extracted from these matrices by an optimized solid phase extraction as discussed in Chapter III. The optimization and validation of the GC-MS method was extensively discussed in chapters V and VI. The GC-MS method with electron ionization is the preferred technique for drug analysis in forensics allowing identification of unknown compounds by comparison of their mass spectrum with a large collection of reference mass spectra in commercially available libraries. However, due to the extensive fragmentation of several ADs in the EI-mode, the positive ion chemical ionization mode (PICI) was chosen to evaluate the post-mortem cases as this technique provides more selectivity in complex matrices such as brain tissue. Trazodone and its metabolite m-chlorophenylpiperazine were analyzed using a HPLC-DAD method due to chromatographic problems of trazodone in the GC-MS analysis.

<u>Table VIII.3.</u> Summary of the AD concentrations found in blood, brain and hair for the different cases

nd, not detected; italic, concentration < LOQ

Case		1	2	3		4		5
Sex		male	female	male		male		female
Age		39	40	27		43		92
Brain weight (g)		1400	1220	1550		1700		1135
Cause of death		hanging	respiratory depression	respiratory depression		arrhythmias and respiratory depression		sudden cardiac death
Compound		Ser / DMSer	Fluox / DMF	Fluox / DMF	Traz / mcpp	Ser / DMSer	Traz / mcpp	Cit / DMC	Cit/DMC
Blood conc. (ng/ml)		600 /	nd	1640 /	nd	93 / 185	nd	191 / 104	*14/18*
Brain conc. (ng/g)	Temporal lobe	11781 / 4336	127 / 63	4454 /3762	75 / 26	1466 / 3624	492 / 112	53 / 64	*27/24*
	Parietal lobe	9684 / 2909	306 / 159	4611 / 3800	85 / 50	1924 / 4517	119 / nd	95 / 59	187/43
	Occipital lobe	10858 / 3294	135 / 76	4673 / 4228	115 / 34	2008 / 4280	661 / 138	251 / 72	148/43
	Frontal lobe	8544 / 2893	63 / *49*	4979 / 4312	90 / 21	1750 / 4392	556 / 139	196 / 54	*30/22*
	Stem	9297 / 1955	106 / 68	4822 / 4515	82 / nd	1671 / 3172	77 / nd	174 / 62	107/35
	Cerebellum	11002 / 3391	*18* / nd	3656 / 2556	108 / 24	993 / 2319	85 / nd	162 / 55	125/31
Hair conc. (ng/mg)	segment 1				- / -	0.6 / 0.5			2.5 / 1.9
	segment 2				/ 0.4	0.8 / 1.4			- / -
	segment 3				/ 0.8	1.6 / 2.6			

VIII.3.1. Case 1

A 39-year old male committed suicide by hanging. After screening, sertraline (600 ng/ml) was found in blood in combination with caffeine and cotinine. After analysis of the urine and stomach contents using HPLC-DAD, a concentration of 2600 and 1100 ng/ml was measured, respectively.

According to The International Association of Forensic Toxicologists [17], the therapeutic range of sertraline in plasma ranges from 50-250 ng/ml, but therapeutic concentrations of 500 ng/ml are also observed. Toxic concentrations vary between 290 and 1600 ng/ml. The observed sertraline concentration in this case is above the therapeutic range and could lead to side-effects, but is not the cause of death. Because of the urine and stomach contents concentration, we can suggest a regular intake of sertraline and in addition, a recent intake before the patient's death. Thus, probably a peak steady-state concentration is observed in this case.

Sertraline concentrations were determined in six different locations in the brain. While sertraline binds on specific binding sites in the brain to create an effect, it is clear that in this case it is homogeneously distributed over the brain tissue as shown in Table VIII.3. In this case, the brain concentration of sertraline is 17 times higher than the plasma concentration. Bolo et al. [25] examined the brain/plasma concentration relationship for other SSRI's (fluoxetine and fluvoxamine) in vivo through ^{19}F magnetic resonance spectroscopy. They concluded that the steady-state brain concentration of an SSRI is about 10 times higher than its plasma concentration. This ratio is compatible with the reported distribution volumes of the compounds, indicating a considerable uptake of the SSRI into tissue spaces. We must point out, however, that because of the amphiphilic character of ADs a comparison between brain/blood and brain/plasma ratios is not straightforward as ADs bind to the membranes of red blood cells [18, 19].

In the brain tissue, a small amount of fluoxetine and desmethylfluoxetine was also determined, while these compounds were not detected in blood. This leads to the conclusion that fluoxetine was administered for a certain time in

the past, explaining the lower concentration in the brain tissue. Unfortunately, no hair samples were provided in this case.

Figure VIII.3. GC-MS chromatogram of the six different brain tissue samples (frontal, temporal, parietal, and occipital lobe, cerebellum and stem) in case 1

Sertraline and desmethylsertraline can be observed in high concentrations. In the enlargement, fluoxetine, desmethylfluoxetine and the internal standard Fd_6 (200 ng) can be detected
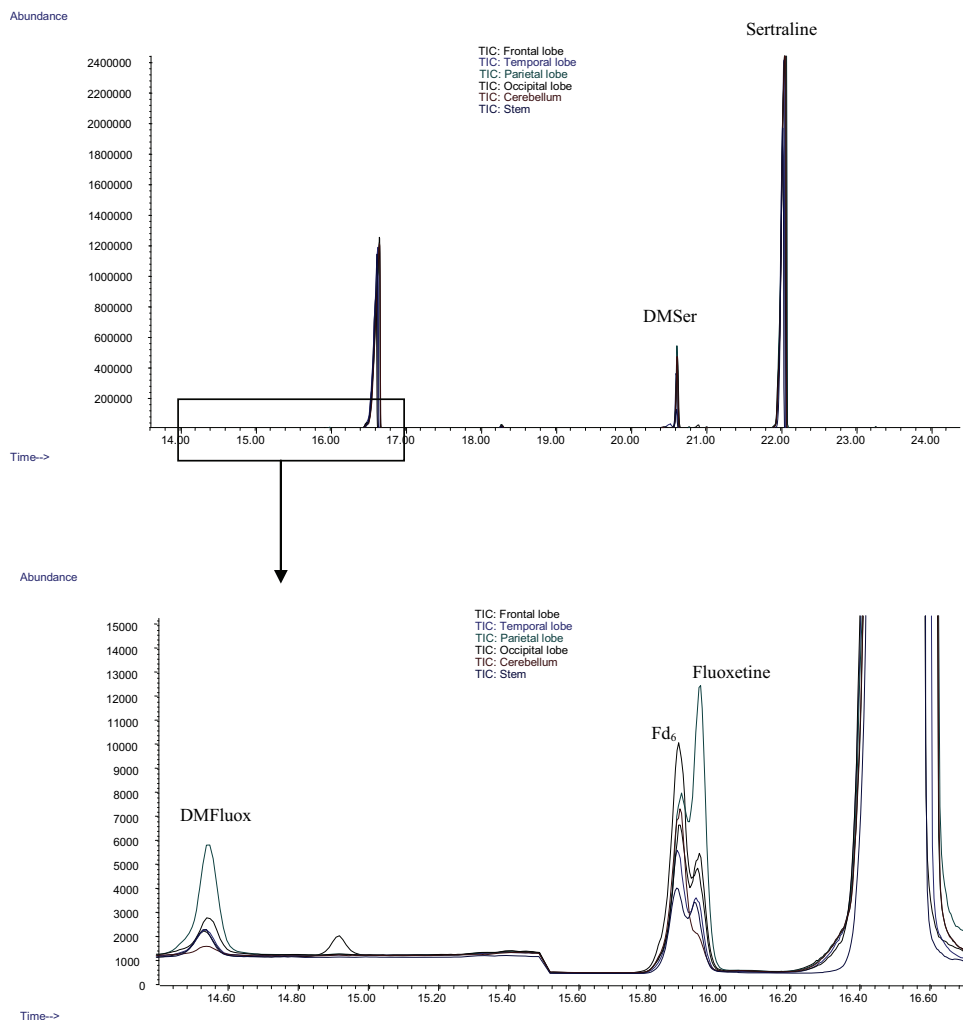
VIII.3.2. Case 2

The cause of death in this case was a polydrug intoxication, namely a combination of bromazepam (160 ng/ml), lorazepam (50 ng/ml), morphine (38 ng/ml), acetaminophen (1430 ng/ml), ethanol (1.36 g/l), clotiapine (600 ng/ml) and fluoxetine (1640 ng/ml). Due to the combined presence of these products in the blood, central nervous system suppression occurred, with a resultant lethal cardio-respiratory depression. The urinary level of fluoxetine was 4750 ng/ml, while in the stomach contents fluoxetine reached the level of 260 ng/ml. Fluoxetine and desmethylfluoxetine were homogenously distributed in the brain with a mean concentration of 4532 and 3862 ng/g, respectively.

The fluoxetine blood concentration is toxic, but not lethal, as the therapeutic concentration ranges between 100 and 450 ng/ml, while toxic concentrations range from 1500 to 2000 ng/ml [17]. According to Bolo et al. [25], the steady-state brain concentration of the sum of fluoxetine and its active metabolite desmethylfluoxetine ranges from 1800 to 6000 ng/g, and is lower than the sum of 8394 ng/g in this case. In addition, the brain concentration of desmethylfluoxetine is almost as high as the fluoxetine concentration which might be explained by the elimination half-life difference, 4 to 6 days for the parent drug and 4-16 days for the metabolite [35]. The brain/blood fluoxetine ratio of 2.8 in our case is comparable to the brain/plasma correlation of 2.6 for the sum of fluoxetine and desmethylfluoxetine found by Renshaw et al. [26]. However, the ratio is much lower than the ratio of 10 described by Bolo et al. [25]. This ratio is compatible with the reported distribution volumes of the compounds, indicating a considerable uptake of the SSRI into tissue compartments. However, as ADs can bind to red blood cell membranes due to their amphiphilic character [18, 19], it is clear that the comparison between brain/blood and brain/plasma results is not obvious.

VIII.3.3. Case 3

The cause of death of this person was a polydrug intoxication, in which high morphine levels were found and thus this decease did in fact not immediately

relate to the ADs concentrations, but was due to a suppression of the central nervous system, with cardio-respiratory depression caused by high amounts of opiates (2.4 µg/ml) in the blood. Sertraline and desmethylsertraline (DMSer) were found in blood at a level of 93 and 185 ng/ml, respectively. The mean brain concentration was 1635 ng/g for sertraline and 3717 ng/g for DMSer. Trazodone and m-cpp were also detected in brain tissue. The quantification of these compounds occurred using HPLC-DAD. A mean concentration of 93 and 31 ng/g was found for trazodone and m-cpp, respectively. In urine, a trazodone concentration of 142.7 ng/ml was monitored, while trazodone was not detected in blood.

In addition, hair samples were analyzed for this case. A hair sample with a length of 5.5 cm was taken from the vertex and cut into 2 fragments of 2 cm and one of 1.5 cm, giving a time window of approximately 2 months per segment. The first fragment, thus closest to the scalp (20 mg) contained 0.6 ng sertraline / mg and 0.5 ng DMSer / mg. The second fragment (61.2 mg) contained 0.8 ng sertraline / mg, 1.4 ng DMSer / mg and 0.4 ng mcpp / mg. The third fragment contained 1.6, 2.6, and 0.8 ng/mg of sertraline, DMSer, and m-cpp, respectively.

According to The International Association of Forensic Toxicologists [17], the therapeutic range of sertraline in plasma ranges from 50-250 ng/ml, but therapeutic concentrations of 500 ng/ml are also observed. Toxic concentrations vary between 290 and 1600 ng/ml. The observed sertraline concentration in this case is thus within the lower therapeutic range. Sertraline was not present in urine nor in the stomach contents and therefore, a non-compliance of the prescribed therapy must be suspected. Sertraline concentrations were determined in 6 different locations in the brain. While sertraline binds on specific binding sites in the brain to create an effect, it is clear that in this case it is homogeneously distributed over the brain tissue as shown in Table VIII.3. Calculation of the brain/blood sertraline ratio provided a value of 17.6. This value is higher, but in the range of the proposed ratio of 10 for SSRI's by Bolo et al. [25]. The ratio of sertraline/DMSer in hair is 1.2 in the first segment, while it was 0.5 and 0.6 for segment 2 and 3, maybe due to stability issues. It is clear from the hair

and urine analysis, that there was a regular but not daily intake of sertraline during the past six months.

<u>Figure VIII.4.</u> GC-MS chromatograms obtained from a blood (A), brain tissue (B) and hair extract (C) for case 3

DMSer, desmethylsertraline; m-cpp, m-chlorophenylpiperazine; Fd_6, deuterated fluoxetine internal standard; Md_3, deuterated mianserin internal standard; Pd_6, deuterated paroxetine internal standard

A
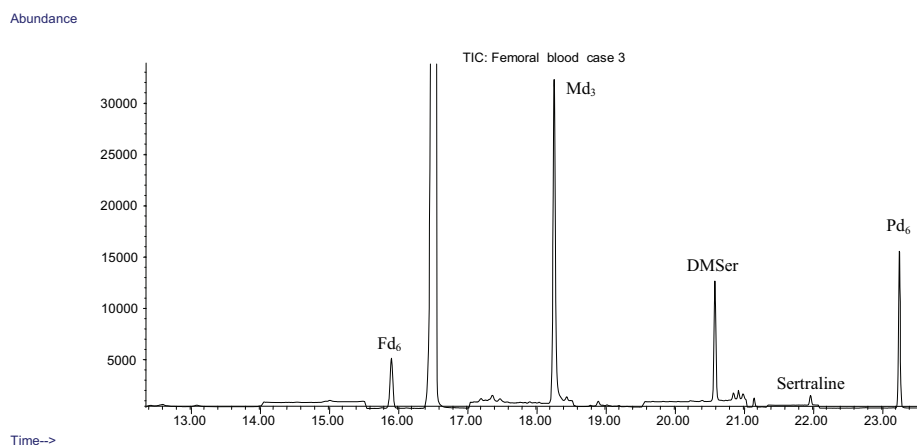
B
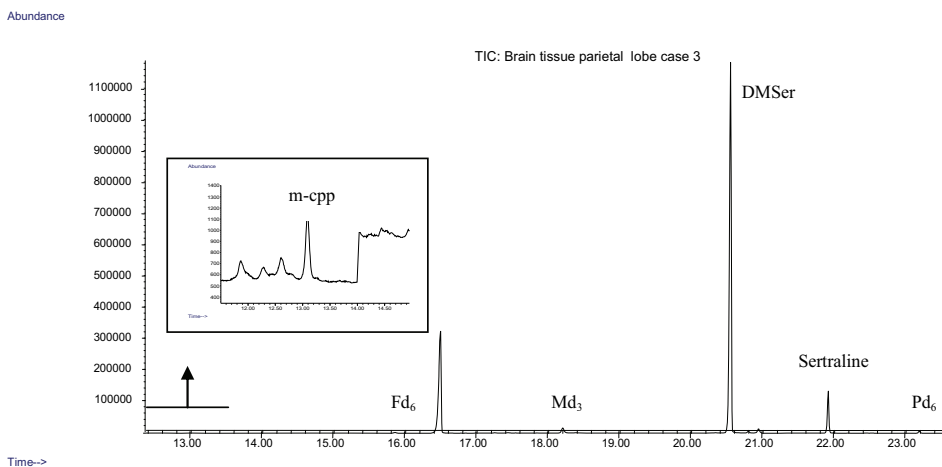
C
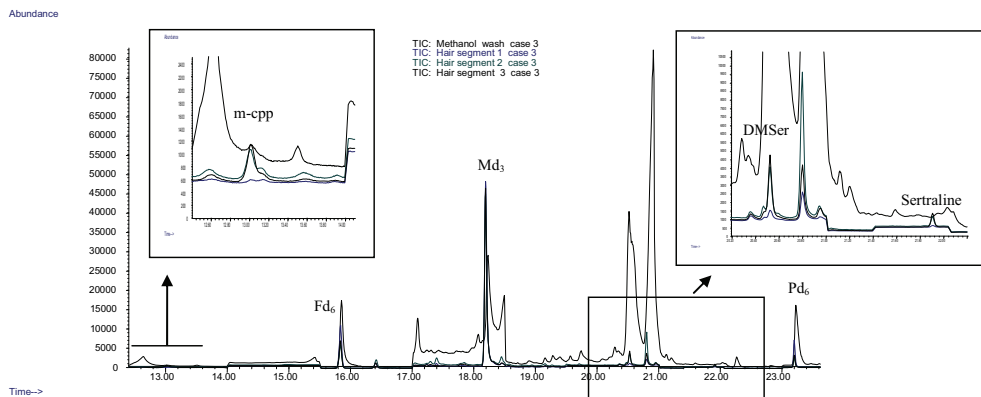
The level of trazodone in brain tissue was 200 to 500 times lower than concentrations found by Martin and Pounder [24]. These authors described intoxications in which about 700 mg of trazodone was ingested, leading to a blood level of 15 000 ng/ml and a urine level of 20 000 ng/ml. In our case, however, neither trazodone nor its metabolite was found in blood. The urinary concentration of trazodone, and the presence of its metabolite m-cpp in hair leads to the conclusion that trazodone was administered at a more postponed point in time, explaining the lower concentration in the brain tissue. This case demonstrates that ADs can still be determined in brain tissue, even when they are no longer present in blood, providing information about the treatment and administration of AD drugs before death.

VIII.3.4. Case 4

In this case large amounts of cocaine (3.43 µg/ml), amphetamine (4.5 µg/ml) and morphine (167 ng/ml) were found in blood which could induce death due to cardiac arrhythmias (cfr. stimulants) and/or respiratory depression (cfr. opiates). Other compounds found in blood were ethanol (0.22 g/l), acetaminophen (1.23 µg/ml), and caffeine (2.6 µg/ml). The urine contained other drugs such as citalopram (5.38 µg/ml), ibuprofen (218 ng/ml), fentanyl (5.6 ng/ml), trazodone metabolites (6.95 µg/ml) and benzodiazepines (1.8 µg/ml). The stomach contents contained morphine

(5.56 μg/ml), cocaine (500 μg/ml), trazodone (115 μg/ml), citalopram (1.12 μg/ml), alprazolam (236 ng/ml), acetaminophen (19.4 μg/ml) and caffeine (0.6 μg/ml). This drug addict had used illegal substances (such as cocaine, amphetamines, and heroin), in combination with ethanol and the ADs, trazodone and citalopram.

Trazodone and m-cpp were detected in brain tissue although they were not found in blood. A mean concentration of 332 ng/g was found for trazodone, while a mean of 130 ng/g was found for m-cpp in the frontal, occipital and temporal lobe. Citalopram and its demethylated metabolite were found in brain tissue with a mean concentration of 155 and 61 ng/g, respectively. Blood concentrations as determined by GC-MS were 194 and 104 ng/ml, respectively.

Dark brown hair with a length of 6 cm was taken from the vertex and cut into 2 fragments of 3 cm because of the limited amount available. The first fragment (closest to the scalp; 23.2 mg) contained 2.5 ng citalopram / mg and 1.9 ng DMC / mg. The second fragment (27.3 mg) did not contain any AD.

ADs use in illegal polydrug abuse (such as cocaine, heroin) is often found. Drug addicts under methadone treatment are often depressed and treated with the low toxic new generation ADs [14, 15]. As trazodone and citalopram were found in the stomach contents, it can be presumed that the drugs were ingested in the hours prior to death leading to an incomplete absorption of the substances. Trazodone was not found in blood, however, it was detected in combination with its metabolite m-cpp in brain tissue and its metabolites were found in urine. Therefore, occasional use of trazodone by this subject is suspected.

Citalopram was detected in blood, brain, urine and stomach contents. The presence of citalopram in the brain could be due to rapid migration and storage in this compartment or rather be an indication of previously consumed citalopram. Moreover, the brain/blood ratio is quite low (0.8) as compared to case 5, which could be explained by the recent and irregular

intake in drug addict, while for case 5 a steady-state AD therapy was presumed. The DMC/Citalopram ratio ranges from 0.3-1.2 with a mean of 0.51, with the highest ratio observed in the temporal lobe. The DMC/Citalopram ratio is comparable to case 5.

Referring to the citalopram concentrations substantiated in the hair fragments, we can conclude that the use of citalopram occurred during the past 3 months.

VIII.3.5. Case 5

A 92-year old lady died suddenly and unexpectedly during admission in hospital. As her death was unforeseen, a forensic autopsy was ordered. This old-age woman was known to be depressive and tired of her life; therefore she received an AD. In urine, 315 ng/ml citalopram was detected, while 114 ng/ml caffeine was measured during screening of the post-mortem blood sample. Analysis of the blood sample with the GC-MS method resulted in a citalopram concentration of 14.1 ng/ml and a desmethylcitalopram (DMC) concentration of 18.3 ng/ml. The mean brain concentration was 104 ng citalopram/g.

The blood levels of citalopram and its metabolite desmethylcitalopram are subtherapeutic as therapeutic concentrations range from 20 till 200 ng/ml [17]. The brain concentrations of these substances were sampling-dependent, with the highest concentrations in the parietal and occipital lobe, and in the cerebellum. The DMC/citalopram ratio ranged from 0.3 till 0.9 with a mean of 0.45. The highest ratio is seen in the temporal lobe. The same ratio is seen in case 4 were DMC/Citalopram ranged from 0.3-1.2 with a mean of 0.51 and again the highest ratio is observed in the temporal lobe. Referring to the brain/blood ratio of 7, it can be concluded that citalopram penetrates the brain rather easily. In addition, it can be presumed by these data that the detection of citalopram and his metabolite might still be possible when these substances are below limit of quantitation in blood.

VIII.4. Conclusion

The developed solid phase extraction and GC-MS method in PICI mode for the simultaneous determination of several new generation ADs and their active metabolites in brain tissue was validated and tested on post-mortem samples. Several ADs were detected and quantified in six brain regions. Although ADs are selectively bound to receptors located in specific brain regions, it was clear that the ADs spread rather homogeneously over the total brain content in most cases. It cannot be excluded that this distribution is also increased due to post-mortem redistribution of the ADs, following liberation from their binding sites. Therefore, in post-mortem analysis, a detailed location of a brain sample is in fact of no importance for the quantitative result as shown by the case reports. However, more case reports with different types of antidepressants should be analyzed in the future to confirm this finding.

A possible advantage of post-mortem toxicological brain analysis is that ADs can still be determined in brain tissue, even when they are no longer present in blood, providing information about the treatment and administration of AD drugs in those cases. However, as described in chapter VI long term stability of low concentrations of ADs is lower as compared to their stability in blood or plasma.

The link between blood levels and the drug-concentration at the effector site (the brain) for a specific clinical response is of importance. For 2 cases, a brain/blood ratio of approximately 17 was seen for sertraline. However, due to the small number of cases, this link could not be determined. In addition, variables such as P-glycoprotein polymorphism, interval between the last time of ingestion and death, treatment period, and patient compliance could alter the brain/blood ratio.

The quantitative results from hair samples are hard to interpret as the link between incorporation in the hair and blood level / effect is not known. In addition, incorporation of the ADs in hair also depends on the type of hair pigmentation and physical state.

However, hair analysis can give more information of the long-term exposure of ADs. While blood is still the preferred matrix to link concentration and effect, analysis of brain tissue and hair can provide additional information. These matrices are certainly of interest to investigate decayed corpses, or to have a longer detection window. Especially, hair samples give information on the consumption pattern of the ADs in the past.

VIII.5. References

[1]   Kincaid RL, McMullin MM, Crookham SB, Rieders F. Report of a fluoxetine fatality. *J. Anal. Toxicol.* 1990; 14: 327-329

[2]   Wenzel S, Aderjan R, Mattern R, Pedal I, Skopp G. Tissue distribution of mirtazapine and desmethylmirtazapine in a case of mirtazapine poisoning. *Forensic Sci. Int.* 2006; 156: 229-236

[3]   Goeringer KE, Raymon L, Christian GD, Logan BK. Postmortem forensic toxicology of selective serotonin reuptake inhibitors: A review of pharmacology and report of 168 cases. *J. Forensic Sci.* 2000; 45: 633-648

[4]   Keller T, Zollinger U. Gas chromatographic examination of postmortem specimens after maprotiline intoxication. *Forensic Sci. Int.* 1997; 88: 117-123

[5]   Luchini D, Morabito G, Centini F. Case report of a fatal intoxication by citalopram. *Am. J. Forensic Med. Path.* 2005; 26: 352-354

[6]   de Meester A, Carbutti G, Gabriel L, Jacques JM. Fatal overdose with trazodone: Case report and literature review. *Acta Clin. Belg.* 2001; 56: 258-261

[7]   Azaz-Livshits T, Hershko A, Ben-Chetrit E. Paroxetine associated hepatotoxicity: A report of 3 cases and a review of the literature *Pharmacopsychiatry* 2002; 35: 112-115

[8]   Goeringer KE, McIntyre IM, Drummer OH. Postmortem tissue concentrations of venlafaxine. *Forensic Sci. Int.* 2001; 121: 70-75

[9]   Kelly CA, Dhaum N, Laing WJ, Strachan FE, Good AM, Bateman DN. Comparative toxicity of citalopram and the newer antidepressants after overdose. *J. Toxicol.-Clin. Toxicol.* 2004; 42: 67-71

[10]   Rogde S, Hilberg T, Teige B. Fatal combined intoxication with new antidepressants. Human cases and an experimental study of postmortem moclobemide redistribution. *Forensic Sci. Int.* 1999; 100: 109-116

[11]   Singer PP, Jones GR. An uncommon fatalilty due to moclobemide and paroxetine. *J. Anal. Toxicol.*1997; 21: 518-520

[12]   McIntyre IM, King VK, Staikos V, Gall J, Drummer OH. A fatality involving moclobeemide, sertraline, and pimozide. *J. Forensic Sci.* 1997; 42: 951-953

[13]   Dams R, Benijts THP, Lambert WE, Van Bocxlaer JF, Van Varenbergh D, Peteghem CV, De Leenheer AP. A fatal case of serotonin syndrome after combined moclobemide-citalopram intoxication. *J. Anal. Toxicol.* 2001; 25: 147-151

[14]   Hamilton SP, Nunes EV, Janal M, Weber L. The effect of sertraline on methadone plasma levels in methadone-maintenance patients. *AM. J. Addict.* 2000; 9: 63-69

[15]   Petrakis I, Carroll KM, Nich C, Gordon L, Kosten T, Rounsaville B. Fluoxetine treatment of depressive disorders in methadone-maintained opioid addicts. *Drug Alcohol Depend.* 1998; 50: 221-226

[16]   Adson DE, Erickson-Birkedahl S, Kotlyar M. An unusual presentation of sertraline and trazodone overdose. *Ann. Pharmacother*. 2001; 35: 1375-1377

[17]   TIAFT. The international association of forensic toxicologists: http: //www. tiaft. org/. *Tiaft bulletin* 26 1S

[18]   Fisar Z, Fuksova K, Sikora J, Kalisova L, Velenovska M, Novotna M. Distribution of antidepressants between plasma and red blood cells. *Neuroendocrinol. Lett.* 2006; 27: 307-313

[19]   Hinderling PH. Red blood cells: a neglected compartment in pharmacokinetics and pharmacodynamics. *Pharmacol. Rev.* 1997; 49: 279-295

[20]   Reis M, Ahlner J, Druid H. Reference concentrations of antidepressants. A compilation of postmortem and therapeutic levels. *J. Anal. Toxicol.* 2007; 31: 254-264

[21]   Stimpfl T, Reichel S. Distribution of drugs of abuse with specific regions of the human brain. *Forensic Sci. Int.* 2007; 170: 179-182

[22]   Löscher W, Potschka H. Role of drug efflex transporters in the brain for drug disposition and treatment of brain diseases. *Prog. Neurobiol.* 2005; 76: 22-76

[23]   Snyder SH. Drugs and the brain. New York: WH. Freeman and Company, 1999, pp 228.

[24]   Martin A, Pounder DJ. Postmortem Toxicokinetics of Trazodone. *Forensic Sci. Int.* 1992; 56: 201-207

[25]   Bolo NR, Hode Y, Nedelec JF, Laine E, Wagner G, Macher JP. Brain pharmacokinetics and tissue distribution in vivo of fluvoxamine and fluoxetine by fluorine magnetic resonance spectroscopy. *Neuropsychopharmacol.* 2000; 23: 428-438

[26]   Renshaw PF, Guimaraes AR, Fava M, Rosenbaum JF, Pearlman JD, Flood JG, Puopolo PR, Clancy K, Gonzalez RG. Accumulation of fluoxetine and norfluoxetine in human brain during therapeutic administration. *Am. J. Psychiatry* 1992; 148: 1592-1594

[27]   Burke MJ, Preskorn SH. Therapeutic drug monitoring of antidepressants - Cost implications and relevance to clinical practice. *Clin. Pharmacokinet.* 1999; 37: 147-165

[28]   Musshoff F, Madea B. Analytical pitfalls in hair testing. *Anal. Bioanal. Chem.* 2007; 388: 1475-1494

[29]   Pragst F, Balikova M. State of the art in hair analysis for detection of drug and alcohol abuse. *Clin. Chim. Acta* 2006; 370: 17-49

[30]   Smyth WF, Leslie JC, McClean S, Hannigan B, McKenna HP, Doherty B, Joyce C, O'Kane E. The characterisation of selected antidepressant drugs using electrospray ionisation with ion trap mass spectrometry and with quadrupole time-of-flight mass spectrometry and their determination by high-performance liquid chromatography/electrospray ionisation tandem mass spectrometry. *Rapid Commun. Mass Spectrom.* 2006; 20: 1637-1642

[31]   Müller C, Vogt S, Goerke R, Kordon A, Weinmann W. Identification of selected psychopharmaceuticals and their metabolites in hair by LC/ESI-CID/MS and LC/MS/MS. *Forensic Sci. Int.* 2000; 113: 415-421

[32]   Couper FJ, McIntyre IM, Drummer OH. Detection of antidepressant and antipsychotic-drugs in postmortem human scalp hair. *J. Forensic Sci.* 1995; 40: 87-90

[33]   Pragst F, Rothe M, Hunger J, Thor S. Structural and concentration effects on the deposition of tricyclic antidepressants in human hair. *Forensic Sci. Int.* 1997; 84: 225-236

[34]   Srogi K. Hair analysis as method for determination of level of drugs and pharmaceutical in human body: review of chromatographic procedures. *Anal. Lett.* 2007; 39: 231-258

[35]   Moffat AC, Osselton MD, Widdop B. Clarke's analysis of drugs and poisons in pharmaceuticals, body fluids and postmortem material. 3th Ed. London: Pharmaceutical Press, 2004, pp 1935.

Chapter IX

General conclusion

According to the World Health Organization, depression will be the second leading contributor to the global burden of disease, calculated for all ages and both sexes by the year 2020. Therefore, the prescription rate of antidepressants will increase, resulting in a growing interest for determination methods in the clinical and forensic field. As a result, in this thesis, a gas chromatographic-mass spectrometric method for the determination of thirteen new generation antidepressants and their metabolites was developed, validated and applied in clinical as well as forensic settings.

The major part of this work is the optimization of the analytical aspects of the method. Because the method had a broad range of possible applications, this thesis reflects possible pros en cons during the different stages in the development and optimization of the method. Antidepressants were extracted using solid phase extraction from different matrixes such as plasma, whole blood, brain and hair tissues for clinical or forensic applications. The mass spectrometric conditions, especially conditions concerning ionization, were thoroughly investigated. While the traditional electron ionization mode is most useful in clinical settings, it is clear that positive ion chemical ionization has its benefits for demanding matrices in forensic settings, while negative ion chemical ionization can lead to extreme sensitivities if necessary. After the optimization of the gas chromatographic-mass spectrometric method, it was validated based on the FDA guidelines to ensure good quantification results. Finally, the usefulness of the method was demonstrated by a preliminary study concerning monitoring of antidepressants in combination with *CYP2D6* genotyping and by analyzing five post-mortem cases.

Although it is clear that not all antidepressants and their metabolites are adequately quantified with this method, we are sure that this thesis can be a helpful guideline to develop a specific method for a specific antidepressant in a specific setting. In addition, it is clear that this method is able to determine antidepressants in different forensic matrices, leading to more information concerning the case. However, in the future, more research should be performed concerning the relationship between antidepressant blood and brain concentrations and the final effect, before interpretation of brain

antidepressant concentrations can be straightforward. Moreover, it is also clear that this method has its purpose in psychiatric clinics as demonstrated by the preliminary study combining the gas chromatographic-mass spectrometric method to determine antidepressant plasma concentrations and the genotyping of the antidepressant metabolizing enzyme CYP2D6. However, we sincerely hope that in the near future, the TDM-GEN method, as described in chapter VII, will be applied in a large scale psychiatric clinic, to evaluate its use.

SUMMARY

This work describes the optimization, validation and application of a gas chromatographic-mass spectrometric method for the quantification of new generation antidepressants and their active metabolites in plasma, blood, brain tissue and hair samples.

In **chapter I** an overview is given of the published literature concerning the new generation antidepressants. This introduction discusses the onset of depression and the treatment, including the action mechanisms, side-effects and toxicity of antidepressants in general. Moreover, the potential values of therapeutic drug monitoring and toxicological assays for these drugs are discussed in relation to their mode of action, drug interactions, metabolism and pharmacokinetic properties. We must not forget that depression affects both economic and social functions of about 121 million people worldwide, leading to substantial impairment in an individual's ability to take care of his or her everyday responsibilities and at its worst can lead to suicide. Although the serious progress in antidepressant drug therapy, there still are a number of problems such as non-responding therapy, poor patient compliance and serious side-effects. Therefore, development of analytical methods to monitor plasma concentration during antidepressant therapy, to investigate forensic cases or to do fundamental research concerning their site of action is of interest.

This work focuses on the development of an analytical method for the quantification of new generation antidepressants and their metabolites. The monitored antidepressants were selected based on their importance in the seven major antidepressant markets (Japan, USA, France, United Kingdom, Italy, Spain, Germany) according to the Cognos Plus Study #11 and on the AGNP-TDM Expert Group Consensus Guidelines. The following anti-depressants and metabolites were monitored: citalopram, fluoxetine, fluvoxamine, maprotiline, melitracen, mianserin, mirtazapine, paroxetine, reboxetine, sertraline, trazodone, venlafaxine, viloxazine, desmethyl-citalopram, didesmethylcitalopram, desmethylfluoxetine, desmethyl-maprotiline, desmethylmianserin, desmethylmirtazapine, desmethyl-sertraline, m-chlorophenylpiperazine, and O-desmethylvenlafaxine.

Chapter II summarizes the objectives of this work. These objectives were first of all the development of a quantitative GC-MS method for the new generation antidepressants, secondly its applicability in clinical as well as forensic settings.

The analytical development of the gas chromatographic-mass spectrometric method was the core of the research subject. The analytical development was discussed in chapters III, IV, and V.

A very important step in the development of an analytical method is the extraction of the compounds of interest from the biological matrix as this will have implications on the overall sensitivity and selectivity of the method. Therefore, extraction of antidepressants using a solid phase extraction (SPE) was throughout discussed in **chapter III**. The SPE was developed by extracting antidepressant spiked water samples, using a high pressure liquid chromatographic method with diode array detection as monitoring technique. Thereafter, the developed SPE procedure was optimized, using the final gas chromatographic method, for biological matrices such as plasma, blood, brain tissue and hair samples, as the extraction of antidepressants from these matrices is of interest in the field of clinical and forensic toxicology. During this optimization factors such as matrix consistence, lipophilicity, protein content and stability were considered to obtain an optimal SPE method for each matrix, finally resulting in high and reproducible antidepressant extraction recoveries.

In **chapter IV**, derivatization of antidepressants was discussed. Derivatization is a common sample preparation technique before gas chromatographic analysis to improve the volatility, peak shape and detector response of the analyte. Different acylation reagents and procedures were compared in this chapter. Heptafluorobutyrylation of antidepressants and their metabolites using heptafluorobutyrylimidazole was finally chosen as this led to a reproducible derivatization with good peak shapes for most antidepressants. In addition, heptafluorobutyrylation led to a single sample preparation for the three possible ionization modes, with a highly sensitive analysis using negative ion chemical ionization because this type of derivatization led to the addition of the seven fluorine-atoms in combination with the carbonyl group after derivatization of the antidepressants. Finally,

heptafluorobutyrylation also led to more volatile derivatives, resulting in a shorter analysis time.

Gas chromatographic and mass spectrometric parameters were optimized in **chapter V**. The separation of the 13 antidepressants and their active metabolites occurred on a non-polar 5% phenylmethyl-polysiloxane column with general purpose dimensions to avoid GC-MS downtime due to column switching in the forensic or clinical routine laboratory. During optimization of the gas chromatographic method most attention was paid to the sample introduction. Splitless vaporization injection was chosen due to sensitivity and robustness concerns. However, as incomplete sample transfer from the injector liner to the column, discrimination, and poor peak focussing on the top of the column are the most widely observed problems in splitless injections, this injection type was evaluated concerning inlet temperature, purge activation time and inlet pressure to ensure minimal negative effects. In order to accelerate and maximize the sample transfer, a pulsed splitless injection was selected in which the high inlet pressure was used to increase the mass transfer to the column and to reduce the band spreading. The discrimination of high boiling compounds was diminished due to optimization of the injector temperature, column temperature, the purge activation time and an increase in inlet pressure during injection.

For the mass spectrometric conditions, optimization and comparison of different ionization modes was of most interest. The second part of chapter V therefore describes the comparison of electron, positive and negative ion chemical ionization and discusses the fragmentation patterns of the antidepressants and their metabolites in these ionization modes. Electron ionization is still the traditional method for comprehensive screening procedures due to the easy library search mechanism. This ionization, however, leads to high fragmentation of citalopram, melitracen, venlafaxine, and O-desmethylvenlafaxine, resulting in the aspecific high abundance quantifier ion at m/z 58 and inherent loss of specificity, especially for demanding matrices such as post-mortem blood and brain tissue. Chemical ionization is a 'softer' ionization technique, thus providing more selectivity through molecular mass information. Negative ion chemical ionization leads to improved sensitivity due to heptafluorobutyrylimidazole derivatization, allowing smaller sample volumes. This could be very interesting in clinical analysis and TDM of samples from children where often only a limited amount

of sample is available. On the other hand, underivatized tertiary amines such as citalopram, melitracen, mianserin, and mirtazapine are not detected.Thus every ionization method has its specific pros and cons and this chapter tries to give a guideline for the choice of ionization modes and parameters to obtain the ideal conditions for a specific antidepressant in a specific setting.

In **chapter VI** the developed GC-MS method for the 13 new generation antidepressants and their metabolites was validated in plasma using different ionization modes according to the FDA guidelines. For blood and brain tissue samples, validation occurred in positive ion chemical ionization mode according to the same guidelines. During validation stability, sensitivity, precision, accuracy, recovery, linearity and selectivity were evaluated. Identification and quantification were based on selected ion monitoring in electron and chemical ionization modes. Calibration by linear and quadratic regression for electron and chemical ionization, respectively, utilized deuterated internal standards and a weighting factor $1/x^2$. Limits of quantitation were established between 5-12.5 ng/ml in electron and positive ion chemical ionization, and 1-6.5 ng/ml in negative ion chemical ionization for plasma. For blood the limit of quantification ranged from 5-20 ng/ml, while the limit of quantification in brain tissue ranged from 25-62.5 ng/g. Accuracy, precision and stability were within the limits set by the guidelines (less than 15 % deviation from target value, less than 15 % relative standard deviation, except at the quantification limit where deviation and RSD of 20 % is allowed) for each ionization mode and for most compounds. While it is clear that not all compounds can be quantified either due to irreproducible validation results and chromatographic problems (trazodone) or due to derivatization problems (O-desmethylvenlafaxine), this method can quantify most new antidepressants in the therapeutic range in plasma in different ionization modes, and in blood and brain tissue.

After the development and validation of the GC-MS method for the new generation antidepressants and their metabolites, the method was evaluated for its usefulness for clinical and forensic toxicological analyses, as described in chapter VII and VIII.
Chapter VII describes a preliminary study concerning personalized anti-depressant treatment. In this study, the developed GC-MS method with

electron ionization is combined with *CYP2D6* genotyping to ensure a good medical treatment. Although the low toxicity of antidepressants, physicians must be aware that depression is a chronic disease leading to a long period of drug intake, in addition, these patients mostly use a whole range of drugs, which increases the risk of adverse effects. Finally, a large variety in therapeutic plasma concentrations due to environmental, physiological and genetic factors occur with antidepressant treatment and identical plasma concentrations often result in different responses to treatment. So far the most of compelling evidence in pharmacogenetics of antidepressants is for an effect of CYP2D6 polymorphisms on antidepressant drug plasma levels, therefore this enzyme was monitored in combination with plasma concentration measurement. A case report was applied to demonstrate the usefulness of the developed GC-MS method and to demonstrate the possibilities of this method in a realistic clinical setting. It also demonstrates that the developed methods work and can be applied. The genotyping of patients is probably of most interest when therapy is started. The phenotype, together with the information concerning the patients depressed state, co-medication and comorbidity can lead to a rational choice of antidepressant therapy and necessary dose. Once therapy is started, TDM can be used to monitor compliance, and to link plasma concentrations with the clinical effect and side-effects of the patient. However, more research has to be done before personalized AD treatment will be state of the art. First of all, dose recommendations based on differences in pharmacokinetics are not automatically helpful for prediction of treatment response, since correlation between plasma concentrations and efficacy is very poor in antidepressant therapy. Secondly, due to the complexity of drug response, single mutations in one gene, such as the *CYP2D6*, are unlikely to cause the continuous variability in response. As result, more information should be obtained concerning polymorphisms of other CYP isoenzymes, variations in targets and transporters. In addition, the proposed method should be evaluated on a large scale population.

In **Chapter VIII** the developed GC-MS method using positive ion chemical ionization is used to quantification of the new generation antidepressants in whole blood, brain tissue and hair samples for interpretation of post-mortem cases. Several antidepressants such as fluoxetine, sertraline and citalopram were detected and quantified in different brain regions. Although

antidepressants are selectively bound to receptors located in specific brain regions, it was clear that the antidepressants spread rather homogeneously over the total brain content in most cases. Therefore, in post-mortem analysis, a detailed location of a brain sample is in fact of no importance for the quantitative result. Analysis of the post-mortem cases also led to the conclusion that a possible advantage of post-mortem toxicological brain analysis is the longer detection window of antidepressants in brain tissue as compared to blood. Because the link between blood levels and the drug-concentration at the effector site (the brain) for a specific clinical response is of importance, blood levels and brain levels were compared in the five cases. For 2 cases, a brain/blood ratio of approximately 17 was seen for sertraline. However, due to the small number of cases, this link could not be determined. In addition, variables such as P-glycoprotein polymorphism, interval between the last time of ingestion and death, treatment period, and patient compliance could alter the brain/blood ratio. Hair samples were also analyzed, especially to confirm the use of antidepressants for a longer period and thus the results of the brain tissue. The quantitative results from hair samples, however, are hard to interpret as the link between incorporation in the hair and blood level / effect is not known. In addition, incorporation of the ADs in hair also depends on the type of hair pigmentation and physical state.

Finally, in **chapter IX** a general conclusion is given. It is clear that the major part of this work is the optimization of the analytical aspects of the method. Because the method has a broad range of possible applications, we hope this thesis can be a guideline for the use of GC-MS analyses for a specific antidepressant in a specific setting. In addition, this work describes the usefulness of the developed GC-MS method for forensic and clinical applications. However, we sincerely hope that in the near future, the developed method will be applied in a large scale forensic or psychiatric clinical setting for further development and evaluation.

SAMENVATTING

Dit doctoraatswerk beschrijft de optimalisatie, validatie en applicatie van een gaschromatografische massaspectrometrische methode voor de bepaling van nieuwe generatie antidepressiva en hun actieve metabolieten in plasma, bloed, hersenweefsel en haar.

In het **eerste hoofdstuk** wordt een overzicht gegeven van de reeds gepubliceerde literatuur omtrent de nieuwe generatie antidepressiva. Deze introductie behandelt de oorzaken van depressie, de mogelijke behandelingen, evenals actiemechanismen, mogelijke nevenwerkingen en toxiciteit van de nieuwe generatie antidepressiva. Daarenboven wordt het belang van antidepressiva plasma spiegel bepaling en van toxicologische analyses voor deze groep geneesmiddelen geargumenteerd. Depressie is immers een ernstige psychische stoornis die het economische en sociale leven van 121 miljoen mensen aantast en kan leiden tot zelfdoding. Ondanks de enorm toegenomen kennis over depressie en de behandelingswijzen zijn er nog heel wat problemen gedurende de medicamenteuze behandeling van depressies zoals slechte therapietrouw, een groot aantal niet-effectieve behandelingen en ernstige bijwerkingen.

Ons onderzoek is voornamelijk gericht op de ontwikkeling van een analytische methode voor de kwantificatie van nieuwe generatie antidepressiva en hun metabolieten. De antidepressiva waarvoor we in dit werk een bepalingsmethode zullen optimaliseren zijn gekozen op basis van hun belang in de zeven landen met het grootste verkoopscijfer van antidepressiva volgens het Cognos Plus Study #11 en het AGNP-TDM Expert Group rapport (Japan, Verenigde Staten, Frankrijk, Verenigd Koninkrijk, Italië, Spanje en Duitsland). De finale selectie omvat citalopam, fluoxetine, fluvoxamine, maprotiline, melitraceen, mianserine, mirtazapine, paroxetine, reboxetine, sertraline, trazodone, venlafaxine, viloxazine, desmethyl-citalopram, didesmethylcitalopram, desmethyfluoxetine, desmethyl-maprotiline, desmethylmianserine, desmethylmirtazapine, desmethyl-sertraline, m-chlorophenylpiperazine en O-desmethylvenlafaxine.

Hoofdstuk II vat de beoogde objectieven voor deze scriptie samen. Eerst en vooral werd de ontwikkeling van een kwantitatieve GC-MS methode voor

nieuwe generatie antidepressiva en hun metabolieten beoogd. Daarnaast moest deze methode zijn nut bewijzen voor zowel forensische als klinische toepassingen.

De analytiek is dus de kern van het onderzoek. De optimalisatie van de analytische methode werd besproken in hoofdstukken III, IV en V.

Eén van de belangrijkste stappen in de ontwikkeling van een analytische methode is de extractie van de componenten die moeten bepaald worden vanuit de biologische matrix. Deze extractiestap zal een invloed hebben op de finale gevoeligheid en selectiviteit van de detectiemethode. Daarom wordt de extractie van de antidepressiva via een vaste fase extractie procedure uitvoerig besproken in **hoofdstuk III**. Eerst werd de keuze van vaste fase, evenals de was- en elutiestap van de extractieprocedure geoptimaliseerd door waterstalen waaraan antidepressiva werden toegevoegd te analyseren via vloeistofchromatografie met diode-array detectie. Nadien werd deze geoptimaliseerde vaste fase extractiemethode aangepast voor matrices zoals plasma, volbloed, hersenweefsel en haarstalen. Er moest vooral rekening gehouden worden met de consistentie, de lipofiliciteit, de proteïnen-concentratie van het staal en ook met de stabiliteit van de componenten gedurende de extractieprocedure om een aangepaste extractiemethode te bekomen voor iedere matrix. Finaal werd voor iedere matrix een reproduceerbaar en hoog extractierendement bekomen.

In **hoofdstuk IV** wordt een ander deel van de staalvoorbereiding beschreven, namelijk de derivatisatieprocedure. Derivatisatie wordt gebruikt om de vluchtigheid, de piekvorm en de detectorrespons van een component te verbeteren. Verschillende acyleringsreacties en producten worden vergeleken in dit hoofdstuk. Finaal werd gekozen voor heptafluorobutyrylatie van de antidepressiva en hun metabolieten via het derivatisatiereagens heptafluorobutyryl imidazol omdat dit product resulteerde in een reproduceerbare reactie met goede piekvormen voor de meeste antidepressiva. Daarenboven kon men via deze derivatisatiereactie zeven fluor-atomen in combinatie met een carbonyl groep toevoegen aan de structuur van de antidepressiva om zo een hogere gevoeligheid te bekomen in de negatieve chemische ionisatiemodus. Heptafluorobutyrylatie resulteerde ook in vluchtige derivaten en dus een kortere analysetijd.

Gaschromatografische massaspectrometrische parameters worden geoptimaliseerd in **hoofdstuk V**. De scheiding van de componenten gebeurde op een niet-polaire 5% phenylmethylpolysiloxaan kolom met algemene kolomdimensies om kolomwisselingen in forensische en klinische laboratoria tot een minimum te beperken. Gedurende de optimalisatie van de methode werd heel wat aandacht besteed aan de staal- introductie op de kolom. Er werd voor de 'splitless vaporization' injectie- techniek geopteerd omdat deze robuuste techniek de nodige gevoeligheid kon verzekeren. Toch werd deze injectietechniek geoptimaliseerd qua injectietemperatuur, inlaatdruk en kolomtemperatuur. Deze optimalisatie was nodig aangezien er een incomplete staaltransfer naar de kolom, discriminatie van hoogkokende componenten en een slechte piekvorm kan ontstaan bij 'splitless' injecties. Het finale resultaat was een 'pulsed splitless' injectie waarbij de inlaatdruk tijdens de injectie, dus voor een korte periode, verhoogd wordt.

Na de scheiding van de antidepressiva op de kolom worden deze gedetecteerd door een massaspectrometer. De condities van deze detector en de verschillende ionisatietechnieken worden beschreven in het tweede deel van hoofdstuk V. De fragmentatiepatronen van alle antidepressiva onder de verschillende ionisatiecondities worden eveneens besproken. Electron- ionisatie is nog steeds de traditionele ionisatietechniek omdat het resulteert in reproduceerbare spectra die kunnen opgezocht worden in commerciële spectrabibliotheken. Deze ionisatietechniek leidt echter wel tot een zeer sterke fragmentatie van componenten zoals citalopram, melitraceen, venlafaxine en O-desmethylvenlafaxine. Dit extreme fragmentatieproces zal leiden tot aspecifieke fragment ionen zoals m/z 58 en dus resulteren in een verlies aan selectiviteit vooral in matrices zoals volbloed en hersenweefsel. Chemische ionisatie kan dit probleem verhelpen omdat het een zachtere ionisatie techniek is en dus resulteert in minder fragmentatie. Hierdoor wordt er meer selectiviteit verkregen via informatie omtrent het moleculair gewicht. De positieve chemische ionisatietechniek boet wel wat in qua gevoeligheid doordat minder hoog abundante fragmentionen gevormd worden. Negatieve chemische ionisatie daarentegen resulteert in een enorme gevoeligheid door de heptafluorobutyryl imidazol derivatisatie. Het grote voordeel van deze enorme gevoeligheid is de mogelijkheid om een kleinere hoeveelheid staal te analyseren. Dit voordeel kan zeker benut worden voor analyses bij kinderen, waar meestal een beperkte hoeveelheid bloed afgenomen wordt. Het is wel

zo dat ongederivatiseerde componenten, zoals de tertiaire amines citalopram, melitraceen, mianserine en mirtazapine, niet gedetecteerd worden in deze ionisatiemode.

In **hoofdstuk VI** wordt de geoptimaliseerde GC-MS methode voor de 13 nieuwe generatie antidepressiva en hun metabolieten gevalideerd in plasma, bloed en hersenweefsel in de verschillende ionisatiemethodes. Hiervoor wordt de FDA regelgeving gevolgd. Tijdens de validatie procedure werden de stabiliteit, gevoeligheid, precisie, accuraatheid, extractierendement, lineariteit en selectiviteit geëvalueerd. Identificatie en kwantificatie van componenten was gebaseerd op het monitoren van enkele specifieke fragmentionen na electron- en chemische ionisatie. Calibratie gebeurde via een lineaire of kwadratische regressiecurve, respectievelijk voor electron- en chemische ionisatie. Gedeutereerde interne standaarden en een wegingsfactor van $1/x^2$ werden steeds toegepast. Kwantificatie limieten voor de antidepressiva in plasma werden vastgezet tussen 5-12,5 ng/ml voor electron en positieve chemische ionisatie, terwijl ze tussen 1-2,5 ng/ml lagen voor negatieve chemische ionisatie. De kwantificatie limieten verhoogden naar 5-20 en 25-62,5 ng/ml voor positieve chemische ionisatie in bloed en hersenweefsel. Accuraatheid, precisie, en stabiliteit waren voor de meeste componenten binnen de limieten vastgesteld door de FDA: niet meer dan 15% verschil met de doelwaarde, minder dan 15% variatie, tenzij voor de kwantificatie limiet waarbij een verschil van 20% aanvaard wordt. De meeste antidepressiva en hun metabolieten voldoen aan deze criteria en kunnen dus adequaat gekwantificeerd worden via deze methode. Enkel trazodone en O-desmethylvenlafaxine kunnen niet gekwantificeerd worden omwille van chromatografische- of derivatisatieproblemen.

Deze gevalideerde methode werd geïmplementeerd in forensische en klinische toepassingen.

Hoofdstuk VII beschrijft een preliminaire studie waarbij de gevalideerde GC-MS methode met electron ionisatie wordt gekoppeld aan een cytochroom 2D6 bepaling om zo de antidepressivatherapie te optimaliseren. Ondanks de lage toxiciteit van de huidige generatie antidepressiva, moeten de behandelende artsen er zich van bewust zijn dat depressie een chronische ziekte is waarbij medicatie heel lang nodig is. Daarenboven worden deze

patiënten met een waaier aan geneesmiddelen behandeld wat kan leiden tot neveneffecten en interacties. Momenteel is er een groeiende interesse naar de variabiliteit in plasmaspiegels en het finaal effect in relatie tot fysiologische, genetische en omgevingsfactoren. De meest bestudeerde factor is het effect van de cytochroom 2D6 polymorfismen op de antidepressiva-plasmaconcentraties. Daarom zal deze genotypering gekoppeld worden aan de ontwikkelde GC-MS methode. Een casus werd besproken in dit hoofdstuk om de haalbaarheid en bruikbaarheid van deze methodes te demonstreren in een reële klinische omgeving. Genotypering van de patiënt gebeurt best voordat een therapie ingesteld wordt. De informatie omtrent het fenotype kan dan tezamen met informatie rond co-medicatie en co-morbiditeit resulteren in een rationele keuze van therapie en dosering. Eens de therapie is opgestart kan het bepalen van plasmaspiegels informatie bezorgen rond therapietrouw en kan er een link gelengd worden tussen plasmaconcentraties en effect. Aan de andere kant zal er meer onderzoek moeten gebeuren om een goed beeld te krijgen over de relatie tussen doseringen, plasmaconcentraties en effect om zo een optimale gepersonaliseerde therapie mogelijk te maken. Daarnaast zal vooral de genotyperingsmethode verder geoptimaliseerd moeten worden aangezien niet alleen het CYP 2D6 enzyme polymorfisme verantwoordelijk is voor de variaties in plasmaconcentraties, maar een hele waaier aan polymorfismen van enzymes en geneesmiddelentransporters.

Een tweede toepassingsgebied van de ontwikkelde methode, in casu het forensische luik, wordt beschreven in **hoofdstuk VIII**. De GC-MS methode werd gebruikt in positive chemische ionisatiemode om antidepressiva op te sporen in volbloed, hersenweefsel en haarstalen in vijf post-mortem casussen. Een aantal antidepressiva waaronder fluoxetine, citalopram en sertraline werden gekwantificeerd in verschillende hersen-regionen. Hieruit bleek dat locatie van staalname geen belang heeft bij antidepressiva analyse en dat de detecteerbaarheid van antidepressiva langer is in hersenweefsel dan in bloed. We hadden graag een verband kunnen aantonen tussen bloed- en hersenconcentraties om zo vat te krijgen op het verband tussen bloedconcentraties en effect. Door het kleine aantal casussen was dit echter onmogelijk. Daarenboven kunnen variabelen zoals P-glycoproteïne poly-morfisme, het tijdsinterval tussen inname en dood, therapieperiode en therapietrouw aanleiding geven tot een andere hersen/bloed concentratie-

ratio. Haar werd ook geanalyseerd om een idee te hebben over therapietrouw en om de resultaten in het hersenweefsel te confirmeren.

Tenslotte wordt in **hoofdstuk IX** een algemene conclusie gegeven. Het is duidelijk dat de kern van het onderzoek de ontwikkeling en validatie van een GC-MS methode voor nieuwe generatie antidepressiva en hun metabolieten inhield. Daarnaast werd het nut van deze methode aangetoond door een klinische en forensische toepassing. Laten we hopen dat de door ons geoptimaliseerde methode in de nabije toekomst in grootschaligere forensische en klinische studies verder zal geëvalueerd worden en zal leiden tot nieuwe inzichten voor antidepressiva therapieën.

CURRICULUM VITAE

Sarah Wille

Pharmacist

Born in Gent on 3 March 1979

Married with Evert Vandeweghe

Education and work experience

2008-……..: Juridical expert at the National Institute of Criminalistics and Criminology in Brussels.

2002-2008: Ph.D. student at the Laboratory of Toxicology, Faculty of Pharmacy, Ghent University under the direction of Prof. Willy Lambert

1997-2002: Pharmacist degree obtained at Ghent University with great distinction.

1991-1997: Science-Maths high school degree at Sint-Jozef Instituut Aalst.

A$_1$ Publications (status 23/08/2008)

2008*:* Sarah M.R. Wille, Els A. De Letter, Michel H.A. Piette, Lien K. Van Overschelde, Carlos H. Van Peteghem, Willy E.E. Lambert, *Determination of new generation antidepressants in human post-mortem blood, brain tissue and hair using a gas chromatographic-mass spectrometric method in positive chemical ionization mode.* International Journal of Legal Medicine (accepted)
Impact factor: 3.030

Sarah M.R. Wille, Sarah G. Cooreman, Hugo M. Neels, Willy E.E. Lambert, *Relevant issues in the monitoring and the toxicology of old and new antidepressants.* Critical Reviews in Clinical Laboratory Sciences 45 (1), 1-66 (2008)
Impact factor: 5.037
Times cited: 1

2007:   Sarah M.R. Wille, Paul Van hee, Hugo M. Neels, Carlos H. Van Peteghem, Willy E. Lambert, *Comparison of electron and chemical ionization modes by validation of a quantitative gas chromatographic-mass spectrometric assay of new generation antidepressants and their active metabolites in plasma.* Journal of Chromatography A 1176, 236-245 (2007)
Impact factor: 3.641

Sarah M.R. Wille and Willy E.E. Lambert, *Recent developments in extraction procedures relevant to analytical toxicology.* Analytical and Bioanalytical Chemistry 388, 1381-1391 (2007)
Impact factor: 2.867
Times cited: 1

Kristof E. Maudens, Sarah M.R. Wille and Willy E.E. Lambert, *Traces of phosgene in chloroform: Consequences for extraction of anthracyclines.* Journal of Chromatography B 848, 384-390 (2007)
Impact factor: 2.935

2005:   Sarah M.R. Wille, Kristof E. Maudens, Carlos H. Van Peteghem and Willy E.E. Lambert, *Development of a solid phase extraction for 13 'new' generation antidepressants and their active metabolites for gas chromatographic-mass spectro-metric analysis.* Journal of Chromatography A 1098, 19-29 (2005)
Impact factor: 3.096
Times cited: 24

2004:   Sarah M.R. Wille and Willy E.E. Lambert, *Volatile substance abuse-post-mortem diagnosis.* Forensic Science International 142, 135-156 (2004)
Impact factor: 1.388
Times cited: 9

Sarah M.R. Wille and Willy E.E. Lambert, *Phenmetrazine or Ephedrine? Fooled by library search.* Journal of Chromatography A 1045, 259-262 (2004)
Impact factor: 3.595
Times cited: 4

Newsletters Publications

2007:   Active as reporter for the IATDMCT Newsletter during the 10th International Congress of Therapeutic Drug Monitoring and Clincal Toxicology, Nice, France, Sept 9-14, 2007

2006:   Sarah M.R. Wille, *Solid Phase Extraction in Clinical and Forensic Toxicology.* IATDMCT Young Scientists Scientific Issues Series in IATDMCT Newsletter.

Referee

Referee of several publications for Journal of Chromatography A and B, Analytical and Bioanalytical Chemistry, Clinical Chemistry and Laboratory Medicine, Journal of Pharmaceutical and Biomedical Analysis and Journal of Separation Science.

Congress Presentations

2008:   Oral presentation at the 46th meeting of The International Association of Forensic Toxicologists (TIAFT), Martinique, French West Indies, June 2-8, 2008
*Quantification of new generation antidepressants using a gas chromatographic-mass spectrometric method. Applications in clinical toxicology (*Sarah M.R. Wille, Paul Van hee, Hugo M. Neels, Carlos H. Van Peteghem, Willy E. E. Lambert)

Oral presentation at the BLT scientific meeting, Brussels, March 11, 2008
Case reports: determination of new generation antidepressants in human post-mortem blood, brain tissue and hair using a gas chromatographic-mass spectrometric method in positive chemical ionization mode (Sarah M.R. Wille, Els A. De Letter, Michel. H.A. Piette, Lien K. Van Overschelde, Carlos H. Van Peteghem, Willy E.E. Lambert)

Poster presentation at the 46th meeting of The International Association of Forensic Toxicologists (TIAFT), Martinique, French West Indies, June 2-8, 2008
Determination of new generation antidepressants in human post-mortem blood, brain tissue and hair using a gas chromatographic-mass spectrometric method in positive chemical ionization mode (Sarah M.R. Wille, Els A. De Letter, Michel H.A. Piette, Lien K. Van Overschelde, Carlos H. Van Peteghem, Willy E.E. Lambert)

2007:   Oral Presentation at the 10th International Congress of Therapeutic Drug Monitoring and Clincal Toxicology, Nice, France, Sept 9-14, 2007
Validation and comparison of a gas chromatographic-mass spectrometric method in electron ionization (EI) and positive chemical ionization mode (PICI) for the simultaneous determination of 13 antidepressants and their active metabolites in plasma (Sarah M.R. Wille, Carlos H. Van Peteghem and Willy E.E. Lambert)

Poster Presentation at the Joint Meeting of International Council on Alcohol, Drugs, and Traffic Safety (ICADTS), The International Association of Forensic Toxicologists (TIAFT), and the 8th Ignition Interlock Symposium (IIS), Seattle, Washington, USA, Aug. 26-30, 2007.
Validation of a GC-MS method for the simultaneous determination of 12 antidepressants and their active metabolites in plasma and application to whole blood, and brain tissue. (Sarah M. Wille, Carlos H. Van Peteghem, Willy E. Lambert)

2005: Oral Presentation at the 43th International Meeting of the International Association of Forensic Toxicologists (TIAFT), Seoul, Korea, Aug 29-Sept 2, 2005.
Development of a solid phase extraction for 13 'new' generation antidepressants and their active metabolites for gas chromatographic-mass spectrometric analysis (Sarah M.R. Wille, Kristof E. Maudens, Carlos H. Van Peteghem and Willy E.E. Lambert)

2004: Poster Presentation at the FBI Laboratory Symposium on Forensic Toxicology and Joint Meeting of the Society of Forensic Toxicologists (SOFT) & The International Association of Forensic Toxicologists (TIAFT), Washington, District of Columbia, USA, Aug. 29-Sept 4, 2004.
Phenmetrazine or Ephedrine? Fooled by library search (Sarah M. Wille, Carlos H. Van Peteghem, Willy E. Lambert)

Memberships

TIAFT   (The International Association of Forensic Toxicologists)

BLT   (The Toxicological Society of Belgium and Luxembourg)

IATDMCT (International Association of Therapeutic Drug Monitoring and Clinical Toxicology)